Copyright is owned by the Author of the thesis. Permission is given for a copy to be downloaded by an individual for the purpose of research and private study only. The thesis may not be reproduced elsewhere without the permission of the Author.

The Hydrogeology of the Pourewa Sub-Catchment, Rangitikei, New Zealand

A thesis presented in partial fulfilment of the requirements for the degree of
Doctor of Philosophy in Earth Science
at Massey University, Palmerston North, New Zealand.



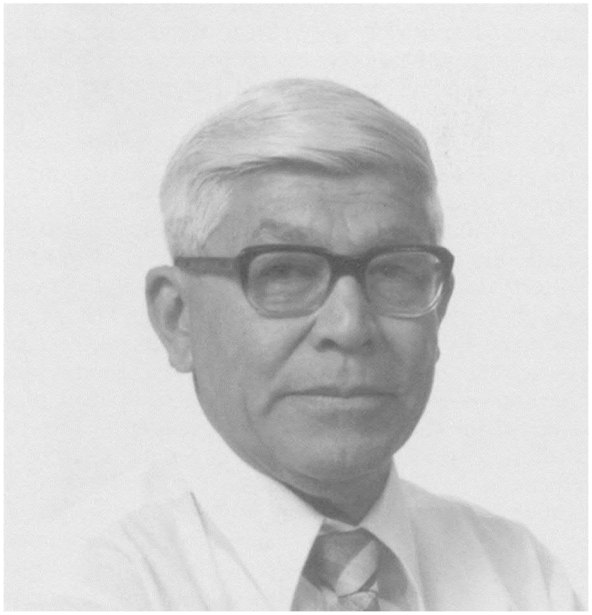
Callum Rees

2020

Volume 1

Dedication

This thesis is dedicated in honour and memory of the late Martin Theodore Te Punga (1921-1989), whose tremendous insights during pioneering work on New Zealand geology are equally as valid today.



Martin Te Punga in 1981, three years before his retirement from the New Zealand Geological Survey. Photo courtesy of GNS.



"I'm fascinated by the narrative of geology and I'm a veritable pack rat of a collector on the road. I keep a rock hammer in my car."

-Marianne Wiggins

Looking north over the broken hill country surrounding Coutts Creek and Mangara Stream during a fine winters morning. Mt Ruapehu can be seen on a good day, Taranaki on an exceptional one.

Abstract

This story begins in the geologically young and active landscapes of the lower North Island of New Zealand, positioned astride the interface between the Pacific and Australian tectonic plates. The chosen field area is located within the onland Whanganui Basin, a Late Miocene-Quaternary marine basin that has undergone uplift, inversion and fluvial incision to form spectacular river valley exposures through the basin succession. The area contains one of the most complete records of Quaternary climate change exposed onland anywhere in the world. Our journey centres on a portion of this uplifted marine basin, characterised by the highly erodible, pastorally farmed hill country of the Rangitikei.

The Pourewa Stream, a tributary of the Rangitikei River provides a cross section through rural landscapes of the lower North Island. The stream's headwaters begin in steep Taihape sheep and beef country, before transitioning into a broad valley with a gentle gradient headed for Hunterville. The lower reaches step down across extensive Late Pleistocene river terraces, providing versatile arable cropping and dairy pasture, until finally joining the Rangitikei River 6 km east of Marton.

Agriculture constitutes 90% of land use in the region, placing pressure on resources required for ongoing agricultural development and production. Recent concerns surrounding the long-term sustainability and potential contamination of freshwater resources have initiated research into the regions groundwater system. Previous studies have taken a broad approach examining large-scale issues surrounding classification, allocation, management and vulnerability of groundwater resources.

This study takes a different approach by examining a single sub-catchment of the Rangitikei River, with the aim of developing a conceptual hydrogeological model for the Pourewa Stream area. The proposed model is underlain by a comprehensive stratigraphic investigation of the Quaternary succession in the central Rangitikei. Geological context is provided through the development of a 1:25 000 geological map series and accompanying structural interpretation. Hydrogeochemical datasets derived from targeted *in situ* and laboratory based analysis provide baseline information. The conceptual hydrogeological model is applied on a wider regional scale to investigate basin history and processes of landscape formation. The project aims to support policy makers, landowners and developers in achieving sustainable management of groundwater resources by the avoidance of over exploitation and contamination.

Acknowledgements

Firstly, I must thank Alan and Julie Palmer. It seems to me we have been discussing the narrative of our geological past for quite some time. I suppose for the both of you it would appear that I have only just entered the conversation.

Alan you old workhorse, starting to show a slight inkling of slowing down, but I can't see any rust on the sharp end of your spade just yet. You never cease to amaze me in your ability to comprehend the wild assortment of variability in the landscape and surmise the simplest, most logical answer, whist I have a million mad ideas fluttering through my brain. Experience knows best.

Julie, I think your genuine interest in students makes you a truly wonderful supervisor for us lucky few. However, one must not be lulled into a false sense of security, when it comes to the hard answer you never shy away. Your imagination and spark stimulate those around you. With the innocent interjection of a fleeting idea, you can derail the thought process, releasing the proverbial hounds in an entirely different direction.

Ranvir, we have a bad habit of crossing wires, as only a geologist and engineer ever could. However, I have built a tremendous respect for your experience and unique perspective and you have been a great asset during my studies.

Special thanks to my co-supervisor John Begg for the support given during my studies. To your colleague Dr Alan Beu once again sir, it is an honor to have had your help. I take great inspiration from your enthusiastic and generous imparting of expertise; you are an irreplaceable wealth of knowledge to us all.

David Feek you old salty dog. Hope you get up to that batch of yours in Motuoapa soon. On behalf of all us useless, late, inexperienced students, I must say you are an irreplaceable addition to our projects and will be sorely missed when you finally get fed up with us all.

To all the Massey technicians and staff Ian Furkert, Glenys Wallace, Bob Toes, Ross Wallace, Dr Roberto Calvelo-Pereira, Dr Qinhua Shen, Dr Anja Mobis, Dr Gabor Kereszturi and Dr Mike Bretherton. You are all a great bunch of people to work with and were it not for your immense collective knowledge us lowly students would be left stranded in the dark, with no prior health and safety approval.

Fellow comrades in arms Hannah 1 and 2, Li Boxin, Celeste, hope your studies go well and you finally realise your tragic mistake in not focusing on the sedimentary geology just past your front doorstep. Driving through your study area whilst mentally testing theories on the surrounding landscape to get bread and milk at the local is a rare opportunity afforded during postgraduate study. To Gere, Li Yang, Atkinson, Ahmed 1 and 2 and other postgraduate students whom I have had the pleasure of meeting over the past three years, thank you all for your help and best wishes for the future.

Johnny Irons, if you spent half as much time writing as you do gas bagging you'd have finished that masters of yours by now! I'll be up to map your farm one day once I have finished with this Whanganui Basin stuff.

To my beloved wife, you have literally kept me alive for the last several years. Your complete disinterest in geology although unfathomable from my perspective has had the effect of keeping me comparatively sane. Helping me to appreciate there are many things in this world just as, if not more wondrous than mere rocks. Likewise, to my family, who have suffered considerably heavier loads than most,

due largely to the constant addition of rocks to your vehicles, thank you. I promise to collect them someday soon.

Finally, to all the farmers in the Rangitikei, Turakina and Manawatu. I've learnt more from you than I ever could've from books. Sometimes I feel like you're the geologist and I'm just a travelling scribe recording your story for you. Hope you enjoy the twist.

Table of Contents

Volume 1

Abstract i

Acknowledgements iii

Table of Contents iv

List of Figures viii

List of Tables xv

List of Equations xvii

Chapter 1: Introduction 1

1.1 Overview 1

1.2 Thesis objectives 5

1.3 Thesis outputs 6

1.4 Thesis organisation 7

Chapter 2: Setting the scene 15

2.1 Introduction 15

2.2 Physiography 18

2.3 Climate 27

2.4 Land use 29

2.5 Geological setting 34

Chapter 3: Geology 71
3.1 Abstract 72
3.2 Introduction 73
3.3 Geological setting 76
3.4 Methods 83
3.5 Stratigraphy 85
3.6 River terraces 101
3.7 Structure 103
3.8 Discussion 111
3.9 Conclusion 119
Chapter 4: Tephrostratigraphy 131
4.1 Abstract 132
4.2 Introduction 133
4.3 Geological setting 139
4.4 Methods 141
4.5 Results 144
4.6 Discussion 152
4.7 Conclusion 162
Chapter 5: Sedimentology 171
5.1 Abstract 172
5.2 Introduction 173
5.3 Geological setting 174
5.4 Methods 182
5.5 Results 184

5.6 Discussion 200
5.7 Conclusion 210
Chapter 6: Hydrogeology 224
6.1 Abstract 225
6.2 Introduction 226
6.3 Geological setting 229
6.4 Climate and physiography 231
6.5 Methods 235
6.6 Results 243
6.7 Discussion 254
6.8 Conclusion 267
Chapter 7: Aquifer Analogues 284
7.1 Abstract 285
7.2 Introduction 286
7.3 The study area - Geological setting 288
7.4 Methods and materials 291
7.5 Results 295
7.6 Discussion 308
7.7 Conclusions 314
Chapter 8: Regional Application 320
8.1 Abstract 321
8.2 Introduction 322
8.3 Study area 324
8.4 Methods 328

8.5 Results 331
8.6 Discussion 339
8.7 Conclusion 353
Chapter 9: Discussion 363
9.1 Conceptual hydrogeological model 366
9.2 Sequence stratigraphy 375
Chapter 10: Conclusion 382
10.1 Future Research 386

List of Figures

Figure 1.1: Location of the Rangitikei study area 3

Figure 2.1: Location of the geological mapping area 16

Figure 2.2: The Rangitikei District Boundary 19

Figure 2.3: The study area showing the Pourewa Stream sub-catchment, local river systems and townships 21

Figure 2.4: Major river systems in close proximity to the study area 23

Figure 2.5: The Rangitikei River catchment 24

Figure 2.6: Average annual rainfall between 1972 -2013 for the lower North Island of New Zealand. 28

Figure 2.7: LUCAS 2012 NZ Land use map of the Rangitikei Catchment. 30

Figure 2.8: LUCAS 2012 NZ land use map of the Pourewa sub-catchment. 31

Figure 2.9: The New Zealand subcontinent, showing the main bathymetric and tectonic features. 36

Figure 2.10: The North Island, New Zealand showing the key regional geological features. 37

Figure 2.11: New Zealand GPS velocities in an Australian Plate fixed reference frame 39

Figure 2.12: The North Island of New Zealand displaying fault lines from the GNS active fault database in relation to the study area and major river systems 44

Figure 2.13: The North Island of New Zealand showing major volcanic areas with reference to the Whanganui Basin 46

Figure 2.14: Distribution of isostatic gravity anomalies in the North Island.....49

Figure 2.15: Tectonostratigraphic basement terranes of New Zealand 51

Figure 2.16: Simplified geology of the Whanganui Basin area 52

Figure 2.17: Coeval uplift and subsidence in the Whanganui and King Country basins 53

Figure 2.18: Distribution of free air gravity anomalies in the North Island.....55

Figure 2.19: The Whanganui-Manawatu area showing major rivers and anticlines across the Manawatu Plains 57

Figure 3.1: A) Location of New Zealand showing Whanganui Basin (WB) in relation to the Taupo Volcanic Zone (TVZ), Hikurangi Trough, Alpine Fault, Pacific and Australian Plates 74

Figure 3.2: Simplified geology of the Whanganui Basin (WB) area 77

Figure 3.3: Composite stratigraphic column of Rangitikei geology 86

Figure 3.4 (facing page): Simplified geological map of central Rangitikei 88

Figure 3.5: Simplified examples of two of the geological cross sections constructed across the geological mapping area, displaying major groups and structures. See Fig. 3.4 for cross section locations. 90

Figure 3.6: Simplified 3D geological model of the study area displaying groups, faults, folds and major rivers.....93

Figure 3.7 (facing page): A) Kaimatira Pumice Sand Formation displaying low angle cross bedding 96

Figure 3.8 (facing page): A) Makirikiri Tuff Formation exposed in a tributary of Pourewa Stream.....98

Figure 3.9: A: View north over a flight of river terraces preserved along Te Houhou Road off SH1.....102

Figure 3.10: 3D image of the Whanganui-Manawatu area showing major rivers and anticlines across the Manawatu Plains 105

Figure 3.11: Interpreted six fold migrated seismic line BL-12 106

Figure 3.12: A: Normal displacement of Makirkiri Tuff Formation along the Nukumaru Fault Zone, near the confluence of Mangatutu Stream and the Rangitikei River 108

Figure 4.1: Map of the North Island showing the study area in relation to the Whanganui Basin (WB) 134

Figure 4.2: Geological map of the study area showing lithological groups, regional structures and the location of the Potaka Pumice and Pakihikura Pumice 142

Figure 4.3: Composition of glass shards from six tephra-fall and/or volcaniclastic deposits in the central Rangitikei 143

Figure 4.4: A) Pakihikura Pumice exposed at a cutting on Turakina Valley Road 148

Figure 4.5: Pleistocene stratigraphic correlations in the central Rangitikei 150

Figure 4.6: A) 25 m thick, clast supported conglomerate. Clasts are sub-rounded pebbles to cobbles of dominantly greywacke 151

Figure 4.7 (facing page): A) Coutts Creek Horizon cropping out along the southern scarp slope of Coutts Creek 154

Figure 4.8 (facing page): Regional correlation of the Pakihikura Pumice toward the main axial range. 158

Figure 4.9: A) Cartoon schematic of lower North Island at c. 1.6 Ma, during an early phase of large-scale rhyolitic eruptions from Mangakino Caldera 161

Figure 5.1: Map displaying the onland portion of the Whanganui Basin (WB) relative to the Taupo Volcanic Zone (TVZ) and Hikurangi margin. 175

Figure 5.2 Stratigraphic log of the proposed type section for the Waitapu Shell Conglomerate 180

Figure 5.3: Mean CaO versus FeOt (wt%) composition of glass shards analysed from tephra-fall and/or volcaniclastic samples.....185

Figure 5.4: The main types of SSDS recognised in the WB and their interpreted processes of deformation. 187

Figure 5.5: Sketch of the proposed Waitapu Shell Conglomerate type section at Waitapu stream.....189

Figure 5.6 (facing page): A) Close up of Liquefaction Zone 1 (LZ1), displaying a site of injection at the Waitapu Stream section. 190

Figure 5.7 (facing page): A) Channelled conglomerate near the base of cycle 37, Beaconsfield Valley 192

Figure 5.8 (facing page): A) Kaimatira Bluff section displaying load and ball and pillow structures.....196

Figure 5.9: Zingg diagram showing clast shape measurements from the Whareroa Conglomerate 199

Figure 5.10 (facing page): A) Schematic cartoon of the WB during the marine transgression of WB cycle 36 (MIS 22) at c. 0.88 Ma.....200

Figure 6.1: Location map of the study area displaying the outline of the Pourewa Stream catchment in yellow and relevant place names along its length 227

Figure 6.2 (facing page): A) Wandering channel morphology within the lower reach of the Pourewa Stream 232

Figure 6.3: Simplified geological map of the study area showing the location of the Pourewa Stream catchment 236

Figure 6.4: Simplified cross sections A to A' and B to B' trending N-S and E-W respectively 237

Figure 6.5 (facing page): A) Groundwater seeps at the contact between Tuha Sandstone and underlying Tikapu Siltstone, Rangitikei Group, exposed in cliffs in the Rangitikei River valley..... 238

Figure 6.6 (facing page): A) Small spring flowing out of Holocene gravels at the base of Leedstown Valley 240

Figure 6.7: A) Photo of the falling head permeameter setup at Massey University, Palmerston North 242

Figure 6.8: Graphs demonstrating key relationships between grain size statistics and hydraulic conductivity. 248

Figure 6.9: Graphs displaying the relationships between porosity and hydraulic conductivity. 249

Figure 6.10: Simplified hydrostratigraphic map of the study area showing the location of the Pourewa Stream catchment..... 253

Figure 6.11: Schematic palinspastic diagram of the lower Pourewa Stream 255

Figure 6.12 (facing page): A) Aerial photograph of paleo-channels observable as micro-topography on the Last Glacial Maximum surface 262

Figure 7.1: Image of the study area (red rectangle) relative to the Rangitikei Catchment (white polygon) and wider physiography of a portion of the lower North Island, New Zealand..... 287

Figure 7.2: Boxplots of the air permeability measurements (millidarcys) for each geological unit 296

Figure 7.3: Cumulative percentage grain size distributions for each hydrostratigraphic unit. 298

Figure 7.4: A) The relationship between hydraulic conductivity derived from falling head permeameter analysis.....299

Figure 7.5: A) Estimated hydraulic conductivity values (K_a) in m per second determined by in situ measurement of air permeability of a weakly consolidated, bioturbated sandstone from Mangarere Formation ...300

Figure 7.6: A) Estimated hydraulic conductivity values (*Ka*) in m per second determined by insitu measurement of air permeability of Mangarere Siltstone 301

Figure 7.7: A) Estimated hydraulic conductivity values (*Ka*) in m per second determined by insitu measurement of air permeability of a high-energy, silty, pumiceous sandstone, Kaimatira Pumice Sand Formation 303

Figure 7.8: A) Estimated hydraulic conductivity values (K_a) in m/s determined by insitu measurement of air permeability of Mangapipi Conglomerate 306

Figure 7.9: A) Estimated hydraulic conductivity values (*Ka*) in m per second determined by in situ measurement of air permeability of Mangaweka Mudstone Formation.....307

Figure 8.1 (facing page): Location map displaying the study area with reference to the Whanganui Basin 322

Figure 8.2: Examples of different types of mass movements 330

Figure 8.3: Example of relict landslide deposits in the Rangitikei.....332

Figure 8.4: A) Digital elevation data of a portion of the Turakina River catchment displaying characteristic landforms developed along strike of the Mangamako Shellbed. 334

Figure 8.5: A) Distribution of 334 deep-seated Late Quaternary relict landslide zones within the study area. 337

Figure 8.6: A) Aspect distribution (%) of all slopes within the study area. 340

Figure 8.7: Comparison of the landslide aspect, total slope aspect and dip direction for selected river catchments within the study area 343

Figure 8.8: A) Comparison of deep-seated Late Quaternary relict landslide aspect with dip direction measurements from WB fill..... 344

Figure 8.9: A) Exposed slip surface beneath a rock rotational slide in Okehu Group 345

Figure 8.10 (facing page): Photos of deformed Okehu Group strata from a deep-seated, relict Quaternary landslide 346

Figure 8.11: Conceptual model for the study area. 348

Figure 8.12: Conceptual model for asymmetric southward plunging anticlines typical of eastern WB. 350

Figure 8.13: A) Location of 1855 Wairarapa earthquake triggered landslide in the Rangitikei Valley 352

Figure 9.1: Conceptual diagrams illustrating observed relationships between rock types and water in the landscape. 368

Figure 9.2: Schematic diagram illustrating the conceptual hydrogeological model. 369

List of Tables

Table 3.1: Proposed new stratigraphic nomenclature for subdivision of Te Pungas' (1952) Upper Rangitikei Formation 82

Table 3.2: Major alluvial terraces in Rangitikei Valley 101

Table 4.1: Proposed stratigraphic nomenclature used in this study (far right) and correlation to other proposed nomenclatures of the eastern and western Whanganui Basin 136

Table 4.2: Selected tephra-fall and/or volcaniclastic deposits and their respective stratigraphic units from the Rangitikei 138

Table 4.3: Electron Probe Microanalyser data for glass shards from the study area, Whanganui Basin 144

Table 5.1: Stratigraphic nomenclature and correlations between the Castlecliff type section 178

Table 6.1: Major aggradational terraces in Rangitikei Valley 230

Table 6.2: Average grain size, hydraulic conductivity (K), bulk density, total porosity and effective porosity measurements 246

Table 6.3: Major element geochemistry (% weight) of respective samples grouped by lithology 250

Table 6.4: Average organic and inorganic carbon contents and clay minerals identified during analysis of respective lithologies 251

Table 7.1: Hydrogeological properties of the main hydrostratigraphic units from the WB, New Zealand 297

Table 8.1: Stratigraphic nomenclature used in this study 325

Table 8.2: Ranges for selected physical and hydraulic properties of WB rock types 329

Table 8.3: Results from the deep-seated Late Quaternary relict landslide zone survey. 338

Table 9.1: List of hydrostratigraphic units within the study area 367

Table 9.2: Stratigraphic nomenclature of the study area including associated Whanganui Basin cyclothems 376

List of Equations

Equation 7.1: Conversion of gas flow rate and gas pressure to gas permeability using a modified form of Darcy's law 291

Equation 7.2: Transfer function to convert air permeability (k_a) to saturated hydraulic conductivity (K_s) by linking air and water permeability and making use of the relation between K_s and intrinsic saturated water permeability ($k_{w,s}$) 292

Equation 7.3: Empircal equation of Iversen et al (2003) to convert air permeability data (k_a) to estimates of saturated hydraulic conductivity (K_s) 294



Chapter 1

Introduction

1.1 Overview

Water is a precious natural resource that supports all living organisms on Earth. Everyday life relies on our ability to access inexpensive, clean water and dispose of it after use (Allan 2011). Sufficient clean water supply is also essential to food production. This is particularly evident in countries like New Zealand that rely on the ability to produce and export food for their economic and social well-being.

Most of the Earths liquid freshwater is found, not on the surface but stored in underground aquifers (Morris et al. 2003). Groundwater is generally cheaper, more convenient and less vulnerable to pollution than surface water (Hiscock 2005). This underground resource goes largely unnoticed by society due to its 'invisible' location within the earth and its seemingly infinite supply.

However, with the advent of steam driven pumps in the 18th century, humanity's ability to pump large quantities of groundwater soon highlighted groundwater as a finite resource (Yannopoulos et al. 2014). Newly established technological advances coupled with an ever-expanding human population intensified pressure on groundwater resources as abstraction for municipal water supply, irrigation, and industrial use increased.

View east across the Rangitikei Valley, taken from a small terrace remnant off Iron Works Road, Mangaonoho.

An increasing human population has also exerted pressure on the agricultural and horticultural industries, as global demand for food products rises. Primary producing nations such as New Zealand have intensified production over the last 30 years to meet new global demands (Williams & Richardson 2004; MacLeod & Moller 2006).

Intensification of land use has led to a greater demand for water, higher use of fertiliser and agricultural chemicals and the need to dispose of large quantities of waste byproducts (Quinn et al. 2009). Anthropogenic activities and their resultant pressure on groundwater resources have led to groundwater degradation.

Groundwater degradation occurs as a result of:

- Excessive exploitation e.g. where groundwater levels fall to an unacceptable level, reducing the available water resource. This can result in adverse and expensive side effects including ground subsidence (Liu et al. 2001) and saline intrusion (Antonellini et al. 2008).
- Major changes in land use e.g. conversion from natural vegetation to intensive farming can lead to elevated nutrient levels in shallow groundwater (Ford & Taylor 2006; Bidwell et al. 2009).
- Inappropriate and/or uncontrolled activities at the land surface e.g. incorrect disposal of waste or spillage of chemicals allowing leachates to enter groundwater (Mor et al. 2006; Moreau et al. 2019).

The Rangitikei District in the western half of the lower North Island, New Zealand is characterised by extensive rolling hill country with good quality groundwater resources suitable for drinking and irrigation purposes (Catalyst-Group 2014). Agriculture constitutes over 90% of the total land use in the region (Zarour 2008). Land-use intensification, marked by the conversion of sheep and beef to dairy farms has been driven by the relative economics of land use in the region (Quinn et al. 2009).



Figure 1.1: Location of the Rangitikei study area (black box). Orange lines indicate state highways; Red polygons represent the location of GNS Science QMAP sheets.

Concerns around the long-term sustainability and potential contamination of the Rangitikei aquifers has initiated research into the groundwater systems of the Rangitikei (Bekesi & McConchie 1999, 2000; Bekesi & McConchie 2002; Roygard & Carlyon 2004; Begg et al. 2005; Collins et al. 2016).

Limited information is available on local-scale hydrogeological settings within the Rangitikei Region (Fig 1.1), including a present knowledge gap concerning the physical and geochemical characteristics of its various rock types. A sound understanding of local hydrogeology is necessary for improved mapping and quantification of the region's groundwater resources. Furthermore, this is essential information for improving our understanding and ability to map and quantify water and nutrient flow pathways from farmlands to receiving waters, informing practices and policies for targeted and effective water quality management. Previous studies in the Rangitikei area have focused on regional groundwater resource classification, allocation, management and vulnerability (Roygard & Carlyon 2004; McCarron & Zarour 2005; McArthur et al. 2007; Wilson 2007; Zarour 2008; Callander & Thomas 2013; Morgenstern et al. 2015; Singh et al. 2017).

This study takes a different approach by focusing on a single sub-catchment of the Rangitikei River. A hydrogeological framework for the Pourewa Stream is presented. The framework is underlain by a comprehensive stratigraphic investigation of the Pliocene–Holocene sedimentary succession of central Rangitikei, New Zealand. This research aims at providing information on the local geology and aquifer characteristics through the development of 1:25 000 geological map, accompanying structural interpretation and 3D geological model. Ultimately with the goal to support policy makers, landowners and developers in achieving sustainable management of groundwater resources by the avoidance of over exploitation and contamination.

1.2 Thesis objectives

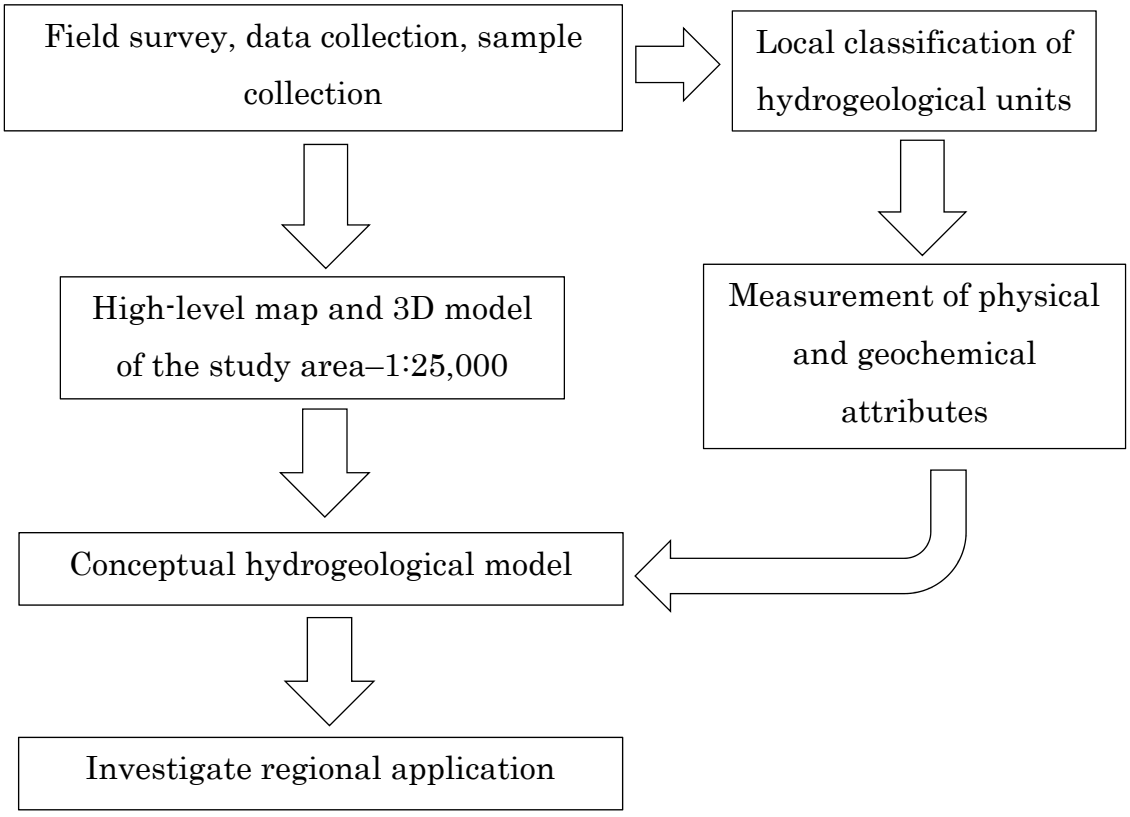
1) Compile all existing data on the geology and hydrogeology of the study area.

2) Document and refine the stratigraphy of the study area. Map the distribution of stratigraphic units and structural features. Construct a 3D geological model of the study area.

3) Subdivide the stratigraphy into broad hydrostratigraphic units. Measure their physical and geochemical attributes.

4) Develop a conceptual hydrogeological model.

5) Investigate wider regional application of the hydrogeological model.



1.3 Thesis outputs

This research includes a 1:25,000 geological mapping survey of the central Rangitikei District. The survey involves logging outcrops, correlating between key sections, analysing tephra and fossil content and integrating the study areas geology into the stratigraphic framework of the Rangitikei (Naish & Kamp 1995) and Whanganui Basin (Naish & Kamp 1995; Naish et al. 1997; Carter & Naish 1998; Abbott et al. 2005; Alloway et al. 2005; Naish et al. 2005; Pillans et al. 2005; Carter et al. 2014).

The resulting geological map series presents the distribution of lithostratigraphic units, faults and folds within the study area, produced within a Geographic Information System (GIS) environment using ArcInfo 10.3. Database design is based on the structure established by the GNS Science QMAP program (Rattenbury & Heron 1997). The database contains a seamless coverage of the study area, enabling maps to be reproduced for any given area. The new map series is presented in Appendix B (Sheets 1-4).

Geological cross-sections trending east-west and north-south across the study area accompany the map sheets. Geological and structural data have also been used in combination with Leapfrog Geo™ software to produce a 3D geological model of the central Rangitikei, complimenting the map sheets and cross sections presented in Appendix B. The model has been designed to be included within a dynamic learning process in which new and existing datasets can be displayed, interpreted and used in the decision making process to optimise future sampling locations and inform the best use of resources. The 3D model is able to be continuously updated and improved, making it a powerful tool for future hydrogeological investigations.

A 1:25,000 hydrogeological map and corresponding cross-sections are also presented in Chapter 6. Subdivision of the Pliocene to Holocene sediments into hydrostratigraphic units was based on a units' ability to store and transmit water. A conceptual hydrogeological model of the study area is presented and discussed in Chapter 9, drawing together work from all previous chapters to compile an overview of the study area's hydrogeology.

1.4 Thesis organisation

This thesis has been arranged into two volumes. The first volume contains ten chapters separated into their respective topics following the flow chart illustrated in the thesis objectives (1.2). Broadly, volume one contains the introduction, background information, geology, tephrostratigraphy, sedimentology, hydrogeology, aquifer analogues, regional application, discussion and conclusion of the thesis.

Volume two contains a variety of information relevant to volume one. It has been presented separately to maintain the chapter order of volume one and to improve clarity. Overall, volume two contains raw data and the new map series of the central Rangitikei.

The following research is styled as a thesis by publication. Each chapter follows an outline typical of a journal article, including a reference list provided at the end of the chapter. This style results in a certain level of repetition as each journal article contains an outline of the study area including its geographic location and regional setting. Despite this drawback, the author is confident that by having taken this approach the quality of the text is of a much higher standard than could otherwise have been achieved.

Included below is a list of the thesis content with a brief description of each chapter and appendix:

Volume 1

Chapter 1: Introduction

The first chapter provides a general overview of the research topic, outlining the proposed objectives, research outputs and describing the thesis layout.

Chapter 2: Setting the scene

Chapter 2 provides an overview of the physiography, climate, land use and geological setting of the study area. The geographic location of the study area is introduced before moving onto the main tectonic elements and geological history of the lower North Island.

Chapter 3: Geology

This chapter is based on a map bulletin in preparation entitled: "Geology of the central Rangitikei, Whanganui Basin, lower North Island, New Zealand". The bulletin summarises the geological work conducted during the course of this PhD, including the compilation of a revised stratigraphic nomenclature and 1:25 000 geological map series of the central Rangitikei.

Chapter 4: Tephrostratigraphy

Chapter 4 presents a journal article entitled: "Tephrostratigraphic constraints on the timing of sedimentation and tectonism in the Whanganui Basin, New Zealand", published in the New Zealand Journal of Geology and Geophysics, Volume 63, Issue 2. This paper discusses the tephra and volcaniclastic marker horizons used during the geological mapping survey, including their identification and application in regional geological mapping.

Chapter 5: Sedimentology

This chapter presents a paper entitled: "Whanganui Basin, an archive of prehistoric earthquakes? Waitapu Shell Conglomerate (C. 0.9 Ma), North Island, New Zealand', published in the New Zealand Journal of Geology and Geophysics, Volume 62, Issue 2. The focus of this paper is to document the Waitapu Shell Conglomerate and follow the unit laterally across the landscape to unravel a single time slice in basin history.

Chapter 6: Hydrogeology

This chapter presents a paper entitled: "Landscape evolution and hydrogeochemical characteristics of the Pourewa Stream catchment, lower North Island, New Zealand", published in the New Zealand Journal of Geology and Geophysics, Volume 62, Issue 2. This manuscript describes the subdivision of the geology into hydrostratigraphic units, their physical and geochemical characteristics and the geological history of the Pourewa Stream area.

Chapter 7: Outcrop analogues of aquifers

Chapter 7 presents a journal article entitled: "Outcrop analogues of lateral variation in aquifer hydraulic conductivity, Whanganui Basin, New Zealand", published in the journal Groundwater, Volume 58, Issue 4. This paper explores variations in hydraulic conductivity within the heterogeneous aquifers and aquitards of the study area. We apply a rapid, *in situ* method for deriving hydraulic conductivity through the application of an air permeameter.

Chapter 8: Regional application

Chapter 8 presents a journal article entitled: "Litho-structural controls on Quaternary landslide distribution in the Rangitikei hill country, North Island, New Zealand", published in the New Zealand Journal of Geology and Geophysics, Volume 63, Issue 1. This paper investigates the relationships between deep-seated Late Quaternary relict landslide zones, geology and geomorphology in the

Rangitikei hill country. It applies the conceptual models developed in this thesis at a regional level.

Chapter 9: Discussion

This chapter focuses on drawing together the combined knowledge of each of the proceeding chapters, discussing relationships observed in the field, presenting the conceptual hydrogeological model for the study area and discussing the application of sequence stratigraphy within this research.

Chapter 10: Conclusion

The final chapter summarises the results of the entire research project. Chapter ten provides a description of ongoing research plans and suggests potential research ideas for other workers in the study area.

Volume 2 (Appendices)

Appendix A: Supplementary data

This appendix presents supplementary datasets for chapters 3, 4, 5 and 7 including marcofossil, grain size and electron probe micro-analyser datasets together with a complete stratigraphic nomenclature for the study area.

Appendix B: Geological map series

Appendix B contains copies of the new 1:25 000 geological map series of the central Rangitikei, together with accompanying geological cross sections.

References

Abbott ST, Naish TR, Carter RM, Pillans BJ 2005. Sequence stratigraphy of the Nukumaruan Stratotype (Pliocene-Pleistocene, c. 2.08–1.63 Ma), Wanganui Basin, New Zealand. Journal of the Royal Society of New Zealand 35(1-2): 123-150.

Allan JA 2011. Virtual Water: Tackling the Threat to Our Planet's Most Precious Resource. I.B Tauris & Co. Ltd, London, United Kingdom. 353 p.

Alloway BV, Pillans BJ, Carter L, Naish TR, Westgate JA 2005. Onshore-offshore correlation of Pleistocene rhyolitic eruptions from New Zealand: Implications for TVZ eruptive history and paleoenvironmental construction. Quaternary Science Reviews 24(14-15): 1601-1622.

Antonellini M, Mollema P, Giambastiani B, Bishop K, Caruso L, Minchio A, Pellegrini L, Sabia M, Ulazzi E, Gabbianelli G 2008. Salt water intrusion in the coastal aquifer of the southern Po Plain, Italy. Hydrogeology Journal 16(8): 1541-1556.

Begg JG, Palmer A, Gyopari M 2005. Geological synopsis of the Manawatu-Horowhenua area for a review of the region's hydrogeology. Institue of Geological and Nucelar Sciences Client Report 2005/172, Lower Hutt, New Zealand. 22 p.

Bekesi G, McConchie J 1999. Groundwater recharge modelling using the Monte Carlo technique, Manawatu region, New Zealand. Journal of Hydrology 224(3-4): 137-148.

Bekesi G, McConchie J 2000. Mapping soil sorption capacity as a measure of regional groundwater vulnerability. Journal of Hydrology New Zealand 39(1): 1-18.

Bekesi G, McConchie J 2002. The use of aquifer-media characteristics to model vulnerability to contamination, Manawatu region, New Zealand. Hydrogeology Journal 10(2): 322-331.

Bidwell V, Ventures L, Thorley M, Canterbury E, Scott D 2009. Nitrate discharge to groundwater from agricultural land use : an initial assessment for the Canterbury Plains. Technical Report commissioned by the Canterbury Water Management Strategy steering group, Christchurch, New Zealand. 16 p.

Callander P, Thomas N 2013. Report on Horizons Groundwater Level Monitoring Network and Groundwater Quantity Management Issues. Horizons Report 2013/EXT/1319, Horizons Regional Council, Palmerston North, New Zealand 9781927250242. 55 p.

Carter RM, Naish TR 1998. A review of Wanganui Basin, New Zealand: Global reference section for shallow marine, Plio-Pleistocene (2.5-0 Ma) cyclostratigraphy. Sedimentary Geology 122(1-4): 37-52.

Carter RM, Abbott ST, Naish TR 2014. Plio-Pleistocene cyclothems from Wanganui Basin , New Zealand : type locality for an astrochronologic time-Scale , or template for recognizing ancient glacio-eustasy. Philosophical Transactions of the Royal Society of London 357(1757): 1861-1872.

Catalyst-Group 2014. Rangitikei Catchment: Surface Water Use and Avaliability. Report No 2014/003 prepared as part of the Rangitikei Strategic Water Assessment project, Palmerston North, New Zealand. 39 p.

Collins S, Singh R, Rivas A, Palmers A, Horne D, Roygard J, Mathews A 2016. Assessment of nitrogen flow pathways and its potential attenuation in shallow groundwaters in the Lower Rangitikei Catchment. In: Currie LD, Singh R ed. Integrated nutrient and water management for sustainable farming, Occassional Report No. 29. Fertilizer and Lime Research Centre, Massey University, Palmerston North, New Zealand. Pp. 1-14.

Ford R, Taylor K 2006. Managing Nitrate Leaching To Groundwater : an Emerging Issue for Canterbury. In: Currie LD, Singh R ed. Proceedings of the Fertiliser and Lime Research Centre Workshop 2006, Massey University, Palmerston North, New Zealand. Pp. 1-9.

Hiscock KM 2005. Hydrogeology: principals and practice. Oxford, United Kingdom, Blackwell Publishing. 377 p.

Liu C, Yu J, Kendy E 2001. Groundwater exploitation and its impact on the environment in the North China Plain. Water International 26(2): 265-272.

MacLeod CJ, Moller H 2006. Intensification and diversification of New Zealand agriculture since 1960: An evaluation of current indicators of land use change. Agriculture, Ecosystems and Environment 115(1-4): 201-218.

McArthur K, Roygard J, Ausseil O, Clark M 2007. Development of Water Management Zones in the Manawatu-Wanganui Region : Technical Report to Support Policy Development, Report No: 2006/EXT/733, Horizons Regional Council, Palmerston North, New Zealand 187741347X. 120 p.

McCarron C, Zarour H 2005. State of the environment of the Manawatu-Wanganui Region – 2005. Technical Report Five – groundwater, 2004/EXT/609. 1-67, Horizons Regional Council, Palmerston North, New Zealand. 73 p.

Mor S, Ravindra K, Dahiya RP, Chandra A 2006. Leachate characterization and assessment of groundwater pollution near municipal solid waste landfill site. Environmental Monitoring and Assessment 118(1-3): 435-456.

Moreau M, Hadfield J, Hughey J, Sanders F, Lapworth DJ, White D, Civil W 2019. A baseline assessment of emerging organic contaminants in New Zealand groundwater. Science of the Total Environment 686: 425-439.

Morgenstern U, Stewart M, Daughney C, Townend D 2015. Transit times of baseflow in New Zealand rivers. European Geosciences Union General Assembly 2015, Vienna, Austria 17: 1-2.

Morris BL, Lawrence AR, Chilton PJ, Adams B, Caylow RC, Klinck BA 2003. Groundwater and its susceptibility to degradation: a global assessment of the problems and options for management. United Nations Environment Program, Early Warning and Assessment Report Series RS. 03-3, Nairobi, Kenya. 120 p.

Naish T, Kamp PJJ, Pillans B 1997. Recurring Global Sea-Level Changes Recorded In Shelf Deposits Near the G/M Polarity Transition, Wanganui Basin, New Zealand: Implications For Redefining The Pliocene-Pleistocene Boundary. Quaternary International 40: 61-71.

Naish TR, Kamp PJJ 1995. Pliocene-Pleistocene marine cyclothems , Wanganui Basin , New Zealand : a lithostratigraphic framework. New Zealand Journal of Geology and Geophysics 38: 223-243.

Naish TR, Field BD, Zhu H, Melhuish A, Carter RM, Abbott ST, Edwards S, Alloway BV, Wilson GS, Niessen F and others 2005. Integrated outcrop, drill core, borehole and seismic stratigraphic architecture of a cyclothemic, shallow marine depositional system, Wanganui Basin, New Zealand. Journal of the Royal Society of New Zealand 35(1-2): 91-122.

Pillans BJ, Alloway B, Naish TR, Westgate J, Abbott S, Palmer AS 2005. Silicic tephras in Pleistocene shallow-marine sediments of Wanganui Basin, New Zealand. Journal of the Royal Society of New Zealand 35(1-2): 43-90.

Quinn JM, Wilcock RJ, Monaghan RM, McDowell RW, Journeaux PR 2009. Grassland farming and water quality in New Zealand. Tearmann: Irish journal of agri-environmental research 7: 69-88.

Rattenbury MS, Heron DW 1997. Revised procedures and specifications for the QMAP GIS, Institute of Geological and Nuclear Sciences science report 97/3, Lower Hutt, New Zealand. 52 p.

Roygard J, Carlyon G 2004. Water Allocation Project Rangitikei River, Water Resource Assessment – Allocation Limits and Minimum Flows. Technical Report

2004/EXT/606. Horizons Regional Council, Palmerston North, New Zealand 1877310557. 178 p.

Singh R, Elwan A, Horne D, Manderson A, Patterson M, Roygard J 2017. Predicting land-based nirtogen loads and attenuation in the Rangitikei River catchment - The model development. In: Currie LD, Hedley MJ ed. Science and policy: nutrient management challenges for the next generation. Fertilizer and Lime Research Center Occassional Report No 30, Massey University, Palmerston North, New Zealand. Pp. 1-13.

Williams JM, Richardson P 2004. Growing for good: Intensive farming, sustainability and New Zealand's environment. In: Stewart G ed. Parliamentary Commissioner for the Environment Report 2004, Wellington, New Zealand. Pp. 84-128.

Wilson S 2007. Reconnaissance vertical electrical sounding survey of the Rangitikei-Manawatu- Horowhenua area, Horizons Regional Council Report No: 2007/EXT/852, Palmerston North, New Zealand. 47 p.

Yannopoulos SI, Lyberatos G, Angelakis AN, Theodossiou N 2014. Water Pumps through the Ages. In: Kalavrouziotis IK, Angelakis AN ed. IWA Regional Symposium on Water, Wastewater and Environment: Traditions and Culture, Hellenic Open University, Patras, Greece. Pp. 22-24.

Zarour H 2008. Groundwater Resources in the Manawatu–Wanganui Region Technical Report 2008/ET/948. Horizons Regional Council, Palmerston North, New Zealand. 262 p.



Chapter 2

Setting the scene

2.1 Introduction

This study focuses on the hydrogeology of the Pourewa Stream sub-catchment in the central Rangitikei District (Fig 2.1). To fully understand and begin to conceptualise the hydrogeology of the study area two key aspects require further consideration. Firstly, an understanding of the local and regional geology is vital for the development of a conceptual hydrogeological model. The research presented in chapters two through five, addresses this objective through the classification and subdivision of local stratigraphy, documentation and interpretation of geological structures and a synthesis of basin and landscape evolutionary history.

Initially, I set a 1,700 km^2 mapping area, fully enclosing the 35 km long Pourewa Stream (Fig. 2.1). The geographic extent and location of the mapping area focuses a high-level geological investigation around the Pourewa sub-catchment. Groundwater does not explicitly follow surface water or topography; instead, it is largely controlled by the structure and composition of the earth. For this reason, I set the mapping area beyond the surface extent of the Pourewa sub-catchment, allowing for a wider interpretation of the regional geology.

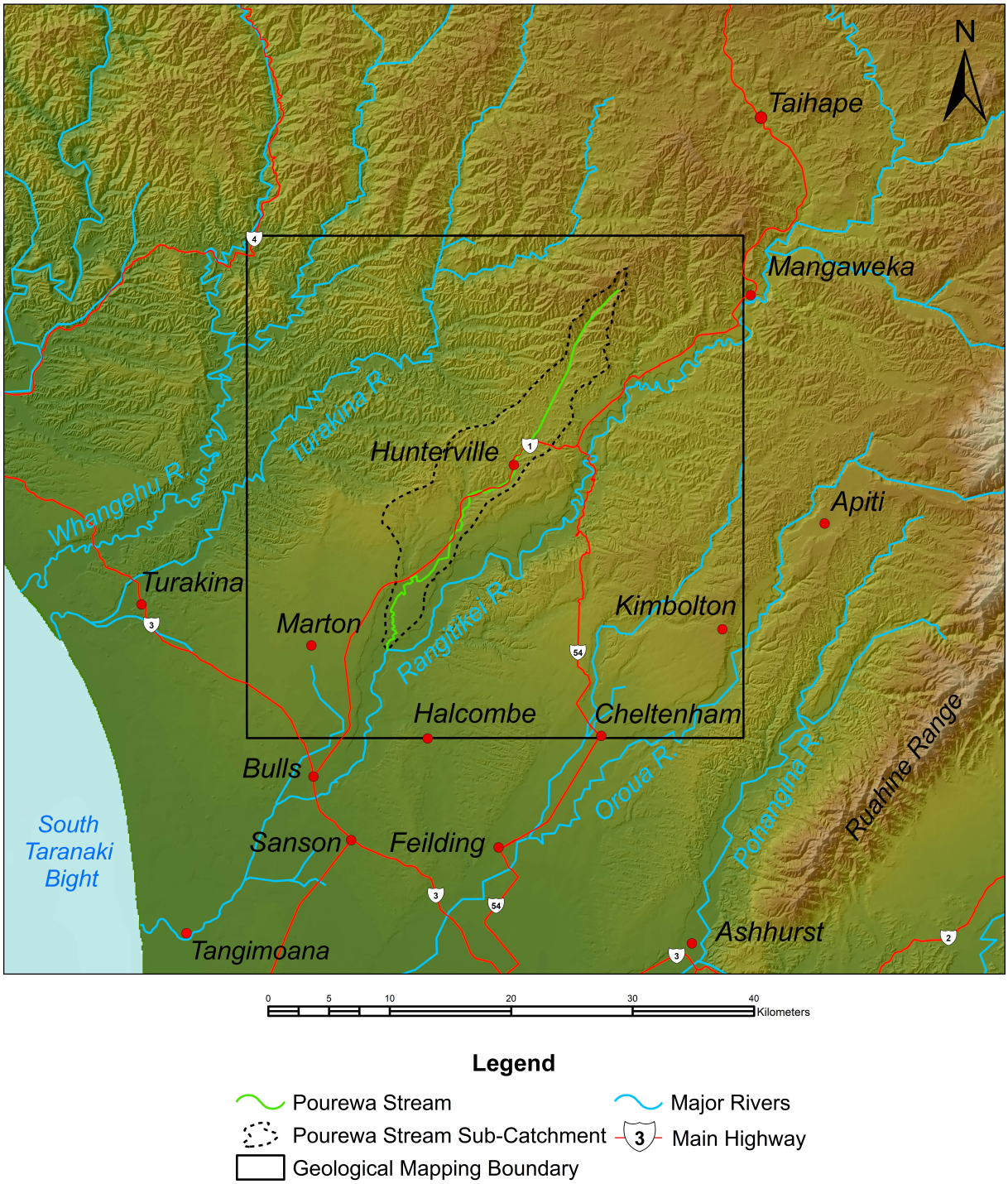


Figure 2.1: Location of the geological mapping area (black box), Pourewa Stream (Green line) and surrounding sub-catchment (dashed black line). Topographic data sourced from LINZ Data Service, Crown Copyright Reserved.

Taking a broader perspective allows for delineation of model boundaries based on changes in geology rather than being constrained to using surface hydrology and topographic boundaries.

The second set of key information is associated with subdivision of the main lithologies into hydrostratigraphic units based on their ability to store and transmit water. In chapters six and seven I investigate the hydrogeology of the Pourewa sub-catchment through a combination of field and laboratory analyses, obtaining physical and geochemical datasets to characterise representative units. A regional application of the ideas and models developed through this thesis is illustrated in chapter eight by investigating land stability within the Rangitikei hill country. Finally, chapter nine presents a conceptual hydrogeological model for the Pourewa sub-catchment, drawing together data and interpretations presented in all previous chapters before considering the direction of future research.

In this chapter, I introduce the Pourewa sub-catchment and geological mapping area within a regional framework. Examining the regional physiography, climate, land use and geological setting of the study area to provide important context for the local geological and hydrogeological investigations to be presented in subsequent chapters. I begin with exploring the location and general characteristics of the Pourewa Stream and Rangitikei District in the lower North Island of New Zealand before moving on to an in depth account of the study area's geological setting.

2.2 Physiography

The Pourewa Stream is a small tributary of the Rangitikei River located in the Rangitikei District on the western side of the lower North Island, New Zealand. I begin this section with an overview of the Rangitikei District and the Pourewa Valley before moving onto descriptions of the major rivers systems encompassed by the study area.

Rangitikei District

The Rangitikei District is a territorial authority located within the Manawatu-Whanganui Region, North Island, New Zealand (Fig. 2.2). The district boundary follows the Rangitikei River SW from the North Island Volcanic Plateau to the South Taranaki Bight, forming a trapezium shaped block with an area of 4,479 km^2, including the towns of Taihape, Bulls, Marton, Hunterville and Mangaweka. Approximately 14,019 people live in the Rangitikei District, with the town of Marton containing the single largest population of 4,548 (Statistics New 2013).

The Rangitikei District comprises a broad range of landscapes from the mountainous central North Island, dominated by the volcanoes of the Tongariro Volcanic Centre and North Island main axial ranges to the extensive coastal dune fields of the Manawatu (Cowie 1963) where the lower reaches of the Rangitikei meander out toward the Tasman sea. The northern Rangitikei District includes the Kaimanawa and Northern Ruahine ranges reaching elevations of >1500 masl. The elevation drops sharply southward from the Central Volcanic Plateau to 500 masl within the Taihape hill country.

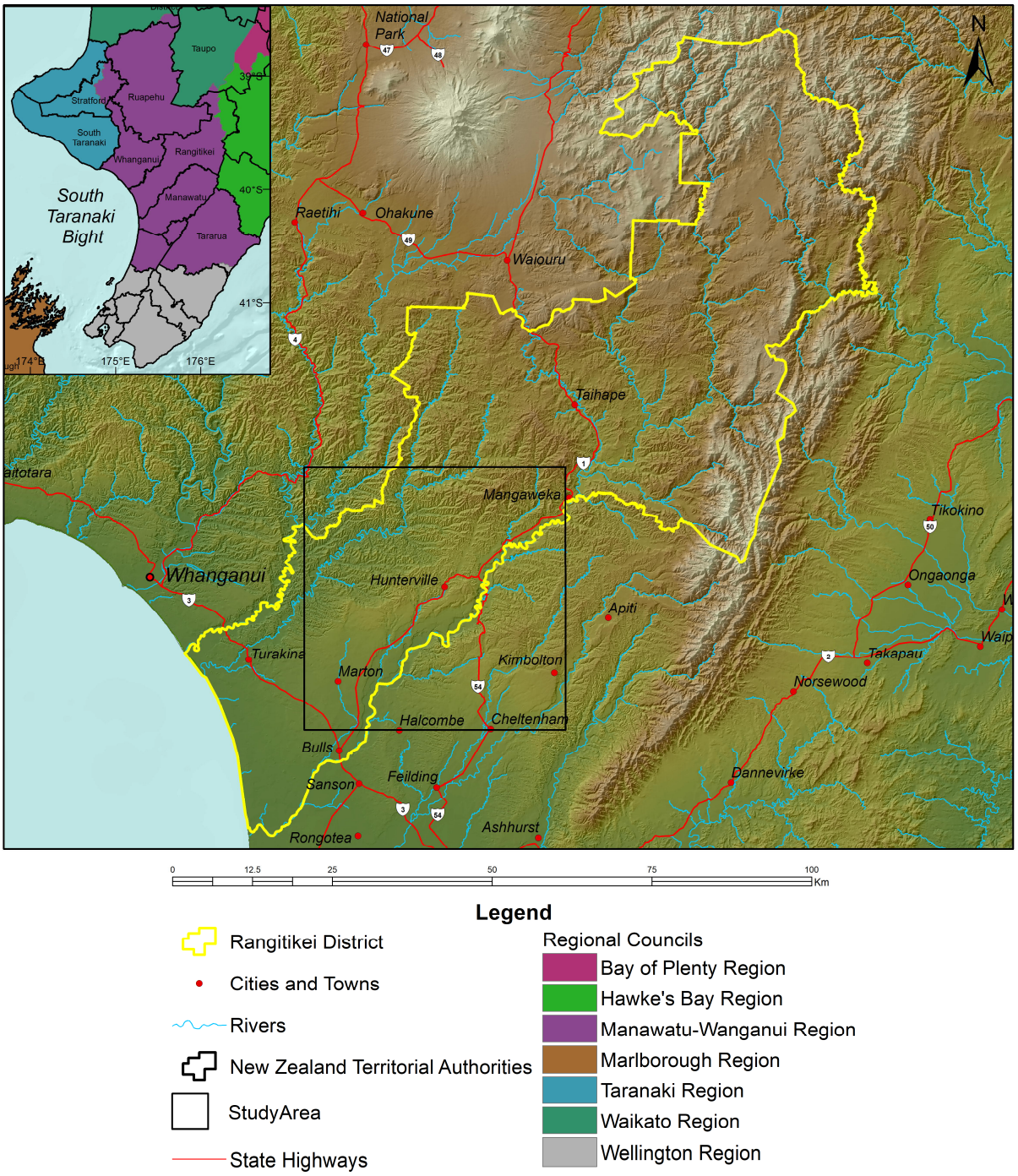


Figure 2.2: The Rangitikei District Boundary. Insert shows the main bordering regions as coloured polygons with individual district boundaries outlined in black. Note the Rangitikei District falls partially within both the Manawatu-Whanganui and Hawkes Bay regions. Also the study area (black rectangle) although centered over the Rangitikei District also partially overlaps into the Manawatu and Whanganui districts. Data sourced from LINZ, 2016.

Here, the Rangitikei River begins to cut deeply into the landscape forming >50 m high cliffs, characteristic of the Rangitikei's scenic middle reaches. South of Taihape the elevation continues to slowly decrease, reaching 350 masl at Hunterville, where the Rangitikei River Valley gradually widens before suddenly giving way to an extensive sequence of river terraces and broad modern day floodplain near the township of Rata.

From Hunterville to Bulls (50 masl) the steep hill country of the Rangitikei gradually passes into gentle rolling hills. The Rangitikei river terraces and modern day flood plain continues to broaden before becoming overlapped by an extensive transgressive dune system reaching 15 km inland from the current shoreline as far inland as Bulls. The sand country (Cowie 1963; Cowie & Rijkse 1977) is characterised by parabolic dune fields and small domed hills interspersed with swampy areas and lakes.

Pourewa Valley

Pourewa stream is a 35 km long tributary of the Rangitikei River (Fig. 2.3). The 170 km^2 catchment comprises steep to gently rolling land on the western side of the main Rangitikei Valley. The stream flows south-westward from steep hill country north of Hunterville, into the gently rolling to flat terrace country of the lower Rangitikei Valley. The confluence of the Rangitikei River and Pourewa stream occurs near Marton, 10 km south of Hunterville, adjacent to State Highway 1 (SH1). SH1 crosses Pourewa Stream several times on its path northeast from Rata to Hunterville, before veering further east and following the Rangitikei Valley north to Mangaweka. The physiography of the Pourewa Valley has been influenced by climatic fluctuations and regional uplift through the Late Quaternary together with a major influence from the Rangitikei River itself, which controls the base levels of its many tributaries. In the case of the Pourewa Stream,

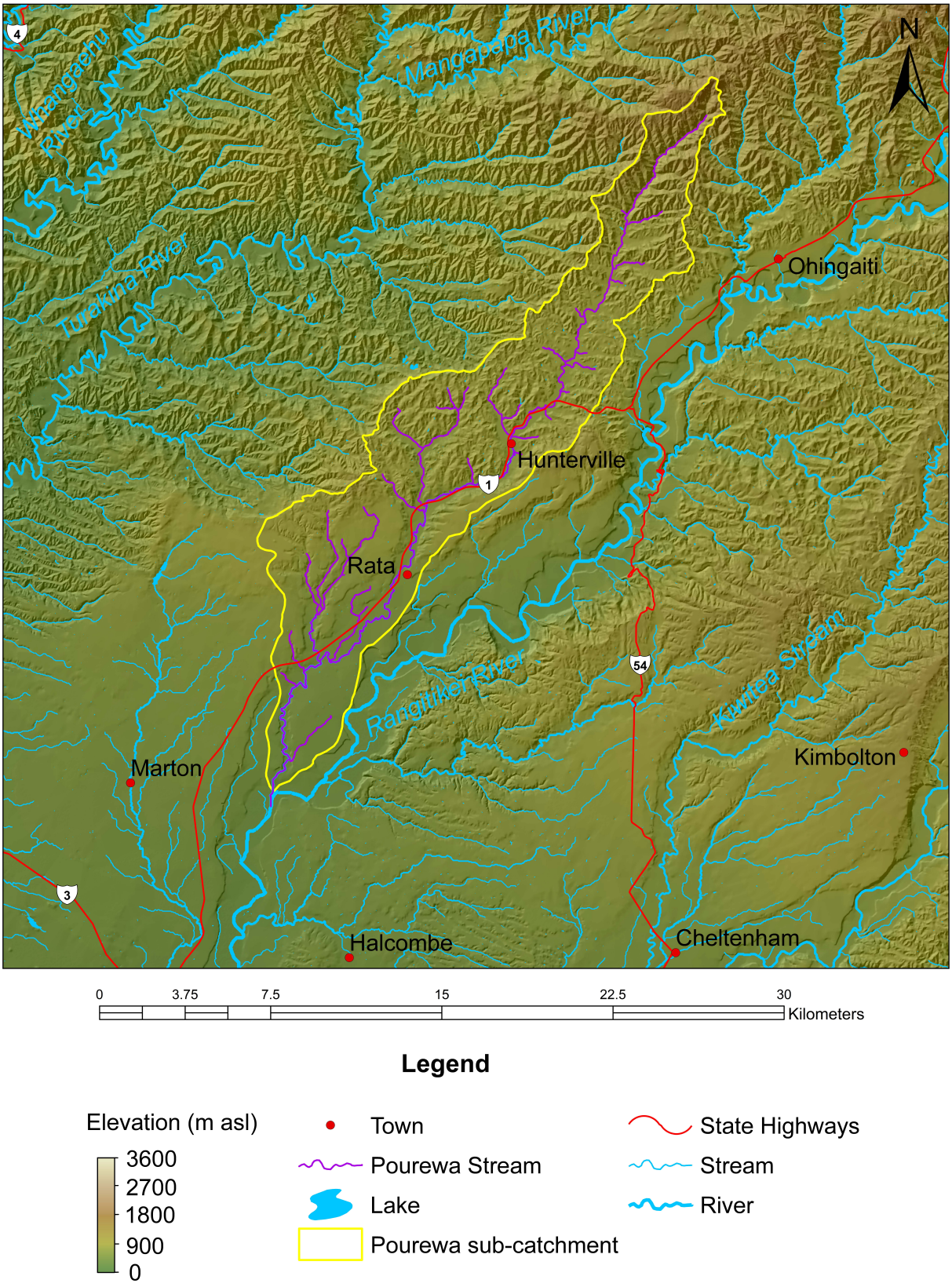


Figure 2.3: The study area showing the Pourewa Stream sub-catchment, local river systems and townships. Data sourced from LINZ, 2016.

the Rangitikei River has created a hanging landscape in which the tributary valley is set above the floor of the main valley as a result of differences in erosion.

Pourewa Stream differs substantially from the Rangitikei River in that its headwaters are located within soft Quaternary sediments, in contrast to the considerably harder basement and volcanic rock comprising the headwaters of the Rangitikei. The upper reaches of the Pourewa stream are characterised by shallow gradients and a sandy mud bed, providing a stark contrast to the fast flowing, relatively steep gravel beds of the adjacent Rangitikei River.

River systems

The study area encompasses small lengths of several major river systems draining the Central Volcanic Plateau and main axial ranges (Fig. 2.4). Although the geological mapping boundary has been positioned centrally around the length of the Pourewa Stream, it is also positioned to make use of the larger valleys of the Oroua, Rangitikei, Turakina and Whangaehu rivers, which offer greater sedimentary exposure, facilitating correlation across the adjoining interfluves. These major fluvial systems are briefly described below, starting with the most pertinent, the Rangitikei River and then working from east to west to cover all four of the major river systems crossing the geological mapping boundary.

Rangitikei's headwaters begin in the Kaimanawa Ranges at an altitude of 1723 m, flowing generally south-west for ca. 150 km to enter the Tasman Sea at Tangimoana. The upper catchment is characterised by the confluence of major river systems draining the eastern volcanic plateau, western Ruahine Ranges and Kaimanawa ranges.

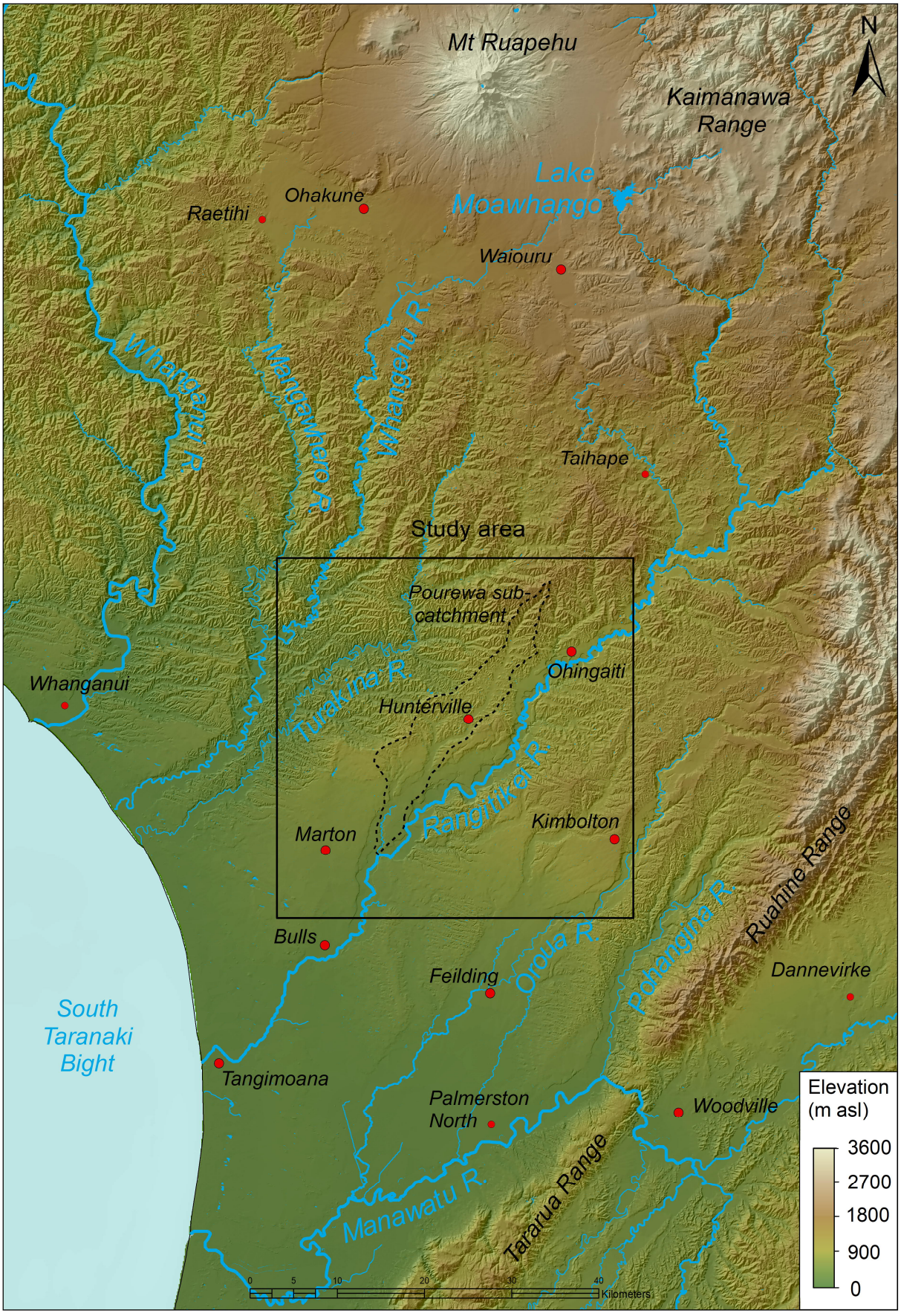


Figure 2.4: Major river systems in close proximity to the study area

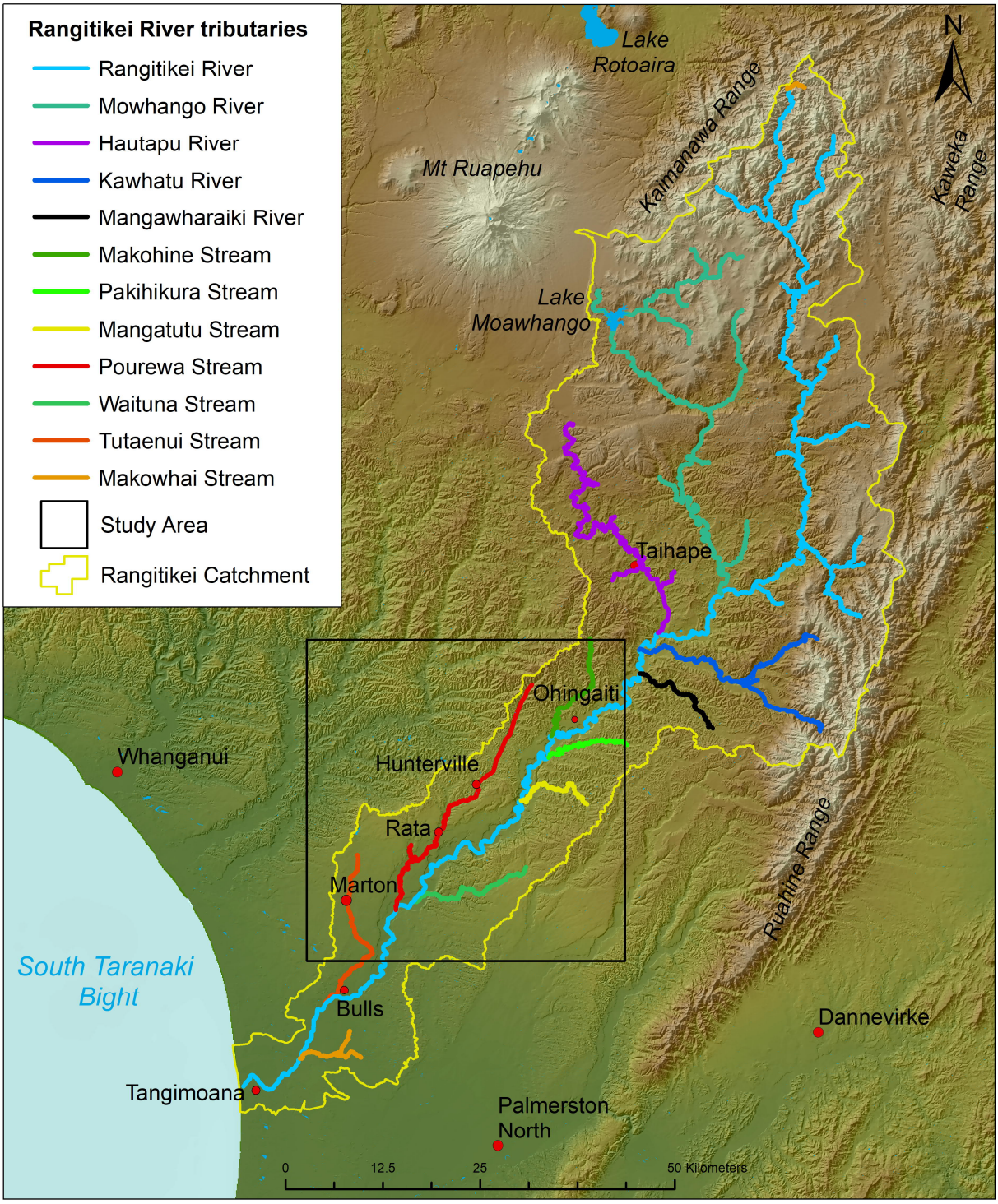


Figure 2.5: The Rangitikei River catchment (outlined in yellow).The Rangitikei River has been separated into its main tributaries, each tributary is highlighted by a different colour (see legend). Data sourced from LINZ and MFE, 2016.

Along its middle reaches, of which this study is primarily concerned, the catchment area narrows as the Rangitikei River becomes deeply entrenched within soft Quaternary sediments of the Whanganui Basin. The fluvial incision is a function of the large catchment area with peak flow rates of up to 135 m^3/s, enabling the river to move around half a million tonnes of sediment per year (Duncan & Woods 2004; Richardson & Fuller 2010), combined with an actively uplifting landscape (Beu et al. 1981; Proust et al. 2005). Several tributary streams draining the Whanganui-Manawatu Hill country including the Pourewa, Makohine, Mangatutu and Pakihikura Streams enter the river along this reach (Fig. 2.5). These side tributaries sit high in the landscape compared with the more incised Rangitikei Valley, unable to match the rate of down cutting achieved by the main river channels.

The Rangitikei River valley begins to open up once again south of Hunterville as the confining Whanganui-Manawatu hill country becomes more subdued giving way to the river aggradation and marine terraces around Marton. Fluvial incision has alternated with aggradation in response to changes in base level during climatically forced cycles over the last ca. 370 ka, (Milne 1973). These climatic cycles together with regional uplift have resulted in preservation of an extensive flight of river terraces across the Rangitikei River Valley between Hunterville and Bulls.

Between Marton and Bulls the hill country gives way entirely, merging into coastal plain, characterised by an immense transgressive dune system reaching 15 km inland as far as Bulls. The sand country and Holocene floodplain of the Rangitikei River forms subdued rolling to flat landscapes, characterised by a progressively decreasing river gradient yet having sufficient fluvial energy to transport gravels to the sea (Milne 1973; Begg et al. 2005).

Oroua River

The headwaters of the Oroua are located in the basement rock of the Ruahine Range, characterised by high rates of uplift (3 mm/yr) and erosion (0.7 mm/yr) (Whitehouse & Pearce 1992). The dissected hill country west of the Ruahine Range, which forms a majority of the Oroua catchment is located within soft Quaternary sediment of the eastern Whanganui Basin (Heerdegen & Shepherd 1992) characterised by relatively high specific sediment yields of up to 850 t/km^2/yr (Hicks et al. 2011). The Oroua flows ca. 70 km southwest from near Rangiwahia through the township of Feilding to join the Manawatu River 17 km southwest of Palmerston North.

River systems draining the western Ruahine Ranges are characterised by steep gradients, gravelly beds, and highly erodible catchments (Fuller et al. 2016). Fuller (2007) suggests the rivers in this region are best defined as wandering (Neill 1973; Ferguson & Werritty 1983), representing a transitional pattern between multithread braided and single-thread meandering channels.

Turakina River

The Turakina River flows ca. 140 km southwestward from its source near Waiouru, entering the Tasman Sea at Koitiata. The rivers headwaters are located within the soft Quaternary sediments of the Whanganui Basin, through which it has become deeply incised. Bedload consists of a mixture of gravels derived from lenses of particularly well cemented calcareous rock with no modern day source of basement rock, in contrast to rivers farther east. The river sits unusually low in the landscape, with a greater level of incision even compared with the larger Rangitikei River, likely related to its position within a structural low, a different response to river aggradation and degradation during glacial cycles and different

bedload composition. The river has moderately high suspended sediment loads including specific sediment yields of up to 415 t/km²/yr (Hicks et al. 2011).

Whangaehu River

The Whangaehu River and its tributary, the Mangawhero, drain the southern slopes of Mt Ruapehu in the south of the central volcanic region (Fig. 2.4). As such eruptive and erosional products from Mt Ruapehu have periodically inundated the valley system, providing an important component of the valley fill (Auer et al. 2012; Tost et al. 2015). The river flows approximately 90 km from Mt Ruapehu to its mouth 7 km southwest of Whangaehu Township.

2.3 Climate

The Rangitikei District is characterised by moderate temperatures without great extremes, including warm summers (15-22°C) and mild winters (1-10°C) (Cowie et al. 1967; Radcliffe 1976; Cowie & Rijkse 1977; Chappell 2015). Average temperatures range from a high of around 18°C in February to a low of around 9°C in July (Chappell 2015). Average daily maximums and minimums are within a few degrees of the average. Typically, rainfall does not show a strong seasonal trend receiving between 1000-1100 mm per year in the study area (Fig. 2.7). The coastal and lowland areas of the Manawatu are one of the driest areas in the North Island, susceptible to summer drought (Hedley & Yule 2009).

Average annual rainfall ranges from ca. 870 mm at the coast to up to 2200 mm in the ranges. On average the annual precipitation for the Rangitikei Catchment is 1215 mm (Roygard & Carlyon 2004). Evapotranspiration in the Rangitikei District follows a seasonal pattern leading to potential soil moisture deficits in summer, depending on the soil type and its ability to retain water (Cowie & Rijkse 1977).

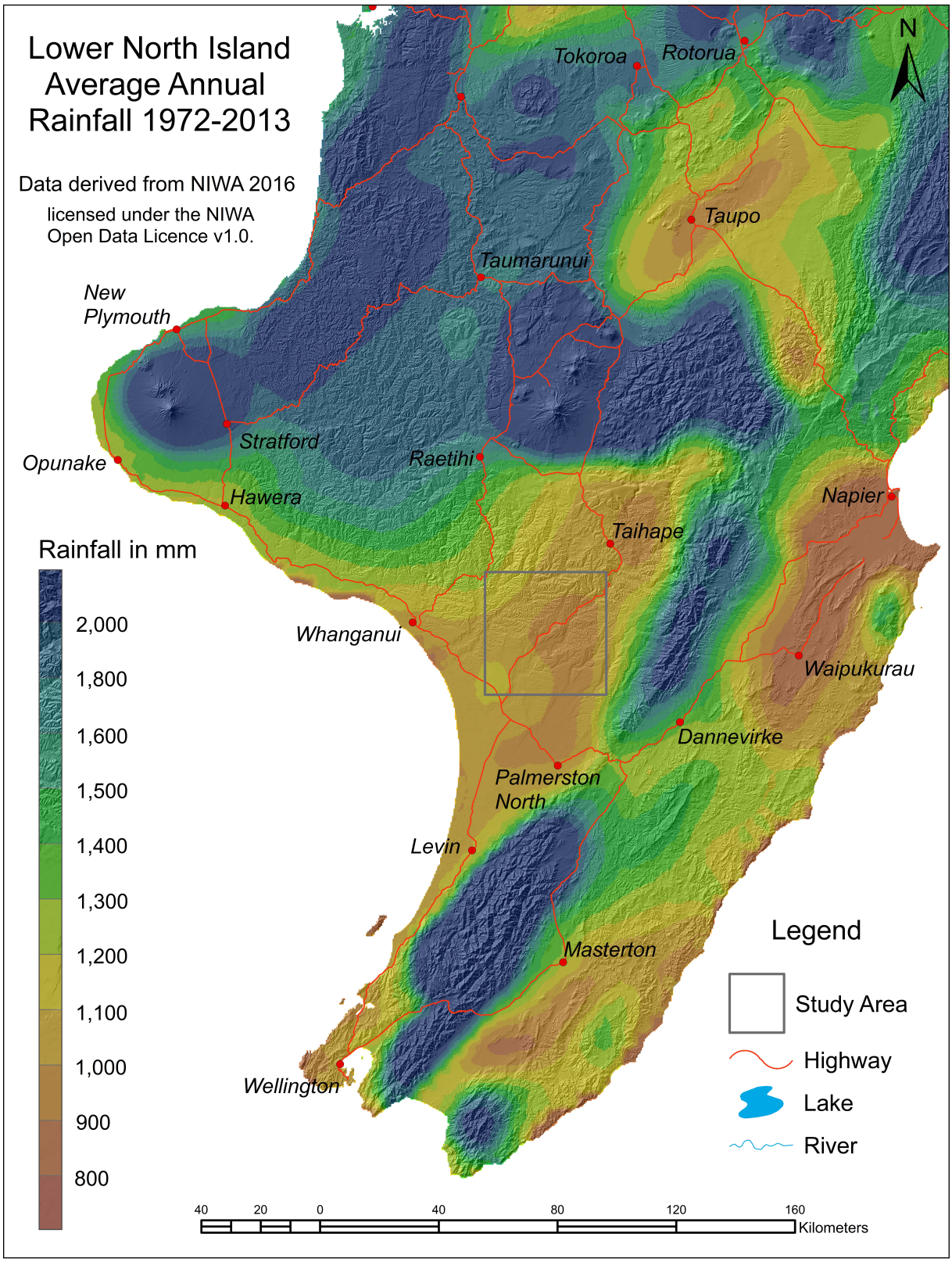


Figure 2.6: Average annual rainfall between 1972 -2013 for the lower North Island of New Zealand. Climate data provided by NIWA, licensed under the NIWA Open Data License v1.0. Topographic data sourced from LINZ Data Service, Crown Copyright Reserved.

Soil moisture deficits occur on average 10-15 days in both January and February and commonly into March and April, with irrigation used to offset the difference (Burgess 1988; Hedley & Yule 2009). The district receives around 2000 sunshine hours per year, with approximately 250 hours received in January and as low as 80 hours in June (Chappell 2015). The prevailing wind is westerly to north westerly occurring 30 to 50 percent of the time (Burgess 1988; Hesp 2001). The average wind speed is usually about 5m/s with wind speeds generally lower in winter and higher in spring (Burgess 1988). The climate supports a range of land uses, though the threat of drought is present during some summers, particularly towards the coast where it can be drier (Heerdegen & Shepherd 1992).

2.4 Land use

Land use in the Rangitikei catchment includes approximately 24% indigenous vegetation (Pre-1990 natural forest, Fig. 2.8), most of which occurs within the Kaimanawa and Ruahine Ranges in the northern and northeastern margins of the catchment. Land in the northwestern portion of the catchment situated on the volcanic plateau is managed by the New Zealand Defense Force and has been estimated as comprising approximately 9% of the total catchment area by Clark and Roygard (2008). A majority of the catchment is under low to high producing grassland (66%), used for agriculture. Clark and Roygard (2008) estimate 54% of the catchment during a 2008 survey was in sheep and beef with only around 4% in dairy. Large blocks of exotic forestry are present along the coastal sand belt,constituting around 1% of the total catchment area. Wetlands and settlements comprise a minor part of the total Rangitikei catchment area at less than 1%.

High producing pasture is mainly concentrated within the lower catchment, where the Rangitikei River emerges from its confined middle reaches onto the broad flat terrace country surrounding Marton.

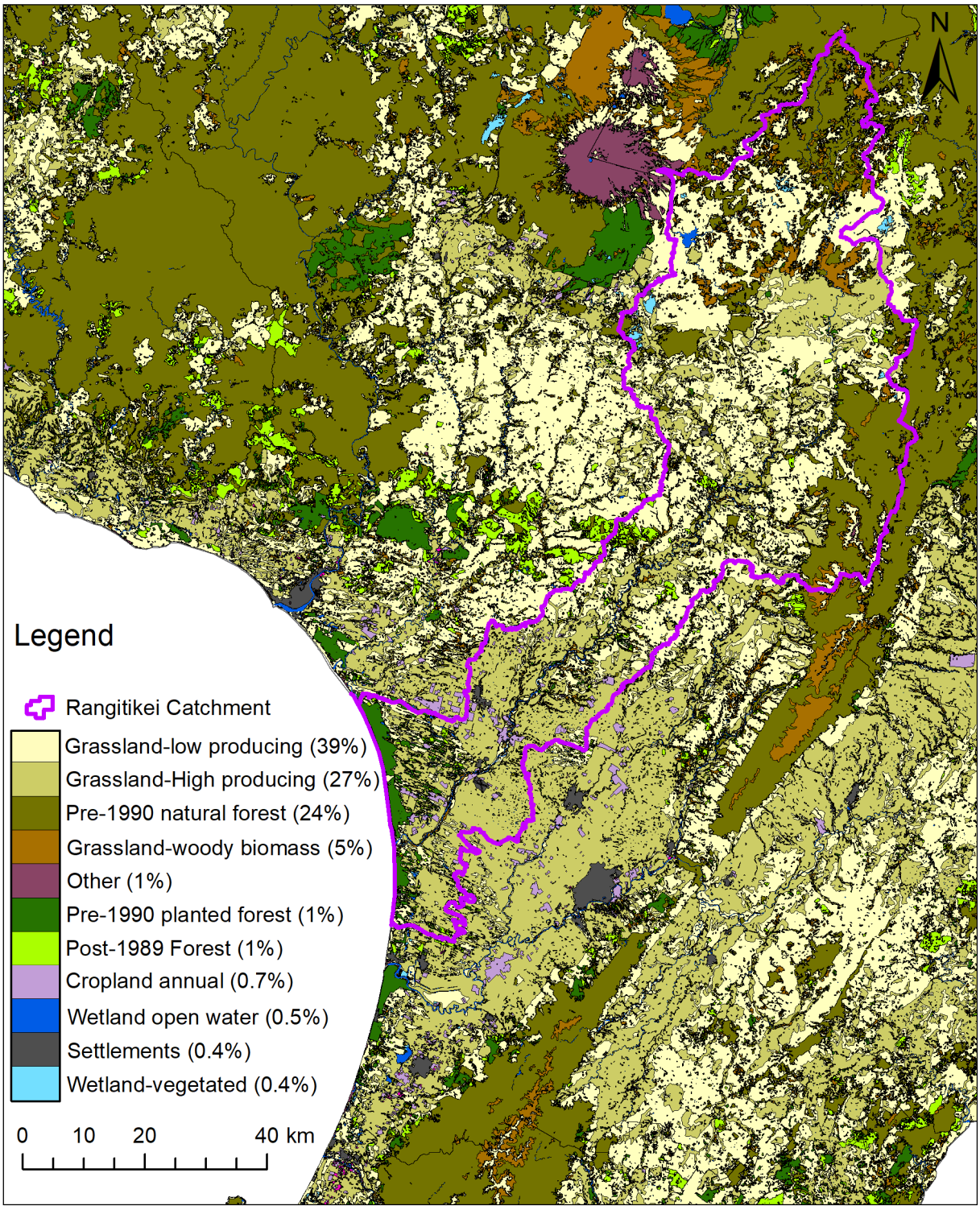


Figure 2.7: LUCAS 2012 NZ Land use map of the Rangitikei Catchment. Percentage values are in terms of total land area of the Rangitikei Catchment (ha). Topographic data sourced from LINZ Data Service, Crown Copyright Reserved. Land use data sourced from MFE under the Creative Commons Attribution 3.0 New Zealand.

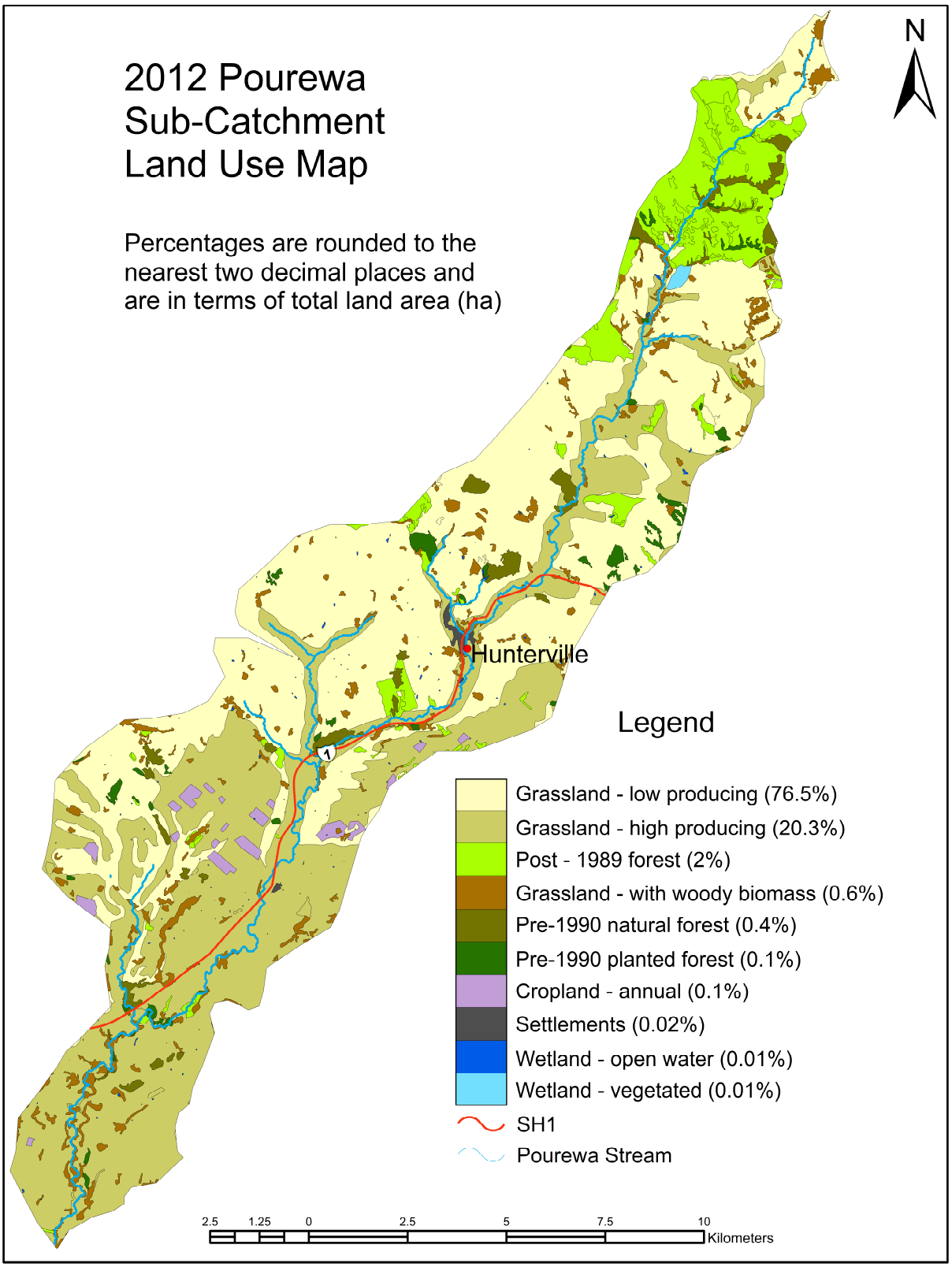


Figure 2.8: LUCAS 2012 NZ land use map of the Pourewa sub-catchment. Topographic data sourced from LINZ Data Service, Crown Copyright Reserved. Land use data sourced from MFE under the Creative Commons Attribution 3.0 New Zealand.

The Rangitikei District economy relies heavily on agriculture, principally sheep and beef farming in the steep hill country and dairying with minor cropping on the more accessible river flats. Changing market values for wool, mutton, beef and dairy products have led to a relative increase in dairy farms within the district (Quinn et al. 2009).

The Pourewa sub-catchment (Fig. 2.9) is dominated by low to high producing grassland (96.8 %), a majority of which is under sheep and beef. Other than diary the only other major land use of note is a block of forestry toward the northern sub-catchment boundary where a sheep and beef farm has been converted into production forestry post 1989.

Dairy farms are concentrated on the high producing grasslands in the southern half of the catchment, centered along strips of alluvial flats bordering the Pourewa Stream and the adjacent Rangitikei River to the east. Vegetable and grain cropland (0.1%) is concentrated on the flat Rangitikei terraces with soils developed in deep loess and volcanic ash cover beds around Leedstown Valley and Rangitira Road. A common secondary income for many famers, particularly within the hill country is leasing land for apiculture. Rare occurrences of horticultural enterprises south of Hunterville include olive groves and kiwi fruit vines.

Water use

A National Water Conservation Order protects parts of the upper and middle Rangitikei catchment, preserving the exceptional wildlife and scenery. The Moawhango River, a major tributary of the Rangitikei River is part of the Tongariro Power Development scheme, established in the 1970's. Water from the southern slopes of Mt Ruapehu is dammed in Lake Moawhango, before draining into the Tongariro River. The Tongariro Power Development scheme is the largest take of water in the Rangitikei catchment, accounting for 16% of the mean annual

low flow (MALF) at Mangaweka (Catalyst-Group 2014a). The operation of the dam has significant effects on flows in the Rangitikei River, including the occurrence of controlled flushes four times per year by Genesis Energy to improve the ecology of the river.

A majority of consented water abstraction from groundwater and surface water in the Rangitikei Catchment is used by agriculture (78 %), with urban drinking water supplies using 15% and industry 7% (Roygard & Carlyon 2004). Approximately 75% of the water used is surface water with the remaining 25% sourced from groundwater. Direct abstraction from waterways provides drinking water for many of the Rangitikei townships, which typically use the same waterway for downstream waste assimilation. Large abstraction takes for irrigation are concentrated within the lower catchment where terrace country is more widespread, suitable for pivot irrigators.

The Hunterville Water Scheme, a rural water supply network, was established in the 1980's to supply stock water to farms. The scheme services approximately 60,700 ha of land from Marton to Ohingaiti with a branch that also e to the Turakina Valley from Hunterville (Catalyst-Group 2014b). A second key component of the scheme is an urban supply to Hunterville. Water for the Hunterville Water Scheme is abstracted from the river by an infiltration gallery and well system before being pumped up to a reservoir and gravity fed along separate branches. Average abstraction is 1350m^3/day (Catalyst-Group 2014b).



2.5 Geological setting

Introduction

The geologically young and active landscapes of New Zealand are largely due to our precarious location at a convergent plate margin and deserve special attention in any field-based study. The following section will begin by discussing the tectonic setting of New Zealand, gradually becoming more specific to focus on the most relevant aspects to this study. In particular, Pliocene to Holocene (5.33 Ma – present day) geology will form a focal point during this review, due to the geologically young landscapes of the Rangitikei that have only fully emerged from the ocean in the last c. 1 Ma. The geological setting has been included as the final section of Chapter 2 rather than as its own chapter for brevity.

Overview

The islands of New Zealand are but the surface expression of a large submerged subcontinent named 'Zealandia' (Adams et al. 2015). This subcontinent sits astride the convergent margin between the Pacific and Australian lithospheric plates (Fig. 2.9). In the northern portion of this plate boundary, oceanic crust of the Pacific plate is obliquely subducted beneath the continental crust of the Australian plate. This subduction interface is expressed as the Hikurangi Trough, which extends north-south from the Kermadec Trench to Kaikoura in the South Island. The Hikurangi subduction zone corresponds to the southern termination of the Tonga-Kermadec subduction (Chanier et al. 1999).

Mt Tongariro pictured on a fine winters day, taken from near the Desert Road.

In the North Island of New Zealand the Pacific and Australian plates are converging obliquely at a rate of around 42 mm yr^{-1} (DeMets et al. 1994). Convergence rates vary from 60mm/yr near Gisborne to 25mm/yr near Wellington (Wallace et al. 2012). This decrease in convergence rate is interpreted to represent the change from subduction to oblique continental collision and strike-slip that occurs between the north and south of New Zealand.

The Hikurangi subduction interface is characterised by unusually thick oceanic crust ranging in thickness from 12 km thick at the Hikurangi Trough (Davy 1992) to 15km thick at the Chatham Rise (Davy & Wood 1994). The plate subducts at an angle of just 12-25° beneath the eastern North Island and is only 15-25 km below the land surface just north of Wellington city (Henrys et al. 2013). This is shallow in comparison to other subduction zones around the world e.g. Japan (Wada et al. 2015).

Tectonic convergence is accommodated by subduction of the Pacific Plate and deformation of the overriding Australian Plate including active uplift of the North Island (Eberhart-Phillips et al. 2008). Uplift is concentrated along the North Island Dextral Fault Belt (NIDFB) trending roughly parallel to the Hikurangi subduction zone NE-SW. The uplift along the NIDFB has resulted in the formation of the North Island's main axial ranges which separate the forearc region from the backarc and volcanic arc regions (Fig. 2.10).

The forearc region of the subduction interface is characterised by an accretionary wedge and forearc basin. This region is bounded to the west by the axial ranges, behind which lies the Whanganui basin, Taupo Volcanic Zone (TVZ), Tongariro Volcanic Centre (TgVC) and Taranaki Volcanic Centre (EgVC). A unique feature of the Hikurangi margin in the North Island of New Zealand is a sharp switch in subduction style within the back-arc area.

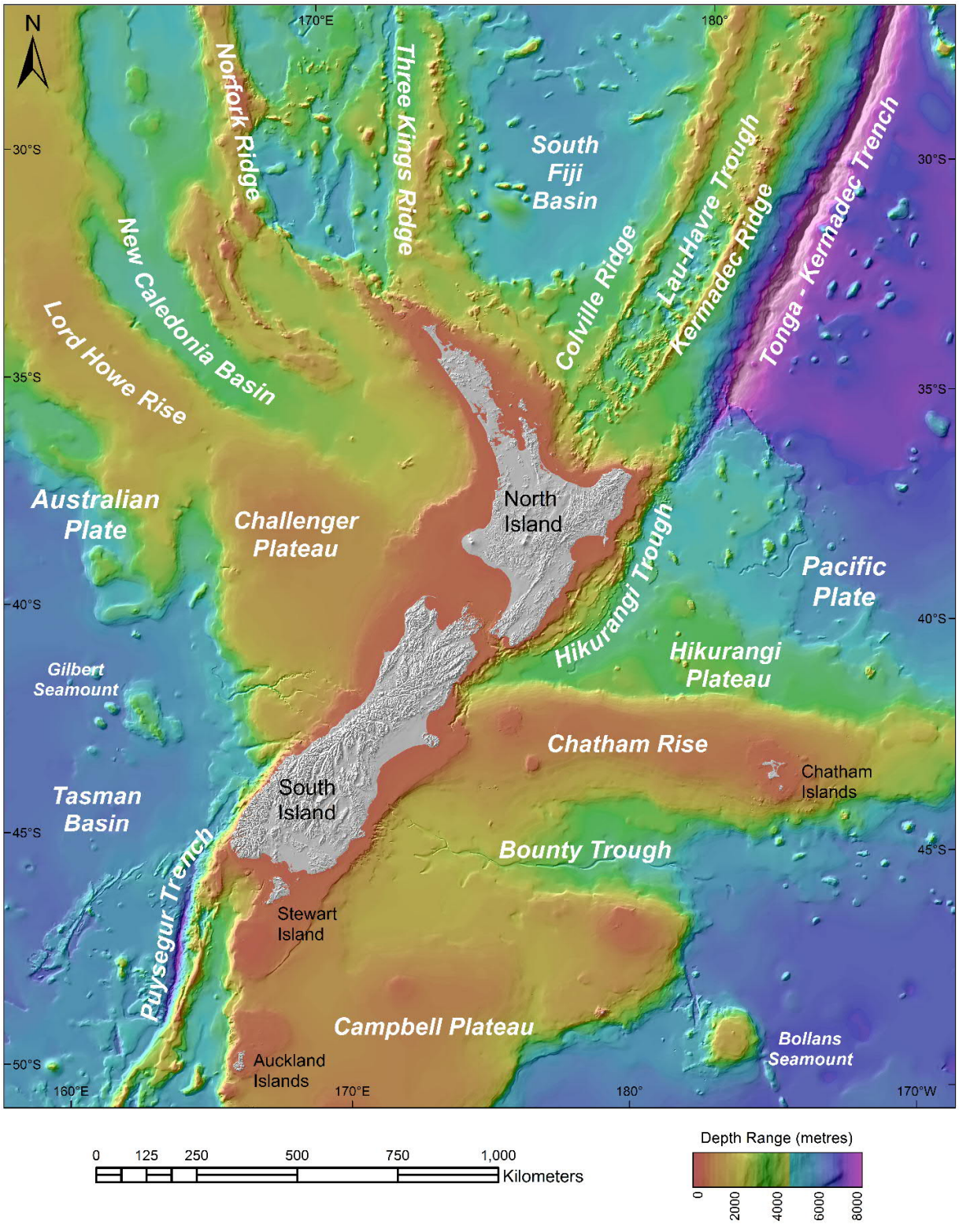


Figure 2.9: The New Zealand subcontinent, showing the main bathymetric and tectonic features. Contains information licensed under the NIWA Open Data License v1.0.

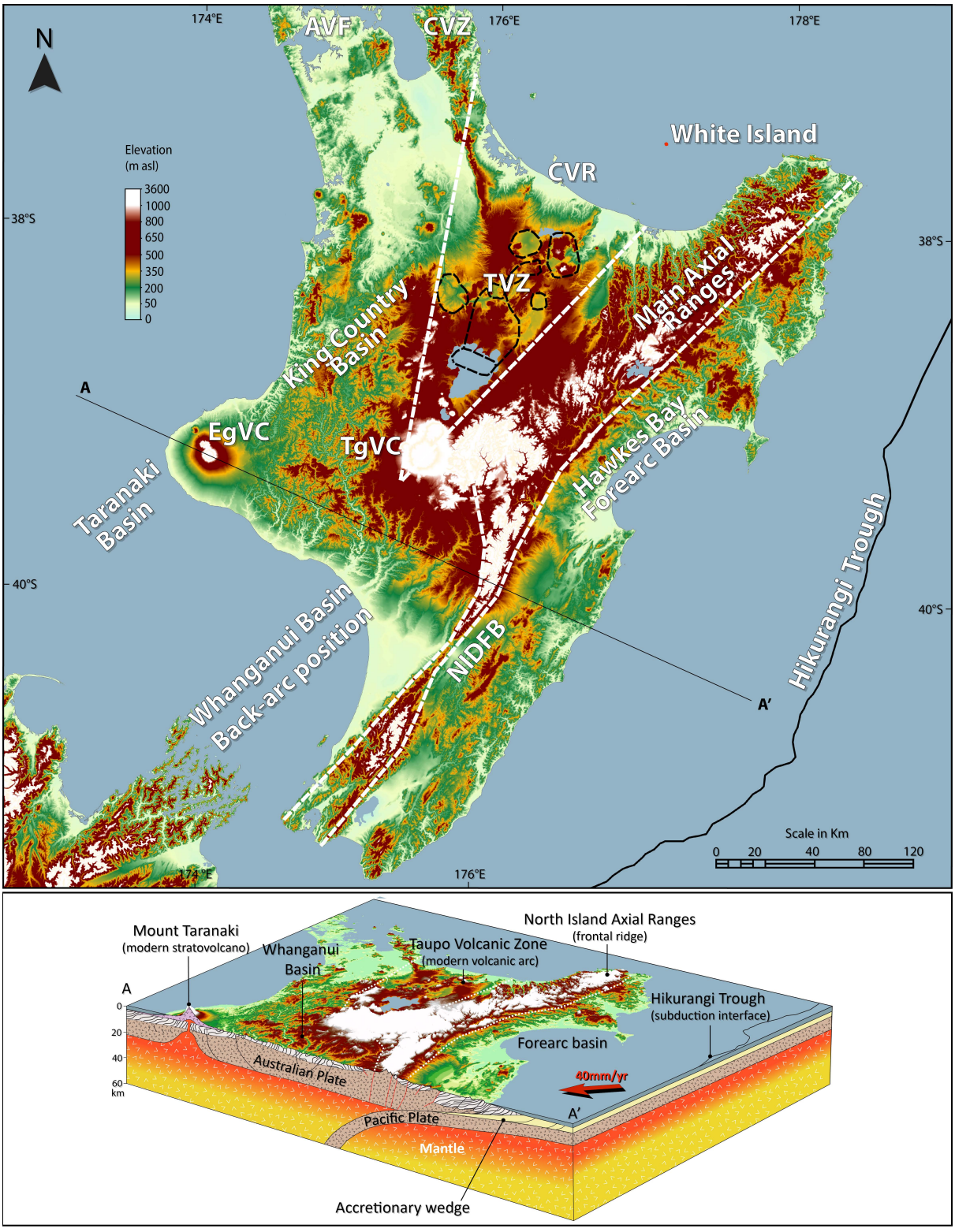


Figure 2.10: The North Island, New Zealand showing the key regional geological features. AVF = Auckland Volcanic Field; CVR = Central Volcanic Region; CVZ = Coromandel Volcanic Zone; TVZ = Taupo Volcanic Zone; TgVC = Tongariro Volcanic Centre; EgVC = Egmont Volcanic Centre; NIDFB = North Island Dextral Fault Belt. Dashed black lines indicate location of the eight major rhyolitic calderas in the TVZ (Spinks et al. 2005). White dashed lines outline the CVR and North Island main axial ranges.

This is characterised by a classic extensional system in the central North Island (TVZ) switching to a mildly compressive regime in the southwest North Island (Whanganui Basin) (Stern et al. 2006).

In the South Island of New Zealand, oblique subduction changes to continent-continent collision. This change in the nature of plate boundary through the North and into the South Island of New Zealand is validated by observing the GPS velocity field data collected by GNS over the last two decades.(Beavan et al. 2016).

Fig. 2.11 clearly shows a rapid clockwise rotation of the eastern North Island (Wallace et al. 2004) developing into strong shear along the Marlborough Fault System at the top of the South Island (Beavan & Haines 2001; Wallace et al. 2007). This change in motion represents a change in the subduction interface as deformation is transferred to strike-slip faulting along the Alpine Fault and Marlborough Fault System (Lamb & Bibby 1989; Beanland 1995).

This central section of the New Zealand plate boundary is characterised by a transform system where continental crust of the Pacific plate obliquely overthrusts continental crust of the Australian plate. The plate boundary can be identified by the surface expression of the Alpine Fault, a prominent linear feature in the landscape. Around 480 km of dextral offset has occurred along the Alpine Fault since the initiation of the New Zealand plate boundary between 30 and 20 Ma (Wellman & Willett 1942; Norris & Cooper 2000). This dextral offset has been accompanied by vertical uplift rates of up to 12mm/yr (Norris & Cooper 2000).

Southwest of the South Island the nature of the plate margin changes yet again to a complex subduction/transform boundary. The Macquarie Ridge and Puysegur Trench mark this southern portion of the subduction interface. Along the northern parts of this section of the plate boundary, Pacific plate crust overrides oceanic crust of the Australian plate (Lebrun et al. 2000).

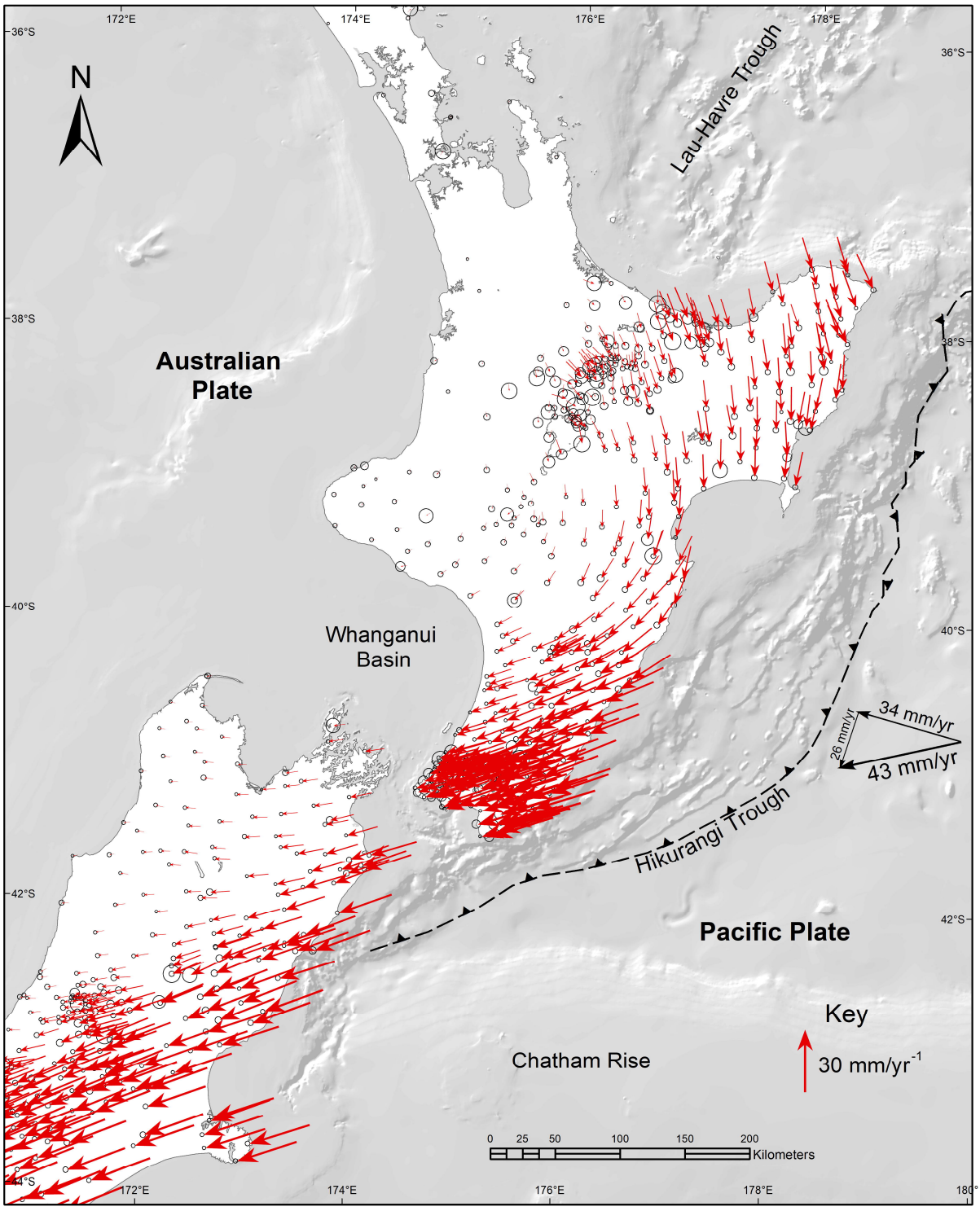


Figure 2.11: New Zealand GPS velocities in an Australian Plate fixed reference frame. Error ellipses display uncertainties (σE and σN). Data provided courtesy of GNS (Beavan et al. 2016). Black vectors represent relative plate convergence of Pacific Plate with respect to the Australian Plate (Beavan et al. 2002).

Imbricate accretionary wedge

West of the Hikurangi trough lies a imbricate accretionary wedge formed by convergence of the Pacific and Australian Plates and the resultant thrust faulting and crustal shortening (Lewis 1980; Sporli 1980). Development of this wedge has occurred during several phases of deformation over the last 25 Ma (Ballance 1988; Rait et al. 1991), characterised by sediment offscraping and fault rupture as the underlying Pacific Plate is driven down below the overriding Australian Plate (Chanier et al. 1999).

The accretionary wedge extends the length of the Hikurangi Margin, mainly located offshore from the East Coast of New Zealand. Onland exposures include the Mahia Peninsula and south of Cape Kidnappers (Pettinga 1982; Beanland 1995). This frontal portion of the subduction zone interface varies from 200 km wide in northern Wairarapa to only 125 km wide north of Mahia Peninsula (Litchfield et al. 2007). Multibeam swath mapping of the continental slope offshore along the Hikurangi Margin has highlighted that the northern section is relatively narrow, steep and characterised by tectonic erosion (Collot et al. 1996). The tectonic erosion is inferred to be the result of numerous seamount impacts, as sea mounts on the Pacific Plate are subducted at the Hikurangi Margin (Litchfield et al. 2007). In contrast the central offshore Hikurangi Margin is characterised by a wide accretionary wedge characterised by numerous thrust faults (Barnes & de Lepinay 1997).

East Coast Forearc Basin

The forearc basin is a major topographic and structural depression bounded by the accretionary wedge to the east and the main axial ranges to the west. The ranges

are composed of Mesozoic basement rocks which separate the forearc basin from the TVZ and back-arc region. Approximately half of the forearc basin is presently above sea level and is being actively uplifted (Beanland 1995). Its location coincides with a line of anomalously low gravity values extending from the Whanganui Basin NE into the Hawkes Bay area.

The forearc basin contains a sequence of mainly marine Miocene-Pleistocene sediments up to 3 km thick overlying an unconformity on Mesozoic basement (Lamarche et al. 1995). The sedimentary fill is moderately deformed by a series of reverse faults, forming anticlines and synclines. Deformation varies in character and intensity across the forearc region with the highest rates of deformation occurring near the axial ranges (uplift of 3 mm/yr) where large dextral reverse faults of the NIDFB significantly offset the basin fill (Beanland & Haines 1998; Wallace et al. 2004).

The North Island Axial Ranges

The forearc basin is bounded to the west by the main axial ranges which trend NNE-SSW through the centre of the lower North Island, rising up to elevations of 1700 m asl. The ranges are composed of uplifted meta-sedimentary terrane rocks including mainly greywacke and argillite. These terrane rocks were accreted and intensely deformed in the accretionary wedge on the eastern margin of Gondwana during the Triassic to Early Cretaceous (Mortimer 2004). Rifting of New Zealand, Australia and Antarctica from Gondwana commenced during the Cretaceous (around 110 Ma) (Mortimer 2004). Later around 80 Ma, New Zealand began rifting from Australia as the Tasman Sea opened (Molnar et al. 1975). This rifting stretched and thinned the New Zealand continental block which became largely submerged between the Cretaceous and Oligocene (Waters & Craw 2006).

The current emergent parts of the New Zealand continental block have been uplifted by collisional tectonism and associated crustal thickening since the initiation of the modern New Zealand plate boundary and Hikurangi subduction system around Oligocene–Early Miocene time (Cooper et al. 1987). Remnants of sedimentary sequences deposited since Late Cretaceous are intermittently preserved unconformably over the Mesozoic basement of the main axial ranges. These sequences provide insights into the development of the Zealandia and North Island of New Zealand (Mazengarb & Speden 2000; Leonard et al. 2010; Lee et al. 2011). Overlying Late Cenozoic marine sediments indicate that the proto axial ranges resided at or about sea level in Oligocene to Miocene time, and have since been uplifted into the modern ranges. A mean surface uplift rate has been calculated for the Axial Ranges of 1-1.3 mm/yr over the last 1-5 Ma (Beu et al. 1981; Pillans 1986; Litchfield & Berryman 2006).

North Island Dextral Fault Belt (NIDFB)

The modern Axial Ranges are cut and bounded by the North Island Dextral Fault Belt (NIDFB) (Beanland 1995). These active dextral strike slip faults extend for 350 km parallel with the strike of the Axial Range. Near Te Urewera the NIDFB reaches its northern termination, represented by a change to N-S trending faults. The most prominent faults in the NIDFB are the Wellington, Mohaka and Whakatane Faults which extend for a combined length of approximately 500 km from Wellington the Bay of Plenty. The Wellington Fault extends north from Wellington to Woodville where it bifurcates into the Ruahine and Mohaka Faults, which then continue northeast through the Hawkes Bay area (Fig. 2.12).

The NIDFB faults commonly form the structural boundary between Mesozoic basement and Cenozoic sediments of the forearc basin. The ranges have a strong NNE-SSW structural and topographic alignment, faulting is generally more prominent along their eastern margin given the presence of the NIDFB. Vertical

displacement rates along the high angle reverse faults bounding the axial range have been estimated to be 2000m since the early Pleistocene (Berryman 1988).

Activation of the NIDFB is thought to have largely occurred over the last 1–2 million years (Reyners 2013) although stratigraphic evidence for earlier phases of uplift have been documented from Kuripapango (Browne 1978; Beu et al. 1981; Browne 2004), Oroua Valley (Milne 1968), Lake Colenso (MacDonald-Creevey 2011) and the Manawatu Saddle (Rees et al. 2018). The southern half of the NIDFB is characterised by high rates of strikeslip movement of over 10mm/year (Nicol et al. 2007). Dip slip on the NIDFB increases towards the TVZ as displacement is transferred into the zone of rifting (Mouslopoulou et al. 2007).

The Central Volcanic Region (CVR) and Taupo Volcanic Zone (TVZ)

The Lau-Havre Trough, a backarc basin behind the Tonga-Kermadec Trench is thought to extend into the North Island of New Zealand (Karig 1970). This continuation is interpreted as the Central Volcanic Region (CVR), formed via extensional tectonics during complex plate interactions at the Hikurangi margin over the past 25-30 Ma (Stratford & Stern 2006; Wilson & Rowland 2016). The CVR is an active extensional zone containing up to 12,000 km^3 of siliceous volcanics within a 2km deep graben (Houghton et al. 1995; Stratford & Stern 2004).

Rhyolitic volcanism has been active in the North Island of New Zealand since 12 Ma (Carter et al. 2003). Between 12 and 4 Ma, rhyolitic eruptions were located in the Coromandel volcanic zone (CVZ), situated in the western CVR (Adams et al. 1994). Onland records of late Cenozoic volcanism are notoriously incomplete. Tectonism, erosion, and burial have resulted in a fragmented onland record, especially within eastern half of the CVR in what is more widely referred to as the Taupo Volcanic Zone (TVZ) (Cole et al. 1995; Wilson et al. 1995).The incomplete onland record has hindered attempts to better gauge the evolution and relationship

of the CVR (Wilson & Rowland 2016). Active andesite and rhyolite volcanism is now confined to the Taupo Volcanic Zone (TVZ).

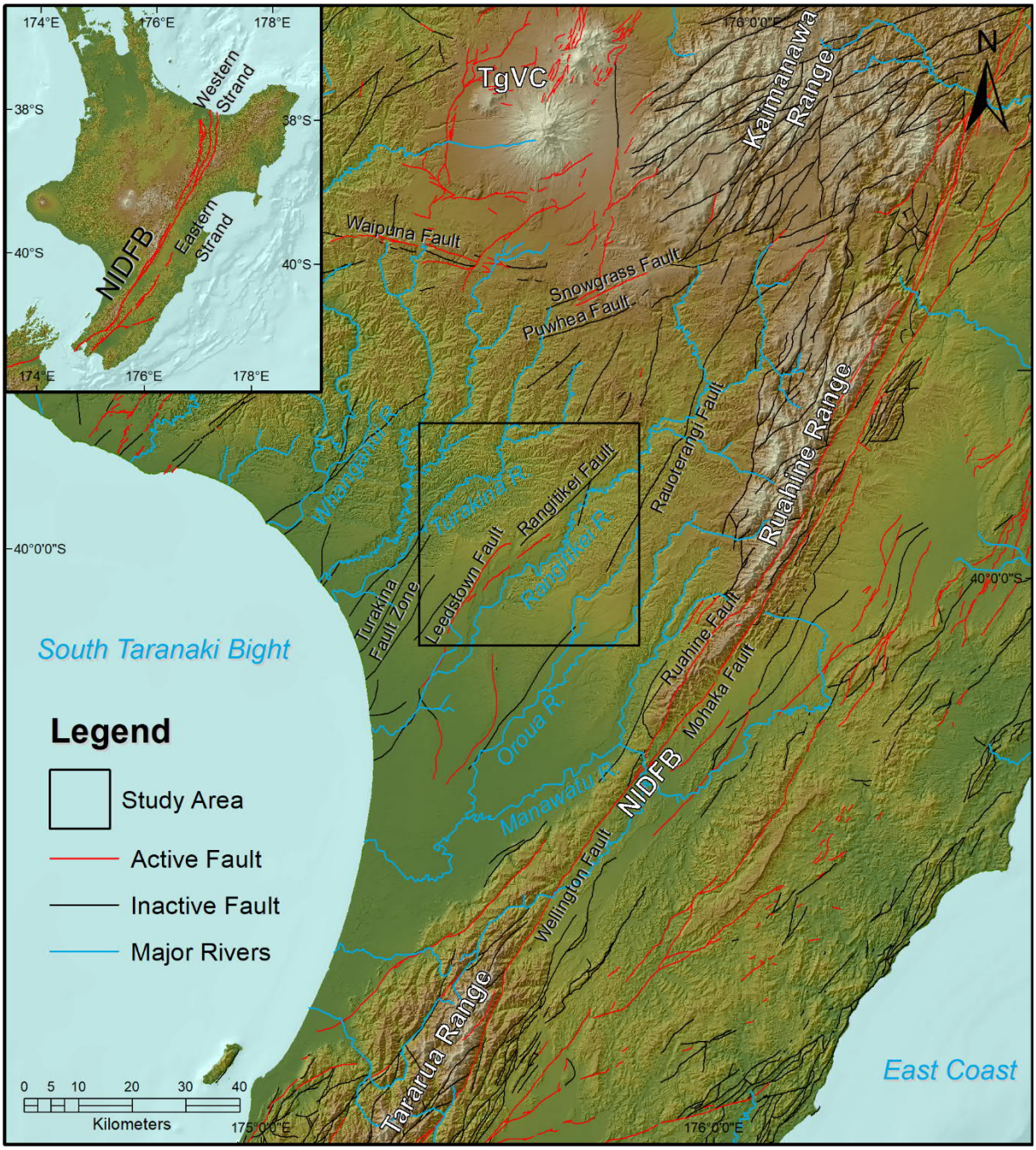


Figure 2.12: The North Island of New Zealand displaying fault lines from the GNS active fault database in relation to the study area and major river systems (Langridge et al. 2016).Insert displays the location of the North Island Dextral Fault Belt (NIDFB).

The Taupo Volcanic Zone (TVZ) is the youngest active part of the CVR (Beanland 1995; Stratford & Stern 2006). It is a seismically active zone of Quaternary calc-alkaline volcanism and intra-arc rifting (Spinks et al. 2005) containing numerous closely spaced northeast striking normal faults, half-grabens and volcanic centres (Wilson et al. 1984). The TVZ marks the present location of intra-arc rifting related to the convergent setting within the North Island, and associated with a highly thinned crust of 15km thickness (Bibby et al. 1995; Spinks et al. 2005).

Volcanic activity commenced in the TVZ about 2 Ma (Houghton et al. 1995; Briggs et al. 2005). The present area of active volcanism is concentrated in a NNE-SSW trending zone 250km long extending from White Island in the northeast to Mount Ruapehu in the southwest (Spinks et al. 2005). This area includes all activity in the past 300 ka (Houghton et al. 1995; Wilson et al. 1995). It can be divided into three parts along its length; 1) A central region with several rhyolitic calderas extending from Okataina to Taupo, 2) the Whakatanae-White Island andesite-dacite extension to the northeast and 3) the andesite-dacite stratovolcanoes of the Tongariro-Ruapehu extension to the southwest (Houghton et al. 1995; Wilson et al. 1995). The central area, formed within continental lithosphere is extremely productive with rhyolitic volcanic (0.28 m^3/s^{-1}) and geothermal (equivalent of c. 4200 MW) fluxes unequalled in the world (Wilson 1996).

Taranaki-Ruapehu Line

The Taranaki-Ruapehu Line (TRL) signifies a major change in the geophysical properties of the lithosphere north and south of the area between Mt Taranaki and Mt Ruapehu (Fig. 2.13). It was first recognized 46 years ago as a deep boundary in the mantle across which seismic attenuation changes abruptly (Hatherton 1970; Mooney 1970). This line marks the southward limit for active volcanism in New Zealand (Reyners 1980; Price et al. 1999).

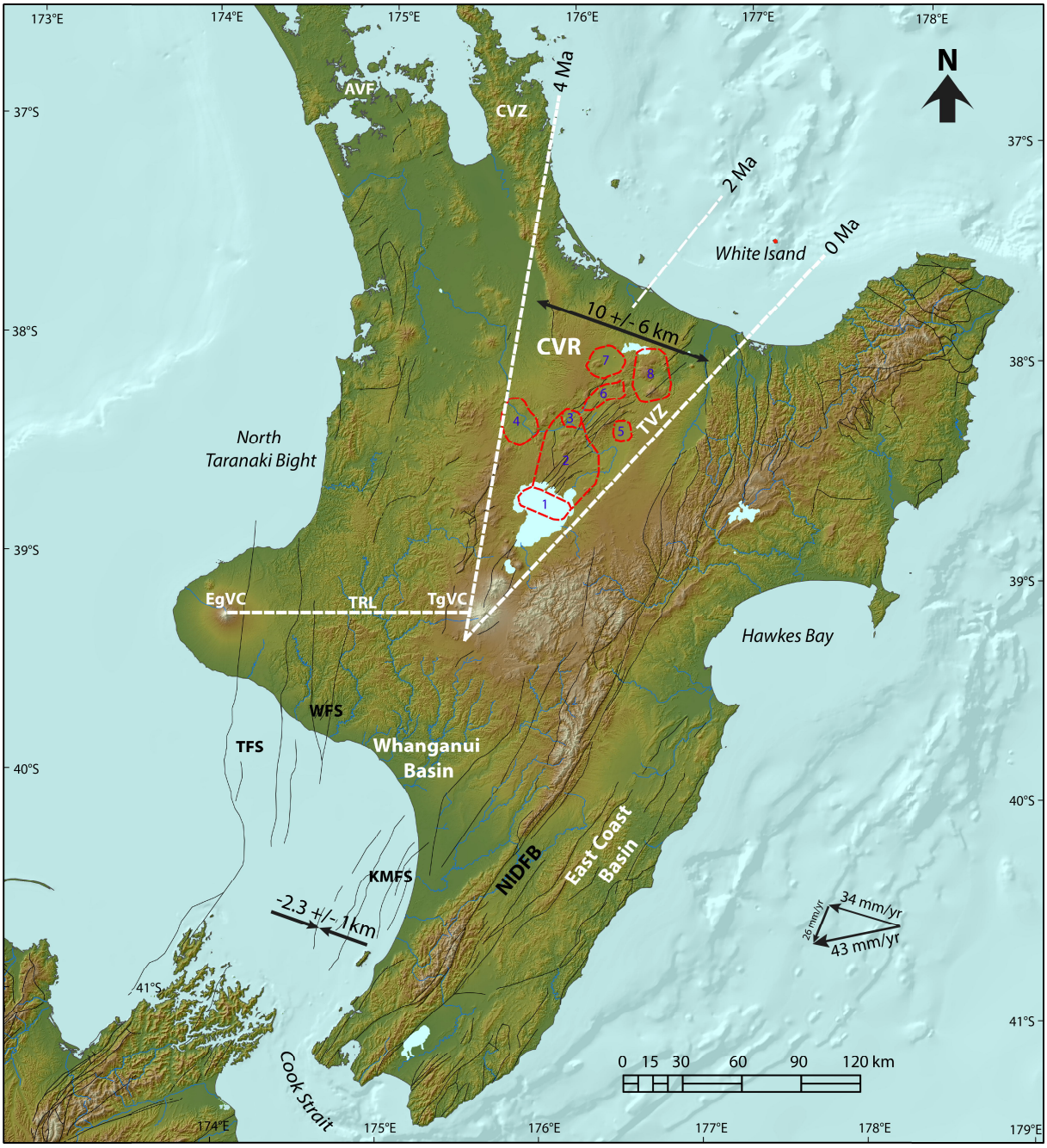


Figure 2.13: The North Island of New Zealand showing major volcanic areas with reference to the Whanganui Basin. Central Volcanic Region (CVR), Coromandel Volcanic Zone (CVZ) and Taupo Volcanic Zone (TVZ). Red dashed outlines represent the 8 major calderas within the TVZ: 1 = Taupo, 2 = Whakamaru, 3 = Maroa, 4 = Mangakino, 5 = Reporoa, 6 = Kapenga, 7 = Rotorua, 8 = Okataina. AVF = Auckland Volcanic Field, TgVC = Tongariro Volcanic Centre, EgVC = Egmont Volcanic Centre, TRL = Taranaki Ruapehu Line. Black arrows indicate Pliocene shortening and extension (Nicol et al. 2007). Black lines indicate major fault lines, TFS = Taranaki Fault System, WFS= Waverly Fault System (Townsend, 1998), KMFS = Kapiti-Manawatu Fault System (Lamarche et al. 2005), NIDFB = North Island Dextral Fault Belt (Beanland and Haines, 1998).

South of the TRL maximum crustal thickness is estimated at 40 km while to the north it thins to 25 km (Holt & Stern 1994; Stratford 2006; Stratford & Stern 2006; Salmon et al. 2011).

Geophysical modelling implies the presence of a 7-10 km crustal step across the TRL (Stern & Davey 1987; Salmon 2008; Seward et al. 2009; Salmon et al. 2011; Tozer 2013). The crustal step is thought to be linked with a step in the mantle lithosphere at the TRL, where the mantle lid is largely absent or heavily thinned under the NW North Island (Stern & Davey 1987; Seward et al. 2009).

The lithospheric step across the TR Line is thought to have formed in Middle to Late Miocene time (15 – 5 Ma) via rapid migration of the plate boundary along the Alpine Fault which extended into the North Island (Bekesi & McConchie 2000; King 2000; Stern et al. 2013). By the Late Miocene, the boundary would have been trans- tensional with the progressive growth of the CVR, which had thin crust and lithosphere. As a result, lithospheric structures of different thicknesses would have been juxtaposed, and an instability developed from this step and migrated southwestward beneath western North Island to its present position beneath the Taranaki-Ruapehu line. Geophysical observations (Stern et al. 2006; Salmon et al. 2011) define the present-day state of this evolved lithospheric step, which now strikes at a high angle to the margin on which it initiated.

Despite several independent studies the structure, dip, and exact position of the TRL is not entirely conclusive. Gravity modelling by Stern et al. (1987) placed the TRL directly between Mt Taranaki and Mt Ruapehu. However, Sherburn and White (2005) suggest the TRL is 25 km north of this location based on changes in crustal earthquake depths near Mt Taranaki, and the assumption that earthquakes do not exist in the mantle.

Whanganui Basin (WB)

The WB is situated in a back-arc position behind the Hikurangi Margin, SW of the active volcanic arc (Fig. 2.14). The basin formed via a combination of sediment loading and frictional shear between the subducting Pacific plate and overriding Australian plate (Stern et al. 1992). Shear force is generated by strong coupling of the Pacific and Australian plates generating a vertical, downwards pull in the overriding Australian plate, along with in-plane stresses. This causes flexural downwarping of the WB basin (Stern et al. 1992, 1993).

The model of the WB as a compressional basin is consistent with high-angle reverse faulting evident in seismic sections, as well as the pattern of crustal earthquakes beneath the southeastern part of the basin (Pillans 1990). Compressional and extensional stresses related to plate bending are generated within the basin and are of sufficient magnitude to cause surface faulting of both normal and reverse sense (Stern et al. 1992; Townsend 1998).

The evolution of the WB is directly linked with the evolution of the Hikurangi subduction zone, believed to have been initiated by Late Oligocene (25 – 28 Ma) (Rait et al. 1991). Plate tectonic reconstructions include substantial Miocene crustal shortening within the WB area (Walcott 1984; King 2000; Wood & Stagpoole 2007; Lamb 2011). Up to 200 km of crustal shortening has been postulated, with maximum shortening occurring in the Miocene between 15-5 Ma (Furlong & Kamp 2009).

Deformation of the southwest North Island may have elevated a large portion of the pre WB basement rock well above sea level during the Miocene (King 2000). This uplifted basement provides a likely explanation for the irregular geometry of the WB basement rock, which in places has the appearance of a submerged mountain range on seismic reflection data (Holt & Stern 1994).

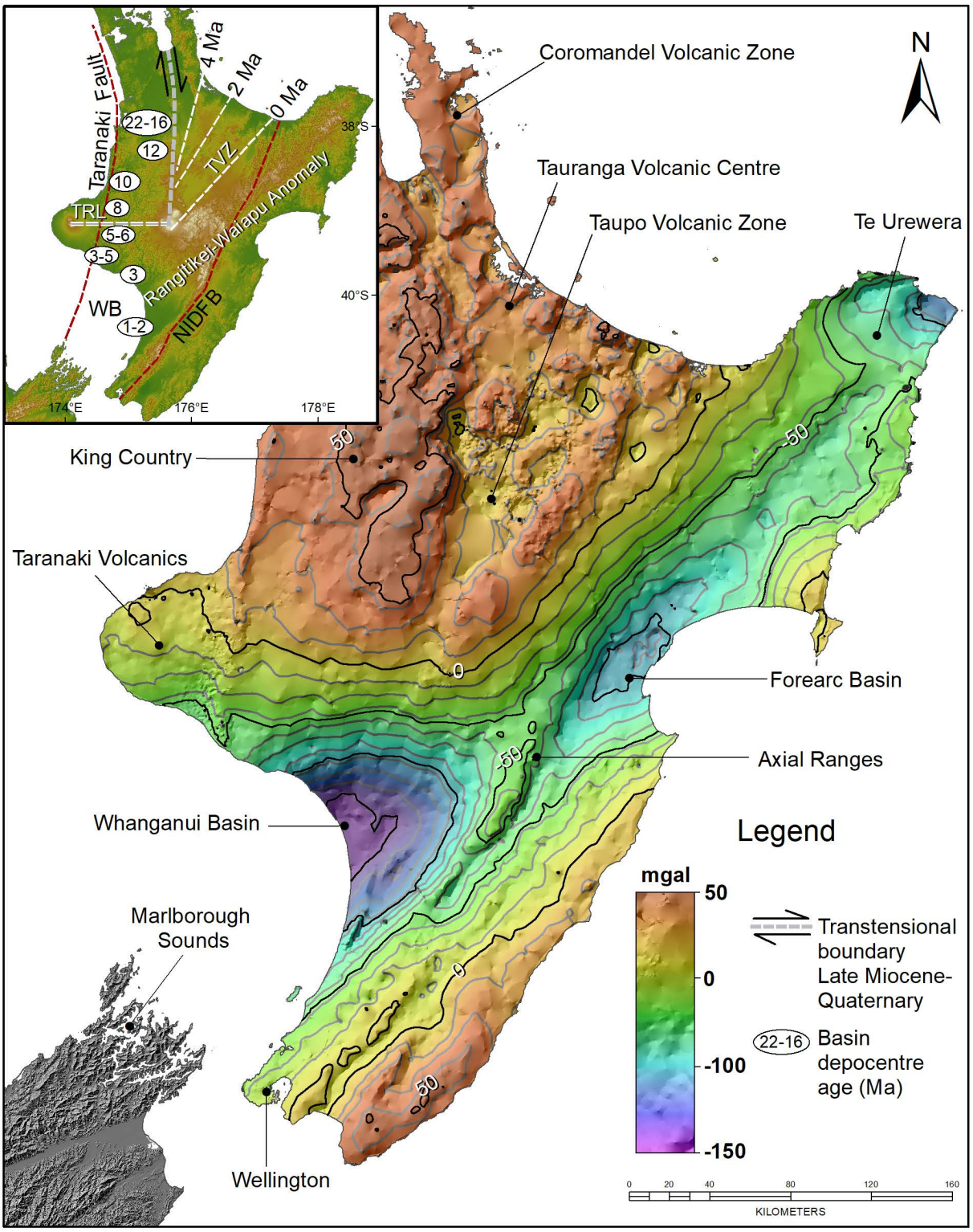


Figure 2.14: Distribution of isostatic gravity anomalies in the North Island. Anomaly values are in mgal (uN/kg). Light grey contour intervals are 15 mgal, black contour intervals are 50 mgal. Gravity values are in terms of the International Gravity Formula 1980 using the conversion of Li and Gotze (2001). Gravity data used in this figure provided courtesy of GNS Science. TRL = Taranaki – Ruapehu Line; WB = Whanganui Basin; NIDFB = North Island Dextral Fault Belt. Basin depocentre data sourced from Stern et al. (2013).

The basement rock of the WB consists primarily of Mesozoic greywacke of the Waipapa and Torlesse composite terranes (Fig. 2.15). Some of the basement greywacke is altered to schist near terrane boundary interfaces (Mortimer 2004).

The basement terrane interfaces were first identified by studies situated on surrounding basement highs, such as the Marlborough sounds (Mortimer 1993). The contacts were then extrapolated offshore using magnetic, marine seismic and petroleum well data (Mortimer et al. 1997). Direct observations of basement rock are limited across most of the WB due to thick Plio-Pleistocene cover rocks. Knowledge of the underlying basement structure is mainly derived from geophysical surveys and limited borehole data.

Late Miocene-Pleistocene sedimentary layers unconformably overlie WB basement terranes (Fig. 2.16) (Fleming 1953). Over 4 km of subsidence has occurred since Late Miocene time. This accommodation space has been rapidly filled by sequences of largely marine Plio-Pleistocene sediments. Through the Plio-Pleistocene, the basin depocentre migrated southward while simultaneous uplift of the northern margin has occurred (Fig. 2.17). This crustal movement has been correlated with the evolution of the modern plate boundary through New Zealand. Successively younger sediments offlap to the south and progressively older (Pliocene) strata are exposed in east-west oriented belts along the northern margin of the basin (Fleming 1953; Journeaux et al. 1996).

WB has developed on top of a geophysically defined crustal down-warp (Robertson & Reilly 1958; Holt & Stern 1994). Subsidence is controlled by a predominantly reverse fault system along the basin's eastern flank named the Kapiti Manawatu Fault System (KMFS). Seismic reflection profiling centered over the onshore portions of the basin reveals active folding (Melhuish et al. 1996), associated with the growth of NNE-SSW striking anticlines (Jackson et al. 1998).

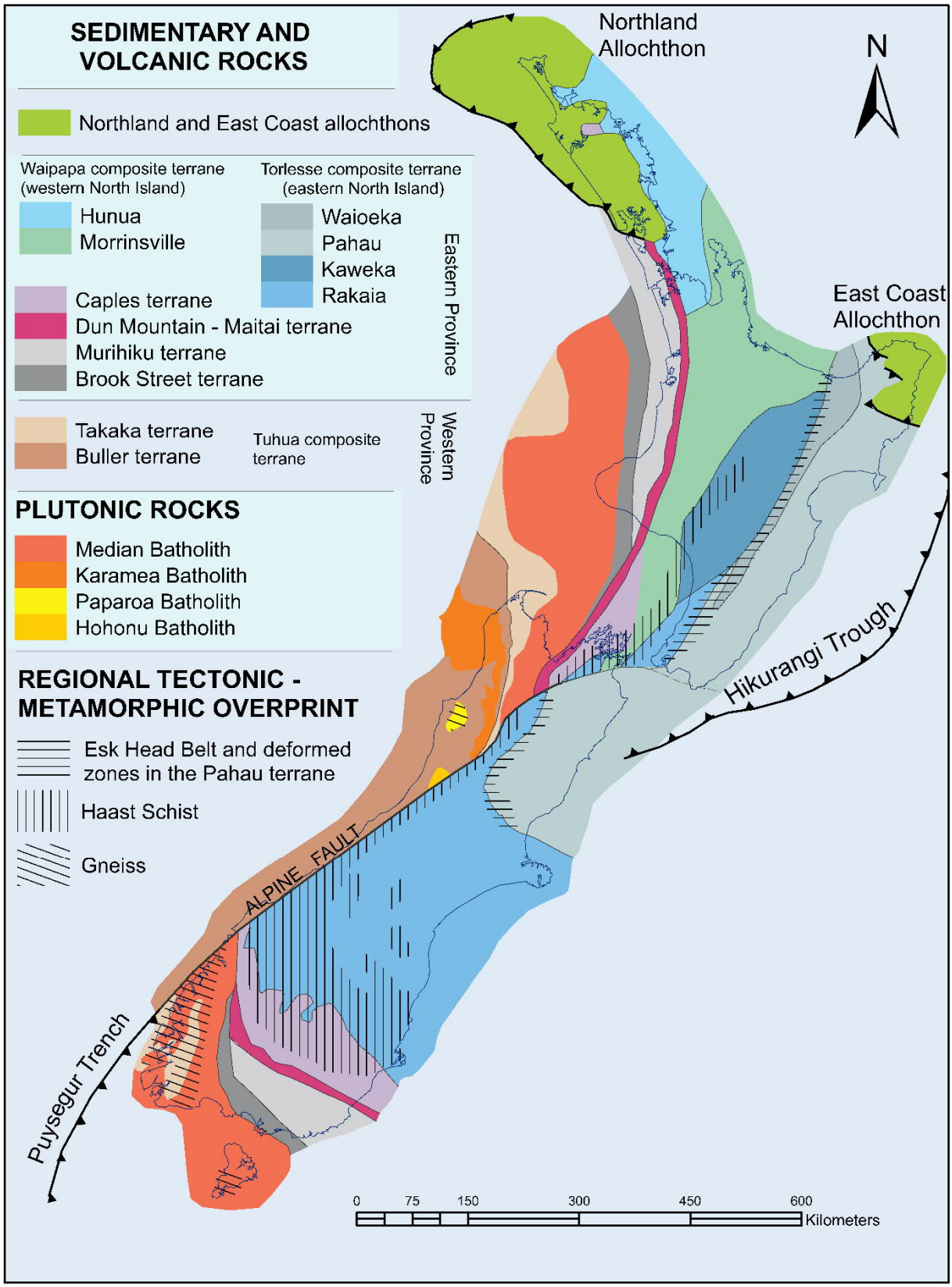


Figure 2.15: Tectonostratigraphic basement terranes of New Zealand (Lee et al. 2011). Basement rocks of the study area comprise Torlesse composite terrane and Waipapa composite terrane.

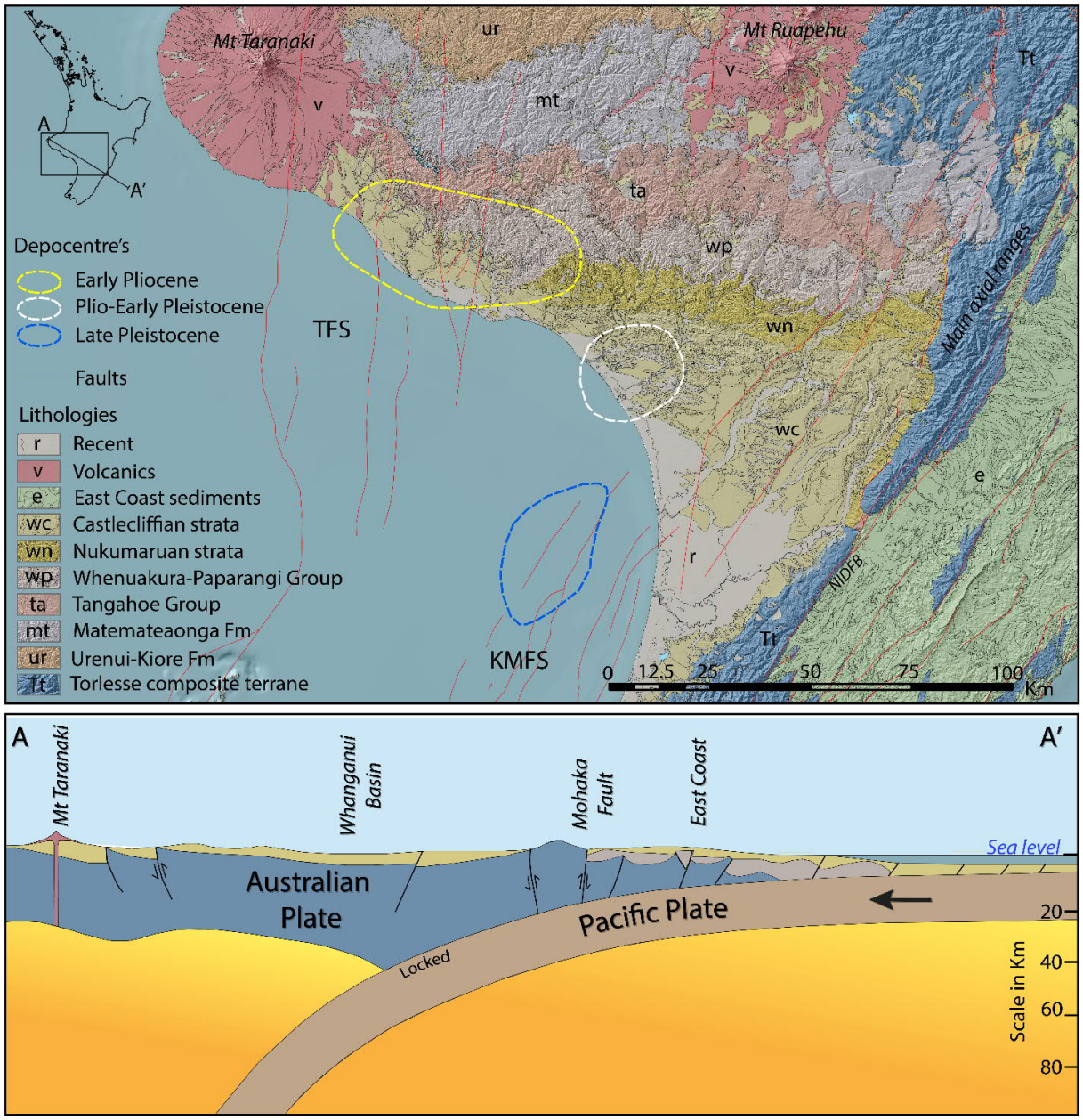


Figure 2.16: Simplified geology of the Whanganui Basin area. Major formations are displayed in increasing age order. Basement rocks of the main axial ranges are dominantly made up of Torlesse composite terrane. Data is derived from Anderton (1981) and Kamp et al. (2002). The cross section is adapted from Nicol and Beavan (2003).

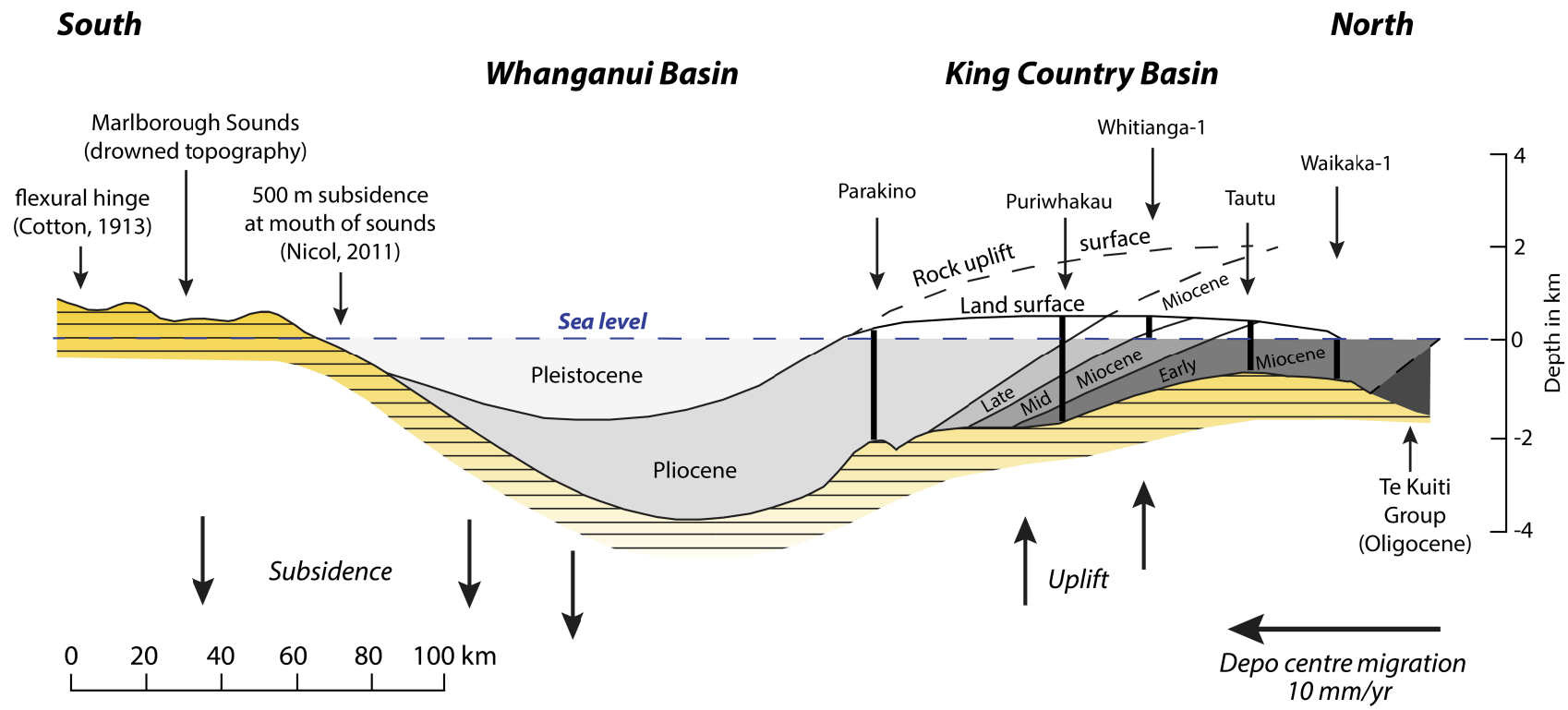


Figure 2.17: Coeval uplift and subsidence in the Whanganui and King Country basins (Cotton 1913; Stern et al. 2006; Nicol 2011).

Shortening across the WB is in the order of 4mm/yr, calculated from GPS measurements gathered over the last decade (Wallace et al. 2004).

The WB is bordered by uplifted Mesozoic basement highs. The western margin is marked by the buried Patea-Tongaporutu High and associated faulting of the Taranaki Fault Zone (Mills 1990; Proust et al. 2005). The southern margin is represented by the drowned topography of the Marlborough Sounds which are actively subsiding as both subsidence and the WB depocentre migrate southward (Nicol 2011). The northern margin is the TRL, characterised by a significant step from the thinned crust of the CVR to the thickened crust of the WB.

The basin's eastern margin is frequently cited as the North Island's main axial ranges e.g. (Nodder et al. 2007; Hughes & Kennedy 2009). However, work by Browne (1978, 1986, 2004) and Rees et al. (2018) demonstrate partial overlap of the Whanganui Basin with the forearc basin across the present day main axial ranges via Plio-Pleistocene marine seaways.

North Island gravity field

The gravity field of the North Island is useful as it offers constraints on the mechanical properties and behavior of the Hikurangi margin (Bland 2006). The most prominent feature of the Bouguer, isostatic and free air gravity maps of the North Island is a large low near Whanganui and its apparent extension northeast towards a low in Hawkes Bay and another north of the Raukumara Peninsula (Fig. 2.18). This feature has been termed the Rangitikei-Waiapu anomaly (Robertson & Reilly 1958). Isostatic anomaly values range from -150 mgal in the Whanganui Basin and -100 mgal in Hawkes Bay to +50 mgal in northwest North Island.

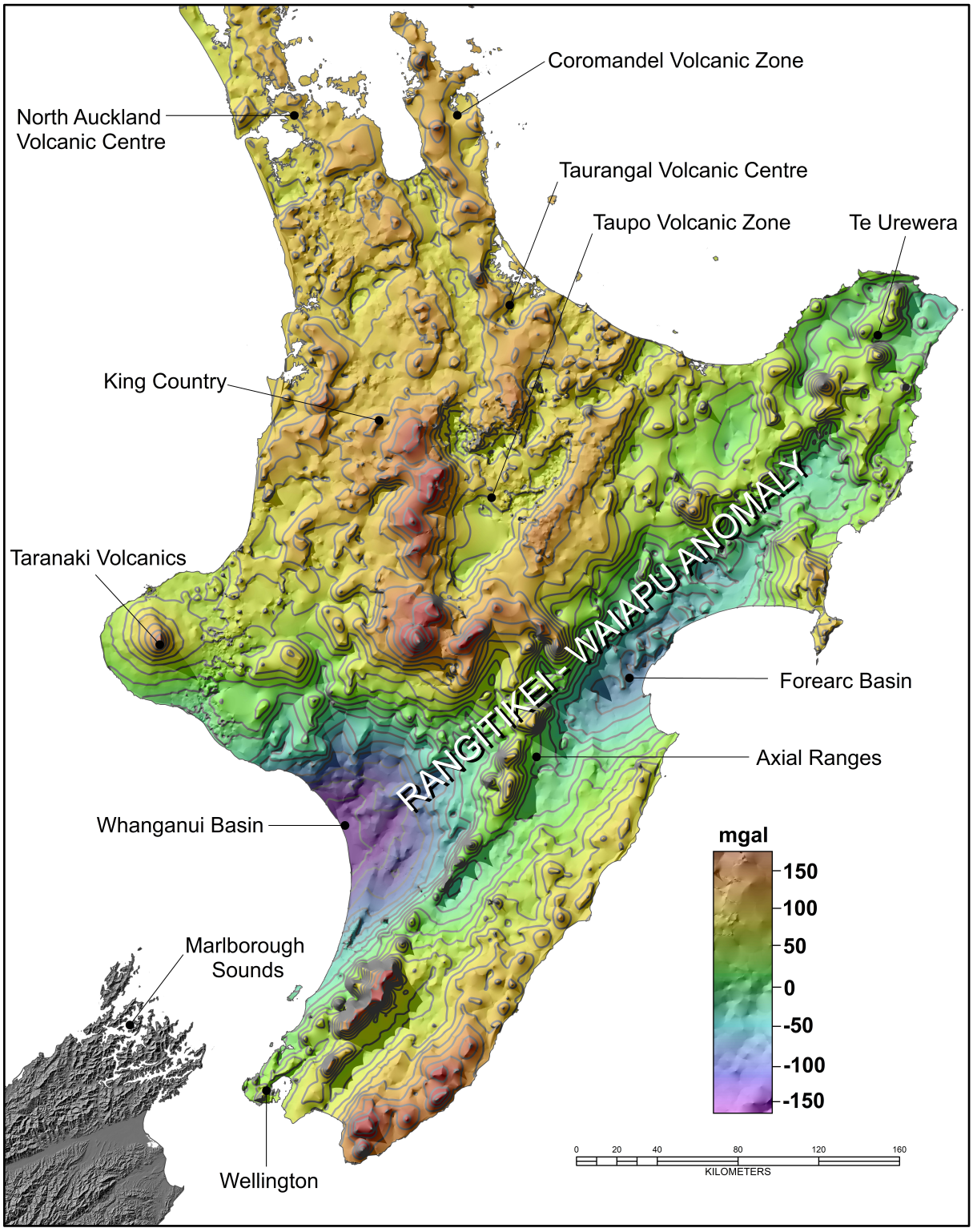


Figure 2.18: Distribution of free air gravity anomalies in the North Island. Anomaly values are in mgal (uN/kg), using the conversion of (Li & Gotze 2001). Contour intervals are 15 mgal. Gravity values are in terms of the International Gravity Formula 1980. Data used in this figure provided courtesy of GNS Science.

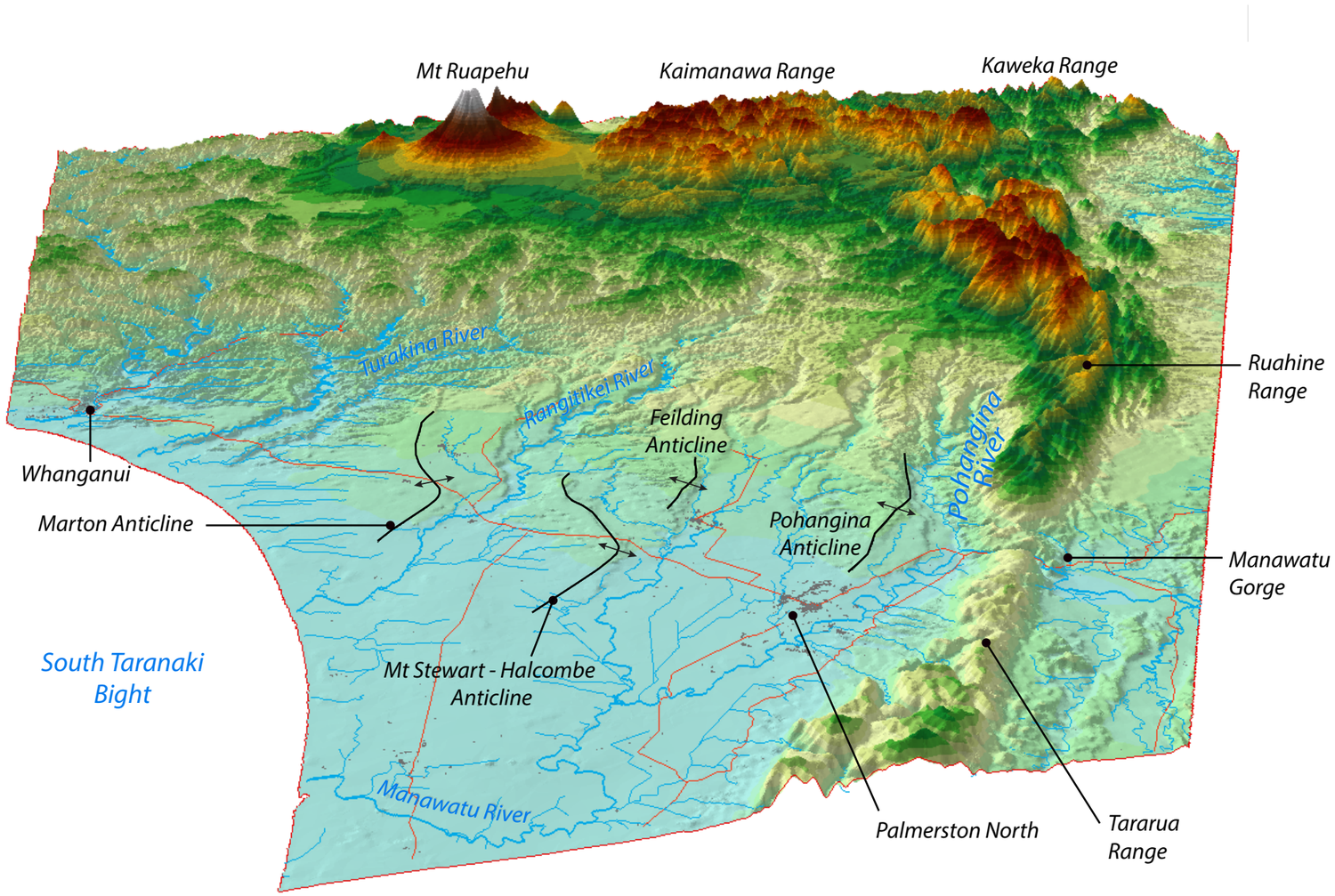
NW of the Rangitikei-Waiapu anomaly is a strong gradient across a lithospheric boundary from Mt Taranaki through Mt Ruapehu to the Bay of Plenty (Stern & Davey 1987). Northwest of this, the Central Volcanic Region is defined by a wedge shaped gravity low (c. 10 mgal) flanked by narrow highs (30 mgal). Southeast of the Rangitikei-Waiapu anomaly are high Bouguer and free air gravity anomalies of up to 80 mgal, located onshore in the southeast of the North Island in a belt striking northeast between the coast and the Hikurangi Trough. A low of -100 mgal lies southeast of Cook Strait, extending to the northeast along the Hikurangi Trough, where values of -30 mgal are typical. Free air anomalies rise to over 40 mgal east of the Trough. Numerous seamounts around New Zealand are marked by prominent, circular gravity highs.

The axial ranges and the North Island Shear belt cut across the large-scale gravity anomaly pattern in the North Island. Along the Rangitikei-Waiapu anomaly the Axial Ranges are associated with slightly higher values between the Whanganui and Hawkes Bay basins and the Hawkes Bay and Raukumara Basins. The higher values 20-50 mgal reflect a lack of sediments at these locations. The Tararua and Ruahine Ranges lie along the northwest-descending gradient from the subduction related high to the Whanganui Basin low.

Anticlines of the west

The Manawatu plains in the eastern Whanganui Basin contain a series of NE-SW trending anticlines, including the Pohangina, Feilding, Marton, Mt Stewart-Halcombe, and Oroua anticlines (Fig. 2.19). These anticlines were first documented in published work by Te Punga (1952, 1957). Seismic reflection profiles demonstrate that the folds are bound on their eastern side by westward dipping reverse faults that only rarely reach the surface (Melhuish et al. 1996; Jackson et al. 1998). The anticlines are asymmetric, characterised by gentle western slopes (typically 2°) and steep eastern slopes (up to 70°).

Figure 2.19: The Whanganui-Manawatu area showing major rivers and anticlines across the Manawatu Plains. Red lines are main highways and grey polygons represent residential areas. DEM sourced from LINZ data service.



Feldmeyer et al. (1943) and Te Punga (1957) both suggested that these anticlines were formed by ridges of basement rock trending approximately parallel with the main axial range. Structural interpretation of the Whanganui-Manawatu area indicates that these folds are still actively growing (Jackli 1957; Te Punga 1957; Lensen 1977).

The Marton Anticline west of the Rangitikei River is the western most of the documented anticlines. It is a broad, subdued fold with well-preserved planar interfluve surfaces. Similar to the other folds in the Manawatu, the Marton Anticline is characterised by a long, parallel stream system on its western flank, approximately perpendicular to the fold axis (Jackson et al. 1998), and steep short stream system on its eastern flank flowing obliquely to the fold axis. A radial drainage pattern is preserved at the southern end just north of Bulls.

References

Adams CJ, Mortimer N, Campbell HJ, Griffin WL 2015. Detrital zircon ages in Buller and Takaka terranes, New Zealand: constraints on early Zelandia history. New Zealand Journal of Geology and Geophysics 58(2): 176-201.

Adams CJ, Graham IJ, Seward D, Skinner DNB, Adams CJ, Skinner DNB, Moore PR 1994. Geochronological and geochemical evolution of late Cenozoic volcanism in the Coromandel Peninsula, New Zealand. New Zealand Journal of Geology and Geophysics 37(3): 359-379.

Anderton PW 1981. Structure and evolution of the South Wanganui Basin, New Zealand. New Zealand Journal of Geology and Geophysics 24(1): 39-63.

Auer A, White JDL, Manville V 2012. Cryptic eruption of Mount Ruapehu revealed by deposits of sediment laden streamflow in a steep mountain valley: The 4 ka Kiwikiwi Formation, Whangaehu Valley, NZ. Journal of Volcanology and Geothermal Research 243-244: 45-58.

Ballance PF 1988. Late Cenozoic time-lines and clac-alkaline volcanic arcs in northern New Zealand - further discussion. Journal of the Royal Society of New Zealand 18(2): 347-358.

Barnes PM, de Lepinay BM 1997. Rates and mechanics of rapid frontal accretion along the very obliquely convergent southern Hikurangi margin , New Zealand. Journal of Geophysical Research 102(B11): 24,931-24,952.

Beanland S 1995. The North Island Dextral Fault Belt, Hikurangi subduction margin, New Zealand. Unpublished PhD thesis, Victoria University, Wellington, New Zealand. 360 p.

Beanland S, Haines J 1998. The kinematics of active deformation in the North Island, New Zealand, determined from geological strain rates. New Zealand Journal of Geology and Geophysics 41(4): 311-323.

Beavan J, Haines J 2001. Contemporary horizontal velocity and strain rate fields of the Pacific-Australian plate boundary zone through New Zealand. Journal of Geophysical Research 106(B1): 741-741.

Beavan J, Wallace LM, Palmer N, Denys P, Ellis S, Fournier N, Hreinsdottir S, Pearson C, Denham M 2016. New Zealand GPS velocity field: 1995–2013. New Zealand Journal of Geology and Geophysics 59(1): 5-14.

Begg JG, Palmer A, Gyopari M 2005. Geological synopsis of the Manawatu-Horowhenua area for a review of the region's hydrogeology. Institue of Geological and Nucelar Sciences Client Report 2005/172, Lower Hutt, New Zealand. 22 p.

Bekesi G, McConchie J 2000. Mapping soil sorption capacity as a measure of regional groundwater vulnerability. Journal of Hydrology New Zealand 39(1): 1-18.

Berryman KR 1988. Tectonic geomorphology at a plate boundary: a transect across Hawke's Bay, New Zealand. Zeitschrift fur Geomorphologie 69: 69-86.

Beu AG, Browne GH, Grant-Taylor TL 1981. New *Chlamys delicatula* localities in the central North Island and uplift of the Ruahine Range. New Zealand Journal of Geology and Geophysics 24(1): 127-132.

Bibby HM, Caldwell TG, Davey FJ, Webb TH 1995. Geophysical evidence on the structure of the Taupo Volcanic Zone and its hydrothermal circulation. Journal of Volcanology and Geothermal Research 68(1-3): 29-58.

Bland KJ 2006. Analysis of the central Hawke's Bay sector of the late Neogene forearc basin, Hikurangi margin , New Zealand., Unpublished PhD thesis, University of Waikato, Hamilton, New Zealand. 289 p.

Briggs RM, Houghton BF, McWilliams M, Wilson CJN 2005. $^{40}Ar/^{39}Ar$ ages of silicic volcanic rocks in the Tauranga Kaimai area, New Zealand: Dating the transition between volcanism in the Coromandel Arc and the Taupo Volcanic Zone. New Zealand Journal of Geology and Geophysics 48(3): 459-469.

Browne GH 1978. Wanganui Strata of the Mangaohane Plateau, Northern Ruahine Range, Taihape. Tane 24: 199-210.

Browne GH 1986. Basement-cover relationships and tectonic significance of Mt Miroroa, western Hawke's Bay. Journal of the Royal Society of New Zealand 16(4): 381-402.

Browne GH 2004. Late Neogene sedimentation adjacent to the tectonically evolving North Island axial ranges: Insights from Kuripapango, western Hawke's Bay. New Zealand Journal of Geology and Geophysics 47(4): 663-674.

Burgess SM 1988. The climate and weather of Manawatu and Horowhenua. New Zealand Meteorological Serivce Miscellaneous Publications 115(18): 1-47.

Carter L, Shane PAR, Alloway BV, Hall IR, Harris SE, Westgate JA 2003. Demise of one volcanic zone and birth of another - A 12 m.y. marine record of major rhyolitic eruptions from New Zealand. Geology 31(6): 493-496.

Catalyst-Group 2014a. Rangitikei Catchment: Surface Water Use and Avaliability. Report No 2014/003 prepared as part of the Rangitikei Strategic Water Assessment project, Palmerston North, New Zealand. 39 p.

Catalyst-Group 2014b. Hunterville Rural Water Supply Scheme: A Review. Report No 2014/003 prepared as part of the Rangitikei Strategic Water Assessment project, Palmerston North, New Zealand. 1-15 p.

Chanier F, Ferrière J, Angelier J 1999. Extensional deformation across an active margin, relations with subsidence, uplift, and rotations: The Hikurangi subduction, New Zealand. Tectonics 18(5): 862-876.

Chappell PR 2015. The Climate and Weather of Manawatu-Wanganui, NIWA Science and Technology Series Number 66, Wellington, New Zealand. 38 p.

Clark M, Roygard J 2008. Land Use and Land Use Capability in the Manawatu-Wanganui Region. Internal Technical Report to Support Policy Development, Horizons Regional Council Report No: 2008/INT/616, Palmerston North, New Zealand. 335 p.

Cole JW, Darby DJ, Stern TA 1995. Taupo Volcanic Zone and Central Volcanic Region backarc structures of North Island, New Zealand. In: Taylor B ed. Backarc Basins: Tectonics and Magmatism. Boston, USA, Springer. Pp. 1-28.

Collot J-Y, Delteil J, Lewis KB, Davy B, Lamarche G, Audru J-C, Barnes P, Chanier F, Chaumillon E, Lallemand S and others 1996. From oblique subduction to intra-continental transpression: Structures of the southern Kermadec-Hikurangi margin from multibeam bathymetry, side-scan sonar and seismic reflection. Marine Geophysical Researches 18(2-4): 357-381.

Cooper AF, Barreiro BA, Kimbrough DL, Mattinson JM 1987. Lamprophyre dike intrusion and the age of the Alpine fault, New Zealand. Geology 15(10): 941-944.

Cotton CA 1913. The Tuamarina valley : A note on the Quaternary history of the Marlborough Sounds district. Transactions of the New Zealand Institute 45: 316-322.

Cowie JD 1963. Dune-building phases in the Manawatu district, New Zealand. New Zealand Journal of Geology and Geophysics 6(6): 268-280.

Cowie JD, Rijkse VIC 1977. Soils Of Manawatu County, North Island, New Zealand. New Zealand Soil Survey Report 30, New Zealand Soil Bureau, Department of Scientific and Industrial Research, Wellington, New Zealand: 1-33.

Cowie JD, Fitzgerald P, Owers W 1967. Soils of the Manawatu-Rangitikei sand country. Soil Bureau Bulletin 29. Department of Scientific and Industrial Research, Wellington, New Zealand. 58 p.

Davy B, Wood R 1994. Gravity and magnetic modelling of the Hikurangi Plateau. Marine Geology 118(1-2): 139-151.

Davy BW 1992. The influence of subducting plate buoyancy on subduction of the Hikurangi-Chatham Plateau beneath the North Island, New Zealand. Advances in the Geology and Geophysics of the Continental Margin, American Association of Petroleum Geologists Memoirs 53, New York, United States of America. 91 p.

DeMets C, Gordon RG, Argus DF, Stein S 1994. Effect of recent revisions to the geomagnetic reversal time scale on estimates of current plate motions. Geophysical Research Letters 21: 2191-2194.

Duncan M, Woods R 2004. Flow regimes. In: Harding JS, Mosely P, Pearson C, Sorrell B ed. Freshwaters of New Zealand, New Zealand Limnological and Hydrological Societies, Christchurch, New Zealand. Pp. 70-80.

Eberhart-Phillips D, Reyners M, Chadwick M, Stuart G 2008. Three-dimensional attenuation structure of the Hikurangi subduction zone in the central North Island, New Zealand. Geophysical Journal International 174(1): 418-434.

Feldmeyer AE, Jones BC, Firth CW, Knight J 1943. The geology of the Palmerston-Wanganui Basin, "West side", North Island, New Zealand. Unpublished Report of the Superior Oil Company of New Zealand, Petroleum Report Series 171, Ministry of Economic Development, Wellington, New Zealand. 46 p.

Ferguson RI, Werritty A 1983. Bar development and channel changes in the gravelly River Feshie. In: Collinson JD, Lewin J ed. Modern and Ancient Fluvial Systems. International Association of Sedimentologists Speical Publication 6, Oxford, United Kingdom, Wiley-Blackwell. Pp. 133-143.

Fleming CA 1953. The geology of Wanganui subdivision. New Zealand Geological Survey Bulletin 52. Wellington, New Zealand. 362 p.

Fuller IC 2007. Geomorphic work during a "150-year" storm: Contrasting behaviors of river channels in a New Zealand catchment. Annals of the Association of American Geographers 97(4): 665-676.

Fuller IC, Riedler RA, Bell R, Marden M, Glade T 2016. Landslide-driven erosion and slope–channel coupling in steep, forested terrain, Ruahine Ranges, New Zealand, 1946–2011. Catena 142: 252-268.

Furlong KP, Kamp PJJ 2009. The lithospheric geodynamics of plate boundary transpression in New Zealand: Initiating and emplacing subduction along the Hikurangi margin, and the tectonic evolution of the Alpine Fault system. Tectonophysics 474(3-4): 449-462.

Hatherton T 1970. Upper mantle inhomogenity beneath New Zealand: surface manifestations. Journal of Geophysical Research 75(2): 269-284.

Hedley CB, Yule IJ 2009. A method for spatial prediction of daily soil water status for precise irrigation scheduling. Agricultural Water Management 96: 1737-1745.

Heerdegen RG, Shepherd MJ 1992. Manawatu landforms: Product of tectonism, climate change and process. In: Soons JM, Selby MJ ed. Landforms of New Zealand. 2nd ed. Auckland, New Zealand, Longman. Pp. 33-308.

Henrys S, Wech A, Sutherland R, Stern T, Savage M, Sato H, Mochizuki K, Iwasaki T, Okaya D, Seward A and others 2013. SAHKE geophysical transect reveals crustal and subduction zone structure at the southern Hikurangi margin, New Zealand. Geochemistry, Geophysics, Geosystems 14(7): 2063-2083.

Hesp PA 2001. The Manawatu Dunefield: Environmental Change and Human Impacts. New Zealand Geographer 57(2): 1-8.

Hicks DM, Shankar U, McKerchar AI, Basher L, Jessen M, Lynn I, Page M 2011. Suspended sediment yields from New Zealand rivers. Journal of Hydrology 50(1): 81-142.

Holt WE, Stern TA 1994. Subduction, platform subsidence, and foreland thrust loading: The late Tertiary development of Taranaki Basin, New Zealand. Tectonics 13(5): 1068-1092.

Houghton BF, Wilson CJN, McWilliams MO, Lanphere MA, Weaver SD, Briggs RM, Pringles MS 1995. Chronology and dynamics of a large silicic magmatic system : Central Taupo Volcanic Zone , New Zealand. Geology 23(1): 13-16.

Hughes GR, Kennedy DM 2009. Late Pleistocene sea-level oscillations (MIS 10-2) recorded in shallow marine and coastal plain sediments of the southern Wanganui Basin, New Zealand. Quaternary Research 71(3): 477-489.

Jackli R 1957. Review of the Superior Oil Company report on the Rangitikei area. Shell, D'Arcy and Todd Oil Serivces Geological Report 7. Unpublished, held as open-file petroleum report 410 by the Institute of Geological and Nucelar Sciences, Lower Hutt, New Zealand. 43 p.

Jackson J, van Dissen R, Berryman KR 1998. Tilting of active folds and faults in the Manawatu region, New Zealand: Evidence from surface drainage patterns. New Zealand Journal of Geology and Geophysics 41(4): 377-385.

Journeaux TD, Kamp PJJ, Naish TR 1996. Middle Pliocene cyclothems , Mangaweka region , Wanganui Basin , New Zealand : A lithostratigraphic framework. New Zealand Journal of Geology and Geophysics 39(1): 135-149.

Kamp PJJ, Vonk A, Bland K, Griffin A 2002. Megasequence architecture of Taranaki, Wanganui, and King Country basins and Neogene progradation of two continental margin wedges across western New Zealand. New Zealand Petroleum Conference Proceedings 2002, Auckland, New Zealand. Pp. 464-481.

Karig DE 1970. Kermadec arc—New Zealand tectonic confluence. New Zealand Journal of Geology and Geophysics 13(1): 21-29.

King PR 2000. Tectonic reconstructions of New Zealand: 40 Ma to the Present. New Zealand Journal of Geology & Geophysics 434(43): 611-638.

Lamarche G, Beanland S, Ravens J 1995. Deformation style and history of the Eketahuna region, Hikurangi forearc, New Zealand, from shallow seismic reflection data. New Zealand Journal of Geology and Geophysics 38(1): 105-115.

Lamb S 2011. Cenozoic tectonic evolution of the New Zealand plate-boundary zone: A paleomagnetic perspective. Tectonophysics 509(3-4): 135-164.

Lamb SH, Bibby HM 1989. The last 25 Ma of rotational deformation in part of the New Zealand plate-boundary zone. Journal of Structural Geology 11: 473-492.

Langridge RM, Ries WF, Litchfield NJ, Villamor P, Van Dissen RJ, Barrell DJA, Rattenbury MS, Heron DW, Haubrock S, Townsend DB and others 2016. The New Zealand Active Faults Database. New Zealand Journal of Geology and Geophysics 59(1): 89-96.

Lebrun JF, Lamarche G, Collot JY, Delteil J 2000. Abrupt strike-slip fault to subduction transition: The alpine fault-puysegur trench connection, New Zealand. Tectonics 19(4): 688-706.

Lee JM, Bland KJ, Townsend DB, Kamp PJJ, (compilers) 2011. Geology of the Hawke's Bay area. Institue of Geological & Nuclear Sciences 1:250,000 geological map 8. Lower Hutt, New Zealand. GNS Science. 1 sheet + 93 p.

Lensen GJ 1977. Late Quaternary Tectonic Map of New Zealand 1 : 2 ,000,000. New Zealand Geological Survey Miscellaneous Series Map 12, Lower Hutt, New Zealand: 1 sheet.

Leonard GS, Begg JG, Wilson CJN 2010. Geology of the Rotorua area. Institue of Geological and Nucelar Sciences 1:250 000 geological map 5, Lower Hutt, New Zealand: 1 sheet + 102 pp.

Lewis KB 1980. Quaternary sedimentation on the Hikurangi oblique-subduction and transform margin, New Zealand. Special Publication of the International Association of Sedmentologists 4: 171-189.

Li X, Gotze HJ 2001. Ellipsoid, geoid, gravity, geodesy, and geophysics. Geophysics 66(6): 1660-1668.

Litchfield N, Berryman KR 2006. Relations between postglacial fluvial incision rates and uplift rates in the North Island, New Zealand. Journal of Geophysical Research: Earth Surface 111(2): 1-15.

Litchfield N, Ellis S, Berryman KR, Nicol A 2007. Insights into subduction-related uplift along the Hikurangi Margin, New Zealand, using numerical modeling. Journal of Geophysical Research: Earth Surface 112(2): 1-17.

MacDonald-Creevey AM 2011. Late Holocene environmental record and geological history of the Lake Colenso area, North-western Ruahine Range, New Zealand. Unpublished MSc thesis, Massey University, Palmerston North, New Zealand. 159 p.

Mazengarb C, Speden IG 2000. Geology of the Raukumara Area, Institute of Geological and Nuclear Science, Lower Hutt, New Zealand. 1 sheet+60 p.

Melhuish A, van Dissen R, Berryman KR 1996. Mount Stewart-Halcombe Anticline: A look inside a growing fold in the Manawatu region, New Zealand. New Zealand Journal of Geology and Geophysics 39: 123-133.

Mills C 1990. Gravity expression of the Patea – Tongaporutu High and subsequent model for the Taranaki Basin margin. Proceedings of the 1989 New Zealand Oil Exploration Conference, Petroleum Geothermal Unit, Energy Resource Division, Ministry of Commerce, Wellington, New Zealand. Pp. 191-200.

Milne JDG 1968. The geology and soils of the Apiti District. Unpublished MSc thesis, Victoria Universtiy of Wellington, New Zealand. 122 p.

Milne JDG 1973. Upper Quaternary geology of the Rangitikei drainage basin, North Island, New Zealand. Unpublished PhD Thesis. Victoria University of Wellington, Wellington, New Zealand. 472 p.

Molnar P, Atwater T, Mammerickx J, Smith SM 1975. Magnetic Anomalies, Bathymetry and the Tectonic Evolution of the South Pacific since the Late Cretaceous. Geophysical Journal Of The Royal Astronomical Society 40: 383-320.

Mooney HM 1970. Upper mantle inhomogenity beneath New Zealand: seismic evidence. Journal of Geophysical Research 75(2): 285-309.

Mortimer N 1993. Jurassic tectonic history of the Otago schist, New Zealand. Tectonics 12(1): 237-244.

Mortimer N 2004. New Zealand's Geological Foundations. Gondwana Research 7(1): 261-272.

Mortimer N, Tulloch aJ, Ireland TR 1997. Basement geology of Taranaki and Wanganui Basins, New Zealand. New Zealand Journal of Geology and Geophysics 40(2): 223-236.

Mouslopoulou V, Nicol A, Little TA, Walsh JJ 2007. Displacement transfer between intersecting regional strike-slip and extensional fault systems. Journal of Structural Geology 29(1): 100-116.

Neill CR 1973. Hydraulic and morphologic characteristics of Athabasca River near Forth Assiniboine-the anatomy of a wandering gravel bed river. Report REH/73/8. Alberta Research Council, Highways and River Engineering Division, Edmonton, United States of America. 23 p.

Nicol A 2011. Landscape history of the Marlborough Sounds, New Zealand. New Zealand Journal of Geology and Geophysics 54(2): 195-208.

Nicol A, Beavan J 2003. Shortening of an overriding plate and its implications for slip on a subduction thrust, central Hikurangi Margin, New Zealand. Tectonics 22(6): 1070-1084.

Nicol A, Mazengarb C, Chanier F, Rait G, Uruski CI, Wallace L 2007. Tectonic evolution of the active Hikurangi subduction margin, New Zealand, since the Oligocene. Tectonics 26(4): 1-24.

Nodder SD, Lamarche G, Proust JNl, Stirling M 2007. Characterizing earthquake recurrence parameters for offshore faults in the low-strain, compressional Kapiti-Manawatu Fault System, New Zealand. Journal of Geophysical Research: Solid Earth 112(12): 1-25.

Norris RJ, Cooper AF 2000. Late Quaternary slip rates and slip partitioning on the Alpine Fault, New Zealand. Journal of Structural Geology 23(2-3): 507-520.

Pettinga JR 1982. Upper Cenozoic structural history, coastal Southern Hawke's Bay, New Zealand. New Zealand Journal of Geology and Geophysics 25: 149-191.

Pillans BJ 1986. A late Quaternary uplift map for North Island, New Zealand. Royal Society of New Zealand Bulletin 24: 409-417.

Pillans BJ 1990. Vertical displacement rates on Quaternary faults, Wanganui basin. New Zealand Journal of Geology and Geophysics 33(2): 271-275.

Price RC, Stewart RB, Woodhead JD, Smith IEM 1999. Petrogenesis of High-K Arc Magmas: Evidence from Egmont Volcano, North Island, New Zealand. Journal of Petrology 40(1): 167-197.

Proust JN, Lamarche G, Nodder S, Kamp PJJ 2005. Sedimentary architecture of a Plio-Pleistocene proto-back-arc basin: Wanganui Basin, New Zealand. Sedimentary Geology 181(3-4): 107-145.

Quinn JM, Wilcock RJ, Monaghan RM, McDowell RW, Journeaux PR 2009. Grassland farming and water quality in New Zealand. Tearmann: Irish journal of agri-environmental research 7: 69-88.

Radcliffe JE 1976. Seasonal distribution of pasture production in New Zealand, Rangitikei District. New Zealand Journal of Experimental Agriculture 4(2): 163-170.

Rait G, Chanier F, Waters DW 1991. Landward- and seaward-directed thrusting accompanying the onset of subduction beneath New Zealand. Geology 19(3): 230-233.

Rees CJ, Palmer JA, Palmer AS 2018. Plio-Pleistocene Geology of the Lower Pohangina Valley, New Zealand. New Zealand Journal of Geology and Geophysics 61(1): 44-63.

Reyners M 1980. A Micro-Earthquake Study Of The Plate Boundary, {North-Island, New-Zealand}. Geophysical Journal Of The Royal Astronomical Society 63(1): 1-22.

Reyners M 2013. The central role of the Hikurangi Plateau in the Cenozoic tectonics of New Zealand and the Southwest Pacific. Earth and Planetary Science Letters 361: 460-468.

Richardson JM, Fuller IC 2010. Quantification of channel planform change on the lower Rangitikei River, New Zealand, 1949-2007: response to management? GeoScience: A Working Paper Series in Physical Geography, Massey University, Palmerston North, New Zealand 2: 3-26.

Robertson EI, Reilly WI 1958. Bouguer anomaly map of New Zealand. New Zealand Journal of Geology and Geophysics 1(3): 560-564.

Roygard J, Carlyon G 2004. Water Allocation Project Rangitikei River, Water Resource Assessment – Allocation Limits and Minimum Flows. Technical Report

2004/EXT/606. Horizons Regional Council, Palmerston North, New Zealand 1877310557. 178 p.

Salmon ML 2008. Crust and Upper Mantle Inhomogeneities Beneath Western North Island, New Zealand: Evidence from Seismological and Electromagnetic Data. Unpublished PhD Thesis, Victoria University of Wellington, New Zealand. 171 p.

Salmon ML, Stern TA, Savage MK 2011. A major step in the continental Moho and its geodynamic consequences: The Taranaki-Ruapehu line, New Zealand. Geophysical Journal International 186(1): 32-44.

Seward AM, Henderson CM, Smith EGC 2009. Models of the upper mantle beneath the central North Island, New Zealand, from speeds and anisotropy of subhorizontal P waves (Pn). Journal of Geophysical Research: Solid Earth 114(1): 1-22.

Sherburn S, White RS 2005. Crustal seismicity in Taranaki, New Zealand using accurate hypocentres from a dense network. Geophysical Journal International 162(2): 494-506.

Spinks KD, Acocella V, Cole JW, Bassett KN 2005. Structural control of volcanism and caldera development in the transtensional Taupo Volcanic Zone, New Zealand. Journal of Volcanology and Geothermal Research 144(1): 7-22.

Sporli KB 1980. Sedimentation in oblique-slip mobile zones. Special Publication of the Internation Association of Sedimentologists 4: 1-265.

Statistics New Z 2013. New Zealand Census Data licenced by Statistics New Zealand under the Creative Commons Attribution 4.0 International licence.

Stern T, Smith EGC, Davey FJ, Muirhead KJ 1987. Crustal and upper mantle structure of the northwestern North Island, New Zealand, from seismic refraction data. Geophysical Journal International 91(3): 913-936.

Stern TA, Davey FJ 1987. A seismic investigation of the crustal and upper mantle structure within the Central Volcanic Region of New Zealand. New Zealand Journal of Geology and Geophysics 30(January 2015): 217-231.

Stern TA, Quinlan GM, Holt WE 1992. Basin formation behind an active subduction zone: Three dimensional flexural modelling of Wanganui Basin, New Zealand. Basin research 4(3-4): 197-214.

Stern TA, Quinlan GM, Holt WE 1993. Crustal dynamics associated with the formation of Wanganui Basin, New Zealand. In: Ballance PF ed. South Pacific

Sedimentary Basins: Sedimentary Basins of the World 2. Amsterdam, Elsevier. Pp. 213-223.

Stern TA, Stratford WR, Salmon ML 2006. Subduction Evolution and Mantle Dynamics At a Continental Margin : Central North Island , New Zealand. Review of Geophysics 44(2005): 1-36.

Stern TA, Houseman G, Salmon ML, Evans L 2013. Instability of a lithospheric step beneath western North Island , New Zealand. Geology 41(4): 423-426.

Stratford WR 2006. Lithospheric Structure of a Continental Back-Arc: Central Volcanic Region, New Zealand. Unpublished PhD Thesis, Victoria University of Wellington. 405 p.

Stratford WR, Stern TA 2004. Strong seismic reflections and melts in the mantle of a continental back-arc basin. Geophysical Research Letters 31(6): 1-5.

Stratford WR, Stern TA 2006. Crust and upper mantle structure of a continental backarc: central North Island, New Zealand. Geophysical Journal International 166(1): 469-484.

Te Punga MT 1952. The geology of Rangitikei Valley. New Zealand Geological Survey Memoir 8, Wellington, New Zealand. 46 p.

Te Punga MT 1957. Live anticlines in western Wellington. New Zealand Journal of Science and Technology(38): 433-466.

Tost M, Cronin SJ, Procter JN, Smith IEM, Neall VE, Price RC 2015. Impacts of catastrophic volcanic collapse on the erosion and morphology of a distal fl uvial landscape: Hautapu River, Mount Ruapehu, New Zealand. Bulletin of the Geological Society of America 127(1-2): 266-280.

Townsend T 1998. Paleoseismology of the Waverley fault zone and implications for earthquake hazard in South Taranaki, New Zealand. New Zealand Journal of Geology and Geophysics 41(4): 467-474.

Tozer B 2013. Crustal Structure of Wanganui Basin: Implications for Back-Arc Formation. Unpublished MSc Thesis, Victoria University of Wellington. 276 p.

Wada I, He J, Hasegawa A, Nakajima J 2015. Mantle wedge flow pattern and thermal structure in Northeast Japan: Effects of oblique subduction and 3-D slab geometry. Earth and Planetary Science Letters(426): 76-88.

Walcott RI 1984. Reconstructions Of The New Zealand Region For The Neogene. Palaeogeography, Palaeoclimatology, Palaeoecology 46: 217-231.

Wallace LM, Beavan J, McCaffrey R, Darby D 2004. Subduction zone coupling and tectonic block rotations in the North Island, New Zealand. Journal of Geophysical Research B: Solid Earth 109(12): 1-21.

Wallace LM, Beavan J, McCaffrey R, Berryman KR, Denys P 2007. Balancing the plate motion budget in the South Island, New Zealand using GPS, geological and seismological datas. Geophysical Journal International 168(1): 332-352.

Wallace LM, Barnes P, Beavan J, Van Dissen R, Litchfield N, Mountjoy J, Langridge R, Lamarche G, Pondard N 2012. The kinematics of a transition from subduction to strike-slip: An example from the central New Zealand plate boundary. Journal of Geophysical Research 117(2): 1-24.

Waters JM, Craw D 2006. Goodbye Gondwana? New Zealand biogeography, geology, and the problem of circularity. Systematic biology 55(2): 351-356.

Wellman HW, Willett RW 1942. The geology of the west coast from Abut Head to Milford Sound. Transactions and Proceedings of the Royal Society of New Zealand 71: 282-306.

Whitehouse IE, Pearce AJ 1992. Shaping the Mountains of New Zealand. In: Soons JM, Selby MJ ed. Landforms of New Zealand. 2nd Edition ed. Auckland, New Zealand, Longman Paul. Pp. 144-160.

Wilson CJ 1996. Taupo's atypical arc. Nature(379): 27-28.

Wilson CJN, Rowland JV 2016. The volcanic, magmatic and tectonic setting of the Taupo Volcanic Zone, New Zealand, reviewed from a geothermal perspective. Geothermics 59: 168-187.

Wilson CJN, Rogan AM, Smith IEM, Northey DJ, Nairn IA, Houghton BF 1984. Caldera volcanoes of the Taupo volcanic zone, New Zealand. Journal of Geophysical Research: Soild Earth 89(B10): 8463-8484.

Wilson CJN, Houghton BF, McWIlliams MO, Lanphere MA, Weaver SD, Briggs RM 1995. Volcanic and structural evolution of Taupo Volcanic Zone, New Zealand: a review. Journal of Volcanology and Geothermal Research 68: 1-28.

Wood RA, Stagpoole VM 2007. Validation of tectonic reconstructions by crustal volume balance: New Zealand through the Cenozoic. Bulletin of the Geological Society of America 119(7-8): 933-943.



Chapter 3

Geology

The following chapter contains a map bulletin intended for publication. Here we capture thesis objective two by summarising the stratigraphy of the central Rangitikei District, including a collation of all existing work and presentation of a revised stratigraphic nomenclature. Chapter 3 provides an important foundation for subsequent subdivision of the succession into hydrostratigraphic units including:

- Recognition of marker horizons and positioning within the sedimentary succession.
- Revision of existing stratigraphic correlations.
- Fusion of a complete lithostratigraphic framework, encompassing the entire succession at a similar level of detail.

Both traditional and digital techniques are employed to perform a structural and stratigraphic analysis of the regional geology, providing a framework to conceptualise the hydrogeology of the Pourewa Stream sub-catchment.

Ohingaiti Sandstone exposed in cliffs along the Rangitikei River, taken from a small island of Pleistocene sediment within the Rangitikei Valley near Ohingaiti.

Geology of central Rangitikei Whanganui Basin, lower North Island New Zealand

Callum Rees[1], Julie Palmer[1], Alan Palmer[1]

[1]*Environmental Sciences, School of Agriculture and Environment, Massey University, Palmerston North, New Zealand*

3.1 Abstract

Central Rangitikei provides a cross section through the Plio-Pleistocene succession of the eastern Whanganui Basin, Lower North Island, New Zealand. The sedimentary units exposed in the cliffs of the Rangitikei River by downcutting and ongoing regional uplift provide part of one of the most comprehensive onland Quaternary stratigraphic records in the world. Lithofacies and their associated fossil assemblages form the basis for stratigraphic subdivision. Contemporary counterparts persisting around modern day New Zealand waters provide palaeoenvironmental analogues. The succession contains a Plio-Pleistocene volcanic record derived from early eruptive products of the Taupo Volcanic Zone. Geochemical 'fingerprinting' of tephra and volcaniclastic beds allow identification of chronostratigraphic horizons, facilitating basin wide correlations. The work of authors over the last 75 years is summarised, drawing together several studies to compile a revised stratigraphic framework for the central Rangitikei. The new research presented includes a set of 1:25 000 geological maps encompassing the

central Rangitikei area. Accompanying structural interpretation includes a summary of work to date and presents new data collected from the complex of en echelon structures that dissect this section of actively uplifting marine basin. Emphasis is placed on a proposed stratigraphic nomenclature with the aim of providing a framework designed for local geological mapping. Tephrochronology and biostratigraphy are used to tie the local stratigraphy into the well-documented chronostratigraphic framework of the Whanganui Basin, allowing correlation with the high resolution astronomically tuned $\delta^{18}O$ records and geomagnetic polarity timescale. We outline the development of a 3D geological model using Leapfrog Geo™ software aiming to provide an updatable resource for future geological investigations and a stratigraphic framework to incorporate and visualise an array of other data sets, relevant to the hydrogeological setting of the Rangitikei District.

Keywords: Plio-Pleistocene, Stratigraphy, Biostratigraphy, Tephrochronology, Whanganui Basin, Geological map.

3.2 Introduction

The geology of the Rangitikei Valley, situated in the heart of the Whanganui Basin (WB) has been well documented by several authors over the last century (Feldmeyer et al. 1943; Te Punga 1952; Fleming 1953; Seward 1974b; Bussell 1984; Potter 1984; Naish & Kamp 1995; Journeaux et al. 1996). Interest in the area has largely been driven by the recognition of one of the most comprehensive onland Quaternary stratigraphic records in the world (Pillans 2017), well exposed along the north-western Whanganui coastline and within the major river valleys draining the central North Island; including from west to east the Whanganui, Whangehu, Turakina, Rangitikei, Oroua and Pohangina rivers (Fig. 3.1).

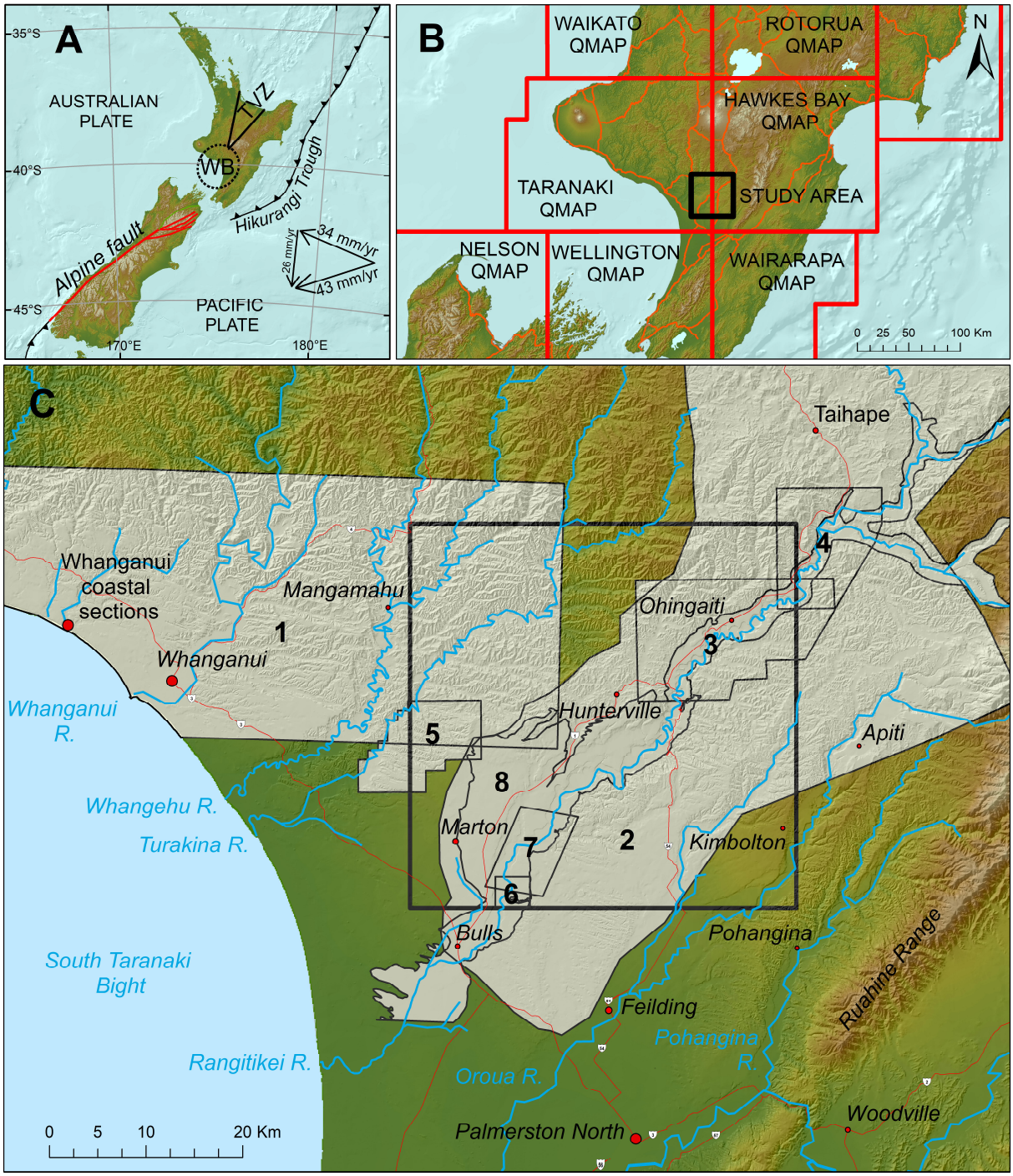


Figure 3.1: A) Location of New Zealand showing Whanganui Basin (WB) in relation to the Taupo Volcanic Zone (TVZ), Hikurangi Trough, Alpine Fault, Pacific and Australian Plates. B) Regional location map showing QMAP national mapping boundaries over the central and lower North Island of New Zealand. Black rectangle displays the location of the new geological mapping series presented in this paper. C) Location Map displaying the location of major studies in the Rangitikei Region (yellow polygons with black outlines) including the location of the new geological map series (bold black rectangle). 1: Fleming (1953); 2: Te Punga (1952); 3: Naish and Kamp (1995); 4: Journeaux et al. (1996); 5: van der Neut (1996); 6: Bussell (1984); 7: Potter (1984); 8: Milne (1973a).

Good exposure of WB strata occurs in the steep cliffs of the Rangitikei River valley and its many tributaries. Here, authors have incorporated the local stratigraphic record into a basin wide chronostratigraphic framework based on: biostratigraphy (Te Punga 1952; Fleming 1953; Beu & Edwards 1984; Bussell 1984; Potter 1984; Naish & Kamp 1995; Journeaux et al. 1996); magnetostratigraphy (Seward & Lienert 1986; Turner & Kamp 1990; Pillans et al. 1994; Naish et al. 1996; Turner et al. 2005); tephrochronology (Seward 1974a, 1976; Boellstorff & Te Punga 1977; Seward 1979; Shane 1991; Kohn et al. 1992; Alloway et al. 1993; Pillans et al. 1994; Naish et al. 1996; Shane et al. 1996b; Alloway et al. 2005; Pillans et al. 2005) and correlation with high resolution astronomically tuned $\delta^{18}O$ records (Pillans 1994; Naish et al. 1996; Naish et al. 1998; Alloway et al. 2005; Naish et al. 2005).

This paper summarises the existing wealth of knowledge on Rangitikei geology together with new field data and digital mapping techniques employed to compile a revised stratigraphic nomenclature specific to the central Rangitikei District and apply it in a 1:25 000 geological mapping project. The new nomenclature encompasses groups, formations and members proposed by several different authors (Table 3.1). We place particular emphasis and recognition on the suite of early Pleistocene volcaniclastic sediments particularly well preserved in eastern WB, which have been the focus of research following the development and application of isothermal plateau fission track dating and electron microprobe techniques in the WB (Seward 1974a; Boellstorff & Te Punga 1977; Seward 1979; Kohn et al. 1992; Alloway et al. 1993; Naish et al. 1996; Pillans et al. 1996; Shane et al. 1996b; Alloway et al. 2005; Pillans et al. 2005). We present a new set of 1:25 000 geological maps with accompanying cross sections, drawing from several existing studies that cover various portions of the mapping area (Fig. 3.1).

3.3 Geological setting

Whanganui Basin (WB)

The WB is an approximately 200 x 200 km, ovoid sedimentary basin situated in the back-arc region behind the modern Australian-Pacific plate boundary, lower North Island, New Zealand (Fig. 3.1). The Taupo Volcanic Zone (TVZ) located to the northeast has been an important source of alluvial sediment and tephras to the WB during Pleistocene to Recent time, resulting in deposition of important volcanic marker horizons within the basin fill. The WB formed via a combination of sediment loading and frictional shear between the subducting Pacific plate and overriding Australian plate (Fig. 3.2) (Stern et al. 1992). Sedimentation has largely kept pace with subsidence throughout the Plio-Pleistocene, leading to the preservation of c. 4 km of basin fill (Anderton 1981; Carter & Naish 1998). Uplift has produced key onland exposures through the shallow marine to marginal marine fill, particularly along the Whanganui coastline and within major river valleys draining the central North Island (Fig. 3.1). The basin depocentre has tracked south-east through geologic time (Fig. 3.2) (Anderton 1981) resulting in relatively deep water marine environments existing over eastern WB during Late Pliocene-Early Pleistocene time and a general shallowing pattern observed in sediments of the same age to the west.

The basin fill comprises unconformity bound cyclothemic strata deposited during transgressive, highstand and regressive parts of glacio-eustatic sea-level fluctuations. Forty seven recognised cyclothems have been correlated to odd numbered Marine Isotope Stages 100-3 spanning the entire Quaternary period (Carter & Naish 1998; Saul et al. 1999). Stages 17 to 3 are represented by a suite of young marine terraces best preserved along the coastal section northwest of Whanganui city (Pillans 1981, 1991). While to the east within the Rangitikei

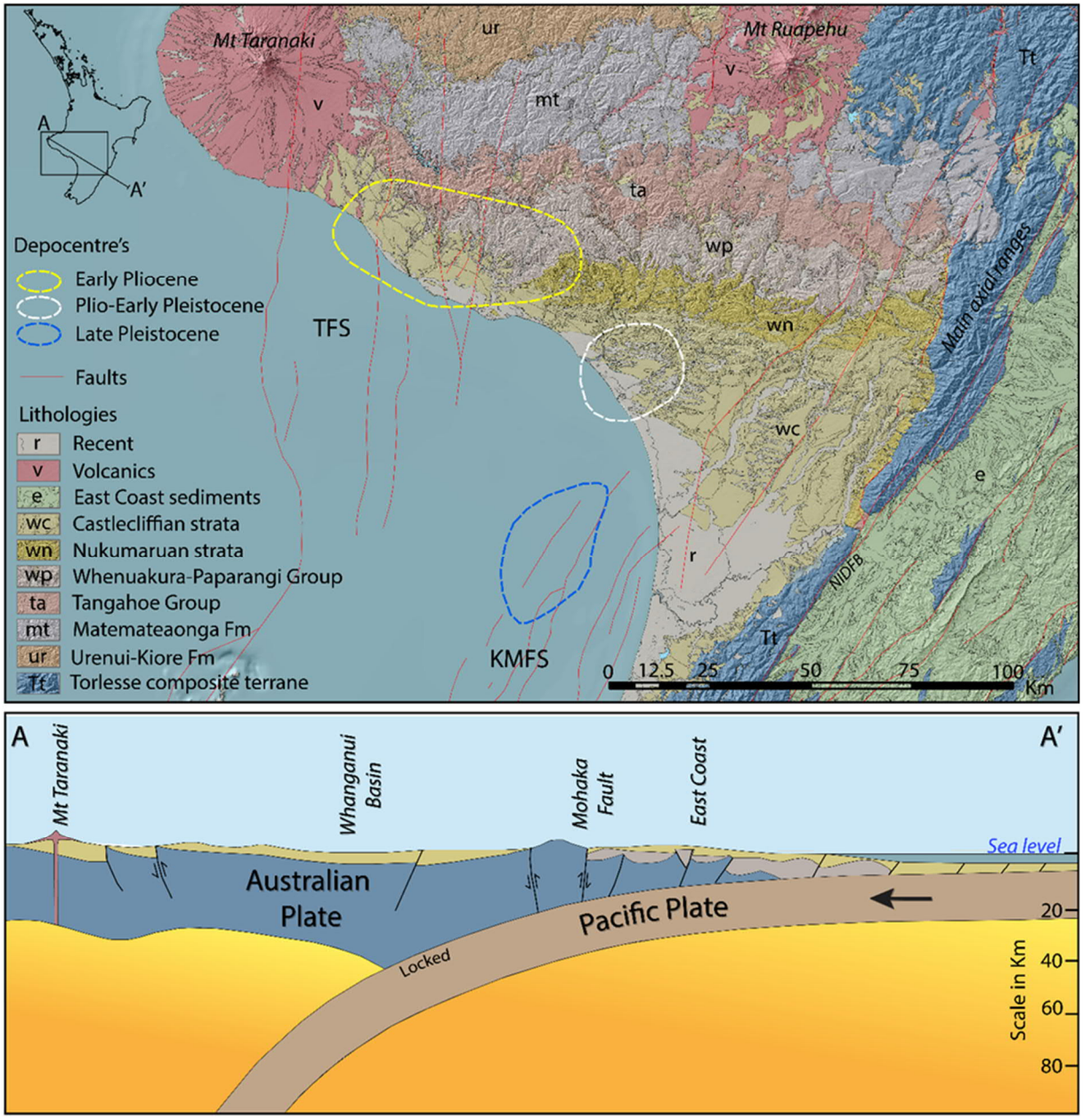


Figure 3.2: Simplified geology of the Whanganui Basin (WB) area. Major formations are displayed in increasing order of age. Basement rocks of the main axial ranges are dominantly made up of Torlesse composite terrane. Data is derived from Anderton (1981); and Kamp et al. (2002). Cross section is adapted from Nicol and Beavan (2003).

Region, a well preserved flight of aggradational river terraces has been correlated to stages 10 to 2 (Milne 1973a, c, b).

Well-preserved fossil fauna within the basin fill have attracted the attention of palaeontologists since the 19th century (Carter & Naish 1998). The relatively young age of the succession allows modern analogues to be drawn with similar environments and inhabitant fauna occurring around the New Zealand coast and shelf today (Beu 1978; Beu et al. 1981; Beu et al. 1987; Beu 1995; Johnson & Curry 2001; Naish et al. 2005; Beu 2012). Biostratigraphy provides an important means of relative dating in the basin and allows for palaeoenvironmental interpretation including accurate paleodepth reconstruction tied to glacio-eustatic fluctuations (Abbott 1994; Naish & Kamp 1996; Abbott 1997; Abbott & Carter 1997).

Proximity to the TVZ has facilitated preservation of volcanic products from multiple eruption phases, recorded in the WB succession as either fallout or reworked volcaniclastic sediment. The first influx of pumice rich alluvial sediments and tephra layers recognised during early mapping of Feldmeyer et al. (1943); Fleming (1953); and Te Punga (1952) have now been dated by isothermal plateau fission track dating (ITPFT), magnetostratigraphy and orbitally tuned cyclostratigraphy (Alloway et al. 1993; Pillans et al. 2005). Detailed stratigraphic logging, dating and chemical analysis of 28 volcaniclastic and tephra horizons throughout WB by Alloway et al. (1993); Pillans et al. (1994); Shane (1994); Naish et al. (1996); Shane et al. (1996b); Pillans et al. (2005) and Pillans (2017) allows local geological mapping to be constrained to a greater level through the application of tephrochronology. This is especially important for the Pleistocene succession in eastern WB where a thick volcaniclastic record is preserved, allowing for widespread correlation through to the eastern side of the current day main axial range (Shane 1991; Rees et al. 2018).

A coherent magnetostratigraphic framework has been proposed for the WB based largely on the analyses of blue grey siltstones which occur cyclically throughout the succession yielding clear paleomagnetic signatures (Seward & Lienert 1986; Pillans & Wright 1990; Turner & Kamp 1990; Naish et al. 1996; Turner et al.

2005). Paleomagnetic reversals have been identified and used to correlate sections to the marine oxygen isotope record (Carter & Naish 1998).

Rangitikei Geology

Feldmeyer et al. (1943) mapped the onland WB and acquired onshore seismic lines over the moderate relief of the coastal plains. This pivotal work included the identification of many of the marker horizons used in WB stratigraphy today albeit with revised names in some cases. Feldmeyer et al. (1943) mapped structures trending up the Rangitikei River valley and observed the series of anticlines trending approximately NE-SW across the coastal plains.

Te Punga provided the first detailed descriptions and maps specifically dealing with the geology of the Rangitikei Valley during field investigations for the New Zealand Geological Survey (Te Punga 1952). He incorporated biostratigraphy, allowing correlation to other study areas such as Turakina and the Whanganui coastal sections and documented several volcanic marker horizons and the well-preserved flight of river terraces in the Rangitikei River valley.

Fleming (1953) was the first to note the cyclothemic nature of Plio-Pleistocene sediments in the Whanganui sequences, later linking the cause of relative sea level fluctuations to glacio-eustasy (Fleming 1975). This correlation was made soon after the proposal by Shackleton and Opdyke (1973) that the Plio-Pleistocene had been characterised by repeated glacio-eustatically controlled sea level fluctuations. Early recognition by Fleming allowed Beu and Edwards (1984) and Pillans (1991) to publish more detailed and accurate correlations of the Whanganui succession with the international oxygen isotope scale. By the early 90's WB was firmly established as an outstanding example of the interaction between sedimentation, tectonics and fluctuations in eustatic sea level, becoming a southern hemisphere reference section for Plio-Pleistocene stratigraphy (Carter & Naish 1998).

Calibration of the WB cyclostratigraphy with radiometric and paleomagnetic ages allows direct correlation to the oxygen isotope timescale (Naish et al. 1996; Alloway et al. 2005; Pillans et al. 2005; Turner et al. 2005; Hansen & Kamp 2006). The age of stratigraphic horizons such as cyclothem and biostratigraphic boundaries can then be estimated (Carter & Naish 1998; Carter et al. 2014)

Seward (1974a, 1974b, 1976, 1978, 1979) applied paleomagnetic, fission-track, and isotopic dating techniques during her research, allowing for chronostratigraphic correlation across the WB. Fission-track ages from these early studies were later revised due to the un-resolved problem of partial track annealing in early analyses (Alloway et al. 1993). These techniques together with chemical fingerprinting of tephra by electron microprobe analysis led to the development of a detailed chronostratigraphic framework enabling correlation of the Whanganui succession to the international oxygen isotope record and deep sea cores (Beu & Edwards 1984; Pillans 1994; Turner et al. 2005).

Naish and Kamp (1995) recognised twenty cyclothems within the sedimentary sequences exposed in the Rangitikei Valley. This detailed study resulted in the introduction of six new formations and a redefinition of the Middle Rangitikei Group of Te Punga (1952). Naish and Kamp (1995) mapped the Ohingaiti area covering part of the NE section of this mapping exercise, presenting a stratigraphic framework for sedimentary units between the Te Rimu Sand (Mangarere Formation) and Vinegar Hill Formation (2.5 -1.75 Ma). The detailed geological map presented by Naish and Kamp (1995) includes cross sections and a structural interpretation for the area using extensive investigation of the stratigraphy exposed by the Rangitikei River. We note in the present study that Naish and Kamp (1995) retain the earlier work of Pillans et al. (1994) and Seward and Lienert (1986) that correlates the 'Upper Rangitikei Group' strata of Te Punga (1952) to the stratigraphic nomenclature of Fleming (1953) through the application of tephrochronology, magnetostratigraphy and biostratigraphy. This allows the

group names of Fleming (1953) e.g. Maxwell Group to be used for strata above the Rangitikei Group of Naish and Kamp (1995) (Table 3.1).

Journeaux et al. (1996) presented a similar redefinition of earlier work by Te Punga (1952), subdividing Te Punga's 'Lower Rangitikei Group' into the Utiku and Paparangi groups (3.6 -2.5 Ma). Journeaux et al. (1996) present a new geological map and cross section of the Mangaweka area, together with a detailed microfaunal and textural analysis of the Utiku and Paparangi groups in which eleven cycles are recognised attributed to glacio-eustatic sea level fluctuations.

van der Neut (1996) investigated the sequence stratigraphy of the lower Turakina Valley correlating ten cycles to the well documented cyclothems preserved in the Castlecliff section. This work includes a 1:25 000 map outlining the spatial distribution of the 10 cycles between the Turakina River in the west to the Galpin Fault. The map covers a portion of the southwestern corner of the current study area.

Bussell (1984, 1986, 1988, 1990) documented the geology and paleobotany of the Rangitawa Stream area, including detailed stratigraphic logging of key sections in the area and the introduction of new stratigraphic units resulting in the partial subdivision of the Upper Rangitikei Formation of Te Punga (1952). Potter (1984) also investigated the geology of the lower Rangitikei Valley together with Bussell (1984) resulting in a detailed stratigraphic subdivision of the Late Pleistocene sediments of the Rangitikei Valley.

Table 3.1: Proposed new stratigraphic nomenclature for subdivision of Te Pungas' (1952) Upper Rangitikei Formation. See Supplementary Data File 3A (Appendix A) for table of entire stratigraphic nomenclature used in this study.

Fleming (1953) Whanganui		Te Punga (1952) Rangitikei		Potter (1984) Bussell (1984) Rangitikei		This study Rangitikei	
POUAKAI GROUP	Papaiti Alluvium St Johns Alluvium Rapanui Frm. Brunswick Frm. Kaiatea Frm	UPPER RANGITIKEI FORMATION	Mangaone Sandstone Halcombe Conglomerate Waituna Conglomerate	POUAKAI GROUP	Westoe Frm. Halcombe Conglomerate Frm.	POUAKAI GROUP	Westoe Frm. Halcombe Conglomerate Frm.
SHAKESPEARE GROUP	Landguard Frm Putiki Shellbed Mosstown Sand Karaka Siltstone Upper Castlecliff Shellbed Shakespeare Cliff Sand Shakespeare Cliff SIltstone Tainui Shellbed Pinnacle Sand Lower Castlecliff Shellbed Seafield Sand		Rangitawa Fossil Beds Kakariki Conglomerate Ruamahanga Conglomerate Onepuhi Fossil Beds Toms Conglomerate	SHAKESPEARE GROUP	*Mingaroa Fossil Bed Mb.* *Upper Kakariki Shell Conglomerate Mb.* *Te Hiri Shellbed Mb.* *Rangitawa Fossil Bed Mb.* Mangatapu Frm *Kakariki Conglomerate Mb.* *Pryce Shellbed Mb.* *Ruamahanga Conglomerate Mb.* *Otapatu Shellbed Mb.* *Onepuhi Fossil Beds Mb.* Tokorangi Frm *Toms Shellbeds Mb.* *Toms Conglomerate Mb.*	SHAKESPEARE GROUP	*Mangatapu Frm.* *Ruamahanga Conglomerate Mb.* *Tokorangi Frm.* *Toms Conglomerate Mb.*
KAI IWI GROUP	Upper Kai Iwi Siltstone Kupe Frm Upper Westmere Siltstone Kaikokopu Frm. Lower Westmere Siltstone Omapu Shellbed Lower Kai Iwi Siltstone Kaimatira Pumice Sand		Shell Creek Fossil Beds Waitapu Shell Conglomerate Potaka Pumice		*Shell Creek Fossil Bed Mb.* Reu Reu Frm. Waiomio Frm. (Abbott 1992)	KAI IWI GROUP	Reu Reu Frm. *Waiomio Shellbed Mb.* Waiomio Frm. *Waitapu Shell Conglomerate Mb.* Kaimatira Pumice Sand Frm. *Potaka Pumice Mb.*
OKEHU GROUP	Upper Okehu Siltstone Okehu Shell Grit Lower Okehu Siltstone Butlers Shell Conglomerate Makirikiri Tuff		Mangapipi Fossil Beds Pakihikura Pumice		Undifferentiated	OKEHU GROUP	*Rewa Frm.* *Mangapipi Conglomerate Mb.* *Mangapipi Mb.* Makirikiri Tuff Frm *Pakihikura Mb.*
MAXWELL GROUP	Upper Maxwell Frm Mangahou Siltstone Middle Maxwell Frm Pukekiwi Shell Sand Lower Maxwell Frm Tewkesbury Frm					MAXWELL GROUP	Upper Maxwell Frm Rataiti Frm

3.4 Methods

During this study, we compiled a stratigraphic framework (Table 3.1, Fig. 3.3) and 1:25 000 geological map of the central Rangitikei area (Fig. 3.4), incorporating previous works by Feldmeyer et al. (1943), Te Punga (1952), Fleming (1953), Seward (1976), Potter (1984), Bussell (1984), Abbott (1992), Naish and Kamp (1995), Journeaux et al. (1996), and Van Der Neut (1996). The present authors between 2016 and 2018 undertook fieldwork, including the collection of structural data; fossil, tephra and sediment samples; logging key sections together with the identification and mapping of marker horizons. During this time, we scanned or uploaded data collected in the field into a master geodatabase constructed to facilitate map compilation.

We constructed the geological map within a Geographic Information System (GIS), producing a single digital coverage of the study area using the database schema outlined in Rattenbury and Heron (1997). Historic maps were georeferenced and used to aid with interpretation, gathering all available information into a single database (Te Punga 1952; Fleming 1953; Milne 1973a; Bussell 1984; Potter 1984; Naish & Kamp 1995; Journeaux et al. 1996; Van Der Neut 1996). A 0.4m rural aerial photograph dataset from Land Information New Zealand was used to interpret and map landslips, terrace treads and prominent lithologies in the landscape.

Six 40 km long cross-sections trending north-south and east-west were constructed across the 1600 km^2 geological mapping area (Fig. 3.5). These sections were used together with available borehole information as the primary data source for the development of a 3D geological model within Leapfrog Geo™ software (Fig. 3.6). The model was constructed from comma separated value files containing x, y, z coordinates and depth to lithology data from 14 points along each cross section.

Horizons Regional Council supplied the local borehole data, including 78 logged boreholes ranging from a depth of 7 to 446 m.

Lithostratigraphic units (groups) were modelled as a stratigraphic sequence in LeapFrog. Faults were modelled as 3D planes with specific attitudes, having the effect of splitting the model into separate fault blocks. Due to inherent limitations with modelling, it is necessary to have faults either terminate against one another or end at the model boundary. This resulted in a compromise between including fault detail from the geological map and maintaining a suitable geometry within the model reflective of the structures observed in the field.

Volcaniclastic and primary airfall horizons were sampled in sections during stratigraphic logging, with particular attention paid to documenting the environment of deposition and facies changes between outcrops. Samples were washed through a 63 µm sieve, discarding silt and clay sized particles. Following drying, samples were then dry sieved collecting the 125-250 µm fraction for mounting. Samples were set in epoxy plugs, ground and finally polished to 1 µm using diamond paste. Glass shard major elements were determined using a JEOL JXA-8230 Electron Probe Microanalyser (EPMA) at Victoria University, Wellington. Analyses were determined using an 8 nAmp beam current, 10 µm beam diameter and glass standards. All analyses are presented as weight percent, recalculated to 100% on a water free basis (Table 3.2). Total Fe (FeOt) was calculated as FeO while H_2O was calculated by the difference from 100%. Individual shard analyses allow the homogeneity of the glass to be assessed as well as chemically fingerprinted. Ternary and bivariate plots were constructed using FeO: 1/3 K_2O: CaO Wt% and FeO Vs CaO Wt % respectively, to aid tephra correlation with the existing published datasets of Pillans et al. (2005). Recognition of key glass chemistries proved vital for the correct identification of marker horizons given the amount of lateral facies variation, which occurs within the early transgressive deposits of the WB.

3.5 Stratigraphy

A stratigraphic framework for WB sediments was first established in early works by Feldmeyer et al. (1943); Fleming (1947, 1953); and Te Punga (1952). Of particular importance is the geological bulletin on the 'Geology of the Wanganui subdivision' by Fleming (1953), which details the Plio-Pleistocene exposures along the Whanganui coastline. This work included early recognition of the interplay between Quaternary subsidence, sedimentation and eustatic sea level fluctuations. Fleming's stratigraphic framework was based on biostratigraphy and lithostratigraphy. He mapped units inland to the Turakina River valley. This work remains the basis of all stratigraphic subdivision today (Carter & Naish 1998). Te Punga (1952) pioneered work in the Rangitikei Valley to the east, subdividing the stratigraphy into three broad groups the Upper, Lower and Middle Rangitikei groups, based on biostratigraphy and lithostratigraphy. Te Punga's work included the early recognition of the important tephra/volcaniclastic sequences and aggradational river terraces preserved within the Rangitikei Valley.

More recently Journeaux et al. (1996) and Naish and Kamp (1995) have revised Te Punga's 'Lower' and 'Middle' Rangitikei group's documenting the middle Pliocene to earliest Pleistocene stratigraphy in more detail, interpreting 20 sixth order (41 ka) cyclothems, dating and chemically analysing six tephras, and correlating the stratigraphy to the marine $\delta^{18}O$ record. Work by Bussell (1984) and Potter (1984) in the lower Rangitikei Valley has refined parts of the 'Upper Rangitikei Group' providing a new stratigraphic framework for the late Pleistocene succession. It is the aim of this paper to tie these detailed works into a single framework through the compilation of existing literature and the addition of new field mapping and stratigraphic correlation (Table 3.1, Fig. 3.3).

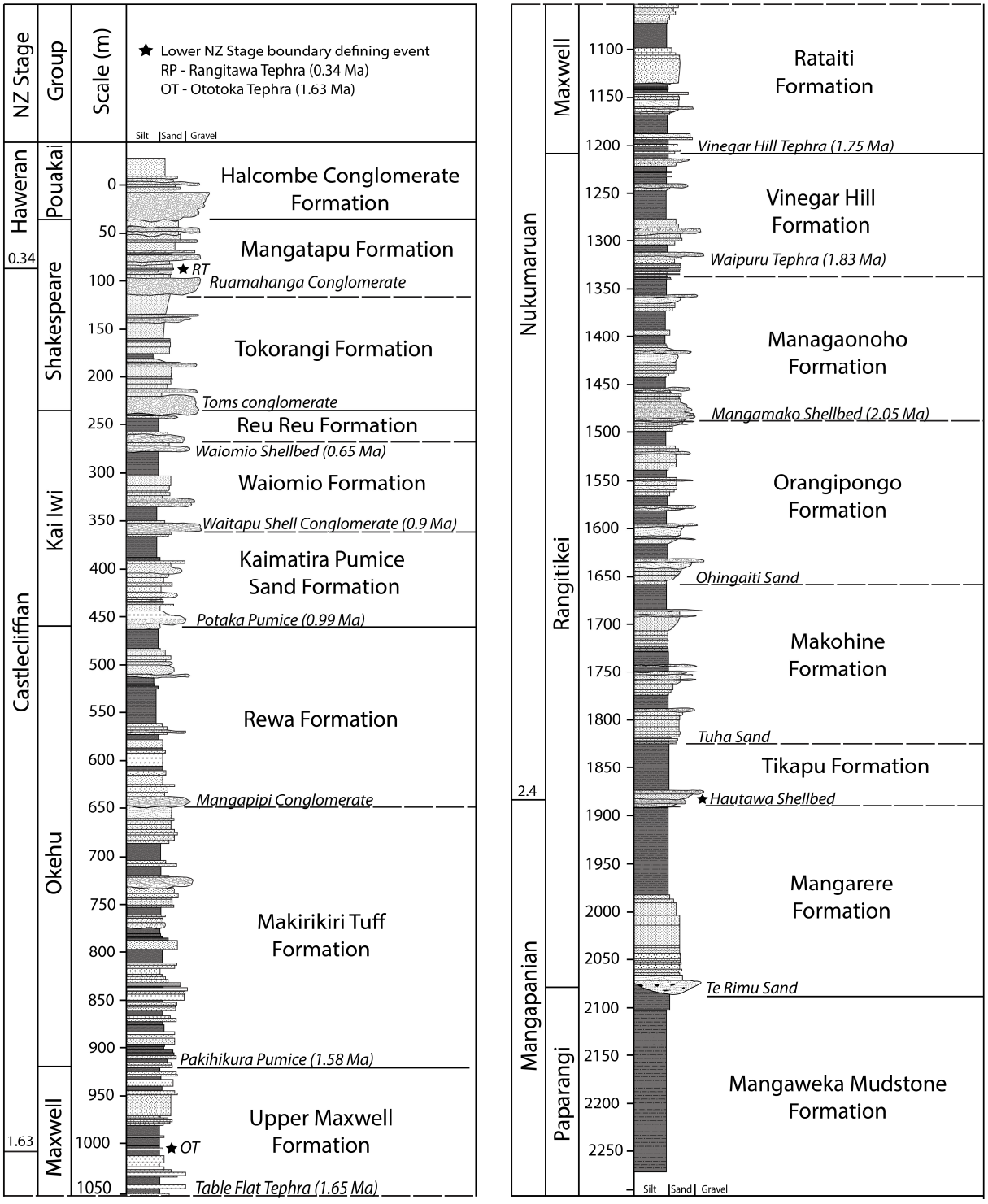


Figure 3.3: Composite stratigraphic column of Rangitikei geology with proposed new formation boundaries based on marker horizons.

Various stratigraphic nomenclature is used from eastern WB to west. We suggest this issue is a result of the spatio-temporal variations observed across the WB. Typically, each main river valley has its own set of stratigraphic units and corresponding nomenclature. Many of these units have been correlated across the basin (Seward 1976; Abbott 1994; van der Neut 1996; Pillans et al. 2005) while others pinch out or are represented by unconformities in other parts of the basin. Chemical fingerprinting of volcaniclastic deposits preserved in key sections of the major river valleys across the WB have shown Kaimatira Pumice Sand Formation (Fleming 1953), the base of which is defined by the first influx of Potaka Pumice 0.99 Ma into the sedimentary record, diverges to the east (Abbott 1994). This divergence is due to a greater amount of preservation between 1.64 – 1.19 Ma in eastern WB, with multiple eruption events recorded leading to misidentification of volcaniclastic units (Abbott 1994). In essence, the central and eastern WB contains a Mid Pleistocene (1.64 – 1.19 Ma) volcaniclastic record absent from sections of similar age to the west along the Whanganui coastline.

Researchers have noted key differences in the amount and style of preservation within middle Pleistocene sediments of the WB (Te Punga 1952; Fleming 1953; Seward 1974b; Abbott 1994), This has resulted in formation of a composite stratigraphy using the Rangitikei sections that contain a thick volcaniclastic record during the 450 ka unconformity at the base of the Butlers Shell Conglomerate in the coastal Whanganui section (Pillans et al. 2005; Pillans 2017).

A comprehensive basin wide chronostratigraphic framework of the WB (Naish et al. 1998; Naish et al. 2005; Pillans et al. 2005; Turner et al. 2005) is crucial for understanding broad scale patterns of climate change and basin history. Given the spatio-temporal variability of the WB sediments a separation of distinct local stratigraphy with unique nomenclature is warranted with the provision for overarching group names allowing for integration within the well-established basin wide chronostratigraphic framework.

Paparangi Group

Paparangi Group (c. 3.7 - 2.58 Ma) are the oldest sediments cropping out in the mapping area. Fleming (1953) originally defined the group, setting a type section in the Waitotara River Valley, 30 km NW of Whanganui City. Fleming correlated the Mangaweka Mudstone Formation in the east as the lateral equivalent of the Paparangi Sandstone Formation to the west at the type section.

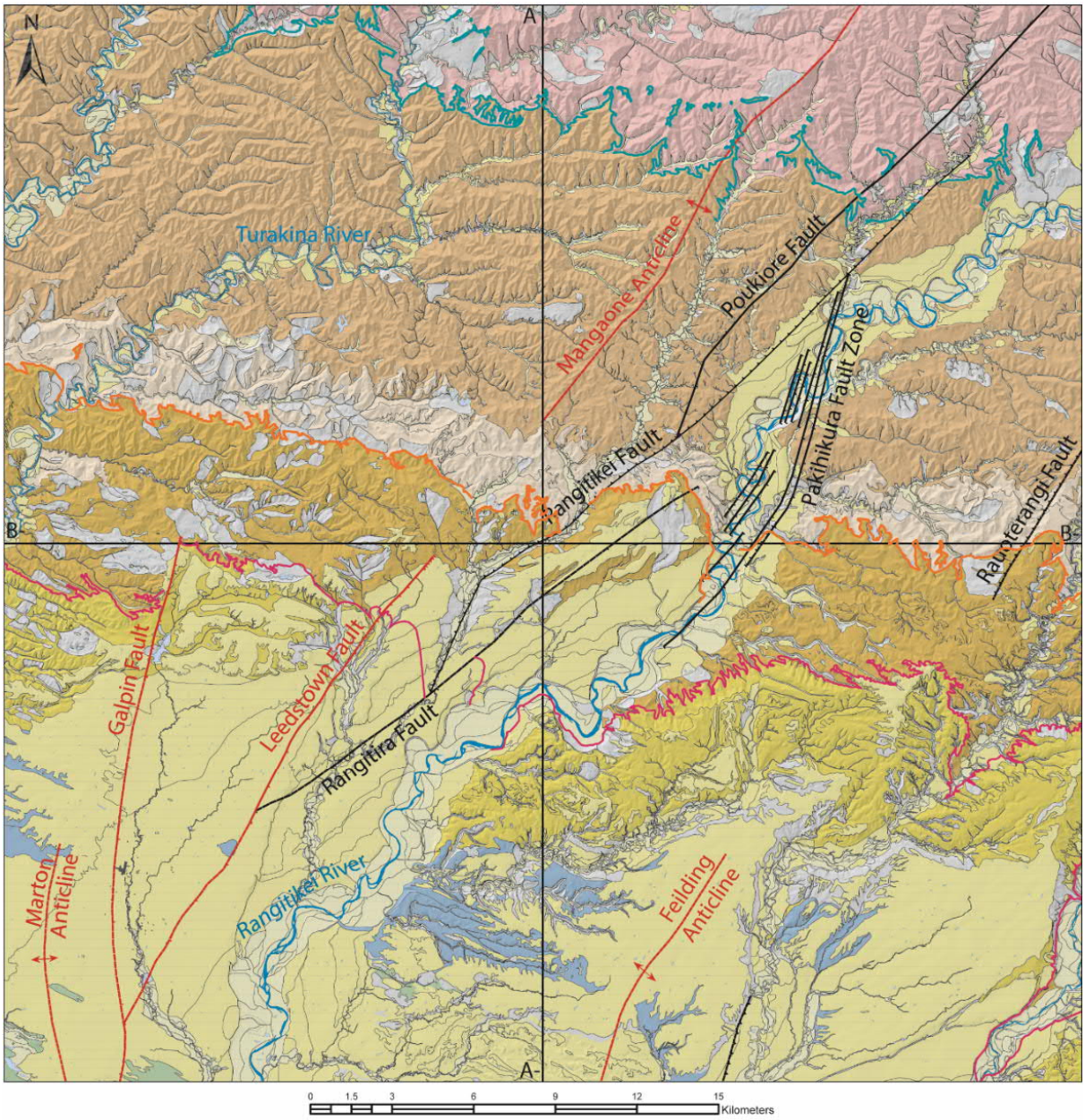
Journeaux et al. (1996) mapped the extent of the Paparangi Group in the Mangaweka area, Rangitikei District, setting the lower boundary at the contact with underlying Manui Formation, Utiku Group. The upper contact was set at the Te Rimu Sand Member of the Mangarere Formation, Rangitikei Group (Naish & Kamp 1995).

Mangaweka Mudstone Formation comprises massive siltstone and sandstone, which is well exposed in the Rangitikei River section 300 m south of the South Rangitikei Viaduct (Journeaux et al. 1996). The Eagle Hill and Kowhai tephras occur as thin silicic tephra beds within the lower half of the Mangaweka Formation, estimated at 2.88 Ma from paleomagnetic chronology and correlations with the astronomically calibrated oxygen isotope timescale (Naish et al. 1996).

Rangitikei Group

Rangitikei Group (c. 2.58 – 1.75 Ma) occurs extensively through the Ohingaiti hill country north of the township of Hunterville.

Figure 3.4 (facing page): Simplified geological map of central Rangitikei . The geological mapping area has been split into four sheets including Turakina, Hunterville, Marton, and Waituna available from the corresponding author in full detail including formations and members at 1:25 000 scale. See Fig. 3.5 for cross sections A-A' and B-B'.



LEGEND

- Holocene
- Quaternary Terraces
- Landslides
- Pouakai Group
- Shakespeare Group
- Kai Iwi Group
- Okehu Group
- Maxwell Group
- Rangitikei Group
- Paparangi Group

Horizons
- Potaka Pumice
- Pakihikura Pumice
- Te Rimu Sand

Inactive
- Approximate normal fault (ticks on downthown side)
- Accurate normal fault (ticks on downthown side)
- Approximate reverse fault (teeth on overthrust side)
- Accurate reverse fault (teeth on overthrust side)

Active
- Approximate normal fault (ticks on downthown side)
- Approximate anticline
- Accurate normal fault (ticks on downthown side)

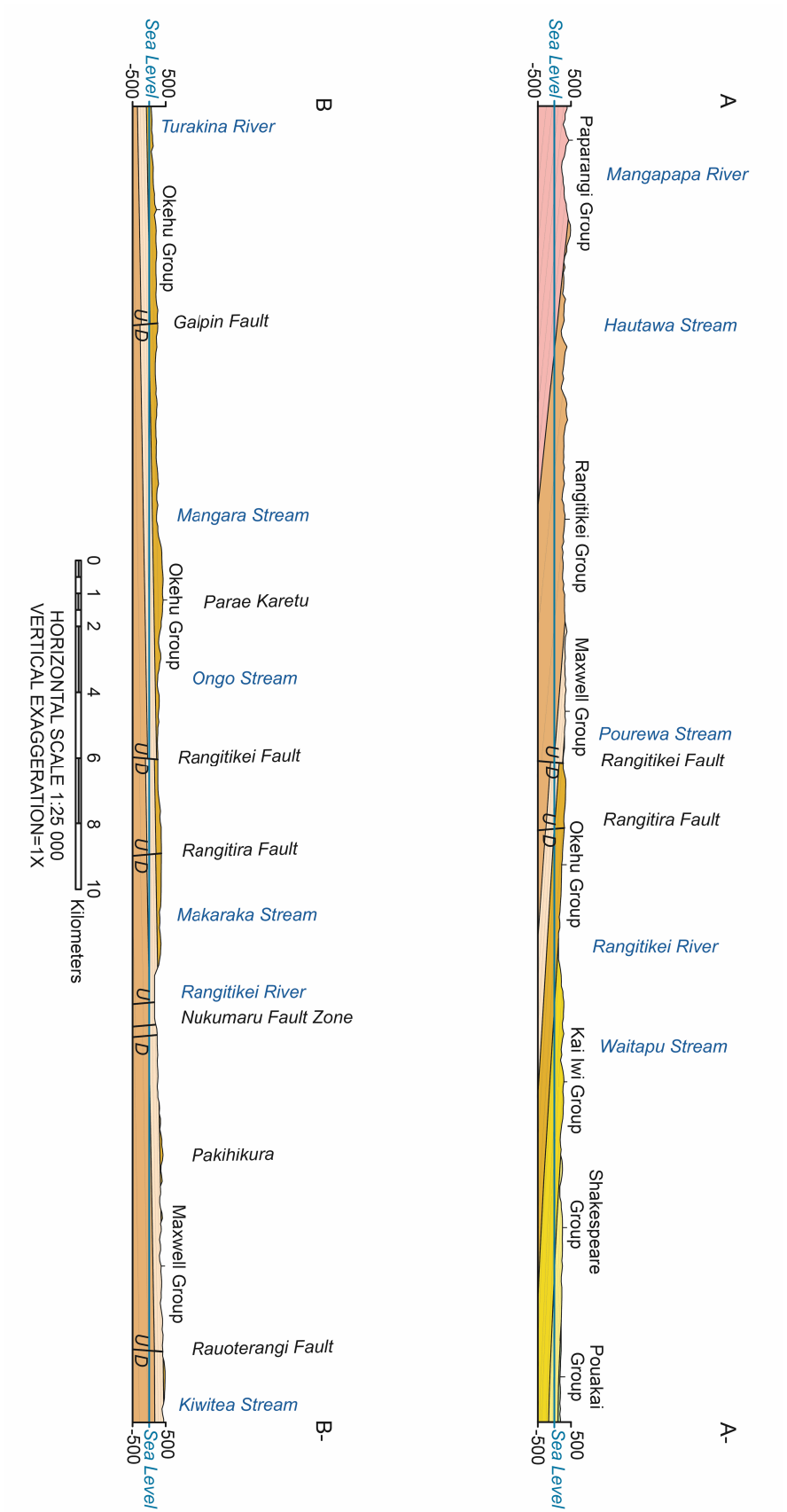


Figure 3.5: Simplified examples of two of the geological cross sections constructed across the geological mapping area, displaying major groups and structures. See Fig. 3.4 for cross section locations.

Naish and Kamp (1995) defined the group, merging the time equivalent strata of Nukumaru and Okiwa groups (Fleming 1953) in the Rangitikei section due to dramatic lithological changes across the WB.

The type section is set in the Rangitikei Valley section from Mangarere Road to Vinegar Hill Bridge (Naish and Kamp, 1995). The Rangitikei Group's lower contact is the between Te Rimu Sand Member, Mangarere Formation with the underlying Mangaweka Formation, Paparangi Group. The upper contact is placed at the Vinegar Hill Tephra (1.75 Ma) within the Vinegar Hill Formation.

Naish and Kamp (1995) subdivided the Rangitikei Group into six formations with accompanying members. Four tephra beds were recognised within the upper portion of the group and dated using the isothermal plateau fission-track (ITPFT) technique (Naish et al. 1996).

The Rangitikei Group includes cyclothemic strata consisting of alternating sets of siliciclastic siltstone and sandstone with shellbed lenses. Notably the group contains the Hautawa Shell Bed containing the first occurrence of cold-water indicator *Zygochlamys delicatula* within WB strata (Beu et al. 1981), indicating the onset of major global glaciations and marking the Mangapanian–Nukumaruan stage boundary.

The Plio-Pleistocene and Tertiary-Quaternary boundaries are set slightly below the Hautawa Shell bed at the Gauss/Matuyama boundary, 2.588 Ma (Gibbard et al. 2007) located in the upper Mangaweka Mudstone Formation (Journeaux 1995; Journeaux et al. 1996; Naish et al. 1996; Naish et al. 1998).

Maxwell Group

Maxwell Group (c. 1.75 -1.58 Ma) outcrops in the hill country surrounding Hunterville extending in a band of heavily eroded country toward Upokongaro 9 km NE of Whanganui City. Fleming (1953) defined the group setting a type section on the Whanganui coast between Nukumaru Beach and Ototoka Stream. The lower contact was set at the top of the Nukumaru Brown Sand in the western WB and the top of the Waipuru shellbed in the eastern WB, Nukumaru Group.

More recent redefinition of the lower contact in the Rangitikei section by Naish and Kamp (1995) has set the lower contact of the Maxwell Group at the Vinegar Hill Tephra (1.75 Ma). This tephra is recognised in the Rangitikei section and at a section on Brunswick Road 12.3 Km NW of Whanganui City (Pillans et al. 2005). Here we adopt the framework of Naish and Kamp (1995), although it is pertinent to note that using a tephra recognised in only two sections 58 km apart as a group boundary is problematic and further work to establish Vinegar Hill tephra in other sections between Whanganui and Rangitikei is needed. The use of the Waipuru Shellbed as a group boundary was dismissed by Naish and Kamp (1995) due to several similar shellbeds occurring in close stratigraphic proximity, however, the collective shellbeds as mapped by Feldmeyer et al. (1943) and in the present study do represent a distinctive change in the stratigraphy, attain prominence in the landscape and are recognised in all major sections. For this reason we map the Waipuru Shellbeds as a horizon within the Vinegar Hill Formation.

Maxwell Group contains alternating siliciclastic sandstone and siltstone with carbonaceous lenticular to flaser bedded units, thin shell and lignite beds (Fig. 3.7E). Here we separate the Maxwell Group of the Rangitikei section into the Rataiti (new) and Upper Maxwell formations based on biostratigraphy, tephrochronology and changes in depositional style. The last occurrence of *Patro undatus* within upper Rataiti Formation correlates to the Pukeiwi Shell Sand at

the type section where Fleming interprets a local marine incursion between non-marine conditions within his Lower and Middle Maxwell Formations. The boundary between Rataiti and Upper Maxwell formations is set at the first influx of Table Flat glass chemistry (1.65 Ma) into the stratigraphy at which point non-marine to estuarine beds with frequent *Austrovenus stutchburyi* begin to dominate the succession. In the field this is a broad lithological separation based on a change from shallow marine to marginal/non marine depositional environments, considerable reworking of Table Flat pumice and glass chemistry within higher beds occurs in the succession, care is needed to be taken to identify its first influx within the basin (Pillans et al. 2005). The upper contact of the Maxwell Group is set at the Pakihikura Pumice (1.58 Ma) within Makirikiri Tuff Formation (Fleming 1953), Okehu Group. Makirikiri Tuff formation is absent from the coastal type section where Maxwell Group is overlain by the Butlers Shell Conglomerate, Okehu Group.

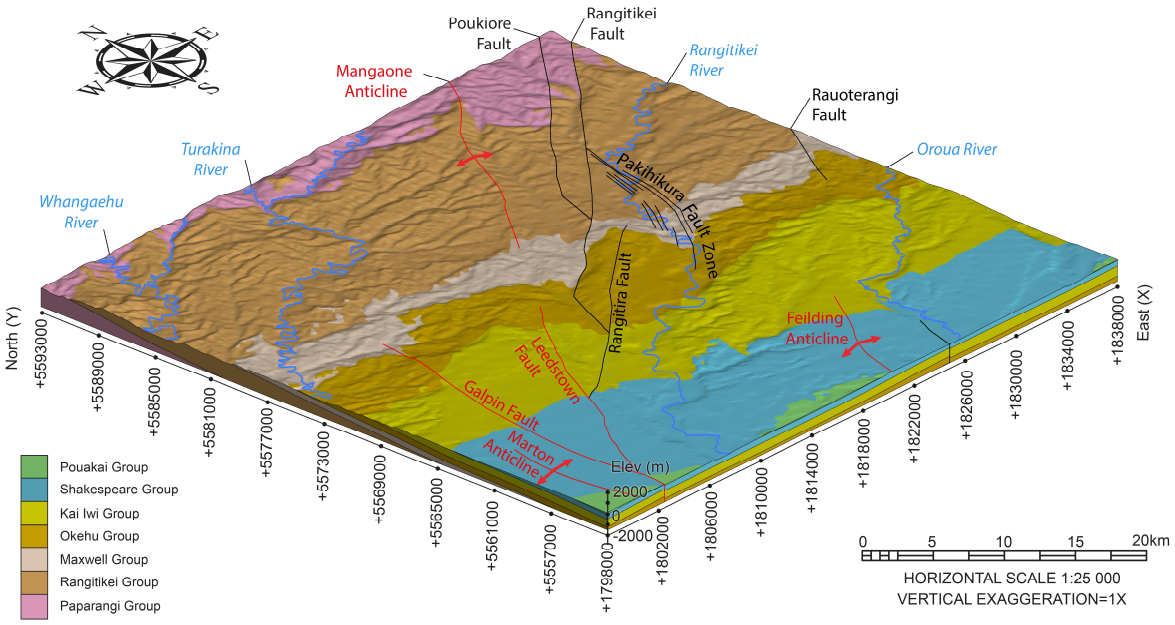


Figure 3.6: Simplified 3D geological model of the study area displaying groups, faults, folds and major rivers.

Maxwell Group marks a major change in the WB succession from marine dominated deposition of Rangitikei, Nukumaru and Okiwa Groups to the non-marine units of the Maxwell Group, characterised by seams of lignite and an absence of marine fossils. Direct correlation between the type section on the Whanganui coast and the present study area is difficult although glass chemistries similar to Table Flat Tephra have been reported in three levels within the Mangahou Siltstone and Middle Maxwell Formation of Fleming (1953) (Shane 1993; Pillans et al. 2005).

Okehu Group

Okehu Group (c. 1.58 – 0.99 Ma) sediments occur through the broken hill country 15 km north of Marton. At the Whanganui coastal section Fleming (1953) defined Okehu Group as the formations cropping out from Ototoka Stream to Kai Iwi Stream. The lower contact of the Okehu Group is set at the base of the Butlers Shell Conglomerate at the coastal type section, the lateral equivalent of the Makirikiri Tuff Formation to the east. The upper contact is set at the base of the Kaimatira Pumice Sand Formation, Kai Iwi Group, representing a major rhyolitic eruption that resulted in WB being flooded with volcaniclastic sediments.

Fleming notes unconformities at the base of the Butlers Shell Conglomerate and Makirirkiri Tuff Formation where the thickness of the underlying Maxwell Group varies from the thickness predicted using parallel bedding. Butlers Shell Conglomerate and Makirikiri Tuff Formation interfinger and alternate with one another in the Mowhanau Stream area until near the Whanganui Valley where the Butlers Shell Conglomerate completely pinches out and is replaced by the Makirikiri Tuff Formation (Fleming, 1953). From this point, Feldmeyer et al. (1943) traced the pumiceous alluvium across the basin as the 'Basal Castlecliffian Ash'. Makirikiri Tuff Formation was named by Fleming (1953) from its outcrop on either side of Whanganui Valley near Makirkiri. Seward (1976) correlated the

Makirikiri Tuff Formation of Fleming (1953) to the Pakihikura Pumice of Te Punga (1952). Seward (1976) recognised Mangapipi Tephra, Ridge Tephra and Pakihikura Pumice formally placing them within the Makirikiri Tuff Formation.

Fleming notes the Okehu Group thickens considerably and becomes finer grained from west to east, which make recognition of the same units defined in the coastal section untenable to the east. In the east of the subdivision, Fleming leaves the Okehu Group as undifferentiated Okehu Siltstone.

Here we propose the Rewa Formation (new) for the strata between Makirikiri Tuff Formation and the base of the Kai Iwi Group. The lower contact of Rewa Formation is set at the Mangapipi Conglomerate Member (Fig. 3.8) which we trace east from Rangiwahia Rd to the Mangatutu/ upper Mangapipi Stream area and farther west to the Turakina valley where it is named Mangara Shell Conglomerate (van der Neut 1996). We place the upper contact at the first influx of Potaka Pumice into the sedimentary record.

Kai Iwi Group

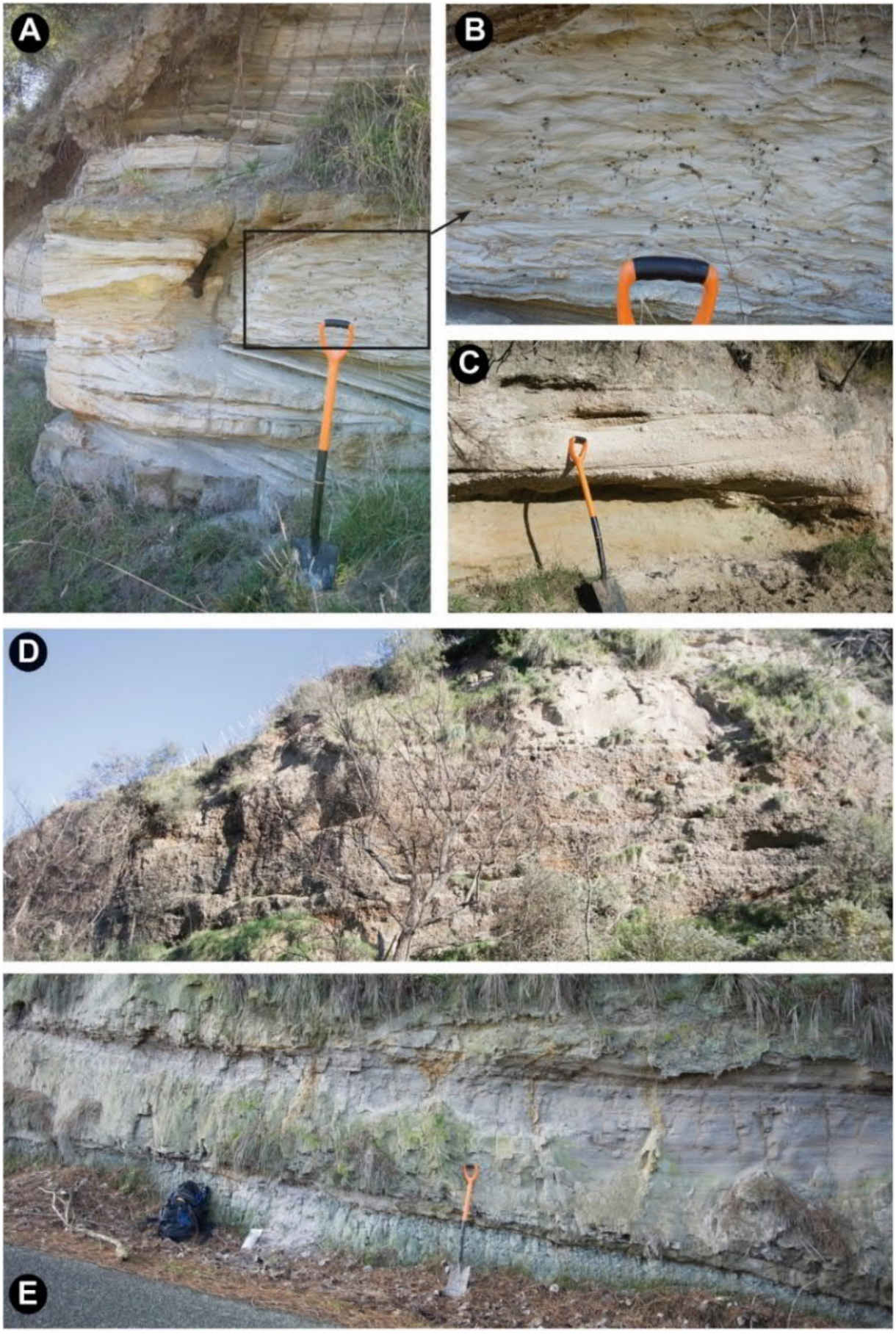
Kai Iwi Group (c. 0.99 – 0.6 Ma) crops out across the steep hill country of Waituna West eastward to the Turakina valley where it is offset across the Galpin Fault. Fleming (1953) nominated a type section for Kai Iwi Group at the Whanganui coastal section between Okehu Stream and halfway between Kai Iwi and Castlecliff beach. The basal contact is set at the base of the Kaimatira Pumice Sand Formation, characterised by the first influx of Potaka Pumice into the WB at c. 0.99 Ma (Pillans 2017). The upper contact is defined by the base of the Toms conglomerate, Shakespeare Group, a unit defined by Te Punga (1952) in the Rangitikei section and west of the Turakina River by Fleming (1953) in the basal portion of the Seafield Sand.

In the present study we adopt and combine the nomenclature of several authors including Te Punga (1952), Fleming (1953) and Abbott (1992) to subdivide the Kai Iwi Group in the Rangitikei section into three formations, namely the Kaimatira Pumice Sand Formation, Waiomio Formation and Reu Reu Formation in order of decreasing age.

We lower the rank of Abbott's (1992) Waiomio Formation to Waiomio Shell Bed Member and redefine the Waiomio Formation as consisting of all strata between the Waitapu Shell Conglomerate (Kaukatea Pumice and/or Tephra, 0.9 Ma) and Waiomio Shell Bed Member (Kupe Pumice and/or Tephra, 0.65 Ma) (Fig. 3.3). This emendation allows coarse-grained, transgressive marker horizons (members) to form the boundaries between separate formations of the Kai Iwi Group in the Rangitikei section aiding with mapping due to their visibility in the landscape. In turn, Abbott's (1992) Reu Reu Formation consists of all strata between the Waiomio Shell Bed Member and Toms Conglomerate Member (base of the Shakespeare Group).

Kaimatira Pumice Sand Formation has received considerable attention since its definition by Fleming (1953) in the succession near Okehu Stream, Kai Iwi Beach, Whanganui. With the advent and application of electron microprobe analysis and isothermal plateau fission track dating together with systematic logging and sampling of sections in the Whangehu, Turakina, Rangitikei and Oroua Rivers by

Figure 3.7 (facing page): A) Kaimatira Pumice Sand Formation displaying low angle cross bedding, ripple troughs and overlying planar bed sets near Te Houhou Rd (NZGD2000 -40.0075 S, 175.526547 E). B) Close up of ripple troughs from photo A. C) Basal Potaka Pumice Member representing a basal conglomerate facies of Kaimatira Pumice Sand Formation taken 400m NE of photo A. D) Toms Conglomerate observed in a cliff exposure on western side of the Rangitikei River (NZGD2000 -40.057282 S, 175.491529 E). E) Tephric silts and sands with interbedded thin (<10cm) lignite typical of Upper Maxwell Formation exposed in a road cutting on Makahou Road (NZGD2000 -39.911777 S, 175.42737 E).


A
B
C
D
E

Seward (1974a), Seward (1979), Shane (1993), Pillans (1994), Shane (1994), Naish et al. (1996), Pillans et al. (1996), Shane et al. (1996a), Alloway et al. (2005), Pillans et al. (2005) a comprehensive stratigraphic framework of early Pleistocene eruptive products in the WB has been established.

This work by previous authors has led to the recognition of a potential miscorrelation of the Kaimatira Pumice Sand Formation eastward from its type section on the Whanganui coastline and resulting in grouping of Rewa Pumice within basal Kaimatira Pumice Sand Formation in the Rangitikei and Turakina areas. In this study we use Potaka Pumice Member, also known as Deepdem Conglomerate in the Turakina section to delineate the base of the Kaimatira Pumice Sand Formation, Kai Iwi Group. The Kaimatira Pumice Sand Formation therefore consists of all strata between the Potaka Pumice Member and Waitapu Shell Conglomerate Member, which contains Kaukatea Pumice and/or Tephra (0.9 Ma) (Fig. 3.3, 3.7 and 3.8).

Shakespeare Group

Shakespeare Group (0.6 – 0.34 Ma) is well exposed in the cliffs of the Rangitikei River and lower Pourewa Stream. Fleming (1953) defined a type section for the Shakespeare Group at the coastal section near Castlecliff Beach, Whanganui. The basal contact in the type section is set at the base of the Seafield Sand, which

Figure 3.8 (facing page): A) Makirikiri Tuff Formation exposed in a tributary of Pourewa Stream 1.5 km SSW of Hunterville with typical tephric rich silts containing thin shell beds of stunted *Austrovenus stuchburyi*; the erosion resistant nature of these consolidated silts makes them an excellent marker horizons for mapping (NZGD2000 -39.949688 S, 175.556631 E). B) Mangapipi Conglomerate Member exposed on Putorino Rd (NZGD2000 175.584912E, -39.990339S, displaying cross-bedded shell hash and coarse sands. C) Hautawa Shellbed exposed on the interfluve between Hautawa and Kaitatara streams (NZGD -39.83095 S, 175.54443 E). D) Waitapu Shell Conglomerate exposed in Waitapu Stream, Potaka Station (NZGD2000 -40.028797 S, 175.529723 E). E) Ohingaiti Sand exposed in the cliffs of the Rangitikei River near Ohingaiti (NZGD -39.877007 S, 175.676236 E).


A
B
C
D
E

Fleming mapped eastward noting the presence of a basal conglomerate west of the Whanganui at the same stratigraphic position as Te Punga's (1952) Tom's Conglomerate. The upper contact is the top of the Landguard Formation exposed at Landguard Bluff on the east side of the Whanganui River in Whanganui City (Fleming 1953; Pillans et al. 1988), and 5 km southeast at a section in the Kaitoke area toward the Whangehu River (Fleming 1953; Beu & Edwards 1984).

Here we adopt the nomenclature introduced by Te Punga (1952), Potter (1984) and Bussell (1984) in describing the Shakespeare Group sediments exposed in Rangitawa Stream, Pourewa Stream and Rangitikei sections. For brevity we have omitted several members of Potter (1984) and Bussell (1984), instead only mapping members that are formational boundaries and attain prominence in the landscape i.e. Ruamahanga Conglomerate. For a full description of members contained within the Shakespeare and Pouakai groups in the Rangitikei section readers are referred to the detailed accounts of Potter (1984) and Bussell (1984). Tokorangi Formation consists of the strata between Toms Conglomerate Member and Ruamahanga Conglomerate including the Onepuhi Pumice and/or Tephra (0.57 Ma). Mangatapu Formation comprises the strata between Ruamahanga Conglomerate Member and the overlying Halcombe Conglomerate Formation, Pouakai Group, including the widespread Rangitawa Pumice and/or Tephra (0.34 Ma).

Pouakai Group

Pouakai Group (0.34 – 0.31? Ma) includes fluvial, aeolian and terrace cover bed deposits with limited exposure at the southern boundary of the present study area. Outcrops at Kakariki and Mingaroa 5 Km NW and SW respectively from the township of Halcombe, provide sections for the Halcombe Conglomerate Formation (Te Punga 1952, 1957b) and Westoe Formation (Bussell 1984), including the Griffins Road, Kakariki and Fordell tephras.

3.6 River terraces

The most complete sequence of river terraces within the WB occurs in the Rangitikei Valley (Te Punga 1952; Milne 1973a, b) (Fig. 3.9). Te Punga (1952) recognised seven episodes of terrace formation within the Rangitikei, matching heights of terrace treads on either side of the present river channel and linking these episodes to changes in relative base level, suggesting this was a result of regional uplift combined with a concurrent lowering of sea level.

Table 3.2: Major alluvial terraces in Rangitikei Valley

Terrace	Age (Milne 1973a; Pillans et al. 1993; Pillans et al. 1996)
Ohakea III	10 ka
Ohakea II	12 ka
Ohakea I	18 ka
Rata	30-50 ka
Pourewa	70-80 ka
Cliff	90-100 ka
Greatford	110-120 ka
Marton	140-170 ka
Burnand	240-280 ka
Aldworth	340-350 ka
Waituna	360-370 ka



Figure 3.9: A: View north over a flight of river terraces preserved along Te Houhou Road off SH1, Rangitikei Valley (NZGD2000 -40.015685 S, 175.514145 S). B: View of the angular discordance between the last glacial aggradational surface (Ohakea 2 Terrace) and gently dipping Pleistocene beds of the Kai Iwi Group forming a dip plane in the landscape on Potaka Station, Rangitikei Valley (NZGD2000 -40.005035 S, 175.546031 E).

Milne (1973a) mapped the Rangitikei river terraces in detail, recognising nine major terrace sets and subdividing them into aggradational and degradational terraces. Terraces with typically greater than 3m of alluvial gravels were defined as aggradational, while those with less than 3m of gravels were defined as degradational (Milne 1973a; Pillans 1994). This definition was guided by the maximum thickness of alluvium on clearly degradational terraces younger than the Ohakean terrace set (Milne 1973a).

Aggradational terraces are associated with glacial and stadial periods during the Quaternary, predicted as a response to increased sediment yields from deforested highlands during cold periods (Milne 1973a; Pillans 1994). This correlation between glacial/stadial periods and river aggradation is based on dating of Ohakean terrace alluvium (Milne 1973a; Marden & Neall 1990; Pillans et al. 1993; Vandergoes et al. 2013; Lowe et al. 2015) and the occurrence of subalpine pollen assemblages in Marton terrace alluvium south of Levin (Barnett 1984).

The Rangitikei valley terrace chronology of Milne (1973a) depended on the glass fission-track age of 230 ±30 ka for the Mount Curl Tephra. This tephra was later correlated to the Rangitawa Pumice (Seward 1976; Boellstorff & Te Punga 1977) and is referred to now as Rangitawa Tephra (Kohn et al. 1992). More recent re-dating of the Rangitawa Tephra has yielded an age of 345 ±12 ka (Pillans et al. 1996). We present the approximate ages for terraces recognised in the Rangitikei Valley in Table 3.2, taking into account a revised age for the Rangitawa Tephra.

3.7 Structure

The structure of the central Rangitikei is surprisingly complex. Despite a relatively simple post depositional structure characterised by dips of between 2-10°, the area is home to large scale faulting made difficult to map by the weakly lithified nature of the lithologies which are prone to slumping. Two major westward dipping reverse faults, the Rangitikei and Rauoterangi faults are attributed to active folding on the Manawatu Plains (Melhuish et al. 1996; Begg et al. 2005) and have been mapped extending SW-NE up the Rangitikei River and its adjoining interfluves (Feldmeyer et al. 1943; Naish & Kamp 1995).

The structure of the Plio-Pleistocene succession follows the patterns of the basins depocentre through time, illustrated by Anderton (1981). During Late Pliocene - earliest Pleistocene time the basin depocentre was situated around the present day lower Turakina River valley, represented by thickening and fining of sediments of this age toward Turakina (Naish & Kamp 1995; Townsend et al. 2008). Correlative strata exposed at the basin margins are thinner and generally coarser grained (Fleming 1953). Through time as the depocentre continued to migrate south due to flexural uplift in the north, a general shoaling occurred within the sedimentary succession, characterised by progressively less tilted strata dipping toward the present position of the depocentre offshore from Foxton.

Folds

The Manawatu plains in eastern WB contain a series of approximately NE-SW trending anticlines, including the Pohangina, Feilding, Marton, Mt Stewart-Halcombe, and Oroua anticlines (Fig. 3.10). These anticlines were first documented in published work by Feldmeyer et al. (1943) and Te Punga (1952, 1957).

They are bounded on their eastern flank by westward dipping reverse faults that only rarely reach the surface (Begg et al. 2005) and have been identified by seismic reflection surveys (Feldmeyer et al. 1943; Anderton 1981; Melhuish et al. 1996; Jackson et al. 1998; Nicol & Beavan 2003; Lamarche et al. 2005). The anticlines are asymmetric, characterised by gentle western slopes (typically 2-5°) and steep eastern slopes (up to 70°). Their asymmetric geometry is interpreted to reflect the westward dipping, shallow reverse faults beneath (Jackson et al. 1998). Feldmeyer et al. (1943) and Te Punga (1957) both suggested that these anticlines were formed by ridges of basement rock trending approximately parallel with the main axial range.

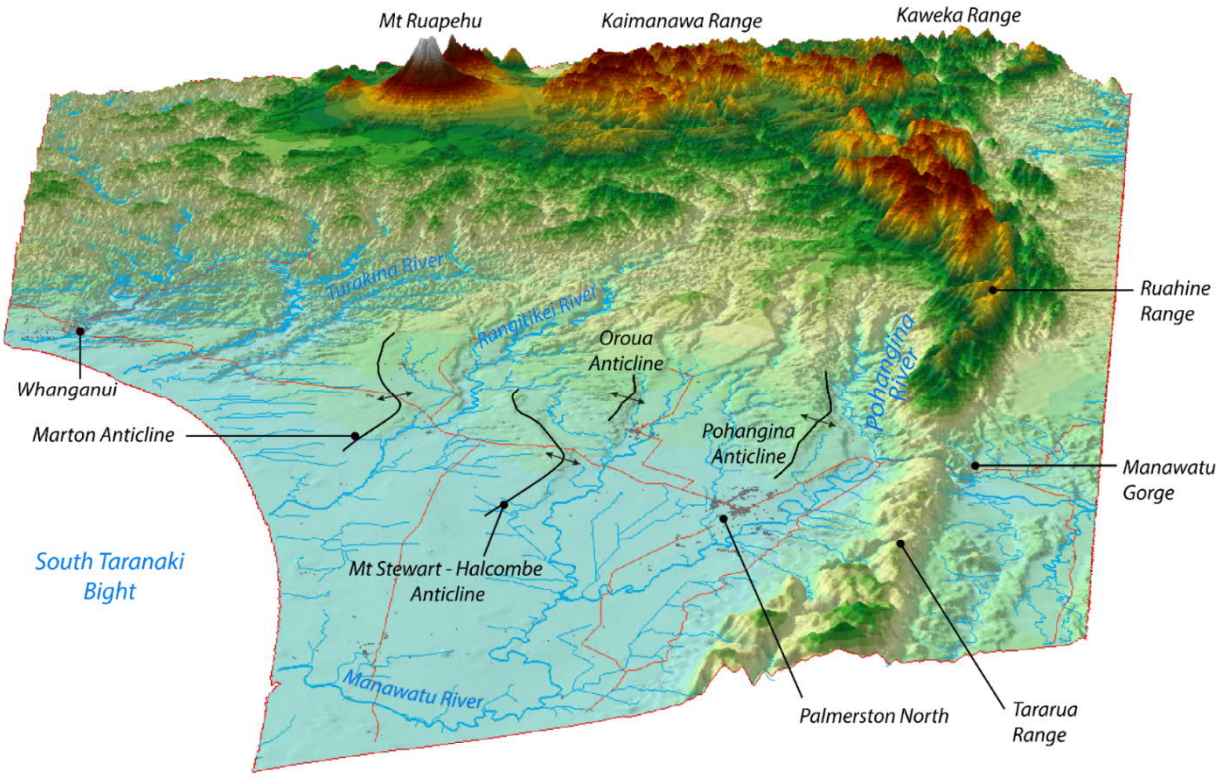


Figure 3.10: 3D image of the Whanganui-Manawatu area showing major rivers and anticlines across the Manawatu Plains. DEM sourced from LINZ, 2016.

Structural interpretation of the Whanganui-Manawatu area indicates that these folds are still actively growing (Jackli 1957; Te Punga 1957; Lensen 1977). Preservation of the 310 ka Brunswick marine terrace tread (Pillans 1983; Pillans 2017) on the anticlines together with seismic reflection evidence of faulting within underlying Plio-Pleistocene sediments (Melhuish et al. 1996) suggests these features are long lived and have been growing since at least Pliocene time with a majority of the present day topography forming over the last c. 300 ka. The Marton Anticline west of the Rangitikei River is the western most of the documented anticlines occurring within the southwestern portion of the present study area. It is a broad, subdued fold with well-preserved planar interfluve surfaces.

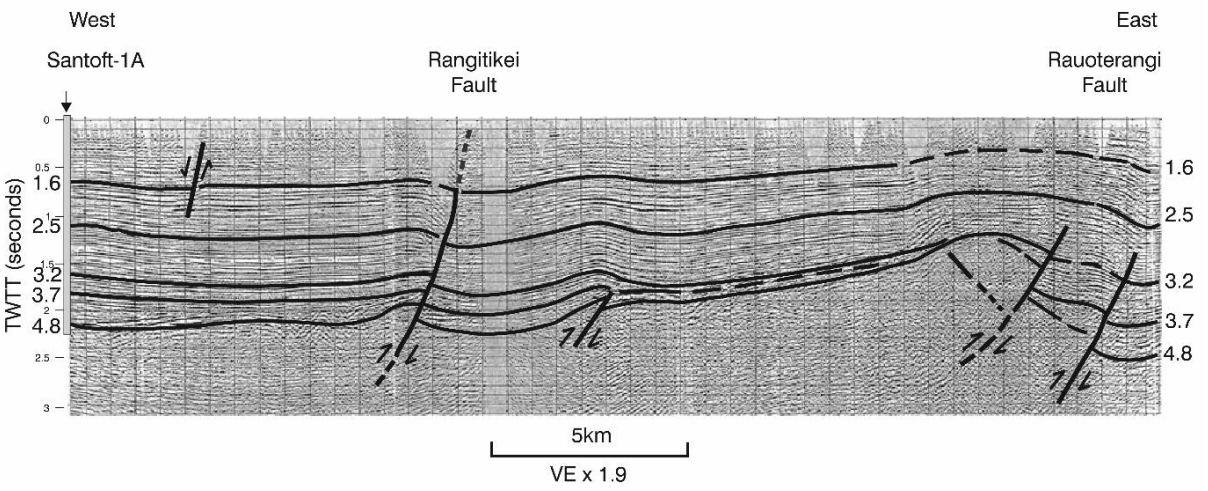


Figure 3.11: Interpreted six fold migrated seismic line BL-12. Horizons were correlated from biostratigraphy in Sandtoft-1A well (Nicol & Beavan 2003). Note the steeply dipping Rangitikei and Rauoterangi reverse faults downthrown to the east.

Similar to the other folds in the Manawatu, the Marton Anticline is characterised by a long, parallel stream system on its western flank, approximately perpendicular to the fold axis (Jackson et al. 1998), and steep short stream system on its eastern flank flowing obliquely to the fold axis. A radial drainage pattern is preserved at the southern end just north of Bulls.

The Mt Stewart-Halcombe Anticline is situated 5km north of Mt Stewart, with its northern end occurring in the southeastern portion of the present study area. The anticline is characterised by a strikingly sigmoidal shape, defined by the drainage divide running along its axis (Melhuish et al. 1996; Jackson et al. 1998). With the valley systems and streams comprising a typical consequent drainage pattern. Rangitawa Stream cuts through its northern end exposing Mangatapu Formation dipping gently at 3-5 ° NE to NW off the anticlinal dome.

Mangaone Anticline was mapped by Feldmeyer et al. (1943) for c. 13 km from Mataroa trig, NW of Taihape to Tauporae trig in the northern portion of the present study area on Te Kumu Station. Here we trace this southward plunging anticline a further 19 km toward Aldworth Road, 3 km NW of Hunterville. This

fold forms the western ridge of the Pourewa Stream Valley separating Rangitikei and Paparangi Group rocks dipping 10-5° SE on its eastern limb from equivalent strata dipping 10-5° SWW into a downwarp occupied by the Turakina River. This downwarp within the Plio-Pleistocene sediments together with differing sedimentary provenance of the contributing headwater catchments is suggested here to be the reason for the Turakina River sitting on average c. 130 m lower in the landscape when compared to the Rangitikei at the same latitude.

Faults

Superior Oil Company geologists first mapped the Galpin Fault (Synonymy: Ngaruru Fault, North Marton Fault) west of Marton, documenting a high angle normal fault downthrown 30 m to the east (Feldmeyer et al. 1943). This initial observation was supported by the works of Fleming (1953) and Milne (1973) who both recorded 30 m offsets on the Galpin Fault near the Galpin trig station, 9 km north of Marton township. Furthermore, seismic conducted by Anderton (1981) supports this sense of throw.

Pillans (1990) investigated Quaternary fault displacement across the WB including the Leedstown and Galpin faults, documenting a 15 m vertical offset across the Ararata marine terrace where it is intersected by the Galpin Fault. Hellstrom (1993) investigated the timing and nature of movements on the Galpin Fault, noting an offset across the Brunswick Terrace of 20 m and a larger offset of 30 m across a pre-Aldworth (340-350 ka) surface near the Marton reservoirs. We follow the detailed mapping of Hellstrom (1993) in the present study and refer readers to his thesis for a more detailed account of the Galpin Fault. The Galpin and Leedstown faults occur on the west and east flanks, respectively of the Marton Anticline (Fleming 1953; Milne 1973a). A vertical displacement of 10 m was noted by Milne (1973a) where the Leedstown Fault crosses the Marton river terrace.

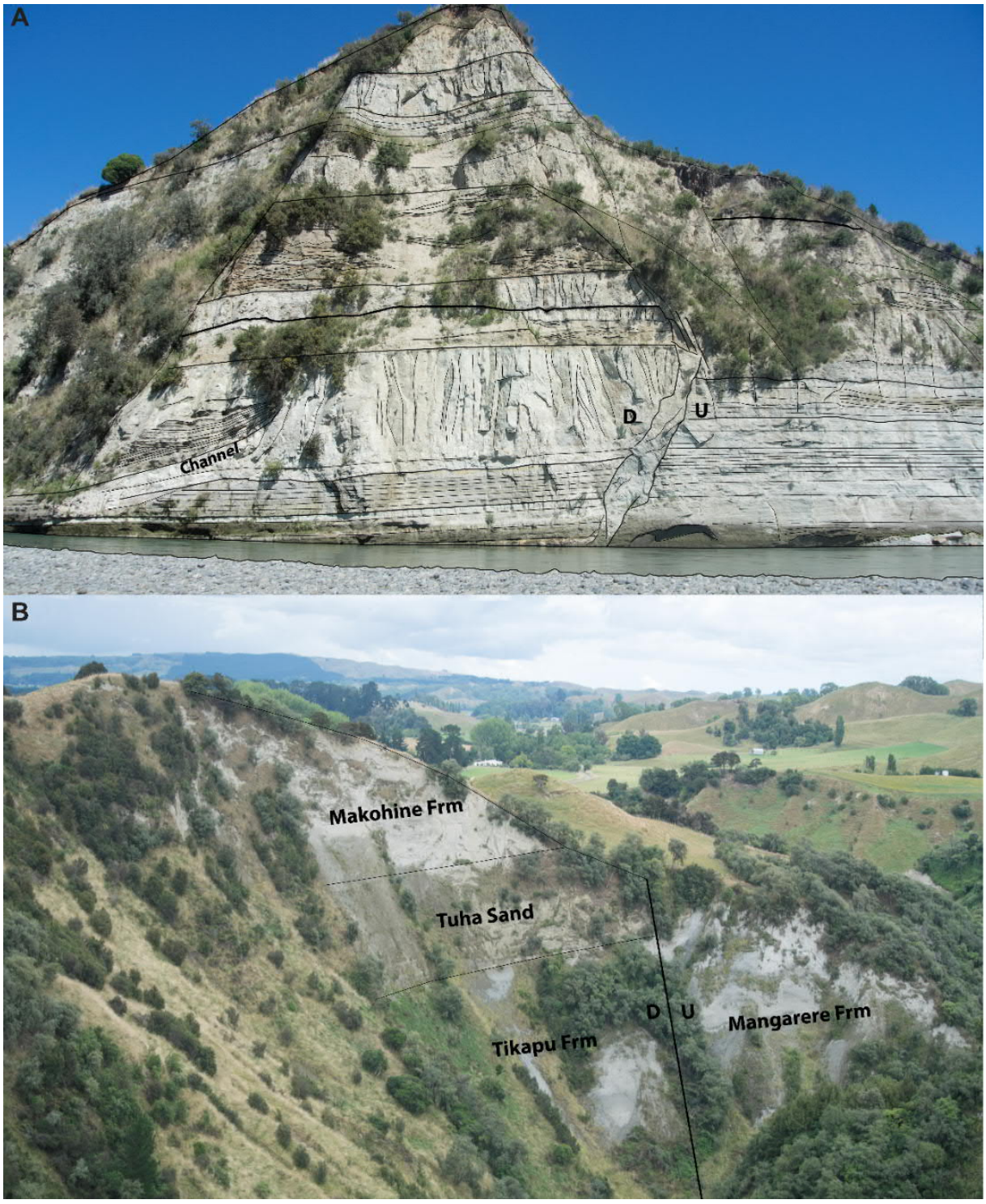


Figure 3.12: A: Normal displacement of Makirkiri Tuff Formation along the Nukumaru Fault Zone, near the confluence of Mangatutu Stream and the Rangitikei River (NZGD2000 -39.978337 S, 175.62242 E). B: Reverse displacement of Rangitikei Group sediments along the Rangitikei Fault exposed in the Makohine Stream Valley near Ohingaiti (NZGD -39.861263 S, 175.686364 E).

The trace of the Leedstown Fault is unusual compared to other faults in the region due to having a near continuous scarp for several kilometers. Milne (1973) suggests the linear nature of the scarp and the presence of the same loess sequence mantling treads on either side rules out the potential of it simply being a terrace riser. In this study we have followed Milnes (1973) mapping of the Leedstown Fault with no amendments.

Milne (1973a) also mapped the Rangitira and Putorino faults as splinter faults of the Leedstown Fault, downthrown to the east and trending approximately SW-NE across the Marton Terrace tread east of Marton. Milne (1973) noted poorly defined parallel scarps both approximately 5 m high on the Marton Terrace and an unusually linear valley cut north of Rangitira Road attributed to offset across the Rangitira Fault. Here we note a fracture zone exposed within the Pourewa Stream Valley across which the bedding attitude of Reu Reu Formation siltstone changes markedly. We map this linear fracture zone as the Rangitira Fault noting a marked change in the physiography of Pourewa Stream, which flows in an elevated position in the landscape along this fault zone for some 4.5 km from Rata SW to the junction with Leedstown Valley. Eventually crossing over onto the downthrown block of the fault at which point the stream rapidly incises into its valley, cutting down to join the Rangitikei River at Onepuhi. Another fracture zone in line with the Rangitira Fault is noted here on Rathmoy Station east of Hunterville where small offsets of less than 1 m occur within Makirikiri Tuff Member. No evidence is found in the present study for the Putorino Fault where it crosses the Pourewa Valley despite the presence of good outcrop; therefore, we have omitted this fault from our map compilation.

Naish and Kamp (1995) defined the Rangitikei Fault previously mapped by authors as the Hunterville (Feldmeyer et al. 1943) and Pourewa (Te Punga (1952) Fault as a high angle westward dipping reverse fault, downthrown to the east (Fig. 3.11). Two exposures have been documented, the first by Feldmeyer et al. (1943)

describes a section at Vinegar Hill north of Hunterville township where a maximum displacement of 180 m is recorded, downthrown to the east. The second by Naish and Kamp (1995) documents a scarp east of Hunterville where it displaces the Vinegar Hill Tephra with a calculated throw of 100 m. Here we provide an additional outcrop at the confluence of Makohine Stream Valley (NZTM2000 182°97'97" E, 55°84'21" S) where the Rangitikei Fault displaces Mangarere Formation adjacent to Tuha Sand, Makohine Formation (Fig. 3.12). The fault plane itself, dipping c. 80°W is poorly exposed in this section due to the unstable nature of the Makohine Stream Valley, however, clear stratigraphic offset is visible. Cross sections drawn through this area provide an estimated throw of c. 70 m.

Feldmeyer et al. (1943) were the first to recognise a series of small relatively small en-echelon faults occurring within a 1.5 km wide zone exposed in the cliffs of the Rangitikei River. Naish and Kamp (1995) mapped the zone as the Pakihikura fault zone, describing the complex of high angle reverse and normal faults which extend from Vinegar Hill to Mangaonoho. Recording throws of between 10 to 30 m on major faults of this zone, all faults being downthown to the east and suggesting the zone may be related to minor dextral strike slip movement along the Rangitikei Fault (Naish & Kamp 1995). In the present study we map the zone a further 6 km south from Vinegar Hill to Rata where multiple high angle normal faults downthrown to the east are observed in the cliffs of the Rangitikei River (Fig. 3.12). The attitude of beds within Makirikiri Tuff Formation change across the southern portion of the Pakihikura Fault Zone with strikes rotating from SW on the upthown side to SEE on the downthrown side of the zone and dips locally increasing up to 12°. This change in attitude is attributed to drag associated with subordinate dextral movement along the complex of en-echlon faults.

Feldmeyer et al. (1943) mapped the Omatane fault for 60 km from Otuareiawa Stream 12 km east of Taihape southward to where it terminates in Castlecliffian

sediments 8 km north of Beaconsfield. Anderton (1981) later introduced the name Rauoterangi for this fault mapping it from seismic surveys in the WB. The Rauoterangi Fault was mapped onshore by Naish and Kamp (1995) and Journeaux et al. (1996) east of Ohingaiti to the Kawhatau River where it offsets strata of the lower Rangitikei and Paparangi groups. Naish and Kamp (1995) describe the Rauoterangi Fault at an exposure on Mangarere Road, where it is characterised by a high angle reverse sense with a throw of c. 200 m, upthrown to the west. Here we find no new evidence of faulting in the study area, adopting the work of Naish and Kamp (1995) and Journeaux et al. (1996) and interpret the Rauoterangi Fault as becoming obscured by overlying Castlecliffian sediments south of the known exposures.

Seismic reflection profiles taken across areas of the WB (Fig. 3.11) clearly display westward dipping reverse faults (Rangitikei and Rauoterangi faults) downthrown to the east (Nicol & Beavan 2003), supporting the interpretation of Naish and Kamp (1995) and Journeaux et al. (1996). It is noted that correlating faults mapped onshore with those identified through offshore seismic (Anderton 1981; Nicol & Beavan 2003; Lamarche et al. 2005) is difficult due to paucity of outcrop and widespread slumping within the Rangitikei Hill country, combined with faults that don't propagate to the surface or display mappable surface expression in the landscape.

3.8 Discussion

3D model

A preliminary 3D geological model of the central Rangitikei District was developed during the present study from borehole data provided by Horizons Regional Council and field data taken during the course of mapping (2016 – 2018). The

model displays a 3D representation of the 1:25 000 geological map and interpreted sub-surface geology illustrated on accompanying cross sections. Two main difficulties were encountered during model development. The first involved interpreting lithological information from driller logs taken during water borehole installation. This issue arises from inconsistencies in boreholes logs by different driller operators, logs that require interpretation to link the recorded descriptions to known lithological units. The second problem involved incorporating the correct amount of structural deformation to make the model reflect patterns observed in the field, while not creating unrealistic geometries as a result of the inherent limitations of modelling. This issue arises primarily due to the necessity within the modelling environment for faults to terminate either against one another or against the model boundary rather than abruptly ending in 3D space, a phenomenon that unfortunately occurs frequently on geological maps. Ways of minimizing this issue included leaving minor faults out of the model and in some cases extending faults for a short distance in order to have them terminate against one another.

The modelling process, including the construction of cross sections that provide a component of the input data, proved useful in a variety of ways. Modelling helped with the conceptualisation of changes in throw along the complex of en echlon, wrench type structures present in the study area (Firth & Feldmeyer 1943; Naish & Kamp 1995). The amount of throw along the fault is able to change along the length of the structure within the modelling software to in order to conform to the input point data set. The model also enables visualisation of lateral changes in formation thickness from east to west. This is especially useful for the Rangitikei Group sediments deposited during a time when the sedimentary depocentre was located near Turakina resulting in a locally thick and fine-grained succession. The software's ability to rapidly trial inclusion or exclusion of different data sets, test relationships between units and structures and change the attitude of various

elements within the geological model is a useful way to explore and develop ideas formed in the field.

Paleogeographic interpretation

The Plio-Pleistocene sediments of central Rangitikei District record a portion of the geological history of the eastern WB over the last 3 Ma. Paparangi Group strata, the oldest rocks in the mapping area, were deposited in outer shelf depths of 150-200 m (Journeaux et al. 1996). The basin during this time was undergoing active subsidence with sediments being derived from North Island Mesozoic Torlesse Terrane and South Island schist and granitoid terranes (Gillespie & Nelson 1996; Mortimer et al. 1997). During deposition of the Mangaweka Mudstone Formation the basin depocentre was located between the Mangawhero and Turakina Rivers (Anderton 1981; Townsend et al. 2008) where thick fine grained sediments were deposited; sediments becoming thinner and coarser grained toward the basin margins (Feldmeyer et al. 1943; Fleming 1953). Feldmeyer et al. (1943) mapped locally developed conglomeratic shell-limestones within Mangaweka Mudstone Formation to the east, suggesting a shallow shoreline existed along the foot of the present day main axial range. Similarly, Fleming (1953) suggests a fluctuating shoreline existed to the west of the depocentre where Paparangi Sandstone and its basal shell conglomerate member was deposited in the Waitotara area.

The Rangitikei Group marks a substantial change within the succession correlated to the first of the major northern hemisphere continental glaciations during MIS 100 at c. 2.52 Ma (Naish & Kamp 1995; Naish et al. 1996; Naish et al. 1997). Hautawa Shellbed marks the first occurence of cold water species *Zygochlamys delicatula* and *Jacquinotia edwardsii*, last occurrence of *Phialopecten triphooki, Crassostrea ignens*, planktic foraminfera *Truncorotalia crassula* and the top of the upper dextral coiling zone of *Truncorotalia oceanica* within WB strata (Fleming

1953; Beu et al. 1981; Raine et al. 2015). The appearance of *Zygochlamys delicatula* represents the earliest faunal evidence of climatic cooling in New Zealand's Plio-Pleistocene marine sequences (Fleming 1953; Naish et al. 1998).

Rangitikei Group sediments are composed of alternating sandstone units deposited within inner most shelf to shoreface depositional environments and massive siltstone units deposited within mid shelf environments. Shell bed members represent stratigraphically condensed beds whereby locally areas on the sea floor are enriched in carbonate material through a combination of terrigenous sediment bypass or sorting and winnowing away of fine material by current action. Naish and Kamp (1995) recognise 20 cylothems within Rangitikei Group between Te Rimu Sand and Vinegar Hill Tephra (1.75 Ma), attributing the cycles to glacio-eustatic sea level changes during Quaternary glaciations.

During this phase, the basin depocentre shifted eastward toward Rangitikei as evidenced by the thickness and distribution of siltstone within the Rangitikei section relative to other sections in the WB. Pebbles observed within the Ohingaiti Sandstone to the west where it interfingers with the lower Nukumaru Limestone are larger than any observed within older deposits (Fleming 1953). Feldmeyer et al. (1943) mapped increasingly coarser beds toward the Ruahine Range including conglomeratic limestone members. Early Nukumaruan sediments preserved on the Manawatu Saddle comprise 80+ m of conglomerate beds displaying fan delta structure (Rees et al. 2017a). These deposits suggest uplift accelerated in Early Nukumaruan time leading to higher relief on either side of the basin and supplying coarse grained sediments to basins margins. This uplift is likely to have had a corresponding effect on the migration of the depocentre and conversely the locus of subsidence and available accommodation space in the Turakina–Rangitikei area, reflected in the increasing proportion of siltstone within the cyclothems described by Naish and Kamp (1995).

The sediments of the upper Rangitikei Group become progressively thinner and coarser grained up section, demonstrating a general shallowing of depositional environments within the area, likely a response to ongoing migration of the basin depocentre driven by uplift along the basin's northern and eastern margins. This shallowing pattern is mirrored in the Whanganui section albeit beginning slightly earlier, so that by the time the Maxwell Group was deposited around c. 1.75 Ma (Vinegar Hill Tephra) shallow water, intertidal mud flat and estuarine environments prevailed in the Whanganui area (Fleming 1953). Progradation, perhaps in part due to increased sedimentary supply from the actively uplifting basin margins, forced a temporary basinward retreat of the coastline allowing the non-marine beds of Maxwell Group to be preserved.

Maxwell Group sediments are pinch and swell across the WB, with a greater amount of preservation occurring in the east where tephras and pumiceous alluvium lying between Ototoka Tephra (1.64 Ma) and Pakihikura Pumice (1.58) are preserved within a 100m+ sequence of alternating carbonaceous siltstone with occasional thin lignite bands and common *Austrovenus stutchburyi*. At the coastal type section, Butlers Shell Conglomerate, Okehu Group unconformably overlies sediments containing Ototoka Tephra (1.64 Ma). Cyclothem sequences 22 to 30, representing c. 450 ka are missing from the section (Pillans et al. 2005). We interpret this unconformity as representing aerial exposure of the far western portion of the WB to active erosion whilst an extensive coastal plain extending eastward toward the emerging paleo-axial ranges facilitated preservation of tephric rich carbonaceous silts within nearshore-estuarine and floodplain environments, similar to the Kairanga Plains today.

Makirikiri Tuff Formation signals the initiation of renewed silicic arc volcanism in central North Island, contributing large quantities of primary airfall and secondary volcaniclastic material into Whanganui and other New Zealand sedimentary basins. Fluvial systems draining the central North Island built large

fluvio-deltaic plains from Whanganui to the emerging paleo-axial range, evidenced by mapping of Makirikiri Tuff Formation by Feldmeyer et al. (1943) (Basal Castlecliffian Ash), Fleming (1953), Seward (1976) and this study across the WB. Commonly thin shell beds containing stunted *Austrovenus stutchburyi* (Fig. 3.8) are found within the tephric rich silts, interpreted as showing some marine incursions. The shells are interpreted to be stunted due to high sedimentation rates as fluvial systems were choked with volcaniclastic debris (Te Punga 1952). The extensive coastal plain during this time was host to backwater swamps and active flood plains where organic matter and airfall tephra preservation ensued as demonstrated by the characteristic thin lignite beds and carbonaceous silts enclosing tephra horizons within Makirikiri Tuff Formation (Shane 1993; Pillans et al. 2005). West of Whanganui a local high formed the western boundary of the coastal plain whilst to the east the newly emerging hinterland of the paleo-axial ranges formed the eastern boundary (Rees et al. 2017b). We suggest here that the increased rate of sediment supply during deposition of the Makirikiri Tuff Formation (starting c. 1.58 Ma) forced progradation of the coastline resulting in a delayed return to marine conditions in eastern WB until well after deposition of Mangapipi Tephra (1.54 Ma).

The deposition of the Butlers Shell Conglomerate, Okehu Group at the Whanganui coastal section signals a return to shallow marine conditions following deposition of the underlying mainly non-marine Maxwell Group. The Butlers Shell Conglomerate broadly correlates to sediments 50 – 100 m below the Potaka Pumice and Deepdem Conglomerate in the Rangitikei and Turakina sections respectively, based on the interpreted position of the Jaramillo Subchron (Turner & Kamp 1990; Pillans et al. 2005; Turner et al. 2005). A change to marine conditions is seen earlier in the Rangitikei and Turakina sections where sediments above the Mangapipi Tephra (1.54 Ma), upper Makirikiri Tuff Formation including the Mangapipi and Mangara shell conglomerates display shallow marine characteristics. This equivalent period of time is absent from the Whanganui

coastal section, where the sediments have not been preserved either due to non-deposition or erosion. Fleming (1953) notes faults in the coastal section which together with the slight 1° angular unconformity at the base of the Butlers Shell Conglomerate provides support for tectonic movement in the area after deposition of Maxwell Group. This movement could have resulted in subaerial erosion and cannibalism of sediments on a near shore coastal platform, resulting in the mix of fauna observed by Fleming (1953) in the Butlers Shell Conglomerate including species presumed transported far from their original environments and/or derived from underlying rocks.

Kaimatira Pumice Sand Formation marks a renewed influx of volcaniclastic sediment into the WB at c. 0.99 Ma. This influx is correlated to the Whanganui cyclothem cycle 34, MIS 27 (Pillans et al. 2005) during which time it generated high sediment supply rates able to keep pace with the rising sea level leading to deposition of a particularly thick transgressive systems tract. Changing facies within Kaimatira Pumice Sand Formation east-west across the basin (Lewis 2007) demonstrate higher rates of subsidence were occurring within the eastern WB at this time (Abbott 1994) where an extensive fluvio-deltaic plain built out into the shallow marine environments of the basin derived from paleo-river systems draining the central north island. This change in the basins depositional regime is associated with continued southward migration of the depocentre, which at 1 Ma was approximately located offshore from Tangimoana (Anderton 1981).

Potaka Pumice thickens substantially toward the Oroua River where in Kiwitea Stream it consists of ca 8+ m of pure vitric coarse pumiceous alluvium. Fluvial conglomerates also become more frequent, thicker and appear earlier in the succession toward Kiwitea Stream. Convolute layers typically associated with sediment loading due to rapid deposition (Abbott 1994; Lewis 2007) have been found directly overlying small faults and sand dykes displaying structures typical of liquefaction following large earthquakes within a saturated fluvio-deltaic plain

setting. We interpret that renewed volcanic activity at c. 0.99 Ma was associated with renewed tectonic activity within the eastern WB manifested as rupture on the Rangitikei and Rauoterangi faults, resulting in widespread liquefaction following earthquake events on the coastal plain. Simultaneous uplift on the North Island Dextral Fault Belt resulted in greater relief within the paleo-fluvial headwaters draining the emerging axial range, supplying fresh greywacke detritus in climatically driven pulses to the eastern fluvial-deltaic wedge of the WB.

Typically, eustatic sea level cycles over the last 1 Ma are characterised by a marked asymmetry, including a rapid sea level rise from low stand and a corresponding slow regression as sea level returns to a glacial low stand (Williams et al. 1988). This asymmetry results in transgressive systems tracts (TST) in Kai Iwi Group averaging 3.5 m and high stand systems tracts (HST) averaging 10.8 m at the coastal Whanganui section (Abbott 1994). Conversely, in the Rangitikei section, subsidence rates up to three times greater than those farther west resulted in an average TST of 29.3 m and an average HST of 20.1m (Abbott 1994). We interpret increased sedimentation rates to the east of the Rangitikei area based on thickness of the strata and proximity to actively uplifting basement. The increased sedimentation in the far eastern WB is due to periodic pulses of greywacke-argillite detritus from the emerging axial range and deposition of volcaniclastic sediment following eruptions on the volcanic plateau. These inputs mask the effects of eustatic sea level rise as sedimentation keeps pace or exceeds accommodation space. This has lead to difficulties in identifying systems tracts in the east (Brackley 1999; Rees et al. 2018)

During deposition of Shakespeare Group uplift along the northern margins of the WB and along the eastern front of the main axial range continued, leading to a general shallowing of the basin (Fleming 1953; Bussell 1984). Andesite first appears in the middle of the Shakespeare Group within Ruamahanga Conglomerate and is common in the Kakariki Conglomerate, indicating andesitic

lava from the Tongariro Volcanic Centre became a source of sediment at this time (Te Punga 1952). An extensive apron of gravel (Waituna) extended from the Ruahine Range west to the Rangitikei Valley, now found capping the interfluves between major valleys. Time control is provided by Rangitawa Tephra (340 ka) within Aldworth loess overlying the Waituna gravels. Fluvial systems draining the Ruahine and Kaimanawa Ranges were systematically captured and forced south along the trend of basement highs forming the crests of growing anticlines across the coastal plain.

The Manawatu River maintained its antecedent pathway across the uplifting main axial range, becoming confined and forced to deposit a majority of its load on the eastern side of the present day Manawatu gorge, leading to Late Quaternary infilling of the lacustrine to alluvial plain upper Pahiatua and Dannevirke basins. The paleo-Oroua River began to erode extensive quantities of greywacke-argillite from the western paleo-axial range, mirroring the eastern headwaters of the paleo-Manawatu River. The paleo-Oroua acted as the dominant source of sediment to the western Manawatu River catchment, delivering a vast majority of the sediment comprising the Late Quaternary fill of the Kairanga Plains. This is due to the 'bottle neck' at the Manawatu Gorge that has allowed a single fluvial system to infill two structurally separate Late Quaternary basins on either side of the main axial range.

3.9 Conclusion

The geology of the Central Rangitikei District has been documented here through the compilation of existing literature, additional fieldwork and application of digital mapping techniques. We present a revised stratigraphic nomenclature, drawing from work introduced by authors over the last 75 years to create a specific framework for the Rangitikei section whilst keeping overarching group names tied

to their stratotype sections. Useful marker horizons are recognised and used as formation boundaries due to their visibility in the landscape.

A 1:25 000 geological map comprising 4 sheets is presented with accompanying structural interpretation, based on the collation of existing work, including onshore and offshore seismic data and surface data gathered in the field. We include a preliminary 3D geological model portraying the interpreted subsurface geology, facilitating consolidation and development of ideas around the study areas geology and history.

The Rangitikei Valley contains an important cross section through eastern WB recording the interplay between sedimentation rate, tectonics and glacio-eustatic fluctuations. Rangitikei Group marks the onset of the major continental glaciations (c. 2.52 Ma). The first occurence of cold-water species *Zygochlamys delicatula* at ca. 2.4 Ma represents the earliest faunal evidence of climatic cooling in New Zealand's Plio-Pleistocene marine sequences.

Early Nukumaruan sediments preserved on the basin margins suggest onset of uplift in Early Nukumaruan time leading to higher relief on either side of the basin and supplying coarse-grained sediments. This phase of uplift likely had a corresponding effect on the migration of the depocentre and conversely the locus of subsidence and available accommodation space in the Turakina–Rangitikei area.

A greater rate of preservation occurred in the eastern WB during deposition of Maxwell and Okehu Groups due to aerial exposure and erosion of the far western portion of the WB, while extensive coastal plains developed extending eastward toward the emerging paleo-axial ranges.

Makirikiri Tuff Formation signals the initiation of renewed silicic arc volcanism in central North Island, contributing large quantities of volcanic material to WB.

Fluvial systems draining the central North Island built large fluvio-deltaic plains from Whanganui to the emerging paleo-axial range.

The deposition of Potaka Pumice c. 0.99 Ma coincided with renewed tectonic activity in the eastern WB. Rupture on the Rangitikei and Rauoterangi faults, resulted in widespread liquefaction following earthquake events on the coastal plain. Simultaneous uplift on the North Island Dextral Fault Belt resulted in greater relief within the paleo-fluvial headwaters draining the emerging axial range, suppling fresh greywacke-argillite detritus in tectonically and/or climatically driven pulses to the eastern fluvial-deltaic wedge of the WB.

During deposition of Shakespeare Group Tongariro Volcanic Centre became an active source of sediment. An extensive apron of gravel extended from the Ruahine Range west to the Rangitikei Valley. Fluvial systems draining the Ruahine and Kaimanawa Ranges were systematically captured and forced south along the trend of basement highs forming the crests of growing anticlines across the coastal plain. Uplift of the main axial range resulted in a sedimentary 'bottle neck' at present day Manawatu Gorge resulting in simultaneous fluvial infilling of two related yet structurally isolated Late Quaternary fills by a single and unique fluvial system crossing the North Islands' main divide.

Acknowledgments

We thank the residents in the Central Rangitikei District for granting land access. This work was financially supported by a Massey University Doctorate Scholarship, Horizons Regional Council Don Linklater Bursary Research Grant, Helen E Akers PhD Scholarship and C V Fife Memorial Scholarship from the Institute of Agriculture and Environment, Massey University.

This paper uses the spelling 'Whanganui' rather than 'Wanganui' as recommended by the New Zealand Geographic Board (Ngā Pou Taunaha o Aotearoa). The spelling of 'Pourewa Stream' rather than 'Porewa Stream' is used as recommended by Ngāti Hauiti.

References

Abbott ST 1994. Sequence Stratigraphy, Sedimentology and Paleoecology of Pleistocene Cyclothems in the Castlecliff Section, Wanganui Basin, New Zealand, Unpublished PhD Thesis. James Cook University of Northern Queensland, Australia. 297 p.

Abbott ST 1997. Foraminiferal Paleobathymetry and Mid-Cycle Architecture of Mid-Pleistocene Depositional Sequences, Wanganui Basin, New Zealand. Palaios 12(3): 267-281.

Abbott ST, Carter RM 1997. Macrofossil Associations from Mid-Pleistocene Cyclothems, Castlecliff Section, New Zealand: Implications for Sequence Stratigraphy. Palaios 12(2): 188-210.

Alloway BV, Pillans BJ, Sandhu AS, Westgate JA 1993. Revision of the marine chronology of the Wanganui Basin, New Zealand, based on the isothermal plateau fission-track dating of tephra horizons. Sedimentary Geology 82(1-4): 299-310.

Alloway BV, Pillans BJ, Carter L, Naish TR, Westgate JA 2005. Onshore-offshore correlation of Pleistocene rhyolitic eruptions from New Zealand: Implications for TVZ eruptive history and paleoenvironmental construction. Quaternary Science Reviews 24(14-15): 1601-1622.

Anderton PW 1981. Structure and evolution of the South Wanganui Basin, New Zealand. New Zealand Journal of Geology and Geophysics 24(1): 39-63.

Barnett R 1984. Upper Quaternary stratigraphy in the Otaki district, Unpublished BSc (Hons) Thesis. Victoria University of Wellington, Wellington, New Zealand. 112 p.

Begg JG, Palmer A, Gyopari M 2005. Geological synopsis of the Manawatu-Horowhenua area for a review of the region's hydrogeology. Institue of Geological and Nucelar Sciences Client Report 2005/172, Lower Hutt, New Zealand. 22 p.

Beu AG 1978. Taxonomy and biostratigraphy of large New Zealand Pliocene Pectinidae (Phialopecten and Mesopeplum). New Zealand Journal of Geology and Geophysics 21(2): 243-269.

Beu AG 1995. Pliocene limestones and their scallops. Lithostratigraphy, pectinid biostratigraphy and paleogeography of eastern North Island late Neogene limestone. Institute of Geological and Nuclear Sciences Monograph 10(68): 1-243.

Beu AG 2012. Marine Mollusca of the last 2 million years in New Zealand . Part 5 . Summary. Journal of the Royal Society of New Zealand 42(1): 1-47.

Beu AG, Edwards AR 1984. New Zealand Pleistocene and Late Pliocene Glacio-Eustatic Cycles. Paleogeography, Palaeoclimatology, Palaeoecology 46: 119-142.

Beu AG, Browne GH, Grant-Taylor TL 1981. New *Chlamys delicatula* localities in the central North Island and uplift of the Ruahine Range. New Zealand Journal of Geology and Geophysics 24(1): 127-132.

Beu AG, Edwards AR, Pillans BJ 1987. A review of New Zealand Pleistocene stratigraphy , with emphasis on the marine rocks. In: Itihara M, Kamei T ed. Proceedings of the First International Colloquium on Quaternary Stratigraphy of Asia and the Pacific Areas, Science Council of Japan, Osaka, Japan. Pp. 250-269.

Boellstorff JD, Te Punga MT 1977. Fission track age and correlation of middle and lower Pleistocene sequences from Nebraska and New Zealand. New Zealand Journal of Geology and Geophysics 20: 47-58.

Brackley H 1999. The Stratigraphy and Environments of Deposition of Early-Mid Pleistocene Sediments of the Pohangina Region, Eastern Wanganui Basin, New Zealand., Unpublished MSc thesis, Massey University, Palmerston North, New Zealand. 113 p.

Bussell MR 1984. Geology and Paleobotany of the Rangitawa Stream area, Southeast Wanganui Basin, Unpublished BSc (Hons) Thesis. Victoria University of Wellington, Wellington, New Zealand. 181 p.

Bussell MR 1986. Palynological evidence for upper Putikian (middle Pleistocene) interglacial and glacial climates at Rangitawa Stream , South Wanganui Basin , New Zealand. New Zealand Journal of Geology & Geophysics 4(29): 471-479.

Bussell MR 1988. Mid and late Holocene pollen diagrams and Polynesian deforestation , Wanganui district , New Zealand Mid and late Holocene pollen diagrams and Polynesian deforestation , Wanganui district , New Zealand. New Zealand Journal of Botany 26(3): 431-451.

Bussell MR 1990. Palynology of Oxygen Isotope Stage 6 and Substage 5e from the Cover Beds of a Marine Terrace, Taranaki, New Zealand. Quaternary Research 34(1): 86-100.

Carter RM, Naish TR 1998. A review of Wanganui Basin, New Zealand: Global reference section for shallow marine, Plio-Pleistocene (2.5-0 Ma) cyclostratigraphy. Sedimentary Geology 122(1-4): 37-52.

Carter RM, Abbott ST, Naish TR 2014. Plio-Pleistocene cyclothems from Wanganui Basin , New Zealand : type locality for an astrochronologic time-Scale , or template for recognizing ancient glacio-eustasy. Philosophical Transactions of the Royal Society of London 357(1757): 1861-1872.

Feldmeyer AE, Jones BC, Firth CW, Knight J 1943. The geology of the Palmerston-Wanganui Basin, "West side", North Island, New Zealand. Unpublished Report of the Superior Oil Company of New Zealand, Petroleum Report Series 171, Ministry of Economic Development, Wellington, New Zealand. 46 p.

Firth GH, Feldmeyer AE 1943. The geology of the Pahiatua-Dannevirke Basin "East Side" North Island. Unpublished Petroleum Report 166, The Superior Oil Company of New Zealand, Ministry of Economic Development, Wellington, New Zealand. 250 p.

Fleming CA 1947. Standard sections and subdivisions of the Castlecliffian and Nukumaruan Stages in the New Zealand Pliocene. Transactions of the Royal Society of New Zealand. 76: 300-326.

Fleming CA 1953. The geology of Wanganui subdivision. New Zealand Geological Survey Bulletin 52. Wellington, New Zealand. 362 p.

Fleming CA 1975. The Quaternary record of New Zealand and Australia. The Royal Society of New Zealand Bulletin 13: 1-20.

Gibbard PL, Head MJ, Walker CJ 2007. Formal ratification of the Quaternary System/Period and the Pleistocene Series/Epoch with a base at 2.58 Ma. Journal of Quaternary Science 22(8): 801-815.

Hansen RJ, Kamp PJJ 2006. An integrated biostratigraphy and seismic stratigraphy for the late Neogene continental margin succession in northern Taranaki Basin, New Zealand. New Zealand Journal of Geology and Geophysics 49(1): 39-56.

Jackli R 1957. Review of the Superior Oil Company report on the Rangitikei area. Shell, D'Arcy and Todd Oil Serivces Geological Report 7. Unpublished, held as open-file petroleum report 410 by the Institute of Geological and Nucelar Sciences, Lower Hutt, New Zealand. 43 p.

Jackson J, van Dissen R, Berryman KR 1998. Tilting of active folds and faults in the Manawatu region, New Zealand: Evidence from surface drainage patterns. New Zealand Journal of Geology and Geophysics 41(4): 377-385.

Johnson KG, Curry GB 2001. Regional biotic turnover dynamics in the Plio-Pleistocene molluscan fauna of the Wanganui Basin, New Zealand. Palaeogeography, Palaeoclimatology, Palaeoecology 172(1): 39-51.

Journeaux TD 1995. Lithostratigraphy, foraminiferal paleoecology and sequence stratigraphy of middle Pliocene strata, Wanganui Basin. Unpublished MSc Thesis, The University of Waikato, Hamilton, New Zealand. 130 p.

Journeaux TD, Kamp PJJ, Naish TR 1996. Middle Pliocene cyclothems , Mangaweka region , Wanganui Basin , New Zealand : A lithostratigraphic framework. New Zealand Journal of Geology and Geophysics 39(1): 135-149.

Kamp PJJ, Vonk A, Bland K, Griffin A 2002. Megasequence architecture of Taranaki, Wanganui, and King Country basins and Neogene progradation of two continental margin wedges across western New Zealand. New Zealand Petroleum Conference Proceedings 2002, Auckland, New Zealand. Pp. 464-481.

Kohn BP, Pillans B, McGlone MS 1992. Zircon fission track age for middle Pleistocene Rangitawa Tephra, New Zealand: Stratigraphic and paleoclimatic significance. Palaeogeography, Palaeoclimatology, Palaeoecology 95: 73-94.

Lamarche G, Proust JN, Nodder SD 2005. Long-term slip rates and fault interactions under low contractional strain, Wanganui Basin, New Zealand. Tectonics 24(4): 1-30.

Lensen GJ 1977. Late Quaternary Tectonic Map of New Zealand 1 : 2 ,000,000. New Zealand Geological Survey Miscellaneous Series Map 12, Lower Hutt, New Zealand: 1 sheet.

Lowe DJ, Alloway BV, Shane PAR 2015. Far-flown markers. In: Graham IJ ed. 2nd ed, Geoscience Society of New Zealand in association with GNS Science, Wellington, New Zealand. 172-175.

Marden M, Neall VE 1990. Dated Ohakean terraces offset by the Wellington Fault , near Woodville , New Zealand. New Zealand Journal of Geology and Geophysics 33(3): 449-453.

Melhuish A, van Dissen R, Berryman KR 1996. Mount Stewart-Halcombe Anticline: A look inside a growing fold in the Manawatu region, New Zealand. New Zealand Journal of Geology and Geophysics 39: 123-133.

Milne JDG 1973a. Upper Quaternary geology of the Rangitikei drainage basin, North Island, New Zealand. Unpublished PhD Thesis. Victoria University of Wellington, Wellington, New Zealand. 472 p.

Milne JDG 1973b. Map and sections of river terraces in the Rangitikei Basin, North Island, New Zealand. New Zealand Soil Survey Report 4, Wellington, New Zealand: 3 sheets+10p.

Milne JDG 1973c. Mount Curl Tephra , a 230000-year-old implications for quaternary chronology marker bed in New Zealand, and its implications for Quaternary Chronology. New Zealand Journal of Geology and Geophysics 16(3): 519-532.

Naish TR, Kamp PJJ 1995. Pliocene-Pleistocene marine cyclothems , Wanganui Basin , New Zealand : a lithostratigraphic framework. New Zealand Journal of Geology and Geophysics 38: 223-243.

Naish TR, Kamp PJJ 1996. Foraminiferal depth palaeoecology of Late Pliocene shelf sequences and systems tracts , Wanganui Basin , New Zealand. Sedimentary Geology(110): 237-255.

Naish TR, Kamp PJJ, Alloway BV, Pillans BJ, Wilson GS, Westgate JA 1996. Integrated tephrochronology and magnetostratigraphy for cyclothemic marine strata, Wanganui Basin: Implications for the Pliocene-Pleistocene boundary in New Zealand. Quaternary International 34-36(95): 29-48.

Naish TR, Abbott ST, Alloway BV, Beu AG, Carter RM, Edwards AR, Journeaux TD, Kamp PJJ, Pillans BJ, Saul G and others 1998. Astronomical calibration of a southern hemisphere Plio-Pleistocene reference section, Wanganui Basin, New Zealand. Quaternary Science Reviews 17(8): 695-710.

Naish TR, Field BD, Zhu H, Melhuish A, Carter RM, Abbott ST, Edwards S, Alloway BV, Wilson GS, Niessen F and others 2005. Integrated outcrop, drill core, borehole and seismic stratigraphic architecture of a cyclothemic, shallow marine depositional system, Wanganui Basin, New Zealand. Journal of the Royal Society of New Zealand 35(1-2): 91-122.

Nicol A, Beavan J 2003. Shortening of an overriding plate and its implications for slip on a subduction thrust, central Hikurangi Margin, New Zealand. Tectonics 22(6): 1070-1084.

Pillans B, Holgate G, McGlone M 1988. Climate and Sea Level during Oxygen Isotope Stage 7b: On-Land Evidence from New Zealand. Quaternary Research 29: 176-185.

Pillans BJ 1981. Upper Quaternary landscape evolution in South Taranaki, New Zealand. Unpublished PhD Thesis, Australian National University, Canberra, Australia. 221 p.

Pillans BJ 1983. Upper Quaternary marine terrace chronology and deformation, South Taranaki , New Zealand. Geology(May): 292-297.

Pillans BJ 1991. New Zealand Quaternary Stratigraphy: An Overview. Quaternary Science Reviews 10(1984): 405-418.

Pillans BJ 1994. Direct marine-terrestrial correlations, Wanganui Basin, New Zealand: The last 1 million years. Quaternary Science Reviews 13(3): 189-200.

Pillans BJ 2017. Quaternary Stratigraphy of Whanganui Basin-A Globally Significant Archive. In: Schulmeister J ed. Landscape and Quaternary Environmental Change in New Zealand. Brisbane, Australia, Atlantis Press. Pp. 141-170.

Pillans BJ, Wright I 1990. 500,000-Year Paleomagnetic Record from New Zealand Loess. Quaternary Research 33(2): 178-187.

Pillans BJ, Kohn BP, Berger G 1996. Multi-method dating comparison for Mid-Pleistocene Rangitawa Tephra, New Zealand. Quaternary Science Reviews 15: 641-653.

Pillans BJ, Roberts AP, Wilson GS, Abbott ST, Alloway BV 1994. Mangnetostratigraphic, lithostratigraphic and tephrostratigraphic constraints on Lower and Middle Pleistocene sea-level changes, Wanganui Basin, New Zealand. Earth and planetary science letters 121: 81-98.

Pillans BJ, McGlone M, Palmer A, Mildenhall D, Alloway B, Berger G 1993. The Last Glacial Maximum in central and southern North Island, New Zealand: a paleoenvironmental reconstruction using the Kawakawa Tephra Formation as a chronostratigraphic marker. Palaeogeography, Palaeoclimatology, Palaeoecology 101(3): 283-304.

Pillans BJ, Alloway B, Naish TR, Westgate J, Abbott S, Palmer AS 2005. Silicic tephras in Pleistocene shallow-marine sediments of Wanganui Basin, New Zealand. Journal of the Royal Society of New Zealand 35(1-2): 43-90.

Potter WD 1984. Upper Quaternary Geology of part of the lower Rangitikei Valley, Unpublished BSc (hons) Thesis. Victoria University of Wellington, Wellington, New Zealand. 84 p.

Rees CJ, Palmer JA, Palmer AS 2018. Plio-Pleistocene Geology of the Lower Pohangina Valley, New Zealand. New Zealand Journal of Geology and Geophysics 61(1): 44-63.

Saul G, Naish TR, Abbott ST, Carter RM 1999. Sedimentary cyclicity in the marine Pliocene-Pleistocene of the Wanganui basin (New Zealand): Sequence stratigraphic motifs characteristic of the past 2.5 m.y. Geological Society Of America Bulletin 111(4): 524-537.

Seward D 1974a. Age of New Zealand Pleistocene substages by fission-track dating of glass shards from tephra horizons. Earth and planetary science letters 24(2): 242-248.

Seward D 1974b. Some Aspects of Sedimentology of the Wanganui Basin, North Island, New Zealand., Unpublished PhD thesis, Victoria University of Wellington, Wellington, New Zealand. 285 p.

Seward D 1976. Tephrostratigraphy of the marine sediments in the Wanganui Basin , New Zealand. New Zealand Journal of Geology and Geophysics 19(1): 9-20.

Seward D 1978. Palaeosalinities and palaeotemperatures from carbon and oxygen isotopes of carbonate shells in three Quaternary formations, Wanganui Basin, New Zealand. Palaeogeography, Palaeoclimatology, Palaeoecology(23): 47-55.

Seward D 1979. Comparison of zircon and glass fission-track ages from tephra horizons. Geology 7(10): 479-482.

Seward D, Lienert B 1986. Magnetic polarity stratigraphy of a Plio- Pleistocene marine sequence of North Island , New Zealand. Earth and Planetary Science Letters 80(3-4): 353-360.

Shackleton NJ, Opdyke ND 1973. Oxygen isotope and palaeomagnetic stratigraphy of Equatorial Pacific core V28-238: Oxygen isotope temperatures and ice volumes on a 105 year and 106 year scale. Quaternary Research 3: 39-55.

Shane PA, Black TM, Alloway BV, Westgate JA 1996a. Early to middle Pleistocene tephrochronology of North Island, New Zealand: implications for volcanism, tectonism, and paleoenvironments. Geological Society of America Bulletin 108(8): 915-925.

Shane PAR 1991. Remobilised silicic tuffs in middle Pleistocene fluvial sediments , southern North Island, New Zealand. New Zealand Journal of Geology and Geophysics 34(4): 489-499.

Shane PAR 1993. Tephrostratigraphy, magnetostratigraphy and geochronology of some early and middle Pleistocene deposits in New Zealand, Unpublished PhD Thesis. Victoria University of Wellington, Wellington, New Zealand. 136 p.

Shane PAR 1994. A widespread , early Pleistocene tephra (Potaka tephra, 1 Ma) in New Zealand: Character, distribution, and implications. New Zealand Journal of Geology and Geophysics 37(1): 25-35.

Shane PAR, Alloway B, Black T, Westgate J 1996b. Isothermal plateau fission-track ages of tephra beds in an Early-Middle Pleistocene marine and terrestrial sequence, Cape Kidnappers, New Zealand. Quaternary International 34(36): 49-53.

Stern TA, Quinlan GM, Holt WE 1992. Basin formation behind an active subduction zone: Three dimensional flexural modelling of Wanganui Basin, New Zealand. Basin research 4(3-4): 197-214.

Te Punga MT 1952. The geology of Rangitikei Valley. New Zealand Geological Survey Memoir 8, Wellington, New Zealand. 46 p.

Te Punga MT 1957. Live anticlines in western Wellington. New Zealand Journal of Science and Technology(38): 433-466.

Townsend D, Vonk A, Kamp PJJ 2008. Geology of the Taranaki area: scale 1:250,000. Lower Hutt, GNS Science. Institute of Geological and Nuclear Sciences 1:250,000 geological map 7, Lower Hutt, New Zealand: 1 sheet+77p.

Turner GM, Kamp PJJ 1990. Palaeomagnetic location of the Jaramillo Subchron and the Matuyama-Brunhes transition in the Castlecliffian stratotype section, Wanganui Basin, New Zealand. Earth and Planetary Science Letters 100(1-3): 42-50.

Turner GM, Kamp PJJ, McIntyre AP, Hayton S, McGuire DM, Wilson GS 2005. A coherent middle Pliocene magnetostratigraphy, Wanganui Basin, New Zealand. Journal of the Royal Society of New Zealand 35(1-2): 197-227.

van der Neut M 1996. Sequence Stratigraphy of Plio-Pleistocene Sediments in Lower Turakina Valley, Wanganui Basin, New Zealand. Unpublished MSc Thesis. Massey Univeristy, Palmerston North, New Zealand. 149 p.

Vandergoes MJ, Hogg AG, Lowe DJ, Newnham RM, Denton GH, Southon J, Barrell DJA, Wilson CJN, McGlone MS, Allan ASR and others 2013. A revised age for the Kawakawa / Oruanui tephra , a key marker for the Last Glacial Maximum in New Zealand. Quaternary Science Reviews 74: 195-201.



Chapter 4

Tephrostratigraphy

The following chapter contains a journal article published in the New Zealand Journal of Geology and Geophysics, Volume 63, Issue 2. Marker beds are crucial for mapping in the Whanganui Basin. They comprise essential tie points that enable us to begin to conceptualise the hydrogeology of the Pourewa Stream sub-catchment. This paper facilitates the capture of thesis objectives two and three by investigating tephrochronology and tephrostratigraphy in the Whanganui Basin and providing the vital chronostratigraphic framework for all subsequent chapters. Key discussion points include:

- Kaimatira Pumice Sand Formation
- Coutts Creek Horizon
- Makirikiri Tuff Formation
- Paleogeography

We use new geochemical datasets and fieldwork to refine existing stratigraphic correlations in central Rangitikei, providing an update on existing work and linking this research to datasets gathered from the eastern basin margin.

Looking south down the Rangitikei River off Saddon Block Road, Mangaonoho Formation exposed in the cliffs to the left.

Tephrostratigraphic constraints on sedimentation and tectonism in the Whanganui Basin, New Zealand

Callum Rees[1], Julie Palmer[1], Alan Palmer[1],

[1]*School of Agriculture and Environment, Massey University, Palmerston North, New Zealand*

4.1 Abstract

We apply digital mapping techniques and tephrostratigraphy to correlate marker horizons across the Whanganui Basin, culminating in a new 1:25 000 geological map of the central Rangitikei District. This is achieved by (1) compilation of existing research, (2) correlation of major element glass shard datasets to known eruptive products and (3) completion of a three-year field survey. We update and refine existing stratigraphic correlations, focusing on two critical units within the basin succession; namely the Makirikiri Tuff (1.6 Ma) and Kaimatira Pumice Sand (1 Ma) formations. Okehu Group is proposed to cover all strata from Pakihikura to Potaka pumice. Rewa Pumice is placed within its own formation bridging the Makirikiri Tuff and Kaimatira Pumice Sand formations. Mapping and analysis facilitates placement of Coutts Creek Horizon within Rewa Formation. Sub-aerial surfaces and influxes of greywacke and volcaniclastic detritus from c. 1.6 Ma onward provide evidence for an alluvial plain developing at the foot of the uplifting, paleo-axial range. We suggest uplift in the paleo-axial range occurred

contemporaneously with the onset of rhyolitic volcanism at Mangakino caldera (c. 1.6 Ma), so that the first influxes of fluvial conglomerate and volcaniclastics occur in close proximity within the eastern basin succession.

Keywords: Pleistocene, Quaternary, Stratigraphy, Whanganui Basin, Taupo Volcanic Zone, Tephrostratigraphy, Potaka Pumice, Kidnappers, Pakihikura Pumice

4.2 Introduction

Tephrochronology and tephrostratigraphy are powerful tools that have been applied since the late 19th century to date and correlate New Zealand geological successions (Lowe 1990). A focus of central and lower North Island research has been the Taupo Volcanic Zone (TVZ), one of the most frequently active rhyolitic centres on Earth, with eruptions that have dispersed tephra for thousands of kilometers from source (Wilson & Rowland 2016). South of the TVZ lies the Late Miocene-Quaternary, Whanganui Basin, providing an important sedimentary archive of volcanic history (Fig. 4.1). Plio-Pleistocene sedimentation broadly matched subsidence in the Whanganui Basin, leading to preservation of a multitude of volcanic products related to the initial development and maturation of the TVZ.

The chronostratigraphic framework of the Whanganui Basin is based on biostratigraphy (Beu 2006), tephrostratigraphy (Pillans et al. 2005) and magnetostratigraphy (Turner et al. 2005). Mapping of the basin fill involves detailed description of key sections and recognition of marker horizons. The most recent maps covering the basin are the Taranaki and Hawkes Bay QMAP sheets at 1:250 000 (Townsend et al. 2008; Lee et al. 2011), and isolated areas covered at

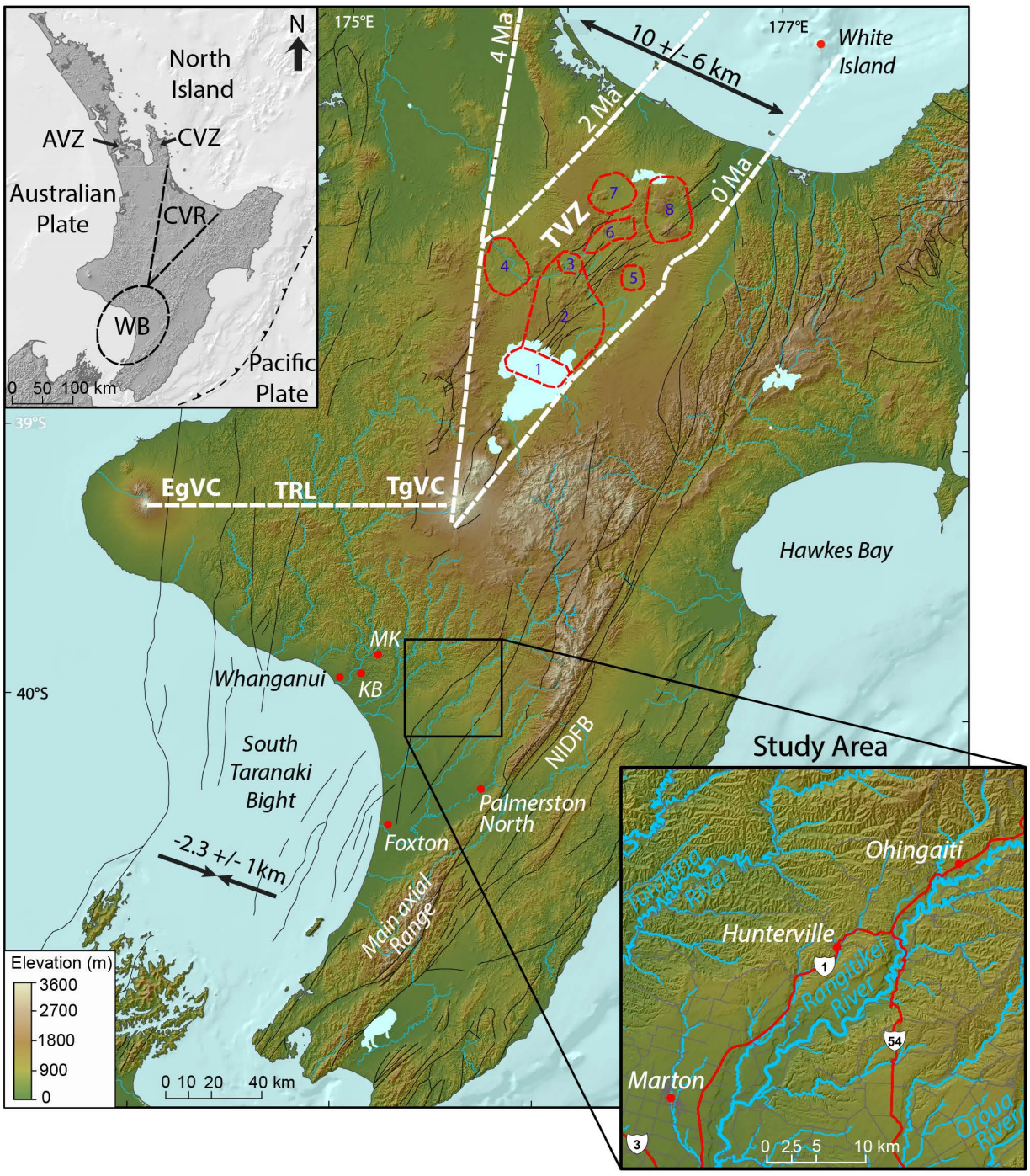


Figure 4.1: Map of the North Island showing the study area in relation to the Whanganui Basin (WB), Auckland Volcanic Zone (AVZ), Coromandel Volcanic Zone (CVZ), Central Volcanic Region (CVR), Taupo Volcanic Zone (TVZ), main axial range, Whanganui City, Makirikiri Valley (MK), Kaimatira Bluff (KB), Foxton township, Palmerston North and major river systems. Red outlines represent the eight major calderas within the TVZ: 1 = Taupo, 2 = Whakamaru, 3 = Ohakuri, 4 = Mangakino, 5 = Reporoa, 6 = Kapenga, 7 = Rotorua, 8 = Okataina (Wilson & Rowland 2016). TgVC = Tongariro Volcanic Centre, EgVC = Egmont Volcanic Centre, TRL = Taranaki Ruapehu, NIDFB = North Island Dextral Fault Belt. Black arrows indicate Pliocene shortening and extension (Nicol et al. 2007). Black lines indicate faults.

smaller scales (Milne 1968; Carter 1972; Naish & Kamp 1995; Journeaux et al. 1996; van der Neut 1996; McIntyre & Kamp 1998; Rees et al. 2018b). Currently, there is a need to update the maps in the basin. We address this by compiling and formally defining stratigraphic nomenclature in the Whanganui Basin, resolving historic miscorrelations and applying tephrostratigraphy to produce a new map of the central Rangitikei District. Stratigraphic sections from the Oroua (Beaconsfield Valley), Rangitikei (Pourewa Stream) and Turakina (Coutts Creek) catchments are presented alongside new geochemical datasets. We investigate spatio-temporal patterns of sedimentation within the basin succession, exploring evidence for the paleogeographic development of the lower North Island.

Nomenclature

Volcaniclastic units are common in the Whanganui Basin succession and we follow recommendations by Schmid (1981) and Froggatt and Lowe (1990) in our terminology, describing epiclastic sediments dominated by volcanic detritus as 'tephric'. The original stratigraphic names 'Potaka Pumice' and 'Pakihikura Pumice', as set out by Te Punga (1952), are retained here in preference to other terms used to encompass a variety of reworked tephric silts, sands and pumice. The name 'Makirikiri Tuff Formation' of Fleming (1953) is adopted here to retain historic precedence.

Mapping the Whanganui Basin

Geological mapping of the Whanganui Basin in the mid-20th century by geologists of the New Zealand Superior Oil Company and New Zealand Geological Survey quickly made use of conspicuous volcaniclastic marker horizons, tracing their extent across a large portion of the basin.

Table 4.1: Proposed stratigraphic nomenclature used in this study (far right) and correlation to other proposed nomenclatures of the eastern and western Whanganui Basin

Western Whanganui Basin				Eastern Whanganui Basin				Approximate age (Ma)
Fleming (1953) Abbott and Carter (1999) Castlecliff type section		Superior Oil Company NZ (1943)		Te Punga (1952)		Potter (1984); Bussel (1984) Naish & Kamp (1995); This study		
POUAKAI GROUP	Papaiti Alluvium St Johns Alluvium Rapanui Fm. Brunswick Fm. Kaiatea Fm.	RECENT	Sand dunes and alluvium	UPPER RANGITIKEI FORMATION	Mangaone Sandstone Halcombe Conglomerate Waituna Conglomerate	POUAKAI GROUP	Westoe Fm. Halcombe Conglomerate Fm.	0.31 Ma
SHAKESPEARE GROUP	Landguard Fm. Putiki Shellbed Mosstown Sand Karaka Siltstone Upper Castlecliff Shellbed Shakespeare Cliff Sand Shakespeare Cliff Siltstone Tainui Shellbed Pinnacle Sand Lower Castlecliff Shellbed Seafield Sand	OTAKI	? — ? — ?		Rangitawa Fossil Beds Kakariki Conglomerate Ruamahanga Conglomerate Onepuhi Fossil Beds Toms Conglomerate Shell Creek Fossil Beds	SHAKESPEARE GROUP	Mangatapu Fm. *Ruamahanga Conglomerate Mb.* Tokorangi Fm. *Toms Conglomerate Mb.*	0.34 Ma 0.57 Ma
KAI IWI GROUP	Upper Kai Iwi Siltstone Kupe Frm Upper Westmere Siltstone Kaikokopu Frm. Lower Westmere Siltstone Omapu Shellbed Lower Kai Iwi Siltstone Kaimatira Pumice Sand	CASTLECLIFFIAN	Kimbolton Ash		Waitapu Shell Conglomerate Potaka Pumice	KAI IWI GROUP	Reu Reu Frm. *Waiomio Shellbed Mb.* Waiomio Fm. *Waitapu Shell Conglomerate Mb.* Kaimatira Pumice Sand Fm. *Potaka Pumice Mb.*	0.65 Ma 0.9 Ma 1 Ma
OKEHU GROUP	Upper Okehu Siltstone Okehu Shell Grit Lower Okehu Siltstone Butlers Shell Conglomerate Makirikiri Tuff		Coutts Creek Horizon Basal Ash		Mangapipi Fossil Beds Pakihikura Pumice	OKEHU GROUP	Rewa Fm. *Mangapipi Conglomerate* *Mangapipi Mb.* Makirikiri Tuff Fm. *Pakihikura Pumice Mb.*	1.2 Ma 1.5 Ma 1.6 Ma
MAXWELL GROUP	Upper Maxwell Fm. Mangahou Siltstone Middle Maxwell Fm. Pukekiwi Shell Sand Lower Maxwell Fm. Tewkesbury Fm.			MIDDLE RANGITIKEI FORMATION	Vinegar Hill Fossils	MAXWELL GROUP	Upper Maxwell Fm. Rataiti Fm.	1.65 Ma 1.75 Ma
NUKUMARU GROUP	Waipuru Shellbed Nukumaru Brown Sand Mangamako Shellbed Nukumaru Limestone Nukumaru Fm. Ohingaiti Sand	NUKUMARUAN	Waipuru Shellbed Mangamako Shellbed Ohingaiti Sand		Mudstone Waipuru Fossil Beds Mangamako Fossil Beds Ohingaiti Sandstone	RANGITIKEI GROUP	Vinegar Hill Fm. *Waipuru Shellbed Mb.* Mangaonoho Fm. *Mangamako Shellbed Mb.* Orangipongo Fm. *Ohingaiti Sand Mb.*	1.83 Ma 2 Ma
OKIWA GROUP	Kuranui Limestone Hautawa Shellbed Te Rama Shellbed Parihauhau Shellbed Te Rimu Sand		Tuha Sand Hautawa Shellbed Basal Sand		Tuha Sandstone Basal Sandstone		Makohine Fm. *Tuha Sand Mb.* Tikapu Fm. *Hautawa Shellbed Mb.* Mangarere Fm. *Te Rimu Sand Mb.*	2.4 Ma
PAPARANGI GROUP	Wilkies Shellbed Makokako Sand Mangaweka Mudstone Paparangi Sandstone *Mangapani Shell Conglomerate Mb.*	WAITOTARAN	Mangamahu Concretions Mangaweka Mudstone Fm.	LOWER RANGITIKEI	Mangaweka Concretionary Mudstone	PAPARANGI GROUP	Mangaweka Mudstone Fm	Plio-Pleist. 2.58 Ma 2.8 Ma

The literature and related nomenclature introduced during this time is still used as the basis for stratigraphic subdivision today, including early recognition of the role of eustatic sea level fluctuations (Fleming 1953), identification of important regional structures (Feldmeyer et al. 1943; Te Punga 1957) and development of a basin history (Te Punga 1952; Fleming 1953).

Advances in the application of radiometric (Milne 1973a; Marden & Neall 1990; Pillans et al. 1993), paleomagnetic (Seward & Lienert 1986; McGuirre 1989; Turner & Kamp 1990), fission track (Milne 1973b; Seward 1974a; Boellstorff & Te Punga 1977; Seward 1979; Pillans & Kohn 1981) and isotopic (Seward 1978; Stevens & Vella 1981) dating techniques came to the forefront of Whanganui Basin research as technology became more widely available toward the end of the 20th century. This led to the ongoing development and refinement of a basin wide chronostratigraphic framework, culminating in the correlation of the Whanganui Basin succession to the high resolution, astronomically tuned $\delta^{18}O$ record (Naish et al. 1998).

Initial work using fission track dating on volcanic glass (Seward 1974a, 1976; Boellstorff & Te Punga 1977) underestimated ages because the method didn't accounted for partial track annealing (Naish et al. 1996). Alloway et al. (1993) used the isothermal plateau fission track (ITPFT) technique to correct for track annealing thereby synchronising it with revised magnetostratigraphic records (Pillans et al. 1994), $^{40}Ar/^{39}Ar$ dating (Shane et al. 1992) and orbitally tuned cyclostratigraphy (Naish et al. 1998) to provide refined glass ages in the Whanganui Basin. Studies of tephra-fall and/or volcaniclastic horizons within the Whanganui Basin were presented by Naish et al. (1996), Shane et al. (1996) and Pillans et al. (2005). We develop this work by incorporating marker horizons into a formal stratigraphic nomenclature and augmenting existing geochemical datasets through addition of new data from less frequented sections.

Table 4.2: Selected tephra-fall and/or volcaniclastic deposits and their respective stratigraphic units from the Rangitikei. Ages derived from Alloway et al. (2004), Pillans et al. (1994), Naish et al. (1996), Shane et al. (1996), Seward and Kohn (1997), Naish et al. (1998), McIntyre (2002), Pillans et al. (2005) and Grant et al. (2018).

Group	Formation	Member	Glass	Age
Shakespeare	Mangatapu	Rangitawa Pumice	Rangitawa	340 ka
	Tokorangi	–	Onepuhi	0.57 Ma
Kai Iwi	Reu Reu	–		
	Waiomio	Waiomio Shellbed	Kupe	0.65 Ma
		Waitapu Shell Conglomerate	Kaukatea	0.90 Ma
	Kaimatira Pumice Sand	Potaka Pumice	Potaka	0.99 Ma
Okehu	Rewa	Rewa Pumice	Rewa	1.19 Ma
	Makirikiri Tuff	Mangapipi	Mangapipi	1.54 Ma
		–	Ridge	1.56 Ma
		Pakihikura Pumice	Pakihikura	1.58 Ma
Maxwell	Upper Maxwell	–	Birdgrove	1.6 Ma
			Mangahaou	1.63 Ma
			Maranoa	1.63 Ma
			Ototoka	1.64 Ma
			Table Flat	1.65 Ma
	Rataiti	–		
Rangitikei	Vinegar Hill Formation	–	Vinegar Hill	1.75 Ma
		Waipuru Shellbed	Waipuru	1.83 Ma
	Mangaonoho	Mangamako Shellbed	Mangamako	2.05 Ma
	Orangipongo	Ohingaiti Sand	Ohingaiti	2.17 Ma
	Makohine	Tuha Sand	–	
	Tikapu	Hautawa Shellbed	–	
	Mangarere	Te Rimu Sand	–	
Paparangi	Mangaweka Mudstone Formation	–	Eagle Hill	2.88 Ma

4.3 Geological setting

Whanganui Basin

The study area is located within the Whanganui Basin c. 200 km behind the Hikurangi subduction zone (Fig. 4.1). During Miocene to early Pleistocene time, the southern North Island was characterised by a series of marine basins connected by seaways across a shallow basement high in the location of the present day main axial range (Beu 1995). Sediments derived from the Central Volcanic Region, Torlesse Terrane of the paleo-axial ranges and South Island granites and schist were transported into peripheral sedimentary basins, where they were deposited throughout climatically forced Quaternary eustatic sea level fluctuations. Up to 4.5 km of basin fill has been preserved within the Whanganui Basin, including coarse-grained transgressive (TST) and fined-grained highstand (HST) deposits separated by sequence bounding unconformities. Consequent uplift along the northern and eastern basin margins has resulted in shore-normal tilting of the Late Miocene-Pleistocene units.

The revised stratigraphic nomenclature of the Whanganui Basin and its relationship to previous work is summarised in Table 4.1. The basin succession varies from east to west, characterised by changes in the style of deposition and extent of preservation. The best outcrop occurs along coastal exposures NW of Whanganui (Fig. 4.1) and down NE-SW oriented river valleys draining the central North Island. Each major river valley is characterised by locally specific members and formations. The recognition of key marker horizons facilitates basin wide correlations and the definition of groups. At the Whanganui type section, a particularly prominent 450 ka unconformity occurs at the base of the Butlers Shell Conglomerate, Okehu Group. East of Whanganui the unconformity is not present, at least to the same extent, replaced by 150 + m of marginal to non-marine beds of

the Makirikiri Tuff Formation (Table 4.1). The Okehu Group, east of Whanganui is difficult to interpret in terms of sequence stratigraphy due to its marginal to non-marine cycle motifs (Naish et al. 2005), including preservation of lowstand systems tracts (LST), conglomerates and sub-aerial surfaces, such as paleosols and lignite.

The Central Volcanic Region and Taupo Volcanic Zone

The Central Volcanic Region (CRV) (Fig. 4.1) is characterised by andesite volcanoes, rhyolitic calderas and negative gravity anomalies resulting from production of c. 12,000 km^3 of Plio-Pleistocene siliceous volcanics (Gravley et al. 2016). Active rhyolitic volcanism within the CVR began in the Coromandel Volcanic Zone (CVZ) from 12-4 Ma (Carter et al. 2003). By c. 2 Ma volcanism had migrated southeast to the younger TVZ, reflecting the evolution of an arc-related magmatic province (Wilson & Rowland 2016). Onland records of late Cenozoic volcanism are incomplete due to tectonism, erosion, and burial, especially within the TVZ where widespread Whakamaru ignimbrite (c. 350 ka) often obscures evidence for older activity (Downs et al. 2014b). Mangakino caldera (Fig. 4.1) is the westernmost and oldest rhyolitic caldera in the TVZ, active during two periods of caldera forming activity from 1.68-1.53 and 1.21-0.95 Ma, respectively (Krippner et al. 1998). Voluminous widespread welded and non-welded ignimbrites and fall deposits originating from the Mangakino Volcanic Centre provided an important source of sediment to the Whanganui Basin during Pleistocene time (Table 4.2).

Correlation between Whanganui Basin volcaniclastic horizons and their corresponding proximal source deposits is problematic due to limited exposure, partial welding and extensive vapour-phase alteration of these ignimbrite sheets. Pakihikura Pumice is chronologically equivalent to Ngaroma Ignimbrite and ignimbrite Unit-B from the Mangakino Volcanic Centre, erupted during an early phase of rhyolitic activity within the TVZ (Wilson et al.2009). Potaka Pumice (c. 1

Ma), base of the Kaimatira Pumice Sand Formation (Fleming 1953), is correlated to the Rocky Hill and Kidnappers ignimbrites (Cooper et al.2017), also originating from the Mangakino Volcanic Centre.

4.4 Methods

We compiled a 1:25 000 geological map of the central Rangitikei (Fig. 4.2). Ortho-rectified aerial photograph datasets from LINZ and digital elevation data acquired from Horizons Regional Council and Columbus et al. (2011) were used to aid mapping within a Geographic Information System (GIS) environment. Database design was based on the structure established by the GNS Science QMAP program (Rattenbury & Heron 1997). We placed particular emphasis on linking existing works (Feldmeyer et al. 1943; Te Punga 1952; Fleming 1953; Bussell 1984; Potter 1984; Naish & Kamp 1995; van der Neut 1996) into a single nomenclature under the umbrella of stratigraphic groups laid down by Fleming (1953), with type sections near Whanganui (Fig. 4.1, Table 4.1). Mapping was assisted by the detailed stratigraphic studies of Seward (1974b), Abbott (1994), Naish and Kamp (1995) and Pillans et al. (2005). Key marker horizons were recognised in the field and traced laterally across the landscape. Particularly prominent horizons in the landscape and/or section were selected as formation and group boundaries within the proposed stratigraphic framework (Table 4.1). We logged and sampled stratigraphic sections within the tributaries and interfluves of the Turakina, Rangitikei and Oroua catchments (Supplementary Data File A). An effort was made to visit type localities of important marker units and trace them laterally over interfluves into adjoining tributaries, in order to gain an understanding of facies changes and variability across the basin.

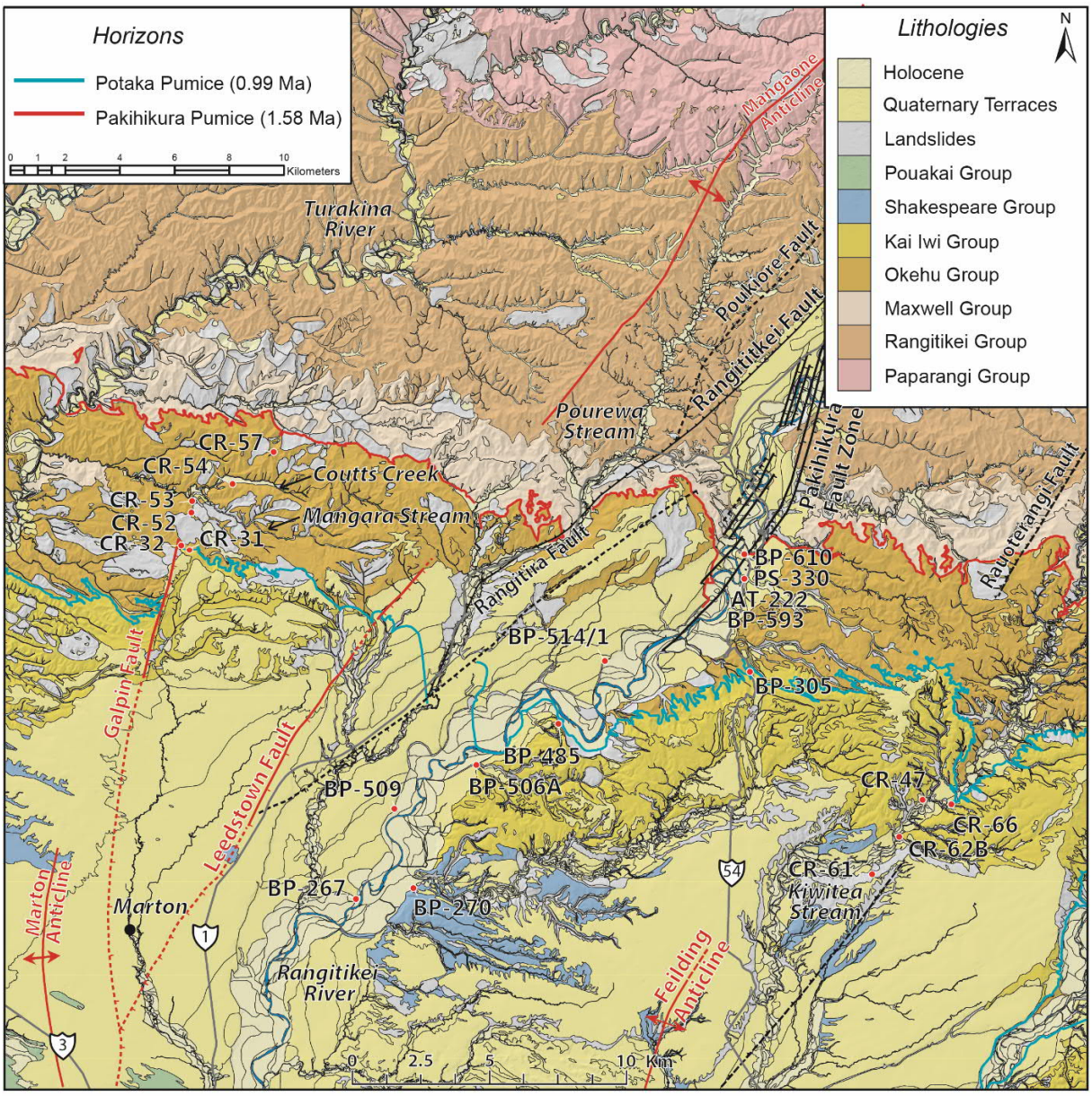


Figure 4.2: Geological map of the study area showing lithological groups, regional structures and the location of the Potaka Pumice and Pakihikura Pumice; two widespread regional marker horizons used to define the base of the Kai Iwi and Okehu Groups respectively. Sample points are shown from Pillans et al. 2005 and this study, state highways are shown in grey. This work draws from the geological maps of Feldmeyer et al. (1943), Te Punga (1952), Fleming (1953), Milne (1973), Naish and Kamp (1995), van der Neut (1996), Townsend et al. (2008), Lee et al. (2011).

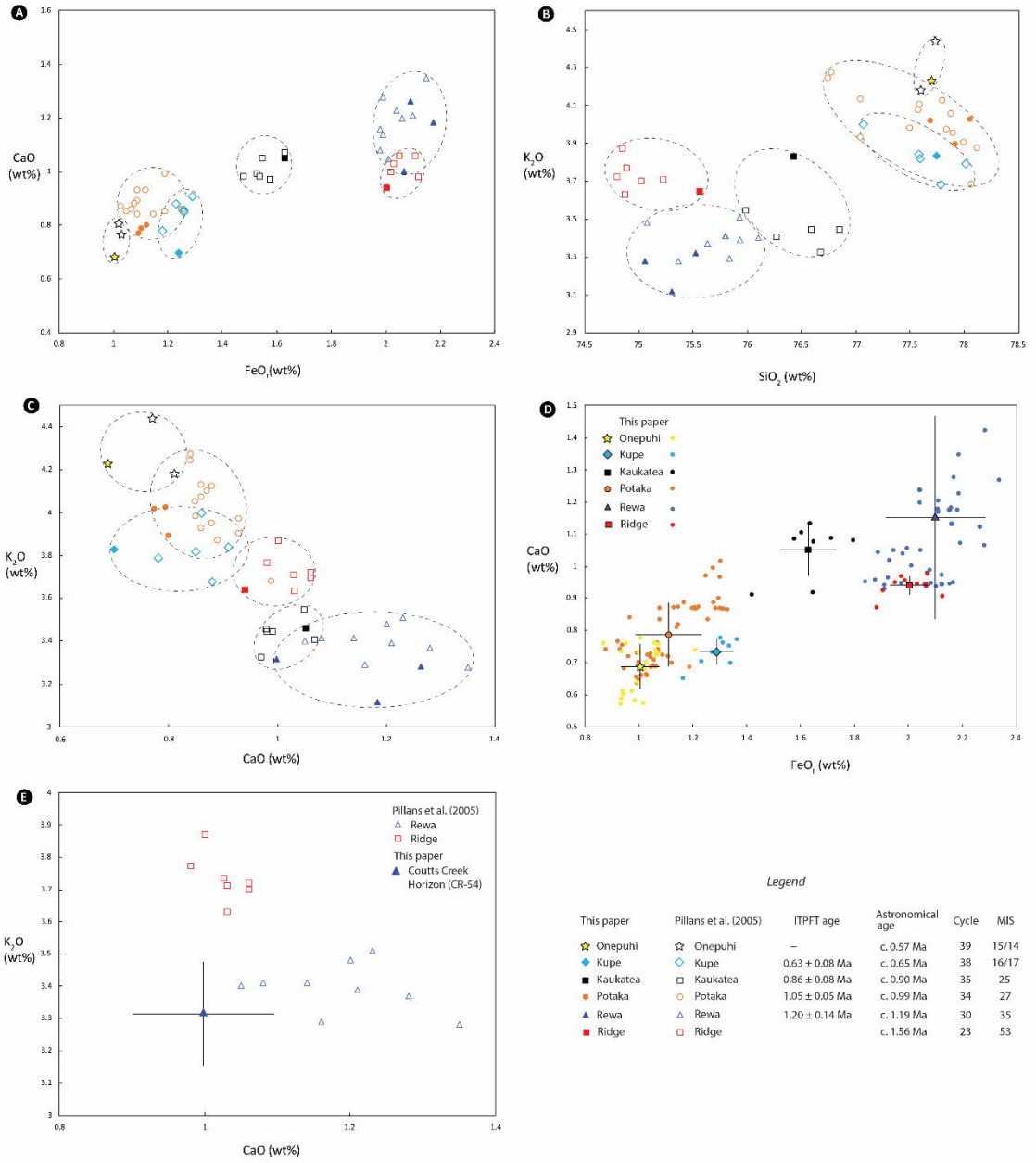


Figure 4.3: Composition of glass shards from six tephra-fall and/or volcaniclastic deposits in the central Rangitikei and correlation to the published datasets of Pillans et al. (2005). A) Mean CaO versus FeO_t (wt%), B) Mean K_2O versus SiO_2 (wt%), C) Mean K_2O versus CaO (wt%), D) CaO versus FeO_t (wt%) composition of glass shards from this study including mean analyses with error bars representing one standard deviation, E) Mean K_2O versus CaO (wt%) for Coutts Creek horizon (CR-54) and correlation to the datasets of Pillans et al (2005). Note some overlap in major element, glass shard geochemistry occurs between the different deposits. Correlations are based on stratigraphic position, EPMA analysis and geological mapping.

Volcaniclastic and primary tephra-fall horizons were sampled at sections, targeting beds composed entirely of glass or alternatively picking pumice clasts from volcaniclastic deposits. Pumice clasts were cleaned and gently crushed during sample preparation. The glass was washed through a 63 µm sieve, discarding silt and clay sized particles. After drying samples were sieved; the 125-250 µm fraction was collected and set in epoxy plugs, ground and finally polished using 1 µm diamond paste. Glass-shard major elements were determined using a JEOL JXA-8230 Electron Probe Microanalyser (EPMA) at Victoria University of Wellington. Analyses were determined using an 8 nA beam current, 10 µm beam diameter. Matrix-matched glass standards ATHO-G from the MPI-DING collection (Jochum et al. 2006) and VG568 (Jarosewich et al. 1980) were used and run every 10 samples to monitor instrumental drift. Accuracy of the analyses was within 3.5% of published values, apart from Ti and Cl that had offsets of 26.94% and 68.88% respectively. Large offsets for Ti and Cl are attributed to the low wt% (<0.35 wt%) within the chosen standards. Ti and Cl were not used for the basis of tephrostratigraphic correlation. All analyses are presented as weight percent, recalculated to 100% on a water-free basis (Table 4.3, Supplementary Data File B). Total Fe (FeO_t) was calculated as FeO while the analytical sum prior to recalculation on an anhydrous basis is the difference from 100%. Bivariate plots were constructed to aid tephra correlation with existing published datasets (Fig. 4.3).

4.5 Results

Geological map of the central Rangitikei

The geology of the study area has been mapped at 1:25 000 (Fig. 4.2, Supplementary Data File C). This survey resulted in the amalgamation of several formal and informal stratigraphic nomenclatures introduced in the literature over

the last 75 years (Table 4.1). Pakihikura Pumice (Table 4.1, Fig. 4.2 and Fig. 4.4) marks the first widespread influx of volcaniclastic detritus into the basin at c. 1.6 Ma. Potaka Pumice represents the second major influx of volcaniclastic detritus into the basin at c. 1 Ma. Both units are prominent in section (Fig. 4.4 A, D and E) and represent important marker horizons within the basin succession.

Geological structures have been identified, including the Poukiore Fault (Fig. 4.2) and a southern extension of the Mangaone Anticline (Feldmeyer et al. 1943). Major regional reverse faults, the Rangitikei and Rauoterangi faults with maximum-recorded throws of 182 and 293 m, respectively (upthrown west), drive deformation of the Plio-Pleistocene succession, associated with zones of antithetic, normal faulting (Pakihikura and Poukiore faults). In the south of the mapping area, the actively growing Marton and Feilding anticlines are related to faulting at depth (Melhuish et al. 1996). Surface features (scarps), stratigraphy and structure contours have been used to map fault locations during the survey. Both sense and throw vary considerably along the length of these faults. They are commonly en echelon, associated with scissor movement and minor antithetic normal faulting. Folds are dome shaped, plunge southward and are often observed to change laterally. Where the underlying faults break to the surface, they offset rather than fold strata. Conversely, faults are also observed to pass laterally into fold structures. No major offsets were noted across the southern end of the Rauoterangi Fault, although a change in dip direction from SW to SE in this area suggests folding of the strata has occurred. Deformation is likely related to the Rauoterangi Fault as it plunges south beneath the Pleistocene strata, with offset accommodated as folding.

The distribution of the Pouakai to Paparangi groups (c. 3 – 0.3 Ma) is related to the depositional history, stratigraphic architecture and tectonic regime of the Whanganui Basin through the Plio-Pleistocene. The general east-west distribution of geological units reflects the gentle shore-normal tilt (2-11°) of the succession

Table 4.3: Electron Probe Microanalyser data for glass shards from the study area, Whanganui Basin

	Sample	Grid Ref.	SiO_2	Al_2O_3	TiO_2	FeO_t	MgO	CaO	Na_2O	K_2O	Cl	H_2O	n
Onepuhi													
	CR-61	BL35 302 620	77.70 (0.42)	12.58 (0.26)	0.10 (0.07)	1.00 (0.07)	0.08 (0.02)	0.69 (0.07)	3.40 (0.31)	4.23 (0.18)	0.23 (0.03)	3.92 (1.66)	22
Kupe													
	CR-62B	BL35 313 638	77.74 (0.24)	12.35 (0.04)	0.19 (0.05)	1.24 (0.11)	0.09 (0.02)	0.70 (0.08)	3.63 (0.12)	3.83 (0.19)	0.23 (0.01)	4.50 (0.65)	10
Kaukatea													
	CR-47	BL35 320 647	76.43 (0.68)	0.22 (0.06)	13.18 (0.16)	1.63 (0.10)	0.14 (0.02)	1.05 (0.08)	3.71 (0.52)	3.46 (0.17)	0.17 (0.01)	5.35 (0.62)	8
Potaka													
	CR-66	BL35 330 646	77.68 (0.24)	12.53 (0.11)	0.12 (0.07)	1.10 (0.12)	0.09 (0.02)	0.77 (0.09)	3.47 (0.11)	4.02 (0.12)	0.22 (0.01)	3.26 (0.39)	24
	CR-31	BL34 052 739	78.05 (0.23)	12.54 (0.07)	0.01 (0.01)	1.10 (0.14)	0.09 (0.02)	0.79 (0.08)	3.14 (0.11)	4.03 (0.15)	0.24 (0.01)	3.92 (0.56)	5
	CR-32	BL34 049 741	77.91 (0.39)	12.65 (0.12)	0.01 (0.01)	1.12 (0.12)	0.10 (0.02)	0.80 (0.11)	3.26 (0.36)	3.89 (0.31)	0.24 (0.01)	4.86 (1.08)	24
Rewa													
	CR-52	BL34 053 753	75.05 (1.23)	13.45 (0.91)	0.27 (0.08)	2.09 (0.22)	0.17 (0.10)	1.26 (0.44)	4.23 (0.31)	3.28 (0.31)	0.20 (0.06)	4.01 (2.16)	19
	CR-53	BL34 053 757	75.30 (0.26)	13.42 (0.09)	0.31 (0.08)	2.17 (0.11)	0.14 (0.02)	1.18 (0.03)	4.16 (0.08)	3.11 (0.18)	0.20 (0.01)	4.93 (0.71)	9
Ridge Tephra													
	CR-54	BL34 068 763	75.23 (1.27)	13.49 (1.08)	0.26 (0.09)	2.01 (0.29)	0.12 (0.03)	1.10 (0.43)	4.36 (0.30)	3.26 (0.27)	0.18 (0.01)	4.53 (1.23)	17
	CR-57	BL34 083 775	75.55 (0.26)	13.10 (0.15)	0.30 (0.08)	2.01 (0.08)	0.12 (0.02)	0.94 (0.03)	4.14 (0.31)	3.64 (0.42)	0.19 (0.02)	4.02 (2.05)	10
ATHO-G													
	ATHO-G	n/a	75.80 (0.19)	12.30 (0.08)	0.32 (0.05)	3.25 (0.09)	0.10 (0.01)	1.74 (0.03)	3.73 (0.15)	2.70 (0.06)	0.04 (0.01)	0.24 (0.34)	21
VG568													
	VG568	n/a	77.51 (0.20)	12.22 (0.06)	0.06 (0.04)	1.13 (0.17)	0.03 (0.01)	0.44 (0.01)	3.62 (0.10)	4.88 (0.09)	0.10 (0.01)	0.70 (0.32)	24

Notes: Oxide values recalculated to 100% on a water-free basis. Total Fe (FeO_t) calculated as FeO. H2O calculated by the difference from 100%. ± 1 standard deviation presented in parentheses. Grid references refer to NZ Topo50 map sheets.

toward the basin depocentre, located offshore. Quaternary river terraces represent climatically controlled aggradational episodes preserved by ongoing regional uplift over the last c. 370 ka (Pillans 1994). The terraces fan out in the lower Rangitikei Valley where the river emerges from its confined middle reaches onto the coastal plain. Holocene valley fill is restricted to the main valleys where the rivers have incised into the Plio-Pleistocene marine succession.

Marine terraces are present in the southern portion of the study area, occurring broadly parallel to and c. 30 km inland from the modern coastline. Pillans (1983) mapped and named 12 terraces along the southern Taranaki coastline northwest of Whanganui (Fig. 4.1), developing a terrace chronology and model of terrace deformation. Each marine terrace comprises a wave cut surface with a fossil sea cliff at its inner margin, representing the paleo-shoreline at maximum transgression during past warm climate episodes. Marine sediments directly overlie the wave cut surface, followed by a range of non-marine coverbed deposits typically comprising loess, dune sand and tephra (Palmer & Pillans 1996). Terrace chronology relies on fission track dating of the c. 340 ka Rangitawa Tephra (Alloway et al. 1993). Loess stratigraphy of coverbed deposits facilitates dating and correlation of landforms. Loess is associated with aggrading river flood plains and the production of abundant fine sediment during Late Quaternary stadial and glacial periods. Interstadial and interglacial periods are associated with landscape stabilisation and soil development, represented by paleosols within the coverbed succession.

Stratigraphy

The Pleistocene succession (Okehu-Shakespeare groups) of the study area (Fig. 4.5) was deposited toward the eastern basin margin as the sedimentary depocentre migrated from Turakina Valley to its present position offshore of Foxton (Fig. 4.1).

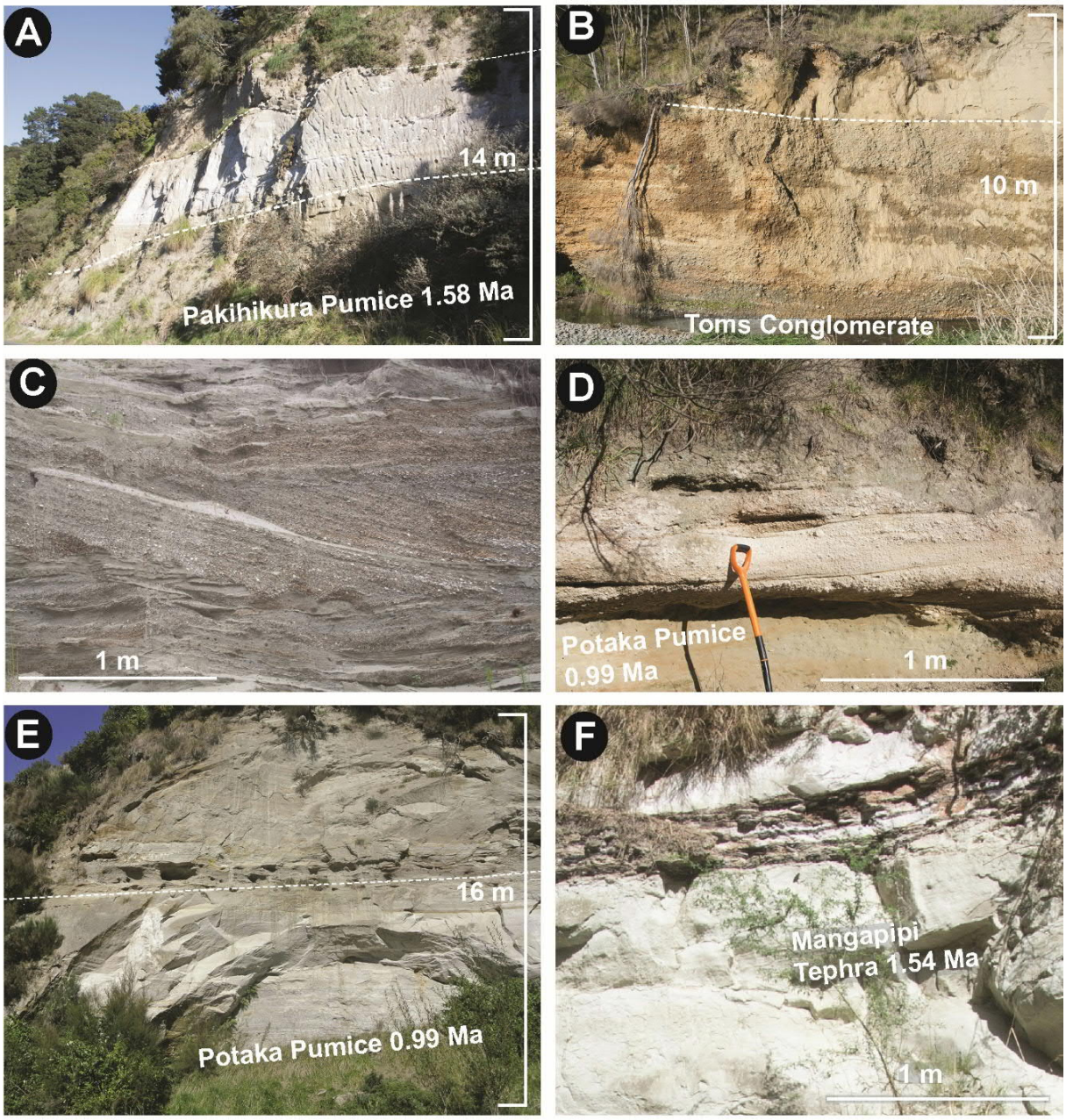


Figure 4.4: A) Pakihikura Pumice exposed at a cutting on Turakina Valley Road (BL33 0135 7932). B) Toms conglomerate in the Pourewa Stream section (BL34 0997 6438). C) Waitapu Shell Conglomerate, a typical cross-bedded shell conglomerate within the Rangitikei succession (BL34 1595 6589). D) Potaka Pumice exposed on farm track, western side of Rangitikei Valley (BL34 1586 6860). E) Potaka Pumice exposed in Kiwitea Stream (BL35 3296 6451). F) Mangapipi Tephra enclosed by lignite near Mangapipi Stream on the eastern side of the Rangitikei River (BL34 2539 7275).

Alternations between coarse-grained (TST) and fine-grained (HST) sedimentary units represent climatically forced changes in water depth of approximately 120 m (Nicol 2011). The identification of these textural couplets allows for cycle matching between key sections (Abbott 1994), whereby packages of sediment are grouped and ordered into cycles based on sequence stratigraphic concepts. The number of cycles above or below a known marker horizon can then be used to position oneself within the succession at outcrop.

The Whanganui Basin Pleistocene succession consists of cross-bedded pebbly shell conglomerates (Type A shellbeds) (Fig. 4.4 C), heterolithic, often pumiceous and pebbly transgressive units and massive to laminated highstand siltstones with sparse, *in situ* fossils (Abbott 1994). Overall, the succession coarsens upwards, becoming increasingly dominated by sandstone and conglomerate units. Shellbeds generally form a minor component of the dominantly siliciclastic succession.

Tephrostratigraphy in the Whanganui Basin is based on the first influx of a new glass chemistry within the succession. These changes in provenance have been coupled with biostratigraphic datums to facilitate correlation across the mapping area (Fig. 4.5). Here, we observe some dramatic changes in sedimentation over relatively short distances (<10 km) within the basin. Particularly pronounced, is the influx of abundant greywacke gravels within the sedimentary record, occurring earlier within the succession and at increasing frequency toward the east. In contrast, the relative concentration of bioclastic material within the succession systematically reduces eastward. For instance, the entire Kai Iwi Group (Potaka Pumice to Toms Conglomerate) is devoid of shell material within Beaconsfield Valley (Oroua Catchment), where we have relied upon tephrostratigraphic and lithostratigraphic correlation.

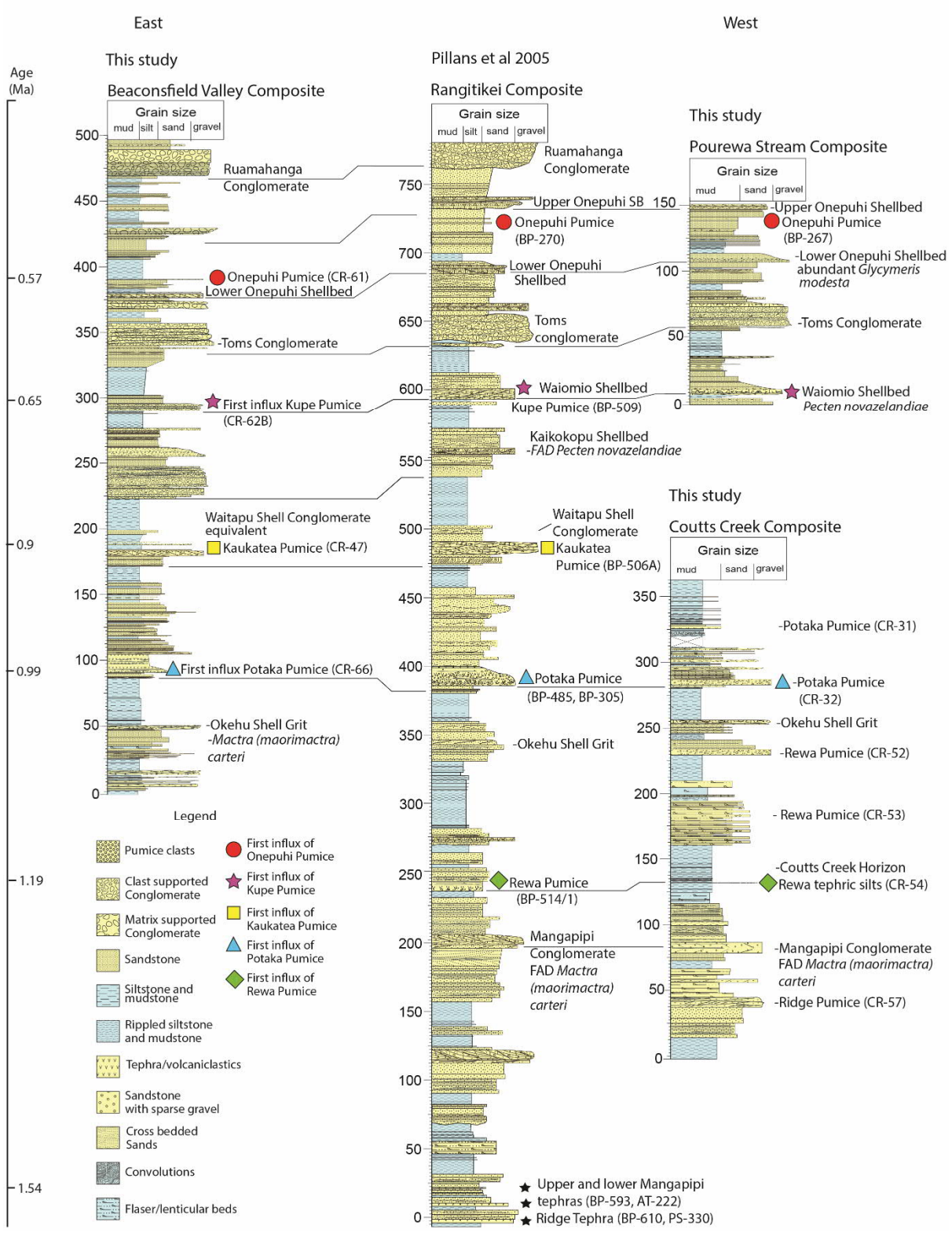


Figure 4.5: Pleistocene stratigraphic correlations in the central Rangitikei. Rangitikei composite data from Pillans et al. (2005), Beaconsfield Valley composite, Pourewa Stream composite and Coutts Creek composite data from this study.

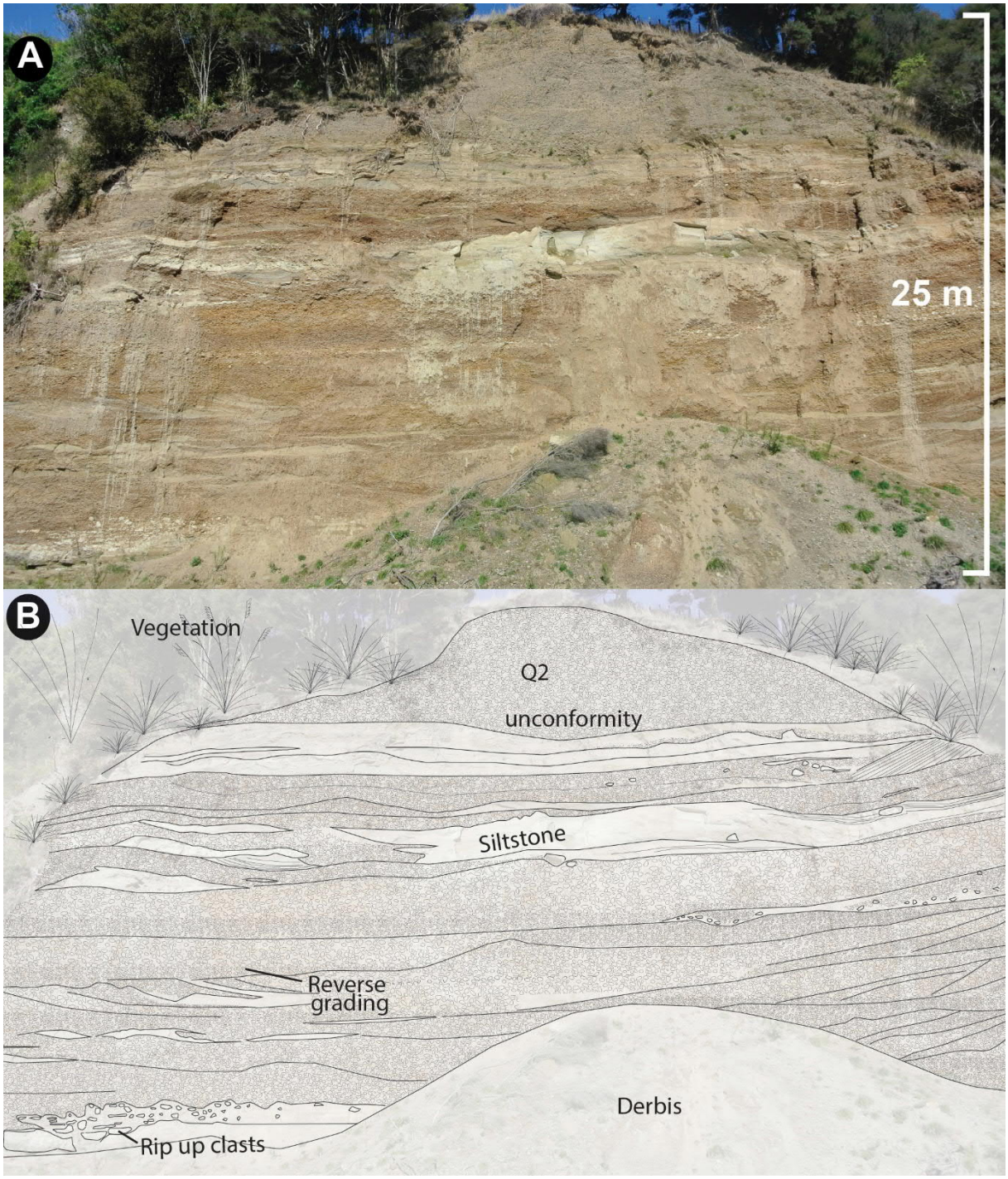


Figure 4.6: A) 25 m thick, clast supported conglomerate. Clasts are sub-rounded pebbles to cobbles of dominantly greywacke Common channel cut and fill, rip up clasts and interbedded lenses of siltstone. Occurs between Kaukatea (0.9 Ma) and Kupe (0.65) pumice in Beaconsfield Valley (BL35 3194 6425). B) Sketch to illustrate structures within the conglomerate.

Conglomerate deposits (Fig. 4.6) occur shortly after deposition of Kaukatea Pumice (0.9 Ma) within Beaconsfield Valley (Rees et al. 2019). These conglomerates are clast supported, contain sub-angular to sub-rounded, pebble to cobbled sized clasts of greywacke with intercalated siltstone and sandstone lenses. Low angle cross-bedding with associated channel cut and fill is present together with reverse graded beds. Abundant rip up clasts of siltstone up to 500 mm in diameter occur, associated with scouring and erosion of underlying beds. The first occurrence of a similar conglomerate within the adjacent Rangitikei section c. 10 km west is Toms Conglomerate (Fig. 4.4 B), occurring between the Kupe (0.65 Ma) and Onepuhi (0.57 Ma) pumices. These conglomerates are devoid of shell material and contain large clasts (up to 500 mm), being similar in nature to the Late Quaternary terrace deposits of the Rangitikei and Manawatu districts (Milne 1973a) although distinguishable by their stratigraphic position, dip angle and degree of weathering (Fig. 4.6).

4.6 Discussion

Kaimatira Pumice Sand Formation – Potaka Pumice

Fleming (1953) defined the Kaimatira Pumice Sand Formation, mapping it eastward from its designated type section at Kaimatira Bluff in Whanganui to the Turakina catchment (Fig. 4.1). Fleming correlated the Kaimatira Pumice Sand Formation to the Coutts Creek Horizon of Feldmeyer et al. (1943), noting it outcropping c. 90 m above the Makirikiri Tuff Formation on the southern ridge of Makirikiri Valley (Fig. 4.1). Fleming (1953) notes the thickness of the formation increases toward the east and that distinguishing individual formations east of the Whangehu Valley is inhibited by extensive landslides and lateral facies variation.

Te Punga (1952) defined the Potaka Pumice in his geological survey of the Rangitikei District. Describing a strongly current-bedded 18 m thick pumice unit with clasts between 50–180 mm in diameter, clearly exposed in the cliffs of the Rangitikei, north of the confluence with Waitapu Stream (Fig. 4.2: BP 485).

Seward (1976) correlated the Potaka Pumice of Te Punga (1952) to the Kaimatira Pumice Sand Formation. Documenting similar ferromagnesian mineral assemblages and chemistry between samples at the type section of Potaka Pumice on Rewa Hill (Fig. 4.2) and the type section of the Kaimatira Pumice Sand Formation at Kaimatira Bluff (Fig. 4.1). Originally, both Rewa Pumice and Potaka Pumice were included within the Kaimatira Pumice Sand Formation (Seward 1976). However, following additional geochemical analysis of the Kaimatira Bluff and Rewa Hill type sections (Pillans et al. 2005) it was found that Rewa Pumice is absent from the Kaimatira Pumice Sand Formation type section in Whanganui, resulting in a necessary subdivision. The Kaimatira Pumice Sand Formation is now defined by the first influx of Potaka Pumice into the Whanganui Basin succession (Table 4.1).

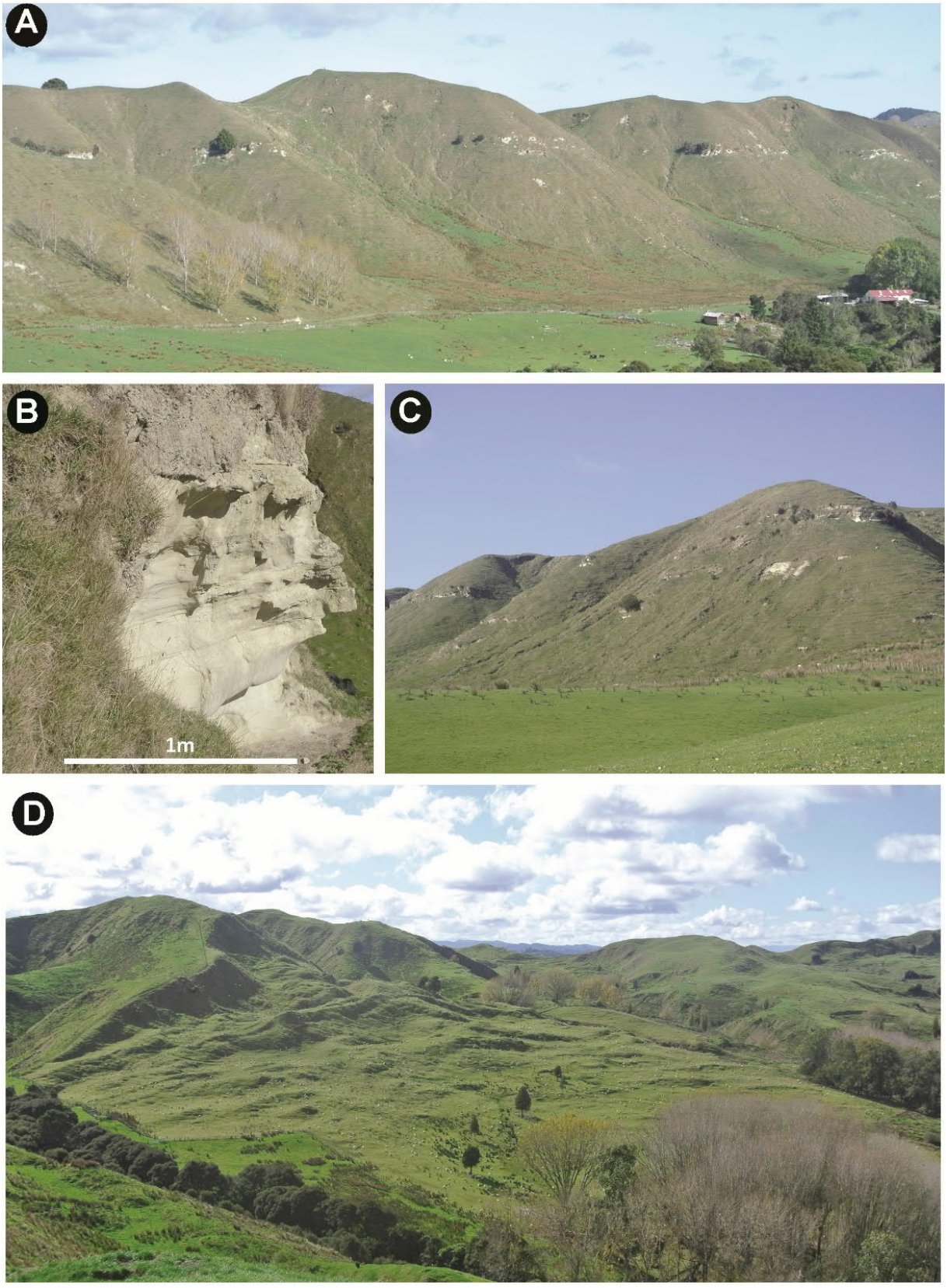
We sampled Potaka Pumice at the Coutts Creek and Beaconsifield Valley sections (Fig. 4.3 and Fig. 4.5), mapping the horizon between the Turakina (Deepdem Conglomerate of van der Neut, 1996), Rangitikei and Oroua sections (Fig. 4.2). Considerable effort was placed on finding the first influx of Potaka glass chemistry at the Coutts Creek locality to establish group and formation boundaries within this area. The localities on Taurimu Road (Fig. 4.2: CR-32) described by Hellstrom (1993) and van der Neut (1996) are supported by our work as containing the first influx of Potaka Pumice. Substantial landslides off the scarp slope above Mangara Stream (Fig. 4.2) where the terrace country suddenly gives way to broken hill country need to be treated with caution. Rock rotational slides of Kaimatira Pumice Sand Formation frequent the base of this scarp slope. However, logging and sampling

of insitu material along Ngaruru Road (Fig. 4.2: CR-52, CR-53) indicates the area is underlain by Rewa Formation (Fig. 4.5, Coutts Creek Composite).

Shane (1991) and Rees et al. (2018b) have documented Potaka Pumice in the Manawatu and Pohangina valleys, enabling correlation of local stratigraphic units to the Kaimatira Pumice Sand Formation of Fleming (1953). Potaka Pumice has also been found cropping out across the Pohangina-Oroua interfluve (Brackley 1999), where it is able to be traced as a mappable unit across the Pohangina Anticline westward to the Oroua River. This horizon correlates to the Kimbolton Ash horizon mapped by Feldmeyer et al. (1943). Here we adopt Seward's (1976) correlation of the Kimbolton Ash to Potaka Pumice without emendation. We note substantial lateral facies variation within the Potaka Pumice moving east from the Turakina toward the Oroua Valley, including a marked increase in the concentration of glass, thickness of the basal unit (up to 10 m) and the prominence it attains in the landscape (Fig. 4.4 E).

Although Seward's (1976) initial ages for the pumiceous sands mapped by Rich (1959) south of the Manawatu Gorge (Fig. 4.1) were substantially younger than the c. 1 Ma Potaka Pumice, we suggest here a strong likelihood that the band of Castlecliffian volcaniclastics mapped along the Pohangina Monocline (Rees et al. 2018b) continue to the south, east of Palmerston North (Rich 1959). This correlation is solely based on stratigraphic position and mapping conducted farther north.

Figure 4.7 (facing page): A) Coutts Creek Horizon cropping out along the southern scarp slope of Coutts Creek, approximately 15km North of the township of Marton (BL34 2539 7275). B) Close up of Coutts Creek Horizon at the Coutts Creek locality. C) Coutts Creek Horizon forming a conspicuous ledge in the landscape, note the vegetation growing along the ledge, accentuating its position on the slope D) An example of a rock planar slide on a gentle southern dip slope, northern side of Coutts Creek, Rangitikei District (BL34 0862 7724).


A
B
1m
C
D

Coutts Creek Horizon – Rewa Formation

Feldmeyer et al. (1943) mapped the Coutts Creek Horizon west from Hunterville into the Makirikiri Valley, 10 km NE of Whanganui (Fig. 4.1). They described 45 m of very fine, interbedded tephric sand and silt that is hard and well consolidated, resulting in good exposure (Fig. 4.7). The succession thins from Rangitikei west toward Whanganui, with the stratigraphic distance between the Coutts Creek Horizon and the underlying Pakihikura Pumice reducing from c. 180 to 90 m respectively. West of Whanganui, the horizon becomes unmappable, merging laterally into siliciclastic sediments of the upper Okehu Siltstone, western Whanganui Basin.

In this study, we logged Coutts Creek and adjacent sections forming a composite column (Fig. 4.5) and correlating samples to the published geochemical datasets of Pillans et al. (2005) (Fig. 4.3). The Coutts Creek Horizon is particularly well exposed, especially considering the nature of the heavily eroded country it crosses (Fig. 4.7 D). This horizon typically outcrops on the steep northern scarp slopes, where the strata are dipping south, into the slope. The southern dip slopes in comparison are characterised by extensive landslides, related to bedding plane failures within the gently dipping strata.

Coutts Creek horizon was initially incorporated into the Kaimatira Pumice Sand Formation by Fleming (1953) and Seward (1976). However, the designated type section of the Kaimatira Pumice Sand Formation near Whanganui is defined by the first influx of Potaka glass chemistry into the Whanganui Basin (Hellstrom 1993; Pillans et al. 2005; Rees et al. 2018b). The first influx of Potaka Pumice occurs c. 120 m above the Coutts Creek Horizon in the Coutts Creek succession. EPMA analysis of tephric silts from Coutts Creek are correlated to Rewa glass chemistry (Fig. 4.3 E). The first occurrence of Mactra (Maorimactra) carteri occurs

30 m below Coutts Creek horizon. Therefore, we suggest Coutts Creek Horizon falls within the Rewa Formation, Okehu Group (Table 4.1).

Makirikiri Tuff Formation – Pakihikura Pumice

Fleming (1953) originally proposed Makirikiri Tuff Formation for the basal Castlecliffian ash of Feldmeyer et al. (1943), reasoning that the use of 'Castlecliff' for a deposit that does not crop out at Castlecliff would be undesirable. Fleming (1953) also suggested the use of the term 'tuff' would be more suitable than 'ash', a sentiment reflected in later papers by Schmid (1981) and Froggatt and Lowe (1990). The formation was described as white, fine to medium-grained tephric sands interfingering with lenses of coarse, pebbly sand and conglomerate. Fleming (1953) described the Makirikiri Tuff Formation as the eastern correlative of the Butlers Shell Conglomerate. These two units interfinger with one another in the Okehu Stream area before the shell conglomerate is completely replaced by Makirikiri Tuff Formation in the Whanganui River Valley near Makirikiri Valley (Fig. 4.1). The base of the Makirikiri Tuff Formation was noted to be unconformable, similar to the Butlers Shell Conglomerate. The Makirikiri Tuff Formation thickens to the east, reflecting the location of the paleo-depocentre.

Difficulties have arisen from the application of stratigraphic nomenclature based on type sections near Whanganui to a succession that thickens and becomes somewhat more complete to the east. The presence of a long-lived 450 ka unconformity at the base of the Okehu Group, Whanganui type section, not present to the same extent in eastern Whanganui Basin, requires acknowledgment and suitable provision for regional mapping. We suggest here all groups introduced by Fleming (1953) are retained, with a simple redefinition of group boundaries within the central and eastern Whanganui Basin to incorporate new stratigraphic data gathered over the past 65 years. We adopt Pakihikura Pumice (base of Makirikiri

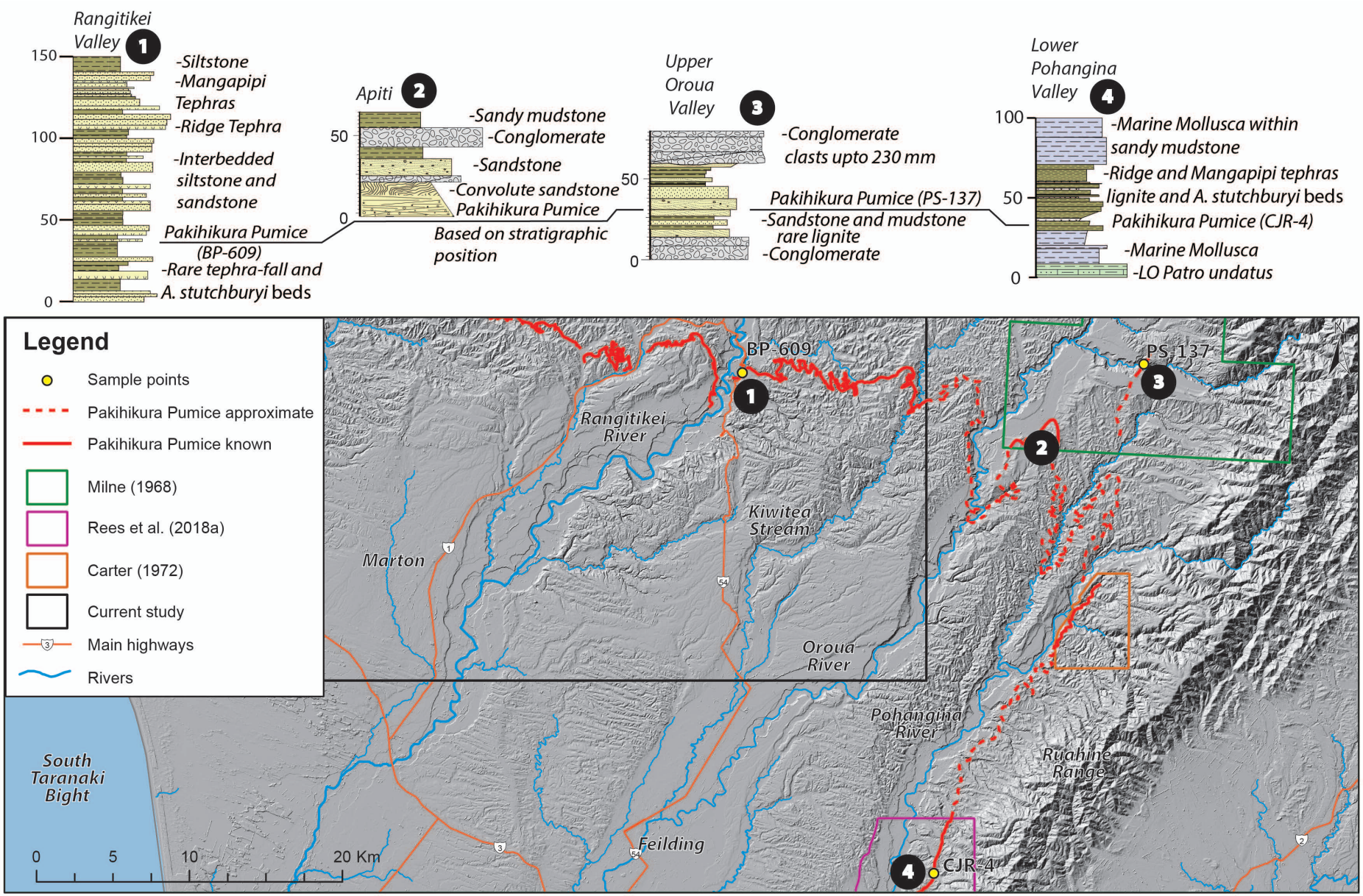
Tuff Formation) as the base of the Okehu Group as originally suggested by Fleming (1953) (Table 4.1).

This redefinition results in Okehu Group encompassing a considerably thicker succession in the east, covering all strata from Pakihikura Pumice to Potaka Pumice. This allows Seward's (1976) correlation of Pakihikura Pumice, Ridge and Mangapipi tephras to Makirikiri Tuff Formation to be retained, however, necessitates an amendment of Seward's (1976) definition of Kaimatira Pumice Sand Formation from including Rewa Pumice to being defined by the first influx of Potaka Pumice. Rewa Pumice is then suggested to be placed within its own formation bridging the Makirikiri Tuff Formation and Kaimatira Pumice Sand Formation (Table 4.1).

Paleogeographic interpretation

The first influx of fluvial conglomerate within the Whanganui Basin succession occurs progressively earlier toward the east. The conglomerates become increasingly frequent, thicker (10–200 m) and are associated with heterolithic intervals devoid of any marine fossils, including the common occurrence of lignite, wood, and siltstone beds dominated entirely by small, stunted *Austrovenus stutchburyi*. This pattern within the succession is known to continue and become more dramatic within the upper Oroua catchment, where Feldmeyer et al. (1943), Milne (1968), Seward (1974b) and Shane et al. (1996) note the occurrence of conglomerate above and below the Pakihikura Pumice (Fig. 4.8). Feldmeyer et al. (1943) and Milne (1968) who mapped this upper portion of the Oroua Valley in detail suggest the conglomerates become increasingly prominent toward the

Figure 4.8 (facing page): Regional correlation of the Pakihikura Pumice toward the main axial range. Data, including the geochemical data from CJR-4, PS-137 and BP-609 are sourced from Milne (1968), Carter (1972), Shane et al. (1996), Pillans et al. (2005), Rees et al. (2018) and this study.


Rangitikei Valley
1
150
100
50
0
-Siltstone
-Mangapipi Tephras
-Ridge Tephra
-Interbedded siltstone and sandstone
Pakihikura Pumice (BP-609)
-Rare tephra-fall and A. stutchburyi beds
Apiti
2
50
0
-Sandy mudstone
-Conglomerate
-Sandstone
-Convolute sandstone
Pakihikura Pumice
Based on stratigraphic position
Upper Oroua Valley
3
50
0
-Conglomerate clasts upto 230 mm
Pakihikura Pumice (PS-137)
-Sandstone and mudstone rare lignite
-Conglomerate
Lower Pohangina Valley
4
100
50
0
-Marine Mollusca within sandy mudstone
-Ridge and Mangapipi tephras lignite and A. stutchburyi beds
Pakihikura Pumice (CJR-4)
-Marine Mollusca
-LO Patro undatus
Legend
Sample points
Pakihikura Pumice approximate
Pakihikura Pumice known
Milne (1968)
Rees et al. (2018a)
Carter (1972)
Current study
Main highways
Rivers
BP-609
PS-137
CJR-4
Rangitikei River
Kiwitea Stream
Marton
Oroua River
Pohangina River
Ruahine Range
Feilding
South Taranaki Bight
0
5
10
20 Km

Ruahine Range reaching thicknesses of c. 200 m. The conglomerates described in this area have an erosive lower contact cut into the underling sediments, large clasts (up to 230 mm) and grade upward into strongly current bedded pebbly sandstones with rare interbedded lignite (Milne 1968).

We suggest the conglomerates recognised in the upper Oroua Valley are part of a shared facies to those we document in the Rangitikei and Beaconsfield Valley successions (Fig. 4.4 B and Fig. 4.6), interfingering with the dominantly marine Whanganui Basin succession from a northeast direction. We interpret the common intercalated siltstone and lignite, channel cut and fill and total absence of marine fossils within these conglomerates to be typical of terrestrial deposits, characteristic of a braided alluvial plain system.

The first influx of fluvial conglomerate within the Whanganui Basin between the Whanganui and Rangitikei rivers does not occur until Toms Conglomerate, Shakespeare Group (c. 0.6 Ma); whilst in the Oroua Valley we have evidence for influxes as early as c. 1.6 Ma (Fig. 4.8). This trend is confirmed in the Pohangina Valley, where a change to non-marine sedimentation occurs at c. 1.6 Ma. We suggest progressive influxes of coarse greywacke detritus were intermittently prograding southwestwards into the Whanganui Basin during sea level low stands, likely forming an alluvial plain about the emergent base of the paleo-axial ranges. Low stand periods being characterised by a lowering of the tree line in the ranges, increased mechanical breakdown and erosion, overloading of river headwaters with detritus and fluvial aggradation (Palmer & Pillans 1996). Incision of the Whanganui Basin fill occurred during marine transgression, as the climate warmed, erosion rates lowered in headwater catchments and paleo-rivers formed localised valleys that retreated landward as sea level continued to rise. Substantial erosion and reworking is evidenced by common rip up clasts, channels and erosive contacts (Fig. 4.6). Progressive flooding of the eastern basin margin during marine transgression and high stand infilled local valley systems, such that they were

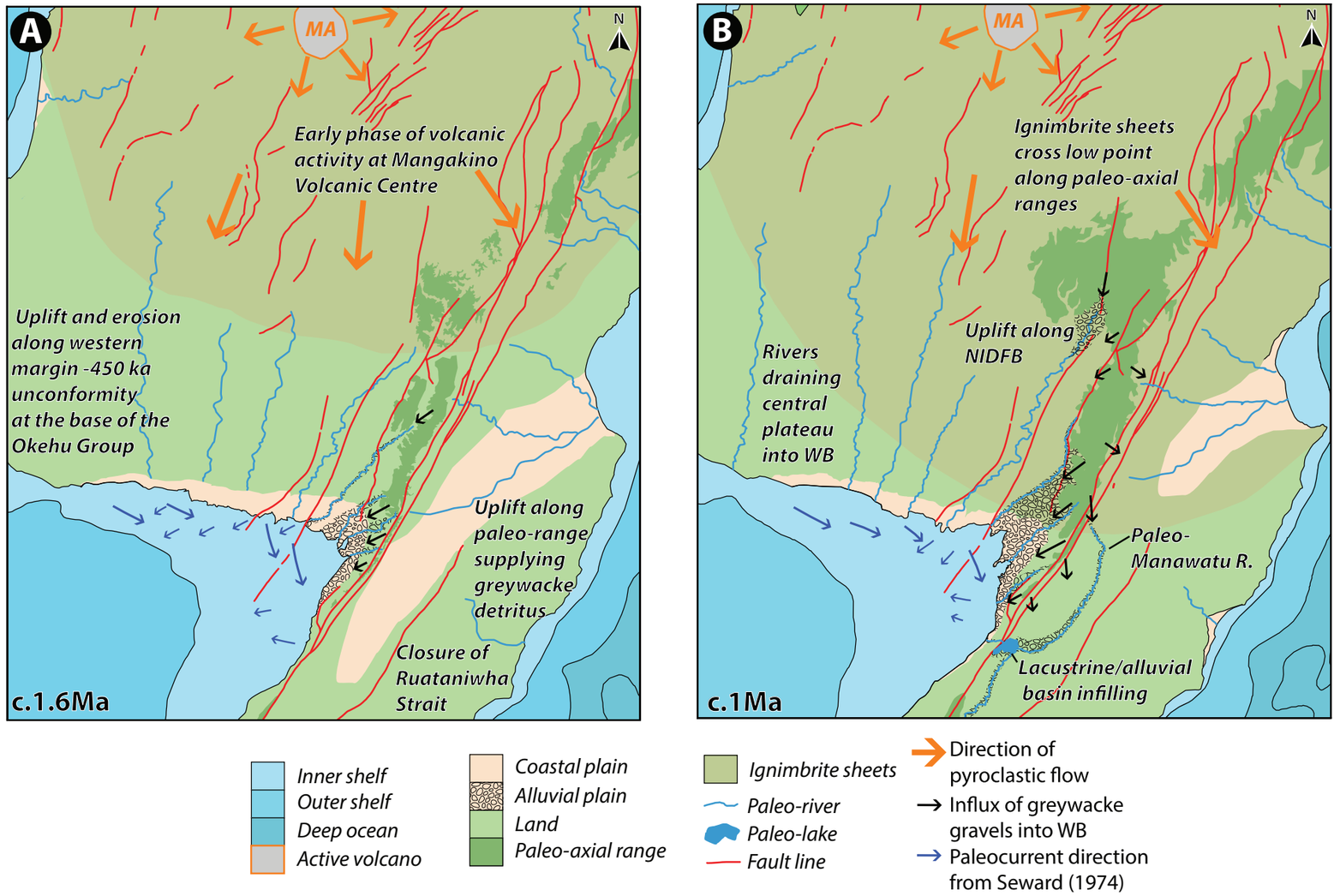


Figure 4.9: A) Cartoon schematic of lower North Island at c. 1.6 Ma, during an early phase of large-scale rhyolitic eruptions from Mangakino Caldera (MA). Uplift along the paleo-axial range to the east and the western margin of the Whanganui Basin occurs during this time resulting in interbedded conglomeratic and volcaniclastic units being deposited within eastern Whanganui Basin and formation of a long-lived 450 ka unconformity in the western Whanganui Basin. B) Cartoon schematic of lower North Island at c. 1 Ma, during emplacement of Rocky Hill and Cape Kidnappers ignimbrites from Mangakino Caldera (MA). Sources of information include (Seward 1974; Beu 1995; King & Thrasher 1996; Field et al. 1997; King 2000; Kamp et al. 2004; Kamp & Furlong 2006; Bunce et al. 2009; Cooper et al. 2012; Trewick & Bland 2012; Downs et al. 2014; Gravley et al. 2016). Cartoons depict sea level highstands.

transient, short-lived features on a shallow gradient coastline. Heterolithic deposition occurred within coastal plain to marginal margin environments, including common back swamp environments where preservation of organic matter and tephra-fall beds occurred (Fig. 4.4 F).

A partially emergent, alluvial and coastal plain along the Whanganui Basin's eastern margin during Castlecliffian time (Fig. 4.9) is consistent with strata observed in the lower Pohangina Valley (Rees et al. 2018b; Rees et al. 2018a), Ruahine Range (MacDonald-Creevey 2011) and Kuripapango (Browne 2004) suggesting uplift of the North Island axial range began as early as Late Miocene time. Uplift along the Whanganui Basin's eastern margin has resulted in pulses of greywacke detritus prograding into local eastern depocentres (Rees et al. 2018a). We suggest uplift in the axial range occurred contemporaneously with commencement of volcanic activity at the Mangakino Volcanic Centre c. 1.6 Ma. Such that the first influxes of fluvial conglomerate and volcaniclastics occur in close proximity within the eastern Whanganui Basin succession. The intercalation of siliciclastic and volcaniclastic sediment along the modern range front provides important constraint on the timing of uplift within the paleo-axial range.

4.7 Conclusion

The eastern Whanganui Basin contains a Pleistocene record of sedimentation along the emerging margin of the Whanganui Basin and paleo axial-range. Tephra-fall and volcaniclastic deposits provide useful chronostratigraphic marker horizons, enabling correlation between sections within the Whanganui Basin.

Lateral changes in sedimentary preservation across the Whanganui Basin have led to difficulties with correlation, resulting in nomenclatural issues. We present a revised version of the Whanganui Basin stratigraphic nomenclature, enabling

historic precedence to be maintained, whilst incorporating modern techniques and new datasets. We correlate Coutts Creek Horizon to Rewa Formation and formally propose Okehu Group to cover all strata from Pakihikura to Potaka Pumice. We recommend Rewa Pumice is placed within its own formation bridging the Makirikiri Tuff Formation and Kaimatira Pumice Sand Formation.

Influxes of conglomeratic and carbonaceous rich heterolithic facies within the basin succession are interpreted to be a feature of an alluvial and coastal plain adjacent to the paleo-axial range. The first influx of fluvial conglomerate occurs shortly before the Pakihikura Pumice (c. 1.6 Ma) within the upper Oroua catchment, whilst within the Rangitikei there is a delay until around Toms Conglomerate (c. 0.6 Ma). We suggest gravels derived from uplifting basement in the position of the main axial range were entering the Whanganui Basin from the northeast. Sea level low stands being characterised by aggradation and progradation of broad fans of greywacke gravel forming an apron of sediment about the paleo-axial range front. Marine transgression is characterised by a warmer climate, reduction of erosion in headwater catchments and fluvial incision into and reworking of LST deposits. Landward migration of the coastal plain and fluvial distributary systems during rising sea level resulted in sedimentary infilling of channels and valleys. We suggest uplift in the main axial range occurred contemporaneously with the onset of volcanic activity at Mangakino caldera, so that the first influxes of fluvial conglomerate and volcaniclastics occur in close proximity within the eastern Whanganui Basin succession.

Acknowledgements

We thank the residents in the Rangitikei and Manawatu districts for granting land access. This work is part of an overarching PhD project on the groundwater of the Pourewa Stream undertaken by CJR. Thanks are extended to Dr Ranvir Singh and Dr John Begg for the support and direction given during the course of this research.

References

Abbott ST 1992. The Mid Pleistocene Waiomio Shellbed (Castlecliffian, c. 550-600 ky), Wanganui Basin, New Zealand. Alcheringa: An Australasian Journal of Palaeontology 16(2): 171-180.

Abbott ST 1994. Sequence Stratigraphy, Sedimentology and Paleoecology of Pleistocene Cyclothems in the Castlecliff Section, Wanganui Basin, New Zealand, Unpublished PhD Thesis. James Cook University of Northern Queensland, Australia. 297 p.

Alloway BV, Pillans BJ, Sandhu AS, Westgate JA 1993. Revision of the marine chronology of the Wanganui Basin, New Zealand, based on the isothermal plateau fission-track dating of tephra horizons. Sedimentary Geology 82(1-4): 299-310.

Anderton PW 1981. Structure and evolution of the South Wanganui Basin, New Zealand. New Zealand Journal of Geology and Geophysics 24(1): 39-63.

Beu AG 1995. Pliocene limestones and their scallops. Lithostratigraphy, pectinid biostratigraphy and paleogeography of eastern North Island late Neogene limestone. Institute of Geological and Nuclear Sciences Monograph 10(68): 1-243.

Beu AG 2006. Marine Mollusca of oxygen isotope stages of the last 2 million years in New Zealand. Part 2 . Biostratigraphically useful and new Pliocene to recent bivalves. Journal of the Royal Society of New Zealand 36(4): 151-338.

Boellstorff JD, Te Punga MT 1977. Fission track age and correlation of middle and lower Pleistocene sequences from Nebraska and New Zealand. New Zealand Journal of Geology and Geophysics 20: 47-58.

Brackley H 1999. The Stratigraphy and Environments of Deposition of Early-Mid Pleistocene Sediments of the Pohangina Region, Eastern Wanganui Basin, New Zealand., Unpublished MSc thesis, Massey University, Palmerston North, New Zealand. 113 p.

Browne GH 1986. Basement-cover relationships and tectonic significance of Mt Miroroa, western Hawke's Bay. Journal of the Royal Society of New Zealand 16(4): 381-402.

Browne GH 2004. Late Neogene sedimentation adjacent to the tectonically evolving North Island axial ranges: Insights from Kuripapango, western Hawke's Bay. New Zealand Journal of Geology and Geophysics 47(4): 663-674.

Bussell MR 1984. Geology and Paleobotany of the Rangitawa Stream area, Southeast Wanganui Basin, Unpublished BSc (Hons) Thesis. Victoria University of Wellington, Wellington, New Zealand. 181 p.

Carter L, Shane PAR, Alloway BV, Hall IR, Harris SE, Westgate JA 2003. Demise of one volcanic zone and birth of another - A 12 m.y. marine record of major rhyolitic eruptions from New Zealand. Geology 31(6): 493-496.

Cooper GF, Morgan DJ, Wilson CJN 2017. Rapid assembly and rejuvenation of a large silicic magmatic system: Insights from mineral diffusive profiles in the Kidnappers and Rocky Hill deposits, New Zealand. Earth and Planetary Science Letters 473: 1-13.

Downs DT, Wilson CJN, Cole JW, Rowland JV, Calvert AT, Leonard GS, Keall JM 2014. Age and eruptive center of the Paeroa Subgroup ignimbrites (Whakamaru Group) within the Taupo Volcanic Zone of New Zealand. Geological Society of America Bulletin 126(9/10): 1131-1144.

Feldmeyer AE, Jones BC, Firth CW, Knight J 1943. The geology of the Palmerston-Wanganui Basin, "West side", North Island, New Zealand. Unpublished Report of the Superior Oil Company of New Zealand, Petroleum Report Series 171, Ministry of Economic Development, Wellington, New Zealand. 46 p.

Fleming CA 1953. The geology of Wanganui subdivision. New Zealand Geological Survey Bulletin 52. Wellington, New Zealand. 362 p.

Froggatt PC, Lowe DJ 1990. A review of late Quaternary silicic and some other tephra formations from New Zealand: their stratigraphy, nomenclature, distribution, volume, and age. New Zealand Journal of Geology and Geophysics 33: 89-109.

Gravley DM, Deering CD, Leonard GS, Rowland JV 2016. Ignimbrite flare-ups and their drivers: A New Zealand perspective. Earth-Science Reviews 162: 65-82.

Hellstrom JC 1993. An investigation of the Galpin Fault, Marton, Rangitikei Unpublished BSc (Hons) Thesis. Victoria University of Wellington, Wellington, New Zealand. 89 p.

Jarosewich E, Nelen JA, Norberg JA 1980. Reference Samples for Electron Microprobe Analysis. Geostandards Newsletter 4(1): 43-47.

Jochum KP, Stoll B, Herwig K, Willbold M, Hofmann AW, Amini M, Aarburg S, Abouchami W, Hellebrand E, Mocek B and others 2006. MPI-DING reference glasses for in sity microanalysis: New reference values for element concentrations and isotope ratios. Geochemistry, Geophysics, Geosystems 7(2): 1-44.

Krippner SJP, Briggs RM, Wilson CJN, Cole JW 1998. Petrography and geochemistry of lithic fragments in ignimbrites from the Mangakino Volcanic Centre: Implications for the composition of subvolcanic crust in western Taupo Volcanic Zone, New Zealand. New Zealand Journal of Geology and Geophysics 41(2): 187-199.

Lee JM, Bland KJ, Townsend DB, Kamp PJJ, (compilers) 2011. Geology of the Hawke's Bay area. Institue of Geological & Nuclear Sciences 1:250,000 geological map 8. Lower Hutt, New Zealand. GNS Science. 1 sheet + 93 p.

Lowe DJ 2011. Tephrochronology and its application: A review. Quaternary Geochronology 6: 107-153.

MacDonald-Creevey AM 2011. Late Holocene environmental record and geological history of the Lake Colenso area, North-western Ruahine Range, New Zealand. Unpublished MSc thesis, Massey University, Palmerston North, New Zealand. 159 p.

Marden M, Neall VE 1990. Dated Ohakean terraces offset by the Wellington Fault , near Woodville , New Zealand. New Zealand Journal of Geology and Geophysics 33(3): 449-453.

Melhuish A, van Dissen R, Berryman KR 1996. Mount Stewart-Halcombe Anticline: A look inside a growing fold in the Manawatu region, New Zealand. New Zealand Journal of Geology and Geophysics 39: 123-133.

Milne JDG 1968. The geology and soils of the Apiti District. Unpublished MSc thesis, Victoria Universtiy of Wellington, New Zealand. 122 p.

Milne JDG 1973a. Mount Curl Tephra , a 230000-year-old implications for quaternary chronology marker bed in New Zealand, and its implications for Quaternary Chronology. New Zealand Journal of Geology and Geophysics 16(3): 519-532.

Milne JDG 1973b. Upper Quaternary geology of the Rangitikei drainage basin, North Island, New Zealand. Unpublished PhD Thesis. Victoria University of Wellington, Wellington, New Zealand. 472 p.

Naish TR, Kamp PJJ 1995. Pliocene-Pleistocene marine cyclothems , Wanganui Basin , New Zealand : a lithostratigraphic framework. New Zealand Journal of Geology and Geophysics 38: 223-243.

Naish TR, Kamp PJJ, Alloway BV, Pillans BJ, Wilson GS, Westgate JA 1996. Integrated tephrochronology and magnetostratigraphy for cyclothemic marine strata, Wanganui Basin: Implications for the Pliocene-Pleistocene boundary in New Zealand. Quaternary International 34-36(95): 29-48.

Naish TR, Abbott ST, Alloway BV, Beu AG, Carter RM, Edwards AR, Journeaux TD, Kamp PJJ, Pillans BJ, Saul G and others 1998. Astronomical calibration of a southern hemisphere Plio-Pleistocene reference section, Wanganui Basin, New Zealand. Quaternary Science Reviews 17(8): 695-710.

Naish TR, Field BD, Zhu H, Melhuish A, Carter RM, Abbott ST, Edwards S, Alloway BV, Wilson GS, Niessen F and others 2005. Integrated outcrop, drill core, borehole and seismic stratigraphic architecture of a cyclothemic, shallow marine depositional system, Wanganui Basin, New Zealand. Journal of the Royal Society of New Zealand 35(1-2): 91-122.

Palmer AS, Pillans BJ 1996. Record of Climatic Fluctuations from ca. 500 Ka Loess Deposits And Paleosols Near Wanganui, New Zealand. Quaternary International 34-36: 155-162.

Pillans B, Kohn B 1981. Rangitawa Pumice: a widespread (?) Quaternary marker bed in Taranaki-Wanganui. Victoria University of Wellington Geology Department Publication 20: 94-104.

Pillans BJ 1994. Direct marine-terrestrial correlations, Wanganui Basin, New Zealand: The last 1 million years. Quaternary Science Reviews 13(3): 189-200.

Pillans BJ, Roberts AP, Wilson GS, Abbott ST, Alloway BV 1994. Mangnetostratigraphic, lithostratigraphic and tephrostratigraphic constraints on Lower and Middle Pleistocene sea-level changes, Wanganui Basin, New Zealand. Earth and planetary science letters 121: 81-98.

Pillans BJ, McGlone M, Palmer A, Mildenhall D, Alloway B, Berger G 1993. The Last Glacial Maximum in central and southern North Island, New Zealand: a paleoenvironmental reconstruction using the Kawakawa Tephra Formation as a chronostratigraphic marker. Palaeogeography, Palaeoclimatology, Palaeoecology 101(3): 283-304.

Pillans BJ, Alloway B, Naish TR, Westgate J, Abbott S, Palmer AS 2005. Silicic tephras in Pleistocene shallow-marine sediments of Wanganui Basin, New Zealand. Journal of the Royal Society of New Zealand 35(1-2): 43-90.

Potter WD 1984. Upper Quaternary Geology of part of the lower Rangitikei Valley, Unpublished BSc (hons) Thesis. Victoria University of Wellington, Wellington, New Zealand. 84 p.

Rees CJ, Palmer JA, Palmer AS 2018a. Plio-Pleistocene Geology of the Lower Pohangina Valley, New Zealand. New Zealand Journal of Geology and Geophysics 61(1): 44-63.

Rees CJ, Palmer JA, Palmer AS 2018b. Gilbert-Style Pleistocene Fan Delta Reveals Tectonic Development of North Island Axial Ranges, New Zealand. New Zealand Journal of Geology and Geophysics 61(1): 64-78.

Rich CC 1959. Late Cenozoic geology of the lower Manawatu valley , New Zealand. Harvard University, Cambridge, Massachusetts, USA. 188 p.

Saul G, Naish TR, Abbott ST, Carter RM 1999. Sedimentary cyclicity in the marine Pliocene-Pleistocene of the Wanganui basin (New Zealand): Sequence stratigraphic motifs characteristic of the past 2.5 m.y. Geological Society Of America Bulletin 111(4): 524-537.

Schmid R 1981. Descriptive nomenclature and classification of pyroclastic deposits and fragments: Recommendations of the IUGS Subcommission on the Systematics of Igneous Rocks. Geology 9: 41-43.

Seward D 1974a. Age of New Zealand Pleistocene substages by fission-track dating of glass shards from tephra horizons. Earth and planetary science letters 24(2): 242-248.

Seward D 1974b. Some Aspects of Sedimentology of the Wanganui Basin, North Island, New Zealand., Unpublished PhD thesis, Victoria University of Wellington, Wellington, New Zealand. 285 p.

Seward D 1976. Tephrostratigraphy of the marine sediments in the Wanganui Basin , New Zealand. New Zealand Journal of Geology and Geophysics 19(1): 9-20.

Seward D 1978. Palaeosalinities and palaeotemperatures from carbon and oxygen isotopes of carbonate shells in three Quaternary formations, Wanganui Basin, New Zealand. Palaeogeography, Palaeoclimatology, Palaeoecology(23): 47-55.

Seward D 1979. Comparison of zircon and glass fission-track ages from tephra horizons. Geology 7(10): 479-482.

Seward D, Lienert B 1986. Magnetic polarity stratigraphy of a Plio- Pleistocene marine sequence of North Island , New Zealand. Earth and Planetary Science Letters 80(3-4): 353-360.

Shane PA, Black TM, Alloway BV, Westgate JA 1996. Early to middle Pleistocene tephrochronology of North Island, New Zealand: implications for volcanism, tectonism, and paleoenvironments. Geological Society of America Bulletin 108(8): 915-925.

Shane PAR 1991. Remobilised silicic tuffs in middle Pleistocene fluvial sediments , southern North Island, New Zealand. New Zealand Journal of Geology and Geophysics 34(4): 489-499.

Shane PAR 1993. Tephrostratigraphy, magnetostratigraphy and geochronology of some early and middle Pleistocene deposits in New Zealand, Unpublished PhD Thesis. Victoria University of Wellington, Wellington, New Zealand. 136 p.

Shane PAR, Froggatt PC 1991. Glass chemistry, paleomagnetism, and correlation of middle Pleistocene tuffs in southern North Island, New Zealand, and Western Pacific. New Zealand Journal of Geology and Geophysics 34: 203-211.

Shane PAR, Walter R, Froggatt P 1992. 40Ar/39Ar ages of Pleistocene silicic tephras in New Zealand: implications for the age of the Jaramillo Subchron. Geological Society of New Zealand Miscellaneous Publication 63A: 1-139.

Stevens KF, Vella P 1981. Paleoclimatic interpretation of stable isotope ratios in molluscan fossils from Middle Pleistocene marine strata, Wanganui, New Zealand. Palaeogeography, Palaeoclimatology, Palaeoecology 34: 257-265.

Te Punga MT 1952. The geology of Rangitikei Valley. New Zealand Geological Survey Memoir 8, Wellington, New Zealand. 46 p.

Te Punga Mt 1953. A late Pleistocene land bridge across Cook Strait, New Zealand. NZ Journal of Science and Technology(35): 161-192.

Te Punga MT 1957. Live anticlines in western Wellington. New Zealand Journal of Science and Technology(38): 433-466.

Townsend D, Vonk A, Kamp PJJ 2008. Geology of the Taranaki area: scale 1:250,000. Lower Hutt, GNS Science. Institute of Geological and Nuclear Sciences 1:250,000 geological map 7, Lower Hutt, New Zealand: 1 sheet+77p.

Turner GM, Kamp PJJ 1990. Palaeomagnetic location of the Jaramillo Subchron and the Matuyama-Brunhes transition in the Castlecliffian stratotype section, Wanganui Basin, New Zealand. Earth and Planetary Science Letters 100(1-3): 42-50.

Turner GM, Kamp PJJ, McIntyre AP, Hayton S, McGuire DM, Wilson GS 2005. A coherent middle Pliocene magnetostratigraphy, Wanganui Basin, New Zealand. Journal of the Royal Society of New Zealand 35(1-2): 197-227.

van der Neut M 1996. Sequence Stratigraphy of Plio-Pleistocene Sediments in Lower Turakina Valley, Wanganui Basin, New Zealand. Unpublished MSc Thesis. Massey Univeristy, Palmerston North, New Zealand. 149 p.

Vella P 1963. Upper Pleistocene succession in the inland part of Wairarapa valley, New Zealand. Transactions of the Royal Society of New Zealand. Geology 2: 63-78.

Wilson CJN, Rowland JV 2016. The volcanic, magmatic and tectonic setting of the Taupo Volcanic Zone, New Zealand, reviewed from a geothermal perspective. Geothermics 59: 168-187.

Wilson CJN, Rowland JV, Gravley DM 2008. The Taupo Volcanic Zone, New Zealand: A Geological and Geophysical Review with an Emphasis on its Central Segment. Institue of Earth Science and Engineering, University of Auckland, New Zealand, Report 2-2008.06: 1-134.

Wilson CJN, Gravley DM, Leonard GS, Rowland JV 2009. Volcanism in the central Taupo Volcanic Zone, New Zealand: temp, styles and controls. In: Thordarson T, Self S, Larsen G, Rowland SK, Hoskuldsson A ed. Studies in Volcanology: The Legacy of George Walker, Special Publications of IAVCEI, Geological Society, London, United Kingdom. Pp. 225-247.

Wolfe KJ 1987. The geology of the Turakina-Whangaehu interfluve. Unpublished Honours Thesis. Victoria University of Wellington, Wellington, New Zealand. 118 p.



Chapter 5

Sedimentology

The following chapter contains a peer-reviewed journal article published in the New Zealand Journal of Geology and Geophysics, Volume 62, Issue 2. The focus of this paper is to document the Waitapu Shell Conglomerate. We follow this marker horizon laterally across the landscape, unravelling a single slice through geological time to demonstrate:

- Tephrostratigraphy
- Facies analysis
- Variability within the basin fill
- Wider paleogeographic implications

This chapter provides important data for interpreting the local and regional groundwater system, volcaniclastic processes and basin history. The Waitapu Shell Conglomerate represents a single example of a transgressive aquifer deposit within the Whanganui Basin's Pleistocene succession. We continue to explore these deposits within Chapter 7, where rapid *in situ* analysis allows a glimpse into their complexity. Chapter 5 satisfies thesis objectives four and five by supporting the development of our conceptual hydrogeological model and illustrating a regional application within a basin wide context.

View west across the Rangitikei Valley, taken opposite Rathmoy Station. Remnant cut-off spur of Bulls Terrace can be seen in middle ground below the Ohakean 3 terrace.

Whanganui Basin, an archive of prehistoric earthquakes?

Waitapu Shell Conglomerate (c. 0.9 Ma), North Island New Zealand

Callum Rees[1], Julie Palmer[1], and Alan Palmer[1]

[1]*Environmental Sciences, School of Agriculture and Environment, Massey University, Palmerston North, New Zealand*

5.1 Abstract

The Waitapu Shell Conglomerate is an important marker horizon in the eastern Whanganui Basin, occurring within a Pleistocene volcaniclastic record that contains early eruption products from the Taupo Volcanic Zone. The unit comprises a cross-bedded pebbly-shell conglomerate containing the first influx of Kaukatea Pumice (c. 0.9 Ma) within the Rangitikei succession. We document soft sediment deformation structures that occur in close stratigraphic proximity to the Waitapu Shell Conglomerate and other laterally equivalent units within the basin's Castlecliffian outcrop belt. Soft sediment deformation structures formed through a combination of liquefaction and fluidisation, triggered by a range of mechanisms, including evidence of high sedimentation rates, loading, slope instability and potential for wave and earthquake induced seismicity. Lateral changes in depositional style toward the basins eastern margin relate to relative position on the paleo-shelf, reduction of accommodation space, intermittent preservation of low stand deposits and proximity to the uplifting paleo-axial range.

Keywords: Pleistocene, Castlecliffian, biostratigraphy, Whanganui Basin, seismicity, liquefaction, fluidisation, submarine landslides, loading

5.2 Introduction

The formation of soft sediment deformation structures (SSDS) is typically associated with rapid sedimentation, where loading of water-saturated sediments results in expulsion of water and deformation of bedding (Bailey & Carr 1994; Manville et al. 2005; Owen & Moretti 2011). These structures have also been attributed to settling, sliding or slumping within an unstable, water-saturated environment (Fleming 1953; Lewis 1971; Collinson 1996; Strachan 2008). Potential paleo-seismic origins are indicated by studies in the Bay of Plenty and Waikato (Carr 1984; Bailey & Carr 1994; Kleyburg et al. 2015), including the distal volcaniclastic equivalent of the Matahina Ignimbrite where SSDS are attributed to liquefaction following rupture along the Waiohau Fault (Bailey & Carr 1994).

SSDS in the Plio-Pleistocene succession of the Whanganui Basin (WB) have been recorded during numerous studies (Fleming 1953; Seward 1974; Shane 1991; Abbott 1994; van der Neut 1996; Brackley 1999; Pillans et al. 2005). A majority of this work has focused on the western and central WB where recognition of cyclic sedimentation corresponding to Quaternary climatic events has driven research interest (Carter et al. 1991; Pillans 1994). The east of the basin has received considerably less attention. We address this knowledge gap by formally defining the Waitapu Shell Conglomerate and documenting the SSDS that occur in close stratigraphic proximity. The Waitapu Shell Conglomerate is correlated between sections using tephrostratigraphy and biostratigraphy, enabling recognition of laterally equivalent units and providing some perspective into the nature and extent of SSDS within the WB's Castlecliffian outcrop belt.

Waitapu Shell Conglomerate contains abundant reworked charcoal and pumice, recording a major rhyolitic eruption in the central North Island and resultant first influx of Kaukatea Pumice within the Rangitikei succession at c. 0.9 Ma. Directly beneath and some 25 m above the base of the conglomerate, lie SSDS that can be traced as a zone of deformation. Waitapu Shell conglomerate crops out within the steep hill country of the lower Rangitikei District northeast of Marton (Fig. 5.1). The stratigraphy dips gently south and is locally offset and gently folded about a series of actively growing anticlines that traverse the Manawatu Plains (Te Punga 1957; Melhuish et al. 1996; Jackson et al. 1998).

5.3 Geological setting

The study area is located in the WB, positioned c. 200 km west of the convergent margin between the Pacific and Australian plates (Fig. 5.1). Volcanism and extension in the central North Island are related to subduction at the Hikurangi Margin (Houghton et al. 1995; Stratford & Stern 2004). Volcanism has migrated southeast through time, commencing in the Taupo Volcanic Zone (TVZ) at c. 2 Ma (Briggs et al. 2005). Subsidence of the western lower North Island has facilitated sedimentary preservation of volcanic and climatic signals spanning the entire Quaternary Period (Stern et al. 1992, 1993; Pillans 2017). Volcanic activity at the Mangakino volcanic centre in the western TVZ was initiated during two periods of caldera-forming activity from 1.68–1.53 and 1.21–0.95 Ma, respectively, providing an important source of sediment to the WB during Castlecliffian time (Briggs et al. 1993; Shane 1993; Houghton et al. 1995; Krippner et al. 1998; Pillans et al. 2005).

Subsidence of the WB approximately kept pace with sedimentation throughout the Plio-Pleistocene, resulting in preservation of a c. 4.5 km-thick sedimentary succession (Carter & Naish 1998). Regional tilting of the basin fill is a result of

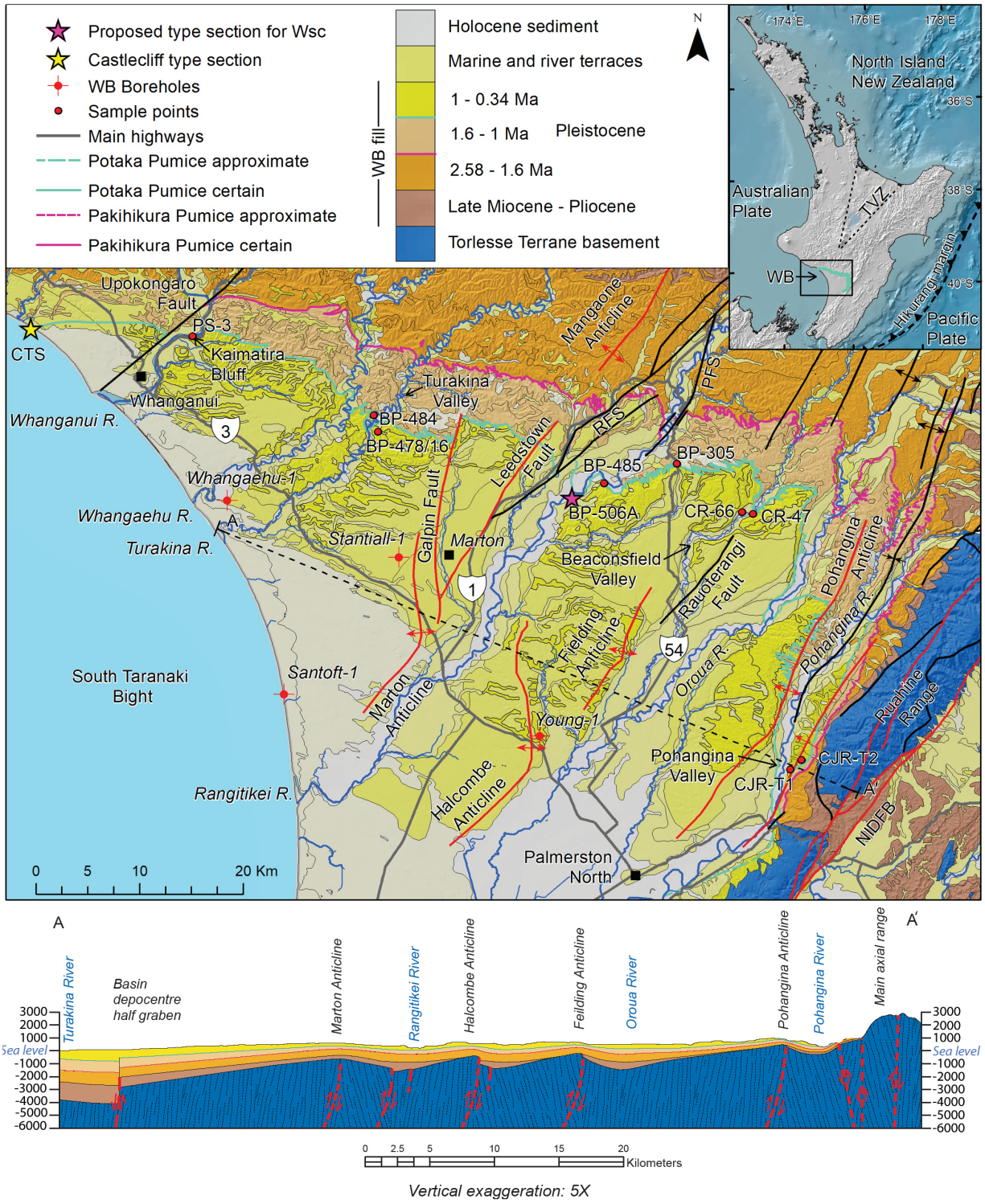


Figure 5.1: Map displaying the onland portion of the Whanganui Basin (WB) relative to the Taupo Volcanic Zone (TVZ) and Hikurangi margin. Sample and section locations are shown, including the proposed type section for the Waitapu Shell Conglomerate (Wsc). The North Island Dextral Fault Belt (NIDFB), Castlecliff type section (CTS), Rangitikei Fault System (RFS) and the Pakihikura Fault System (PFS) are displayed. A simplified cross section A to A' illustrates the undulating basement surface beneath the Late Miocene - Pleistocene basin fill, constrained by available borehole data. Data sourced from Feldmeyer et al 1943; Te Punga (1952); Fleming (1953); Milne (1968); Seward (1976); Anderton (1981); Melhuish et al. (1996); Pillans et al. (2005), GNS Science and this study.

southward migration of the basin depocentre and simultaneous uplift along the northern and eastern margins. Late Quaternary uplift has been calculated at a rate of 0.3–0.5 m/ka in the location of the modern coastline and c. 1–3 m/ka adjacent to the axial range (Pillans 1986). This tectonic regime has resulted in exposure of gently dipping (2–15°) marine strata along coastal cliffs and river valleys (Fleming 1953; Abbott 1994) and the preservation of extensive flights of marine (Pillans 1990a) and river terraces (Te Punga 1952; Milne 1973). Orbitally driven climatic cycles have been linked to sedimentary deposition of the basin fill, corresponding to fifth (100 ka) and sixth (40 ka) order sequences.

Forty-seven unconformity-bounded cycles are recognised and correlated to oxygen isotope stages 100–3 (Naish & Kamp 1995; Carter & Naish 1998; Abbott & Carter 1999). Each cycle relates to a glacial/interglacial couplet, represented by a transgressive (TST), highstand (HST) and in some cases, regressive (RST) and lowstand (LST) systems tracts. At the Castlecliff type section, near Whanganui City (Fig. 5.1) preservation of TSTs and HSTs occurs with bounding sequence surfaces represented by erosional unconformities, formed during subaerial exposure at sea-level low-stands and subsequent transgressive marine ravinement. During the Pleistocene, particularly towards the eastern margin of the basin, preservation of incised valley fill (Rees et al. 2018b) and coastal plain facies (Te Punga 1952; Milne 1968) occurred during marine regressions and sea-level low-stands, complicating sequence stratigraphic interpretation (Naish et al. 2005; Pillans et al. 2005).

Stratigraphy

The middle Kai Iwi Group sediments surrounding the Waitapu Shell Conglomerate form the focus of this study, encompassing a portion of the Waiomio and Kaimaitra Pumice Sand formations (Table 5.1). The Kai Iwi Group comprises five cyclothems (WB cycles 34 – 38) deposited between c. 0.99 and 0.6 Ma (Pillans

et al. 2005). The base of the group is defined by the first influx of Potaka Pumice into the sedimentary record, during the transgression of cycle 34 (Pillans et al. 2005; Rees et al. 2018a). We correlate the Waitapu Shell Conglomerate to the early transgression of cycle 36, marking the first influx of Kaukatea Pumice into the Rangitikei succession and positioned one cycle below the first appearance datum of *Pecten novaezelandiae* (Fig. 5.2C). Primary Kaukatea Tephra is intermittently preserved within cycle 35, including at Turakina (van der Neut 1996), Pohangina (Rees et al. 2018b), Whanganui (Kershaw 1989) (Fig 2 B and E) and in the Castlecliff-1/1A drillcore (Naish et al. 2005). The first influx of Kaukatea Pumice is recognised in a majority of WB sections (Pillans et al. 2005) highlighting its value as a chronostratigraphic marker horizon. The first influx of a new pumice geochemistry into the WB is not entirely isochronous, given lateral changes in preservation across the basin. Specifically, preservation of low stand deposits, below the ravinement surface (RS) in the far eastern basin predate Type A1 shellbeds (Abbott & Carter, 1994), positioned above the RS in the central and western basin sequences. However, for working purposes the two are deemed lateral equivalents (Pillans et al. 2005).

Major element glass shard analysis (Fig. 5.3, Supplementary Data File 5A, Appendix A) and field mapping within the Beaconsfield and Pohangina valleys (Fig. 5.1) allows for the recognition of lateral equivalents of the Waitapu Shell Conglomerate within eastern WB sections (Fig. 5.2 D and E). Previous correlations of Kershaw (1989), Abbott (1994), Pillans et al. (1994), van der Neut (1996) and Pillans et al. (2005) are compiled in Fig. 5.2, allowing for addition of and comparison to the Turakina and Kaimatira Bluff sections.

Table 5.1: Stratigraphic nomenclature and correlations between the Castlecliff type section(Fleming, 1953; Abbott and Carter, 1999) and the Rangitikei section in eastern WB (Te Punga, 1952; Potter, 1984; Bussell, 1984; Abbott, 1992; and this study).

Fleming (1953) Abbott and Carter (1999) Castlecliff type section		Te Punga (1952) Rangitikei		Potter (1984) Bussell (1984) Rangitikei		This study Rangitikei	
POUAKAI GROUP	Papaiti Alluvium St Johns Alluvium Rapanui Frm. Brunswick Frm. Kaiatea Frm	UPPER RANGITIKEI FORMATION	Mangaone Sandstone Halcombe Conglomerate Waituna Conglomerate	POUAKAI GROUP	Westoe Frm. Halcombe Conglomerate Frm.	POUAKAI GROUP	Westoe Frm. Halcombe Conglomerate Frm.
SHAKESPEARE GROUP	Landguard Frm Putiki Shellbed Mosstown Sand Karaka Siltstone Upper Castlecliff Shellbed Shakespeare Cliff Sand Shakespeare Cliff SIltstone Tainui Shellbed Pinnacle Sand Lower Castlecliff Shellbed Seafield Sand		Rangitawa Fossil Beds Kakariki Conglomerate Ruamahanga Conglomerate Onepuhi Fossil Beds Toms Conglomerate	SHAKESPEARE GROUP	*Mingaroa Fossil Bed Mb.* *Upper Kakariki Shell Conglomerate Mb.* *Te Hiri Shellbed Mb.* *Rangitawa Fossil Bed Mb.* Mangatapu Frm *Kakariki Conglomerate Mb.* *Pryce Shellbed Mb.* *Ruamahanga Conglomerate Mb.* *Otapatu Shellbed Mb.* *Onepuhi Fossil Beds Mb.* Tokorangi Frm *Toms Shellbeds Mb.* *Toms Conglomerate Mb.*	SHAKESPEARE GROUP	*Mangatapu Frm.* *Ruamahanga Conglomerate Mb.* *Tokorangi Frm.* *Toms Conglomerate Mb.*
KAI IWI GROUP	Upper Kai Iwi Siltstone Kupe Frm Upper Westmere Siltstone Kaikokopu Frm. Lower Westmere Siltstone Omapu Shellbed Lower Kai Iwi Siltstone Kaimatira Pumice Sand		Shell Creek Fossil Beds Waitapu Shell Conglomerate Potaka Pumice		*Shell Creek Fossil Bed Mb.* Reu Reu Frm. Waiomio Frm. (Abbott 1992)	KAI IWI GROUP	Reu Reu Frm. *Waiomio Shellbed Mb.* Waiomio Frm. *Waitapu Shell Conglomerate Mb.* Kaimatira Pumice Sand Frm. *Potaka Pumice Mb.*
OKEHU GROUP	Upper Okehu Siltstone Okehu Shell Grit Lower Okehu Siltstone Butlers Shell Conglomerate Makirikiri Tuff		Mangapipi Fossil Beds Pakihikura Pumice		Undifferentiated	OKEHU GROUP	*Rewa Frm.* *Mangapipi Conglomerate Mb.* *Mangapipi Mb.* Makirikiri Tuff Frm *Pakihikura Pumice Mb.*

Paleo-liquefaction

Liquidisation involves the formation of fluidised sediment, whereby sediment experiences a complete loss of shear strength and behaves as a cohesionless, viscous fluid (Allen 1977, 1982; Davenport & Ringrose 1987). The common mechanisms of liquidisation are liquefaction and fluidisation (Alfaro et al. 2002; Onorato et al. 2016). Liquefaction is associated with an increase in pore fluid pressure and a reduction of shear strength (Owen & Moretti 2011; Quigley et al. 2013). Sediment liquefies as excess pore-water pressures exceed the static confining pressure, causing large strains and sediment flow together with a breakdown of the grain fabric (Seed & Lee 1966; Seed & Idriss 1982; Idriss & Boulanger 2008).

Fluidisation is the mechanism where a liquid-like condition is achieved by forcing a fluid from an external source upward through the sediment, until the immersed weight of the grains is balanced by the total fluid drag (Molina et al. 1998). A distinction is made in the literature between liquefied systems, in which solids settle downward through the fluid, and fluidised beds in which fluids move upward through the solids, suspending them without net downward movement (Lowe 1976).

Paleo-liquefaction within sediments is commonly recognised by injection structures forming sand dykes or sills and severely distorted or offset bedding (Bastin et al. 2015; Kleyburg et al. 2015). Liquefaction develops through the action of a trigger, including seismic events, waves, rapid deposition/loading of sediment, slope instability or groundwater movement (Owen & Moretti 2011).

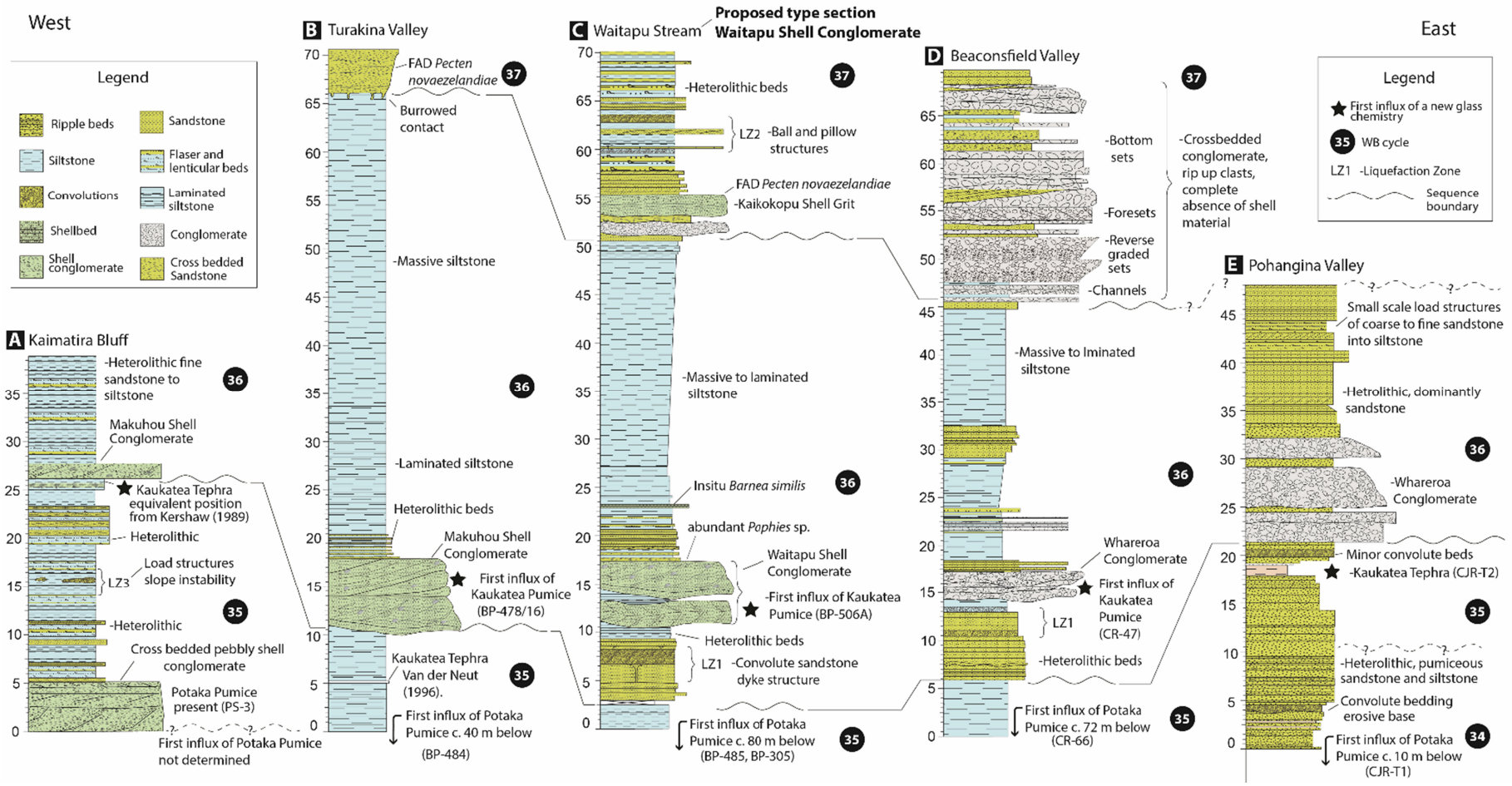


Figure 5.2 Stratigraphic log of the proposed type section for the Waitapu Shell Conglomerate near the mouth of Waitapu Stream, Rangitikei Valley (BL34 1582 6596) and other laterally equivalent sections from across the basin. Data sourced from Kershaw (1989), Abbott (1994), Shane (1994) van der Neut (1996), Pillans (2005), Rees (2018a) and this study.

Liquefaction associated with recent seismic events has been highlighted in New Zealand (Ward et al. 2011), demonstrating the susceptibility of our environment to this potentially destructive process. Recent seismic events in Canterbury (Cubrinovski et al. 2011) , Italy (Alessio et al. 2013) and Japan (Yasuda et al. 2012) have provided case studies, stimulating research into liquefaction susceptibility (Green et al. 2011; Green et al. 2014) and its relationship to environments of deposition (Giona Bucci et al. 2017; Giona Bucci et al. 2018).

Historic evidence of liquefaction in the Whanganui-Manawatu and Horowhenua-Wellington areas has been documented by Eiby (1968) and Fairless and Berrill (1984). These records include evidence of liquefaction within coastal to marginal marine environments where observations have been made of cracking, sand boils and cockles rising to the surface following the 1843 Whanganui, 1848 Marlborough and 1855 Wairarapa earthquakes.

Marine sediments have potential for liquefaction due to their unconsolidated, water-saturated nature at the seabed (Alfaro et al. 2002). However, reworking of seabed deposits by tides, wave action and surface bioturbation leads to low preservation potential for surficial SSDS and a relative dominance of subsurface SSDS within the geological record (Reid et al. 2012; Giona Bucci et al. 2017). Given the tectonic setting of the WB, it is probable that the basin contains evidence of past earthquakes within its shallow to marginal marine facies, characterised by fine-grained, saturated sediments with high liquefaction potential. However, confidently identifying the trigger mechanism for SSDS can be difficult (Owen & Moretti 2011), presenting a challenge for paleoseismic investigations in the WB.

5.4 Methods

During fieldwork, we identified common SSDS within a particular interval of the WB's Castlecliffian succession (c. 1–0.9 Ma), extending from Pohangina Valley c. 70 km west to Kaimatira Bluff (Fig. 5.1). Recognition and description of the main types of SSDS within this stratigraphic interval (Fig. 5.4) proceeded during geological mapping in the eastern WB (Rees et al. 2018a; Rees et al. 2019). Mapping involved compilation and revision of local stratigraphic nomenclature (Feldmeyer et al. 1943; Te Punga 1952; Fleming 1953; Seward 1976; Bussell 1984; Potter 1984; Abbott 1992; Naish & Kamp 1995; van der Neut 1996). Table 5.1 outlines the revised nomenclature and its relationship to the Castlecliff type section (Fig. 5.1) near Whanganui City (Fleming 1953; Abbott & Carter 1999).

The use of marker horizons was paramount for correlation between the sections. Mid-Pleistocene marker horizons in the Rangitikei District typically comprise a TST; pebbly shell conglomerate containing reworked fossils from estuarine to offshore environments and volcaniclastic sediment that in many cases represents the first influx of a new pumice geochemistry into the basin (Type A1 shellbed of Abbott & Carter, 1994). Many of these units are prominent in the landscape, allowing for ease of mapping.

We chose to document the Waitapu Shell Conglomerate, as it is well constrained by the WB chronostratigraphic framework, is associated with large scale SSDS and displays interesting lateral variation across relatively short distances (<16 km). The Waitapu Shell Conglomerate is a unit that marks the boundary between the Kaimatira Pumice Sand Formation (Fleming 1953) and newly revised Waiomio Formation in the Rangitikei District (Table 5.1). In this study we propose a type section for the Waitapu Shell Conglomerate, following the detailed works of Te Punga (1952) and Abbott (1994), specifying an easily accessible outcrop at the

entrance to Waitapu Stream, Potaka Station (NZ Topo50 map reference BL34 1582 6599).

We logged stratigraphic sections (Fig. 5.2), collecting fossils and samples from primary tephra-fall and volcaniclastic beds. Sample locations were marked by handheld GPS (Fig 1). Fossil identification and paleo-environmental interpretation was greatly aided by Dr Alan Beu (GNS Science) (Supplementary Data File 5B, Appendix A). The Waitapu Shell Conglomerate and its correlatives within each section were assessed for clast shape, size and composition. The short (S), intermediate (I) and long (L) axes of fifty clasts from each unit were measured with a pair of digital calipers (Supplementary Data File 5C, Appendix A).

Tephrostratigraphy and field mapping was used to trace the lateral equivalent of the Waitapu Shell Conglomerate eastwards into the Beaconsfield and Pohangina valleys (Fig. 5.1 and 5.2), documenting facies changes towards the Ruahine Range (Fig. 5.1). Beds composed entirely of glass were targeted when available. Pumice clasts were sampled from conglomerate beds, before being gently crushed during sample preparation. Samples were washed through a 63 µm sieve, discarding silt and clay sized particles. Following drying, samples were then dry sieved to collect the 125-250 µm fraction for mounting in epoxy plugs. Glass shard major elements were determined using a JEOL JXA-8230 Electron Probe Microanalyser (EPMA) at Victoria University, Wellington. Analyses were determined using an 8 nA beam current, 10 µm beam diameter, and the glass standards ATHO-G from the MPI-DING collection (Jochum et al. 2006) and VG568 (Jarosewich et al. 1980). All analyses presented are weight percent, recalculated to 100% on a water free basis (Supplementary Data File 5A, Appendix A). Total Fe (FeO_t) was calculated as FeO while H_2O was calculated by the difference from 100%. Bivariate plots were constructed using FeO_t Vs CaO Wt % to aid tephra correlation with published datasets (Fig. 5.3).

5.5 Results

Section descriptions

Waitapu Stream – Proposed type section

The Waitapu Shell Conglomerate (Fig. 5.2C) contains a heterolithic mixture of bioclastic and siliciclastic sediments, with clasts typically of pebble size in a matrix of coarse sands and granules. The basal contact is erosive with channels up to 1 m deep carved into the underlying laminated to lenticular bedded siltstone and fine sandstone (Fig. 5.5). Large-scale, low-angle, trough cross-bedded sets 1-2 m thick contain large (up to 400 mm), angular rip-up clasts of the laminated to lenticular bedded siltstone and fine sandstone. Lenses of siltstone, 0.1 – 0.3 m thick, drape the crossbeds, pinching out laterally. The rip-up clasts contain original laminated to lenticular bedding formed prior to reworking (Fig. 5.6B) and appear to be derived from the heterolithic beds immediately beneath the cross-bedded sets.

Clasts are dominantly pebbles of sub-rounded, disc to blade-shaped, greywacke, pumice, rhyolite and ignimbrite 2–64 mm in diameter, with rare larger clasts >100 mm (Supplementary Data File 5C, Appendix A). Clasts are typically weakly aligned along the cross-bed sets. Rare charcoal is particularly evident within the lower-most channelled cross-bed sets, occurring as pockets of rounded clasts up to 70 mm in diameter. Variable concentration and composition of clasts occurs throughout the deposit, with particular cross-bedded sets enriched in bioclastic material, greywacke pebbles and pumiceous alluvium. Lenses of distinctive, coarse to granular quartz- and ferromagnesian-rich sands occur locally, displaying strong sorting and resultant mineral separation by density.

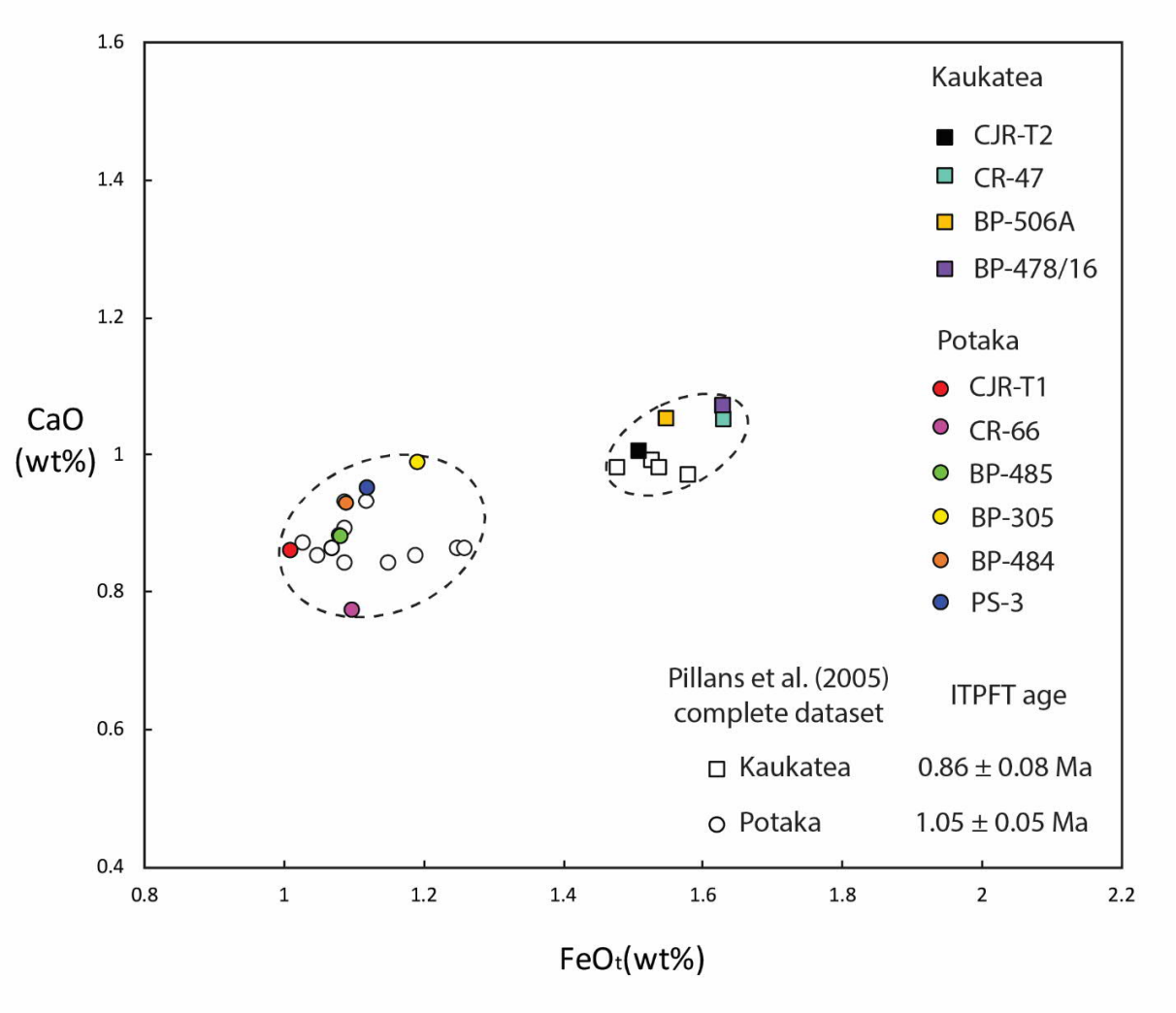


Figure 5.3: Mean CaO versus FeOt (wt%) composition of glass shards analysed from tephra-fall and/or volcaniclastic samples and correlation to the complete dataset of Pillans et al (2005). Data sourced from Shane (1994), Pillans (2005) and Rees (2018a).

Bioclastic material is highly worn, comprising approximately equal proportions of granule-sized debris and variably preserved fossil Mollusca dominated by *Paphies* sp. Particular lenses of highly enriched bioclastic material occur, in which shell fragments and whole shells comprise up to 80% of the material in a siliciclastic matrix. Similarly, other lenses are enriched in pumiceous sediment containing abundant sub-rounded pumice clasts up to 150 mm in diameter. The largest pumice clasts significantly outsize clasts of any other lithology.

Large-scale convolute, water escape and injection structures (LZ1) occur 1-2 m below the Waitapu Shell Conglomerate (Fig. 5.5, 5.6 A and D) underlying a locally channelled unit of laminated to lenticular siltstone and fine sandstone. LZ1 SSDS are characterised by an injection structure originating from an area of deformation within fine laminated to massive sandstone 2 m below the main zone of convolute bedding (Fig. 5.5). The 1.5 m-high injection structure is characterised by consolidated medium to fine grained sandstone at its core, displaying a funnel-shaped contact with the intensely convoluted fine sandstone to coarse siltstone above. The dyke geometry is 0.2 m wide near its base and increases in width to 1 m at the upper funnel shaped contact. The interval of intense convolution overlying the dyke structure contains multiple smaller sites of injection with a majority of the convolute bedding centered in the lowermost portion of fine sandstone, grading upwards into wavy-laminated fine sandstone to coarse siltstone. During repeat visits, the outcrop face was observed to be actively eroding, revealing other dyke structures originating from LZ1 located 6-10 m from the dyke sketched in Fig. 5.5.

A gradual fining upward sequence occurs above the Waitapu Shell Conglomerate (Fig. 5.2C), changing from heterolithic sediments with rare shell debris to massive, sparsely fossiliferous siltstone. Overlying the fine-grained massive siltstone is a conglomeratic unit. The base is characterised by a 1 m thick, well sorted, un-fossiliferous, clast-supported greywacke conglomerate overlain by coarse to granule sandstone. A cross-bedded shell conglomerate, locally scours into this greywacke conglomerate-sandstone unit. The first appearance of *Pecten novaezelandiae* within the shell conglomerate allows correlation to the Kaikokopu Shell Grit (Abbott 1994). The Kaikokopu Shell Grit passes upwards into a complex of heterolithic, interbedded sandstone, siltstone and 0.2–0.5 m thick beds of coarse shell debris and sandstone displaying unidirectional cross-bedding.

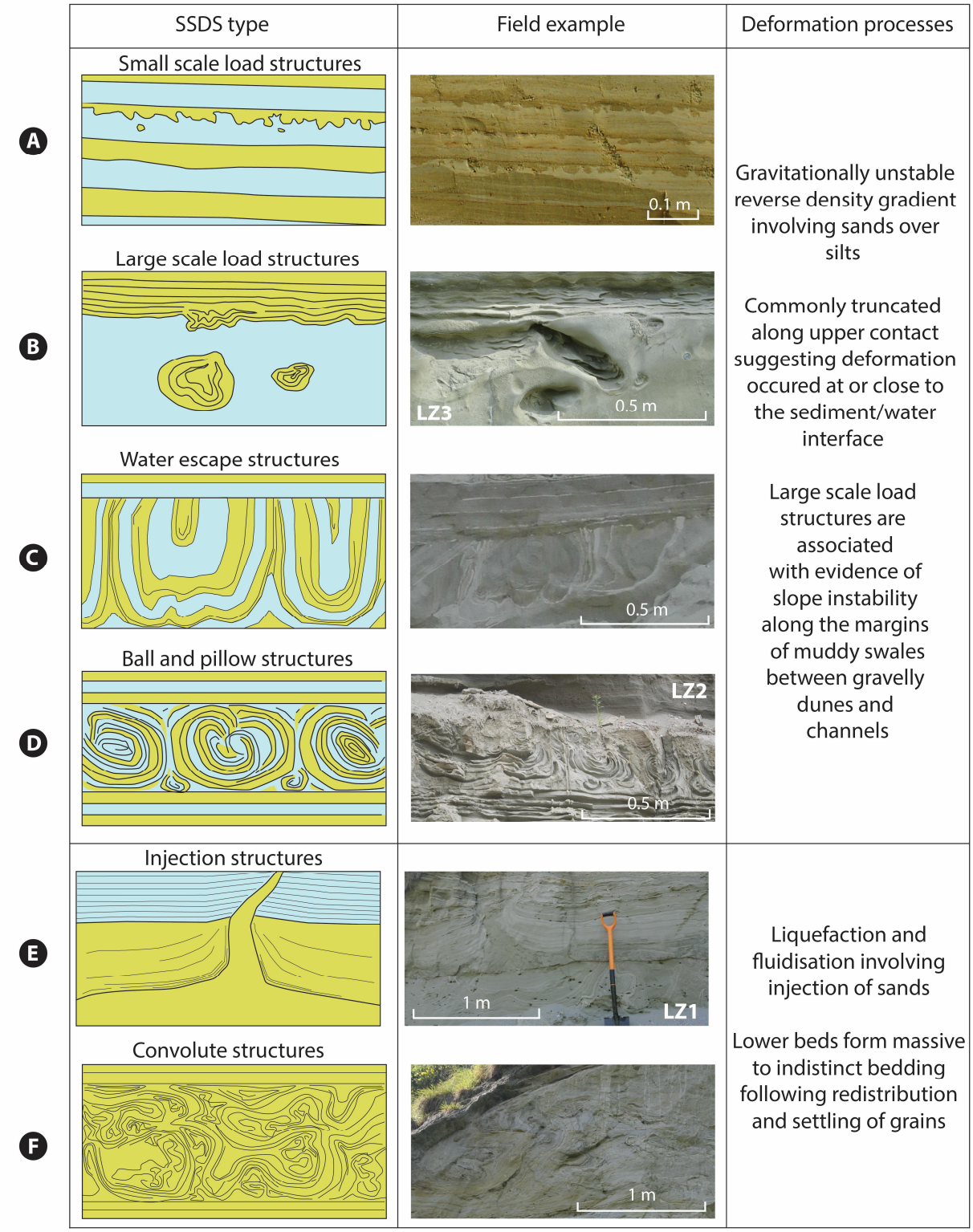


Figure 5.4: The main types of SSDS recognised in the WB and their interpreted processes of deformation.

LZ2 occurs c. 25 m above the Waitapu Shell Conglomerate and is interbedded with rare lenses of shell debris and massive siltstone (Fig. 5.6 C and E). Here two distinctive beds of soft sediment deformation, 0.3 and 0.6 m thick, occur within a highly variable succession of alternating lenticular fine sandstone and siltstone with rare, thin lenses of shell debris. These beds are characterised by ball and pillow structures (Fig. 5.6 E) comprising fine sandstone to siltstone tightly folded into concentric layers with some lateral variation in grain-size and patterns of deformation. LZ2 can be traced for 1 km farther east as the Waitapu Stream cuts across the strike of the gently dipping Pleistocene units (1-3° SSE). Beyond this point, the beds are not exposed, dipping beneath the late Quaternary fill. The heterolithic units gradually fine upward with rare 10–50 mm coarse to granule sandstone layers present, until near the top of the succession where structureless siltstone dominates.

The Waitapu Shell Conglomerate contains a diverse assemblage of fossils (Supplementary Data File 5B, Appendix A). Shells are often moderately to severely worn. Approximately 50% of fossils occur as fragments with rare lenses containing well-preserved diverse faunal assemblages. Estuarine species are rare and their shells are extremely abraded. The assemblage is dominated by open coast to sandy nearshore species, particularly *Paphies donacina* and *P. delta*.

Beaconsfield Valley

In Beaconsfield Valley (Fig. 5.1 and 5.2D), we correlate the Waitapu Shell Conglomerate to an equivalent unit, the Whareroa Conglomerate (Rees et al. 2018a), based on the first occurrence of Kaukatea Pumice (Fig. 5.2D and 5.3). Whareroa Conglomerate occurs in this section as a clast supported conglomerate displaying 1-2 m thick trough crossbed sets above an erosional lower contact

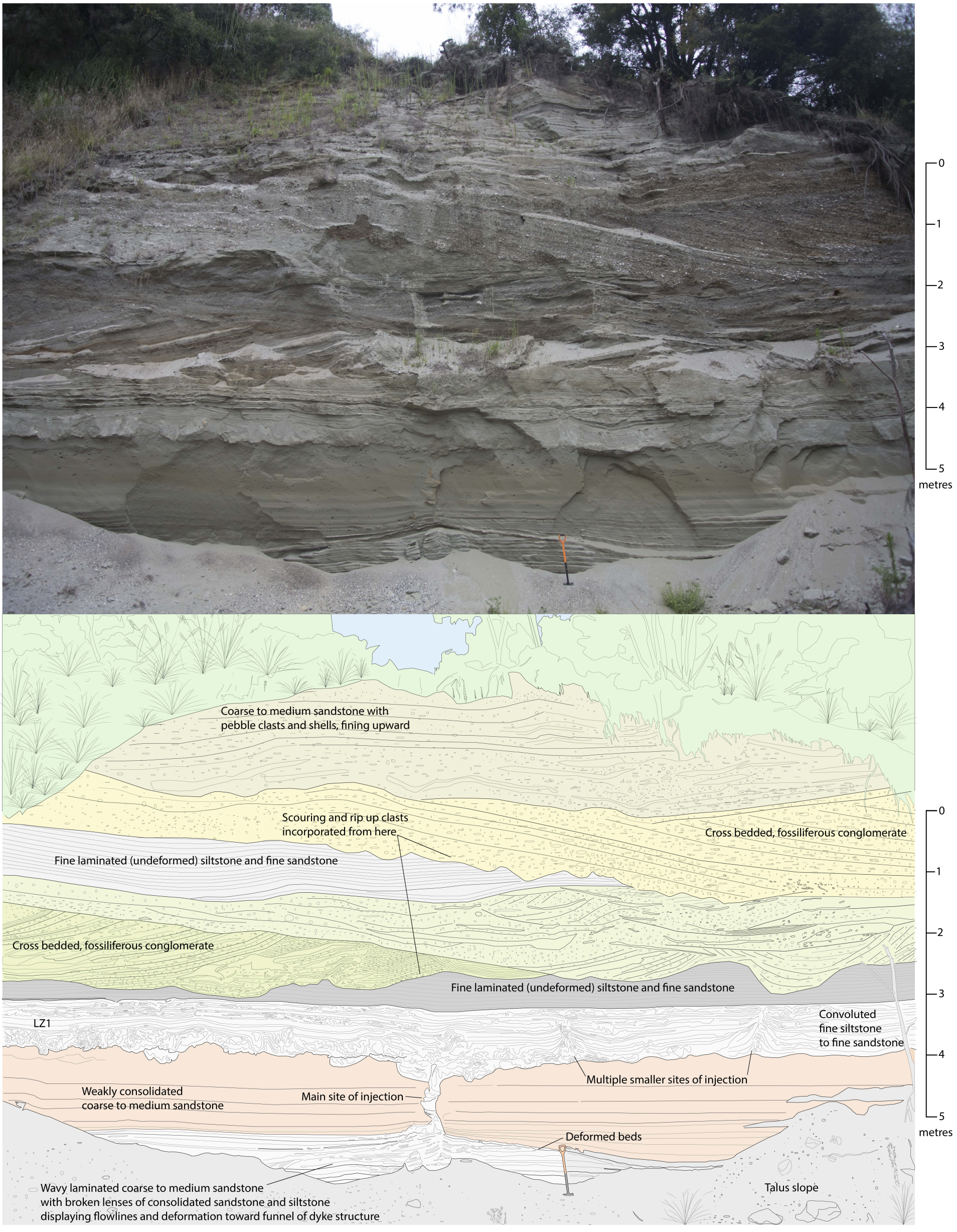


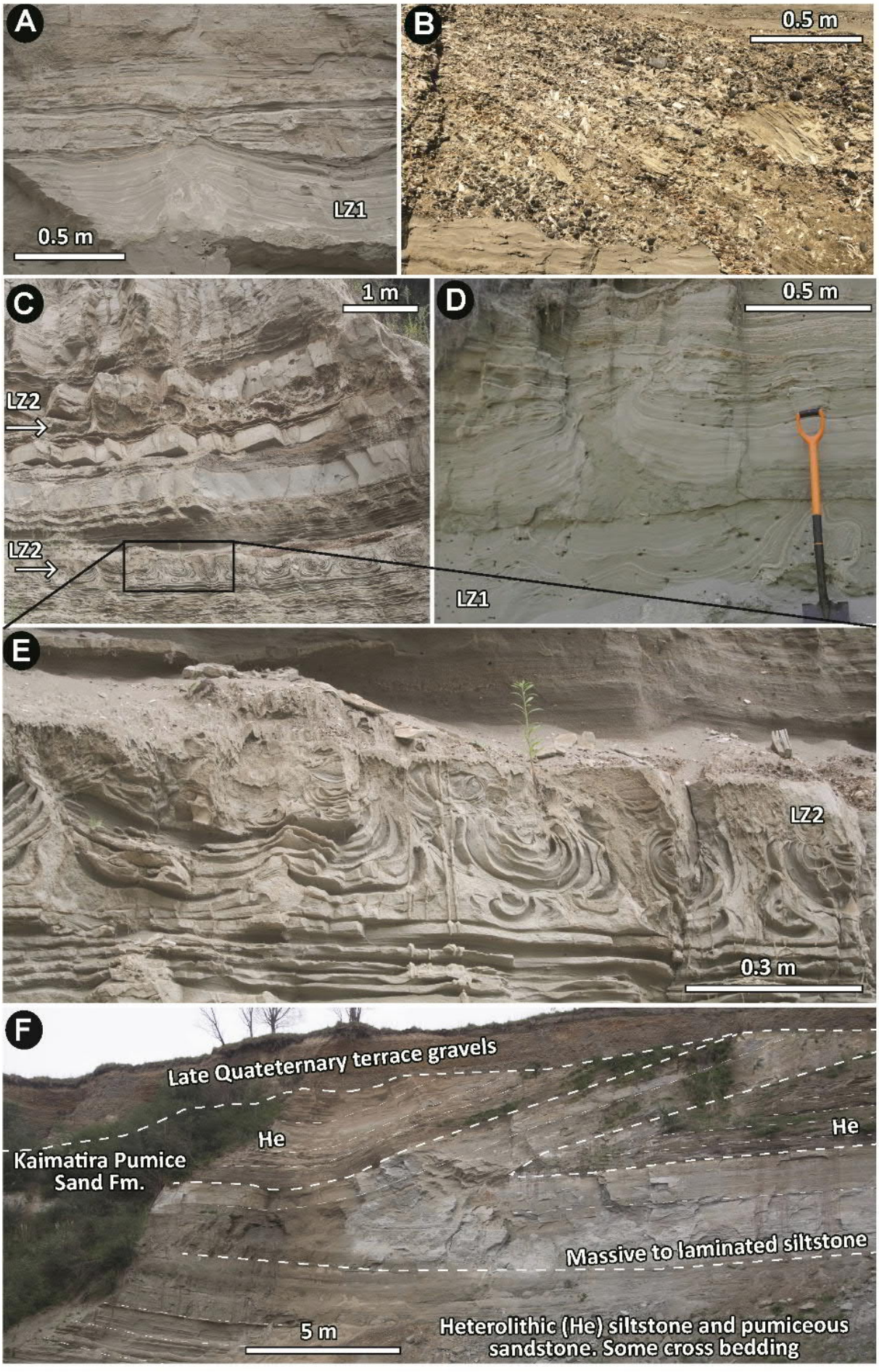
Figure 5.5: Sketch of the proposed Waitapu Shell Conglomerate type section at Waitapu stream (BL34 1584 6597). Spade is 1 m high, note lift in top of laminated sandstone to left of spade grading upwards into a zone of massive fine sandstone. The injection structure starts at the apex of this lift before funneling into the overlying intensely convolute fine sandstone and siltstone of Liquefaction Zone 1 (LZ1).

(Fig. 5.7). Clasts are rounded to sub-rounded, comprising a mixture of equant to disc shaped pebbles (13-50 mm). They are dominated by greywacke with locally enriched lenses of pumice. Isolated larger clasts of pumice and charcoal occur up to 60 mm in diameter. No shell material is identified within this interval of the Beaconsfield succession. Crossbed sets often show normal grading with erosive lower contacts and basal lags containing isolated large clasts (45-60 mm). We note 10-60 mm tear shaped load structures consisting of sub-round clasts of granule to small pebbles within a 1 m thick massive siltstone immediately underlying Whareroa Conglomerate. The load clasts penetrate the siltstone to a maximum depth of 90 mm. A 300 mm lignite bed is found locally overlying the Whareroa Conglomerate, pinching and swelling laterally (Fig. 5.7D).

Beneath Whareroa Conglomerate lies c. 8 m of massive to laminated fine sandstone and siltstone with occasional wavy lenses of coarse sand to granule sized pumice and greywacke clasts. Two beds, 0.3 to 0.5 m thick, contain convolute structures (LZ1), observed 1 and 3 m below the conglomerate unit, occurring within siltstone and fine sandstone, respectively (Fig. 5.2D and 5.7). The convolute structures are truncated at their upper contacts by sharp bedding planes.

15 m of heterolithic beds overlie Whareroa Conglomerate, including five lenses of pebble conglomerate, 0.2-0.15 m thick, interbedded with siltstone and fine sandstone beds. Occasional beds of pumiceous conglomerate 0.5-0.6 m occur,

Figure 5.6 (facing page): A) Close up of Liquefaction Zone 1 (LZ1), displaying a site of injection at the Waitapu Stream section. B) Rip up clasts of laminated to wavy lenticular coarse siltstone and fine sandstone within the Waitapu Shell Conglomerate, retaining bedding. C) Liquefaction Zone 2 (LZ2), c. 40 m above the base of the Waitapu Shell Conglomerate displaying two beds with ball and pillow structures (BL34 1675 6563). D) An injection structure exposed within LZ1. E) Close up of photo B, LZ2 , showing ball and pillow structures formed in fine sandstone and siltstone. F) Interpreted slope instability within Kaimatira Pumice Sand Formation, stratigraphically below Waitapu Shell Conglomerate. This outcrop is located c. 800 m NE of the proposed type section for the Waitapu Shell Conglomerate (BL34 1664 6643).


A
LZ1
0.5 m
B
0.5 m
C
1 m
LZ2
LZ2
D
0.5 m
LZ1
E
LZ2
0.3 m
F
Late Quateternary terrace gravels
He
He
Kaimatira Pumice Sand Fm.
Massive to laminated siltstone
5 m
Heterolithic (He) siltstone and pumiceous sandstone. Some cross bedding

containing abundant reworked pumice, dominated by Potaka geochemistry (determined by EPMA analysis). A 12 m interval of massive to laminated siltstone separates the heterolithic beds from a 25 m thick conglomerate unit interbedded with medium to coarse sandstone and abundant rip up clasts of siltstone. Clasts are rounded to sub-rounded, disc to equant in shape and are largely composed of greywacke with lesser amounts of ignimbrite, pumice and siltstone (25-100 mm in diameter). The conglomerate unit grades from 2.5 m of low angle cross beds with associated channel cut and fill structures and abundant rip up clasts into 2-2.5 m thick reverse graded sets (Fig. 5.7 A and B). Foresets composed of laminated, clast-supported conglomerate beds 100-300 mm thick overlie the reverse graded sets (Fig 5.7D). The foreset unit is a total of 1-2.5 m thick; the individual beds dip between 16-20° S and are truncated along their upper contact by the overlying heterolithic bottom sets. Lenses of siltstone up to 1 m thick become more frequent within the upper part of the conglomerate, interbedded with low angle cross-stratified to laminated pebble conglomerate.

Pohangina Valley

The Pohangina Valley section (Fig. 5.2E) contains a heterolithic succession dominated by fine sandstone. Primary Kaukatea tephra-fall and the first influx of Potaka Pumice has been documented by Rees et al. (2018b), enabling correlation to the other sections. The basal 10 m of this section is characterised by 20-60 mm

Figure 5.7 (facing page): A) Channelled conglomerate near the base of cycle 37, Beaconsfield Valley (BL35 3194 6423). B) Reverse graded sets located above the channeled conglomerate in A. C) A 30 cm thick lignite locally capping Whareroa Conglomerate in Beaconsfield Valley (BL35 3250 6465). D) Foresets overlying the reverse graded sets pictured in B. E) Sketch of the Whareroa Conglomerate exposed in Beaconsfield Valley, soft sediment deformation occurs 0.5 and 1.5 m (LZ1) below this lateral equivalent of the Waitapu Shell Conglomerate c. 16 km east of the Waitapu Stream section. Rare load clasts 50 – 300 mm in diameter occur directly beneath the conglomerate at this outcrop, consisting of coarse conglomerate material sinking and forming balls within the massive siltstone. F) Photo used to produce sketch in E. G) close up of LZ1 below the Whareroa Conglomerate in Beaconsfield Valley.

A
2 m
B
2 m
C
0.3 m
D
0.3 m
2 m
E
Cross bedded pumiceous conglomerate
First influx of Kaukatea Pumice (CR-47)
Loading and scouring
Weathering on outcrop face
Massive siltstone
Thick sets of massive siltstone
LZ1
Kiwitea Stream
1 m
F
Whareroa Conglomerate
G

beds of rippled to laminated, pumiceous sandstone and siltstone. Ripples are commonly highlighted by coarse sand to granule sized pumice clasts. Basal contacts are often erosional within occasional inclusion of sub-rounded rip up clasts of siltstone 20-35 mm thick. Water escape and convolute structures are apparent within a 0.5-0.8 m bed of fine pumiceous sandstone and siltstone located toward the base of section (Fig. 5.2 E). The SSDS are truncated by sharp upper contacts.

The heterolithic pumiceous sandstone and siltstone grades upward into 8 m of laminated sandstone with sets between 5 and 150 mm thick. The siliciclastic component in the sandstone increases as volcaniclastic material become less frequent. The beds fine upward into silty fine sandstone with occasional 10-30 mm lenses of carbonaceous siltstone and a 300 mm tephra-fall bed correlated to Kaukatea Tephra (CJR-T2, Fig. 5.3). 0.6 m of fine laminated sandstone separates Kaukatea Tephra from a 0.5 m bed of minor convolute structures within coarse to fine grained pumiceous sandstone.

Laminated medium to coarse sandstone, 0.5-0.8 m thick, separates the convolute bed from the overlying Whareroa Conglomerate (Fig. 5.2E). The lower contact of the conglomerate is wavy and erosional. The conglomerate is 10.5 m thick, poorly sorted, consisting of alternating sets of matrix supported and clast supported conglomerate with common rip up clasts (20-150 mm in diameter) and discontinuous lenses of siltstone (up to 200 mm thick). Clasts consist of dominantly equant, rounded to sub-rounded greywacke between 3-60 mm with rare cobbles up to 68 mm. Low angle cross bedding grades upward into thick laminated sets 1 -2.4 m thick. No shell material is present within this part of the Pohangina succession. The conglomerate displays lateral facies variation between outcrops, changing within 2 km to a moderately well sorted, dominantly clast supported, pebbly conglomerate with little to no siltstone lenses, apart from rip up clasts (20-300 mm) occurring along the erosional lower contact. Pumice clasts are typically rare in the

described section; however, within laterally equivalent units pumice becomes a prominent feature.

A 16 m thick, heterolithic succession of coarse to fine siliciclastic sandstone and siltstone occurs above Whareroa Conglomerate. Planar beds 10-60 mm thick alternate with lenticular sandstone/siltstone couplets and 300-400 mm thick crossbed sets of medium to coarse-grained sandstone. Thirteen metres above the sharp contact with Whareroa Conglomerate, small-scale load structures occur within wavy, planar and lenticular bed sets (Fig. 5.4A), comprising fine to medium-grained sandstone within massive siltstone.

Turakina Valley

The Turakina Valley section was described by Abbott (1994) and van der Neut (1996). The Makuhou Shell Conglomerate represents the first influx of Kaukatea Pumice into the Turakina succession (Pillans et al. 2005), laterally equivalent to the Waitapu Shell Conglomerate in the Rangitikei Valley (Fig. 5.2). Primary Kaukatea Tephra occurs within massive to laminated siltstone approximately 5 m below the Makuhou Shell Conglomerate within cycle 35 (Fig. 5.2B). The Makuhou Shell Conglomerate consists of 7 m of cross-bedded, pebbly shell conglomerate. The lower contact is sharp with low relief. Mud drapes occur along the crossbed foresets. Clasts comprise sub-rounded, disk, blade and roller shaped pebbles (22-50 mm) with rare larger pebbles up to 60 mm. The clasts are composed of greywacke and pumice that occur together with whole shells within a fine to coarse sand and shell debris matrix. Whole shells comprise approximately 30-40 % of the conglomerate, concentrated within bioclastic rich lenses.

The Makuhou Shell Conglomerate contains a mixed assemblage of fossils, similar to the Waitapu Shell Conglomerate (van der Neut, 1996, Supplementary Data File 5B, Appendix A). The assemblage is dominated by *Paphies sp.* with common

Gastropoda including *Maoricolpus sp., Stiracolpus sp.* and *Maoricrypta sp.* There are a range of rocky intertidal species within the assemblage including *Ostrea chilensis, Anomia trigonopsis* and *Buccinulum sp.,* however, no estuarine/lagoonal species were identified by van der Neut (1996).

Heterolithic beds of laminated to lenticular fine sandstone and siltstone occur above the Makuhou Shell Conglomerate, grading into c. 40 m of massive siltstone. Cross-bedded fossiliferous sandstone rests above the massive siltstone, separated by a burrowed, wavy contact. The FAD of *Pecten novaezelandiae* within the fossiliferous sandstone facilitates correlation to the Kaikokopu Shell Grit, defined at the Castlecliff type section (Abbott 1994). No SSDS are noted at this stratigraphic interval within the Turakina Section, although convolute beds are present within the middle Kaimatira Pumice Sand Formation (van der Neut 1996).

Kaimatira Bluff

Well exposed strata at Kaimatira Bluff (Fig. 5.1) and the surrounding area have been well described by Kershaw (1989) and Abbott (1994) and compiled within Fig. 5.2A. At the base of the section, 5 m of cross bedded, pebbly shell conglomerate contains clasts of Potaka Pumice (Shane 1994), enabling correlation to the Kaimatira Pumice Sand Formation. However, the first occurrence of Potaka Pumice at this section has not been established due to limited exposure. The shell conglomerate contains disarticulated, often broken and fragmented *Paphies sp* and *Cyclomactra tristis.* Clasts consist of sub-rounded, disc, blade and roller shaped

Figure 5.8 (facing page): A) Kaimatira Bluff section displaying load and ball and pillow structures. Massive siltstone occupies swales between dunes composed of cross-bedded pebbly shell conglomerate (BL32 7887 8156). Progressive downslope deformation of the heterolithic bed within the siltstone swale is interpreted as evidence of slope instability. B) Close up photo of deformed beds. C) A sketch of Photo A. D) Makuhou Shell Conglomerate occurring on a hillside near Kaimatira Bluff (BL32 7934 8150). E) Basal condensed shellbed at the base of Makuhou Shell Conglomerate within the Kaimatira Bluff section.

A
B
0.2 m
C
Heterolithic siltstone and granule beds, also forming load clasts within the underlying siltstone
Massive siltstone
Heterolithic siltstone to fine sandstone
Heterolithic siltstone and granule to small pebble foresets
1 m
D
0.3 m
E
0.4 m

granules to pebbles of greywacke 1-60 mm in diameter. Rare larger cobbles upto 67 mm are present.

Heterolithic siltstone to coarse sandstone beds with lenses of granule greywacke and shell debris occur as lenticular to planar bed sets 20 -60 mm thick above the basal conglomerate. These beds truncate the underlying conglomerate cross beds at an undulating, erosive lower contact. A massive to laminated bed of siltstone (Fig. 5.8) occurs as a broad 11 m wide swale structure above the heterolithic beds, pinching and swelling from 0.1 to 1.2 m in height. A highly deformed 300 mm lens of ball and pillow structures occurs at the southern edge of this structure, swelling from 50 to 300 mm and becoming progressively more deformed down dip (Fig. 5.8). The SSDS are composed of circular convolutions of interbedded siltstone and fine to coarse sandstone with thin seams of shell hash and pebbles. The outer layer is composed of consolidated siltstone, forming an erosion resistant rind that accentuates the structures at outcrop.

Above the massive siltstone lies 3.5 m of heterolithic, cross-bedded siltstone with fine to coarse sandstone and lenses of shell debris and pebbles. These beds are similar in lithology to the SSDS present within the underlying massive siltstone. The lower contact surface contains convolute bedding and load structures, ranging from 50 to 400 mm in size, typically tear shaped or horizontally elongated.

Massive to laminated siltstone separates the heterolithic beds from a 2.5 m thick fossiliferous unit, containing a lower condensed shellbed dominated by *Ostrea chilensis* and *Talochlamys gemmulata* (Fig. 5.8E) and overlying cross-bedded shell conglomerate (Fig. 5.8D) with abundant *Paphies sp.* The approximate stratigraphic position of the Kaukatea Tephra is located between the condensed shellbed and the erosive base of the overlying cross-bedded shell conglomerate (Kershaw 1989; Abbott 1994). This allows for correlation of the shell conglomerate to the Makuhou Shell Conglomerate of Abbott (1994) and van der Neut (1996).

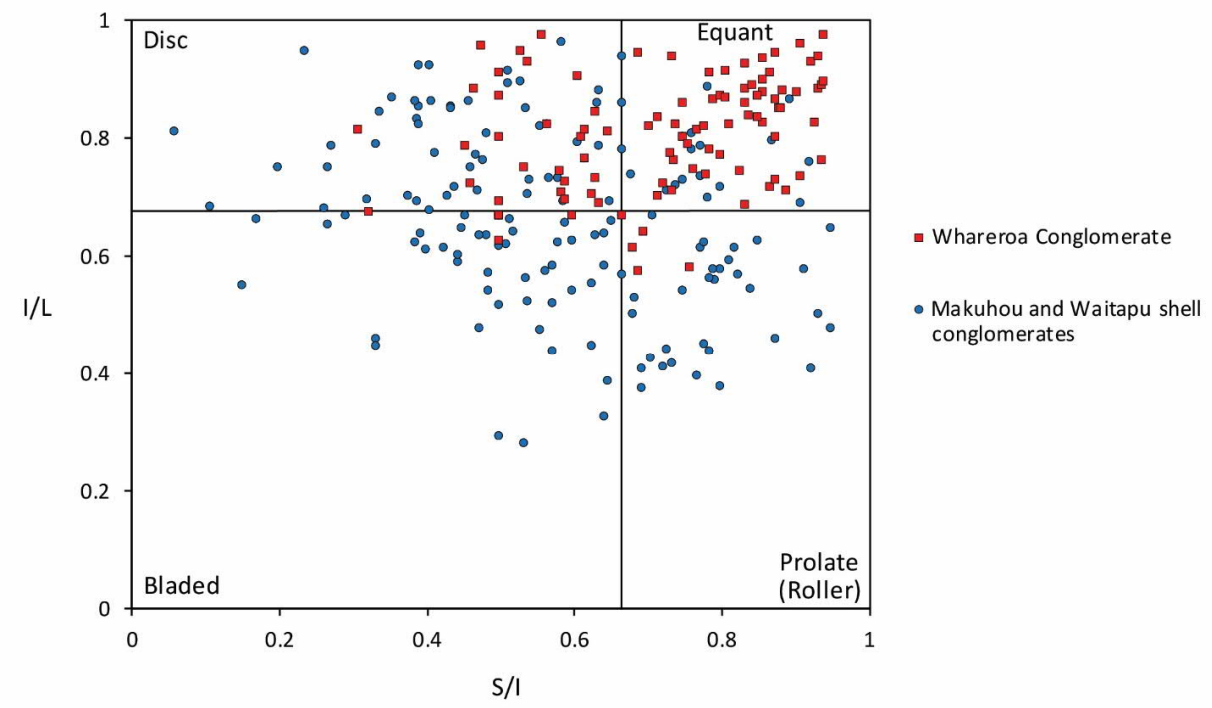


Figure 5.9: Zingg diagram showing clast shape measurements from the Whareroa Conglomerate (Pohangina and Beaconsfield valley sections) and the Makuhou and Waitapu shell conglomerates (Kaimatira Bluff, Turakina and Waitapu Stream sections).

The Makuhou Shell Conglomerate at Kaimatira Bluff displays mud draped crossbeds 0.5-1 m thick, merging into lenticular to flaser bedded siltstone bottom sets. Clasts are sub-rounded, dominantly disc shaped pebbles of greywacke, 19- 64 mm in diameter with rare cobbles up to 120 mm. The matrix is composed of equal portions crushed shell debris and coarse to granule sands. Isolated large clasts of pumice occur, up to 100 mm in diameter. Shells are often abraded and worn with rare lenses of well-preserved diverse assemblages including *Paphies* sp., *Xymene expansus*, *Talochlamys gemmulata*, *Barbatia novaezelandiae*, *Zethalia zelandica*, *Trochus taratus*, *Nucula nitidula*, *Alcithoe fusus* and *Alcithoe arabica.*

Heterolithic, siltstone and fine- to medium-grained sandstone, 12 m thick, occurs above the Makuhou Shell Conglomerate. Beds comprise rippled to planar sets 20 - 60 mm thick.

5.6 Discussion

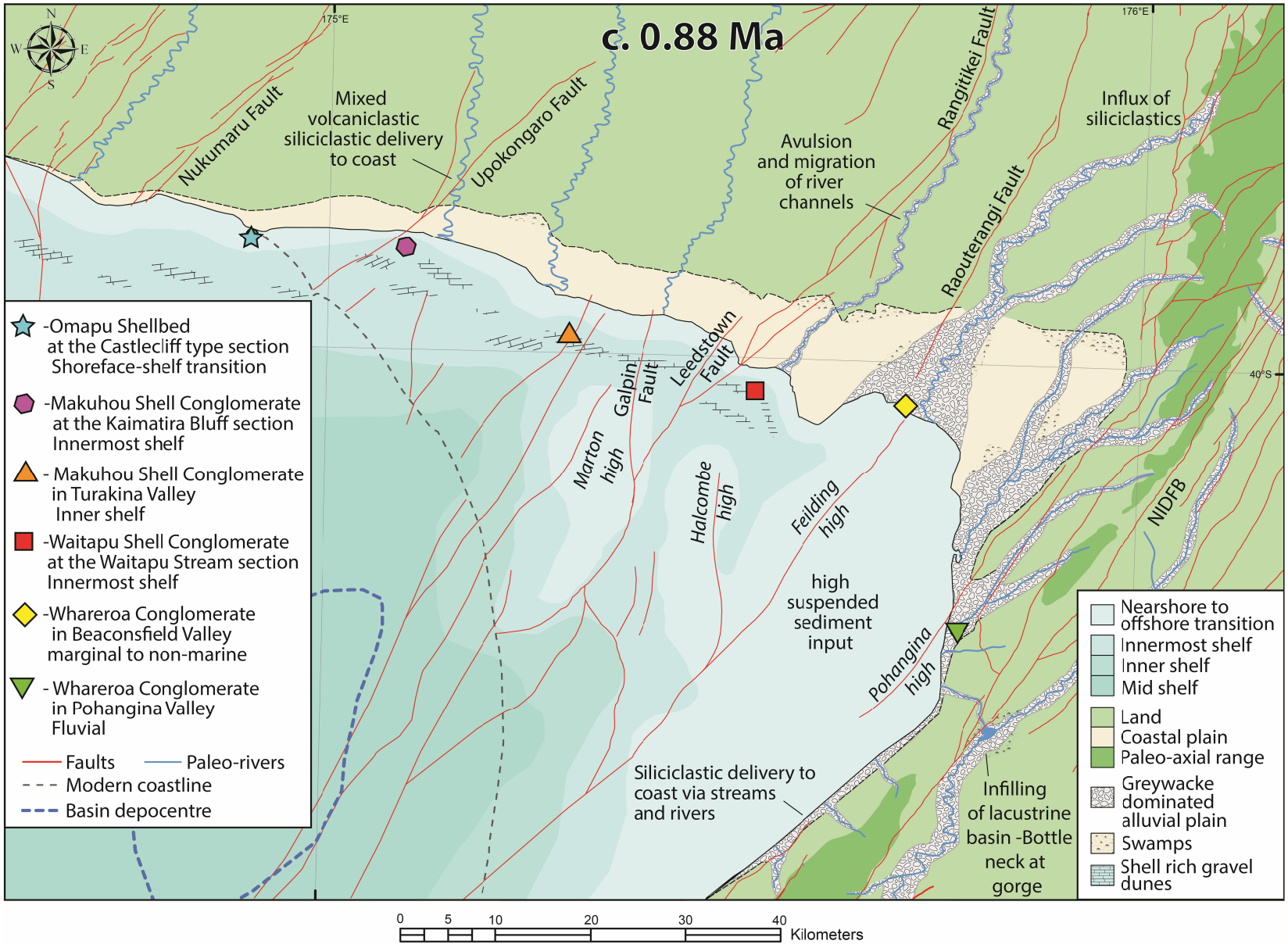
Stratigraphy and sedimentology

Waitapu Shell Conglomerate

The Waitapu Shell Conglomerate contains fossils representative of a wide variety of depositional environments (Supplementary Data File 5B, Appendix A). Shells are well mixed, broken and abraded, typical of reworking by waves and tidal currents. Trough cross-bedding indicates dune bed forms produced by strong unidirectional currents (Harms et al. 1982; Duke et al. 1991). Set thicknesses of up to 2 m implies the influence of strong tidal and/or storm-driven currents (Abbott 1998; Le Bot & Trentsaux 2004). Mud draped crossbed foresets (Fig. 5.5) indicate fluctuating energy conditions, including slack water/quiescent periods where finer particles settled from suspension. The channelled erosion surface below the crossbed sets was likely formed by strong storm/tidal action, possibly related to a reduction in the mean wave base and localised scour and fill of sediments (Dott & Bourgeois 1982).

The Waitapu Shell Conglomerate is analogous to the basal TST shell conglomerates described at the Castlecliff section (Abbott 1998), interpreted to represent deposition on a storm-dominated, muddy innermost shelf (Abbott & Carter 1994). We infer the presence of a fluvial outlet in close proximity to the depositional site, with headwaters located in the present day central North Island,

Figure 5.10 (facing page): A) Schematic cartoon of the WB during the marine transgression of WB cycle 36 (MIS 22) at c. 0.88 Ma (Bowen et al. 1998; Lisiecki & Raymo 2005). The location of time equivalent strata are displayed across the basin to demonstrate the approximate position of the paleo-shoreline and transition into greywacke dominated conglomerate toward the paleo-axial range. Data from Feldmeyer (1943), Piyasin (1966), Milne, (1968), Seward (1974), Anderton (1981), Abbott (1994), van der Neut (1996), Brackley (1999) and GNS Science.


c. 0.88 Ma
N
W
E
S
175°E
176°E
40°S
Nukumaru Fault
Mixed volcaniclastic siliciclastic delivery to coast
Upokongaro Fault
Avulsion and migration of river channels
Rangitikei Fault
Raouterangi Fault
Influx of siliciclastics
Leedstown Fault
Galpin Fault
Marton high
Halcombe high
Feilding high
high suspended sediment input
Pohangina high
NIDFB
Siliciclastic delivery to coast via streams and rivers
Infilling of lacustrine basin -Bottle neck at gorge
-Omapu Shellbed at the Castlecliff type section Shoreface-shelf transition
-Makuhou Shell Conglomerate at the Kaimatira Bluff section Innermost shelf
- Makuhou Shell Conglomerate in Turakina Valley Inner shelf
-Waitapu Shell Conglomerate at the Waitapu Stream section Innermost shelf
-Whareroa Conglomerate in Beaconsfield Valley marginal to non-marine
- Whareroa Conglomerate in Pohangina Valley Fluvial
Faults
Paleo-rivers
Modern coastline
Basin depocentre
Nearshore to offshore transition
Innermost shelf
Inner shelf
Mid shelf
Land
Coastal plain
Paleo-axial range
Greywacke dominated alluvial plain
Swamps
Shell rich gravel dunes
0 5 10 20 30 40
Kilometers

supplying abundant greywacke and volcaniclastic detritus to the coast. This is consistent with the lateral changes observed within the Waitapu Shell Conglomerate, as it grades into an eastern margin conglomerate facies, characterised by a lack of marine fossils, rare lignite and equant greywacke clasts, suggesting closer proximity to and influence from fluvial systems draining the uplifting paleo-axial range (Fig 9 and 10).

At the WBs eastern margin, we envision braid plains, delta fronts and gravelly beaches to have developed during sea level low stand, locally incising through the previous HST, as evidenced by delta type architecture above undulating surfaces of erosion within eastern margin conglomerate deposits (Fig. 5.7 A, B and D). Nearby land was likely deforested and sediment input particularly high (Beu et al. 1981; Lewis et al. 1994). Low stand deposits were later scoured and eroded during transgressive ravinement, reworked into shelly gravel dunes at inner-most shelf depths (Abbott 1998). Local preservation of low stand deposits in eastern WB (Abbott 1992), suggests transgressive ravinement was either not as destructive or that low stand incision was more pervasive along the eastern basin margin.

Marine transgression and associated shoreface retreat triggered sedimentary infilling of the valleys incised during the previous low stand (Rees et al. 2018b). Estuarine systems developed, hosting a wide range of species, including *Cyclomactra tristis, Austrovenus stutchburyi, Paphies australis* and *Cominella adspersa* (Supplementary Data File 5B, Appendix A), the shells of which were transported into the marine environment by rivers (Hayward & Stilwell 1995) or became entrained during transgressive ravinement and sedimentary reworking (Abbott 1998).

The abundant unweathered pumice within the Waitapu Shell conglomerate is typically of a much larger clast size than the accompanying clasts of greywacke, suggesting that a phase of important eruptions in the TVZ preceded and perhaps

accompanied its deposition (Te Punga 1952). This is consistent with the incorporation of clasts of charcoal within the lowest beds of the Waitapu Shell Conglomerate. In the Pohangina, Turakina and Whanganui valleys (Fig. 5.1), Kaukatea Tephra is preserved within marginal to shallow marine deposits just below the stratigraphic position of the Waitapu Shell Conglomerate, suggesting that volcanic activity closely preceded deposition of Waitapu Shell Conglomerate, occurring within cycle 35 (Naish et al. 2005; Pillans et al. 2005).

Whareroa Conglomerate

We correlate the Whareroa Conglomerate west from Pohangina Valley to Beaconsfield Valley (Fig. 5.1 and 5.2D). The name introduced in Rees et al. (2018a) is adopted in Beaconsfield Valley to describe a similar eastern margin conglomerate facies occupying the same stratigraphic position and to negate the unnecessary introduction of further nomenclature.

The most notable change within the Kai Iwi Group from the Waitapu Stream to Beaconsfield Valley (Rangitikei and Oroua catchments, Fig. 5.1) is a total absence of marine Mollusca. The last shellbed noted in the succession is below the Rewa Pumice (c. 1.19 Ma), and marine fossils are not encountered again until the Onepuhi Fossil Beds (c. 570 ka). This change is mirrored in the Pohangina Valley succession where the last shellbed containing marine Mollusca occurs below the Rewa Pumice.

The absence of fossils within the Whareroa Conglomerate occurs together with a change in clast shape, characterised by a greater proportion of equant clasts (Fig. 5.9). We interpret the Whareroa Conglomerate in the Beaconsfield section to occupy a more landward position relative to the Waitapu Shell Conglomerate, with more of a direct influence from a paleo-fluvial outlet. The lignite bed, locally capping the Whareroa Conglomerate (Fig. 5.7C), suggests a marginal to non-

marine setting, where organic matter preservation occurred in coastal wetlands developing on an outer alluvial floodplain or coastal plain (Fig. 5.10).

Makuhou Shell Conglomerate

The Makuhou Shell Conglomerate and overlying heterolithic to massive siltstone beds in Turakina Valley represent an ideal WB sequence as defined by Abbott (1998), recording progressively deeper water deposition above a transgressive ravinement surface. The basal cross-bedded shell conglomerate is considered to have formed seaward of the transgressive shoreface (Abbott 1994). Shell material was derived from contemporary shoreface (Paphies sp.) to marginal marine/estuarine environments together with a reworked component from the underlying rocks. Siliciclastic and volcaniclastic pebbles derived from paleo-rivers draining the central North Island and paleo-axial range were incorporated during reworking of LST coastal plain and alluvial facies and were supplied contemporaneously by rivers feeding the coast. Seaward of the reworked gravel deposits heterolithic silt and sands were deposited on a storm-dominated, muddy, inner shelf (Abbott 2000). During sea level high stand, massive to laminated siltstone accumulated at inner- to mid-shelf depths (Abbott 1997).

Soft Sediment Deformation Structures (SSDS)

LZ1

The soft sediment deformation of LZ1 (Fig. 5.2C) originates from a fine sandstone bed displaying water escape structures and a related sand dyke. We interpret paleo-liquefaction as having occurred within this fine sandstone, resulting in subsequent settling and the formation of indistinct to massive bedding, associated with re-distribution of grain-to-grain contacts. No evidence of bioturbation is present within this unit. Subsequent fluidisation above this basal sand is apparent

within the overlying intensely convolute beds where multiple smaller sites of injection occur (Fig. 5.6 A). The overlying sandstone typically contains a higher proportion of coarse silt, a greater level of consolidation and displays wavy to convolute bedding in contrast to the underlying massive, unconsolidated sandstone. Evidence of fluidisation includes multiple sites of injection, resulting from pore fluid expulsion from the underlying sandstone. As the pore-fluid has travelled up through the sediment, it has entrained particles resulting in convolute bedding displaying a moderate degree of sorting and separation of grains by density (Fig. 5.5 and 5.6A).

Large (400 mm) sub-angular, rip-up clasts of laminated to lenticular siltstone and sandstone display original bedding structures, demonstrating that the sediments were already moderately consolidated, prior to subsequent scouring and erosion (Fig. 5.6 B). These clasts appear to be derived from the heterolithic facies directly beneath the cross bed sets. We do not observe any loading structures along the contact between the Waitapu Shell Conglomerate and underlying heterolithic beds. Therefore, the storm/tidal activity involved in the deposition of Waitapu Shell Conglomerate is unlikely to have caused the LZ1 soft-sediment deformation, as the sediment would be required to be in a soft, unconsolidated and water-saturated state for wave-induced liquefaction to occur (Mory et al. 2007). Loading during deposition does not appear to have caused the LZ1 SSDS at the Waitapu Stream section. Rare load structures are preserved directly below the Whareroa Conglomerate in Beaconsfield Valley (Fig. 5.7). These structures occur in massive siltstone stratigraphically above LZ1. We suggest the silt that Whareroa Conglomerate was deposited onto at the Beaconsfield section, was in an unconsolidated, water-saturated state, prone to deformation during loading, conditions that do not appear to have existed during deposition of the Waitapu Shell Conglomerate c. 16 km farther west.

LZ2

The base of cycle 37 at the Waitapu Stream section (Fig. 5.2C) is marked by the Kaikokopu Shell Grit, grading upward into a heterolithic succession with interbedded SSDS (LZ2). We interpret this heterolithic succession as having been deposited on a storm-dominated, muddy innermost shelf with strong tidal currents, evidenced by unidirectional cross-bedding and the occurrence of abundant laminated coarse siltstone and fine sandstone. The pillow and ball structures of LZ2 are truncated along their upper contacts, suggesting they formed at or close to the sediment/water interface. They are separated by undeformed beds, 0.4 to 1 m thick, including 0.2 m beds of broken shells (shell debris), characteristic of a high rate of sediment supply and a high-energy environment (Figueiredo et al. 1982). The interpreted environment of deposition is well within the known range of the mean storm wave base on the modern Manawatu coast (c. 40 m, Dunbar & Barrett, 2005). Wave energy has been shown through experimental work (Okusa 1985; Lindenberg et al. 1989; Sassa & Sekiguchi 2001) and field studies to be capable of producing similar structures (Seed & Rahman 1977; Dalrymple 1979; Alfaro et al. 2002). Therefore, we cannot conclusively rule out the possibility of loading from rapid deposition (Kerr & Eyles 1991; Hildebrandt & Egenhoff 2007) or storm wave-induced liquefaction (Molina et al. 1998; Alfaro et al. 2002; Mory et al. 2007) during formation of LZ2.

LZ3

Toward the western basin margin at Kaimatira Bluff, we observe a prominent change in SSDS, associated with heterolithic facies of the Kaimatira Pumice Sand Formation. Cross-bedded, pebbly shell conglomerates occur as a series of gravel dunes or waves with intervening swale and interdune silts and muds (Fig. 5.8). Seafloor instability is indicated by the SSDS, where progressive down slope deformation occurs along the margins of the swales (Fig. 5.8). This suggests the

interdune sediments behaved as fluid mud into which coarse grained sands and granule material were able to sink, forming load and ball and pillow structures. Down slope, flow is indicated within the SSDS gradually decreasing toward the centre of the swale where the siltstone becomes structureless. We suggest paleo-slope instability is related to and perhaps a control on the formation of LZ3.

We observe similar relationships within Kai Iwi Group strata exposed in the Rangitikei and Beaconsfield valleys where evidence of slope instability occurs together with load structures, convolute bedding and channels (Fig. 5.6F). Slope instability appears to be particularly common within Kaimatira Pumice Sand Formation, suggesting increased sediment delivery to the coast following emplacement of the Kidnappers ignimbrite led to rapid deposition, loading and instability within the nearshore shelf environments of the WB.

Seismicity

We examined our SSDS data against the widely accepted criteria for identifying a seismic trigger presented by Seilacher (1969), Sims (1973, 1975), Obermeier et al. (1990) and Obermeier (1996). Here, we review the criteria and examine our observations in relation to each criterion.

1: SSDS occur within a seismically active area, including known faults distributed throughout the WB Castlecliffian outcrop belt (Beu et al. 1981; Pillans 1986; Pillans 1990b; Begg et al. 2005). Active faults include the Leedstown (Pillans 1990b), Galpin (Hellstrom 1993) and faults underlying the Halcombe Anticline (Melhuish et al. 1996). Major reverse faults, the Rangitikei and Rauoterangi faults (Fig. 5.10) displace Plio-Pleistocene strata by up to 293 m (Feldmeyer et al. 1943; Naish & Kamp 1995). These faults are suggested to have been active through the Plio-Pleistocene, with a renewed phase of uplift occurring at c. 1 Ma, coinciding

with a phase of volcanic activity within TVZ from 1.21-0.95 Ma (Briggs et al. 1993; Houghton et al. 1995; Krippner et al. 1998).

2: The SSDS we describe are restricted to specific stratigraphic horizons and are interbedded between units that remain undeformed.

3: SSDS can be traced over a wide lateral extent. In this paper we present evidence of liquefaction that can be traced beneath correlatives of the Waitapu Shell Conglomerate for 16 km from Beaconsfield Valley to the Rangitikei Valley (Fig. 5.1). Furthermore, the occurrence of SSDS can be traced more loosely within an intermittent zone from Pohangina Valley to Kaimatira Bluff in the Whanganui Valley, a distance of c. 70 km.

4: The structures described here are similar to those produced experimentally under conditions of earthquake-induced shaking (Nichols et al. 1994; Owen 1996). They are also comparable to SSDS reported in the literature within areas of known seismic activity (Obermeier et al. 1987; Blanc et al. 1998; Matsuda 2000; Perucca et al. 2014) and modern-day features of liquefaction documented following seismic events in New Zealand (Reid et al. 2012; Villamor et al. 2016), Japan (Lin 1997; Ishihara et al. 2014) and Italy (Ninfo et al. 2012; Rodriguez-Pascua et al. 2015).

5: There is evidence of an upward-directed strong hydraulic force that acted suddenly within LZ1, including multiple sites of injection. This sudden hydraulic force is also interpreted as having been brief, as it only affects a particular horizon, with overlying laminated to lenticular siltstone and sandstone remaining undisturbed.

6: There is no evidence of artesian springs or groundwater movement within the succession. The rise and fall in sea level associated with mid-Pleistocene 100 ka cycles following the mid-Pleistocene transition (c. 950 ka) (Medina-Elizalde & Lea

2005) occur on a longer timescale and are unlikely to initiate soft sediment deformation. The SSDS described in this paper are considered to have formed almost instantaneously.

Given the evidence stated above, combined with records of coastal liquefaction from relatively recent earthquakes (1848 Marlborough, 1855 Wairarapa earthquake) within the Whanganui-Manawatu Region (Fairless & Berrill 1984), we suggest that LZ1 has been induced by seismic events associated with tectonic and volcanic activity within the central and lower North Island.

Loading, rapid deposition and slope failure

There is evidence of slope failure within the Kai Iwi Group strata (Fig. 5.6F and 5.8). The failures are particularly common toward the base of the group, likely related to a increased sedimentation rate following emplacement of the Cape Kidnappers and Rocky Hill ignimbrite sheets (c. 1 Ma) (Cooper et al. 2017). Sedimentary response to ignimbrite emplacement involves inundation of river and coastal settings, causing valley aggradation, river avulsion, infilling of coastal embayment's and coastal progradation (Manville & Wilson 2004; Kataoka 2011). A dramatic flood of volcaniclastic sediment entered the WB occurred at c. 1 Ma (Potaka Pumice of Te Punga, 1952). This influx of volcaniclastic sediment forms one of the thickest TSTs documented within the WB (Pillans et al. 2005) and resulted in coastal progradation (Lewis 2007). We correlate the instability associated with LZ3 to this episode of increased sedimentation (Fig. 5.2A and 5.3), characterised by an abundance of unstable, water saturated sediment entering the WB, creating a hydraulically active seafloor environment (Abbott & Carter 1999).

Large-scale load structures (LZ3) and convolute bedding in particular are common along the margins of slope failures. Slope failure appears to exert a control on these structures and perhaps provide a triggering mechanism. Failure itself could be

related to rapid deposition and resultant instability within a shallow marine environment. Indeed evidence of loading, associated with LZ3 would corroborate this. Initiation of slope failure by wave or earthquake induced seismic activity is a possibility (Stigall & Dugan 2010), however, attribution of SSDS to seismicity relies on elimination of all other possible trigger mechanisms (Moretti & van Loon 2014) and is therefore unviable for LZ3.

5.7 Conclusion

The Waitapu Shell Conglomerate is an important chronostratigraphic marker horizon in the eastern WB. We formally designate a type section at Waitapu Stream, Rangitikei Valley. The fossil assemblage contains a mixture of estuarine to offshore species including a component derived from underlying rocks. Deposition took place seaward of a transgressive shoreline on a storm-dominated, muddy, innermost shelf, characterised by migrating gravel dunes interfingering with deeper water heterolithic facies. The abundance of fresh pumice and charcoal indicates deposition closely followed a major TVZ eruption within a phase of renewed volcanic activity from the Mangakino Volcanic Centre at c. 0.9 Ma.

We infer the presence of a fluvial outlet in close proximity to the depositional site, with headwaters located in the present-day central North Island and paleo-axial range, supplying abundant greywacke and volcaniclastic detritus to the coast. This is consistent with lateral changes observed within the Waitapu Shell Conglomerate, as it grades into an eastern margin conglomerate facies, suggesting closer proximity to and influence from fluvial systems draining the uplifting paleo-axial range.

We interpret liquefaction to have occurred within LZ1 beneath the Waitapu Shell Conglomerate, resulting in settling and the occurrence of indistinct to massive

bedding following re-distribution of grain-to-grain contacts. The overlying intensely convolute beds contain multiple injection sites attributed to successive fluidisation above the basal sandstone. We trace LZ1 east into Beaconsfield Valley and relate formation to earthquake-triggered seismicity, given an absence of load structures or signs of slope instability.

LZ2 occurs within a heterolithic succession typical of a high rate of sediment supply. The SSDS are truncated along their upper contact, suggesting they formed close to the sediment/water interface. The interpreted environment of deposition is within the known range of the mean storm wave base. A variety of possible trigger mechanisms are proposed, including rapid deposition, loading and storm wave-induced liquefaction.

The basal Kai Iwi Group contains common evidence for seafloor instability and associated soft sediment deformation (LZ3). We relate LZ3 to an increased sedimentation rate following emplacement of the Cape Kidnappers and Rocky Hill ignimbrite sheets (c. 1 Ma). Sedimentary response to ignimbrite emplacement involved inundation of river and coastal settings, causing valley aggradation, river avulsion, infilling and loading of the Whanganui coastal embayment and formation of a hydraulically active seafloor.

Acknowledgements

Alan G. Beu greatly aided with fossil identification, paleo-environmental interpretation and kindly reviewed the text. Extramural, undergraduate students and Boxin Li from Massey University, under the supervision of Julie Palmer aided in fossil collection from the Waitapu Shell Conglomerate. The manuscript was substantially improved following comments by Steve Abbott and an anonymous reviewer.

This paper uses the spelling ‘Whanganui’ rather than ‘Wanganui’ as recommended by the New Zealand Geographic Board (Ngā Pou Taunaha o Aotearoa).

References

Abbott ST 1992. The Mid Pleistocene Waiomio Shellbed (Castlecliffian, c. 550-600 ky), Wanganui Basin, New Zealand. Alcheringa: An Australasian Journal of Palaeontology 16(2): 171-180.

Abbott ST 1994. Sequence Stratigraphy, Sedimentology and Paleoecology of Pleistocene Cyclothems in the Castlecliff Section, Wanganui Basin, New Zealand, Unpublished PhD Thesis. James Cook University of Northern Queensland, Australia. 297 p.

Abbott ST 1997. Foraminiferal Paleobathymetry and Mid-Cycle Architecture of Mid-Pleistocene Depositional Sequences, Wanganui Basin, New Zealand. Palaios 12(3): 267-281.

Abbott ST 1998. Transgressive systems tracts and onlap shellbeds from mid-Pleistocene sequences, Wanganui Basin, New Zealand. Journal of Sedimentary Research 68: 253-268.

Abbott ST 2000. Detached mud prism origin of highstand systems tracts from mid-Pleistocene sequences, Wanganui Basin, New Zealand. Sedimentology 47(1): 15-29.

Abbott ST, Carter RM 1994. The sequence architecture of mid-Pleistocene (c. 1.1-0.4 Ma) cyclothems from New Zealand: facies development during a period of orbital control on sea-level cyclicity. In: De Boer PL, Smith DG ed. Oribital Forcing and Cyclic Sequences, Special Publication of the International Association of Sedimentologists. Oxford, John Wiley & Sons. Pp. 367-394.

Abbott ST, Carter RM 1999. Stratigraphy of the Castlecliffian type section: 10 mid-Pleistocene sequences from the Wanganui coast, New Zealand. New Zealand Journal of Geology and Geophysics 42(1): 91-111.

Alessio G, Alfonsi L, Brunori CA, Burrato P, Casula G, Cinti FR, Civico R, Colini L, Cucci L, De Martini PM and others 2013. Liquefaction phenomena associated with the Emilia earthquake sequence of May-June 2012 (Northern Italy). Natural Hazards and Earth System Sciences 13: 935-947.

Alfaro P, Delgado J, Estevez A, Molina JM, Moretti M, Soria JM 2002. Liquefaction and fluidization structures in Messinian storm deposits (Bajo Segura Basin, Betic Cordillera, southern Spain). Internation Journal of Earth Sciences 91(3): 505-513.

Allen JRL 1977. The possible mechanics of convolute lamination in graded sand beds. Journal of the Geological Society, London 134(1): 19-31.

Allen JRL 1982. Sedimentary structures: their character and physical basis, Elsevier, New York.

Bailey RA, Carr RG 1994. Physical geology and eruptive history of the Matahina Ignimbrite, Taupo Volcanic Zone, North Island, New Zealand. New Zealand Journal of Geology and Geophysics 37(3): 319-344.

Bastin SH, Quigley MC, Bassett K 2015. Paleoliquifaction in Christchurch, New Zealand Geological Society Of America Bulletin 127(9/10): 1348-1365.

Begg JG, Palmer A, Gyopari M 2005. Geological synopsis of the Manawatu-Horowhenua area for a review of the region's hydrogeology. Institue of Geological and Nucelar Sciences Client Report 2005/172, Lower Hutt, New Zealand. 22 p.

Beu AG, Browne GH, Grant-Taylor TL 1981. New *Chlamys delicatula* localities in the central North Island and uplift of the Ruahine Range. New Zealand Journal of Geology and Geophysics 24(1): 127-132.

Blanc EJP, Blanc-Aletru MC, Mojon PO 1998. Soft-sediment deformation structures interpreted as seismites in the uppermost Aptian to lowermost Albian transgressive deposits of the Chihuahua basin (Mexico). Geologische Rundschau 86: 875-883.

Bowen DQ, Pillans B, Sykes GA, Beu AG, Edwards AR, Kamp PJJ, Hull AG 1998. Amino acid geochronology of Pleistocene marine sediments in the Wanganui Basin: a New Zealand framework for correlation and dating. Journal of the Geological Society 155(3): 439-446.

Brackley H 1999. The Stratigraphy and Environments of Deposition of Early-Mid Pleistocene Sediments of the Pohangina Region, Eastern Wanganui Basin, New Zealand., Unpublished MSc thesis, Massey University, Palmerston North, New Zealand. 113 p.

Briggs RM, Houghton BF, McWilliams M, Wilson CJN 2005. $^{40}Ar/^{39}Ar$ ages of silicic volcanic rocks in the Tauranga Kaimai area, New Zealand: Dating the transition between volcanism in the Coromandel Arc and the Taupo Volcanic Zone. New Zealand Journal of Geology and Geophysics 48(3): 459-469.

Briggs RM, Gifford MG, Moyle AR, Taylor SR, Norman MD, Houghton BF, Wilson CJN 1993. Geochemical zoning and eruptive mixing in ignimbrites from Mangakino volcano, Taupo Volcanic Zone, New Zealand. Journal of Volcanology and Geothermal Research 56: 175-203.

Bussell MR 1984. Geology and Paleobotany of the Rangitawa Stream area, Southeast Wanganui Basin, Unpublished BSc (Hons) Thesis. Victoria University of Wellington, Wellington, New Zealand. 181 p.

Carr RG 1984. The Matahina Ignimbrite: Its Evolution Including its Eruption and Post Depositional Changes. Unpublished PhD Thesis, University of Auckland, New Zealand. 1-254 p.

Carter RM, Naish TR 1998. A review of Wanganui Basin, New Zealand: Global reference section for shallow marine, Plio-Pleistocene (2.5-0 Ma) cyclostratigraphy. Sedimentary Geology 122(1-4): 37-52.

Carter RM, Abbott ST, Fulthorpe CS, Haywick DW, Henderson RA 1991. Application of Global Sea - Level and Sequence - Stratigraphic Models in Southern Hemisphere Neogene Strata from New Zealand. Special Publication of the International Association of Sedimentologists(12): 41-65.

Collinson JD 1996. Alluvial sediments. In: Reading HG ed. Sedimentary Environments: Processes, Facies and Stratigraphy, Blackwell, Oxford. Pp. 37-82.

Cooper GF, Morgan DJ, Wilson CJN 2017. Rapid assembly and rejuvenation of a large silicic magmatic system: Insights from mineral diffusive profiles in the Kidnappers and Rocky Hill deposits, New Zealand. Earth and Planetary Science Letters 473: 1-13.

Cubrinovski M, Bray JD, Taylor M, Giorgini S, Bradley B, Wotherspoon L, Zupan J 2011. Soil Liquefaction Effects in the Central Business District during the February 2011 Christchurch Earthquake. Seismological Research Letters 82(6): 893-904.

Dalrymple RW 1979. Wave-induced liquefaction: a modern example from the Bay of Fundy. Sedimentology 26: 835-844.

Davenport CA, Ringrose PS 1987. Deformation of Sediments and Sedimentary Rocks. Geological Society, London, Special Publications 29: 299-314.

Dott RH, Bourgeois J 1982. Hummocky stratification: Significance of its variable bedding sequences. Geological Society Of America Bulletin 93: 663-680.

Duke WL, Arnott RWC, Cheel RJ 1991. Shelf sandstones and hummocky cross-stratification: New insights on a stormy debate. Geology 19: 625-628.

Dunbar GB, Barrett PJ 2005. Estimating palaeobathymetry of wave-graded continental shelves from sediment texture. Sedimentology 52: 253-269.

Eiby GA 1968. A descriptive catalogue of New Zealand earthquakes. New Zealand Journal of Geology and Geophysics 11(1): 16-40.

Fairless GJ, Berrill JB 1984. Liquefaction during historic earthquakes in New Zealand. Earthquake Engineering 17(4): 280-291.

Feldmeyer AE, Jones BC, Firth CW, Knight J 1943. The geology of the Palmerston-Wanganui Basin, "West side", North Island, New Zealand. Unpublished Report of the Superior Oil Company of New Zealand, Petroleum Report Series 171, Ministry of Economic Development, Wellington, New Zealand. 46 p.

Figueiredo AG, Sanders JE, Swift DJP 1982. Storm-graded layers on inner continental shelves: Examples from southern Brazil and the Atlantic Coast of the Central United States. Sedimentary Geology 31: 171-190.

Fleming CA 1953. The geology of Wanganui subdivision. New Zealand Geological Survey Bulletin 52. Wellington, New Zealand. 362 p.

Giona Bucci M, Villamor P, Almond P, Tuttle M, Stringer M, Ries W, Smith C, Hodge M, Watson M 2018. Associations between sediment architecture and liquefaction suceptibility in fluvial settings: The 2010-2011 Canterbury Earthquake Sequence, New Zealand. Engineering Geology 237: 181-197.

Giona Bucci M, Almond P, Villamor P, Tuttle M, Stringer M, Smith C, Ries W, Bourgeois J, Loame R, Howarth J and others 2017. Which sedimentary environment best preserves paleoliquefaction features? PATA DAYS 2017: 8th International Workshop on Paleoseismology, Active Tectonics and Archeoseismology, 13th - 16th November, Blenheim, New Zealand. Pp. 1-4.

Green RA, Cubrinovski M, Cox B, Wood C, Wotherspoon L, Bradley B, Maurer B 2014. Select liquefaction case histories from the 2010-2011 Canterbury earthquake sequence. Earthquake Spectra 30(1): 131-153.

Green RA, Wood C, Cox B, Cubrinovski M, Wotherspoon L, Bradley B, Algie T, Allen J, Bradshaw A, Rix G 2011. Use of DCP and SASW Tests to Evaluate Liquefaction Potential: Predictions vs. Observations during the Recent New Zealand Earthquakes. Seismological Research Letters 82(6): 927-938.

Harms JC, Southard JB, Walker RG 1982. Structures and sequences in clastic rocks. Society of Economic Paleontologists and Mineralogists, Short Course No. 9: 1-249.

Hayward BW, Stilwell JD 1995. Floating cockle shells (*Austrovenus stutchburyi*) - Their significance to paleoenvironmental assessments. Tane 35: 143-148.

Hellstrom JC 1993. An investigation of the Galpin Fault, Marton, Rangitikei Unpublished BSc (Hons) Thesis. Victoria University of Wellington, Wellington, New Zealand. 89 p.

Hildebrandt C, Egenhoff S 2007. Shallow-marine massive sandstone sheets as indicators of palaeoseismic liquefaction - An example from the Ordovician shelf of Central Bolivia. Sedimentary Geology 202: 581-595.

Houghton BF, Wilson CJN, McWilliams MO, Lanphere MA, Weaver SD, Briggs RM, Pringles MS 1995. Chronology and dynamics of a large silicic magmatic system : Central Taupo Volcanic Zone , New Zealand. Geology 23(1): 13-16.

Idriss IM, Boulanger RW 2008. Soil Liquefaction during Earthquakes. Monograph Series: Oakland, California, Earthquake Engineering Research Institute 1-261.

Ishihara K, Araki K, Toshiyuki K 2014. Liquefaction in Tokyo bay and Kanto regions in the 2011 great east Japan earthquake. The 2011 Great East Japan Earthquake. Earthquake Geotechnical Engineering Design, Springer International Publishing. Pp. 93-140.

Jackson J, van Dissen R, Berryman KR 1998. Tilting of active folds and faults in the Manawatu region, New Zealand: Evidence from surface drainage patterns. New Zealand Journal of Geology and Geophysics 41(4): 377-385.

Jarosewich E, Nelen JA, Norberg JA 1980. Reference Samples for Electron Microprobe Analysis. Geostandards Newsletter 4(1): 43-47.

Jochum KP, Stoll B, Herwig K, Willbold M, Hofmann AW, Amini M, Aarburg S, Abouchami W, Hellebrand E, Mocek B and others 2006. MPI-DING reference glasses for in sity microanalysis: New reference values for element concentrations and isotope ratios. Geochemistry, Geophysics, Geosystems 7(2): 1-44.

Kataoka KS 2011. Geomorphic and sedimentary evidence of a gigantic outburst flood from Towada caldera after the 15 ka Towada-Hachinohe ignimbrite eruption, northeast Japan. Geomorphology 125: 11-26.

Kerr M, Eyles N 1991. Storm-deposited sandstones (tempestites) and related ichnofossils of the Late Ordovician Georgian Bay Formation, southern Ontario, Canada. Canadian Journal of Earth Science 28: 266-282.

Kershaw C 1989. The geology of the area around Kaimatira Bluff, Wanganui, New Zealand. Unpublished BSc (Hons) thesis, Victoria University of Wellington.

Kleyburg MA, Moon VG, Lowe DJ, Nelson CS 2015. Paleoliquefaction in Late Pleistocene alluvial sediments in Hauraki and Hamilton basins, and implications for paleoseismicity Proceedings of the 12th Australia New Zealand Conference on Geomechanics (ANZ 2015), 22-25 February 2015, Wellington, New Zealand: 524-531.

Krippner SJP, Briggs RM, Wilson CJN, Cole JW 1998. Petrography and geochemistry of lithic fragments in ignimbrites from the Mangakino Volcanic Centre: Implications for the composition of subvolcanic crust in western Taupo

Volcanic Zone, New Zealand. New Zealand Journal of Geology and Geophysics 41(2): 187-199.

Le Bot S, Trentsaux A 2004. Types of internal structure and external morphology of submarine dunes under the influence of tide- and wind-driven processes (Dover Strait, northern France). Marine Geology 211: 143-168.

Lewis B 2007. Eruptive Source and Depositional Characteristics of the Potaka Tephra, Wanganui Basin, New Zealand. University of Otago, Dunedin, New Zealand, Unpublished. 304 p.

Lewis KB 1971. Slumping on a continental slope inclined at 1°-4°. Sedimentology 16: 97-110.

Lewis KB, Carter L, Davey FJ 1994. The opening of Cook Strait: Interglacial tidal scour and aligning basins at a subduction to transform plate edge. Marine Geology 116: 293-312.

Lin A 1997. Instantaneous-shaking liquefaction induced by the M7.2 1995 Southern Hyogo Prefecture earthquake, Japan. Geology 25(5): 435-438.

Lindenberg J, van Rijn LC, Winterwerp JC 1989. Some Experiments on Wave-induced Liquefaction of Soft Cohesive Soils. Journal of Coastal Research(Special Issue no 5): 127-137.

Lisiecki LE, Raymo ME 2005. A Pliocene-Pleistocene stack of 57 globally distributed benthic $\delta^{18}O$ records. Paleoceanography 20(PA1003): 1-17.

Lowe DR 1976. Subaqueous liquefied and fluidized sediment flows and their deposits. Sedimentology 23: 285-308.

Manville V, Wilson CJN 2004. The 26.5 ka Oruanui eruption, New Zealand: A review of the roles of volcanism and climate in the post-eruptive sedimentary response. New Zealand Journal of Geology and Geophysics 47(3): 525-547.

Manville V, Newton EH, White JDL 2005. Fluvial responses to volcanisim: resedimentation of the 1800a Taupo ignimbrite eruption in the Rangitaiki River catchment, North Island, New Zealand. Geomorphology 65: 49-70.

Matsuda J 2000. Seismic deformation structures of the post-2300 a BP muddy sediments in Kawachi lowland plain, Osaka, Japan. Sedimentary Geology 135: 99-116.

Medina-Elizalde M, Lea DW 2005. The Mid-Pleistocene Transition in the Tropical Pacific. Science 310(1009-1012).

Melhuish A, van Dissen R, Berryman KR 1996. Mount Stewart-Halcombe Anticline: A look inside a growing fold in the Manawatu region, New Zealand. New Zealand Journal of Geology and Geophysics 39: 123-133.

Milne JDG 1968. The geology and soils of the Apiti District. Unpublished MSc thesis, Victoria Universtiy of Wellington, New Zealand. 122 p.

Milne JDG 1973. Upper Quaternary geology of the Rangitikei drainage basin, North Island, New Zealand. Unpublished PhD Thesis. Victoria University of Wellington, Wellington, New Zealand. 472 p.

Molina JM, Alfaro P, Moretti M, Soria JM 1998. Soft-sediment deformation structures induced by cyclic stress of storm waves in tempestites (Miocene, Guadalquivir Basin, Spain). Terra Nova 10: 145-150.

Moretti M, van Loon AJ 2014. Restrictions to the application of 'diagnostic' criteria for recognizing ancient seismites. Journal of Palaeogeography 3(2): 162-173.

Mory M, Michallet H, Bonjean D, Piedra-Cueva I, Barnoud JM, Foray PB, P. 2007. A field study of momentary liquefaction caused by waves around a coastal structure. Journal of waterway, port, coastal, and ocean engineering 133(1): 28-38.

Naish TR, Kamp PJJ 1995. Pliocene-Pleistocene marine cyclothems , Wanganui Basin , New Zealand : a lithostratigraphic framework. New Zealand Journal of Geology and Geophysics 38: 223-243.

Naish TR, Field BD, Zhu H, Melhuish A, Carter RM, Abbott ST, Edwards S, Alloway BV, Wilson GS, Niessen F and others 2005. Integrated outcrop, drill core, borehole and seismic stratigraphic architecture of a cyclothemic, shallow marine depositional system, Wanganui Basin, New Zealand. Journal of the Royal Society of New Zealand 35(1-2): 91-122.

Nichols RJ, Sparks RSJ, Wilson CJN 1994. Experimental studies of the fluidization of layered sediments and the formation of fluid escape structures. Sedimentology 41: 233-253.

Ninfo A, Zizioli D, Meisina C, Castaldini D, Zucca F, Luzi L, De Amicis M 2012. The survey and mapping of sand-boil landforms related to the Emilia 2012 earthquakes: preliminary results. Annals of Geophysics 55(4): 735-742.

Obermeier SF 1996. Use of liquefaction-induced features for paleoseismic analysis - An overview of how seismic liquefaction features can be distinguished from other features and how their regional distribution and properties of source sediment can be used to infer the location and strength of Holocene paleo-earthquakes. Engineering Geology 44: 1-76.

Obermeier SF, Weems RE, Jacobson RB 1987. Earthquake-induced liquefaction features in the coastal South Carolina region. Department of the Interior, US Geological Survey Open File Report 87-504: 480-493.

Obermeier SF, Jacobson RB, Smoot JP, Weems RE, Gohn GS, Monroe JE, Powars DS 1990. Earthquake-induced liquefaction features in the coastal setting of South Carolina and in th fluvial setting of the New Madrid seismic zone. United States Geological Survey Professional Paper 1504: 1-44.

Okusa S 1985. Wave-induced stresses in unsaturated submarine sediments. Geotechnique 35(4): 517-532.

Onorato MR, Perucca L, Coronato A, Rabassa J, Lopez R 2016. Seismically-induced soft-sediment deformation structures associated with the Magallanes-Fagnano Fault System (Isla Grande de Tierra del Fugeo, Argentina). Sedimentary Geology 344: 135-144.

Owen G 1996. Experimental soft-sediment deformation: structures formed by the liquefaction of unconsolidated sands and some ancient examples. Sedimentology 43: 279-293.

Owen G, Moretti M 2011. Identifying triggers for liquefaction-induced soft-sediment deformation in sands. Sedimentary Geology 235: 141-147.

Perucca LP, Godoy E, Pantano A 2014. Late Pleistocene-Holocene earthquake-induced slumps and soft-sediment deformation structures in the Acequion River valley, Central Precordillera, Argentina. Geologos 20(2): 147-156.

Pillans BJ 1986. A late Quaternary uplift map for North Island, New Zealand. Royal Society of New Zealand Bulletin 24: 409-417.

Pillans BJ 1990a. Pleistocene marine terraces in New Zealand : A review. New Zealand Journal of Geology and Geophysics 33(2): 219-231.

Pillans BJ 1990b. Vertical displacement rates on Quaternary faults, Wanganui basin. New Zealand Journal of Geology and Geophysics 33(2): 271-275.

Pillans BJ 1994. Direct marine-terrestrial correlations, Wanganui Basin, New Zealand: The last 1 million years. Quaternary Science Reviews 13(3): 189-200.

Pillans BJ 2017. Quaternary Stratigraphy of Whanganui Basin-A Globally Significant Archive. In: Schulmeister J ed. Landscape and Quaternary Environmental Change in New Zealand. Brisbane, Australia, Atlantis Press. Pp. 141-170.

Pillans BJ, Roberts AP, Wilson GS, Abbott ST, Alloway BV 1994. Mangnetostratigraphic, lithostratigraphic and tephrostratigraphic constraints on Lower and Middle Pleistocene sea-level changes, Wanganui Basin, New Zealand. Earth and planetary science letters 121: 81-98.

Pillans BJ, Alloway B, Naish TR, Westgate J, Abbott S, Palmer AS 2005. Silicic tephras in Pleistocene shallow-marine sediments of Wanganui Basin, New Zealand. Journal of the Royal Society of New Zealand 35(1-2): 43-90.

Potter WD 1984. Upper Quaternary Geology of part of the lower Rangitikei Valley, Unpublished BSc (hons) Thesis. Victoria University of Wellington, Wellington, New Zealand. 84 p.

Quigley MC, Bastin SH, Bradley BA 2013. Recurrent liquefaction in Christchurch, New Zealand, during the Canterbury earthquake sequence. Geology 41(4): 419-422.

Rees CJ, Palmer JA, Palmer AS 2018a. Plio-Pleistocene Geology of the Lower Pohangina Valley, New Zealand. New Zealand Journal of Geology and Geophysics 61(1): 44-63.

Rees CJ, Palmer JA, Palmer AS 2018b. Quaternary sedimentology and tephrostratigraphy of the lower Pohangina Valley, New Zealand. New Zealand Journal of Geology and Geophysics 62(2): 171-194. DOI: 10.1080/00288306.2018.1547321.

Rees CJ, Palmer JA, Palmer AS, Singh R 2019. Landscape evolution and hydrogeochemical characteristics of the Pourewa Stream catchment, Lower North Island, New Zealand. New Zealand Journal of Geology and Geophysics 62(2): 147-170. DOI: 10.1080/00288306.2018.1541812

Reid CM, Thompson NK, Irvine JRM, Laird TE 2012. Sand volcanoes in the Avon-Heathcote Estuary produced by the 2010-2011 Christchurch Earthquakes: implications for geological preservation and expression. New Zealand Journal of Geology and Geophysics 55(3): 249-254.

Rodriguez-Pascua MA, Silva PG, Lopez RP, Giner-Robles JL, Martin-Gonzalez F, Moral BD 2015. Polygenetic sand volcanoes: On the features of liquefaction processes generated by a single event (2012 Emilia Romagna 5.9 Mw earthquake, Italy). Quaternary International 357: 329-335.

Sassa S, Sekiguchi H 2001. Analysis of wave-induced liquefaction of sand beds. Geotechnique 51(2): 115-126.

Seed HB, Lee KL 1966. Liquefaction of Saturated Sands During Cyclic Loading. Journal of the Soil Mechanics and Foundations Divsion 92(6): 105-134.

Seed HB, Rahman MS 1977. Wave-induced pore pressure in relation to ocean floor stability of cohesionless soils. Marine Geotechnology 3: 123-150.

Seed HB, Idriss IM 1982. Ground Motions and Soil Liquefaction during Earthquakes, Monograph Series: Berkeley, California, Earthquake Engineering Research Institute. 1-134.

Seilacher A 1969. Fault-graded beds interpreted as seismites. Sedimentology 13: 15-159.

Seward D 1974. Some Aspects of Sedimentology of the Wanganui Basin, North Island, New Zealand., Unpublished PhD thesis, Victoria University of Wellington, Wellington, New Zealand. 285 p.

Seward D 1976. Tephrostratigraphy of the marine sediments in the Wanganui Basin , New Zealand. New Zealand Journal of Geology and Geophysics 19(1): 9-20.

Shane PAR 1991. Remobilised silicic tuffs in middle Pleistocene fluvial sediments , southern North Island, New Zealand. New Zealand Journal of Geology and Geophysics 34(4): 489-499.

Shane PAR 1993. Tephrostratigraphy, magnetostratigraphy and geochronology of some early and middle Pleistocene deposits in New Zealand, Unpublished PhD Thesis. Victoria University of Wellington, Wellington, New Zealand. 136 p.

Shane PAR 1994. A widespread , early Pleistocene tephra (Potaka tephra, 1 Ma) in New Zealand: Character, distribution, and implications. New Zealand Journal of Geology and Geophysics 37(1): 25-35.

Sims JD 1973. Earthquake-induced structures in sediments of Van Norman Lake, San Fernando, California. Science 182(4108): 161-163.

Sims JD 1975. Determining earthquake recurrence intervals from deformational structures in young lacustrine sediments. Tectonophysics 29: 141-152.

Stern TA, Quinlan GM, Holt WE 1992. Basin formation behind an active subduction zone: Three dimensional flexural modelling of Wanganui Basin, New Zealand. Basin research 4(3-4): 197-214.

Stern TA, Quinlan GM, Holt WE 1993. Crustal dynamics associated with the formation of Wanganui Basin, New Zealand. In: Ballance PF ed. South Pacific Sedimentary Basins: Sedimentary Basins of the World 2. Amsterdam, Elsevier. Pp. 213-223.

Stigall J, Dugan B 2010. Overpressure and earthquake initiated slope failure in the Ursa region, northern Gulf of Mexico. Journal of Geophysical Research 115: 1-11.

Strachan LJ 2008. Flow transformations in slumps: a case study from the Waitemata Basin, New Zealand. Sedimentology 55: 1311-1332.

Stratford WR, Stern TA 2004. Strong seismic reflections and melts in the mantle of a continental back-arc basin. Geophysical Research Letters 31(6): 1-5.

Te Punga MT 1952. The geology of Rangitikei Valley. New Zealand Geological Survey Memoir 8, Wellington, New Zealand. 46 p.

Te Punga MT 1957. Live anticlines in western Wellington. New Zealand Journal of Science and Technology(38): 433-466.

van der Neut M 1996. Sequence Stratigraphy of Plio-Pleistocene Sediments in Lower Turakina Valley, Wanganui Basin, New Zealand. Unpublished MSc Thesis. Massey Univeristy, Palmerston North, New Zealand. 149 p.

Villamor P, Almond P, Tuttle MP, Giona-Bucci M, Langridge RM, Clark K, Ries W, Bastin SH, Eger A, Vandergoes M and others 2016. Liquefaction Features Produced by the 2010-2011 Canterbury Earthquake Sequence in Southwest Christchurch, New Zealand, and Preliminary Assessment of Paleoliquefaction Features. Bulletin of the Seismological Society of America 106(4): 1-25.

Ward SD, Brown MKH, Brown IR, Larkin TJ 2011. Geological engineering study of liquefaction after the 2010 Darfield earthquake in an area of complex fluvial geology. Proceedings of the Ninth Pacific Conference on Earthquake Engineering: Building an Earthquake-Resilient Society, Auckland, New Zealand 14-16 April 2011, Paper Number 053: 1-8.

Yasuda S, Harada K, Ishikawa K, Kanemaru Y 2012. Characteristics of liquefaction in Tokyo Bay area by the 2011 Great East Japan Earthquake. Soils and Foundations 52(5): 793-810.



Chapter 6

Hydrogeology

The following chapter contains a peer-reviewed journal article published in the New Zealand Journal of Geology and Geophysics, Volume 62, Issue 2. In this chapter, we satisfy thesis objective three by subdividing the stratigraphy of the central Rangitikei into broad hydrostratigraphic units and taking representative samples. A wide range of analyses are then performed to characterise each unit and understand the important factors controlling a sample's hydraulic conductivity. We present a 1:25 000 hydrogeological map and corresponding structural interpretation. Key discussion points include:

- Landscape evolution
- Hydrostratigraphy
- Denitrification
- Springs

This chapter provides an overview of the study area's hydrogeology, establishing a firm base upon which to launch a targeted and detailed analysis of key hydrostratigraphic units, the results of which are presented in Chapter 7.

Rangitikei River flowing over carbonaceous mudstone of the Makirikiri Tuff Formation during summer low-flow.

Landscape evolution and hydrogeochemical characteristics of the Pourewa Stream catchment, lower North Island, New Zealand

Callum Rees[1], Julie Palmer[1], Alan Palmer[1] and Ranvir Singh[1]

[1]*Environmental Sciences, School of Agriculture and Environment, Massey University, Palmerston North, New Zealand*

6.1 Abstract

The Pourewa Stream, a tributary of the Rangitikei River, drains sheep and beef hill country before flowing through the township of Hunterville toward the intensively farmed Rangitikei terraces. Recent issues regarding water quality and supply have been raised, following ongoing landuse change and associated demand for freshwater within an agriculturally driven local economy. Nitrogen loss from farms due to rapid leaching of nitrate into the subsurface has increased in conjunction with landuse intensification. The Pourewa stream dissects a portion of the Plio-Pleistocene Whanganui Basin fill, including cyclothems of alternating coarse and fine-grained sediments that form interbedded aquifers, aquitards, seeps and springs within a geologically young landscape. The Rangitikei River dominates the landscape, forming a series of aggradational terraces in this actively uplifting marine basin. Coarse Torlesse Terrane and andesite gravels entrained from the Rangitikei's central North Island headwaters form an important constituent of the Late Quaternary valley fill. En echelon fault lines and

corresponding basement highs run approximately NE–SW up the Rangitikei Valley, providing a control on both the underlying Plio-Pleistocene stratigraphic architecture and modern day drainage network. A 1: 25 000 hydrogeological map and corresponding structural interpretation are presented. Analysis of representative catchment lithologies demonstrates the importance of fines content, mean grain size, effective porosity and age in dictating hydraulic conductivity. Organic carbon, illite and glauconite present within the hydrostratigraphic succession indicate natural attenuation of nitrate within the local groundwater system is taking place.

Keywords: Plio-Pleistocene, Stratigraphy, Hydrogeology, Whanganui Basin, Aquifer.

6.2 Introduction

Agriculture constitutes 90% of landuse in the Rangitikei region (Zarour 2008), placing pressure on fresh water resources required for ongoing agricultural development and production. Recent concerns around the availability and long-term sustainability of freshwater resources have initiated research into the region's groundwater systems (Roygard & Carlyon 2004; Begg et al. 2005; McArthur et al. 2007; Wilson 2007; Collins et al. 2017). Limited knowledge and information is available on local-scale hydrogeological settings within the Rangitikei Region. A sound understanding of local hydrogeology is necessary for improved mapping and quantification of the region's groundwater resources. Furthermore, information on local hydrogeological settings is essential for improving our understanding and ability to map and quantify water and nutrient flow pathways and attenuation from farmlands to receiving waters, informing practices and policies for targeted and effective water quality management.

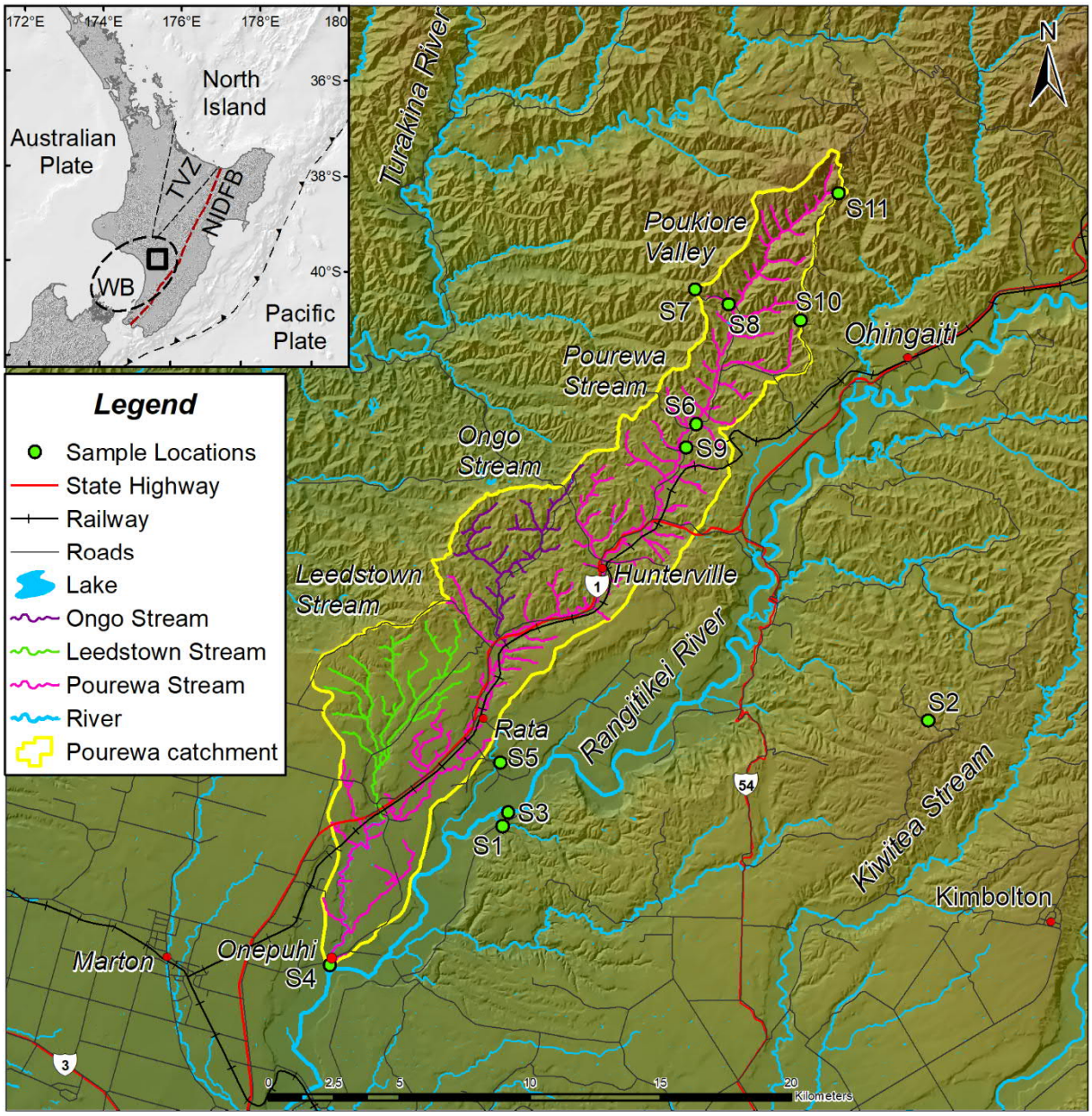


Figure 6.1: Location map of the study area displaying the outline of the Pourewa Stream catchment in yellow and relevant place names along its length. Sample locations: S1–Waitapu Shell Conglomerate, S2-Rewa Pumice, S3-Rangitikei River gravel, S4-Pourewa Stream gravel, S5-Potaka Pumice, S6-Mangamako Shellbed, S7-Mangarere Siltstone, S8-Te Rimu Sandstone, S9-Mangamako Sandstone, S10-Hautawa Shellbed, S11-Mangaweka Mudstone Formation. Inset displays location of the study area within Whanganui Basin (WB) and its location relative to the Taupo Volcanic Zone (TVZ), North Island Dextral Fault Belt (NIDFB) and the Australian–Pacific plate interface.

Previous studies have taken a broad approach examining classification, allocation, management and vulnerability of groundwater resources (Roygard & Carlyon 2004; McCarron & Zarour 2005; McArthur et al. 2007; Wilson 2007; Zarour 2008;

Callander & Thomas 2013; Morgenstern et al. 2015; Singh et al. 2017). There is a knowledge gap concerning the hydrogeochemical characteristics of the various rock types within the Rangitikei District. This study addresses that knowledge gap in a sub-catchment of the Rangitikei.

Our approach centres on geological mapping and development of a conceptual understanding of basin history and landscape evolution. This forms the rationale behind our sampling design and targeted hydrogeochemical analysis of representative catchment lithologies. Although the Pourewa catchment is the focus of this study, we consider a wider perspective is required to both effectively explore and document catchment development through time and understand how regional geology and structure influence the local groundwater system. For these reasons, the geological mapping boundary covers a 1,600-km^2 portion of the central Rangitikei District centred around the Pourewa Stream (Fig. 6.1). A particularly important factor considered whilst setting the field area was the need to capture and explore the adjacent Rangitikei River, a feature that has played a significant role in landscape evolution.

This paper presents data from a range of analyses, providing information on the ability of local lithologies to store and transmit water. We relate organic carbon together with structural and exchangeable ferrous iron (Fe^{2+}) to environments of deposition, providing evidence for the subsurface reduction of nitrate within the Pourewa Catchment. Evolution of the landscape is tied to eastward migration of the Rangitikei River, tectonics and climatically controlled, Late Quaternary aggradation. The occurrence of freshwater springs are related to geological structure, paleo-channels within the Late Quaternary valley fill and basin architecture, providing evidence for confined aquifers within the study area.

The Pourewa Stream is a c. 35 km long tributary of the Rangitikei River, located in the central Rangitikei District, Lower North Island, New Zealand (Fig. 6.1). The

stream drains a 170-km^2 catchment that begins in steep hill country northeast of Hunterville forming a shallow gradient stream channel before meandering out onto the Rangitikei terrace country at Rata. The stream then continues in a SE direction adjacent to the Rangitikei River before eventually cutting down through the underlying Plio-Pleistocene sediments to its confluence at Onepuhi (Fig. 6.1).

6.3 Geological setting

The islands of New Zealand are but the surface expression of a large submerged subcontinent named 'Zealandia'. This subcontinent sits astride the convergent margin between the Pacific and Australian lithospheric plates (Fig. 6.1). Tectonic convergence is accommodated by subduction of the Pacific Plate and deformation of the overriding Australian Plate, resulting in active uplift of the North Island (Eberhart-Phillips et al. 2008). Uplift is concentrated along the North Island Dextral Fault Belt (NIDFB) trending roughly parallel to the Hikurangi subduction zone. Uplift along the NIDFB has resulted in the formation of the North Island's main axial ranges, separating the forearc region from the backarc and volcanic arc regions. The Whanganui Basin (WB) is situated in the back-arc region behind the plate interface, southwest of the Taupo Volcanic Zone (TVZ) (Fig. 6.1).

Whanganui Basin (WB)

The WB is an approximately 200 x 200 km sedimentary basin located in the south-western North Island of New Zealand (Anderton 1981) containing a c. 4.5 km thick Late Miocene-Pleistocene fill. Basin formation is attributed to lithospheric loading in combination with compressional downwarping driven by coupling of the overriding and subducting plates (Stern et al. 1992, 1993; Tozer 2013). Southward migration of the basin depocentre through the Plio-Pleistocene occurred in combination with uplift along the northern and eastern margins, resulting in

present day onland exposures of gently dipping marine to marginal marine strata. Well-preserved fossil Mollusca, foraminifera and nannofossils are used to subdivide and date the basin succession and provide important paleo-environmental information (Beu et al. 2004; Beu 2006). Proximity to the TVZ has resulted in periodic influxes of volcanic products over the last ca. 2 Ma (Houghton et al. 1995; Briggs et al. 2005). These volcanic beds establish isochrons used to date and correlate between basin successions (Naish et al. 1996; Pillans et al. 2005).

The most complete sequence of river terraces within the WB occurs in the Rangitikei Valley (Te Punga 1952; Milne 1973a). Te Punga (1952) recognised seven episodes of terrace formation within the Rangitikei, matching heights of terrace treads on either side of the present day river channel and linking these episodes to changes in relative base level. Milne (1973a) mapped the Rangitikei river terraces in detail, subdividing them into aggradational and degradational and recognising nine major terrace sets (Table 6.1).

Table 6.1: Major aggradational terraces in Rangitikei Valley. Ages from Milne (1973), Pillans et al. (1993) and Pillans et al. (1996).

Terrace	Age
Ohakea	10-30 ka
Rata	30-50 ka
Pourewa	70-80 ka
Cliff	90-100 ka
Greatford	110-120 ka
Marton	140-170 ka
Burnand	240-280 ka
Aldworth	340-350 ka
Waituna	360-370 ka

Aggradational terraces are associated with glacial and stadial periods during the Quaternary, predicted as a response to increased sediment yields from deforested highlands during cold periods (Milne 1973a; Pillans 1994). The correlation between glacial/stadial periods and river aggradation is based on dating of Ohakean terrace alluvium (Milne 1973a; Marden & Neall 1990; Pillans et al. 1993; Pillans et al. 1996; Vandergoes et al. 2013; Lowe et al. 2015) and the occurrence of subalpine pollen assemblages in Marton terrace alluvium south of Levin (Barnett 1984).

6.4 Climate and physiography

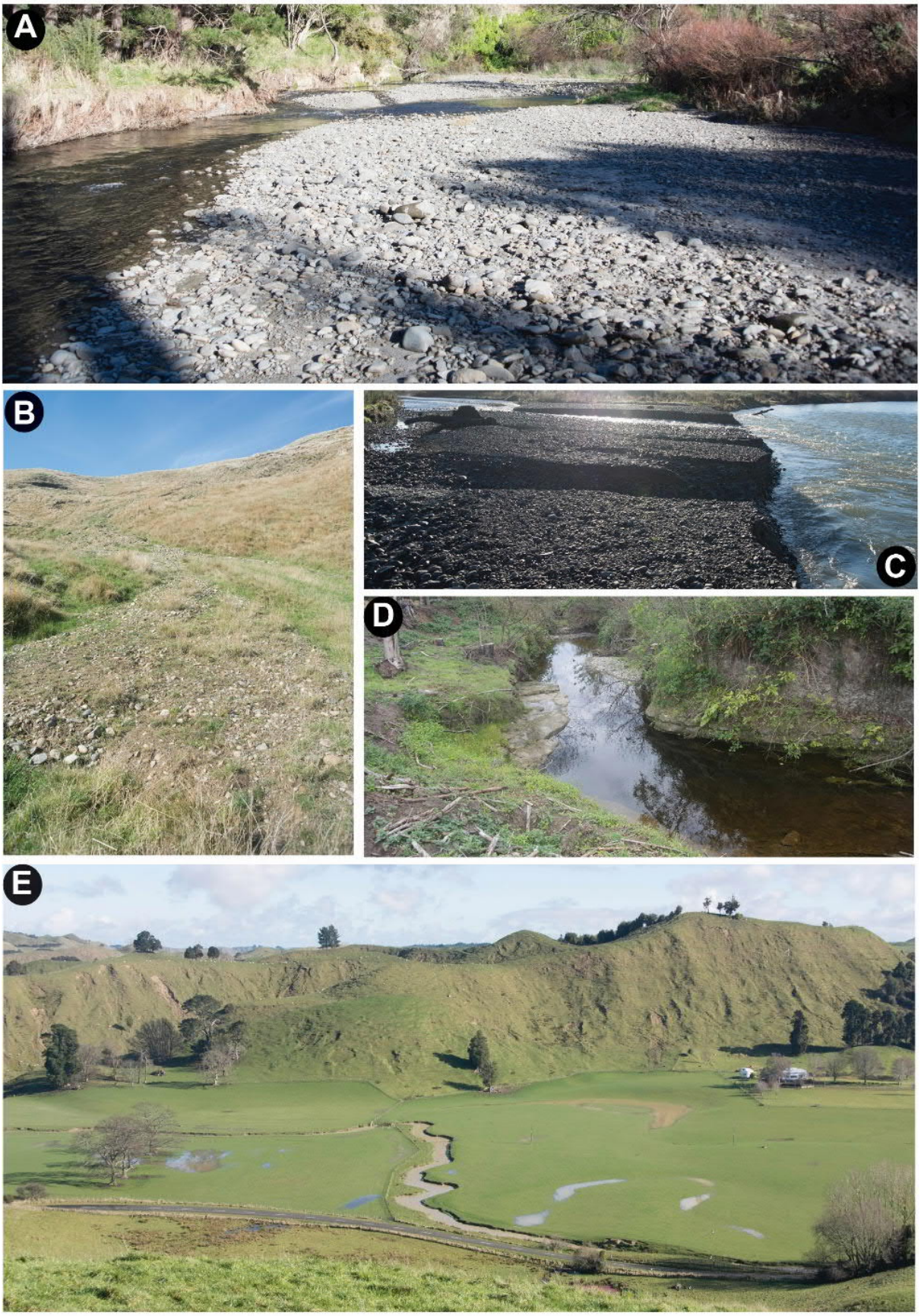
The Rangitikei District is characterised by moderate temperatures without great extremes including warm summers (15 -22°C) and mild winters (1-10°C) (Radcliffe 1976; Cowie & Rijkse 1977; Chappell 2015). The climate supports a range of land uses with sheep and beef farming dominating in the Rangitikei River and Pourewa Stream catchments. The threat of drought is present during some summers, particularly towards the coast where it can be drier (Heerdegen & Shepherd 1992). Average temperatures range from a high of around 18°C in February to a low of around 9°C in July (Chappell 2015). On average rainfall does not show a strong seasonal trend; the catchment receives between 1000-1100 mm per year. Evapotranspiration follows a seasonal pattern leading to potential soil moisture deficits in summer, depending on the soil type and its ability to retain water (Cowie & Rijkse 1977). Soil moisture deficits occur on average 10-15 days in both January and February and commonly into March and April, with irrigation used to offset the difference (Burgess 1988; Hedley & Yule 2009). The Rangitikei region is exposed to prevailing west to northwest winds that occur 30-50 percent of the time.

The physiography of the Pourewa Valley has been influenced by the same set of processes and forcing mechanisms as the Rangitikei River valley, with the Rangitikei River itself also playing an influential role during landscape

development. The Pourewa Stream differs substantially from the Rangitikei River in that its headwaters are located within the soft Plio-Pleistocene sediments of the WB, in contrast to the considerably harder Torlesse greywacke and volcanic rock comprising the headwaters of the Rangitikei River. The Pourewa stream has a shallow gradient, meandering planform with a sandy mud bed until near Hunterville where large quantities of reworked gravel enter the stream from tributaries draining the Rangitikei River terraces (Fig. 6.2). The terraces form extensive cropping and grazing land on the eastern interfluve c. 100 m above the bed of the Pourewa stream. From this point onward, the Pourewa Stream displays a wandering planform (Neill 1973; Ferguson & Werritty 1983; Fuller 2008) similar to the Rangitikei River albeit on a much smaller scale. Flood control works installed from the 1950's onward have played an important role in constraining the lower Rangitikei River and Pourewa Stream, limiting substantial natural avulsion processes evident from geological mapping (Te Punga 1952; Fleming 1953; Richardson & Fuller 2010; Rees et al. 2018a).

Major tributaries, Ongo Stream and the informally named Leedstown Valley Stream (Fig. 6.1) drain the western side of the Pourewa catchment providing large contributions to the catchment's otherwise narrow area. The Pourewa stream sits high in the landscape, flowing SW across its Late Pleistocene–Holocene valley fill. The stream pattern is unusually linear, running approximately parallel to the

Figure 6.2 (facing page): A) Wandering channel morphology within the lower reach of the Pourewa Stream (NZGD2000 -40.046606 S, 175.456338 E). B) Influx of Late Quaternary gravels from uplifted Rangitikei terraces capping hills within the central Pourewa catchment 2 km east of Hunterville (NZGD2000 -39.944884 S, 175.581436 E). C) Confluence between Pourewa Stream and the Rangitikei River displaying a gravel fan, note this fluvial interface undergoes rapid change (NZGD2000 -40.079352 S, 175.452476 E). D) Pourewa Stream cutting overtop of 'basement' composed of carbonaceous siltstone containing the estuarine dwelling cockle *Austrovenus stutchburyi,* Okehu Group (c. 1.58 – 0.99 Mxa) (NZGD2000 -39.953241 S, 175.563025 E). E) Typical meandering bed form of the Pourewa Stream within its upper reach, note photograph taken following moderate rain which has led to surface water pooling within paleo-channels across Poukiore Valley (NZGD2000 -39.886163 S, 175.609932 E).


A
B
C
D
E

more deeply incised Rangitikei River for c. 30 km. The Manawatu plains in the eastern Whanganui Basin contain a series of NE-SW trending anticlines, including the Pohangina, Feilding, Marton, Mt Stewart-Halcombe, and Oroua anticlines (Feldmeyer et al. 1943; Te Punga 1952, 1957). They are bounded on their eastern side by westward dipping reverse faults that only rarely reach the surface (Melhuish et al. 1996; Jackson et al. 1998; Begg et al. 2005). The anticlines are asymmetric, characterised by gentle western slopes (c. 2°) and steep eastern slopes (up to 70°), a geometry interpreted to reflect the underlying reverse faults (Jackson et al. 1998).

Feldmeyer et al. (1943) and Te Punga, (1957) both suggested that these anticlines were formed by ridges of basement rock trending approximately parallel with the main axial range. Structural interpretation of the Whanganui-Manawatu area indicates that these folds are long lived structures that are still actively growing (Jackli, 1957; Lensen, 1977; Te Punga, 1957). Preservation of the 310 ka Brunswick marine terrace tread (Pillans 1983, 1990, 1994) on the anticline crests suggests a majority of the present day topography has formed over the last c. 300 ka.

The Pourewa Stream extends across several different physiographic zones, originating in steep mudstone hill country of the upper Poukiore Valley (Fig. 6.1) to Rata where the stream meanders out over a broad flight of Rangitikei River terraces before finally becoming deeply entrenched as it grades to the Rangitikei River.

6.5 Methods

During this study, we compiled a 1:25 000 geological map of the central Rangitikei area, a simplified version of which is displayed in Fig. 6.3, presenting the main geological groups and important regional structures. This map compilation incorporated studies by Feldmeyer et al. (1943), Te Punga (1952), Fleming (1953), Naish and Kamp (1995), Journeaux et al. (1996), van der Neut (1996), Potter (1984) and Bussell (1984). We constructed geological cross sections trending east-west and north-south across the study area to aid with structural interpretation (Fig. 6.4). Details of the new 1:25 000 geological map and corresponding geological cross sections of the Central Rangitikei District are described in Rees et al. (2018a). This work was the result of an extensive field campaign from 2016 – 2018.

During the fieldwork phase of this study, particular focus was placed on observing the movement of water in the landscape and exploring relationships between water flow and the local geology. Springs, seeps and water bearing layers were noted with GPS (Fig. 6.5 and 6.6) and all available stratigraphic sections logged. Particular lithologies were targeted for sediment sampling and analysis, selected to be representative of key elements within the large suite of sediments encompassed by the mapping area. Samples were taken with a percussion corer to a depth of typically 1 – 2 m and with stainless steel rings able to be driven into an outcrop by hammer to take smaller 50 – 150 mm long cores.

Due to the wide range of sedimentary deposits within the c. 2000 m of WB strata that the Pourewa Stream cuts through and time constraints on field work, it was necessary to adopt a simplified approach to sediment sampling and analysis. We subdivided the lithologies into broad groups based on grain size and petrography, initially selecting a set of representative sandstone, siltstone, shellbed, pumiceous and conglomerate units. Following initial sediment sampling and analysis, other

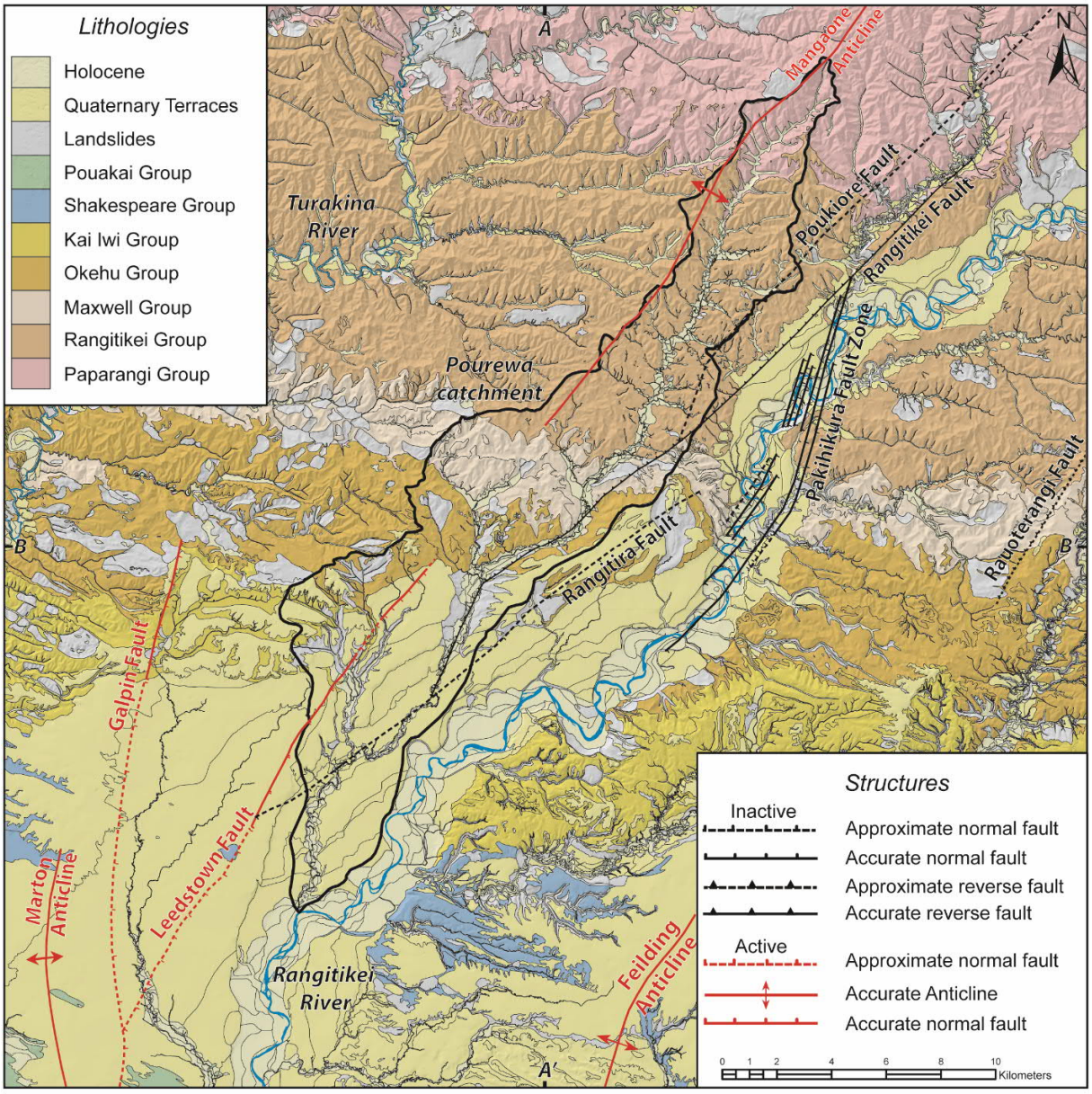


Figure 6.3: Simplified geological map of the study area showing the location of the Pourewa Stream catchment outlined in black in relation to major regional structures and lithological groups.

samples from the main categories outlined above were collected in order to measure some of the variability observed in outcrop. Three samples were also taken from a modern day gravel bed of the Pourewa Stream in three locations moving away from the stream, allowing for collection of samples containing low, moderate and high percentage of fines for later comparison. A single sample from a modern day Rangitikei River gravel bed was also sampled for comparison. The

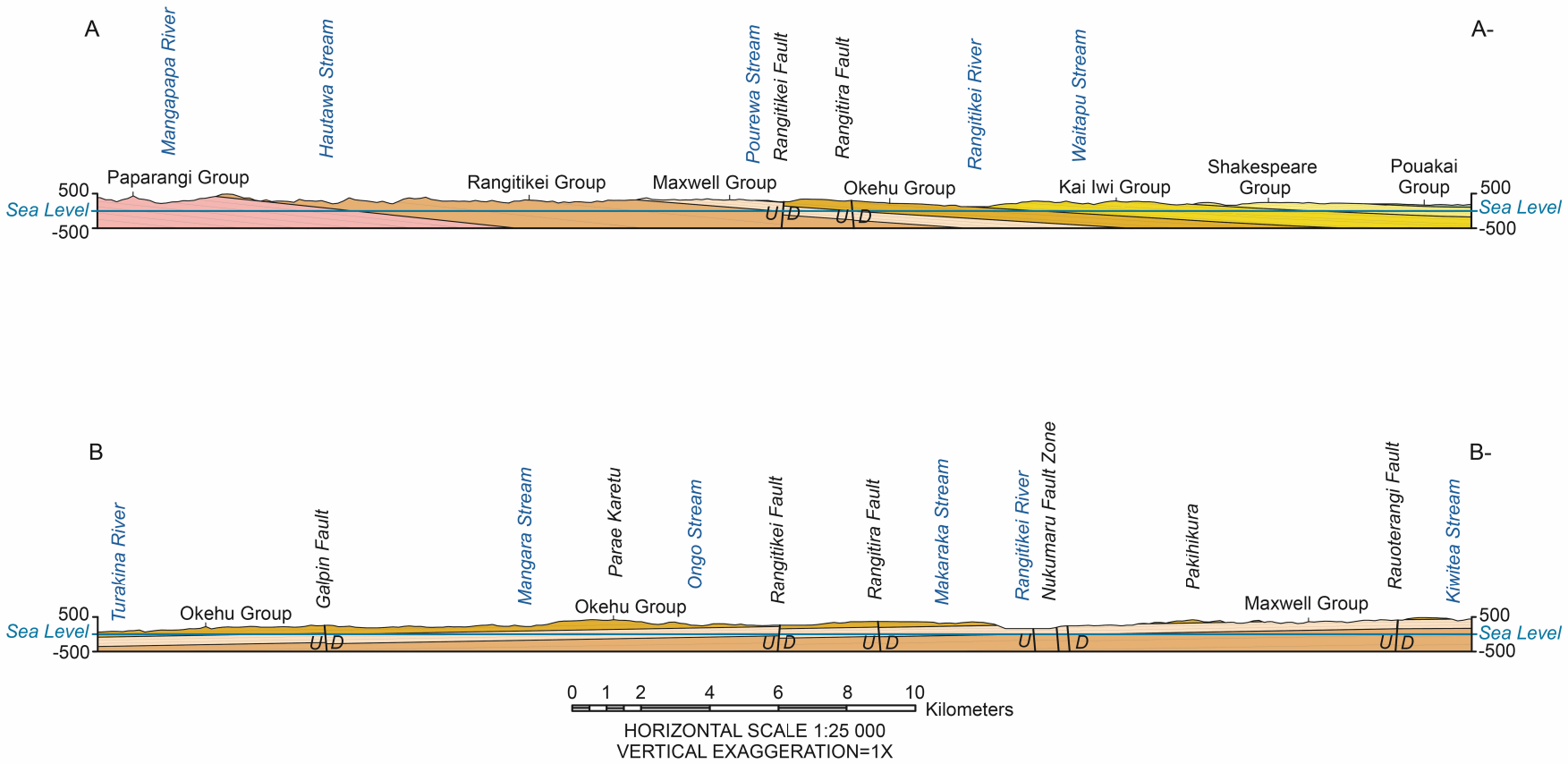
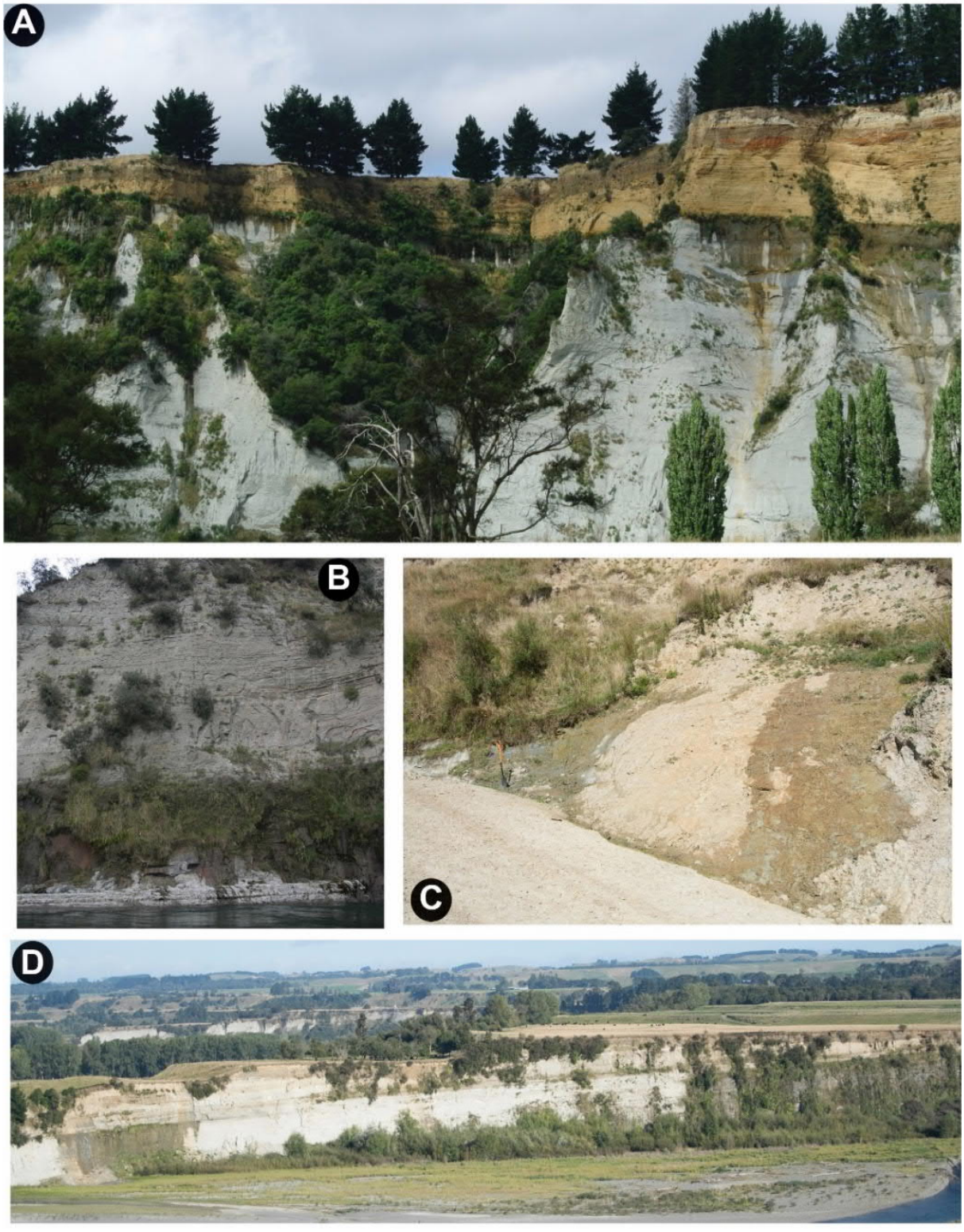


Figure 6.4: Simplified cross sections A to A' and B to B' trending N-S and E-W respectively, displaying the main geological structures of the Rangitikei District. Geological units have been ordered into their respective groups.

goal of the sampling regime was to provide a preliminary overview of the study areas hydrogeological units by outlining their modal characteristics.

Three 50 x 46 mm sub-samples were taken for triplicate dry bulk density, gravimetric and volumetric water content, total and effective porosity and particle density determinations using methods outlined in Gradwell and Birrell (1979), Claydon (1997) and Rayment and Lyons (2011). Three 150 x 46 mm sub-samples were taken for triplicate measurements of hydraulic conductivity using a falling head permeameter (Fig. 6.7). The falling head permeameter consisted of a 6 m long standpipe with an inside diameter of 50 mm. The standpipe then enters a series of 90° bends before connecting to a sample chamber consisting of a 150 mm length of core with a 46 mm inside diameter. Filter cloth is placed above and below the sample chamber to stop debris falling into the pipe then clamped into place using a combination of hose clamps and rubber sleeves. Samples were first allowed to saturate and reach a steady state of flow before the test was run. Incremental measurements were made of the head in the stand pipe using a water level sounder over time as the head reduced. The timing of measurements was based on the rate of flow for the particular sample; for example coarse grained units required more frequent minute to hourly measurement intervals whilst siltstone and mudstone units were measured twice daily. Hydraulic conductivities were calculated using Darcy's equation as outlined in Landon et al. (2001).

Figure 6.5 (facing page): A) Groundwater seeps at the contact between Tuha Sandstone and underlying Tikapu Siltstone, Rangitikei Group, exposed in cliffs in the Rangitikei River valley (NZGD2000 -39.877205 S, 175.721254 E). B) Groundwater seeps at a particularly coarse sandstone overtop of a hard well consolidated siltstone forming the ledge in the lower part of the section, Vinegar Hill Formation, Rangitikei Group (NZGD2000 -39.92932 S, 175.642462 E). C) Groundwater seeps within Mangaonoho Formation, Rangitikei Group at contact with laminated sandstone over massive siltstone (NZGD2000 -39.911645 S, 175.620189 E). D) Groundwater seeps along the contact between a sandstone and underlying siltstone unit within Rewa Formation, Okehu Group (NZGD2000 -40.008355 S, 175.589676 E).

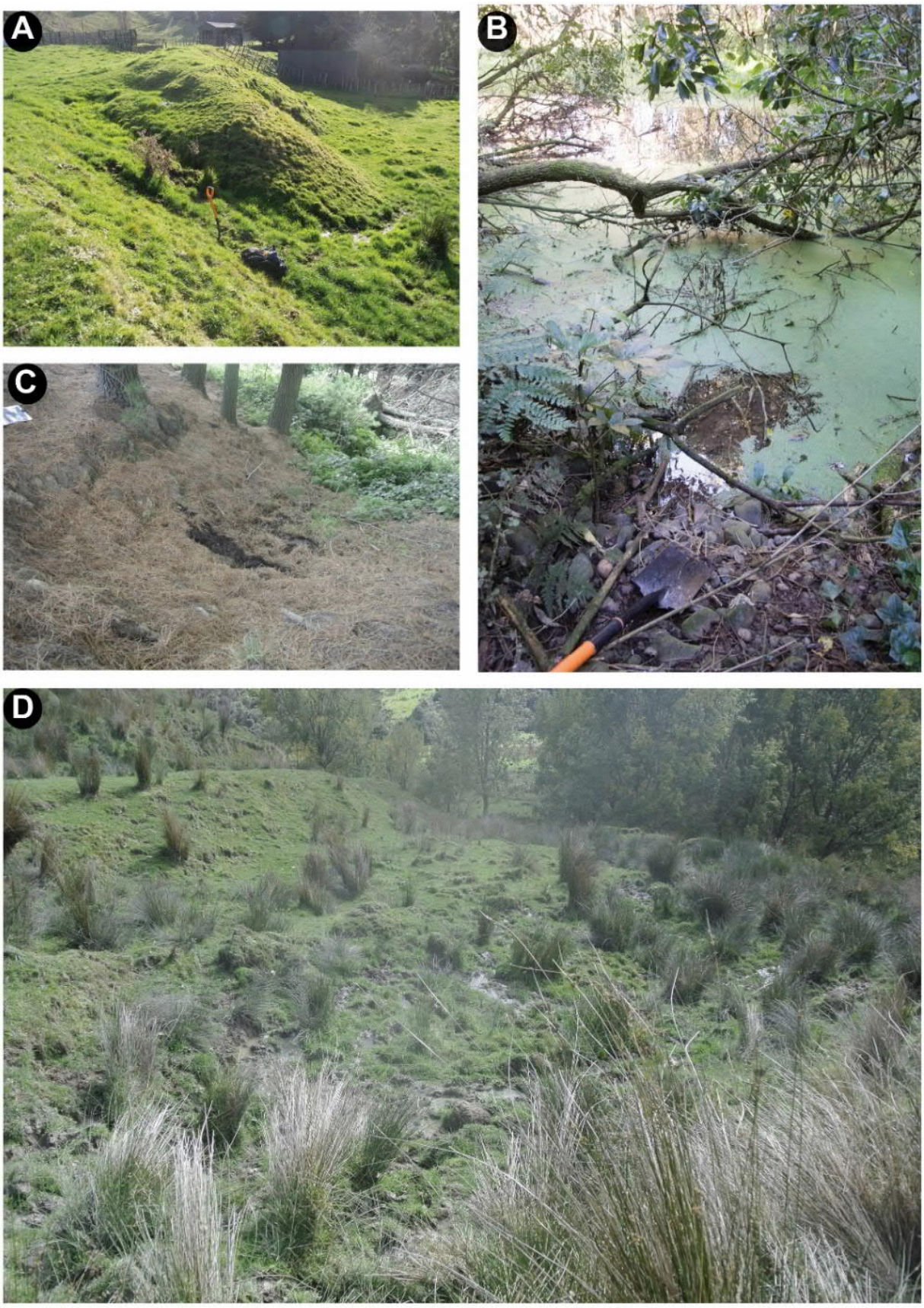

A
B
C
D

Three subsamples of typically 100 g were taken for grain size analysis. Grain size analysis was undertaken by dry sieving the >63 micron fraction using a set of sieves at half phi increments. The <63 micron fraction was determined in solution using a Horiba Partica LA-950V2 laser particle analyser, a refractive index of 1.52 and an absorption value of 0.1 was used for the sample material, based on a mixed mineral assemblage of dominantly marine sediments (Rothwell et al. 2006).

Grain mounts were made from the 125-250 µm fraction in each representative lithology and 400 grains were counted to determine the general mineralogy of the sediments. All samples were analysed for major and trace elements by X-ray fluorescence spectroscopy (XRF) at Massey University following procedures and analytical techniques outlined in Kimura and Yamada (1996) and Lee et al. (1997) using a Bruker S8 TIGER with Bruker SPECTRA-plus software. H_2O and loss on ignition (LOI) were calculated from the weighed samples.

The general clay mineralogy of samples was determined from suspension-oriented x-ray diffraction (XRD) samples using the sample preparation techniques outlined in Whitton and Churchman (1987). Measurements were made using a GBC Scientific EMMA diffractometer operating at 35 kV and 20 mA, using monochromatic Co Kα radiation and a scanning rate of 2° 2θ/minute, scanning from 5° to 40° 2θ. Triplicate suspensions for each sample were prepared including non-saturated, K saturated and Mg saturated. Following initial XRD runs, Mg

Figure 6.6 (facing page): A) Small spring flowing out of Holocene gravels at the base of Leedstown Valley (NZGD2000 -40.019826 S, 175.471315 E). B Large set of springs along contact between Ratan Gravels and underlying siltstone of Waiomio Formation, Kai Iwi Group on the immediate up thrown side of Rangitira Fault (NZGD2000 -40.023638 S, 175.479813 E). C) Large set of springs emerging mid to top slope beneath the tread of the Greatford Terrace (MIS 5) (NZD2000 -39.989024 S, 175.511184 E). D) Medium to small spring emerging from coarse pumiceous sediments overlying fine-grained Coutts Creek Horizon, Okehu Group. Note the typical landform of hummocky landslip topography with water logged soil tolerant species such as rushes and tussock prevalent, typical of a spring site (NZGD2000 -39.940442 S, 175.432777 E).


A
B
C
D

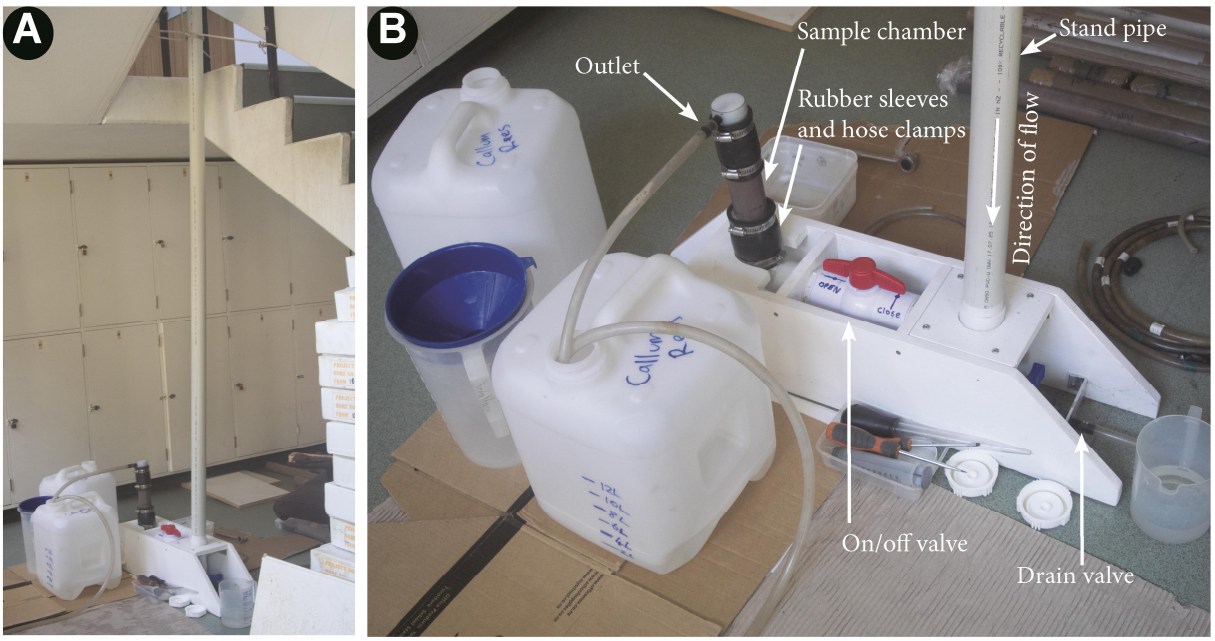


Figure 6.7: A) Photo of the falling head permeameter setup at Massey University, Palmerston North, consisting of a 6 m standpipe tied to the railing within the stair well. B) Close up of the base where the standpipe enters two 90-degree bends and a main shut off valve before entering the 150 x 46 mm sample housed in piping attached by rubber sleeves and hose clamps. The outlet at the top of the sample is epoxied into a plug allowing the outflow of water to enter the 20L water container. Note a second valve on the right of the base positioned low, allowing all water to be drained from the system following a successful run.

saturated samples were sprayed with glycerol and analysed until complete expansion of smectites was achieved, followed by heating to 550°C and repeat analysis. Resulting XRD patterns were compared with the International Centre for Diffraction Data (ICDD) library to aid with identification of clay minerals.

Total carbon, nitrogen, hydrogen and sulfur concentrations were determined using the elementar® (vario MICRO cube) at Massey University. Inorganic carbon was determined by digestion of samples with hydrochloric acid within a vacuum chamber following the methods outlined by Bundy and Bremner (1972) and Tiessen et al. (1983). Inorganic carbon and total carbon determinations were used to calculate organic carbon content of each sample.

6.6 Results

Geology

The geology of the Central Rangitikei has been mapped at 1:25 000, a simplified version of which is presented in Fig. 6.3 with accompanying structural interpretation (Fig. 6.4). This mapping resulted in the fusion of several formal and informal stratigraphic nomenclatures introduced in the literature over the last 75 years, including work by Feldmeyer et al. (1943), Te Punga (1952), Fleming (1953), Milne (1973a), Seward (1976), Potter (1984), Bussell (1984), Abbott (1992), Naish and Kamp (1995) and van der Neut (1996). New regional structures including the Poukiore Fault and a southern extension of the Mangaone Anticline (Feldmeyer et al. 1943) have been identified during the field survey. Major regional reverse faults, the Rangitikei and Rauoterangi faults with maximum-recorded throws of 100 and 200 m west respectively (Naish & Kamp 1995), drive deformation of the Plio-Pleistocene succession, with associated zones of antithetic, normal faulting (Pakihikura and Poukiore faults). In the south of the mapping area the actively growing Marton and Feilding anticlines are observed, related to faulting at depth (Melhuish et al. 1996; Jackson et al. 1998; Begg et al. 2005).

The distribution of the Pouakai to Paparangi group succession (c. 3 – 0.3 Ma) is related to the depositional history and stratigraphic architecture of the WB through the Plio-Pleistocene. A general east-west alignment reflects the gentle dip (2-10°) of the succession toward the basin depocentre, located to the south. Quaternary terraces represent climatically controlled aggradational episodes preserved by ongoing regional uplift over the last c. 370 ka (Pillans 1994). The terraces fan out in the lower Rangitikei Valley where they dominate the southern portion of the mapping area. Holocene valley fill is restricted to the main valleys where the rivers have incised through the Plio-Pleistocene marine succession.

An important relationship observed in the field is the general increase in level of compaction and cementation with age, reflecting progressively greater depth of burial and level of diagenesis. Mudstones and siltstones typically have a higher level of cohesion and consolidation due to a greater proportion of silt to clay sized particles and tight grain fabric, imbuing them with higher average strength (45–180 KPa) relative to their sandstone counterparts (9 – 90 KPa) (Ker 1970; Thompson 1982; Ker 1991). For instance, Thompson (1982) reports an average strength determined by point load tests of 156 KPa for Mangaweka Mudstone Formation and conversely 7 to 68 KPa for sandstones of the Rangitikei Group, relating this change to relative levels of consolidation. Conglomerate and gravel units are frequently cemented by iron oxide; typically, these deposits are <1.6 Ma and are dominated by greywacke clasts, with the level of cementation observed to increase with age (Te Punga 1952; Fleming 1953; Milne 1973a). Locally, shell and sandstone beds are cemented by calcite, dramatically increasing their strength (upto 2,857 KPa); however, these deposits form a small proportion of the entire succession (Thompson 1982). Hydraulic conductivity gradually decreases with increasing age (Begg et al. 2005), reflecting an increase in compaction, consolidation and cementation as a function of diagenesis (Houseknecht 1987).

Analyses

Grain size statistics were calculated using the Folk and Ward method (Folk & Ward 1957) and compared with the hydraulic conductivity measurements (Table 6.2, Fig. 6.8). Increasing hydraulic conductivity is associated with an increase in mean grain size and a reduction in the presence of a fine tail fraction. The samples are typically poorly to very poorly sorted; however, the sample with the highest hydraulic conductivity is moderately well sorted. Overall the hydraulic conductivity measurements range from 5 to 20379 m/day. Coarse grained gravel, shellbed and pumice deposits obtain the highest hydraulic conductivities of between 351 to 20379 m/day, consistent with gravel to granular sediment values

documented by Freeze and Cherry (1979), Domenico and Schwartz (1998), Fetter (2001) and New Zealand based studies (White 1986; Thorpe 1992; Davidson & Wilson 2011). Mudstone and siltstone hydraulic conductivities were fairly high at between 5 to 6 m/day, falling between a fine sandstone to silty sandstone range relative to published values (Freeze & Cherry 1979; Fetter 2001). Sandstone units ranged from 18 to 39 m/day, falling within a typical sandstone range when compared with published datasets (Chapuis et al. 1989; Wang et al. 2008).

Average bulk densities of the study units typically range from 1.37 to 1.81 g/cm^3 with particularly low values for pumiceous units (Table 6.2). The sedimentary units measured in this study plotted within similar ranges as unconsolidated Holocene (Avnimelech et al. 2001; Rose & Kuehl 2010) to weakly and moderately lithified Pleistocene sediments (Jakobsson et al. 2001; Bahr et al. 2005; Lamb et al. 2007; O'Regan et al. 2008) in the literature. The particle densities of the study units were calculated to be around 2.6 to 2.8 g/cm^3, apart from the pumiceous rich sediments, which were calculated to be around 2.4 g/cm^3. Total porosities ranged from 34 – 66 %, with the highest porosities occurring within pumiceous sediments and coarse shellbed material. Total porosity values obtained in this study are similar to values presented by Halley and Schmoker (1983) and Boving and Grathwohl (2001) for a comparable range of sediments and sedimentary rocks (Table 6.2). Effective porosity values range from 43 to 7 % (Fig. 6.9), comparable to values presented in Dong et al. (2010) and Medina et al. (2011). The siltstone, mudstone and sandstone samples with relatively high total porosity values of 39 to 42 %, have much lower effective porosity values of 7 to 13%, reflecting the presence of small and intermediate sized pores and therefore, low macro-porosity (Dewhurst & Aplin 1998).

Table 6.2: Average grain size, hydraulic conductivity (K), bulk density, total porosity and effective porosity measurements from the representative lithologies of the study area, in order of increasing hydraulic conductivity.

Lithological Unit	Grain size (μm)	Sorting	Hydraulic Conductivity (K) m/day	Average Bulk Density g/cm3	Total porosity (%)	Effective Porosity (%)
Pourewa Stream gravel (no fines)	Coarse gravel (19102)	Moderately well sorted	20379	1.58	44	43
Waitapu Shell Conglomerate	Very coarse sand (1953)	Very poorly sorted	400	1.67	37	33
Mangamako Shellbed	Very coarse sand (1280)	Very poorly sorted	389	1.37	48	32
Potaka Pumice	Medium sand (316)	Poorly sorted	351	0.89	66	7
Pourewa Stream gravel (moderate fines)	Medium gravel (15924)	Poorly sorted	87	1.75	37	31
Pourewa Stream gravel (high fines)	Very fine gravel (3640)	Very poorly sorted	75	1.70	35	28
Hautawa Shell Bed	Fine Sand (125)	Very poorly sorted	51	1.73	35	6
Rangitikei River gravel (High fines)	Medium gravel (9978)	Poorly sorted	48	1.81	31	29
Mangamako Sand	Very fine sand (88)	Poorly sorted	39	1.75	34	9
Te Rimu Sand	Very fine sand (90)	Poorly sorted	24	1.66	38	7
Rewa Pumice	Very fine sand (67)	Very poorly sorted	18	1.24	48	7
Mangaweka Mudstone	Coarse silt (25)	Poorly sorted	6.2	1.61	39	13
Mangarere Siltstone	Coarse silt (22)	Poorly sorted	5	1.54	42	7

Clay mineralogy of the sediments is dominated by illite with lesser amounts of glauconite, kandite and minor smectite. Detrital glauconite grains were also observed as a minor constituent in the 125 to 250 µm fraction of 80% of samples during point counts. The mineralogy determined by point counts was dominated by quartz and highly altered minerals including some chlorite, with lesser amounts of feldspar and minor pyroxene and hornblende. Moderate lithic and opaque grains were also present in several coarse grained samples including Mangamako shellbed, Te Rimu Sandstone, Rangitikei River gravel and Mangamako sandstone. Weathered clear rhyolitic glass shards dominated the pumiceous deposits while lithic shell material dominated the shell beds including minor quantities of foraminifera.

Major element chemistry (Table 6.3) determined by the XRF displays changes in geochemistry consistent with the measured suites of minerals. Sandstones show an enrichment in silica and relative depletion in aluminum, iron, and magnesium compared with mudstone and siltstone samples, representing a relative dominance of quartz within sandstone units and higher proportion of altered clay minerals within the siltstone and mudstone. The siltstone and mudstone units also have slightly elevated levels of titanium and potassium compared with the sandstone units suggesting an increase relative to quartz of potassium feldspar (orthoclase and microcline) and minerals such as pyroxene and mica where titanium can occur as an accessory or substituted element (Murray 2006). Calcium values are highest within the shellbed and shell hash conglomerate units at between 7.4 to 30 %, due to the presence of abundant detrital shell material within these samples. Correspondingly, these samples display the highest loss on ignition due to carbonate volatilisation during combustion. Samples containing a strong greywacke and/or volcanic provenance namely the shell hash conglomerate, Holocene gravels and pumiceous units display relatively high sodium at between 3.5 to 4.4 %, attributed to higher proportions of plagioclase feldspar and vitric rhyolitic glass shards within their respective mineral assemblages.

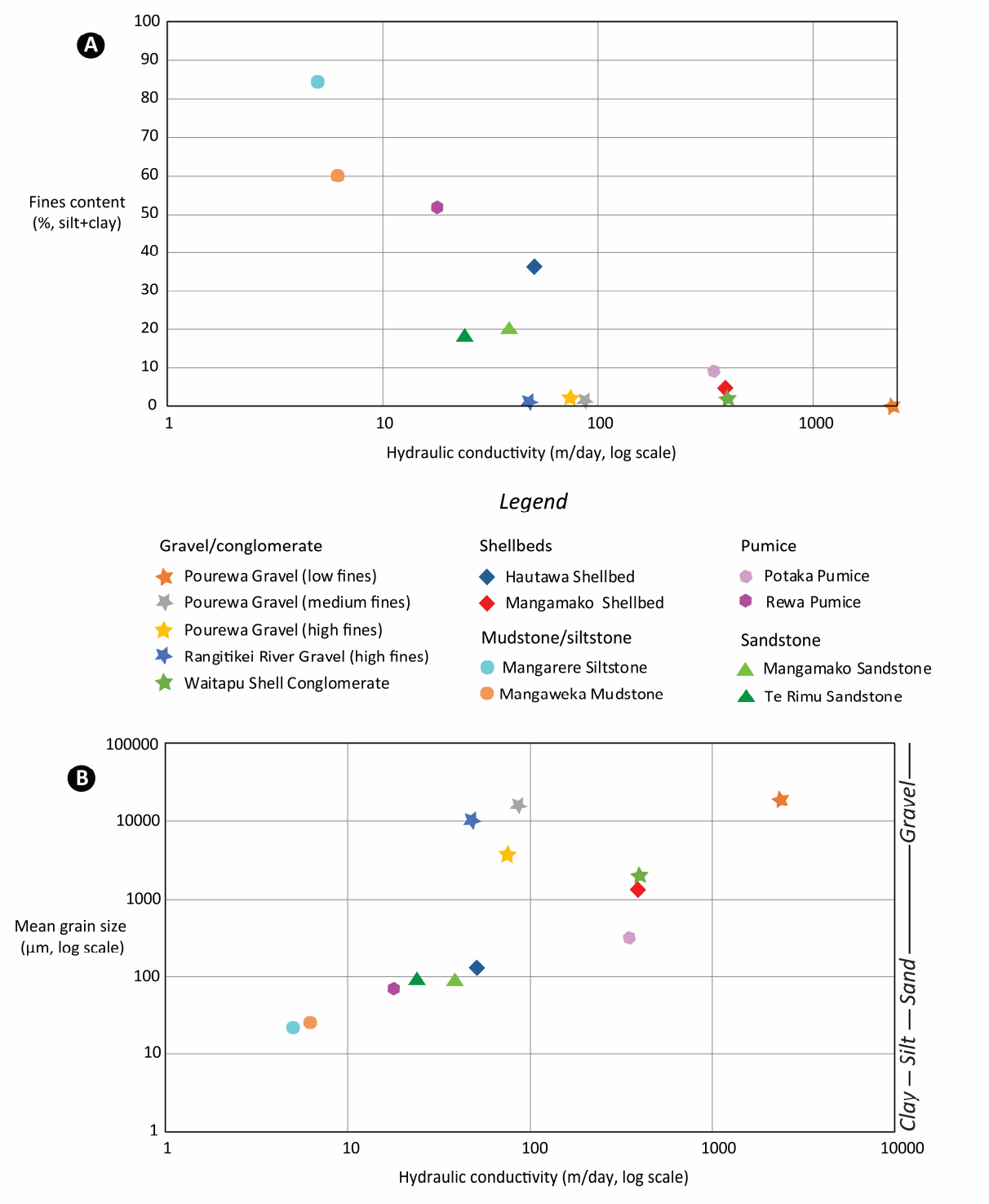


Figure 6.8: Graphs demonstrating key relationships between grain size statistics and hydraulic conductivity. A) Percentage fines content vs hydraulic conductivity (m/day, log scale). B) Mean grain size (µm, log scale) vs hydraulic conductivity (m/day, log scale).

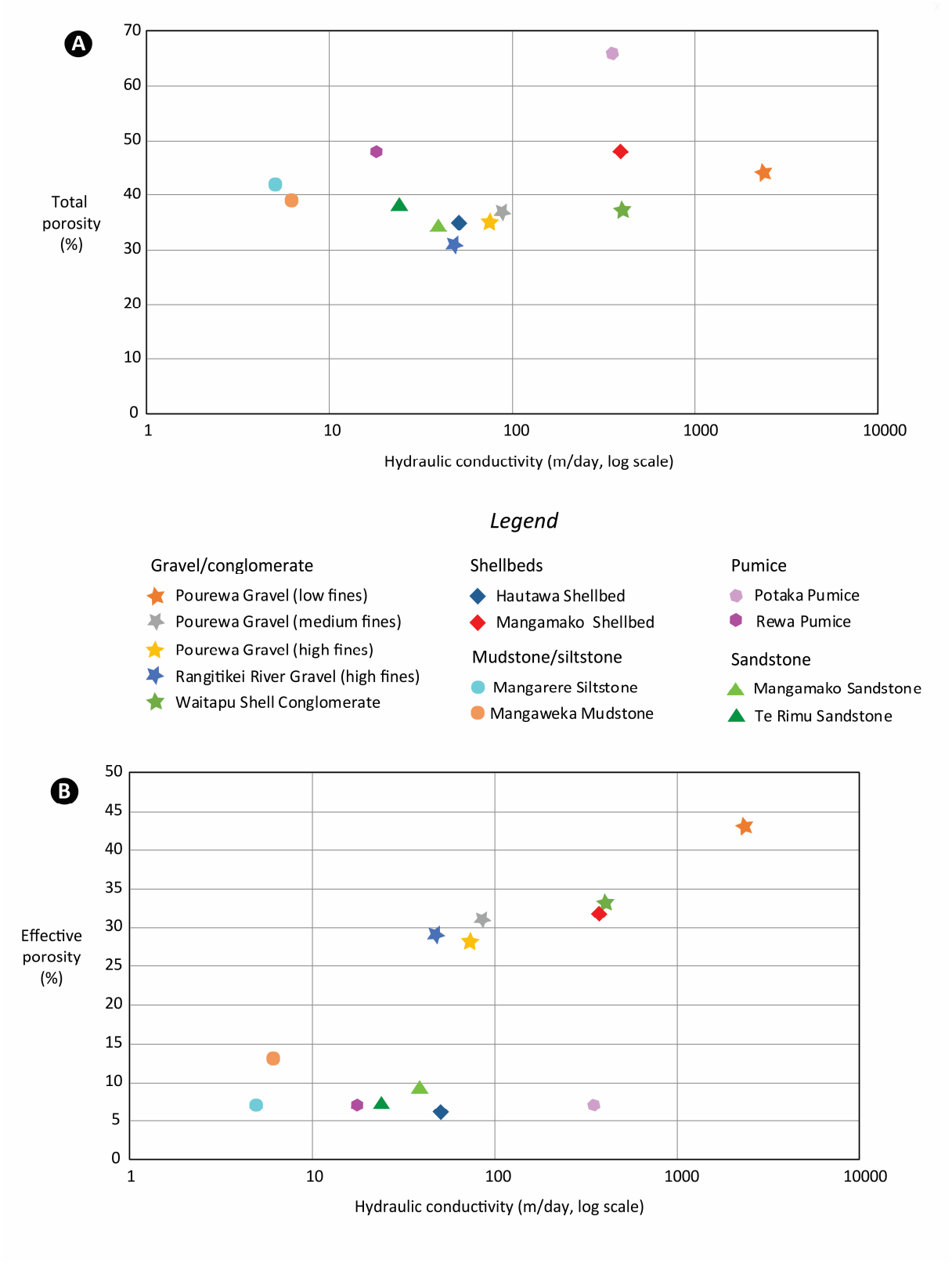


Figure 6.9: Graphs displaying the relationships between porosity and hydraulic conductivity. A) Total porosity (%) vs hydraulic conductivity (m/day, log scale). B) Effective porosity (%) vs hydraulic conductivity (m/day, log scale).

Table 6.3: Major element geochemisty (% weight) of respective samples grouped by lithology. Hu - Hautawa Shell Bed; Mm - Mangamako Shellbed; Ma - Mangamako Sandstone; Tr - Te Rimu Sandstone; Mw - Mangaweka Mudstone; Mg- Mangarere Siltstone; P - Rewa Pumice; Rg - Rangitikei Gravel; Pg - Pourewa Gravel.

Lithological Group	Sample Code	SiO_2	Al_2O_3	TiO_2	MnO	Fe_2O_3	MgO	CaO	Na_2O	K_2O	LOI	Sum
Shellbeds	Hu	61.48	12.54	0.52	0.05	3.80	1.35	7.39	2.60	2.13	8.53	100.53
	Mm	35.05	4.47	0.16	0.04	1.44	0.59	29.98	1.21	0.84	25.36	99.30
Sandstones	Ma	76.97	10.57	0.49	0.04	2.64	0.84	1.25	2.38	1.87	2.48	99.60
	Tr	73.62	12.36	0.54	0.05	3.29	1.19	1.41	2.62	2.32	2.28	99.80
Mudstone	Mw	69.98	14.51	0.65	0.04	3.77	1.37	1.04	2.62	2.36	4.03	100.43
Siltstone	Mg	63.42	16.50	0.67	0.07	5.30	2.03	2.09	2.91	3.11	4.29	100.55
Pumiceous sand	P	68.35	14.20	0.37	0.05	2.78	0.68	2.05	3.50	2.00	4.77	98.81
Gravels	Rg	70.00	14.63	0.43	0.07	3.52	1.22	2.62	4.39	2.00	1.76	100.75
	Pg	75.84	11.39	0.35	0.04	3.01	0.78	1.47	3.48	1.75	2.31	100.50
Shell hash conglomerate	Wai	58.66	12.38	0.34	0.10	3.92	1.54	11.23	3.57	0.99	8.17	101.00

Table 6.4: Average organic and inorganic carbon contents and clay minerals identified during analysis of respective lithologies, in order of increasing organic carbon content. Note we were unable to identify any clay minerals within Waitapu Shell Conglomerate due to poor diffraction patterns.

Lithological Unit	Organic carbon (g of C per kg of sediment)	Inorganic carbon (g of C per Kg of sediment)	Clay minerals present (XRD)	Glauconite as percentage of 125-250 μm fraction.
Mangamako Shellbed	8.60	60.69	Illite, Kandite	2%
Rewa Pumice	8.46	0.43	Glauconite, Illite	0%
Waitapu Shell Conglomerate	3.30	19.29	-	1.5 %
Hautawa Shell Bed	2.67	10.52	Illite, Kandite, Smectite	2.2%
Pourewa Stream gravel	2.15	1.94	Glauconite, Illite, Kandite	1.5%
Mangaweka Mudstone	1.59	0.30	Glauconite, Illite	0%
Mangarere Siltstone	0.88	1.61	Illite, Kandite	0.2%
Mangamako Sandstone	0.63	0.26	Glauconite, Illite, Kandite	0.75%
Te Rimu Sandstone	0.52	0.18	Glauconite, Illite, Kandite	0.5%
Rangitikei River gravel	0.37	1.93	Glauconite, Illite, Kandite	1.5%

Carbon (C) determinations show high amounts of inorganic carbon within the shellbed and shell hash conglomerate units, Mangamako Shellbed being the highest outlier at 60.7 g of C per kg (Table 6.4). The majority of other samples display inorganic carbon values >2 g of C per kg. Pumiceous and shellbed sediments also display the highest organic carbon contents of up to 8.6 g per kg. Sandstones contain less organic carbon at 0.5 to 0.6 g per kg, compared to mudstones and siltstones with higher values of 0.9 to 1.6 g per kg.

Hydrostratigraphy

Fig. 6.10 displays a map of potential aquifers in the central Rangitikei District, separating different geological units into hydrostratigraphic groups based on their age and dominant lithology. Aquifer and aquiclude units were characterised by assigning average hydraulic conductivity, porosity, grain size and bulk density measurements to each geological formation. Given the sampling regime used in this study, it was necessary to assign values derived from a unit's dominant lithology. For instance, Tikapu Formation, Rangitikei Group (Naish & Kamp 1995) contains shellbed and siltstone members yet was assigned average properties from its dominant lithology siltstone, resulting in an aquitard classification. Fig. 6.10 also plots the springs observed during the fieldwork in the study area. The spring data represents only a small portion of total springs and seeps in the study area. The grouping of sedimentary units into aquifer and aquiclude layers is broad and serves only to show general regional trends as opposed to detailed local scale aquifer spatial patterns.

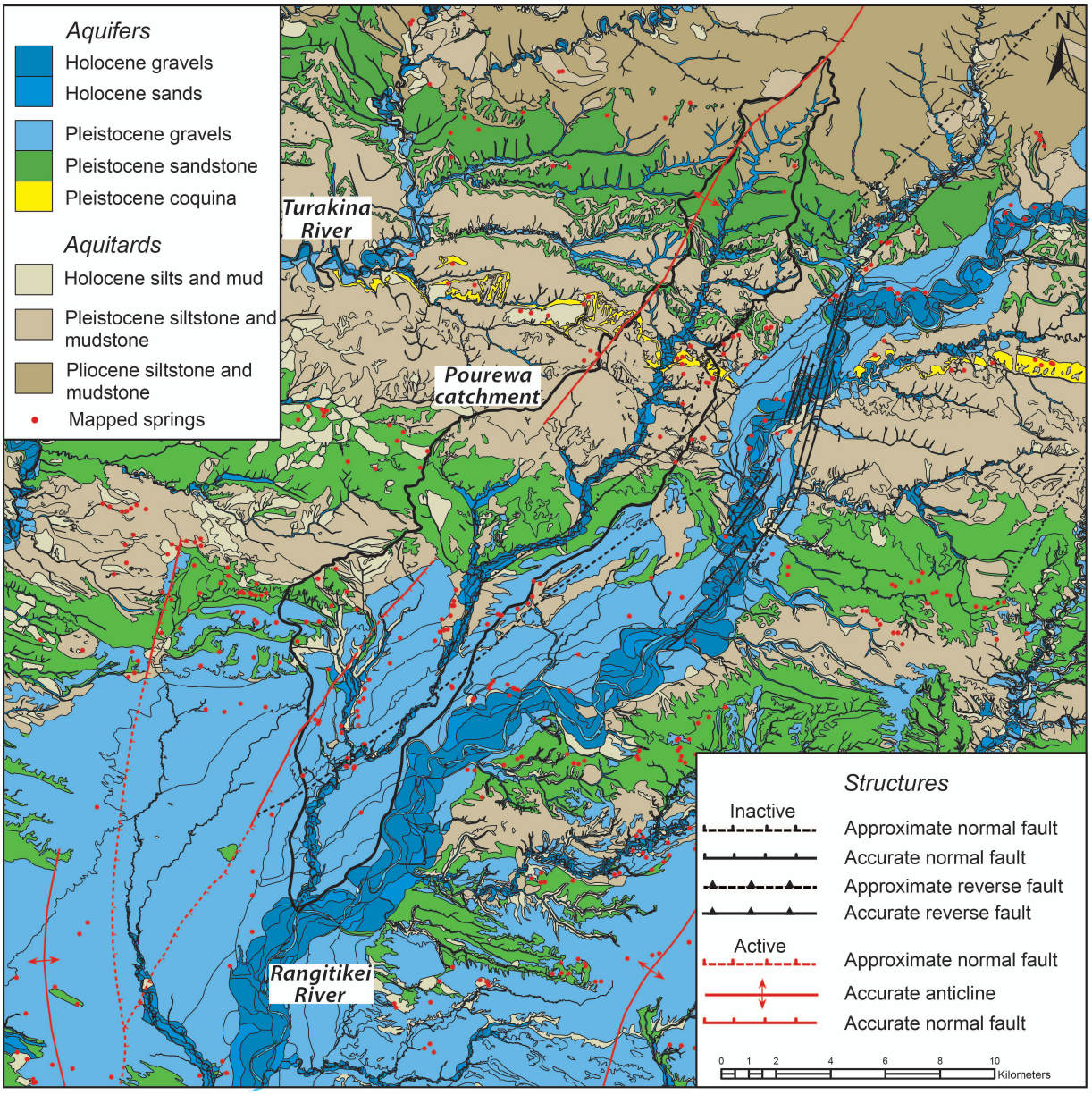


Figure 6.10: Simplified hydrostratigraphic map of the study area showing the location of the Pourewa Stream catchment outlined in black in relation to the local geology. Geological units subdivided based on average grain size, hydraulic properties, age and depositional regime into respective hydrostratigraphic units. Major regional structures are also shown alongside mapped spring locations; note the mapped springs only present a small proportion of the total springs in the area, a majority of which are minor seeps and small springs.

6.7 Discussion

Landscape evolution

The widespread aggradational terraces of the Rangitikei Valley are prominent features in the present day physiography of the Pourewa Stream catchment (Fig. 6.3 and 6.11). Exceptionally thick and widespread Ratan terraces (30-50 ka) occur near Rata (Fig. 6.1) where the Pourewa Stream emerges onto the open, lower Rangitikei River Valley. These gravels are derived from the paleo-Rangitikei River and pre-50 ka Rangitikei valley fills, filling areas of the Pourewa valley to depths of up to 10 m. The confluence of Leedstown Stream and Pourewa Stream is interpreted to have been subjected to major scouring post 50 ka given the occurrence of particularly thick Ratan gravels overlain by rare alluvial dunes formed by wind-blown silt off an aggrading fluvial floodplain during the last glacial maximum (LGM) (Milne 1973b; Palmer & Pillans 1996). These local areas of fluvial scour and fill are observed in the present study to host important shallow ground water reserves, related to large freshwater springs.

The course of the Rangitikei River has been located much further west of its present position within the structural low of the Pakihikura Fault Zone. A series of progressively younger terrace treads stepping down from the land immediately north of Marton to the present day flood plain of the Rangitikei River suggest the river has tracked eastward over the last 370 ka, likely in response to offset along major NE-SW trending faults and increasing confinement by the growing Marton and Mt Stewart-Halcombe anticlines (Fig. 6.3). Fifty thousand years ago, it is likely the Pourewa stream was substantially shorter than present day, exiting its valley carved through the Plio-Pleistocene rocks of the WB at Rata into the paleo-Rangitikei River (Fig. 6.11).

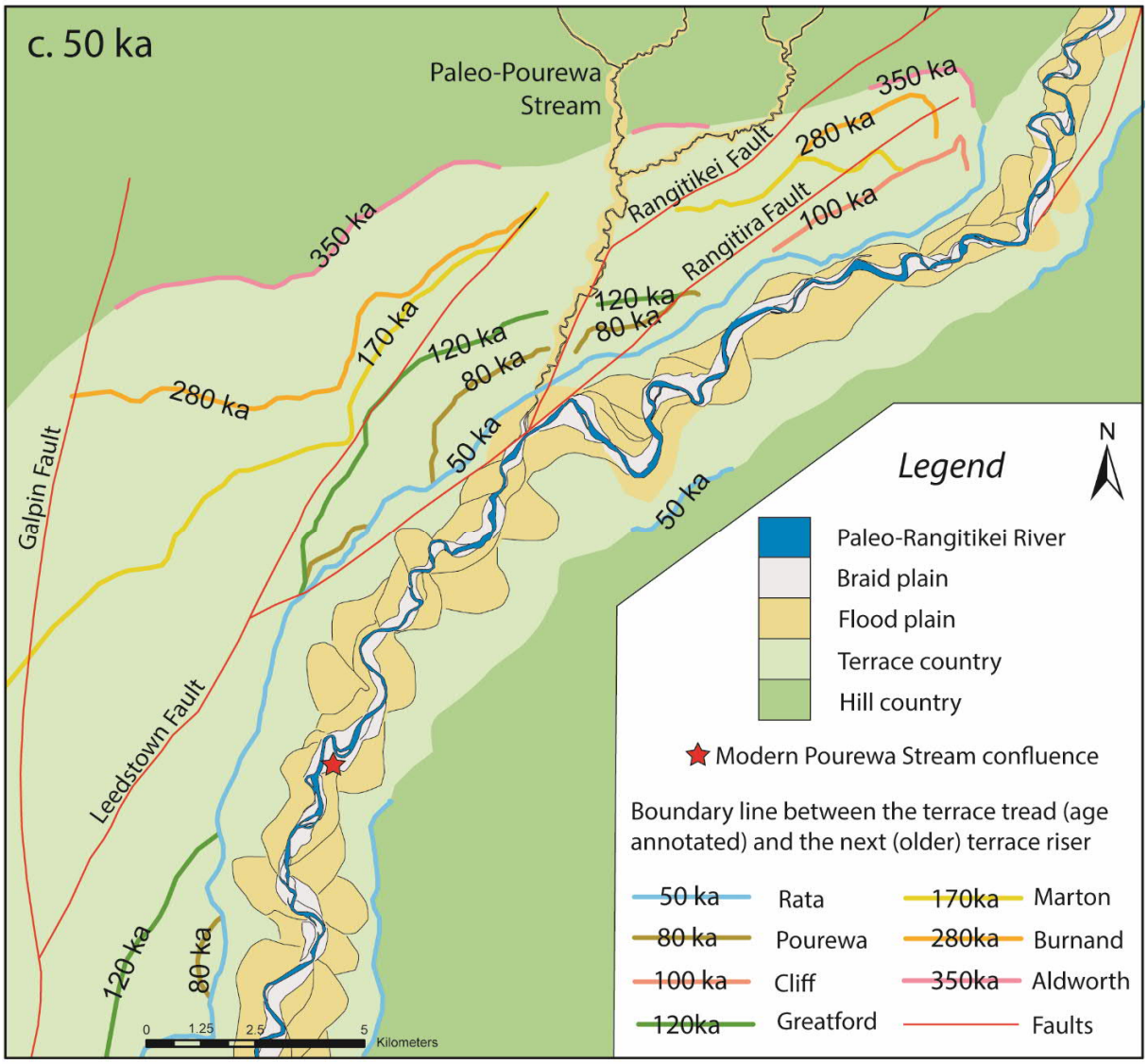


Figure 6.11: Schematic palinspastic diagram of the lower Pourewa Stream displaying the relatively rapid landscape changes which have occurred over the last 50 ka. Outlines of the modern day Rangitikei River terrace treads are displayed representing the maximum preserved extent of the Rangitikei River for each approximate period of time. These lines indicate the boundary between the terrace tread (age annotated) and the terrace riser of the next (older) terrace. In the case of the Aldworth line, this indicates the maximum preserved extent of the tread before it gives way to hill country. The modern day confluence between the Rangitikei River and Pourewa Stream is indicated by a red star illustrating the amount of eastward migration the Rangitikei River has undergone in the last 50 ka contemporaneous with development of the lower Pourewa Stream. Data sourced from Te Punga (1952), Milne (1973), Hellstrom (1993), Pillans (1994) and this study.

Since 50 ka ongoing uplift manifested as offset along regional faults has led to further eastward migration of the Rangitikei River through the LGM aggradation and multiple Holocene degradation episodes. Contemporaneous fluvial development of the Pourewa stream has resulted in a fault controlled extension of the Pourewa stream to the SW, extending from Rata parallel to the Rangitira Fault. We infer the Pourewa stream has preferentially exploited this fault zone as the path of least resistance during its natural inclination of cutting down to meet the Rangitikei River. Another line of thought is that the Rangitikei River itself could have produced the substantial fluvial scouring at the confluence of the modern day Pourewa and Leedstown streams, so that the Pourewa stream is exploiting a topographic low carved into the Pleistocene marine sediments by a paleo-channel of the Rangitikei River.

The Poukiore Valley (Fig. 6.1) at the headwaters of the Pourewa Stream has been influenced by a broad structure in the underlying Plio-Pleistocene sediments. The Mangaone Anticline (Fig. 6.3) forms the western watershed boundary of the Pourewa Stream, defining a marked change in dip direction within the Plio-Pleistocene sediments. Sediments on the eastern side of the structure dip to the SE while equivalent sediments to the west dip W to SWW into a structural low occupied by the Turakina River. Sediments along the western watershed of the Pourewa Stream typically dip to the SE and as a result springs and seeps outcrop extensively on the southern and eastern slopes of this hill country, some providing domestic drinking water.

Hydrostratigraphic map

The hydrostratigraphic map (Fig. 6.10) displays two key relationships that highlight important factors influencing the hydraulic properties of the area's lithologies. Firstly, the age of the sedimentary units is a controlling factor, determining the amount of diagenesis and resulting cementation and compaction

a unit has undergone (Larsen & Chilingar 1983; Bjorlykke 2014). Holocene fluvial deposits formed over the last c. 11 ka (Holocene gravels and sands on Fig. 6.10) represent the least consolidated units in the mapping area with little to no cementation and low compaction, forming the most productive shallow unconfined aquifer within the study area (Begg et al. 2005). In contrast, Te Rimu Sandstone (Pleistocene Sandstone on Fig. 6.10), including the basal sandy Mangarere Formation (Naish & Kamp 1995) represents a succession of locally cemented coarse to fine siliciclastic sandstone that has undergone diagenesis since deposition c. 2.5 Ma (Wilson & Roberts 1999). Because of a relatively high level of compaction and local cementation, this unit contains substantially lower hydraulic conductivity than contemporary Holocene gravelly sands, illustrated by a change from 24 to 75 m/day respectively (Table 6.2).

The second key relationship observed from Fig. 6.10 is the difference in depositional setting within the hydrostratigraphic units. Clearly, the Late Quaternary and Holocene gravels and sands fill the modern day drainage network of the Rangitikei Valley, formed over the last 370 ka, throughout a series of climatically controlled aggradational and degradational episodes (Milne 1973a; Pillans 1994). The abundance of greywacke and andesite gravel within these deposits imparts high hydraulic conductivity.

The increasingly common occurrence of greywacke gravel within the Late Quaternary hydrostratigraphic units of the study area reflects substantial changes in the paleogeography and sediment transport pathways of the Lower North Island (Te Punga 1952; Fleming 1953; Beu et al. 1981; Melhuish et al. 1996; Rees et al. 2018b). Notably, the onset of volcanic activity within the Tongairiro Volcanic Centre (c. 350 ka) (Shane et al. 2017) providing a new provenance for volcaniclastic sediment, delivered by rivers draining the central volcanic plateau. Simultaneous uplift along the main axial range front (Beanland 1995; Jiao et al. 2015) has provided a source of abundant greywacke detritus, as the modern day topography

formed. Localised uplift along a series of regional anticlines (Te Punga 1957) has acted to shape and constrain the emerging fluvial drainage network, funneling a series of high permeability sediments between bounding basement highs.

In contrast, the linear nature of the Plio-Pleistocene marine sediments exposed along depositional strike, record the paleogeography and depositional setting at their time of formation, characterised by shallow marine deposition within a southward migrating marine depocentre adjacent to the uplifting paleo-axial range (Anderton 1981; Rees et al. 2018a). A key difference distinguishing this older marine basin fill from the overlying Late Quaternary sediments, is the occurrence of relatively thick (c. 10-60 m) (Abbott 1994), massive, blue grey, siltstone units representing high stand deposition within inner to mid shelf depths (Carter & Naish 1998). We suggest these units attain enough lateral persistence to act as local confining layers and as such form an important constituent of the hydrostratigraphy.

Physical and hydrogeochemical attributes

The most important factors related to a sample's hydraulic conductivity are the presence of a fine tail grain size fraction followed closely by mean grain size. This correlation is consistent with known relationships between grain size and hydraulic conductivity determined by experimental evidence (Krumbein 1934; Hazen 1983; Alyamani & Sen 1993; Song et al. 2009; Sen 2015) and field studies (Fogg et al. 1998; Odong 2008; Vienken & Dietrich 2011). The general reduction of hydraulic conductivity with a corresponding increase in fine content (Fig. 6.8) has been well documented by Schalchli (1992), Benson and Trast (1995) and Boadu (2000). For example, the three gravel samples taken from Pourewa Stream show an increase in hydraulic conductivity from 75 to 20379 m/day, corresponding to a decrease in fines content from high to no fines (Table 6.2). This marked change

occurs despite the gravel component (size, shape) being similar within all three samples.

While the mean grain size is important, it does not show a 1:1 relationship with hydraulic conductivity. For instance, the Pourewa Stream gravel samples with moderate to high fine content have a larger mean grain size (3640 to 15924 μm) yet have lower hydraulic conductivity than Potaka Pumice (mean grain size 316 μm) (Table 6.2). This could be attributed to the difference in the amount of fines which act to fill voids between the pore spaces, affecting the hydraulic conductivity (Koltermann & Gorelick 1995). Almost all of the samples displayed poor to very poor sorting; however, the sample with the highest hydraulic conductivity (i.e. Pourewa Steam gravels with no fines) was moderately well sorted, demonstrating that sorting is likely another important contributing factor. A wider sampling coverage and increased sampling rate of the sedimentary units within the study area would likely highlight this third key factor.

The siltstone and mudstone units tested in this study exhibited relatively high hydraulic conductivity (5 to 6 m/day) relative to examples from the literature (Freeze & Cherry 1979; Dewhurst & Alpin 1999; Fetter 2001) attaining a closer fit to sandy mudstone and siltstone mixtures documented by Revil and Cathles (1999) and Belcher et al. (2001). This is attributed to a significant component of sand within the mudstone tested, a coarse silt grain size for tested siltstone lithologies and the generally weakly lithified and cemented nature of the WB sediments (Thompson 1982; Ker 1991; Kamp et al. 2004). It is also possible an undetermined amount of bypass flow occurred during permeameter tests, potentially affecting the results and leading to unusually high hydraulic conductivities within the fine-grained sediments measured; however, we consider this error be negligible in our analyses. Methods to combat bypass flow included allowing significant time for the fine sediments to saturate and swell against the sample chamber and the

installation of epoxy around the outside of the lower filter cloth covering the bottom of the sample chamber to channel flow toward the centre of the chamber.

Bulk density values typically range between 1.6 to 1.8 g/cm^3. Particularly low bulk density values are associated with shellbed and pumiceous units, which correspondingly display the highest total porosity of between 48 to 66 %. Generally, total porosity values are high (>30%) and display a weak relationship with hydraulic conductivity indicated by a slight trend of increasing hydraulic conductivity with increasing total porosity (Fig. 6.9). Units containing high total fines e.g. Mangarere Siltstone exhibit high total porosity (42%), a large portion of which is made up of small to intermediate pores with low interconnected macro-porosity (Stephens et al. 1998).

Effective porosity displays a stronger positive correlation with hydraulic conductivity (Fig. 6.9). However, Potaka Pumice, a granular, pure, pumice with high hydraulic conductivity displays unusually low effective porosity. It has proven difficult to determine the correct effective porosity of highly pumiceous sediment during this study. In the laboratory, pumiceous units demonstrate high water holding capacity, resulting in low calculated macroporosity and therefore, effective porosity. However, from our field experience, pumiceous sediments and soils are well drained and prone to drought, rapidly drying in the summer and demonstrating low water holding capacity. The effective porosity values of Potaka Pumice are considered erroneous in this study, due to the difficulties encountered in attaining an accurate, representative measurement in the lab.

Another outlier (Fig. 6.9 B) is Mangaweka Mudstone Formation, displaying a higher effective porosity (13%) than the two sandstone samples; Te Rimu (7%) and Mangamako sandstone (9%). This discrepancy is likely the result of a relatively high sand content within the Mangaweka Mudstone Formation sample, classified as a sandy mudstone during grain size analysis. Potential error within the effective

porosity results may also have contributed to this difference. Hautawa Shellbed displays an unusually low effective porosity (6%) considering its relatively high hydraulic conductivity (51 m/day), considered to be a result of the fine-grained matrix including illite, kandite and smectite clays that provide small to intermediate sized pores and result in high water holding capacity.

Pumiceous units displayed lower bulk density, particle density and higher total porosity than any other sediment type analysed in this study. They also contained low inorganic carbon, but relatively high amounts of organic carbon. This is interpreted to reflect the nature of their depositional environment, typically characterised by rapid fluvial aggradation resulting in potential for organic matter preservation (Gastaldo & Demko 2010), clearly illustrated by the abundance of lignite, charcoal and logs exposed within the volcaniclastic units of the WB (Te Punga 1952; Fleming 1953; Shane 1991; Rees et al. 2018a). Pumiceous units in the WB are the result of episodic ignimbrite emplacement in the central north island (Shane 1991), rapid erosion of the distal unwelded portion of an ignimbrite sheet results in paleo-fluvial systems becoming chocked with volcaniclastic debris (Manville et al. 2009a; Manville et al. 2009b). Drastically increased sedimentation rates following ignimbrite emplacement (von Lichtan et al. 2016) are interpreted to have led to coastal progradation (Lewis 2007) and the formation of extensive coastal plain and marginal marine deposits in the WB succession (Te Punga 1952; Abbott 1994; Shane 1994; Pillans et al. 2005; Rees et al. 2018a). These deposits are often found in close relation with lignite's, carbonaceous mud and stunted *Austrovenus stutchburyi* shellbeds in the Rangitikei District, representing high rates of sedimentation within marginal marine to coastal plain environments (Te Punga 1952; Rees et al. 2018a).

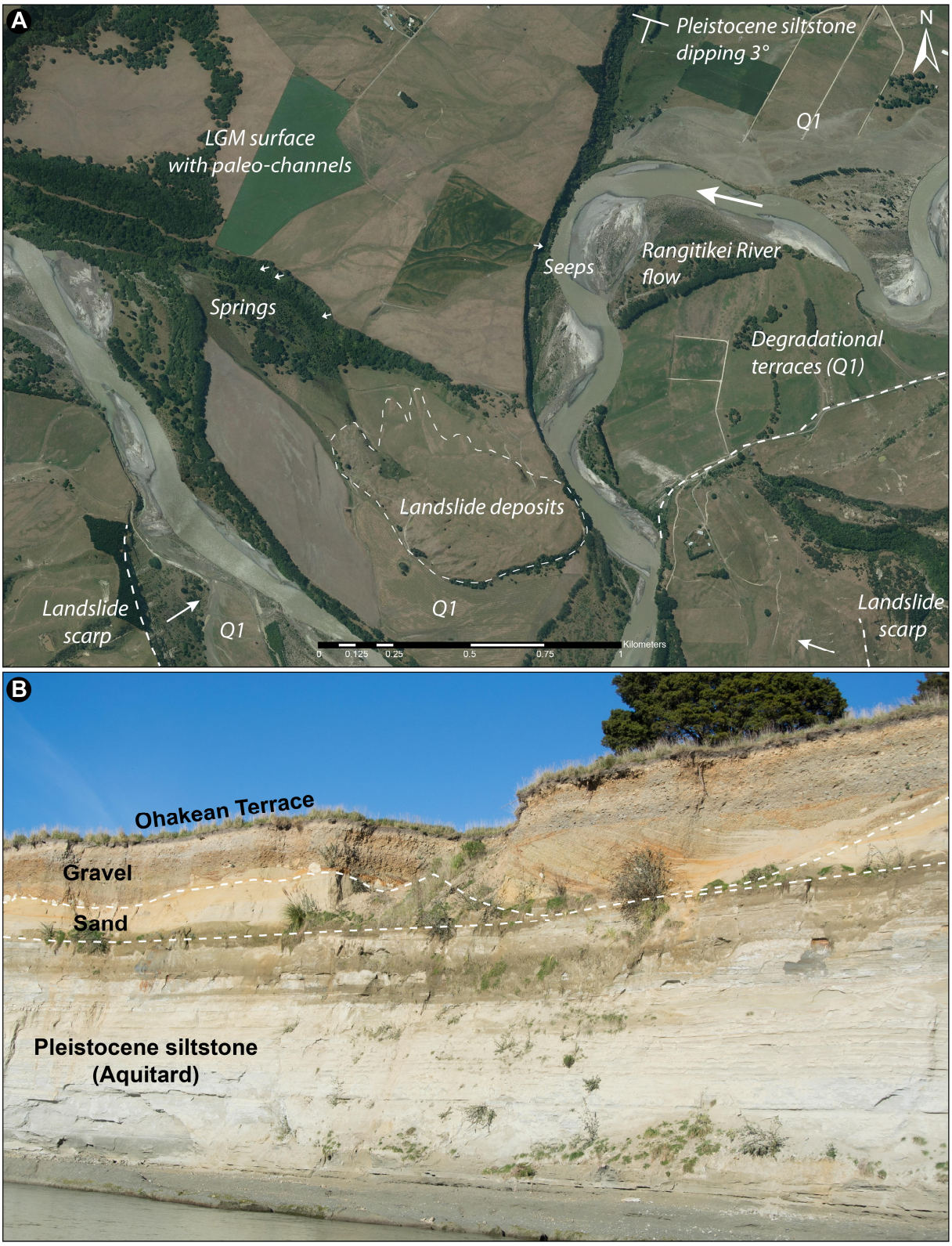
The depositional environments of the pumiceous units in the WB imbues them with an inherent lateral variability, which we suggest here to be mirrored by associated variations in hydraulic conductivity of between 18 and 351 m/day.

Pockets of high porosity clean pumice such as Potaka Pumice are able to store and transmit significant amounts of water; however, it is extremely difficult to predict their lateral extent from outcrop given rapid facies changes. Groundwater from Maxwell Group sediments in which several volcanic/volcaniclastic units occur together with associated lignite and carbonaceous muds are used locally for water supply; however, the water is often stained and considered unpotable (Fleming 1953).

The relationship between a fluvial depositional regime and rapid lateral variations in hydraulic conductivity is also relevant to the Late Quaternary terrace and modern floodplain hydrostratigraphic units, which demonstrate a similar variation in hydraulic conductivity including a change of between 48 to 20379 m/day (Pourewa and Rangitikei gravel samples, Table 6.2). Seams of well-washed gravels are interpreted to occur along both paleo and modern fluvial channels forming pockets of highly permeable sediment with high hydraulic conductivity surrounded by overbank and alluvial flood plain deposits of mixed grain size with considerably lower hydraulic conductivity, despite considerable gravel content.

Water preferentially flows along the channels of modern day rivers largely as a function of gravity and topography (Helton et al 2014; Blume & van Meerveld 2015

Figure 6.12 (facing page): A) Aerial photograph of paleo-channels observable as micro-topography on the Last Glacial Maximum surface (LGM) (NZGD2000 -40.006514 S, 175.576372 E). These channels are related to shallow groundwater springs and seeps where interception occurs by the modern day fluvial erosion of the Rangitikei River and its tributaries. Underlying Pleistocene siltstone dipping gently to the SW creates a sloping aquiclude surface beneath the more permeable Late Quaternary gravels. B) Example of the undulating surface of erosion beneath an Ohakean Terrace (LGM surface) (NZGD2000 -40.081486 S, 175.466938 E); fine to medium grained fluvial sand is intermixed with gravel within channel cut and fill overlain by further gravels. This photo is included to illustrate some of the variability within Late Quaternary Terraces. Terrace deposits have been observed with incorporated logs and boulders highlighting the inherent danger of over-generalising these highly variable hydrostratigraphic units.


A
Pleistocene siltstone dipping 3°
N
Q1
LGM surface with paleo-channels
Seeps
Rangitikei River flow
Springs
Degradational terraces (Q1)
Landslide deposits
Landslide scarp
Q1
Q1
Landslide scarp
0 0.125 0.25 0.5 0.75 1 Kilometers
B
Ohakean Terrace
Gravel
Sand
Pleistocene siltstone (Aquitard)

(Helton et al. 2014; Blume & van Meerveld 2015), moving through the landscape eroding, sorting and re-depositing sediment (Kondolf & Piegay 2003). As a result, braided to wandering rivers with highly indurated source rock catchments, such as those occurring across the Canterbury Plains and draining the North Island main axial range contain riverbeds lined with highly permeable gravels, allowing streams to retreat into their beds during periods of low flow (McHugh et al. 2015). We observe this phenomenon in the gravel bedded streams of the Rangitikei District including the Pourewa Stream, through the summer months.

Denitrification

Nitrogen loss from farms due to rapid leaching of nitrate through the soil profile into the subsurface is an increasingly important environmental issue in rural New Zealand, due to increased use of nitrogen fertiliser associated with land use intensification (Houlbrooke et al. 2004; Parfitt et al. 2006). Subsurface denitrification can result in attenuation of nitrate leaching from agricultural lands (Elwan et al. 2015; Rivas et al. 2015; Collins et al. 2017; Rivas et al. 2017). Natural attenuation of excess nitrate leached from farmland has flow on effects for aquatic systems, reducing water quality impacts and promoting healthy ecosystem functions (Quinn et al. 2009).

The clay mineralogy reported from stratigraphic units in this study are similar to modern day sediments described on the Whanganui shelf (Hume & Nelson 1986; Gillespie 1992; Gillespie & Nelson 1996). Illite imparts natural attenuation within groundwater systems facilitating the adsorption and oxidation/reduction of heavy metal contaminants such as arsenic, cadmium and chromium (Palmer & Puls 1994; Wang & Mulligan 2006; Longe & Enekwechi 2007)

The common occurrence of illite, glauconite and organic matter within the WB sedimentary units and the reworked modern day fluvial deposits of the Pourewa

Stream provides evidence for potential electron donors in the subsurface environment (Puckett 2004; Cundy et al. 2008; Debernardi et al. 2008; Rissmann 2011). Glauconite and illite contain structural and exchangeable ferrous iron (Fe^{2+}) that can facilitate reduction of nitrate (NO_3^-) in the subsurface to N_2O and then N_2 gas during the microbially mediated process of denitrification (Korom 1991; Ernstsen 1996). Organic carbon within the pumiceous (8 g C per kg) and shellbed (8.6 g C per kg) members of the WB succession could also act as a source of electron donors, supporting the denitrification potential of local aquifers. Even the lower quantities of organic carbon measured within the finer grained siltstones and mudstones (0.8 to 1.6 g C per kg) could be important if long ground water residence times (years) along flow paths allow sufficient time for redox reactions to occur, leading to reduction of nitrate in the subsurface environment (Seitzinger et al. 2006). Organic carbon preserved within the shellbeds of the WB is interpreted here to be a result of bypassing of siliciclastic sediment on the areas of sea floor allowing for stratigraphic condensation and preservation of moderately low amounts of organic matter.

Inherent limitations incorporated due to the sparseness of sampling within a texturally complex marine basin and modern day fluvial basin must be acknowledged in this study. Continued research is underway into the groundwater systems of the Rangitikei District, aiming to develop an understanding of the role rock type plays in nitrogen attenuation in the subsurface. This work involves sampling of a wider array of sediments within the WB through the application of rapid *in situ* testing and application of the ideas and concepts developed during this work at a wider regional scale.

Springs

Local residents of the Rangitikei District have made observations of changing rates in spring flow corresponding to changes in atmospheric pressure, with a distinct increase in spring flow occurring during incoming low pressure systems, typically preceding a rainstorm event. Some springs we observed show a visibly higher flow rate following a period of heavy rainfall while others appear to flow at the same despite heavy rain, maintaining a constant flow through winter and summer. These two sets of observations lead us to believe there is possible evidence for confined aquifer springs within the study area. Unconfined aquifer springs typically are not immediately affected by changes in atmospheric pressure due to a delay in transmitting atmospheric pressure through the vadose zone (Rasmussen & Crawford 1997; Spane 2002); their flow rates are also more likely to be affected by seasonal variations in rainfall due to generally faster recharge times and a higher level of connectivity with surface water (Scanlon et al. 2002). Springs being immediately affected by atmospheric pressure and flowing at similar rates through winter and summer provide anecdotal evidence of confined aquifer flow.

Springs have been related to paleo-channels within the Late Quaternary gravels intercepted by a marine cliff in the Horowhenua District (Kampman & Caldwell 1985; Reynolds 1992; Cussins 1994). Here, we document similar relationships in the Rangitikei District where several springs observed on the Ohakean terraces are related to paleo-channels within the terrace gravels (Fig. 6.12). These channels are only obvious on the LGM aggradational surfaces and younger degradational terraces, due to a thick blanketing of cover beds which mask the micro-topography of pre LGM aggradation terraces (Milne 1973a, b). We interpret the channels to be composed of coarse gravels with high hydraulic conductivity effectively funneling the shallow groundwater, which flows along the path of least resistance in the landscape. Underlying Pleistocene siltstone forms a less permeable base promoting horizontal groundwater flow on the interface between the gravel and siltstone

units. Where terrace risers or cliffs cut by modern day streams intercept the paleo-channels, springs emerge at the contact between the gravel and underlying siltstone (Fig. 6.12). These springs are typically utlised by farmers who dam one end of the receiving tributary creating a pond, which can then be used to supply water to animal toughs; or alternatively dig out the head of the spring and line the hole to create a small reservoir, which can then be piped by gravity to a tank.

6.8 Conclusion

The Pourewa catchment lies within the WB and its geology is dominated by alternating coarse and fine-grained sedimentary units deposited during cyclic eustatic sea level fluctuations spanning the entire Quaternary Period. Regional fault zones and related basement highs trending approximately NE-SW exert control on the structure of the Plio-Pleistocene sedimentary units and the development of the modern day fluvial system in the Rangitikei and Pourewa catchments.

Climatically controlled Late Quaternary aggradational episodes have played an important role in the formation of the present day physiography of the Pourewa Stream catchment. At c. 50 ka the Pourewa stream was substantially shorter than at present day, entering the paleo-Rangitikei River near Rata. Since c. 50 ka ongoing uplift manifested as offset along regional fault systems has led to eastward migration of the Rangitikei River. Contemporaneous fluvial development of the Pourewa stream has resulted in a fault controlled extension of the Pourewa stream before its eventual descent to Onepuhi and confluence with the Rangitikei River.

Hydraulic conductivity of the main representative lithologies appears to be governed primarily by presence of a fine tail fraction, mean grain size, effective porosity, sorting and level of cementation and compaction as a function of

diagenesis and age. Rapid lateral facies variations in the Pleistocene succession are interpreted to be reflected by corresponding changes in hydraulic conductivity, porosity and geochemistry.

Clay mineralogy of the sediments is dominated by illite with lesser amounts of glauconite, kandite and minor smectite, similar to modern day sediments on the Whanganui shelf. Geochemical data display changes consistent with the observed mineral assemblages. Organic carbon is highest within pumiceous and shellbed deposits, interpreted to reflect environments of deposition. Common glauconite, illite and moderately low organic carbon are present within the hydrostratigraphic succession facilitating microbially mediated denitrification in the subsurface through provision of electrons. Ongoing research into these subsurface processes aims to capture a wider proportion of the textural variability in the WB, applying the ideas and concepts developed herein at a regional scale.

Some spring flows in the Rangitikei District have been noted to change with season and atmospheric pressure while others remain relatively constant. We interpret this as possible evidence for confined aquifers within the study area. Several springs observed on LGM terraces are related to paleo-channels on the overlying terrace treads. We suggest paleo-channels contain coarse gravels with high hydraulic conductivity, funneling the shallow groundwater, which flows along the path of least resistance in the landscape.

Acknowledgments

We thank the residents in the Central Rangitikei District for granting land access. This work was financially supported by a Massey University Doctorate Scholarship, Horizons Regional Council Don Linklater Bursary Research Grant, Helen E Akers PhD Scholarship and C V Fife Memorial Scholarship from the School of Agriculture and Environment, Massey University.

Special thanks to the Massey University staff and lab technicians including Ian Furkert, Glenys Wallace, Bob Toes, Ross Wallace, David Feek, Dr Roberto Calvelo-Pereira, Dr Qinhua Shen, Dr Anja Mobis, Dr Gabor Kereszturi and Dr Mike Bretherton.

This paper uses the spelling 'Whanganui' rather than 'Wanganui' as recommended by the New Zealand Geographic Board (Ngā Pou Taunaha o Aotearoa). The spelling of 'Pourewa' rather than 'Porewa' is used as recommended by Ngāti Hauiti.

References

Abbott ST 1992. The Mid Pleistocene Waiomio Shellbed (Castlecliffian, c. 550-600 ky), Wanganui Basin, New Zealand. Alcheringa: An Australasian Journal of Palaeontology 16(2): 171-180.

Abbott ST 1994. Sequence Stratigraphy, Sedimentology and Paleoecology of Pleistocene Cyclothems in the Castlecliff Section, Wanganui Basin, New Zealand, Unpublished PhD Thesis. James Cook University of Northern Queensland, Australia. 297 p.

Alyamani MS, Sen Z 1993. Determination of Hydraulic Conductivity from Grain-Size Distribution Curves. Ground Water 31(4): 551-555.

Anderton PW 1981. Structure and evolution of the South Wanganui Basin, New Zealand. New Zealand Journal of Geology and Geophysics 24(1): 39-63.

Avnimelech Y, Ritvo G, Meijer LE, Kochba M 2001. Water content, organic carbon and dry bulk density in flooded sediments. Aquacultural Engineering 25: 25-33.

Bahr A, Wong HK, Yim W-S, Huang G, Ludmann T, Chan LS, Ridley Thomas WN 2005. Stratigraphy of Quaternary inner-shelf sediments in Tai O Bay, Hong Kong, based on ground-truthed seismic profiles. Geo-Marine Letters 25: 20-33.

Barnett R 1984. Upper Quaternary stratigraphy in the Otaki district, Unpublished BSc (Hons) Thesis. Victoria University of Wellington, Wellington, New Zealand. 112 p.

Beanland S 1995. The North Island Dextral Fault Belt, Hikurangi subduction margin, New Zealand. Unpublished PhD thesis, Victoria University, Wellington, New Zealand. 360 p.

Begg JG, Palmer A, Gyopari M 2005. Geological synopsis of the Manawatu-Horowhenua area for a review of the region's hydrogeology. Institue of Geological and Nucelar Sciences Client Report 2005/172, Lower Hutt, New Zealand. 22 p.

Belcher WR, Elliott PE, Geldon AL 2001. Hydraulic-propoerty estimates for use with a transient fround-water flow model of the Death Valley regional ground-water flow system, Nevada and California. US Department of the Interior, US Geological Survery , Water-Resources Investigations Report 01-4120, Nevada, USA: 1-27.

Benson CH, Trast JM 1995. Hydraulic conductivity of thirteen compacted clays. Clays and Clay Minerals 43(6): 669-681.

Beu AG 2006. Marine Mollusca of oxygen isotope stages of the last 2 million years in New Zealand. Part 2 . Biostratigraphically useful and new Pliocene to recent bivalves. Journal of the Royal Society of New Zealand 36(4): 151-338.

Beu AG, Browne GH, Grant-Taylor TL 1981. New *Chlamys delicatula* localities in the central North Island and uplift of the Ruahine Range. New Zealand Journal of Geology and Geophysics 24(1): 127-132.

Beu AG, Alloway BV, Pillans BJ, Naish TR, Westgate JA 2004. Marine Mollusca of oxygen isotope stages of the last 2 million years in New Zealand. Part 1: Revised generic positions and recognition of warm-water and cool-water migrants. Journal of the Royal Society of New Zealand 34(2): 111-256.

Bjorlykke K 2014. Relationships between depositional environments, burial history and rock properties. Some principal aspects of diagenetic process in sedimentary basins. Sedimentary Geology 301: 1-14.

Blume T, van Meerveld HJ 2015. From hillslope to stream: methods to investigate subsurface connectivity. Wiley Interdisciplinary Reviews: Water 2 3: 177-198.

Boadu FK 2000. Hydraulic conductivity of soils from grain-size distribution: new models. Journal of Geotechnical and Geoenvironmental Engineering 126(8): 739-746.

Boving TB, Grathwohl P 2001. Tracer diffusion coefficients in sedimentary rocks: correlation to porosity and hydraulic conductivity. Journal of Contaminant Hydrology 53: 85-100.

Briggs RM, Houghton BF, McWilliams M, Wilson CJN 2005. $^{40}Ar/^{39}Ar$ ages of silicic volcanic rocks in the Tauranga Kaimai area, New Zealand: Dating the transition between volcanism in the Coromandel Arc and the Taupo Volcanic Zone. New Zealand Journal of Geology and Geophysics 48(3): 459-469.

Bundy LG, Bremner JM 1972. A simple titrimetric method for determination of inorganic carbon in soils. Soil Science Society of America Journal 36: 273-275.

Burgess SM 1988. The climate and weather of Manawatu and Horowhenua. New Zealand Meteorological Serivce Miscellaneous Publications 115(18): 1-47.

Bussell MR 1984. Geology and Paleobotany of the Rangitawa Stream area, Southeast Wanganui Basin, Unpublished BSc (Hons) Thesis. Victoria University of Wellington, Wellington, New Zealand. 181 p.

Callander P, Thomas N 2013. Report on Horizons Groundwater Level Monitoring Network and Groundwater Quantity Management Issues. Horizons Report

2013/EXT/1319, Horizons Regional Council, Palmerston North, New Zealand 9781927250242. 55 p.

Carter RM, Naish TR 1998. A review of Wanganui Basin, New Zealand: Global reference section for shallow marine, Plio-Pleistocene (2.5-0 Ma) cyclostratigraphy. Sedimentary Geology 122(1-4): 37-52.

Chappell PR 2015. The Climate and Weather of Manawatu-Wanganui, NIWA Science and Technology Series Number 66, Wellington, New Zealand. 38 p.

Chapuis RP, Gill DE, Baass K 1989. Laboratory permeability tests on sand: influence of compaction method on anisotropy Canadian Geotechnical Journal 26(4): 614-622.

Claydon JJ 1997. Labratory methods for water release and solid/void characterisation of soils. Unpublished Report , Landcare Research, Hamilton, New Zealand: 1-18.

Collins S, Singh R, Rivas A, Palmers A, Horne D, Manderson A, Roygard J 2017. Transport and potential attenuation of nitrogen in shallow groundwaters in the lower Rangitikei catchment, New Zealand. Journal of Contaminant Hydrology 206: 55-66.

Cowie JD, Rijkse VIC 1977. Soils Of Manawatu County, North Island, New Zealand. New Zealand Soil Survey Report 30, New Zealand Soil Bureau, Department of Scientific and Industrial Research, Wellington, New Zealand: 1-33.

Cundy AB, Hopkinson L, Whitby RLD 2008. Use of iron-based technologies in contaminated land and groundwater remediation: A review. Science of the Total Environment 400: 42-51.

Cussins AP 1994. Hydrology and hydraulic characteristics of the unconfined aquifers of the Otaki-Te Horo area. Unpublished MSc Thesis, Victoria University, Wellington, New Zealand. 136 p.

Davidson P, Wilson S 2011. Groundwaters of Marlborough, Marlborough District Council, Marlborough, New Zealand. 302 p.

Debernardi L, De Luca DA, Lasagna M 2008. Correlation between nitrate concentration in groundwater and parameters affecting aquifer intrinsic vulnerability Environmental Geology 55: 539-558.

Dewhurst DN, Aplin AC 1998. Compaction-driven evolution of porosity and permeability in natural mudstones: An experimental study. Journal of Geophysical Research 103(B1): 651-661.

Dewhurst DN, Alpin AC 1999. Influence of clay fraction on pore-scale properties and hydraulic conductivity of experimentally compacted mudstones. Journal of Geophysical Research 104(B12): 29261-29274.

Domenico PA, Schwartz FW 1998. Physical and chemical hydrogeology. New York, USA, Wiley and Sons. 689. 689-689 p.

Dong J-J, Hsu J-Y, Wu W-J, Shimamoto T, Hung J-H, Yeh E-C, Wu Y-H, Sone H 2010. Stress-dependence of the permeability and porosity of sandstone and shale from TCDP Hole-A. International Journal of Rock Mechanics and Mining Science 47: 1141-1157.

Eberhart-Phillips D, Reyners M, Chadwick M, Stuart G 2008. Three-dimensional attenuation structure of the Hikurangi subduction zone in the central North Island, New Zealand. Geophysical Journal International 174(1): 418-434.

Elwan A, Singh R, Horne D, Roygard J, Clothier B 2015. Nitrogen attenuation factor: can it tell a story about the journey of nutrients in different subsurface environments. In: Currie LD, Burkitt LL ed. Moving farm systems to improved attenuation, Occassional Report No 28, Fertilizer and Lime Research Centre, Massey University, Palmerston North. Pp. 1-12.

Ernstsen V 1996. Reduction of nitrate by Fe2+ in clay minerals. Clays and Clay Minerals 44(5): 599-608.

Feldmeyer AE, Jones BC, Firth CW, Knight J 1943. The geology of the Palmerston-Wanganui Basin, "West side", North Island, New Zealand. Unpublished Report of the Superior Oil Company of New Zealand, Petroleum Report Series 171, Ministry of Economic Development, Wellington, New Zealand. 46 p.

Ferguson RI, Werritty A 1983. Bar development and channel changes in the gravelly River Feshie. In: Collinson JD, Lewin J ed. Modern and Ancient Fluvial Systems. International Association of Sedimentologists Speical Publication 6, Oxford, United Kingdom, Wiley-Blackwell. Pp. 133-143.

Fetter CW 2001. Applied Hydrogeology. 4th ed. New Jersey, United States of America, Waveland Press Inc. 588 p.

Fleming CA 1953. The geology of Wanganui subdivision. New Zealand Geological Survey Bulletin 52. Wellington, New Zealand. 362 p.

Fogg GE, Noyes CD, Carle SF 1998. Geologically based model of heterogeneous hydraulic conductivity in an alluvial setting. 131-143.

Folk RL, Ward WC 1957. Brazos River bar: a study in the Significance of grain size parameters. Journal of Sedimentary Petrology 27(1): 3-26.

Freeze RA, Cherry JA 1979. Groundwater. Englewood Cliffs, New Jersey, Prentice-Hall. 604. 604-604 p.

Fuller IC 2008. Geomorphic impacts of a 100-year flood: Kiwitea Stream, Manawatu catchment, New Zealand. Geomorphology 98: 84-95.

Gastaldo RA, Demko TM 2010. The Relationship Between Continental Landscape Evolution and the Plant-Fossil Record: Long Term Hydrologic Controls on Preservation. In: Allison PA, Bottjer DJ ed. Taphonomy: Process and Bias Through Time, Topics in Geobiology 32. 2nd Edition ed, Springer Science and Business Media. Pp. 249-285.

Gradwell MW, Birrell KS 1979. Methods for physical analysis of soils. New Zealand Soil Bureau Scientific Report 10C. DSIR Soil Bureau, Lower Hutt, New Zealand: 1-22.

Halley RB, Schmoker JW 1983. High-porosity Cenozoic carbonate rocks of south Florida: progressive loss of porosity with depth. American Association of Petroleum Geologists Bulletin 67(2): 191-200.

Hazen A 1983. Some physical Properties of Sand and Gravels, with Special Reference to Their Use in Filtration. Twenty Fourth Annual Report, State Board of Health of Massachusetts, United States of America: 541-556.

Hedley CB, Yule IJ 2009. A method for spatial prediction of daily soil water status for precise irrigation scheduling. Agricultural Water Management 96: 1737-1745.

Heerdegen RG, Shepherd MJ 1992. Manawatu landforms: Product of tectonism, climate change and process. In: Soons JM, Selby MJ ed. Landforms of New Zealand. 2nd ed. Auckland, New Zealand, Longman. Pp. 33-308.

Helton AM, Poole GC, Payn RA, Izurieta C, Stanford JA 2014. Relative influences of the river channel, floodplain surface, and alluvial aquifer on simulated hydrologic residence time in a montane river floodplain. Geomorphology 205: 17-26.

Houghton BF, Wilson CJN, McWilliams MO, Lanphere MA, Weaver SD, Briggs RM, Pringles MS 1995. Chronology and dynamics of a large silicic magmatic system : Central Taupo Volcanic Zone , New Zealand. Geology 23(1): 13-16.

Houlbrooke DJ, Horne DJ, Hedley MJ, Hanly JA, Snow VO 2004. A review of literature on the land treatment of farm-dairy effluent in New Zealand and its impact on water quality. New Zealand Journal of Agricultural Research 47(4): 499-511.

Houseknecht DW 1987. Assessing the relative importance of compaction processes and cementation to reduction of porosity in sandstones. American Association of Petroleum Geologists Bulletin 71(6): 633-642.

Jackson J, van Dissen R, Berryman KR 1998. Tilting of active folds and faults in the Manawatu region, New Zealand: Evidence from surface drainage patterns. New Zealand Journal of Geology and Geophysics 41(4): 377-385.

Jakobsson M, Lovlie R, Arnold EM, Backman J, Polyak L, Knutsen J-O, Musatov E 2001. Pleistocene stratigraphy and paleoenvironmental variation from Lomonosov Ridge sediments, central Arctic Ocean. Global and Planetary Change 31: 1-22.

Jiao R, Seward D, Little TA, Kohn BP 2015. Unroofing of fore-arc ranges along the Hikurangi Margin, New Zealand: Constraints from low-temperature thermochronology. Tectonophysics 656: 39-51.

Journeaux TD, Kamp PJJ, Naish TR 1996. Middle Pliocene cyclothems , Mangaweka region , Wanganui Basin , New Zealand : A lithostratigraphic framework. New Zealand Journal of Geology and Geophysics 39(1): 135-149.

Kamp PJJ, Vonk AJ, Bland KJ, Hansen RJ, Hendy AJW, McIntyre AP, Ngatai M, Cartwright SJ, Hayton S, Nelson CS 2004. Neogene stratigraphic architecture and tectonic evolution of Wanganui, King Country, and eastern Taranaki Basins, New Zealand. New Zealand Journal of Geology and Geophysics 47(4): 625-644.

Kampman I, Caldwell KJ 1985. Groundwater Resources of the Waitohu, Otaki and Mangaone. Manawatu Catchment Board Report No 65, Palmerston North, New Zealand. 22 p.

Ker DS 1970. Stratigraphy and engineering geology of the Lower Wanganui Valley, Koriniti to Parakino. New Zealand Journal of Geology and Geophysics 16(2): 189-208.

Ker DS 1991. Provisional geological map of 1:50 000 sheet T21AC (Hautapu). New Zealand Geological Survery Report G144, Lower Hutt, New Zealand: 1-19.

Kimura J-I, Yamada Y 1996. Evaluation of major and trace element XRF analyses using a flux to sample ratio of two to one glass beads. Journal of Mineralogy petrology and economic geology 91: 92-72.

Koltermann CE, Gorelick SM 1995. Fractional packing model for hydraulic conductivity derived from sediment mixtures. Water Resources Research 31(12): 3283-3297.

Kondolf GM, Piegay H 2003. Tools in Fluvial Geomorphology. West Sussex, England, John Wiley and Sons Ltd. 661 p.

Korom SF 1991. Natural denitrification in the saturated zone: a reivew. Water Resources Research 28(6): 1657-1668.

Krumbein WC 1934. Size frequency distribution of sediments. Journal of Sedimentary Geology 4: 65-77.

Lamb HF, Bates CR, Coombes PV, Marshall MH, Umer M, Davies SJ, Dejen E 2007. Late Pleistocene desiccation of Lake Tana, source of the Blue Nile. Quaternary Science Reviews 26: 287-299.

Landon MK, Rus DL, Harvey FE 2001. Comparison of Instream Methods for Measuring Hydraulic Conductivity in Sandy Streambeds. Ground Water 39(6): 870-885.

Larsen G, Chilingar GV 1983. Diagenesis in Sediments and Sedimentary Rocks, 2. Amsterdam, The Netherlands, Elsevier Scientific Publishing Company. 563 p.

Lee CY, Tsai JH, Ho HH, Yang TF, Chung SL, Chen C-H 1997. Quantitative analysis in rock samples by an x-ray fluroscence spectrometer (I) major elements. Annual Meeting of the Geological Society of China, Taipei, Taiwan: 418-420.

Lewis B 2007. Eruptive Source and Depositional Characteristics of the Potaka Tephra, Wanganui Basin, New Zealand. University of Otago, Dunedin, New Zealand, Unpublished. 304 p.

Longe EO, Enekwechi LO 2007. Investigation on potential groundwater impacts and influence of local hydrogeology on natural attenuation of leachate at a municipal landfill. Internation Journal of Environmental Science and Technology 4(1): 133-140.

Lowe DJ, Alloway BV, Shane PAR 2015. Far-flown markers. In: Graham IJ ed. 2nd ed, Geoscience Society of New Zealand in association with GNS Science, Wellington, New Zealand. 172-175.

Manville V, Nemeth K, Kano K 2009a. Source to sink: A review of three decades of progress in the understanding of volcaniclastic processes, deposits, and hazards. Sedimentary Geology 220: 136-161.

Manville V, Segschneider B, Newton E, White JDL, Houghton BF, Wilson CJN 2009b. Environmental impact of the 1.8 ka Taupo eruption, New Zealand: Landscape responses to a large-scale explosive rhyolite eruption. Sedimentary Geology 220: 318-336.

Marden M, Neall VE 1990. Dated Ohakean terraces offset by the Wellington Fault , near Woodville , New Zealand. New Zealand Journal of Geology and Geophysics 33(3): 449-453.

McArthur K, Roygard J, Ausseil O, Clark M 2007. Development of Water Management Zones in the Manawatu-Wanganui Region : Technical Report to Support Policy Development, Report No: 2006/EXT/733, Horizons Regional Council, Palmerston North, New Zealand 187741347X. 120 p.

McCarron C, Zarour H 2005. State of the environment of the Manawatu-Wanganui Region – 2005. Technical Report Five – groundwater, 2004/EXT/609. 1-67, Horizons Regional Council, Palmerston North, New Zealand. 73 p.

Medina CR, Rupp JA, Barnes DA 2011. Effects of reduction in porosity and permeability with depth on storage capacity and injectivity in deep saline aquifers: A case study from the Mount Simon Sandstone aquifer. International Journal of Greenhouse Gas Control 5: 146-156.

Melhuish A, van Dissen R, Berryman KR 1996. Mount Stewart-Halcombe Anticline: A look inside a growing fold in the Manawatu region, New Zealand. New Zealand Journal of Geology and Geophysics 39: 123-133.

Milne JDG 1973a. Upper Quaternary geology of the Rangitikei drainage basin, North Island, New Zealand. Unpublished PhD Thesis. Victoria University of Wellington, Wellington, New Zealand. 472 p.

Milne JDG 1973b. Map and sections of river terraces in the Rangitikei Basin, North Island, New Zealand. New Zealand Soil Survey Report 4, Wellington, New Zealand: 3 sheets+10p.

Morgenstern U, Stewart M, Daughney C, Townend D 2015. Transit times of baseflow in New Zealand rivers. European Geosciences Union General Assembly 2015, Vienna, Austria 17: 1-2.

Murray MH 2006. Structure and composition of the clay minerals and their physical and chemical properties. Developments in clay science 2: 7-31.

Naish TR, Kamp PJJ 1995. Pliocene-Pleistocene marine cyclothems , Wanganui Basin , New Zealand : a lithostratigraphic framework. New Zealand Journal of Geology and Geophysics 38: 223-243.

Naish TR, Kamp PJJ, Alloway BV, Pillans BJ, Wilson GS, Westgate JA 1996. Integrated tephrochronology and magnetostratigraphy for cyclothemic marine strata, Wanganui Basin: Implications for the Pliocene-Pleistocene boundary in New Zealand. Quaternary International 34-36(95): 29-48.

Neill CR 1973. Hydraulic and morphologic characteristics of Athabasca River near Forth Assiniboine-the anatomy of a wandering gravel bed river. Report REH/73/8. Alberta Research Council, Highways and River Engineering Division, Edmonton, United States of America. 23 p.

O'Regan M, Kind J, Backman J, Jakobsson M, Palike H, Moran K, Heil C, Sakamoto T, Cronin TM, Jordan RW 2008. Constraints on the Pleistocene chronology of sediments from the Lomonosov Ridge. Paleoceanography 23: 1-18.

Odong J 2008. Evaluation of Empirical Formulae for Determination of Hydraulic Conductivity based on Grain-Size Analysis. The Journal of American Science 4(1): 1-6.

Palmer AS, Pillans BJ 1996. Record of Climatic Fluctuations from ca. 500 Ka Loess Deposits And Paleosols Near Wanganui, New Zealand. Quaternary International 34-36: 155-162.

Palmer CD, Puls RW 1994. Natural attenuation of hexavalent chromium in groundwater and soils. In: Boulding JR ed. EPA Environmental Assessment Sourcebook. Michigan, USA, Arbor Press. Pp. 57-72.

Parfitt RL, Schipper LA, Baisden WT, Elliott AH 2006. Nitrogen inputs and outputs for New Zealand in 2001 at national and regional scales. Biogeochemistry 80(1): 71-88.

Pillans BJ 1983. Upper Quaternary marine terrace chronology and deformation, South Taranaki , New Zealand. Geology(May): 292-297.

Pillans BJ 1990. Pleistocene marine terraces in New Zealand : A review. New Zealand Journal of Geology and Geophysics 33(2): 219-231.

Pillans BJ 1994. Direct marine-terrestrial correlations, Wanganui Basin, New Zealand: The last 1 million years. Quaternary Science Reviews 13(3): 189-200.

Pillans BJ, Kohn BP, Berger G 1996. Multi-method dating comparison for Mid-Pleistocene Rangitawa Tephra, New Zealand. Quaternary Science Reviews 15: 641-653.

Pillans BJ, McGlone M, Palmer A, Mildenhall D, Alloway B, Berger G 1993. The Last Glacial Maximum in central and southern North Island, New Zealand: a paleoenvironmental reconstruction using the Kawakawa Tephra Formation as a chronostratigraphic marker. Palaeogeography, Palaeoclimatology, Palaeoecology 101(3): 283-304.

Pillans BJ, Alloway B, Naish TR, Westgate J, Abbott S, Palmer AS 2005. Silicic tephras in Pleistocene shallow-marine sediments of Wanganui Basin, New Zealand. Journal of the Royal Society of New Zealand 35(1-2): 43-90.

Potter WD 1984. Upper Quaternary Geology of part of the lower Rangitikei Valley, Unpublished BSc (hons) Thesis. Victoria University of Wellington, Wellington, New Zealand. 84 p.

Puckett LJ 2004. Hydrogeological controls on the transport and fate of nitrate in ground water beneath riparian buffer zones: results from thirteen studies across the United States. Water Science and Technology 49(3): 47-53.

Quinn JM, Wilcock RJ, Monaghan RM, McDowell RW, Journeaux PR 2009. Grassland farming and water quality in New Zealand. Tearmann: Irish journal of agri-environmental research 7: 69-88.

Radcliffe JE 1976. Seasonal distribution of pasture production in New Zealand, Rangitikei District. New Zealand Journal of Experimental Agriculture 4(2): 163-170.

Rasmussen TC, Crawford LA 1997. Identifying and removing barometric pressure effects in confined and unconfined aquifers. Groundwater 35(3): 502-511.

Rayment GE, Lyons DJ 2011. Soil chemical methods: Australasia. Coolingwood, Victoria, Australia, CSIRO Publishing. 330 p.

Rees CJ, Palmer JA, Palmer AS 2018a. Geology of the Central Rangitikei District, Whanganui Basin, Lower North Island, New Zealand. Paper in press: 1-43.

Rees CJ, Palmer JA, Palmer AS 2018b. Plio-Pleistocene Geology of the Lower Pohangina Valley, New Zealand. New Zealand Journal of Geology and Geophysics 61(1): 44-63.

Revil A, Cathles LM 1999. Permeability of shaly sands. Water Resources Research 35(3): 651-662.

Reynolds TI 1992. Kapiti Coast sub-region - Groundwater review. Wellington Regional Council Publication No WRC/CI-T-92/44, Wellington, New Zealand. 44 p.

Richardson JM, Fuller IC 2010. Quantification of channel planform change on the lower Rangitikei River, New Zealand, 1949-2007: response to management? GeoScience: A Working Paper Series in Physical Geography, Massey University, Palmerston North, New Zealand 2: 3-26.

Rissmann C 2011. Regional Mapping of Groundwater Denitrification Potential and Aquifer Sensitivity Regional Mapping of Groundwater Denitrification Potential and Aquifer Sensitivity, Technical Report. Environment Southland Publication No 2011-12: 1-38.

Rivas A, Singh R, Horne D, Roygard J, Matthews A 2017. Denitrification potential in the subsurface environment in the Manawatu River catchment, New Zealand: Indications from oxidation-reduction conditions, hydrogeological factors, and implications for nutrient management. Journal of Environmental Management 197: 476-489.

Rivas A, Singh R, Horne D, Roygard J, Matthews A, Hedley M 2015. An assessment of the denitrification potential in shallow groundwaters of the Manawatu River Catchment. In: Currie LD, Burkitt LL ed. Moving farm systems to improved attenuation, Fertilizer and Lime Research Centre, Massey University, Palmerston North, Occassional Report No 28. Pp. 1-15.

Rose LE, Kuehl SA 2010. Recent sedimentation patterns and facies distribution on the Poverty Shelf, New Zealand. Marine Geology 270: 160-174.

Rothwell RG, Hoogakker B, Thomson J, Croudace IW, Frenz M 2006. New Techniques in Sediment Core Analysis. Geological Society of London Special Publications 267: 79-98.

Roygard J, Carlyon G 2004. Water Allocation Project Rangitikei River, Water Resource Assessment – Allocation Limits and Minimum Flows. Technical Report 2004/EXT/606. Horizons Regional Council, Palmerston North, New Zealand 1877310557. 178 p.

Scanlon BR, Healy RW, Cook PG 2002. Choosing appropriate techniques for quantifying groundwater recharge Hydrogeology Journal 10: 18-39.

Schalchli U 1992. The clogging of coarse gravel river beds by fine sediment Hydrobiologia 235/236: 189-197.

Seitzinger S, Harrison JA, VBohlke JK, Bouwman AF, Lowrance R, Peterson B, Tobias C, Van Drecht G 2006. Denitrification across landscapes and waterscapes: A synthesis. Ecological Applications 16(6): 2064-2090.

Sen Z 2015. Practical and applied hydrogeology 1st edition ed. Oxford, United Kingdom, Elsevier.

Seward D 1976. Tephrostratigraphy of the marine sediments in the Wanganui Basin , New Zealand. New Zealand Journal of Geology and Geophysics 19(1): 9-20.

Shane P, Maas R, Lindsay J 2017. History of Red Crater volcano, Tongariro Volcanic Centre (New Zealand): Abrupt shift in magmatism following recharge and contrasting evolution between neighboring volcanoes. Journal of Volcanology and Geothermal Research 340: 1-15.

Shane PAR 1991. Remobilised silicic tuffs in middle Pleistocene fluvial sediments , southern North Island, New Zealand. New Zealand Journal of Geology and Geophysics 34(4): 489-499.

Shane PAR 1994. A widespread , early Pleistocene tephra (Potaka tephra, 1 Ma) in New Zealand: Character, distribution, and implications. New Zealand Journal of Geology and Geophysics 37(1): 25-35.

Singh R, Elwan A, Horne D, Manderson A, Patterson M, Roygard J 2017. Predicting land-based nirtogen loads and attenuation in the Rangitikei River catchment - The model development. In: Currie LD, Hedley MJ ed. Science and policy: nutrient management challenges for the next generation. Fertilizer and Lime Research Center Occassional Report No 30, Massey University, Palmerston North, New Zealand. Pp. 1-13.

Song J, Chen X, Cheng C, Wang D, Lackey S, Xu Z 2009. Feasibility of grain-size analysis methods for determination of vertical hydraulic conductivity of streambeds. Journal of Hydrology 375: 428-437.

Spane FA 2002. Considering barometric pressure in groundwater flow investigations. Water Resources Research 38(6): 1-18.

Stephens DB, Hsu K-C, Priksat MA, Ankeny MD, Blandford N, Roth TL, Kelsey JA, Whitworth JR 1998. A comparison of estimated and calculated effective porosity. Hydrogeology Journal 6: 156-165.

Stern TA, Quinlan GM, Holt WE 1992. Basin formation behind an active subduction zone: Three dimensional flexural modelling of Wanganui Basin, New Zealand. Basin research 4(3-4): 197-214.

Stern TA, Quinlan GM, Holt WE 1993. Crustal dynamics associated with the formation of Wanganui Basin, New Zealand. In: Ballance PF ed. South Pacific Sedimentary Basins: Sedimentary Basins of the World 2. Amsterdam, Elsevier. Pp. 213-223.

Te Punga MT 1952. The geology of Rangitikei Valley. New Zealand Geological Survey Memoir 8, Wellington, New Zealand. 46 p.

Te Punga MT 1957. Live anticlines in western Wellington. New Zealand Journal of Science and Technology(38): 433-466.

Thompson RC 1982. Relationship of geology to slope failures in soft rocks of the Taihape-Mangaweka area, central North Island, New Zealand. Unpublished PhD Thesis, University of Auckland, Auckland, New Zealand. 330 p.

Thorpe HR 1992. The Hidden Resource. In: Rosen MR, White PA ed. Groundwaters of New Zealand. Wellington, New Zealand, New Zealand Hydrological Society Incorporated. Pp. 161-183.

Tiessen H, Roberts T, Stewart J 1983. Carbonate analysis in soils and minerals by acid digestion and two-endpoint titration. Communications in Soil Science and Plant Analysis 14: 161-166.

Tozer B 2013. Crustal Structure of Wanganui Basin: Implications for Back-Arc Formation. Unpublished MSc Thesis, Victoria University of Wellington. 276 p.

van der Neut M 1996. Sequence Stratigraphy of Plio-Pleistocene Sediments in Lower Turakina Valley, Wanganui Basin, New Zealand. Unpublished MSc Thesis. Massey Univeristy, Palmerston North, New Zealand. 149 p.

Vandergoes MJ, Hogg AG, Lowe DJ, Newnham RM, Denton GH, Southon J, Barrell DJA, Wilson CJN, McGlone MS, Allan ASR and others 2013. A revised age for the Kawakawa / Oruanui tephra , a key marker for the Last Glacial Maximum in New Zealand. Quaternary Science Reviews 74: 195-201.

Vienken T, Dietrich P 2011. Field evaluation of methods for determining hydraulic conductivity from grain size data. Journal of Hydrology 400: 58-71.

von Lichtan IJ, White JDL, Manville V, Ohneiser C 2016. Giant rafted pumice blocks from the most recent eruption of Taupo volcano, New Zealand: Insights from palaeomagnetic and textural data. Journal of Volcanology and Geothermal Research 318: 73-88.

Wang S, Mulligan CN 2006. Natural attenuation processes for remediation of arsenic contaminated soils and groundwater. Journal of Hazardous Materials B138: 459-470.

Wang T, Zlotnik VA, Wedin D, Wally KD 2008. Spatial trends in saturated hydraulic conductivity of vegetated dunes in the Nebraska Sand Hills: Effects of depth and topography. Journal of Hydrology 349: 88-97.

White P 1986. Shallow groundwater flow direction and velocity at the Renwick refuse tip, Marlborough. Report No WS1109, Water and Soil Science Centre Christchurch, Ministry of Works and Development for the National Water and Soil Conservation Organisation: 1-42.

Whitton JS, Churchman GJ 1987. Standard methods for mineral analysis of soil sruvery samples for characterisation and classification in NZ Soil Bureau. NZ Soil Bureau Scientific Report 79: 1-27.

Wilson GS, Roberts AP 1999. Diagenesis of magnetic mineral assemblages in multiply redeposited siliciclastic marine sediments, Wanganui basin, New Zealand. In: Tarling DH, Turner P ed. Palaeomagnetism and Diagenesis in Sediments, Geological Society of London, Special Publication. Pp. 95-108.

Wilson S 2007. Reconnaissance vertical electrical sounding survey of the Rangitikei-Manawatu- Horowhenua area, Horizons Regional Council Report No: 2007/EXT/852, Palmerston North, New Zealand. 47 p.

Zarour H 2008. Groundwater Resources in the Manawatu–Wanganui Region Technical Report 2008/ET/948. Horizons Regional Council, Palmerston North, New Zealand. 262 p.



Chapter 7

Aquifer analogues

The following chapter contains an article published in the journal 'Groundwater', Volume 58, Issue 4. Here we apply air permeameter technology to gather rapid, *in situ* data from a series of hydrostratigraphic units within the Whanganui Basin. The air permeability data are then related to saturated hydraulic conductivity through the application of an empirical equation. Facies analysis is applied to investigate the variation of saturated hydraulic conductivity at outcrop. Key discussion points include:

- Relationship between air permeability and saturated hydraulic conductivity
- Variability of saturated hydraulic conductivity
- Sedimentary structures
- Bioturbation
- Fractures and secondary mineralisation

This chapter satisfies thesis objective three by capturing a portion of the textural variability present within the Whanganui Basin and linking this variability to fundamental hydrogeologic properties and facies within the basin fill.

A flight of river terraces in the Rangitikei River Valley, taken from just north of the Vinegar Hill Bridge.

Variation in saturated hydraulic conductivity at the outcrop scale, the Whanganui Basin, New Zealand

Callum Rees[1], Julie Palmer[1], Alan Palmer[1], Ranvir Singh[1]

[1]*Environmental Sciences, School of Agriculture and Environment*
Massey University, Palmerston North, New Zealand

7.1 Abstract

Groundwater flow and contaminant transport are strongly influenced by hydrogeological spatial variation. Understanding the textural heterogeneity of aquifer and aquitard units is critical for predicting preferential flow pathways, but is often hindered by sparse hydrogeological data, widely spaced data points, and complex stratigraphy. Here we demonstrate the application of air permeameter technology, providing a cost-effective, rapid alternative for characterising hydrostratigraphic units in the field. The aim of this research is to (1) characterize the variation of saturated hydraulic conductivity across shallow-marine hydrostratigraphic units of the Whanganui Basin, New Zealand, and (2) assess the variation of saturated hydraulic conductivity within individual hydrostratigraphic units and relate these changes to facies and depositional environments. Results suggest heterogeneity within fine-grained aquitard units is largely controlled by bioturbation, whereby burrowing, ingestion and defecation results in grainsize segregation and differential micrite cementation. Coarse-grained heterolithic aquifer facies display sharp changes in permeability across planar to crossbed sets, related to current and wave energy fluctuations within shallow-marine

depositional settings. Bedding plane orientation creates high permeability zones that promotes down dip subsurface flow. Down dip gradation of coarse-grained nearshore facies into fine-grained shelf facies along the paleo shoreline-shelf transect is suggested to promote lateral and vertical groundwater flow within the basin fill. Air permeameter techniques have potential for application within other groundwater basins around the world, providing datasets that facilitate greater understanding of groundwater systems, informing practices and policies for targeted water quality management.

Keywords: Groundwater flow, Quaternary, Whanganui Basin, Hydraulic conductivity, Heterogeneity, Spatial variation

7.2 Introduction

Understanding the hydraulic properties of heterogeneous aquifers is crucial for predicating preferential flow pathways, the transport of contaminants and groundwater-surface water interactions (Bowling et al. 2005). Land use intensification in primary producing countries such as New Zealand is leading to an increase in water demand, higher use of fertiliser and agricultural chemicals and the need to dispose of large quantities of byproducts, resulting in groundwater degradation (Quinn et al. 2009). Patterns of landuse change have created a need for improved mapping and quantification of groundwater resources. Information on local hydrogeological settings is essential for improving our understanding and ability to map and quantify water and nutrient flow pathways and attenuation from farmlands to receiving waterways, informing practices and policies for effective water quality management.

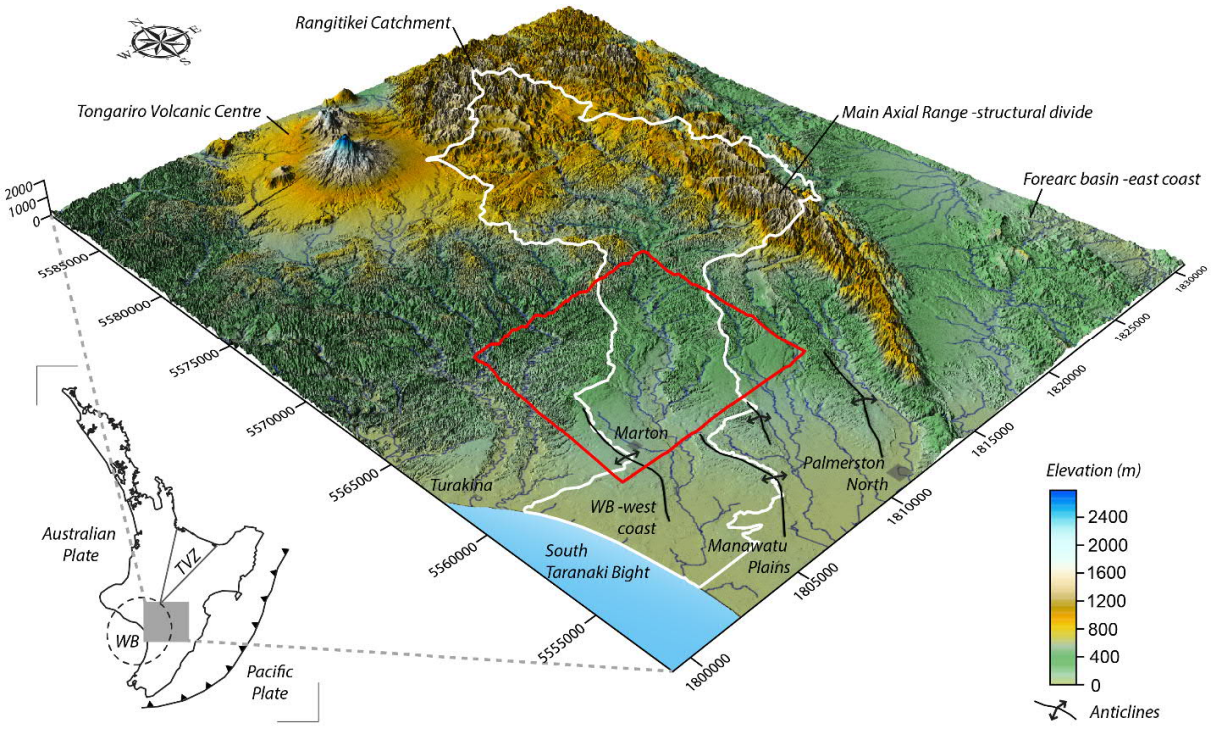


Figure 7.1: Image of the study area (red rectangle) relative to the Rangitikei Catchment (white polygon) and wider physiography of a portion of the lower North Island, New Zealand. Inset displays location of figure with respect to the Whanganui Basin (WB), Taupo Volcanic Zone (TVZ) and Pacific – Australian Plate interface. Coordinates are in meters NZGD2000, heights are in meters above sea level.

Saturated hydraulic conductivity (K_s) is a fundamental hydrogeologic property used to determine groundwater flow and contaminant transport in the subsurface environment. However, its direct measurement is limited and is time consuming to capture, particularly across different hydrogeological settings. The variable nature of sedimentation often results in a highly heterogeneous distribution of K_s within an aquifer, presenting a major challenge to studies on subsurface water flow and contaminant transport pathways (Zhang et al. 2006). Conventional pumping and flowmeter tests provide data at a scale considerably larger than individual facies within a heterogeneous aquifer, while widely space boreholes present issues with lateral correlation despite good vertical resolution (Schulze-Makuch & Cherkauer 1998). These difficulties result in unknown spatial continuity of hydrostratigraphic units within the subsurface.

Here, we apply air permeameter technology to estimate saturated hydraulic conductivity (K_a) from air permeability (k_a) within several hydrostratigraphic units of the Whanganui Basin (WB) fill, New Zealand. The main objectives of the study are to (1) characterize the variation of saturated hydraulic conductivity across shallow-marine hydrostratigraphic units of the WB, and (2) assess the variation of saturated hydraulic conductivity within individual hydrostratigraphic units and relate these changes to facies and depositional environment. We attribute K_a variation within fine-grained hydrostratigraphic units to bioturbation, whereby burrowing, ingestion and defecation results in grainsize segregation and differential micrite cementation. Coarse-grained heterolithic aquifers display sharp changes in grainsize, related to current and wave energy fluctuations within shallow-marine depositional settings, resulting in high permeability zones that facilitate preferential groundwater flow.

7.3 The study area - Geological setting

The study area is located in the lower North Island of New Zealand (Fig. 7.1), sitting astride the obliquely convergent interface between the Australian and Pacific tectonic plates. Convergence since Miocene time has driven regional uplift, forming the main axial range that separates the forearc basin in the east from the Taupo Volcanic Zone (TVZ) and WB to the west (Fig. 7.1). Extension and thinning of the crust in the central North Island has led to formation of one of the most frequently active rhyolitic zones in the world (Wilson et al. 1995). To the south of the TVZ, subsidence associated with frictional shear and downwarping at the plate interface has facilitated sedimentary preservation within the WB (Lamarche et al. 2005).

Whanganui Basin

The WB is a c. 150 km wide, asymmetric sedimentary basin positioned c. 200 km behind the active subduction margin (Fig. 7.1). Subsidence largely kept pace with sedimentation throughout the Plio-Pleistocene resulting in preservation of up to 4.5 km of shallow to marginal marine basin fill. The region has been characterised by a marginally compressional tectonic regime resulting in uplift, basin inversion and excellent onland exposure of the marine succession. Shore-normal tilting (10-3° S) of the basin succession has occurred in response to southward migration of the depocentre and coeval uplift along the basins northern margin. Biostratigraphic analysis of the richly fossiliferous succession allows for basin wide correlation and provides important paleo-environmental information used to reconstruct environments of deposition (Beu & Maxwell 1990). Well-preserved volcaniclastic and primary airfall deposits derived from the TVZ provide chronostratigraphic marker horizons, used to date and subdivide the basin fill.

The WB succession contains cyclic, unconformity bounded strata deposited during glacio-eustatic sea level cycles. Each glacial-interglacial stage couplet is represented by a depositional sequence consisting of a coarse-grained, conglomeratic to heterolithic transgressive systems tract (TST), a fine-grained siltstone to sandy mudstone highstand systems tract (HST) and a coarsening upward silty, fine sandstone regressive system tract (RST). Sea level low stand and subsequent transgressive marine ravinement is associated with erosion of the continental shelf, forming widespread erosional unconformities and sequence bounding surfaces (Abbott 1998). Coarse-grained shellbeds and conglomerates within the WB succession are classified as moderate to high producing aquifers characterised by K_s of 10^{-4} –10^{-2} m/s. Fine-grained siltstones and sandy mudstones represent aquitards characterised by relatively low Ks (10-7–10-5 m/s), providing a barrier to flow and promoting lateral groundwater movement. Sandstones within

the WB succession are classified as moderate to low producing aquifers with Ks values ranging between 10-4–10-3 m/s, respectively.

Two key relationships influence the hydrogeologic properties of the basin fill. Firstly, age is important as it determines the depth to which the unit was buried and the level of compaction and cementation it has undergone. We generally observe a decrease in hydraulic conductivity, effective porosity and permeability with age in the WB succession (Begg et al. 2005). The second key relationship is the unit's depositional environment. Shallow marine nearshore environments are subject to constant wave and tidal action along the modern day South Taranaki Bight (Fig. 7.1), resulting in a relative concentration of high permeability sands, gravel and shell material. Fine-grained relatively low permeability silts and clays are transported in suspension farther basinward accumulating at shelf depth. Relatively deep-water HST units represent fine-grained aquitards whilst shallower marine TST units represent coarse-grained aquifers within the WB succession.

Previous Groundwater Investigations

Groundwater studies within the WB have largely concentrated on the economically relevant late Quaternary groundwater resources of the Manawatu plains (Fig. 7.1) (Taylor et al. 2001). The general consensus to date is that the area is best conceptualised as a semi-confined aquifer system (Zarour et al. 2018). Regional faults and folds control topography, groundwater divides and the spatial distribution of late Quaternary fill, representing the most productive regional aquifer (Begg et al. 2005).

Concerns raised around the effects of land use on freshwater quality and groundwater degradation over the last two decades have stimulated research into

large-scale issues surrounding management of the WB groundwater resources (Singh et al. 2017). However, there is limited information available on local hydrogeological settings to better understand and model spatial and temporal variations in groundwater flow pathways and contaminant transport. Useful examples of outcrop scale models are available from other areas of New Zealand (Burbery et al. 2017), Europe (Klingbeil et al. 1999) and North America (Weissmann et al. 2015), in which Quaternary aquifer and aquitard units have been investigated to gain an understanding of local groundwater systems. Existing nutrient budget models and monitoring of catchment outlets in New Zealand has highlighted significant nitrogen loss between farms and receiving waterways (Singh & Stenger 2018). Understanding where nitrogen attenuation takes place in the landscape and subsurface is important, informing practices and policies for effective and targeted water quality management.

7.4 Methods and materials

Theoretical relationship between air permeability and saturated hydraulic conductivity

An air permeameter is essentially a compressed gas or vacuum cylinder through which gas can be released into or subtracted from a porous media. Compressible, impermeable material is placed at the permeameter tip to prevent leakage from between the cylinder outlet and the porous medium. Gas flow rate and gas pressure are monitored and can be transformed into gas permeability by using a modified form of Darcy's law with a geometrical factor depending on tip seal size, as proposed by Goggin et al. (1988):

$$k_a = \frac{2\mu P_1 Q_1}{((P_1^2 - P_2^2) G_0 a)} \tag{7.1}$$

Where k_a is air permeability (m^2), μ is the gas viscosity at atmospheric pressure, P_1 is injection pressure, P_2 is outflow pressure, Q_1 is the volumetric airflow rate (m^3/s), G_0 is a dimensionless geometric factor and a is the radius of the seal area (m). Transfer functions are available to convert k_a to K_s values by linking air and water permeability and making use of the relation between K_s and intrinsic saturated water permeability $k_{w,s}$:

$$K_s = k_{w,s} \frac{p_w g}{n_w} \tag{7.2}$$

Where K_s is saturated hydraulic conductivity, $k_{w,s}$ is intrinsic saturated water permeability, p_w is the density of water (998.23 kg m^3 at 20°C), g is gravitational acceleration (9.81 m/s^2) and n_w is the dynamic viscosity of water (10^{-3} kg m^{-1} s^{-1} at 20°C). Replacement of $k_{w,s}$ with k_a in equation 2 allows k_a measurements to be used as an indirect method to predict K_s (Loll et al. 1999; Iversen et al. 2003).

In-situ air permeability measurements

We measured the *in-situ* air permeability of selected hydrostratigraphic units within the study area to assess variations in K_s. Preliminary work involved geological mapping and hydrogeochemical analysis of the study area's main rock types (Rees et al. 2019). Here, we focus on three Plio-Pleistocene TST aquifer units, Mangarere Sandstone, Mangapipi Conglomerate and Kaimatira Pumice Sand Formation and two HST aquitard units, Mangaweka Mudstone Formation and Mangarere Siltstone. Sampling locations are provided in Supplementary Data File 7A (Appendix A).

A preliminary analysis of each outcrop involved sampling using hydraulic percussion and ring corer techniques. Sub-samples were taken for triplicate dry bulk density, gravimetric water content, volumetric water content, particle

density, grain size and porosity determinations. Three sub-samples were taken for triplicate measurements of hydraulic conductivity using a falling head permeameter. Darcy's equation was used to determine K_s, as outlined in Landon et al. (2001). All K_s values derived from falling head analysis in this study relate to vertical hydraulic conductivity.

A field campaign for detailed *in-situ* air permeability analysis took place during summer of 2019 to ensure outcrops were as dry as possible and a majority of the pore space was filled with air. The outcrop face was prepared, including removal of any vegetation or weathered material. We then photographed and sketched the outcrop before describing facies. A measured 50x50 mm grid was laid out and pegged to the outcrop face to allow for analysis at regular intervals. Air permeability measurements were taken with a TinyPerm III instrument from New England Research. The instrument consists of a vacuum cylinder, pressure transducer, handle, plunger and android device, which permits wireless data collection. The flexible butyl rubber permeameter tip is pressed against the outcrop face and the plunger is depressed, creating a vacuum causing air to flow from the unsaturated porous outcrop to the device where the gas flow rate and pressure are monitored by the pressure transducer and analysed within the android device. Using signal-processing algorithms, the unsteady state response function of the transient pressure test is computed and related to the samples air permeability. The device has an inner tip diameter of 9 mm, resulting in an investigation depth of 9-18 mm, corresponding to a maximum volume of c. 24 cm^3. Air permeability results are recorded in millidarcy's (mD) and are able to be exported from the device as comma-separated value files.

The air permeability data (k_a) was later used to derive estimates of saturated hydraulic conductivity herein denoted K_a by using the empirical equation of Iversen et al. (2003):

$$K_a = \frac{10^{1.22 x log_{10}(k_a \text{x } 9.86923e^{-16})} + 13.93}{86400} \quad (7.3)$$

Where k_a is in mD and K_a is in m/s. Equation 3 is based on the linear log-log relationship between air permeability (k_a) and saturated hydraulic conductivity (K_s) found by Loll et al. (1999) and Iversen et al. (2003). The conditions for equation 3 require the samples macroporosity to be drained. The K_a values derived in this study are somewhere between an estimate of the true horizontal and vertical K_s, as air flow lines have been shown to have different directions within the sediment during air permeameter analysis (Chief et al. 2008).

The estimation of K_s from air permeability measurements has been validated in studies by Huysmans et al. (2008), Possemiers et al. (2012), Rogiers et al. (2013a, 2013b) and Filomena et al. (2014). Effective sealing of the probe tip to the outcrop face was achieved by placing moderate pressure on the device, depressing the tip against the outcrop. Unusually high values resulting from leakage of air between the tip and the air permeameter were discarded.

Scale and approach to determining in situ saturated hydraulic conductivity

A variety of large-scale methods are available for determining in situ K_s, including slug tests, constant head tests, pumping tests, analysis of pore pressure fluctuations and numerical analysis of local and regional groundwater flow (van der Kamp 2001). Each method is based on simplifying assumptions and has its own advantages and disadvantages (Dawsone & Istok 1992). Traditional pumping and slug tests 'sample' a larger volume of material than laboratory testing or in situ air permeability testing, providing more representative values for large scale aquifer properties. These methods require installation of wells or piezometers and careful test design. Due to a lack of available wells in our study area and the costs associated with drilling and piezometer installation, we have chosen to implement

a sedimentological based approach aimed at understanding small-scale variations in K_s by utilising an air permeameter and excellent outcrop exposures of the hydrostratigraphic succession. Representative TST and HST exposures have been targeted for sampling and analysis, with the intention to characterise the average hydrogeologic properties of a WB cyclothem, enabling upscaling of this detailed analysis to cover a larger portion of the basin succession. The air permeameter is able to capture data at a scale that is unattainable using conventional slug or pumping tests. We aim to link hydrogeologic properties to facies and depositional environments, providing baseline information to ongoing basin wide groundwater studies that will utilize conventional well and wellfield testing approaches.

7.5 Results

Air permeability and grain size data for each hydrostratigraphic unit are displayed in Figs. 7.2–7.4, illustrating their relationships with laboratory derived K_s measurements. Variations in estimated saturated hydraulic conductivity derived from air permeability measurements (K_a) are presented in Figs. 5-9 for each unit. Table 7.1 summarises the measured or estimated hydrogeological properties for each hydrostratigraphic unit, descriptions are provided below.

Mangarere Formation

Mangarere Formation occurs at the base of the Rangitikei Group (Naish & Kamp 1995), with an approximate stratigraphic age of 2.5–2.4 Ma. The formation comprises a range of siliciclastic conglomerate, sandstone and siltstone members deposited within shoreface to inner-shelf environments. Sandstone members are predominantly uncemented, biotrubated, brownish grey and display a range of sedimentary structures from planar to crossbed sets. Siltstone members typically comprise massive to laminated blueish grey concretionary siltstone. During this

study, we selected a TST sandstone and HST siltstone facies from the Mangarere Formation for further analysis, the descriptions of which are provided below.

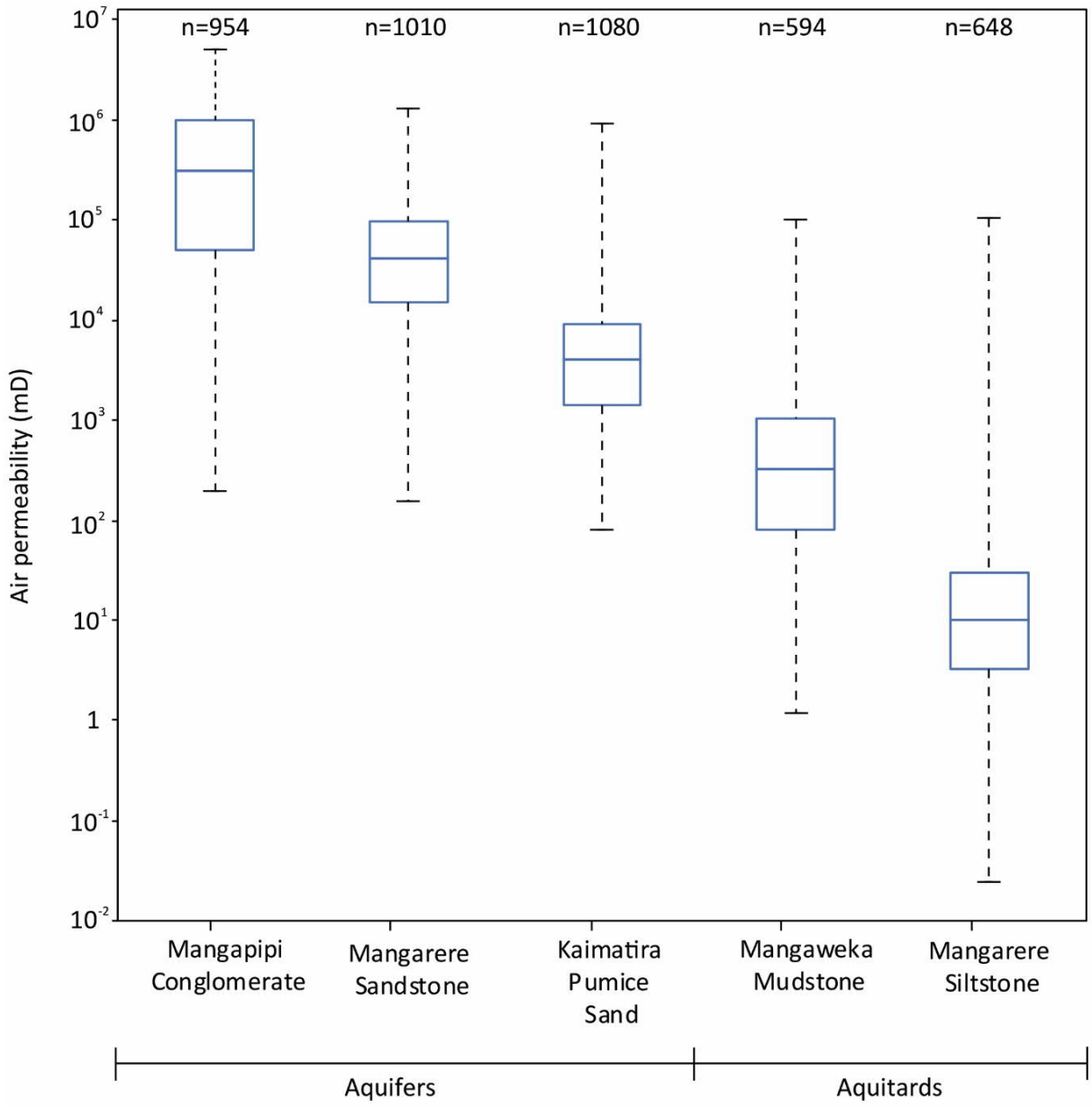


Figure 7.2: Boxplots of the air permeability measurements (millidarcys) for each geological unit. Plots display the minimum, first quartile, median, third quartile and maximum. Whiskers are set at the full data range.

Table 7.1: Hydrogeological properties of the main hydrostratigraphic units from the WB, New Zealand, obtained from a combination of laboratory and field techniques.

Systems tract	Hydrostratigraphic unit	Lithology	Laboratory measurements						In situ air permeameter measurements				
			Average grain size (μm)	Average sorting	Average bulk density g/cm^3	Average total porosity (%)	Average effective porosity (%)	Average saturated hydraulic conductivity (K_s) m/s	No of air permeability measurements	Average air permeability (milliDarcys)	Average estimated saturated hydraulic conductivity (K_a) m/s	Maximum estimated saturated hydraulic conductivity (K_a) m/s	Minimum estimated saturated hydraulic conductivity (K_a) m/s
TST Aquifer	Mangapipi Conglomerate	Fine conglomerate to coarse sandstone	Very coarse sand (1953)	Very poorly sorted	1.70	39	28	$1.1x10^{-2}$	954	476172	$4.7x10^{-3}$	$2.4x10^{-2}$	$3.1x10^{-7}$
	Mangarere Sandstone	Sandstone	Very fine sand (90)	Poorly sorted	1.66	38	7	$2.8x10^{-4}$	1010	52628	$3.2x10^{-4}$	$5.4x10^{-3}$	$2.4x10^{-7}$
	Kaimatira Pumice Sand	Pumiceous sandstone	Very fine sand (67)	Very poorly sorted	1.24	49	7	$2.1x10^{-4}$	1080	9238	$5.0x10^{-5}$	$3.8x10^{-3}$	$1.0x10^{-7}$
HST Aquitard	Mangaweka Mudstone	Mudstone	Coarse silt (25)	Poorly sorted	1.61	39	13	$7.2x10^{-5}$	594	909	$2.8x10^{-6}$	$2.7x10^{-4}$	$5.9x10^{-10}$
	Mangarere Siltstone	Siltstone	Coarse silt (22)	Poorly sorted	1.54	42	7	$5.8x10^{-5}$	648	208	$7.9x10^{-7}$	$2.7x10^{-4}$	$5.3x19^{-12}$

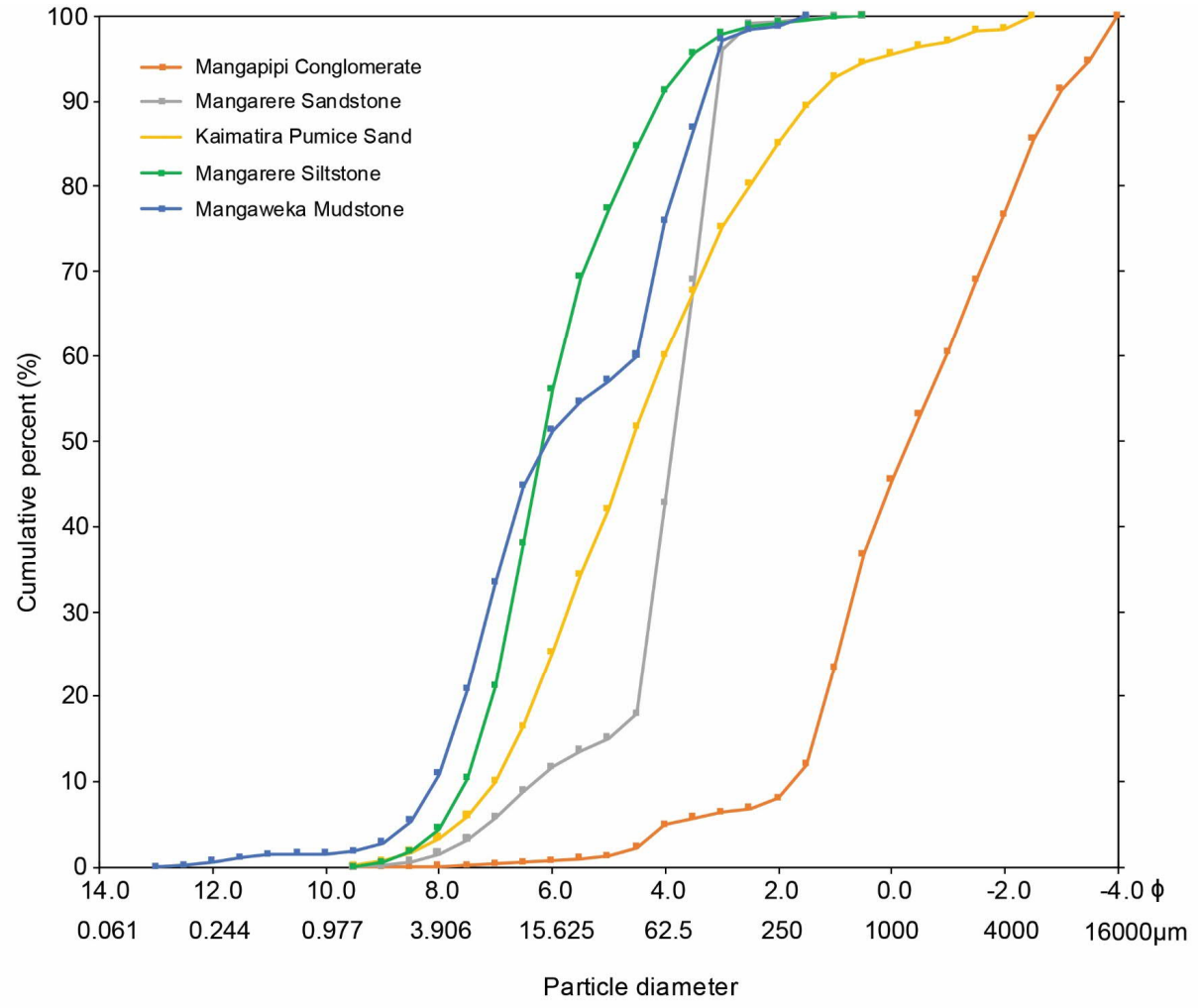


Figure 7.3: Cumulative percentage grain size distributions for each hydrostratigraphic unit.

Mangarere Sandstone facies

Mangarere Sandstone is a finely laminated to massive, light olive grey to brown silty sandstone. It is poorly sorted, very fine skewed and leptokurtic, with a geometric mean grainsize of 90 μm (Table 7.1, Fig. 7.5). Abundant bioturbation is present including common small horizontal to sub-horizontally inclined burrows between 10 and 30 mm long and 5-10 mm in diameter, filled with light coloured fine to medium-grained sandstone. Less common, large burrows up to 100 mm long and 30 mm in diameter are filled with finer grained siltstone and are aligned sub-

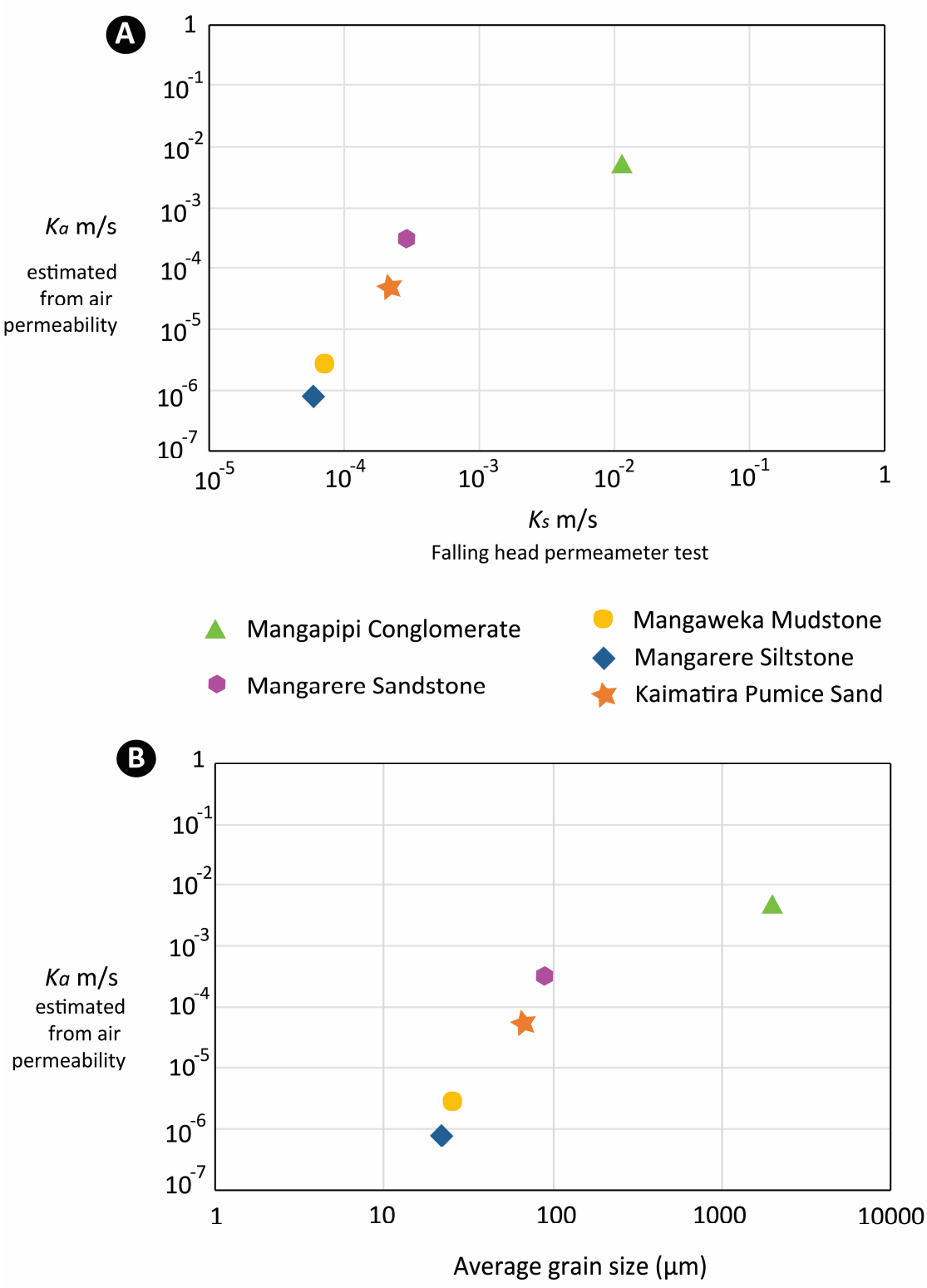


Figure 7.4: A) The relationship between hydraulic conductivity derived from falling head permeameter analysis (K_s in m/s) and hydraulic conductivity derived from air permeability analysis (K_a in m/s). B) Average grain size in µm vs hydraulic conductivity derived from air permeability analysis (K_a in m/s). Note all axes are in log scale.

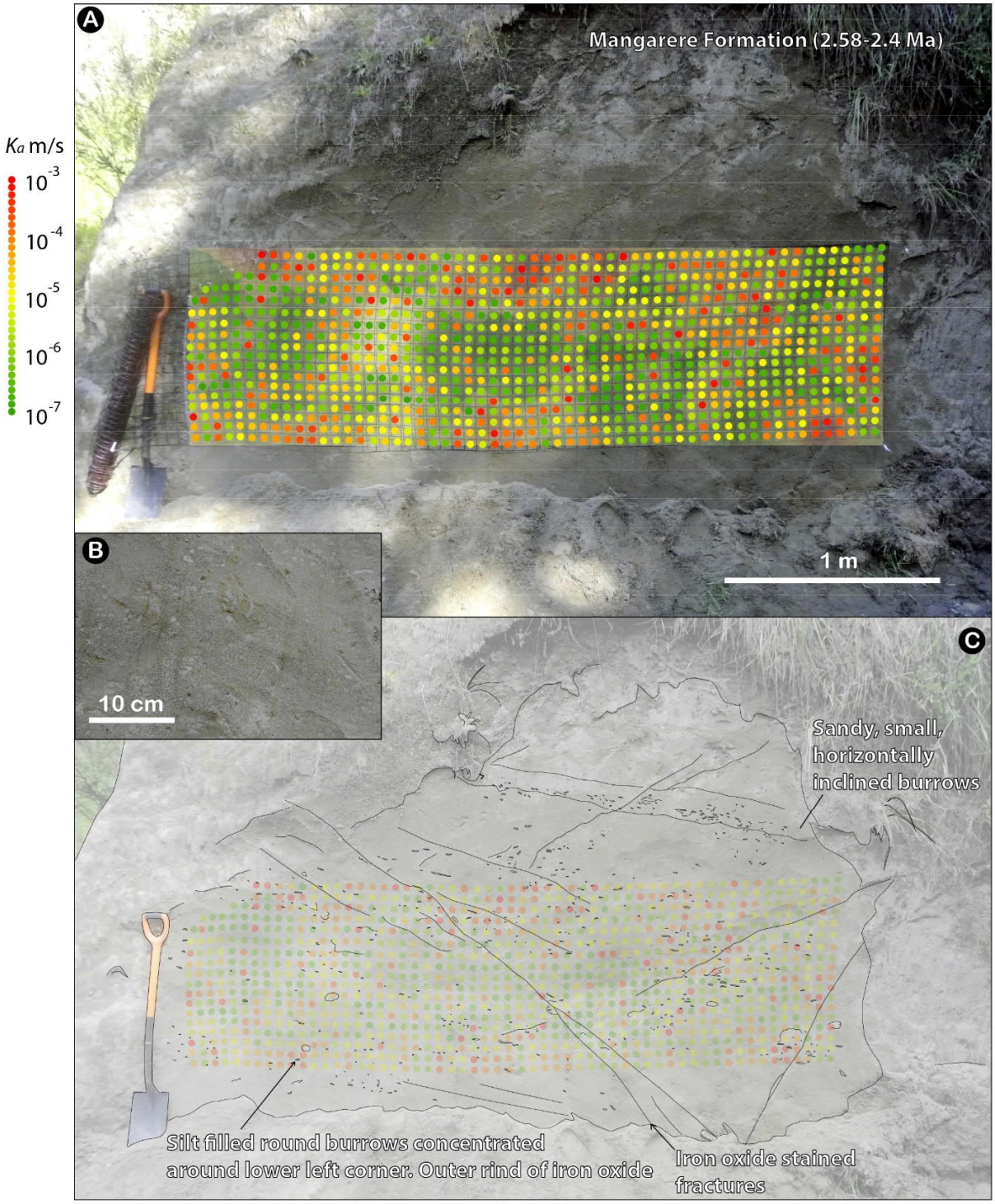


Figure 7.5: A) Estimated hydraulic conductivity values (K_a) in m per second determined by in situ measurement of air permeability of a weakly consolidated, bioturbated sandstone from Mangarere Formation, Rangitikei Group (BK34 2385 8620). B) Close up of bioturbation evident within the sandstone. C) Sketch of the outcrop emphasizing structures. This deposit is interpreted to represent a TST facies deposited at innermost shelf depth.

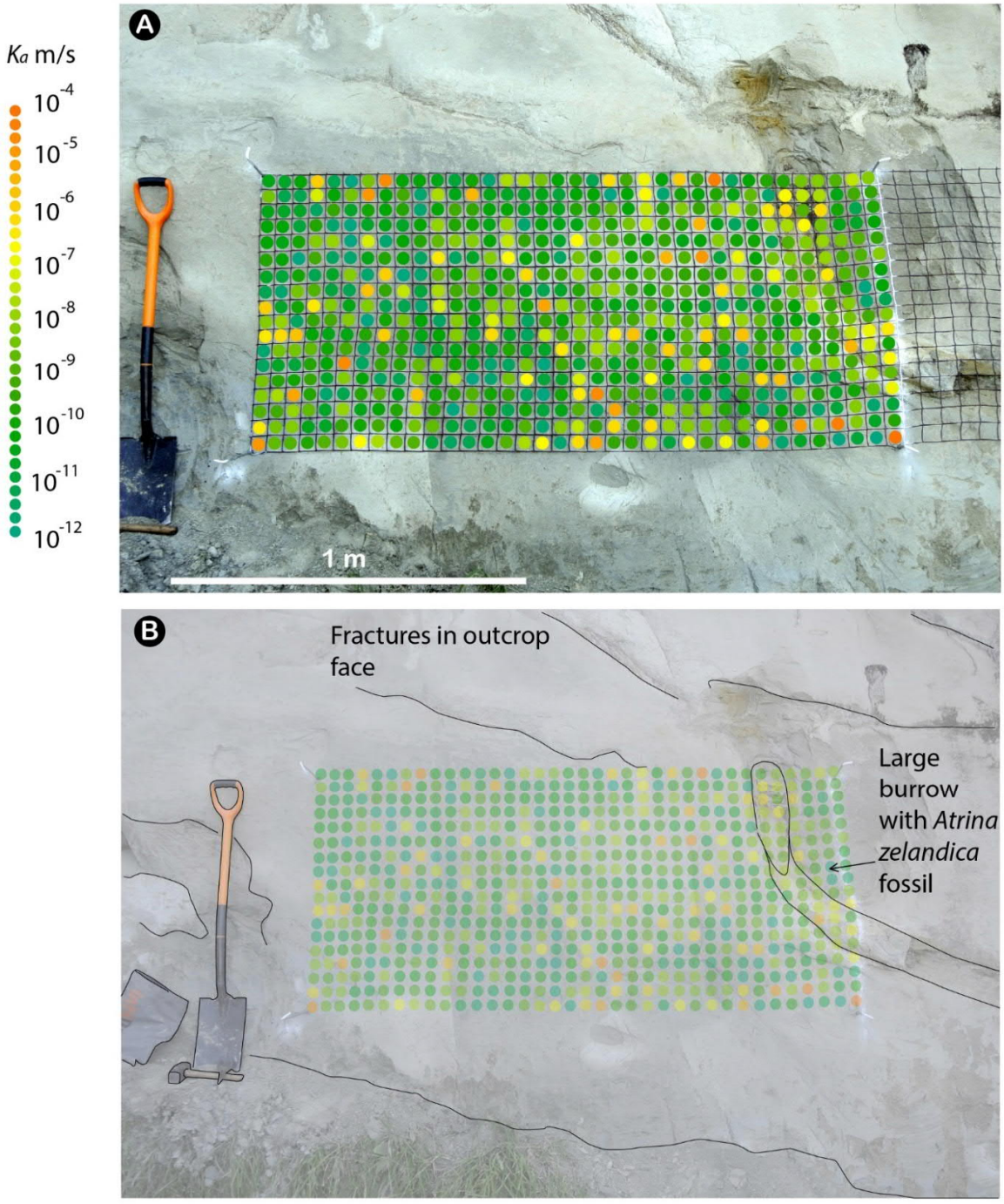


Figure 7.6: A) Estimated hydraulic conductivity values (*Ka*) in m per second determined by insitu measurement of air permeability of Mangarere Siltstone (BK34 2336 8622). B) Field sketch of the outcrop illustrating sedimentary structures. This outcrop is interpreted as a HST siltstone formed at mid shelf depth.

vertically. Thin (<10mm) fractures, aligned oblique to bedding are common at outcrop, stained by iron oxide and cemented by calcite. Effective porosity is relatively low at around 7% and average bulk density is 1.66 g/cm^3. Air permeameter results ranged from 159 to 599,467 millidarcies (mD), corresponding to estimated hydraulic conductivity values (K_a) of between 2.4x10^{-7} to 5.4x10^{-2} m/s (Fig. 7.5). K_a and K_s values for Managarere Sandstone achieved a relatively close match with both datasets averaging around 10^{-4} m/s (Table 7.1).

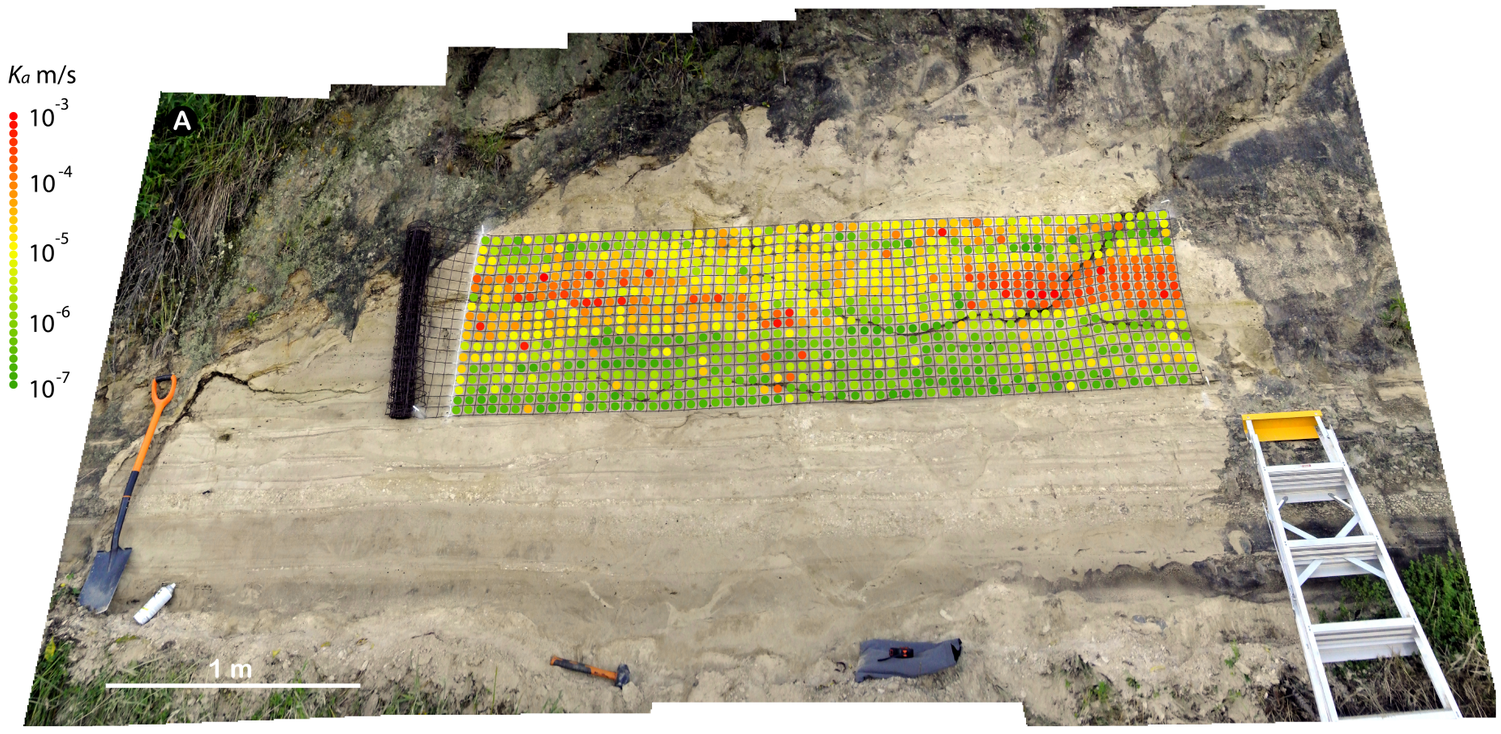
Mangarere Siltstone facies

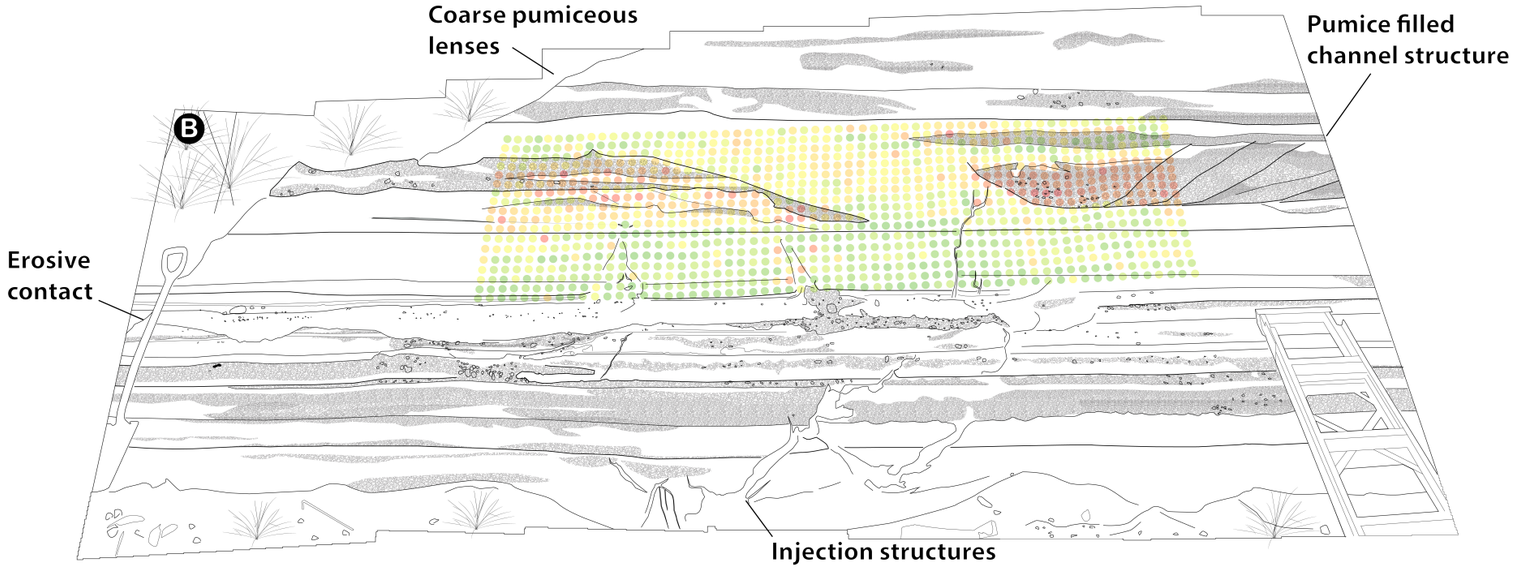
Mangarere Siltstone comprises a light to dark bluish grey massive siltstone (Fig. 7.6). The grain size distribution is poorly sorted, coarse skewed and mesokurtic with a geometric mean of 22 μm. At outcrop rare, sub-vertical burrows 100-180 mm wide and up to 1.2 m long contain the fossil *Atrina zelandica*. Typically, burrows comprise massive siltstone, characterised by a hard calcite cemented outer rind that accentuates these structures in outcrop. The siltstone contains many fractures 2-5 mm wide and extending for 1-3 m. Bulk density and effective porosity are low at 1.54 g/cm^3 and 7%, respectively. Air permeameter results ranged from 0.02 to 51,887 mD corresponding to K_a values of 5.3x10^{-12} to 2.7x10^{-3} m/s. The average K_s and K_a values obtained for Mangarere siltstone (Fig. 7.4) display the highest recorded variance at between 10^{-5} and 10^{-7} m/s, respectively.

Kaimatira Pumice Sand Formation

Kaimatira Pumice Sand Formation occurs at the base of the Kai Iwi Group (Fleming 1953), with an approximate age of 1 Ma. The formation comprises a diverse range of facies from large-scale cross-bedded conglomerate and sandstone to laminated and rippled silty sandstone with carbonaceous lenses. Depositional environments range from shallow marine through to coastal plain settings. Pumice

Figure 7.7: A) Estimated hydraulic conductivity values (Ka) in m per second determined by in situ measurement of air permeability of a high energy, silty, pumiceous sandstone, Kamatira Pumice Sand Formation (BL35 3202 6996). B) Field sketch of the outcrop illustrating the main sedimentary features. This deposit is interpreted to represent a TST heterolithic facies deposited at innermost shelf depth. Channel cut and fill structures present are surrounded by dominantly fine silty pumiceous sandstone.





is an important constituent of the formation, although as a whole the formation is predominantly siliciclastic. We selected a single TST facies from the Kaimatira Pumice Sand Formation for analysis (Fig. 7.7), the description of which is provided below.

The Kaimatira Pumice Sand facies consists of light grey to brown very fine pumiceous sandstone. It is poorly sorted, coarse skewed and mesokurtic with a geometric average grain size of 67 μm. The lower part of the outcrop displays planar bed sets of very fine silty sandstone between 200-300 mm thick. Lenses of granule to small pebble sized pumice clasts between 50-200 mm thick are present. Clasts are 1-25 mm in diameter, rounded to sub-rounded and typically display normal grading within the planar bed sets. In some cases, pumice clasts (1-25 mm in diameter) are incorporated sporadically within the dominantly fine silty pumiceous sandstone. Soft sediment deformation is visible at the base of the outcrop, where 20-50 mm thick injection structures are filled with very fine silty sandstone. The injection structures are often discontinuous, yet as a whole, persist for 1 m towards the centre of the outcrop. Above the planar bed sets lies a 300 mm thick massive fine to medium-grained pumiceous sandstone.

Overlying the massive sandstone is a 500 mm thick by 2.5m long, channeled unit displaying large variations in grain size. The base of the channel structures contain abundant rounded pumice clasts between 1-50 mm in diameter. The channels display normal grading with basal lags comprising poorly sorted coarse pumice with isolated large clasts up to 100 mm. The channels are surrounded by fine silty pumiceous sandstone that appears massive apart from the continuation of thin injection structures that locally cross the bed. Discontinuous, wavy to planar bed sets 200-500 mm thick overly the channeled bed, comprising lenses of granule to small pebble sized pumice clasts within dominantly fine silty pumiceous sandstone. The sandstone is characterised by low bulk density of 1.24 g/cm^3 and low effective porosity (7%). Air permeameter results ranged from 80 to 450,996 mD

corresponding to K_a values of between 1.0×10^{-7} and 3.8×10^{-2} m/s. The average K_s and K_a values for Kaimatira Pumice Sand Formation are compatible with moderate to low variance of between 10^{-4} and 10^{-5} m/s, respectively.

Mangapipi Conglomerate Member, Rewa Formation

Mangapipi Conglomerate Member occurs at the base of the Rewa Formation with an approximate age of 1.5-1.2 Ma. The member comprises a heterolithic mixture of bioclastic and siliclastic sediments deposited within a shallow marine depositional environment (Fig. 7.8). Greywacke clasts and abundant partially crushed shell material is typically of pebble size in a matrix of coarse to fine sands and granules. Sedimentary structures range from large-scale crossbedding to planar and rippled bed sets. We chose a single TST facies from the Mangapipi Conglomerate Member to analyse in further detail, the description of which is provided below.

The Mangapipi Conglomerate facies consists of laminated very coarse sand with abundant granule to small pebble sized shell debris and greywacke clasts. The conglomerate is very poorly sorted and mesokurtic with a geometric mean of 1953 μm. The selected outcrop consists of a series of 10-80 mm thick foresets dipping 18-20° SE. Angular shell debris and rounded clasts of greywacke 10-30 mm in diameter are sporadically spread through the beds, pinching and swelling as discontinuous lenses of coarse material. Occasional 30-50 mm thick lenses of fine siltstone drape the dominantly coarse sandstone beds. The bulk density and effective porosity is relatively high at 1.7 g/cm^3 and 28%, respectively. Air permeameter results range from 200 to 2,040,579 mD corresponding to K_a values of 3.1×10^{-7} to 2.4×10^{-1} m/s. The K_s and K_a values for Mangapipi Conglomerate (Fig. 7.4) achieve a relatively good match with moderate variance of between 10^{-2} and 10^{-3} m/s, respectively.

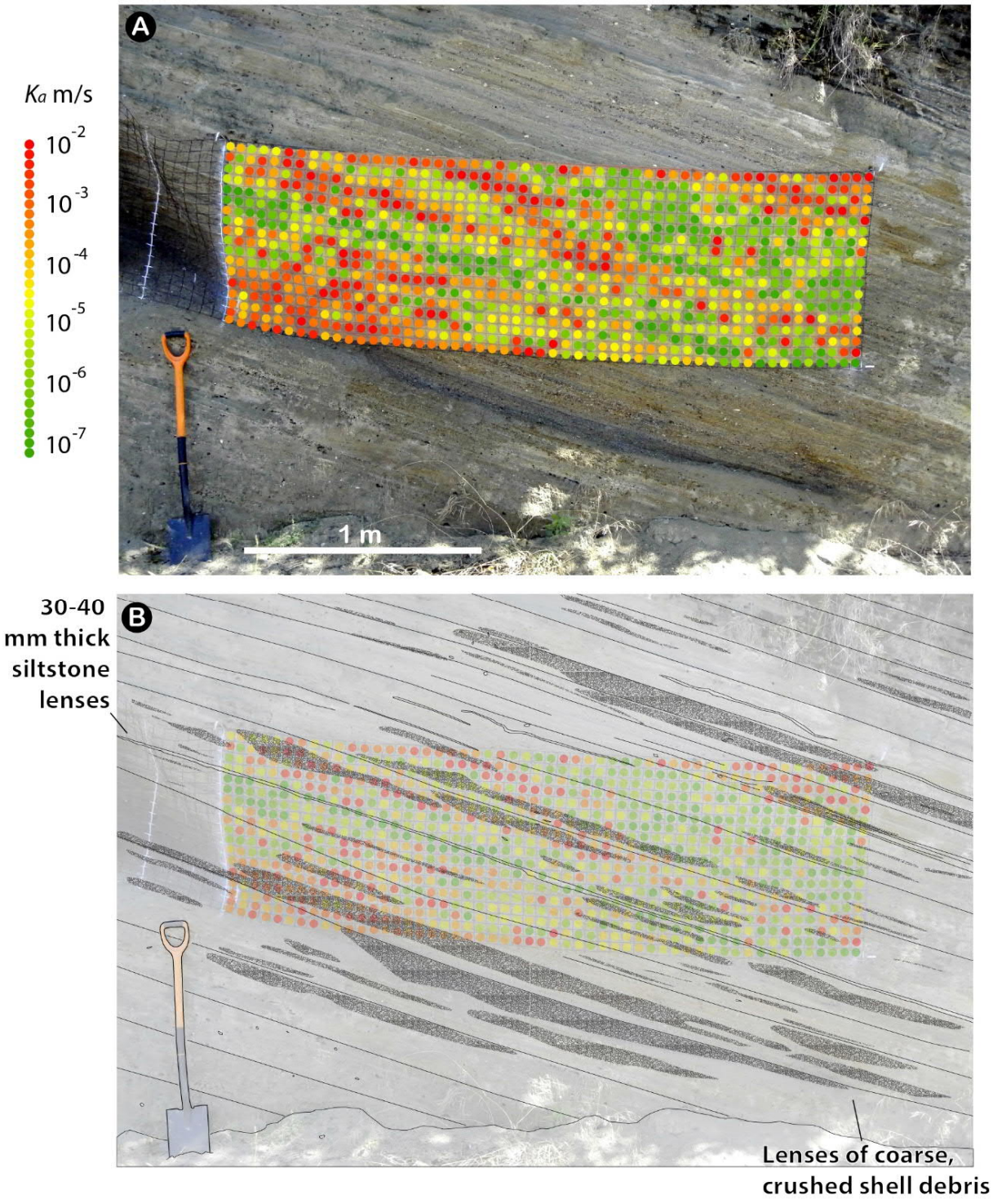


Figure 7.8: A) Estimated hydraulic conductivity values (K_a) in m/s determined by insitu measurement of air permeability of Mangapipi Conglomerate, Rewa Formation (BL34 2074 7013). B) Field sketch of the outcrop illustrating sedimentary structures. This deposit is interpreted to represent a TST dune facies deposited at innermost shelf depth.

Mangaweka Mudstone Formation

Mangaweka Mudstone Formation occurs within Paparangi Group, with an approximate age of 2.8-2.6 Ma (Fig. 7.9). The formation comprises siliciclastic, silty sandstone, siltstone, mudstone and thin tephra members deposited within mid shelf to uppermost slope environments. Members are sparsely fossiliferous, massive and blueish grey in color. We selected a single HST facies of the Mangaweka Mudstone Formation for further analysis, the description of which is provided below.

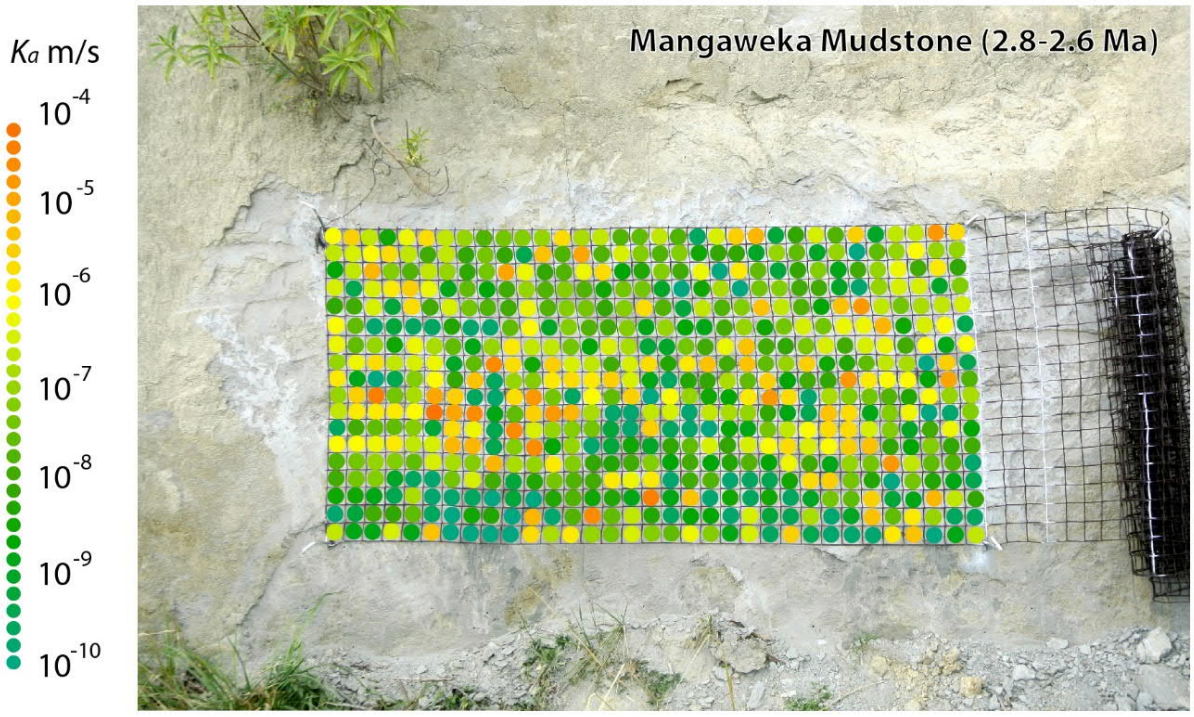


Figure 7.9: A) Estimated hydraulic conductivity values (*Ka*) in m per second determined by in situ measurement of air permeability of Mangaweka Mudstone Formation (BK35 2850 9011). This deposit is interpreted as a HST facies deposited at mid shelf to uppermost slope depth.

The Mangaweka Mudstone facies consists of massive to weakly laminated, blueish grey, fine sandy mudstone (Fig. 7.9). The grain size distribution is poorly sorted, coarse skewed and platykurtic with a geometric mean of 25 μm. At outcrop, sparse fragments of shell material were observed typically <10 mm in size. Horizontally elongated concretions 300-450 mm long are a conspicuous feature of this formation, although none cropped out at the section analysed. Bulk density is 1.61 g/cm^3 with low effective porosity of 13 %. Air permeameter results ranged from 1 to 50,701 mD corresponding to K_a values of 5.9x10^{-10} to 2.6 x10^{-3} m/s. The K_s and K_a values for the Mangaweka Mudstone facies (Fig. 7.4) are comparable with moderate variance at between 10^{-5} and 10^{-6} m/s, respectively.

7.6 Discussion

Relationships between in-situ air permeability and hydraulic conductivity

The average estimated hydraulic conductivity values derived from the air permeability datasets (K_a) were found to be in broad agreement with the saturated hydraulic conductivity (K_s) values determined from laboratory analysis, particularly for Mangarere Sandstone and Kaimatira Pumice Sand Formation (Fig. 7.4 A). The largest mismatch between K_s and K_a values was observed in fine grained hydrostratigraphic units such as Mangarere Siltstone, similar to observations made by Rogiers et al. (2014a) where clay rich units (Kasterleee Clay and Diest Clayey Top) displayed the largest variance between laboratory and air permeameter measurements. The overall range in K_a was from 10^{-12} to 10^{-2} m/s, although a majority of the measurements ranged from 10^{-8} and 10^{-3} m/s, within the verified air permeameter range of Rogiers et al. (2014b). The K_a vs K_s analysis conducted in this study shows a strong log-linear correlation, r=0.83 (Fig. 7.4 A) reflecting a relatively small bias, with predicted K_a values occurring within 1 to 2 orders of magnitude of the K_s values. Coarse-grained facies display sharp changes

in K_a across planar to crossbed sets, related to changes in grain size and porosity. Whilst the variations within fine-grained facies appear to be more chaotic and less well defined, interpreted to be a function of mixing by bioturbation.

The rapid nature of the air permeability analysis facilitates collection of large datasets. We collected a total of 4,286 measurements from the five hydrostratigraphic units, averaging 500-1000 measurements per day. Preparation of the outcrop surface is time consuming, however, and must be taken into consideration when planning fieldwork. The range of values within each dataset is considerable, with the largest K_a variance observed within Mangarere Siltstone of between 10^{-4} and 10^{-12} m/s.

Fine-grained HST units such as Mangaweka Mudstone Formation and Mangarere Siltstone were found to have consistently lower K_a compared to K_s values, particularly the latter that is characterised by a change from an average K_s value of 5.8×10^{-5} m/s to an average K_a value of 7.9×10^{-7} m/s (Table 7.1). This substantially lower K_a value could result from some of the small to intermediate sized pores in the fine-grained siltstone containing interstitial water, therefore producing lower estimates of hydraulic conductivity due a proportion of gas-filled porosity. Another possibility is that the K_s values determined by laboratory analysis could be erroneously high due to introduced error during sampling. Percussion core sampling of the units results in some disturbance and micro-fracturing of the rock. This disturbance could lead to bypass flow during permeameter analysis, resulting in erroneously high hydraulic conductivity values. Rotary core drilling could have alleviated some of this disturbance, but the additional cost of recovering core put this sampling method beyond the allocated budget of this study.

Variability of outcrop scale saturated hydraulic conductivity

Sedimentary structures

Sedimentary structures have been observed to provide an important control on the distribution of air permeability and hydraulic conductivity at the outcrop scale (Huysmans et al. 2008). Hydraulic conductivity and permeability is found by Rosas et al. (2014) and in the present study to increase with increasing grain size and decrease with increasing fines content. Minor changes in the depositional conditions and small-scale stratification of sedimentary rock can cause K_s to vary by a factor of 10 to 100 (Bersezio et al. 1999). This in turn may exert considerable control on the preferential flow of groundwater through an aquifer (Swanson et al. 2006). Alternating fine and coarse grained beds within heterolithic facies act to direct preferential subsurface flow horizontally rather than vertically through the hydrostratigraphic succession (Yager et al. 2009).

In heterolithic facies of the WB, we find closely bedded coarse and fine-grained material, typically related to tidal deposition characterised by fluctuating energy conditions, including slack water/quiescent periods where fine particles settle from suspension. Heterolithic facies are particularly common within transgressive systems tracts, towards the base of cyclothems and are commonly associated with fossiliferous conglomerate and cross-bedded pumiceous rich deposits (Abbott 1998). Transgressive units of the WB form by reworking of material basinward of a landward migrating, erosional shoreface during sea level rise at near-shore to inner shelf depths. Resultant deposits are typically coarser grained and contain a greater variety of grain sizes and sedimentary structures than their highstand counterparts. As such, they form heterogeneous aquifer units within the WB's hydrostratigraphic succession.

Lateral variations in hydraulic conductivity are particularly pronounced within the Kaimatira Pumice Sand Formation (Fig. 7.7) where channels (2.5m long by 0.5m high) filled with abundant granule to small pebble sized pumice clasts (2-8 mm in diameter) are associated with high K_a values of upto 10^{-3} m/s in comparison to the underlying massive fine silty sandstone characterised by lower K_a values of between 10^{-4} to 10^{-7} m/s. The channels only persist laterally for 2.5 m and are surrounded by finer grained deposits that have lower hydraulic conductivity, inhibiting subsurface flow. This rapid change in hydraulic conductivity associated with heterolithic facies highlights the internal heterogeneity within transgressive aquifer units of the WB. High energy, erosional features such as channel cut and fill are interpreted to represent storm wave and tidal action in a shallow marine environment (Abbott 1994).

Muldoon et al. (2001) notes the lateral persistence of bedding or lateral change in depositional environment and resultant facies also influences groundwater flow. This is envisioned to promote latitudinal (E-W subordinate vector) and vertical flow within the basin fill as coarse grained, TST material abuts fine grained, HST material along a longitudinally (N-S principal vector) oriented paleo shoreline-shelf transect, represented by a single chronostratigraphic horizon.

Mangapipi Conglomerate is a typical example of a heterolithic TST facies within the WB Pleistocene succession. This unit is interpreted to represent high energy reworking of sediments during landward migration of a transgressive shoreface and formation of gravelly dune bed forms with mud-draped foresets at innermost shelf depth. Bedding plane orientation within the Mangapipi conglomerate is observed to provide a strong control on K_a distribution (Fig. 7.8). Foreset laminations dipping 18-20° SEE are accentuated by alternations between fine and coarse-grained material. We see a corresponding change in estimated hydraulic conductivity from 10^{-2} to 10^{-7} m/s aligned parallel to the dominant bedding orientation. The paleo-slope orientation of dune foresets is interpreted to create

preferential flow pathways within the subsurface acting to control groundwater movement. The small-scale bedding within coarse grained, TST aquifers creates an internal heterogeneity, observable at outcrop as changes in grain size and sedimentary structures that result in complex aquifer compositions.

Foreset orientation reflects paleo-current direction and may not follow the regional dip of the beds (dominantly south) being independent of modern day topography or surface water flow pathways. Primary controls are paleogeography, direction of principal tidal/storm driven currents, basin inflows and their location relative to sedimentary sources and depocentres (Abbott 1998). Therefore, minor perturbations in subsurface flow direction may be associated with or explained by a combination of paleo-current and paleo-slope orientation in coarse-grained, high permeability, heterolithic TST aquifer units. Although, the spatial extent of these perturbations is possibly insignificant with regard to regional flow patterns.

Bioturbation

Massive to weakly laminated marine siltstone and mudstone units deposited within mid shelf to uppermost slope environments during sea level highstand display variations in hydraulic properties at outcrop that are difficult to attribute to primary lithology or sedimentary structures. A notable feature of these units is bioturbation and this appears to exert control on hydrology as evidenced by changes in the spatial distribution of permeability and estimated hydraulic conductivity around large burrows of *Atrina zelandica* in Mangarere Siltstone (Fig. 7.6).

Bioturbation was observed to provide an important control on the spatial pattern of hydraulic conductivity within Mangarere Sandstone (Fig. 7.5), where zones of concentrated small horizontal to sub-horizontally inclined burrows between 10 and 30 mm long are associated with higher K_a values of up to 10^{-3} m/s. In contrast,

larger burrows up to 100 mm long, filled with fine-grained siltstone are observed to limit hydraulic conductivity, characterised by lower K_a values of 10^{-6}-10^{-7} m/s.

We observe a clear pattern of increased permeability in highly bioturbated zones of Mangarere Sandstone where animal activity has led to a relative concentration of coarse-grained material. Mud filled burrows produce the opposite effect, forming areas of low hydraulic conductivity, locally impeding subsurface flow. The fine-grained, burrows are cemented by micrite Mg-calcite related to deposit feeding organisms that pass sediment through their systems below the sediment water interface (Ekdale & Lewis 1991).

Fracturing and secondary mineralisation

Syn- and post-depositional fracturing and secondary mineralisation are associated with zones of low permeability and hydraulic conductivity. For instance, fractures in the Mangarere Sandstone outcrop display a higher level of calcite cementation and particularly low K_a values of 10^{-7} m/s. We interpret secondary mineralisation and weathering of fractures in the sedimentary rock as inhibiting subsurface flow, forming fine, low permeability seals that obliquely cut the outcrop.

The distinct change in hydraulic conductivity between the fracture zones and unaffected sandstone was noticed during analysis, however, due to the thin width of the fractures (<10 mm) and the scale of the analysis (50x50 mm grid) we were unable to properly assess this relationship. The effect of these fractures on the overall distribution of hydraulic conductivity is therefore difficult to discern from the dataset gathered (Fig. 7.5).

7.7 Conclusions

Saturated hydraulic conductivity (K_s) is a fundamental hydrogeologic property used to determine groundwater flow and contaminant transport in the subsurface environment. Air permeameters provide a rapid, reliable alternative to capture estimates of in situ K_s across different hydrogeological settings. We apply this technology to the texturally diverse Late Miocene-Quaternary WB to characterise glacial/interglacial couplets of coarse and fine-grained aquifer and aquitard units. This research provides baseline hydrogeologic information, linking facies and depositional environments to the hydraulic properties of the WB fill. Our dataset informs ongoing wider scale WB groundwater models by promoting a sedimentological approach based on sequence stratigraphic concepts to improve our understanding and ability to quantify sub-surface flow pathways from farmland to receiving waterways.

Results from our analysis show individual hydrostratigraphic units contain variations in permeability and hydraulic conductivity related to changes in grainsize, porosity, fabric and level of cementation and compaction as a function of diagenesis and age. Bedding plane orientation influences the spatial distribution of hydraulic attributes, creating high permeability zones that promote horizontal subsurface flow in a down dip direction. As such, paleo-slope surfaces, stratigraphic architecture and basin structure provide controls on subsurface flow.

Heterolithic TST aquifers represent high energy reworking of sediments during marine transgression, forming gravelly dune bed forms characterised by strong zonation of hydraulic properties. The preferential subsurface flow pathways within TST aquifers pass down dip into finer-grained deposits, promoting lateral and vertical groundwater flow within the basin fill.

Fine-grained aquitard units deposited within mid shelf to uppermost slope environments during sea level highstand display chaotic variations that are attributed to bioturbation. Mud filled burrows, secondary carbonate mineralisation and weathering about fractures is shown to inhibit subsurface flow, forming fine, low permeability zones at outcrop. In contrast, bioturbated facies where deposit-feeding activity has led to a relative concentration of coarse-grained material generate preferential flow pathways in the subsurface.

Acknowledgments

We thank the residents in the central Rangitikei District for granting land access. Special thanks to the wonderful staff and laboratory technicians at Massey University. This manuscript was greatly improved following the helpful suggestions from the executive editor of Groundwater Thomas Missimer and three anonymous reviewers.

References

Abbott ST 1994. Sequence Stratigraphy, Sedimentology and Paleoecology of Pleistocene Cyclothems in the Castlecliff Section, Wanganui Basin, New Zealand, Unpublished PhD Thesis. James Cook University of Northern Queensland, Australia. 297 p.

Abbott ST 1998. Transgressive systems tracts and onlap shellbeds from mid-Pleistocene sequences, Wanganui Basin, New Zealand. Journal of Sedimentary Research 68: 253-268.

Begg JG, Palmer A, Gyopari M 2005. Geological synopsis of the Manawatu-Horowhenua area for a review of the region's hydrogeology. Institue of Geological and Nucelar Sciences Client Report 2005/172, Lower Hutt, New Zealand. 22 p.

Bersezio R, Bini A, Giudici M 1999. Effects of sedimentary heterogeneity on groundwater flow in a Quaternary pro-glacial delta environment: joining facies analysis and numerical modelling. Sedimentary Geology 129: 327-344.

Beu AG, Maxwell PA 1990. Cenozoic Mollusca of New Zealand. New Zealand Geological Survey Paleontological Bulletin 58: 1-518.

Bowling JC, Rodriguez AB, Harry DL, Zheng C 2005. Delineating alluvial aquifer heterogeneity using resistivity and GPR data. Groundwater 43(6): 890-903.

Burbery LF, Moore CR, Jones MA, Abraham M, Humphries BL, Close ME 2017. Study of connectivity of open framework gravel facies in the Canterbury Plains aquifer using smoke as a tracer. In: Ventra D, Clarke LE ed. Geology and Geomorphology of Alluvial and Fluvial Fans: Terrestrial and Planetary Perspectives, Geological Society of London Special Publication 440, London, United Kingdom. Pp. 1-18.

Chief K, Ferre TPA, Hinnell AC 2008. The effects of anisotropy on in sity air permeability measurements. Vadose Zone Journal 7(3): 941-947.

Dawsone KJ, Istok JD 1992. Aquifer Testing, Design and Analysis of Pumping and Slug Tests. New York, CRC Press, Taylor and Francis Group. 339 p.

Ekdale AA, Lewis DW 1991. Trace fossils and paleoenvironmental control of ichnofacies in a late Quaternary gravel and loess fan delta complex, New Zealand. Palaeogeography, Palaeoclimatology, Palaeoecology 81: 253-279.

Filomena CM, Hornung J, Stollhofen H 2014. Assessing accuracy of gas-driven permeability measurements: a comparative study of diverse Hassler-cell and probe permeameter devices. Solid Earth 5: 1-11.

Fleming CA 1953. The geology of Wanganui subdivision. New Zealand Geological Survey Bulletin 52. Wellington, New Zealand. 362 p.

Goggin DJ, Thrasher RL, Lake LW 1988. A theoretical and experimental analysis of minipermeameter response including gas slippage and high velocity flow effects. In situ 12: 79-116.

Huysmans M, Peeters L, Moermans G, Dassargues A 2008. Relating small-scale sedimentary structures and permeability in a cross-bedded aquifer. Journal of Hydrology 361: 41-51.

Iversen BV, Moldrup P, Schjonning P, Jacobsen OH 2003. Field application of a portable air permeameter to characterize spatial variability in air and water permeability. Vadose Zone Journal 2(4): 618-626.

Klingbeil R, Kleineidam S, Asprion U, Aigner T, Teutsch G 1999. Relating lithofacies to hydrofacies: Outcrop-based hydrogeological characterisation of Quaternary gravel deposits. Sedimentary Geology 129(3-4): 299-310.

Lamarche G, Proust JN, Nodder SD 2005. Long-term slip rates and fault interactions under low contractional strain, Wanganui Basin, New Zealand. Tectonics 24(4): 1-30.

Landon MK, Rus DL, Harvey FE 2001. Comparison of Instream Methods for Measuring Hydraulic Conductivity in Sandy Streambeds. Ground Water 39(6): 870-885.

Loll P, Moldrup P, Schjonning P, Riley H 1999. Predicting saturated hydraulic conductivity from air permeability: Application in stochastic water infiltration modeling. Water Resources Research 35(8): 2387-2400.

Muldoon MA, A. SJ, Bradbury KR 2001. Correlation of hydraulic conductivity with stratigraphy in a fractured-dolomite aquifer, northeastern Wisconsin, USA. Hydrogeology Journal 9: 570-583.

Naish TR, Kamp PJJ 1995. Pliocene-Pleistocene marine cyclothems , Wanganui Basin , New Zealand : a lithostratigraphic framework. New Zealand Journal of Geology and Geophysics 38: 223-243.

Possemiers M, Huysmans M, Peeters L, Batelaan O, Dassargues A 2012. Relationship between sedimentary features and permeability at different scales in the Brussels Sands. Geologica Belgica 15(3): 156-164.

Quinn JM, Wilcock RJ, Monaghan RM, McDowell RW, Journeaux PR 2009. Grassland farming and water quality in New Zealand. Tearmann: Irish journal of agri-environmental research 7: 69-88.

Rees CJ, Palmer JA, Palmer AS, Singh R 2019. Landscape evolution and hydrogeochemical characteristics of the Pourewa Stream catchment, Lower North Island, New Zealand. New Zealand Journal of Geology and Geophysics 62(2): 147-170. DOI: 10.1080/00288306.2018.1541812

Rogiers B, Beerten K, Smeekens T, Mallants D, Gedeon M, Huysmans M, Batelaan O, Dassargues A 2013a. The usefulness of outcrop-analouge air-permeameter measurements for analysing aquifer heterogeneity: testing outcrop hydrogeological parameters with independent borehole data. Hydrology and Earth System Sciences 17: 5155-5166.

Rogiers B, Beerten K, Smeekens T, Mallants D, Gedeon M, Huysmans M, Batelaan O, Dassargues A 2013b. Derivation of flow and transport parameters from outcropping sediments of the Neogene aquifer, Belgium. Geologica Belgica 16(3): 129-148.

Rogiers B, Winters P, Huysmans M, Beerten K, Mallants D, Gedeon M, Batelaan O, Dassargues A 2014a. High resolution saturated hydraulic conductivity logging of borehole cores using air permeability measurements. Hydrogeology Journal 22(6): 1345-1358.

Rogiers B, Beerten K, Smeekens T, Mallants D, Gedeon M, Huysmans M, Batelaan O, Dassargues A 2014b. The usefulness of outcrop analogue air permeameter measurments for analyzing aquifer heterogeneity: quantifying outcrop hydraulic conductivity and its spatial variability. Hydrological Processes 28: 5176-5188.

Rosas J, Lopez O, Missimer TM, Coulibaly KM, Dehwah AHA, Sesler K, Lujan LR, Mantilla D 2014. Determination of Hydraulic Conductivity from Grain-Size Distribution for Different Depositional Environments. Groundwater 52(3): 399-413.

Schulze-Makuch D, Cherkauer DS 1998. Variations in hydraulic conductivity with scale of measurement during aquifer tests in heterogeneous, porous carbonate rocks. Hydrogeology Journal 6: 204-215.

Singh R, Elwan A, Horne D, Manderson A, Patterson M, Roygard J 2017. Predicting land-based nirtogen loads and attenuation in the Rangitikei River catchment - The model development. In: Currie LD, Hedley MJ ed. Science and policy: nutrient management challenges for the next generation. Fertilizer and Lime Research Center Occassional Report No 30, Massey University, Palmerston North, New Zealand. Pp. 1-13.

Singh SK, Stenger R 2018. Indirect methods to elucidate water flows and contaminant transfer pathways through meso-scale catchments-a review. Environmental Processes 5: 683-706.

Swanson SK, Bahr JM, Bradbury KR, Anderson KM 2006. Evidence for preferential flow through sandstone aquifers in Southern Wisconsin. Sedimentary Geology 184: 331-342.

Taylor CB, Trompetter VJ, Brown LJ, Bekesi G 2001. The Manawatu aquifers, North Island, New Zealand: Clarification of hydrogeology using a multidisciplinary environmental tracer approach. Hydrological Processes 15(17): 3269-3286.

van der Kamp G 2001. Methods for determining the in situ hydraulic conductivity of shallow aquitards - an overview. Hydrogeology Journal 9: 5-16.

Weissmann GS, Pickel A, McNamara KC, Frechette JD, Kalinovich I, Allen-King RM, Jankovic I 2015. Characterization and quantification of aquifer heterogeneity using outcrop analogs at the Canadian Forces Base Borden, Ontario, Canada. Geological Society Of America Bulletin 127(7/8): 1021-1035.

Wilson CJN, Houghton BF, McWilliams MO, Lanphere MA, Weaver SD, Briggs RM 1995. Volcanic and structural evolution of Taupo Volcanic Zone, New-Zealand: a review. Journal of Volcanology and Geothermal Research 68(1-3): 1-28.

Yager RM, Voss CI, Southworth S 2009. Comparison of alternative representations of hydraulic-conductivity anisotropy in folded fractured-sedimentary rock: modeling groundwater flow in the Shenandoah Valley (USA). Hydrogeology Journal 17: 1111-1131.

Zarour H, Palmer AS, Begg JG 2018. A novel approach to incorporate heterogeneity in groundwater flow models. In: Rayan MA ed. Twenty-first International Water Technology Conference, IWTC21, Port Said, 28-30 June 2018, Egypt. Pp. 1-6.

Zhang Y, Gable CW, Person M 2006. Equivalent hydraulic conductivity of an experimental stratigraphy: Implications for basin-scale flow simulations. Water Resources Research 42: 1-19.



Chapter 8

Regional Application

The following chapter is a peer-reviewed journal article published in the New Zealand Journal of Geology and Geophysics, Volume 63, Issue 1. This article captures the 5th thesis objective by investigating a wider regional application of the conceptual hydrogeological model. Here, I compare a new inventory of deep-seated Late Quaternary relict landslide zones to the hydraulic, physical and structural properties of the Whanganui Basin fill. The proximity of landslides to geological structures and river systems is analysed before exploring the role of hydrogeology on development of slope morphology and landscape evolution in the Rangitikei hill country. Key discussion points include:

- Stratigraphic control
- Fluvial control
- Structural control
- Earthquakes

Chapter 8 illustrates a regional application of the conceptual models developed during the course of this research. It draws from all previous chapters to generate a synthesis of basin and landscape evolutionary history.

Litho-structural controls on Quaternary landslide distribution in the Rangitikei hill country, North Island, New Zealand

Callum Rees[1], Alan Palmer[1], Julie Palmer[1]

[1]*Environmental Sciences, School of Agriculture and Environment*
Massey University, Palmerston North, New Zealand

8.1 Abstract

The aim of this research is to investigate the influence of stratigraphy and structure on the development of present-day topography in the Rangitikei hill country. This is achieved by (1) comparing a new inventory of deep-seated Late Quaternary relict landslide zones to the hydraulic, physical and structural properties of the Whanganui Basin fill, (2) analysing the proximity of landslides to structures and rivers, and (3) exploring the relationships between geology and slope morphology. Analysis suggests postglacial incision and daylighting of the Whanganui Basin fill is a primary control on landslide distribution, providing the necessary conditions upon which a range of triggering mechanisms operate. Faults display a clear relationship to landslide frequency, suggesting earthquakes are possibly an important triggering mechanism. Landscape evolution involves inversion and denudation of alternating coarse and fine-grained sedimentary units. Frequent, shallow landslides dominate on steep, northern scarp slopes, and deep-seated rock planar slides dominate on gentle, southern dip slopes.

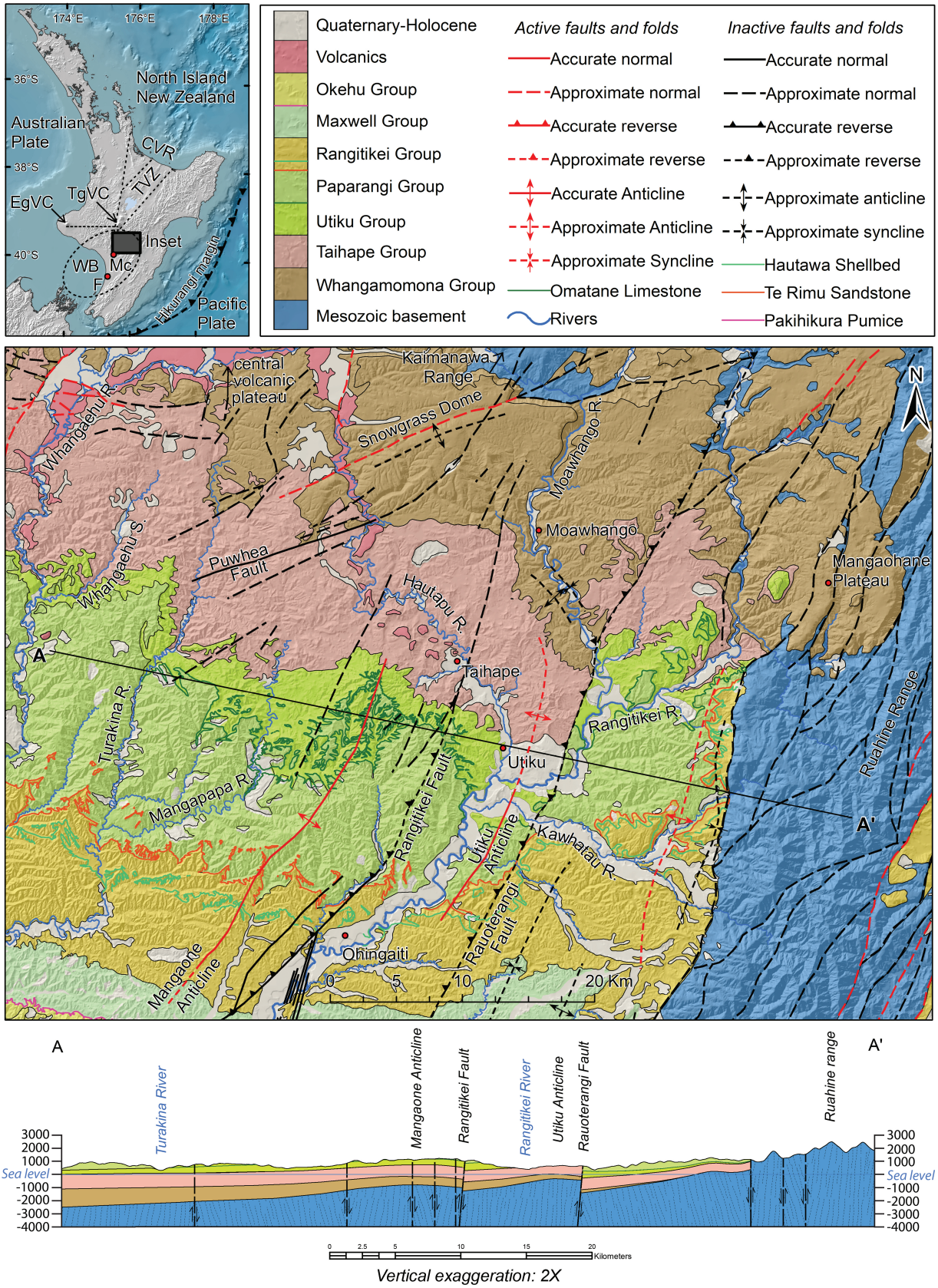
Keywords: Quaternary, Stratigraphy, Whanganui Basin, Landslides, Landscape evolution, Aquifer, Aquitard, Dip slope, Scarp slope

8.2 Introduction

Landslides are the most obvious and important process acting on hillslopes in New Zealand (Crozier et al. 1992). This is particularly evident in the western, lower North Island of New Zealand where geologically young and active landscapes have evolved largely over the last 1 Ma (Beu et al. 1981). Regional tectonic uplift has led to terrestrial exposure of the cyclic Whanganui Basin (WB) fill, one of the most complete Plio-Pleistocene marine stratigraphic records in the world (Pillans 2017).

Weak Cenozoic strata of the WB (Fig. 8.1) is susceptible to episodes of widespread shallow and deep-seated landsliding, following tropical cyclones or prolonged wet winters (Hancox & Wright 2005). Land use intensification has led to concerns regarding the management and sustainability of regional land and groundwater resources (Quinn et al. 2009). Understanding controls on landscape-forming processes is essential for improving our ability to map and quantify natural resources (Al Bakri 2001). Baseline stratigraphic and structural information provides a framework to model sediment, water and nutrient pathways from farmlands to receiving waterways, informing practices and policies for targeted and effective resource management.

Figure 8.1 (facing page): Location map displaying the study area with reference to the Whanganui Basin, Central Volcanic Region (CVR), Tongariro Volcanic Centre (TgVC), Foxton Township (F), Mt Curl (Mc) and the Hikurangi Margin. Simplified geological units and structures are displayed together with major rivers. Hautawa Shellbed (c. 2.4 Ma) and Pakihikura Pumice (c. 1.6 Ma) represent important chronostratigraphic marker horizons. Omatane Limestone and Te Rimu Sandstone mark textural changes within the basin fill. Cross section A to A' displays the faulted and folded Mesozoic basement rock that occurs depth below the Whanganui Basin fill. Data derived from LINZ, GNS Science and this study.


174°E
176°E
178°E
36°S
38°S
40°S
North Island
New Zealand
Australian
Plate
CVR
TVZ
TgVC
EgVC
Inset
WB
Mc
F
Hikurangi margin
Pacific
Plate
Quaternary-Holocene
Volcanics
Okehu Group
Maxwell Group
Rangitikei Group
Paparangi Group
Utiku Group
Taihape Group
Whangamomona Group
Mesozoic basement
Active faults and folds
Accurate normal
Approximate normal
Accurate reverse
Approximate reverse
Accurate Anticline
Approximate Anticline
Approximate Syncline
Omatane Limestone
Rivers
Inactive faults and folds
Accurate normal
Approximate normal
Accurate reverse
Approximate reverse
Approximate anticline
Approximate syncline
Hautawa Shellbed
Te Rimu Sandstone
Pakihikura Pumice
central
volcanic
plateau
Kaimanawa
Range
Snowgrass Dome
Whangaehu R.
Whangaehu S.
Puwhea
Fault
Moawhango R.
Moawhango
Mangaohane
Plateau
Hautapu R.
Taihape
A
A'
Turakina R.
Rangitikei R.
Ruahine Range
Utiku
Mangapapa R.
Rangitikei Fault
Utiku
Anticline
Kawhatau R.
Ohingaiti
Rauoterangi
Fault
Mangaone
Anticline
0
5
10
20 Km
N
A
A'
Turakina River
Mangaone Anticline
Rangitikei Fault
Rangitikei River
Utiku Anticline
Rauoterangi Fault
Ruahine range
3000
2000
1000
Sea level
-1000
-2000
-3000
-4000
0
2.5
5
10
15
20
Kilometers
Vertical exaggeration: 2X

Ker (1970) and Thompson (1982) compared the spatial distribution of deep-seated landslides within the Rangitikei hill country to lithologies within the WB fill. They suggested that the majority of deep-seated landslides occur within the Taihape Group, concentrated near contacts with units of the Utiku and Whangamomona groups (Table 8.1, Fig. 8.1). Slip surfaces at the base of deep-seated landslides have been attributed to clay beds within the Taihape Group (Ker 1970; Thompson 1982; Massey 2010). Moreover, structural control on bedding plane attitude and fractures within the rock mass have been proposed to influence the direction and likelihood of landsliding in the WB (Thompson 1982). Here, we investigate landscape evolution of the Rangitikei hill country, its relationship to the WB fill, and the role of deep-seated Late Quaternary landslides on the formation of present-day topography. We apply a new inventory of deep-seated Late Quaternary relict landslide zones to datasets that characterise the hydraulic, physical and structural properties of WB rock types. The proximity of landslides to structures and river systems is examined, alongside a conceptual model of the relationships between geology and slope morphology.

8.3 Study area

Tectonic setting

The Whanganui Basin (WB) is a partially inverted c. 200 x 200 km Late Miocene-Quaternary marine basin that forms a portion of the western lower North Island of New Zealand (Fig. 8.1). It comprises c. 4.5 km of predominantly marine sedimentary fill. Basin formation possibly involved a combination of lithospheric loading and compressional downwarping driven by coupling of the Pacific and Australian plates (Stern et al. 1993). Through the Miocene-Early Pleistocene, marine seaways at Kuripapaongo (Browne 2004) and the Manawatu Saddle (Rees et al. 2018b) provided sediment transport pathways between the WB and the east

Table 8.1: Stratigraphic nomenclature used in this study and correlation to other proposed nomenclatures of the eastern and western Whanganui Basin and eastern Taranaki Peninsula.

Western Whanganui Basin				Eastern Whanganui Basin			
Fleming (1953)		Superior Oil Company NZ (1943)		Te Punga (1952)		Ker (1991); Naish & Kamp (1995); Journeaux et al. (1996) This study	
OKEHU GROUP	Upper Okehu Siltstone Okehu Shell Grit Lower Okehu Siltstone Butlers Shell Conglomerate Makirikiri Tuff	CASTLECLIFFIAN	Basal Ash	UPPER RANGITIKEI	Mangapipi Fossil Beds Pakihikura Pumice	OKEHU GROUP	Rewa Fm. *Mangapipi Conglomerate* *Mangapipi Mb.* Makirikiri Tuff Fm. *Pakihikura Pumice Mb.*
MAXWELL GROUP	Upper Maxwell Fm. Mangahou Siltstone Middle Maxwell Fm. Pukekiwi Shell Sand Lower Maxwell Fm. Tewkesbury Fm.	NUKUMARUAN		MIDDLE RANGITIKEI FORMATION	Vinegar Hill Fossils Mudstone	MAXWELL GROUP	Upper Maxwell Fm. Rataiti Fm.
NUKUMARU GROUP	Waipuru Shellbed Nukumaru Brown Sand Mangamako Shellbed Nukumaru Limestone Nukumaru Fm. Ohingaiti Sand		Waipuru Shellbed Mangamako Shellbed Ohingaiti Sand		Waipuru Fossil Beds Mangamako Fossil Beds Ohingaiti Sandstone	RANGITIKEI GROUP	Vinegar Hill Fm. *Waipuru Shellbed Mb.* Mangaonoho Fm. *Mangamako Shellbed Mb.* Orangipongo Fm. *Ohingaiti Sand Mb.*
OKIWA GROUP	Kuranui Limestone Hautawa Shellbed Te Rama Shellbed Parihauhau Shellbed Te Rimu Sand		Tuha Sand Hautawa Shellbed Basal Sand		Tuha Sandstone Basal Sandstone		Makohine Fm. *Tuha Sand Mb.* Tikapu Fm. *Hautawa Shellbed Mb.* Mangarere Fm. *Te Rimu Sand Mb.*
PAPARANGI GROUP	Wilkies Shellbed Makokako Sand Mangaweka Mudstone Paparangi Sandstone *Mangapani Shell Conglomerate Mb.*	WAITOTARAN	Mangamahu Concretions Mangaweka Mudstone Fm.	LOWER RANGITIKEI FORMATION	Mangaweka Concretionary Mudstone	PAPARANGI GROUP	Mangaweka Mudstone Fm
WHENUKURA GROUP	Waverley Fm. Waipipi Fm. Rangikura Sandstone Pepper Shell Sand		Conglomeratic Limestone Horizon Utiku Sand		Hautapu Shell Limestone	UTIKU GROUP	*Omatane Limestone Mb.* Manui Fm. Kawhatau Fm. Tarare Fm.
			Mataroa Concretionary mudstone Taihape Sand Taihape Mudstone		Concretionary mudstone	TAIHAPE GROUP	Tangahoe Mudstone Fm.
			No.1. Reef Undifferentiated Reefs Reef-bearing Sands Fm.		Mudstone and Sandstone	WHANGAMOMONA GROUP	Undifferentiated Matemateaonga Fm.

Eastern Taranaki Peninsula	
Thoms (1942); Arnold (1957, 1958); Vonk and Kamp (2004)	
TAIHAPE GROUP	Maungatiti Sandstone Mb. Tangahoe Mudstone Fm.
WHANGAMOMONA GROUP	Umukiwi Mb. Matemateaonga Fm.

coast basins. As a result, successions on both sides of the present day main axial ranges share a similar depositional history, only becoming fully separated during piercement and formation of the modern day topography over the last c. 1 Ma (Beu et al. 1981; Shane 1991; Rees et al. 2018a).

During Late Miocene to Pleistocene time the WB depocentre migrated southeast from between the current Tongariro and Egmont volcanic centres to its present location offshore of Foxton (Fig. 8.1). Depocentre migration occurred together with simultaneous uplift along the northern and eastern basin margins resulting in progressive exhumation and southward tilting (2–15°) of the basin fill. Late Quaternary uplift has been calculated at a rate of 0.3–0.5 m ka in the location of the modern coastline and c. 1–3 m ka adjacent to the axial range (Pillans 1986). This tectonic regime combined with Late Quaternary downcutting has resulted in exposure through the gently dipping marine succession within deeply incised northeast-southwest oriented river valleys (Abbott 1994). The Central Volcanic Region (CVR) (Fig. 8.1), has provided an important source of sediment to the WB, particularly over the last c. 2 Ma.

Whanganui Basin succession

The WB contains a c. 4.5 km predominantly marine succession deposited in shelf, shoreline, and coastal plain depositional environments throughout orbitally-controlled sea level fluctuations (Naish et al. 2005). Seventy depositional cycles have been documented, correlated to Marine Isotope Stages (MIS) M2–3 (Carter & Naish 1998; Grant et al. 2018). Each cycle relates to a glacial/interglacial couplet, represented by vertically stacked, alternating, fine- and coarse-grained sedimentary units. Late Miocene-Pliocene WB fill was deposited in shallow marine to outer shelf/inner-most slope depositional environments (Journeaux et al. 1996; Kamp et al. 1998). These studies indicate two phases of rapid deepening within the WB, located at the Tangahoe Mudstone (between the Whangamomona and

Taihape groups) and the Mangaweka Mudstone Formation (between the Utiku and Paparangi groups).

Geomorphology

The study area consists of c. 3500 km^2 of Rangitikei hill country, bounded by Mesozoic greywacke-argillite rock of the Kaimanawa Mountains and Ruahine Range to the northeast and east, respectively. Quaternary volcanics of the central volcanic plateau are located to the northwest (Fig. 8.1). The hill country comprises subdued to steep (20–40°) slopes, with a dominant south-southwest aspect, formed in Cenozoic sedimentary rock of the WB. Slope morphology is varied, including concave, convex, and rectilinear profiles (Hancox & Wright 2005). Ridges are narrow, sharp and fluted where relatively competent lithologies cap the hilltops (Neall 1982). Ridges, ledges, scarp slopes, dip-slopes and waterfalls within the Rangitikei hill country reflect changes within the WB fill. Relatively competent lithologies resist erosion forming conspicuous ledges, often lined by saturated soil tolerant plant species. Permeability contrasts along bedding planes lead to seeps and springs, facilitating the growth of vegetation and promoting downslope landslides through local increases in pore water pressure (Hodge & Freeze 1977). Distinct topography occurs in the Moawhango area, characterised by the surfaces of the Hihitahi and Mangaohane plateaus, formed by a series of gently westward-dipping fault blocks, covered in extensive tussock vegetation (Browne 1978; Rogers & McGlone 1989) (Fig. 8.1). South of Moawhango, steep hill country extends in a broad band from the western Ruahine Range west, toward Taranaki, dissected by the Rangitikei, Turakina and Whangaehu river valleys (Fig. 8.1, line A to A'). Major tributaries of the Rangitikei River (Moawhango, Hautapu and Kawhatau rivers) rise in the highlands converging toward Utiku (Fig. 8.1), where the river cuts a steep-sided gorge through WB fill. Erosion combined with the c. east-west strike of sedimentary units through this area has formed a degree of uniformity in the landforms, characterised by similar slope angles and summit height

accordance (Molloy 1998). Denudation of the soft, actively uplifting Cenozoic rock has formed a fine dendritic drainage pattern (Neall 1982). The steep Rangitikei hill country gives way to undulating-flat, plateau and inter-montane basins in the northern portion of the study area.

8.4 Methods

This study draws from a 1:25 000 scale hydrogeological survey conducted between 2016-2019 in the Rangitikei hill country (Rees et al. 2019). The survey included a compilation of stratigraphic nomenclature for the study area (Table 8.1). Emphasis was placed on observing the movement of water in the landscape and exploring relationships between springs, seeps, water bearing layers and the local geology. Mapping involved subdivision of the WB fill into broad hydrostratigraphic units, based largely on differences in grain size. Representative samples of hydrostratigraphic units were sampled using percussion and ring corer techniques for analysis at Massey University. Analyses included effective porosity, permeability and hydraulic conductivity (Table 8.2). In addition, 334 deep-seated Late Quaternary relict landslide zones were mapped at 1:10 000 scale using two sets of ortho-rectified aerial photographs (LINZ), digital elevation data (Horizons Regional Council) and ground truthing between 2016-2019. A large portion (244) of these relict landslide zones were re-mapped from existing literature and surveys (Thompson 1982; Ker 1991; Townsend et al. 2008; Massey 2010; Lee et al. 2011; Holdsworth 2018), and the New Zealand landslide database (Rosser et al. 2016). The landslide classification system of Hungr et al. (2014), was used (Fig. 8.2), and focused on large (>50,000 m^2) deep-seated landslides involving bedrock.

Table 8.2: Ranges for selected physical and hydraulic properties of WB rock types Data from Thompson (1982) and this study.

Rock type	Effective porosity %	Hydraulic conductivity m/s	Permeability m^2	Point load Index I_s KPa	Unconfined Compressive Strength KPa
Shellbed – Coquina limestone	6 –32	$5.4x10^{-4} – 5.0x10^{-3}$	$5.5x10^{-11} – 5.1x10^{-10}$	198 – 4738	–
Sandstone	7 – 9	$2.6x10^{-4} – 4.9x10^{-4}$	$2.6x10^{-11} – 5.0x10^{-11}$	7 – 167	62 – 3500
Mudstone	9 – 13	$2.8x10^{-6} – 8.1x10^{-5}$	$2.9x10^{-13} – 8.3x10^{-12}$	37 – 291	974 – 8211
Siltstone	5 – 7	$7.9x10^{-7} – 6.9 x10^{-5}$	$8.1x10^{-14} – 7.1x10^{-12}$		

In some cases, distinguishing individual landslide events and landforms was problematic, due to the amount of denudation in the landscape and occurrence of landslide complexes involving multiple overlapping landslides. Thus, the areas are mapped as "landslide zones" that may encompass multiple individual landslides. Landslide aspect was determined either in the field or through interpretation of orthophotos draped over digital elevation models of the study area.

Where practical, landslide type was assigned in the field by assessing landslide geomorphology. For example, rock rotational slides in the field are characterised by a concave surface of rupture, arcuate head scarp, several internal scarps, back-tilting below the headwall and an aspect that is opposite or oblique to the dip direction of the basin fill (Fig. 8.3 A). Ortho-rectified aerial photograph datasets were obtained from LINZ, including the 0.4 m resolution rural aerial photos of the Manawatu-Whanganui Region taken during the summer period of 2010-2011, with a spatial accuracy of ±2.5 m. The second set of orthophotos was taken in the

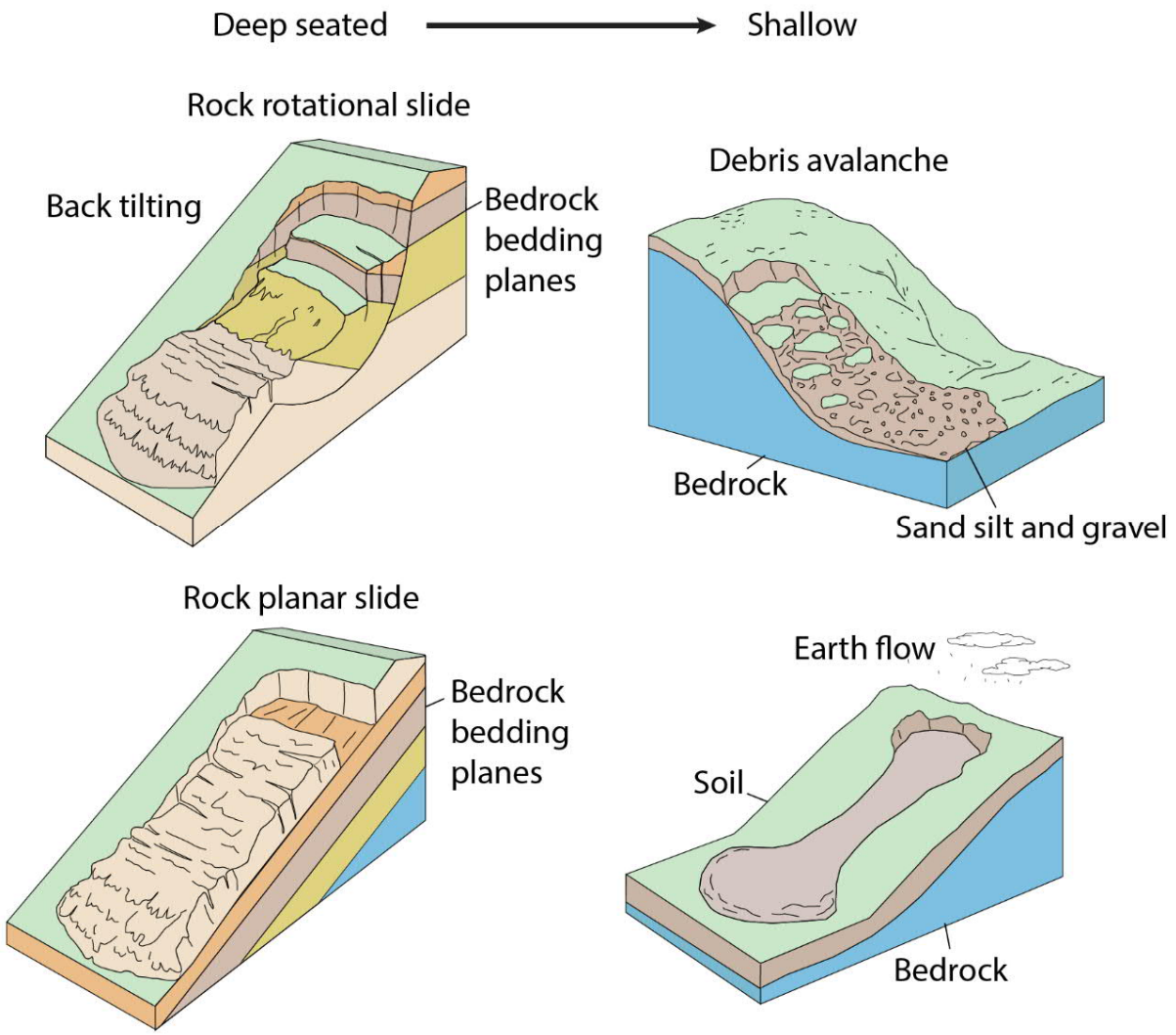


Figure 8.2: Examples of different types of mass movements based on the landslide classification system of Hungr et al (2014).

summer period of 2015-2016 at 0.3 m resolution, and a spatial accuracy of ±0.6 m. Digital elevation data was acquired from several sources: (1) a 10 m digital surface model (DSM) derived from aerial imagery with nominal vertical accuracy of ±0.5 m, (2) a 1 m digital elevation model (DEM) derived from LiDAR, with a nominal vertical accuracy of ±0.15 m, and (3) a 15 m DEM (Columbus et al. 2011) created through interpolation of 20 m contours from the LINZ 1:50 000 topo database. The 1 m DEM coverage was of limited extent, but the 10 m DSM and 15 m DEM had full coverage of the study area. Slope and aspect for the entire study area, along with incision calculations, were derived from the 15 m DEM. Incision was

calculated fitting a surface to the main summit heights of the study area and then subtracting modern topography (Pulford & Stern 2004). Deep-seated Late Quaternary relict landslide zones were digitised as polygons and measurements made of total landslide area, initiation point (centre of main headscarp), vertical drop (initiation point to toe), length (runout) and landslide aspect (principal direction of movement). The geological units and proximity of the initiation point to major rivers, streams and geological structures was also logged. Landslide volume was estimated using the power regression model of Guzzetti et al. (2009).

8.5 Results

Stratigraphy

The stratigraphy of the study area is compiled in Table 8.1. Consequent river valleys oriented NE-SW, perpendicular to strike provide outcrop of the laterally variable WB fill (Fig. 8.1). Each valley is characterised by locally specific members and formations that have been defined during previous studies. Laterally persistent marker horizons and formations have been used to define groups, facilitating regional mapping and correlation. The Taihape and Whangamomona groups have been introduced by Murrell (1998), Oulton (1998), Dickinson (1998) Hendy et al. (2004) and Vonk and Kamp (2004) to replace a range of older nomenclature in the WB. This change raises the name Taihape to group status (Hendy et al. 2004) and necessitates the replacement of Taihape Mudstone (Feldmeyer et al. 1943) with Tangahoe Mudstone Formation of Arnold (1957). Adoption of the relatively new regional stratigraphic nomenclature of Vonk and Kamp (2004) and Hendy et al. (2004) is followed here (Table 8.1).

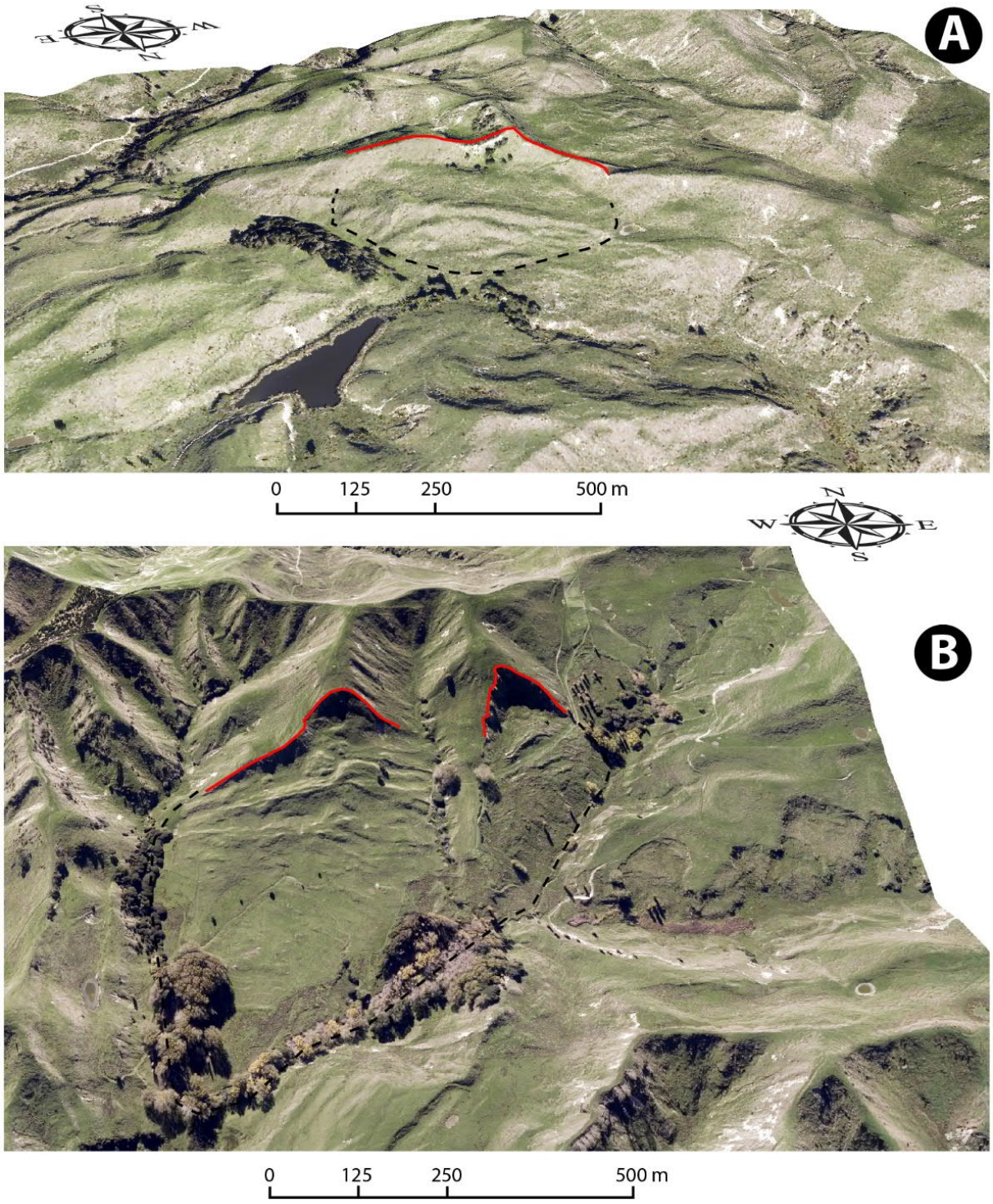


Figure 8.3: Example of relict landslide deposits in the Rangitikei hill country. A) Rock rotational slide in Okehu Group (1803888, 5578163). B) Rock planar slide in Okehu Group (1806138, 5577616). Bedding of the Pleistocene rock is trending 4°/SSW (dip/dip direction).

Lithological properties

WB lithologies are classified as 'extremely weak' to 'weak' (typically <1 to 20 MPa; (Read & Miller 1990) in terms of unconfined compressive strength (UCS), with a UCS of 1 MPa being the threshold between a soil and a rock (NZGS 2005). An observed increase in compaction and cementation occurs with age, reflecting progressively greater depth of burial and level of diagenesis (Rees et al. 2019). Outliers from this observed pattern include Late Quaternary conglomerates that despite their young age can achieve relatively high levels of cementation, principally by iron and manganese oxides, forming cap rock layers in the landscape. Concretionary layers and beds enriched in bioclastic material are locally cemented by fibrous to bladed spar and interstitial micrite Mg-calcite, forming resistant cap rocks despite chemical vulnerability to dissolution. The highest recorded point load strength values for WB strata (Thompson 1982) are assigned to cemented shellbed units, ranging from 198 to 4738 kPa (Table 8.2). Shellbeds and conglomerates within the WB succession are classified as moderate to high, producing aquifers with permeability and hydraulic conductivity values of between 10^{-11}–10^{-9} m^2 and 10^{-4} –10^{-2} m/s, respectively. These units are typically thin (<15 m), form dome-shaped hilltops and outcrop below sharp ridgelines and escarpments.

WB mudstones and siltstones are typically characterised by a higher level of cohesion and consolidation than their sandstone counterparts, due to a greater proportion of silt to clay sized particles and tight grain fabric, with typical point load strengths of between 37 and 291 kPa (Table 8.2). Permeability and hydraulic conductivity values are relatively low at between 10^{-14}–10^{-12} m^2 and 10^{-7}–10^{-5} m/s, respectively. These rock types are classified as aquitards and provide a barrier to flow, promoting lateral rather than vertical groundwater movement (Rees et al. 2019). Groundwater springs and seeps are commonly found above a siltstone or mudstone aquitard where intercepted by topography or a fault. Outcrops are

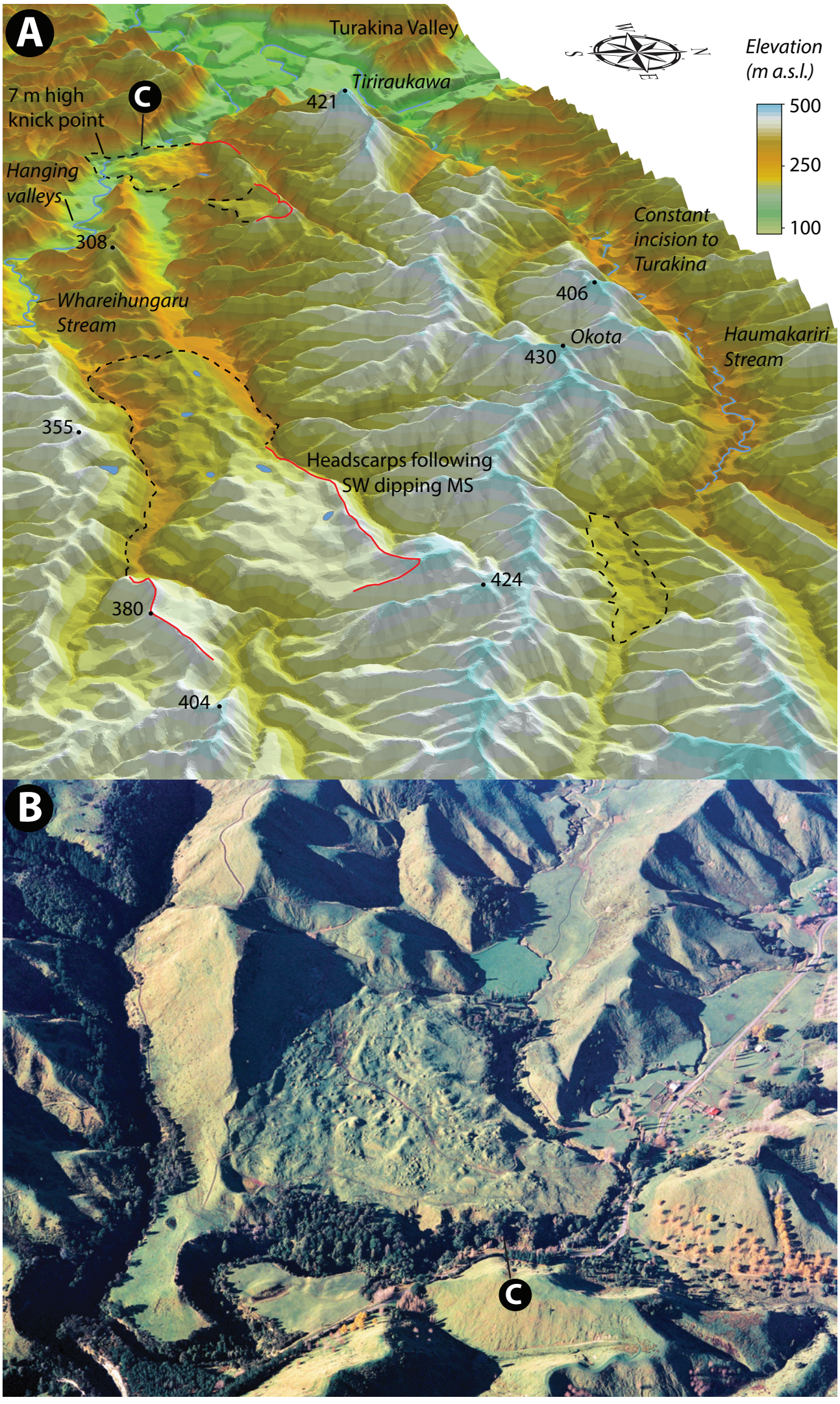


Figure 8.4: A) Digital elevation data of a portion of the Turakina River catchment displaying characteristic landforms developed along strike of the Mangamako Shellbed (MS) and associated weakly consolidated sandstone of the Mangaonoho Frm (Rangitikei Group) (Naish & Kamp 1995). Rock planar slides associated with this dip slope have blocked the Whareihungaru Stream forming hanging valleys above a knickpoint formed by post LGM fluvial incision within the trunk valley. B) Aerial photo from Townsend et al. (2008) displaying landslide topography comprised of blocks of Mangamako Shellbed and fine sandstone and siltstone of Mangaonoho Fm. Note C is positioned in both images to show relative location.

characterised by non-terminating, high angle fractures and fine joints, sometimes forming conjugate couples and contain thin (<20 mm) beds of smectite and illite (Thompson 1982). Spalling and exfoliation are common at weathered outcrops, resulting in surficial, terminating, curved fractures. Cemented shellbed, sandstone and cohesive fine-grained mudstone/siltstone units represent the most erosion resistant strata in the landscape. They commonly form dip slopes and plateau-like surfaces, related to progressive erosion of overlying units (Fig. 8.4).

Sandstones within the WB succession are classified as 'moderate' to 'low' producing aquifers with permeability and hydraulic conductivity values ranging between 10^{-11}–10^{-10} m^2 and 10^{-4}–10^{-3} m/s, respectively. They are characterised by the lowest point load strengths within the succession at 7–167 KPa. Particularly low point load strengths are associated with unconsolidated sandstone members, with relatively high hydraulic conductivity and permeability. Sandstone outcrops contain non-terminating, high-angle fractures and joints that are typically larger (10-100 mm) and more irregular than finer-grained mudstone and siltstone (Thompson 1982). In general, hydraulic conductivity gradually decreases with increasing age (Begg et al. 2005), reflecting an increase in compaction, consolidation and cementation as a function of diagenesis (Houseknecht 1987).

Landslide distribution

The distribution of 334 deep-seated Late Quaternary relict landslide zones mapped in the present study area are displayed in Fig. 8.5 A-D, draped over slope, geological, rock uplift and incision base maps, respectively. These polygons represent a range of landslide types that are dominated by rock planar slides. Landslide distribution clusters around structures, and shows a clear relationship to major rivers. Relict landslide zones range in area from 0.07 to 15.52 km^2, with estimated volumes of between 10^5-10^7 m^3 (Table 8.3). Post-Miocene rock uplift is highest in the northern part of the study area, decreasing southward (Fig. 8.5 C),

associated with topographic doming of the central North Island (Pulford & Stern 2004). Maximum fluvial incision within the WB (Fig. 8.5 D) is associated with a band of topography some 50 km south of the region of maximum rock uplift. The relict landslide zones coincide with areas of relatively high fluvial incision within the Rangitikei, Turakina and Whangaehu river valleys (Fig. 8.5 D).

Slope and Landslide Aspect

Slope aspect was derived from a 15 m DEM (Fig. 8.6 A), and shows a dominant south-southwest trend, with few slopes trending northeast-east. Similarly, of 491 dip direction measurements from the WB fill, the majority (65%) are oriented south-southwest. South-dipping measurements (34%) reflect shore-normal tilting of the basin fill, from uplift along the northern basin margin. Landslide aspect of 386 shallow landslides compiled by Hancox and Wright (2005) following the February 2004 Whanganui-Manawatu storm event is plotted in Fig. 8.6 B. Of those landslides, 46% had a north-northeast aspect, while 11% had a south-southwest aspect. Aspect distribution of the 334 relict landslide zones of this study is shown in Fig. 8.6 D, with 21% oriented southwest, 16% south, and 16% northwest. The southwest alignment accords with the measured dip directions of the WB fill. Fig. 8.7 plots the landslide aspect distribution from this study and that of Hancox and Wright (2005), together with total slope aspect and dip direction, separated by the main catchments (no data exists for the Rangitikei Catchment in Hancox and Wright, 2005). The Turakina, Mangawhero and Whangaehu catchments show clear contrasts in aspect between the relict landslides of the present study and the recent shallow landslides reported by Hancox and Wright (2005). Distribution of slope aspects (Fig. 8.7 C) is similar for all catchments, with a minor dominance of southwest slopes. Dip direction data (Fig. 8.7 D) is southerly trending in the Mangawhero and Rangitikei catchments, while the Whangaehu and Turakina catchments are dominanted by southwest dips. Relict landslide aspect frequency

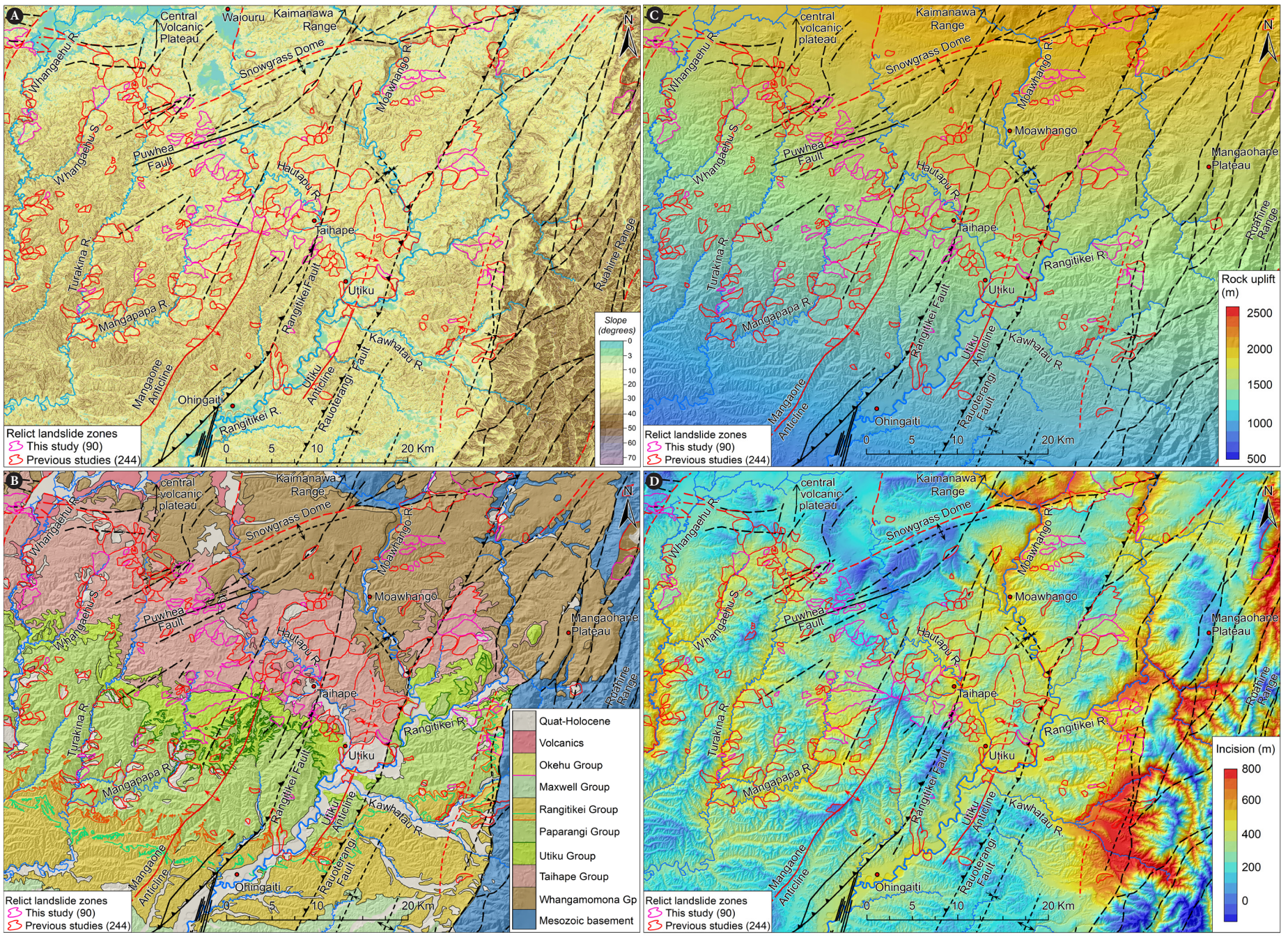


Figure 8.5: A) Distribution of 334 deep-seated Late Quaternary relict landslide zones within the study area. Pink polygons (90) have been mapped during this study, red polygons (244) are derived from existing literature and surveys of Thompson (1982), Ker (1991), Townsend et al. (2008), Massey (2010), Lee et al. (2011), Holdsworth (2018), and the New Zealand landslide database (Rosser et al. 2016). Slope is derived from the 15 m DTM of Columbus et al. (2011). Note slope breaks along strike of the WB fill, best observed around the Mangapapa River (lower left hand corner). Relict landslide zones occupy relatively low gradient areas of the landscape due to denudation and reduction of slope elevation through mass wasting. Structural data from Townsend et al. (2008), Lee et al. (2011) and this study. Particularly prominent dip slopes can be observed on the southern limb of the Snowgrass Dome formed by relatively competent beds of the Whangamomona Group. B) Landslide distribution over geological map, data derived from LINZ, GNS Science and this study. C) Landslide distribution in relation to post Miocene rock uplift calculated by Pulford and Stern (2004). D) Landslide distribution in relation to incision erosion. Incision erosion calculated from 15 m DTM of New Zealand (Columbus et al. 2011) by creating a surface from summit heights and subtracting modern topography from this surface.

and dip direction are plotted in Fig. 8.8 A. A clear relationship between landslide aspect and dip direction exists, both showing southern aspect trends.

Distance to structures and rivers

Distance from relict landslide initiation points to the nearest fault, fold axis and river (order 8-4) is shown in Fig. 8.8 B-E. Both faults and rivers occur in close proximity to the landslide initiation points. All landslide initiation points fall < 8 km of a major river system. In contrast, faults and fold axes can be found >12 km from landslide initiation points. The frequency of landslides with proximity to faults is positively skewed (Fig. 8.8 C), with a high proportion of relict landslides within 250 m of a fault. Similarly, rivers are positively skewed (Fig. 8.8 D), including the highest recorded frequency values, indicative of a strong positive correlation. The proximity of landslide initiation points to fold axes displays an irregular frequency distribution (Fig. 8.8 E).

Table 8.3: Results from the deep-seated Late Quaternary relict landslide zone survey. Statistics include distance to faults, rivers (stream order 8 to 4) and folds (for landslides that occur within a fold zone).

	Area (km^2)	Runout (km)	Volume (m^3)	Distance to fault (m)	Distance to river (m) (Order 4 – 8)	Distance to fold (m) (within fold zone)
Median	0.66	0.84	$2.0x10^7$	2,074	1,567	2,738
Max	15.52	7.06	$2.0x10^9$	12,572	7,833	12,487
Min	0.07	0.15	$8.6x10^5$	9	236	21
Std	2.11	0.99	$2.3x10^8$	2,412	1187	2,864

8.6 Discussion

Stratigraphic control

Initiation of landslides is often attributed to planar surfaces such as bedding, typically between two contrasting lithologies (Hermanns et al. 2004). In the present study, lithological contacts particularly susceptible to failure include: Mangaweka Mudstone Formation (Paparangi Group) and overlying Te Rimu Sandstone Member (Rangitikei Group); Kawhatau Formation and Manui Formation/Omatane Limestone Member (Utiku Group); Tangahoe Mudstone Formation (Taihape Group) and Tarare Formation (Utiku Group); Matemateaonga Formation (Whangamomona Group) and the Tangahoe Mudstone Formation (Taihape Group). Lithological contacts are characterised by physical, geochemical and mineralogical changes (Schon 2015) including factors that control subsurface hydrogeology (e.g. hydraulic conductivity, porosity, cementation and grainsize). For example, Mangaweka Mudstone Formation and overlying Te Rimu Sandstone exhibit a contrast in hydraulic conductivity of between c. 0.03 to 24 m/day (Rees et al. 2019). Water percolates slowly through the sandstone before flowing down-dip (southward) along the contact, facilitated by higher horizontal relative to vertical hydraulic conductivity. Seeps and springs at this contact daylight where groundwater flow is intercepted by topography and/or faults. Saturation of the relatively permeable sandstone generates increased pore water pressure, leading to slope failure (Fleming 1953; Ker 1970).

In the eastern WB, fine-grained, cohesive siltstone and mudstones typically exhibit relatively high shear strength. They commonly form dip slopes overlain by abundant deep-seated landslide topographies formed by progressive failure of the overlying weakly consolidated, sandstone (Table 8.2). In some instances, coarse-grained, lime-cemented sandstone and sandy coquina shellbeds (e.g. Mangamako

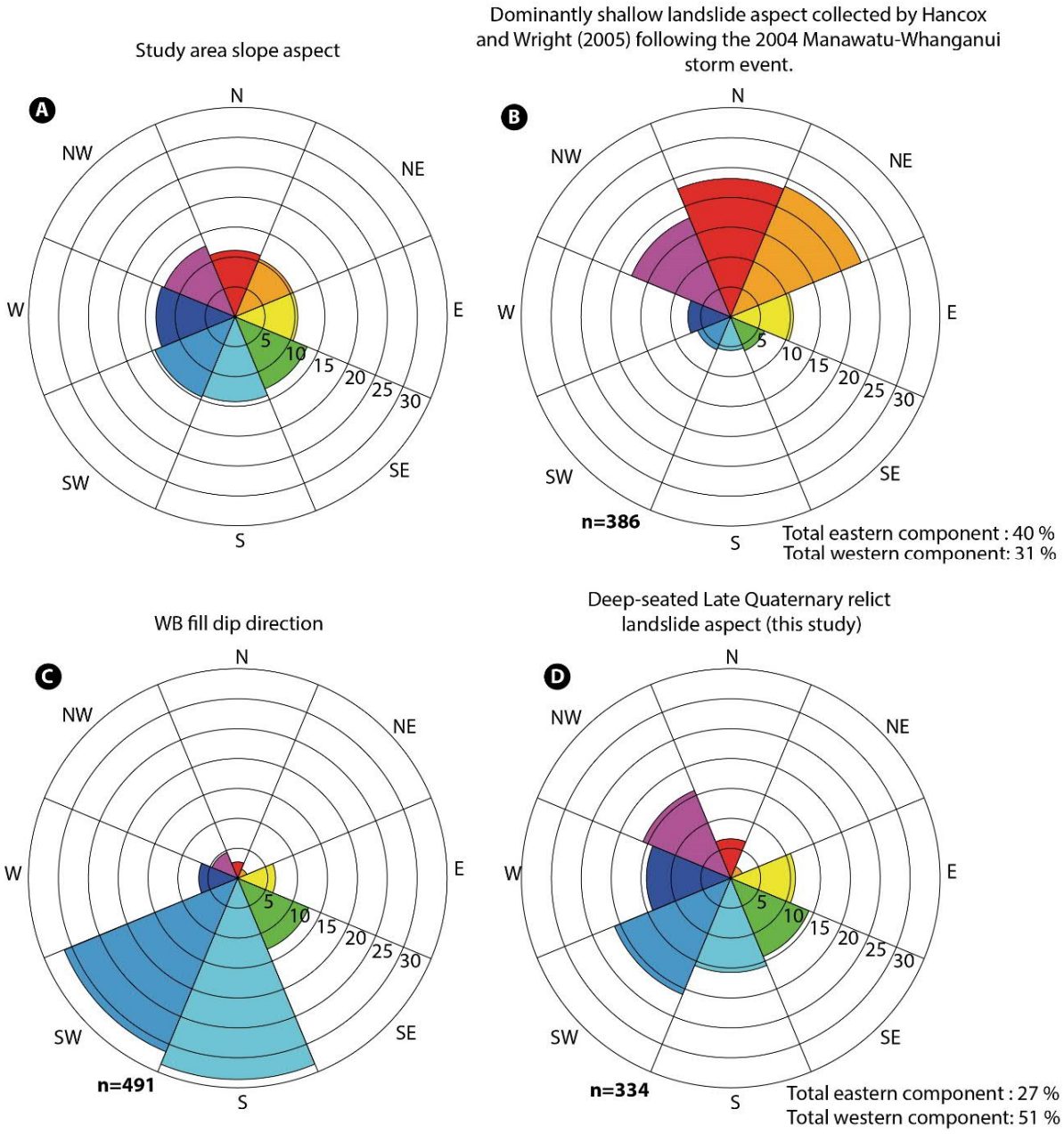


Figure 8.6: A) Aspect distribution (%) of all slopes within the study area. B) Dominantly shallow landslide aspect distribution (%) collected following the 2004 Manawatu-Whanganui storm event (Hancox & Wright 2005). C) Aspect distribution (%) of 491 dip direction measurements taken from the WB fill in the study area. Data derived from Feldmeyer et al. (1943), Te Punga (1952), Fleming (1953), Thompson (1982), (Ker 1991), Naish and Kamp (1995), Journeaux et al. (1996), Oulton (1998), Murrell (1998), Dickinson (1998), Townsend et al. (2008), Lee et al. (2011), and this study. D) Landslide aspect distribution (%) of deep-seated Late Quaternary relict landslide zones within the study area. Colours highlight respective quadrants.

Shellbed Member of the Rangitikei Group; (Naish & Kamp 1995) represent the most competent lithologies, despite chemical vulnerability to dissolution. This competency and resistance to erosion allows for the formation of cap rock atop dip slopes, as erosion and fluvial incision strip away less competent material, forming sharp ridgelines above progressively steeper slopes. Slopes gradually become over-steepened and eventually failure occurs, forming characteristic landslide topographies (Fig. 8.4 B). Similar stratigraphic controls have been observed in the Otago Region by Benson (1940) and Crozier (1968), where Cenozoic sedimentary successions include competent limestone or sandstone beds overlying less competent plastic mudstones. In this situation, the mudstones are prone to failure and are associated with deep-seated landslides (e.g. Abbotsford Landslide; (Hancox 2008).

Fluvial control

Late Quaternary incision of the WB fill is consequent on uplift (Pulford & Stern 2004). The distribution of deep-seated Late Quaternary relict landslide zones mapped in this study coincides with areas of relatively high fluvial incision within the Rangitikei, Turakina and Whangaehu river valleys. This is likely due to daylighting of bedding planes within the >400 m thick Mangaweka and Tangahoe mudstone formations, together with progressive undercutting and removal of toe support for strata dipping out of slope. Where two major tributaries merge, two sides of a bedding plane are exposed and we commonly find concentrations of large, deep-seated landslides.

Structural control and slope morphology

Structural features appear to exert influence on the spatial distribution of deep-seated Late Quaternary relict landslide zones. Large open fractures form side shear on some landslides, and there is the possibility of faults initiating others

(Thompson 1982). Folding and stratigraphic architecture determines bed attitude, and thus the direction of landslide movement. The sedimentary units of the WB have been deposited within a southeastward migrating depocentre and undergone broad regional uplift along the northern and eastern margins. As a result, each geological unit extends approximately east-west along depositional strike, dipping south. Sedimentary units thicken toward the centre of the paleo-depocentre and become finer-grained, reflecting progressively deeper water depositional environments across the paleo-shelf shoreline transect (Fleming 1953).

Deep-seated relict landslides show a dominant southwest trend, which is expected given the dominant southwest aspect of all slopes in the study area. In contrast, the recent, predominantly shallow translational failures reported by Hancox and Wright (2005) following the February 2004 Manawatu-Whanganui storm event, have a north to northeast aspect. The difference in trend between modern day predominantly shallow landsliding and deep-seated relict Late Quaternary landslides reflects processes of landscape formation. Relict landslide deposits occurring on or at the base of northern scarp slopes are either less common or less commonly preserved in the landscape compared to those on southern-oriented dip slopes. This is likely due to subsequent tributary streams flowing parallel to the strike of beds at the base of scarp slopes, actively reworking landslide debris, leading to lower preservation potential (Fig. 8.9). The high frequency of shallow landslides during scarp retreat also acts to remove and obscure evidence of deep-seated landslide scars along northern escarpments.

There are instances in the landscape where abundant deep-seated landslides are preserved below northern scarp slopes, including where the marine terrace country gives way to broken hill country at Mt Curl near the coast (Fig. 8.1). In this instance, deep-seated landslides largely consist of rock rotational slides cutting across multiple bedding planes and are attributed to cemented gravels of the

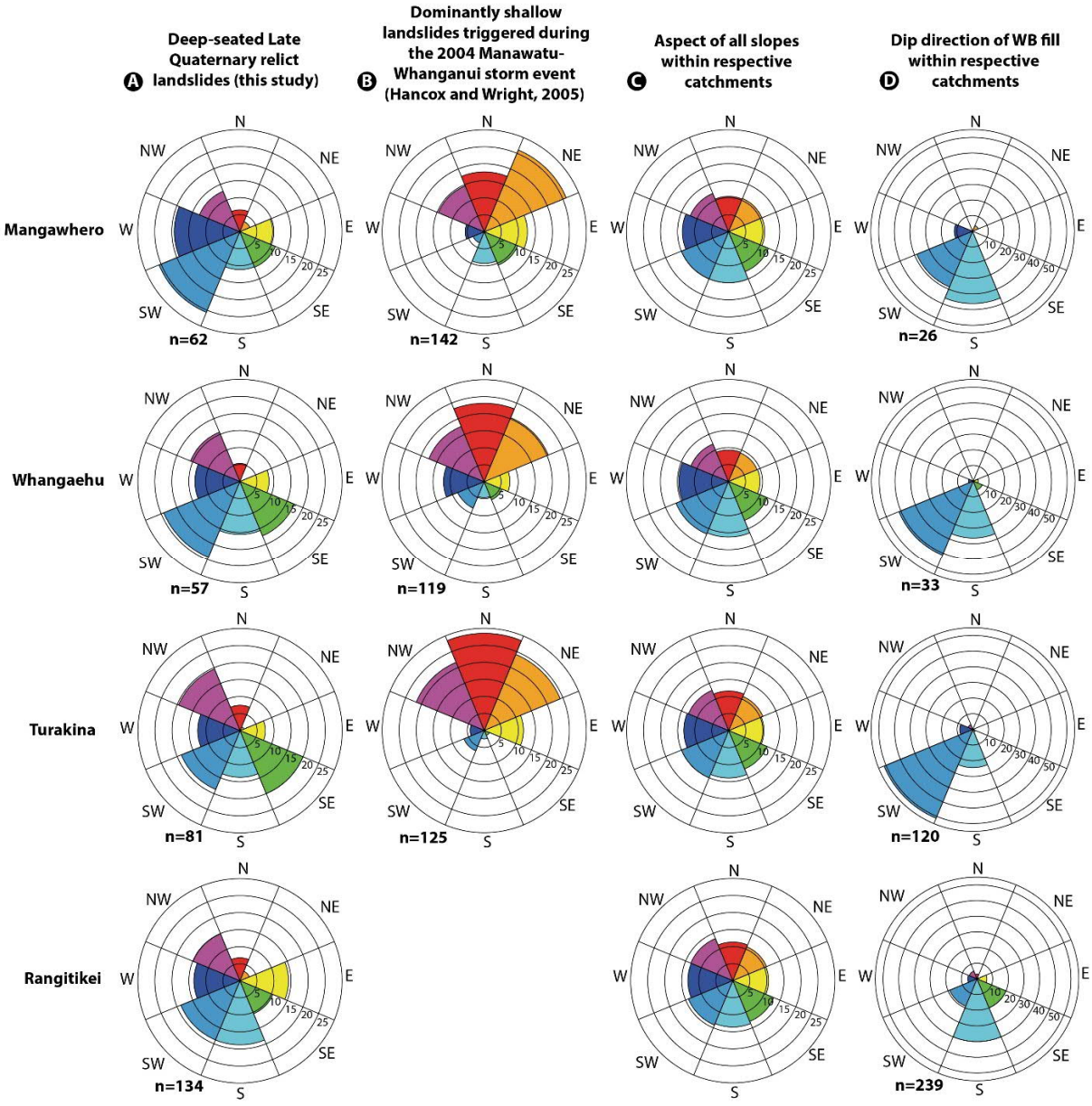


Figure 8.7: Comparison of the landslide aspect, total slope aspect and dip direction for selected river catchments within the study area (%). A) Data from this study displaying the aspect distribution (%) of deep-seated Late Quaternary relict landslide zones. B) Dominantly shallow landslide data derived from Hancox and Wright (2005), following the 2004 Manawatu-Whanganui storm event. C) Total slope aspect within respective catchments. D) Dip direction measurements of WB fill within respective catchments.

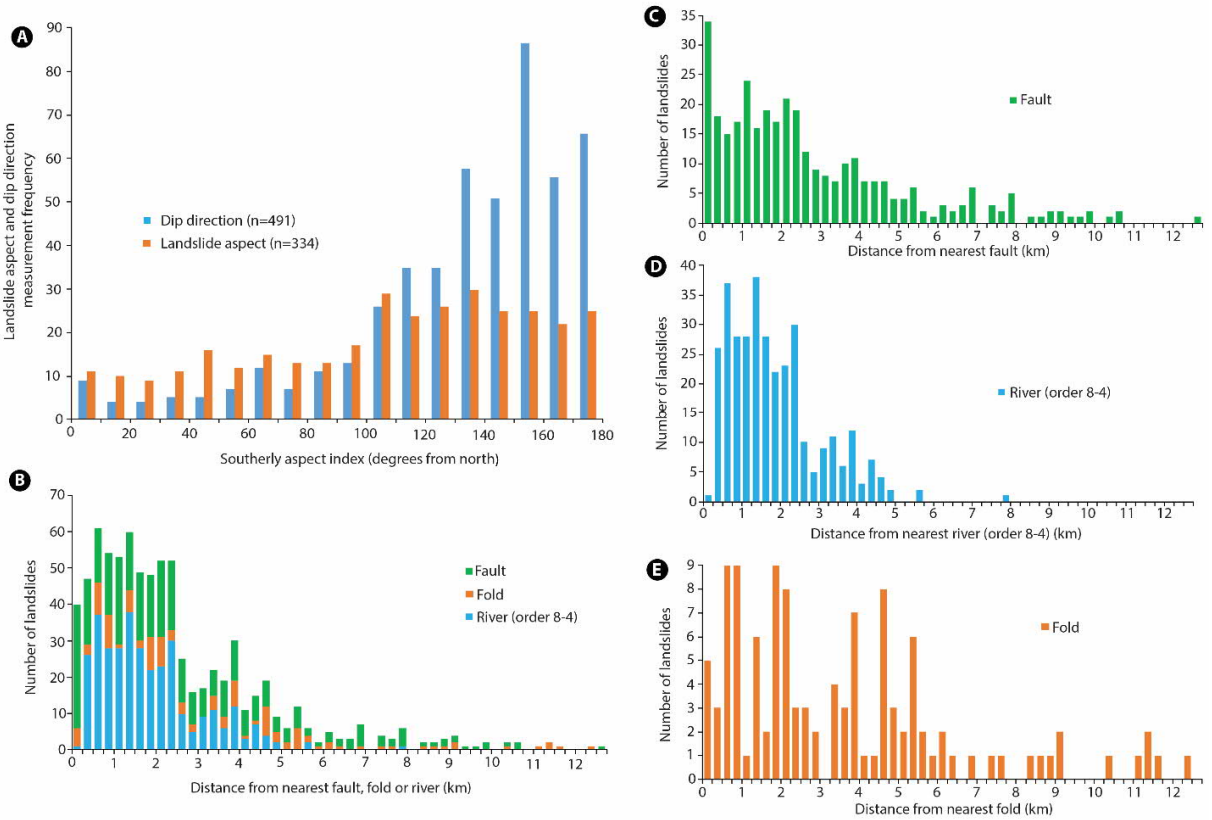


Figure 8.8: A) Comparison of deep-seated Late Quaternary relict landslide aspect with dip direction measurements from WB fill (degrees from north). Structural data compiled from Feldmeyer et al. (1943), Te Punga (1952), Fleming (1953), Thompson (1982), (Ker 1991), Naish and Kamp (1995), Journeaux et al. (1996), Oulton (1998), Murrell (1998), Dickinson (1998), Townsend et al. (2008), Lee et al. (2011), and this study. B) Frequency of landslides with distance from faults, folds and rivers (order 8-4). Distance measured from landslide initiation points. C) Frequency of landslides with distance from faults. D) Frequency of landslides with distance from rivers (order 8-4). E) Frequency of landslides with distance from folds. Note all landslide data in this figure relates to deep-seated Late Quaternary relict landslide zones mapped in the current study.

Aldworth and Waituna terraces (Milne 1973; Hellstrom 1993). The gravels act as a resistant cap rock, promoting oversteepening of the dip slope.

There is some bias introduced into the analysis of landslide aspect presented herein, arising from the Late Quaternary development of the fluvial drainage pattern in eastern WB. Rivers draining the central North Island and emerging main axial range have been progressively constrained by a series of anticlines

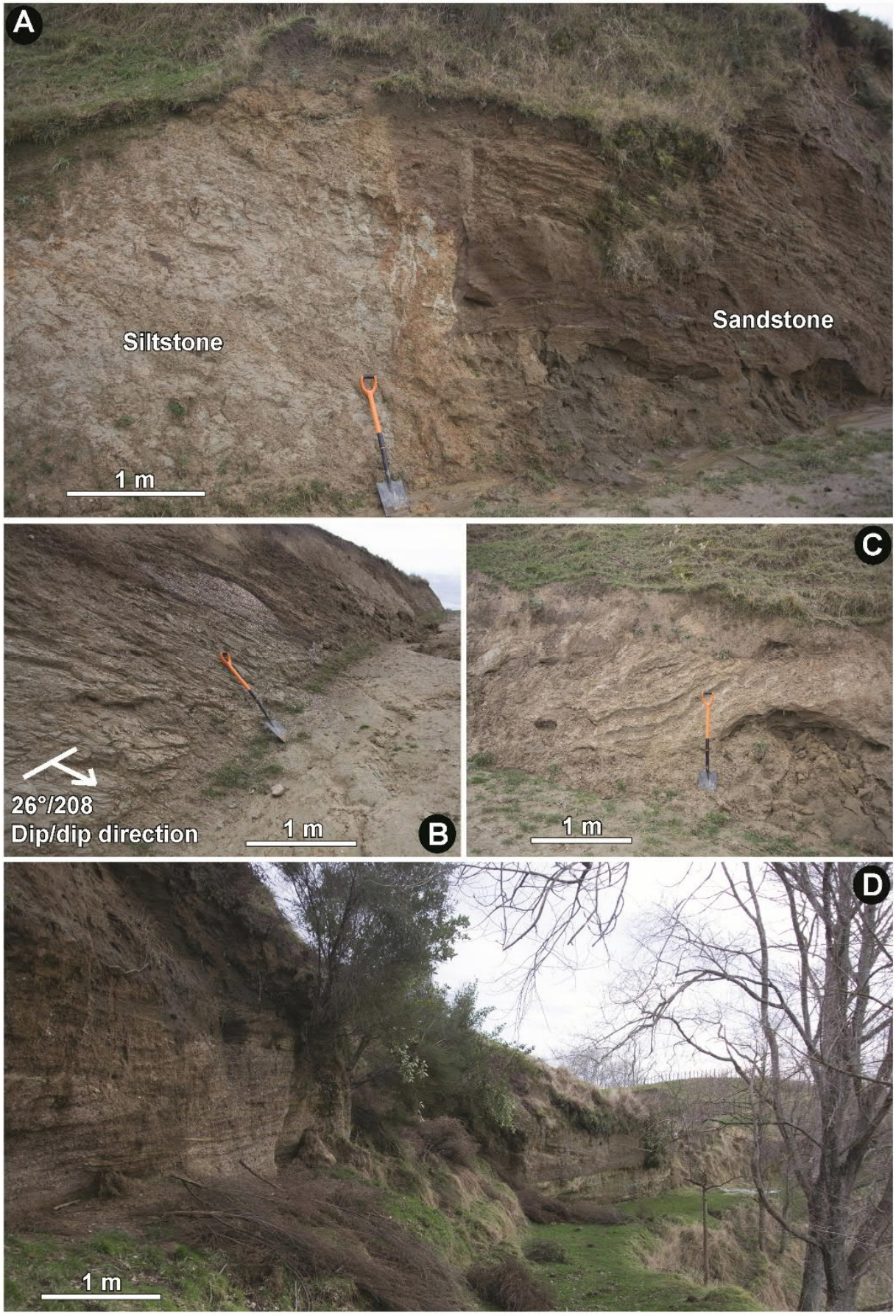


Figure 8.9: A) Exposed slip surface beneath a rock rotational slide in Okehu Group (1818276, 5575417). B) Flat lying, in situ Okehu Group exposed at a northern scarp slope nearby photo A. C) Deformation of Okehu Group related to a deep-seated Quaternary landslide, exposed by fluvial incision within the Mangapipi Stream catchment (1821189, 5575242). D) Photo of a typical northern scarp slope in the WB. Erosion resistant cap rock of Okehu Group exposed along strike indicated by the white arrows. Subsequent stream flows parallel to strike incising into the WB fill, toward the trunk channel of the consequent Turakina River (1809200, 5576187).

trending NNE-SSW (Te Punga 1957). As uplift and anticline growth progressed through the Late Quaternary, flow pathways became further constricted and rivers were pushed eastward. This is reflected in the progressive eastward stepping of Late Quaternary aggradational terraces in the Rangitikei and Oroua valleys (Milne 1973). Today, major tributaries in the eastern WB often incise abruptly into the eastern flank of regional structures. This concentration of fluvial erosion effectively removes evidence of Quaternary landslides from the eastern limb of anticlines, resulting in greater preservation potential on the western limbs.

A maximum age of deep-seated landslides preserved within south Taranaki has been estimated at c. 30 ka by Crozier et al. (1995). In the present study, there is no evidence of Late Quaternary relict landslides having been cut by the Ohakean Terrace (c. 30–10 ka). Rare exposures of Kawakawa Tephra (c. 25 ka) are found preserved within Late Quaternary relict landslide zones of the study area (Thompson 1982). However, this does not necessarily indicate that landsliding pre-dates tephra deposition as blocks of material within the rock planar slides of the study area can remain remarkably intact following landsliding. C^{14} ages derived from landslide-dammed lakes in the study area are all Mid to Late Holocene in age < 10 ka (MacDonald-Creevey 2011). Therefore, we consider a large proportion of the deep-seated Late Quaternary relict landslides mapped in this study to have occurred post-Last Glacial Maximum (LGM). Postglacial accelerated incision and removal of buttressing alluvial fill in response to a decrease in sediment supply are likely to be contributing factors (Johnson et al. 2018).

Figure 8.10 (facing page): Photos of deformed Okehu Group strata from a deep-seated, relict Quaternary landslide exposed by a new farm track (1830361, 5571256). Landslide deposits occupy a southern slope aspect. A) Overturned strata consisting of juxtaposed sandstone and siltstone. B) Beds displaying steep dips of up to 26° in an area typified by dips of < 5°. C) Strata displaying folding and intermixing. D) Exposure along strike on the steep northern scarp slope displaying undeformed, conformable, near horizontal beds.


A
Siltstone
Sandstone
1 m
B
26°/208
Dip/dip direction
1 m
C
1 m
D
1 m

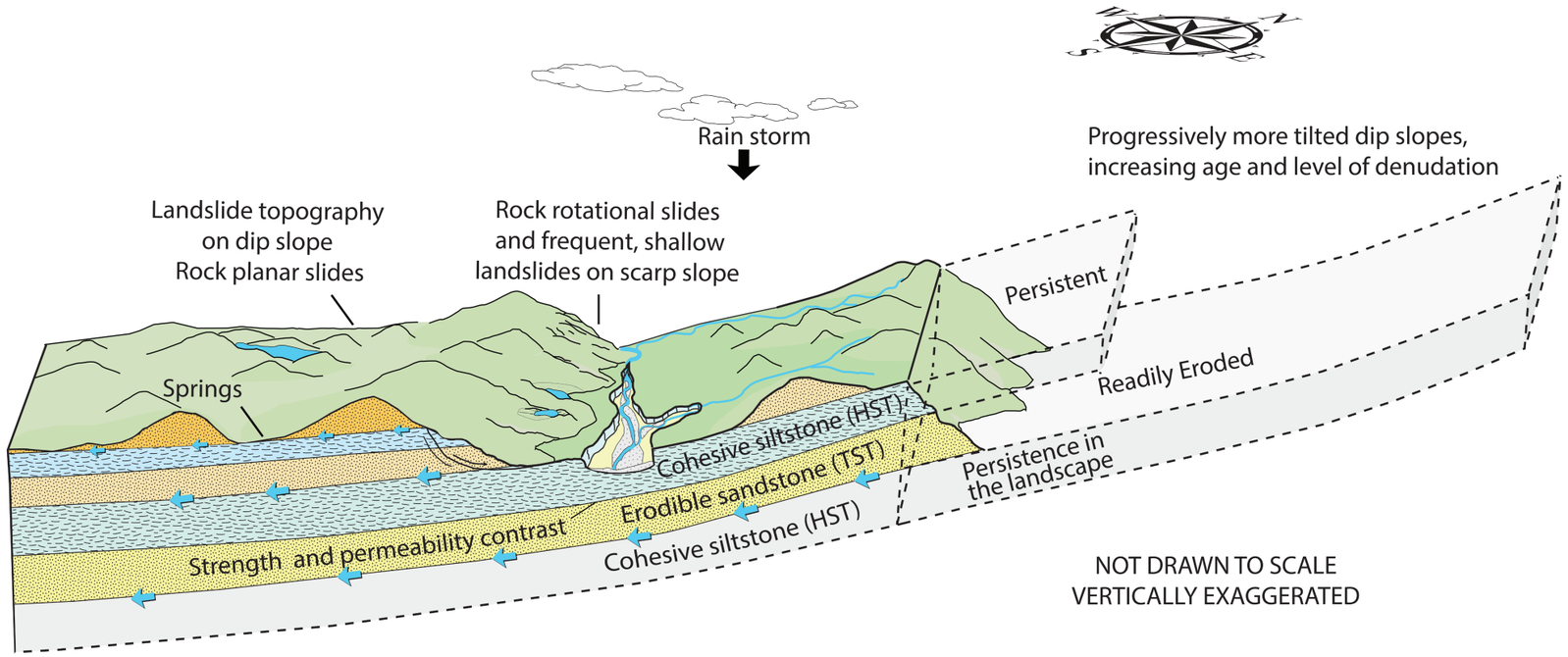


Figure 8.11: Conceptual model for the study area. Note rock planar slides are concentrated on the southern dip slope, whilst rock rotational slides and shallow landslides are concentrated on the steep, northern scarp slopes where they cut across multiple bedding planes. Note a reduction in preservation potential at foot of scarp slope due to fluvial erosion, introducing bias into the record of relict landslide deposits within the landscape. Consequent drainage is directed SW along dip slopes whilst subsequent drainage is directed along the strike of the uplifting basin fill, leading to progressive undercutting and scarp retreat, predominantly as a function of shallow landsliding.

Anticlines

Folds of the WB are formed over 'blind' high angle reverse faults in the underlying Mesozoic greywacke basement (Jackson et al. 1998). These folds are actively growing, as demonstrated by subtle tilting of Late Quaternary river terraces (Milne 1973; Melhuish et al. 1996). Indeed, these structures likely formed sea floor topography, controlling deposition of the Late Miocene-Pleistocene basin fill within a series of extensional half grabens (Fig. 8.12), evidenced by local highs where the basin fill pinches out between intervening basement lows (Feldmeyer et al. 1943; Anderton 1981).

A simple conceptual model for the dominantly southward plunging asymmetric anticlines typical of eastern WB is presented here (Fig. 8.12). This model adapts the fracture orientation prediction model of Price (1966) to illustrate inferred relationships between geology and landscape evolution in the WB. Central to this model is the structural control on Late Miocene-Pleistocene fill, which pinches and swells between successive basement highs, forming groundwater divides. This geometry facilitates bedding plane failures related to lithological contrasts and fracturing produced during basin inversion.

Earthquakes

Earthquake-triggered (i.e. coseismic) landslides are prevalent in New Zealand, a recent example being the 2016 Kaikoura earthquake (Dellow et al. 2017). The WB is tectonically-active, with the eastern basin undergoing Late Quaternary uplift of 1–3 mm/yr (Pillans 1986), and average vertical displacement rates on known active faults of between 0.02 and 0.2 mm/yr (Pillans 1990). Active folding in the eastern WB is driven by blind reverse faults (Melhuish et al. 1996). A long-term Late Quaternary deformation rate of 0.3 mm/yr has been calculated for the Mt Stewart-Halcombe Anticline (Te Punga 1957; Melhuish et al. 1996). Jackson et al. (1998)

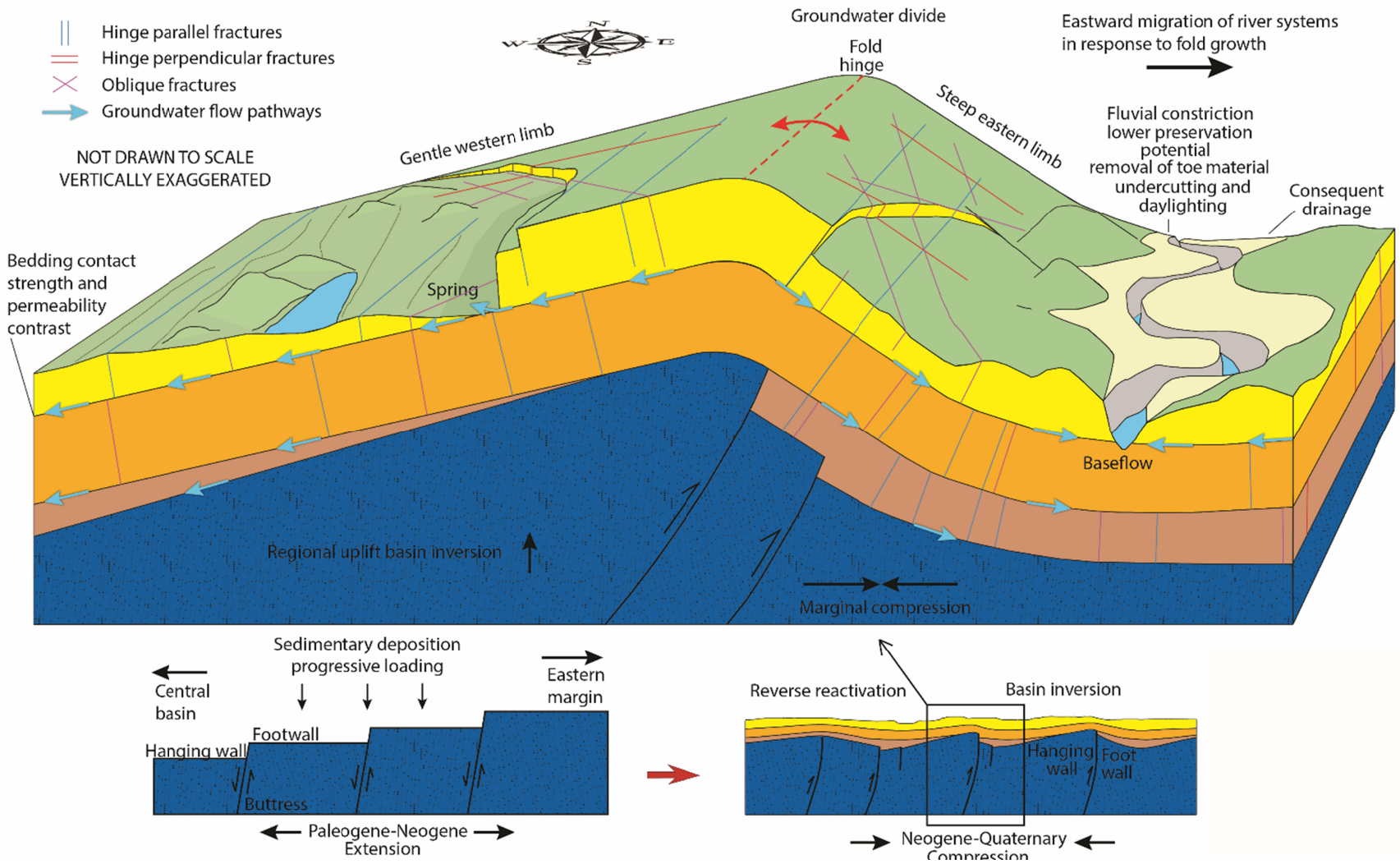


Figure 8.12: Conceptual model for asymmetric southward plunging anticlines typical of eastern WB. Sedimentary deposition has progressed over an uneven Mesozoic basement surface of half grabens before a major change in tectonic regime in the Neogene-Quaternary, resulting in reverse reactivation of old normal, extensional faults and tectonic overprinting. Deformation associated with tectonic uplift includes fracturing of the basin fill providing lateral release to rock planar slides.

postulates the blind reverse faults are capable of producing M6.5–7 earthquakes, based on fold axis lengths of 15–20 km. This suggests the tectonic setting of WB could produce earthquakes of a sufficient magnitude to trigger a geomorphic response (Crozier et al. 1995). Landslide initiation points measured in this study were all <13 km from a fault and on average <3 km (Table 8.3), suggesting a potential relationship between faults and deep-seated Late Quaternary relict landslide zones.

Historic Coseismic Landslides in the lower North Island

Historic coseismic landslides are known to have occurred in the study area. Landslides up to 65 km apart were noted in the Whanganui-Manawatu Region following an earthquake in 1843, estimated at M7.5 (Dowrick et al. 2008). Landslides caused the death of two people in the Makohine Stream valley, Rangitikei Catchment (Eiby 1968). There is some ambiguity surrounding the exact positioning of the historic earthquake epicentre and the assigned magnitude of the event has been estimated using felt intensity reports without instrumentation (Dowrick et al. 2008). The 1855 M8.2 Wairarapa earthquake caused extensive liquefaction and landslides in an area extending over 5000 km^2 from Cape Kidnappers in the east to Whanganui in the west (Grapes & Downes 1997). A coseismic landslide-dammed the Rangitikei River for two days before eventual dam breach, resulting in a catastrophic flood flowing down the lower river valley (Wilson 1914). This landslide probably covered an area of c. 2.5 km^2 and was approximately 8.9 x 10^6 m^3 in volume. This is a broad estimate given that the majority of the evidence of the landslide has been eroded over the last 160 years, although a portion of the landslide toe is preserved on the western side of the Rangitikei River (Fig. 8.13). The M6.2 Eketahuna earthquake occurred on 20th January 2014, with the epicentre located c. 15 km east of Eketahuna at a depth of 34 km. This event triggered rock and debris falls and debris slides in the Whanganui-Manawatu Region. Eyewitness accounts and damage surveys reported

rockfalls along the cliffs of the Whanganui, Rangitikei, Manawatu and Pohangina valleys (Rosser et al. 2014).

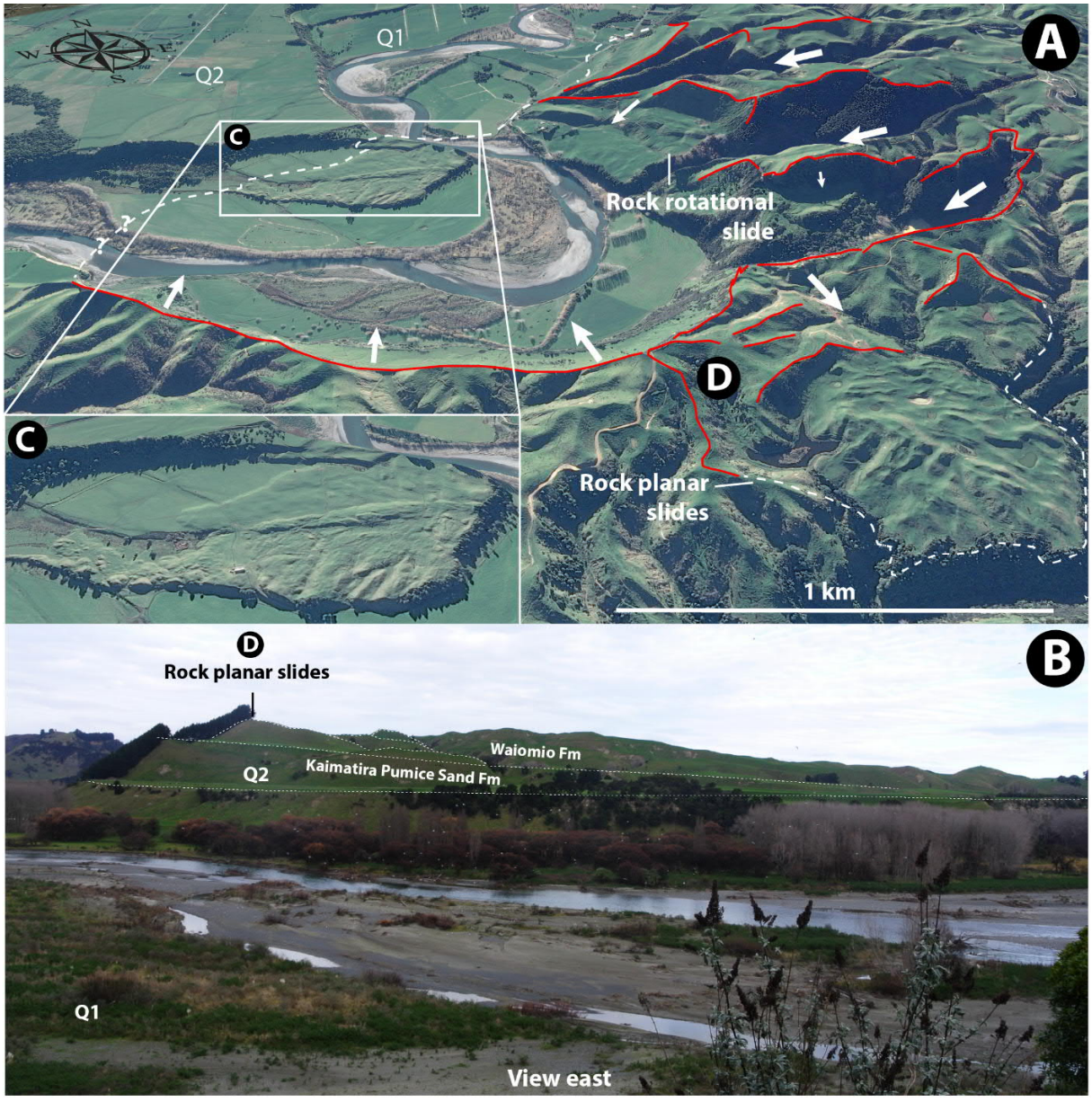


Figure 8.13: A) Location of 1855 Wairarapa earthquake triggered landslide in the Rangitikei Valley, with remnant landslide deposits preserved on western side of the river (Milne 1973). Image derived from DigitalGlobe Inc licenced under the Creative Commons Attribution 4.0 International Licence (1819790, 5567734). B) Photo taken looking east toward the cliffs forming the main scarp slope; note the visible angular unconformity between the Pleistocene dip slope of Kaimatira Pumice Sand Formation (c. 1–0.9 Ma) and the Ohakean Terrace (c. 30–10 ka). C) Close up of landslide debris. D) Relative location of the rock planar slides atop dip slope in photos A and B.

8.7 Conclusion

Landscape evolution in the Rangitikei hill country involves inversion and denudation of the WB fill. Cenozoic lithologies of the WB are susceptible to failure and widespread episodes of deep-seated and shallow landsliding. Mapping and analysis of deep-seated Late Quaternary relict landslide zones and the WB fill indicates some associations between the proximity of landslides to structures and rivers, and relationships between geology and slope morphology.

The predominantly shallow marine WB fill comprises alternating coarse- and fine-grained units related to climatically-forced sea level fluctuations. Lithological units pinch and swell along strike and display facies variation, related to deposition within laterally adjacent environments along a shelf-shoreline transect. Mudstones and siltstones are characterised by a higher level of cohesion and consolidation than their sandstone counterparts due to a greater proportion of silt to clay-sized particles and tight grain fabric. They act as aquitards, providing a barrier to subsurface flow and promoting lateral rather than vertical groundwater movement. Sandstones have the lowest point load strengths, and are classified as moderate to low producing aquifers. In contrast, shellbed, conglomerate, cemented sandstone and cohesive fine-grained mudstone/siltstone units represent the most erosion resistant lithologies. These units form caprocks, dip slopes and plateau-like surfaces, related to slope oversteepening and removal of overlying units through mass-wasting processes.

Shallow landslides dominate on steep, northern scarp slopes and deep-seated rock planar slides dominate on gentle southern dip slopes. Deep-seated rock rotational slides on northern scarp slopes are either less common or less commonly preserved in the landscape. This is likely due to subsequent tributary streams flowing parallel to strike at the base of scarp slopes, actively reworking landslide debris

and scarp retreat removing and obscuring evidence of deep-seated landslide scars. We interpret bias in the preservation of Late Quaternary relict landslide deposits in the landscape, related to abutment of fluvial systems against the steep eastern limbs of regional folds.

Fluvial incision and daylighting of the WB fill is a primary control on landslide distribution, providing the necessary conditions upon which a range of triggering mechanisms operate. A large proportion of the deep-seated Late Quaternary relict landslide zones are considered to have occurred post LGM. Postglacial incision and removal of buttressing alluvial fill in response to a decrease in sediment supply are suggested to be contributing factors. Faults display a clear relationship to landslide frequency, suggesting earthquakes are possibly an important triggering mechanism, consistent with historic case studies.

Acknowledgments

We thank the local residents in the Manawatu-Whanganui Region for land access. Andrew Steffert (Horizons Regional Council) greatly aided with data acquisition. Brenda Rosser kindly facilitated access to the New Zealand landslide database. Many thanks to the Massey University staff and laboratory technicians including Ian Furkert, Glenys Wallace, Bob Toes, Ross Wallace, David Feek, Dr Roberto Calvelo-Pereira, Dr Qinhua Shen, Dr Anja Mobis, Dr Gabor Kereszturi and Dr Mike Bretherton.

This work is part of an overarching PhD project on the groundwater of the Pourewa Stream sub-catchment undertaken by CJR. Thanks are extended to Dr Ranvir Singh and Dr John Begg for the support and direction given during the course of this research. The manuscript benefited greatly from the helpful reviews of Dr Marc-Andre Brideau and an anonymous referee. Special thanks are extended to Dr Martin Brook for his patient handling of the manuscript.

This paper uses the spelling 'Whanganui' rather than 'Wanganui' as recommended by the New Zealand Geographic Board (Ngā Pou Taunaha o Aotearoa).

References

Abbott ST 1994. Sequence Stratigraphy, Sedimentology and Paleoecology of Pleistocene Cyclothems in the Castlecliff Section, Wanganui Basin, New Zealand, Unpublished PhD Thesis. James Cook University of Northern Queensland, Australia. 297 p.

Al Bakri D 2001. Towards developing a geoscientific approach to sustainable agricultural and rural development. Environmental Geology 40(4-5): 543-556.

Anderton PW 1981. Structure and evolution of the South Wanganui Basin, New Zealand. New Zealand Journal of Geology and Geophysics 24(1): 39-63.

Arnold HC 1957. The Pliocene stratigraphy of South Taranaki. Unpublished open-file petroleum report 414. Ministry of Economic Development, Wellington, New Zealand. 19p.

Begg JG, Palmer A, Gyopari M 2005. Geological synopsis of the Manawatu-Horowhenua area for a review of the region's hydrogeology. Institue of Geological and Nucelar Sciences Client Report 2005/172, Lower Hutt, New Zealand. 22 p.

Benson WN 1940. Landslides and allied features in the Dunedin District in relation to geological structure, topography and engineering. Transactions and Proceedings of the Royal Society of New Zealand 70(3): 249-263.

Beu AG, Browne GH, Grant-Taylor TL 1981. New *Chlamys delicatula* localities in the central North Island and uplift of the Ruahine Range. New Zealand Journal of Geology and Geophysics 24(1): 127-132.

Browne GH 1978. Wanganui Strata of the Mangaohane Plateau, Northern Ruahine Range, Taihape. Tane 24: 199-210.

Browne GH 2004. Late Neogene sedimentation adjacent to the tectonically evolving North Island axial ranges: Insights from Kuripapango, western Hawke's Bay. New Zealand Journal of Geology and Geophysics 47(4): 663-674.

Carter RM, Naish TR 1998. A review of Wanganui Basin, New Zealand: Global reference section for shallow marine, Plio-Pleistocene (2.5-0 Ma) cyclostratigraphy. Sedimentary Geology 122(1-4): 37-52.

Columbus J, Sirguey P, Tenzer R 2011. A free fully assessed 15 metre digital elevation model for New Zealand. Survey Quarterly 300(66): 16-19.

Crozier MJ 1968. Earthflows and related environmental factors of eastern Otago. Journal of Hydrology(7): 1-12.

Crozier MJ, Deime MS, Simon JS 1995. Investigation of earthquake triggering for deep-seated landslides, Taranaki, New Zealand. Quaternary International 25: 65-73.

Crozier MJ, Gage M, Pettinga JR, Selby MJ, Wasson RJ 1992. The Stability of Hillslopes. In: Soons JM, Selby MJ ed. Landforms of New Zealand. 2nd Edition ed. Auckland, New Zealand, Longman Paul. Pp. 63-90.

Dellow S, Massey C, Cox S, Archibald G, Begg J, Bruce Z, Carey J, Davidson J, Pasqua FD, Glassey P and others 2017. Landslides caused by the MW7.8 Kaikoura Earthquake and the immediate response. Bulletin of the New Zealand Society for Earthquake Engineering 50(2): 106-116.

Dickinson JA 1998. Stratigraphy and sedimentology of early Pliocene strata, Mangawhero Valley, and subsurface correlations, central Wanganui Basin. Unpublished MSc thesis, University of Waikato, Hamilton, New Zealand 140 p.

Dowrick DJ, Hancox GT, Perrin ND, Dellow GD 2008. The Modeified Mercalli Intensity Scale - Revisions arising from New Zealand experience. Bulletin of the New Zealand National Society for Earthquake Engineering 41(3): 193-205.

Eiby GA 1968. A descriptive catalogue of New Zealand earthquakes. New Zealand Journal of Geology and Geophysics 11(1): 16-40.

Feldmeyer AE, Jones BC, Firth CW, Knight J 1943. The geology of the Palmerston-Wanganui Basin, "West side", North Island, New Zealand. Unpublished Report of the Superior Oil Company of New Zealand, Petroleum Report Series 171, Ministry of Economic Development, Wellington, New Zealand. 46 p.

Fleming CA 1953. The geology of Wanganui subdivision. New Zealand Geological Survey Bulletin 52. Wellington, New Zealand. 362 p.

Grant GR, Sefton JP, Patterson MO, Naish TR, Dunbar GB, Hayward BW, Morgans HEG, Alloway BV, Seward D, Tapia CA and others 2018. Mid- to late Pliocene (3.3-2.6 Ma) global sea-level fluctuations recorded on a continental shelf transect, Whanganui Basin, New Zealand. Quaternary Science Reviews 201: 241-260.

Grapes RH, Downes G 1997. The 1855 Wairarapa earthquake: analysis of historic data. Bulletin of the New Zealand National Society for Earthquake Engineering 30(4): 273-368.

Guzzetti F, Ardizzone F, Cardinali M, Rossi M, Valigi D 2009. Landslide volumes and landslide mobilization rates in Umbria, central Italy. Earth and Planetary Science Letters 279: 222-229.

Hancox GT 2008. The 1979 Abbotsford Landslide, Dunedin, New Zealand: a retrospective look at its nature and causes. Landslides 5: 177-188.

Hancox GT, Wright K 2005. Analysis of landsliding caused by the February 2004 rainstorms in the Wanganui-Manawatu hill country, southern North Island, New Zealand. Institute of Geological and Nuclear Sciences science report 2005/11, Lower Hutt, New Zealand: 1-64.

Hellstrom JC 1993. An investigation of the Galpin Fault, Marton, Rangitikei Unpublished BSc (Hons) Thesis. Victoria University of Wellington, Wellington, New Zealand. 89 p.

Hendy AJW, Kamp PJJ, Kamp PJJ 2004. Late Miocene to early Pliocene biofacies of Wanganui and Taranaki Basins , New Zealand : Applications to paleoenvironmental and sequence stratigraphic analysis. New Zealand Journal of Geology and Geopysics 47(4): 769-785.

Hermanns RL, Niedermann S, Ivy-Ochs S, Kubik PW 2004. Rock avalanching into a landslide-dammed lake causing multiple dam failure in Las Conchas valley (NW Argentina) - evidence from surface exposure dating and stratigraphic analyses. Landslides 1(2): 113-122.

Hodge RAL, Freeze RA 1977. Groundwater flow systems and slope stability. Canadian Geotechnical Journal 14(4): 446-476.

Holdsworth CN 2018. The influence of rainfall and river incision on the movement rate of a slow-moving, soft-rock landslide in the Rangitikei, New Zealand. Unpublished MSc Thesis, Massey University, Palmerston North, New Zealand. 135p.

Houseknecht DW 1987. Assessing the relative importance of compaction processes and cementation to reduction of porosity in sandstones. American Association of Petroleum Geologists Bulletin 71(6): 633-642.

Hungr O, Leroueil S, Picarelli L 2014. The Varnes classification of landslide types, an update. Landslides 11(2): 167-194.

Jackson J, van Dissen R, Berryman KR 1998. Tilting of active folds and faults in the Manawatu region, New Zealand: Evidence from surface drainage patterns. New Zealand Journal of Geology and Geophysics 41(4): 377-385.

Johnson PL, Cotton WE, Shires PO 2018. Alluvium-buttressed landslides: Conceptual model and examples from California. The Geological Society of America Abstracts with Programs, 130th Annual Meeting 4-7 November, Paper No. 249-5. 1p. DOI: 10.1130/abs/2018AM-324970.

Journeaux TD, Kamp PJJ, Naish TR 1996. Middle Pliocene cyclothems , Mangaweka region , Wanganui Basin , New Zealand : A lithostratigraphic framework. New Zealand Journal of Geology and Geophysics 39(1): 135-149.

Kamp PJJ, Journeaux D, T., Morgans HEG 1998. Cyclostratigraphy of middle Pliocene mid shelf to upper slope strata, eastern Wanganui Basin (New Zealand): correlations to the deep sea isotope record. Sedimentary Geology 117: 165-192.

Ker DS 1970. Renewed movement on a slump at Utiku, New Zealand. New Zealand Journal of Geology and Geophysics 13(4): 996-1017.

Ker DS 1991. Provisional geological map of 1:50 000 sheet T21AC (Hautapu). Lower Hutt, DSIR Geology and Geophysics, New Zealand Geological Survey report G 144: 19 p + 1 map.

Lee JM, Bland KJ, Townsend DB, Kamp PJJ, (compilers) 2011. Geology of the Hawke's Bay area. Institue of Geological & Nuclear Sciences 1:250,000 geological map 8. Lower Hutt, New Zealand. GNS Science. 1 sheet + 93 p.

MacDonald-Creevey AM 2011. Late Holocene environmental record and geological history of the Lake Colenso area, North-western Ruahine Range, New Zealand. Unpublished MSc thesis, Massey University, Palmerston North, New Zealand. 159 p.

Massey CI 2010. The dyncamics of reactivated landslides: Utiku and Taihape, North Island, New Zealand. Unpublished PhD thesis, Durham University, Durham, United Kingdom. 319 p.

Melhuish A, van Dissen R, Berryman KR 1996. Mount Stewart-Halcombe Anticline: A look inside a growing fold in the Manawatu region, New Zealand. New Zealand Journal of Geology and Geophysics 39: 123-133.

Milne JDG 1973. Upper Quaternary geology of the Rangitikei drainage basin, North Island, New Zealand. Unpublished PhD Thesis. Victoria University of Wellington, Wellington, New Zealand. 472 p.

Molloy L 1998. Soils in the New Zealand Landscape, the living mantle. 2nd Edition ed. Lincoln Univeristy, Canterbury, New Zealand, The New Zealand Society of Soil Science. 253p.

Murrell G 1998. Lithostratigraphy and sequence stratigraphy of Matemateaonga Formation (Early Pliocene), Moawhango Valley, eastern Wanganui Basin. Unpublished MSc Thesis, University of Waikato, Hamilton, New Zealand. 1-230 p.

Naish TR, Kamp PJJ 1995. Pliocene-Pleistocene marine cyclothems , Wanganui Basin , New Zealand : a lithostratigraphic framework. New Zealand Journal of Geology and Geophysics 38: 223-243.

Naish TR, Field BD, Zhu H, Melhuish A, Carter RM, Abbott ST, Edwards S, Alloway BV, Wilson GS, Niessen F and others 2005. Integrated outcrop, drill core, borehole and seismic stratigraphic architecture of a cyclothemic, shallow marine depositional system, Wanganui Basin, New Zealand. Journal of the Royal Society of New Zealand 35(1-2): 91-122.

Neall VE 1982. Landforms of Taranaki and the Wanganui Lowlands. In: Soons JM, Selby MJ ed. Landforms of New Zealand. Auckland, New Zealand, Longman Paul Ltd. Pp. 193-211.

NZGS 2005. Field description of soil and rock: Guideline for the field classification and description of soil and rock for engineering purposes, New Zealand Geotechnical Society Inc. 38 p.

Oulton D 1998. Stratigraphy and sedimentology of early Pliocene succession, Mangaohane region, eastern Wanganui Basin. Unpublished MSc Thesis, University of Waikato, Hamilton, New Zealand, 115p.

Pillans BJ 1986. A late Quaternary uplift map for North Island, New Zealand. Royal Society of New Zealand Bulletin 24: 409-417.

Pillans BJ 1990. Vertical displacement rates on Quaternary faults, Wanganui basin. New Zealand Journal of Geology and Geophysics 33(2): 271-275.

Pillans BJ 2017. Quaternary Stratigraphy of Whanganui Basin-A Globally Significant Archive. In: Schulmeister J ed. Landscape and Quaternary Environmental Change in New Zealand. Brisbane, Australia, Atlantis Press. Pp. 141-170.

Price NJ 1966. Fault and joint development in Brittle and Semi-brittle Rock. First edition ed. Oxford, United Kingdom, Pergamon Press. 173 p.

Pulford A, Stern T 2004. Pliocene exhumation and landscape evolution of central North Island, New Zealand: The role of the upper mantle. Journal of Geophysical Research: Earth Surface 109(F01016): 1-12.

Quinn JM, Wilcock RJ, Monaghan RM, McDowell RW, Journeaux PR 2009. Grassland farming and water quality in New Zealand. Tearmann: Irish journal of agri-environmental research 7: 69-88.

Read SAL, Miller PJ 1990. Characterisation and classification of New Zealand Teritary age sedimentary soft rocks. Bridge Design and Research Seminar. 1990: Volume 4: Road Engineering in Soft Rock Materials. RRU Bulletin 84. Pp. 1-25.

Rees CJ, Palmer JA, Palmer AS 2018a. Quaternary sedimentology and tephrostratigraphy of the lower Pohangina Valley, New Zealand. New Zealand Journal of Geology and Geophysics 62(2): 171-194. DOI: 10.1080/00288306.2018.1547321.

Rees CJ, Palmer JA, Palmer AS 2018b. Gilbert-Style Pleistocene Fan Delta Reveals Tectonic Development of North Island Axial Ranges, New Zealand. New Zealand Journal of Geology and Geophysics 61(1): 64-78.

Rees CJ, Palmer JA, Palmer AS, Singh R 2019. Landscape evolution and hydrogeochemical characteristics of the Pourewa Stream catchment, Lower North Island, New Zealand. New Zealand Journal of Geology and Geophysics 62(2): 147-170. DOI: 10.1080/00288306.2018.1541812

Rogers GM, McGlone MS 1989. A postglacial vegetation history of the southern-central uplands of North Island, New Zealand. Journal of the Royal Society of New Zealand 19(3): 229-248.

Rosser B, Dellow S, Haubrock S, Glassey P 2016. New Zealand's National Landslide Database. Landslides 14(6): 1949-1959.

Rosser BJ, Townsend D, McSaveney E, Ries W 2014. Landslides and ground damage assoicated with the M6.2 Eketahuna earthquake, 20 January 2014, GNS Science Report 2014/51, Lower Hutt, New Zealand. 34p.

Schon JH 2015. Physical properties of rocks: Fundamentals and principles of petrophysics. Amsterdam, Netherlands, Elsevier. 491 p.

Shane PAR 1991. Remobilised silicic tuffs in middle Pleistocene fluvial sediments , southern North Island, New Zealand. New Zealand Journal of Geology and Geophysics 34(4): 489-499.

Stern TA, Quinlan GM, Holt WE 1993. Crustal dynamics associated with the formation of Wanganui Basin, New Zealand. In: Ballance PF ed. South Pacific Sedimentary Basins: Sedimentary Basins of the World 2. Amsterdam, Elsevier. Pp. 213-223.

Te Punga MT 1957. Live anticlines in western Wellington. New Zealand Journal of Science and Technology(38): 433-466.

Thompson RC 1982. Relationship of geology to slope failures in soft rocks of the Taihape-Mangaweka area, central North Island, New Zealand. Unpublished PhD Thesis, University of Auckland, Auckland, New Zealand. 330 p.

Townsend D, Vonk A, Kamp PJJ 2008. Geology of the Taranaki area: scale 1:250,000. Lower Hutt, GNS Science. Institute of Geological and Nuclear Sciences 1:250,000 geological map 7, Lower Hutt, New Zealand: 1 sheet+77p.

Vonk AJ, Kamp PJJ 2004. Late Miocene-Early Pliocene Matemateaonga Formation in eastern Taranaki Peninsula: A new 1:50,000 geological map and stratigraphic framework. 2004 New Zealand Petroleum Conference proceedings(March): 9p.

Wilson JG 1914. Early Rangitikei, Whitcombe and Tombs, Christchurch, New Zealand. 284 p.



Chapter 9

Discussion

The following chapter provides a short discussion of the hydrogeology of the Pourewa Stream sub-catchment. Here, I strive to avoid repeating the discussion from chapters 3-8, all of which are either published or intended for publication in peer-reviewed journal articles. Instead, I place the focus on new knowledge obtained in relation to the study area's groundwater system, including presentation of a conceptual hydrogeological model to illustrate some of the relationships discussed in the text. Concepts presented herein draw from the entire body of work, rooted in observations made during the fieldwork component of the study. Chapter 9 captures thesis objectives 3, 4 and 5 by presenting a hydrostratigraphic framework, a conceptual hydrogeological model and by placing the study into regional context through discussion of insights gained during the course of this work.

Important insights from this study include:

- Groundwater springs occur in close relationship with fault zones, related to the faulting of aquitards into elevated positions in the landscape.

- Shallow unconfined groundwater flows along paleo-channels within Late Quaternary terrace gravels, emerging as springs where intercepted by topography.

- Siltstone and mudstones within the WB succession act as aquitards, restricting vertical and facilitating horizontal groundwater flow. Springs nearly always emerge on top of an aquitard, suggesting these layers form an important component of the hydrostratigraphy.

- All streams and rivers observed in the study area are effectively cutting over 'basement', in that they are eroding into the underlying marine succession of the WB in a bid to reach sea level. This observation demonstrates that groundwater interactions between Plio-Pleistocene 'basement' could occur along significant reaches of waterways in the study area, likely as fluxes between unconfined shallow alluvial fill and the underlying older marine succession.

- All geological units measured in this study have some ability to store and transmit water, with the classification of local aquifer units being user defined, based on the consumer's definition of a 'significant' volume of water. Useable quantities of water for an irrigation scheme are in large excess to those required to supply stock water or house supply. This is illustrated by the dominance of river abstraction for irrigation supply in the terrace country compared to the frequent utilisation of groundwater springs by sheep and beef farmers to supply small-scale, farm water systems in the hill country.

- Stratigraphic units of the WB, commonly disregarded as hydrogeological 'basement', are texturally diverse sedimentary rocks that play an important role in the groundwater system. A majority of this sedimentary rock has low

potential as a productive aquifer, however, relatively thin layers of coarse sedimentary rock contain hydraulic conductivity values comparable with Quaternary fill. These permeable layers are responsible for some of the artesian water encountered in the study area, often at depths far exceeding the known depth of Quaternary fill. From observing drilling records, artesian water appears notoriously difficult to locate, yet when found can in some instances produce volumes sufficient for irrigation supply. Due to a focus of water bores in discharge zones of the landscape, principally the modern day valley floor, there is a possibility of topographically controlled artesian pressures occurring within unconfined hydrostratigraphic units (Fetter 2001; Gaber 2005).

- Late Quaternary fill represents the most productive aquifer unit in the study area. However, given its close relationship with surface water bodies it also represents the most susceptible to pollution and over exploitation. By tapping the shallow unconfined groundwater present within Quaternary fill, you are effectively abstracting directly from the river, as the two are inseparable.

- Geological structure plays an important role in landscape development, shaping the modern day drainage network we see today. Rivers crossing the Manawatu-Whanganui region have been systematically captured between basement highs aligned roughly NNE-SSW along trend with the main axial range as the WB has emerged from the sea over the last c. 3 Ma. This has two key effects, firstly controlling the depth of Late Miocene-Pleistocene basin fill, which thickens between successive highs and secondly confining drainage pathways, focusing deposition of Late Quaternary to Holocene valley fill. Basement highs act to separate and hydrologically isolate the major river catchments forming groundwater divides.

- Different levels exist within the study area's hydrogeological system, from regional to local flow. This is evidenced by certain springs being immediately affected by rainstorms with an increase in flow whilst others maintain consistent flow throughout the year. Observations of multiple, stratigraphically separate seep and spring lines emerging at cliff exposures is also indicative of a multi-level system, consistent with the stratigraphic 'layer cake' of the encompassing marine basin. In contrast, as proposed by Zarour (2008) overlying Late Quaternary valley fill in the region appears to be semi to unconfined, constantly interacting with surface water bodies and is best conceptualised as a 'leaky' system.

- The presence of abundant Fe^{2+} bearing minerals and low to moderate levels of organic matter within the WB and modern day fluvial basin sediments are likely to be an important source of electron donors during microbially facilitated de-nitrification. These hydrogeochemical and biological processes are likely to be a contributing factor in the unaccounted loss of nitrogen between farmland and receiving waterways.

9.1 Conceptual hydrogeological model

Here I present a conceptual hydrogeological model for the Pourewa sub-catchment (Fig 9.1 and 9.2) incorporating data from chapters 3–8. Mapping of the regional stratigraphy and structure in the central Rangitikei has been fundamental to development of this model, providing a framework for conceptualisation of the local hydrogeology (Chapter 3). Multiple hydrostratigraphic units are identified (Table 9.1) within the study area, capable of storing and transmitting varying quantities of water. Identification has proceeded through lab and *in situ* field-testing of sediments and sedimentary rock, building an overview of typical values present within the mapping area (Chapter 6 and 7).

Table 9.1: List of hydrostratigraphic units within the study area and their associated range of hydraulic conductivity.

Age	Group	Hydrostratigraphy	Classification	Lithology	Hydraulic conductivity m/day
12 - 0 ka	Holocene	Holocene alluvial deposits	Aquifer	Unconsolidated gravel, sand and silt	Clean gravel ↓ Increasing fines 2050 ↓ 25
		Holocene landslides	Aquitard	Dominantly poorly drained due to colluvial processes	Sand ↓ Silt 25 ↓ 5
370-12 ka	Quaternary terraces	Late Quaternary terrace deposits	Aquifer	Cemented gravel, weakly consolidated sand and silt	Clean gravel ↓ Increasing fines 700 ↓ 5
2.58-0 Ma	Undifferentiated Quaternary	Undifferentiated Quaternary landslides	Aquitard	Dominantly poorly drained due to colluvial processes	Sand ↓ Silt 25 ↓ 5
0.31 Ma?	Pouakai Group	Westoe Frm.	Aquifer	Weakly consolidated dune sands	Coarsening → 25 - 50
		Halcombe Conglomerate	Aquifer	Coarse conglomerate	Less fines → 50 - 700
0.34 Ma	Shakespeare Group	Mangatapu Frm.	Aquifer	Frequent conglomerate, shell hash conglomerate and pumiceous horizons subordinate siltstone	Clean gravel ↓ Increasing fines Siltstone 700 ↓ 5
0.57 Ma		Tokorangi Frm.	Aquitard	Dominantly fine grained with minor conglomeratic and shell bed horizons	Sand ↓ Silt 25 ↓ 5
0.65 Ma	Kai Iwi Group	*Toms Conglomerate Mb.*	Aquifer	Coarse conglomerate	Less fines → 50 - 700
		Waiomio and Reu Reu Frm.	Aquitard	Dominantly fine grained, thin conglomeratic and shell hash horizons, generally low hydraulic conductivity	Sand ↓ Silt 25 ↓ 5
0.9 Ma		*Waitapu Shell Conglomerate*	Aquifer	Coarse conglomerate	Less fines → 50 - 700
		Kaimatira Pumice Sand Frm.	Aquitard	Dominantly siltstone	Sand ↓ Silt 25 ↓ 5
0.99 Ma		*Potaka Pumice*	Aquifer	Coarse to granular pumice conglomerate	Less fines → 25 - 400
1.19 Ma	Okehu Group	Rewa Frm.	Aquitard	Dominantly siltstone	Sand ↓ Silt 25 ↓ 5
		Mangapipi Conglomerate	Aquifer	Coarse conglomerate	Less fines → 50 - 700
1.54 Ma		Makirikiri Tuff Frm	Aquitard	Dominantly siltstone	Sand ↓ Silt 25 ↓ 5
1.58 Ma		*Pakihikura Pumice*	Aquifer	Pumiceous sandstone	Granular pumice ↓ Sand 400 ↓ 25
1.6 Ma	Maxwell Group	Upper Maxwell Frm		Pumiceous horizons, sandstone and interbedded silstone. Known to hold water, often stained brown unpotable.	
1.65 Ma		Vinegar Hill and Rataiti Frm	Aquitard	Dominantly siltstone and fine grained sandstones, minor shellbeds	Sand ↓ Silt 25 ↓ 5
1.75 Ma	Rangitikei Group	*Waipuru Shellbed*	Aquifer	Coarse shellbed and sandstone	Coarsening → 25 - 400
1.83 Ma		Mangaonoho Frm	Aquitard	Dominantly siltstone	Sand ↓ Silt 25 ↓ 5
2.05 Ma		*Mangamako Shellbed*	Aquifer	Coarse shellbed and sandstone	Coarsening → 25 - 400
2.17 Ma		Orangipongo Frm	Aquitard	Dominantly siltstone	Sand ↓ Silt 25 ↓ 5
		Ohingaiti Sand	Aquifer	Sandstone	Coarsening → 25 - 50
		Makohine Frm	Aquitard	Dominantly siltstone	Sand ↓ Silt 25 ↓ 5
		Tuha Sand	Aquifer	Sandstone	Coarsening → 25 - 50
2.4 Ma		Tikapu and Upper Mangarere Frm	Aquitard	Dominantly siltstone	Sand ↓ Silt 25 ↓ 5
		Lower Mangarere Frm and *Te Rimu Sand*	Aquifer	Moderately to weakly consolidated sandstone	Coarsening → ← Consolidation 25 - 50
2.8 Ma	Paparangi Group	Mangaweka Mudstone	Aquitard	Siltstone and sandstone, has sandy zones holding water, aquifer layers	Sand ↓ Silt 25 ↓ 5

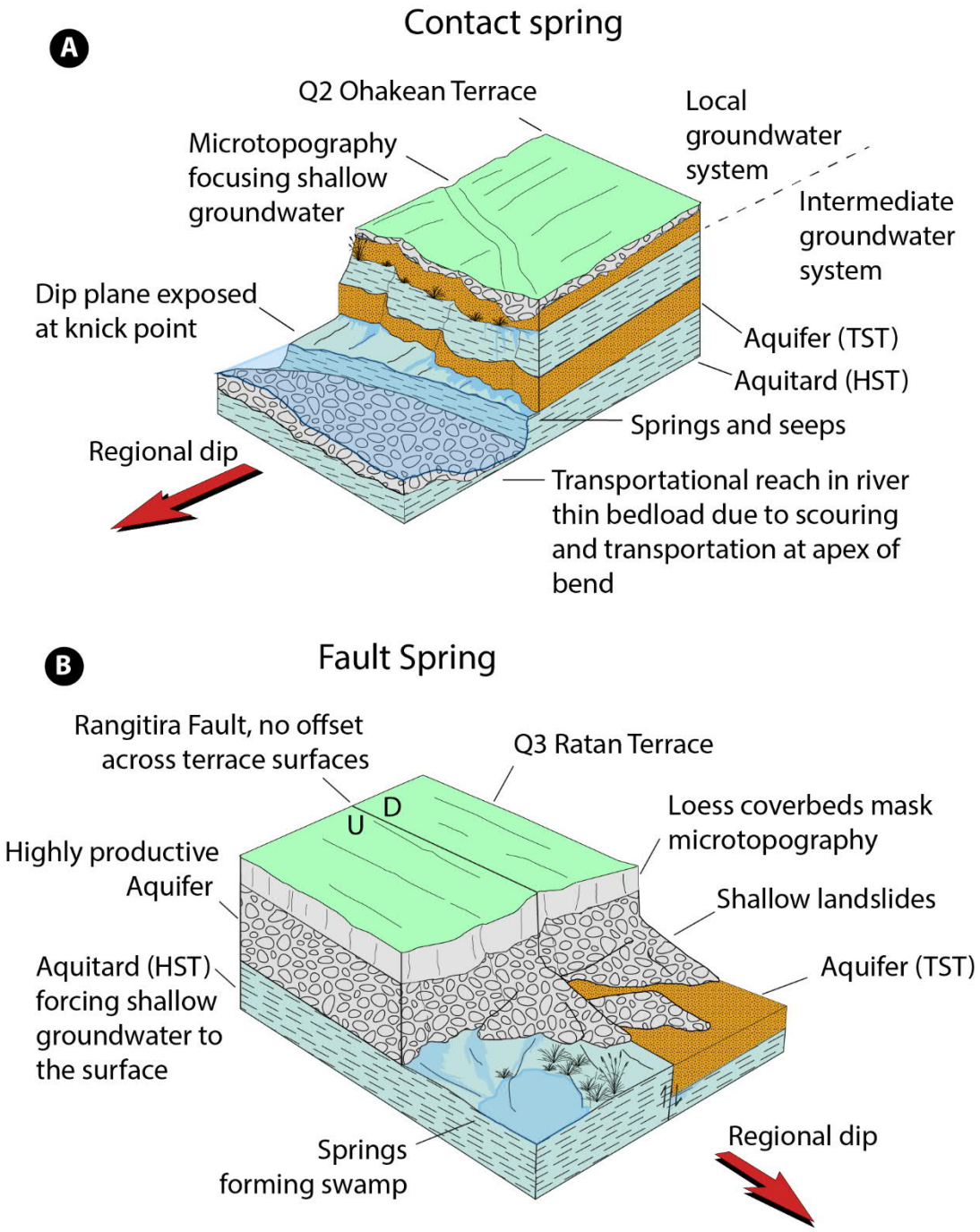


Figure 9.1: Conceptual diagrams illustrating observed relationships between rock types and water in the landscape. A) Typical outcrop in the older Pliocene – Early Pleistocene succession of the WB, alternating fine- and coarse-grained sediments representing transgressive and high stand systems tracts. These cyclothems are spectacularly exposed in the Rangitikei Valley, typically each contact contains a seepage line with vegetation. B) An example of a fault created spring where uplifted siltstone is creating a barrier to flow that is then intercepted by topography. Note diagram A depicts a single field example of an Ohakean 3 Terrace (degradational phase following LGM), typically Q2 aggradational terrace gravels reach greater thickness than Q3 terrace gravels.

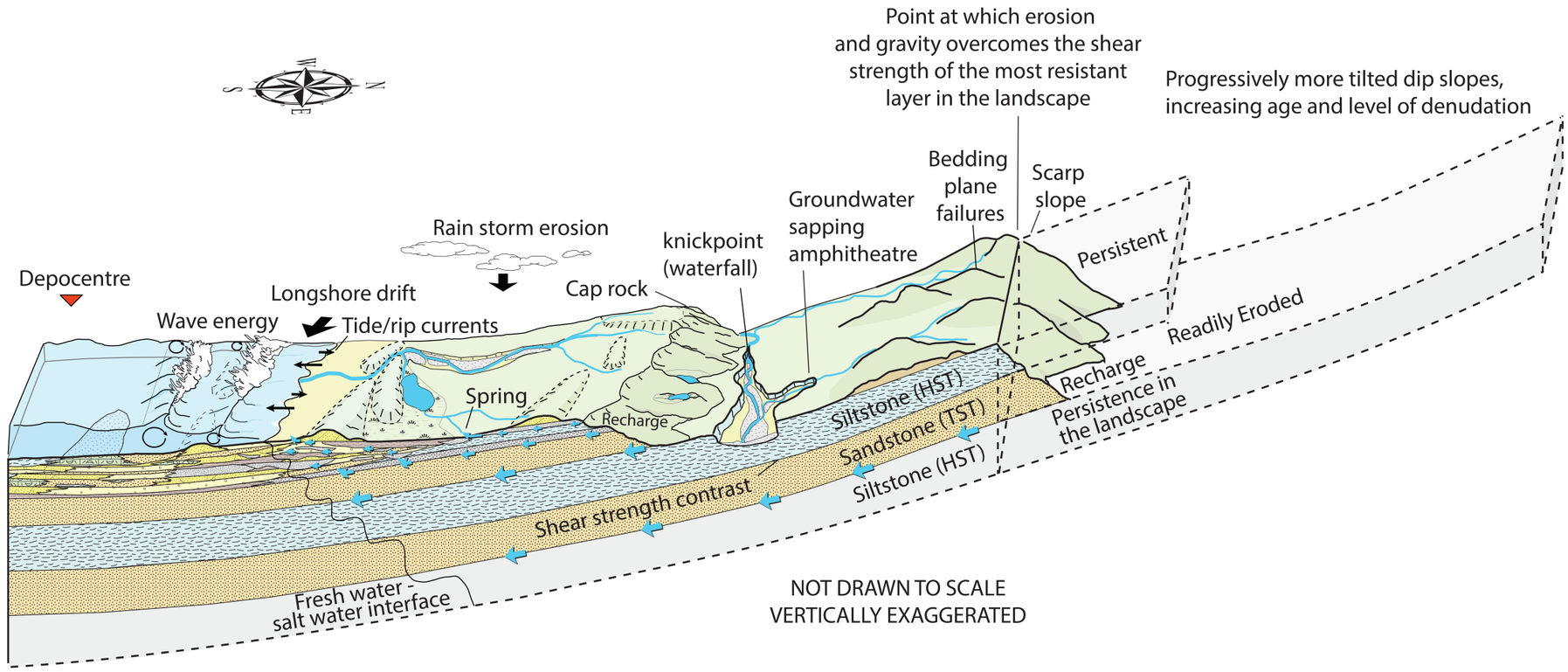


Figure 9.2: Schematic diagram illustrating the conceptual hydrogeological model.

The central Rangitikei's groundwater system is stratified (Fig 9.1 and 9.2), in that it has several different levels, some of which interact with one another and surface water bodies. This is not to refute the proposal by Zarour (2008) that the Late Quaternary fill is best conceptualised as semi-confined (leaky) system, but to emphasize the existence of an older, somewhat more laterally extensive marine succession that in places attains significant hydraulic conductivities. The Late Pliocene and Early Pleistocene units include HST deposits of thick siltstone and mudstone deposited at a time when the sedimentary depocentre was located near to the present study area. These units attain enough lateral persistence and internal homogeneity to act as confining layers to intervening porous, thinner TST deposits.

Despite its massive appearance, the Pliocene Mangaweka Mudstone Formation is texturally diverse, containing variations in grain size associated with sea level cycles (Journeaux et al. 1996). It has been noted during field survey and discussion with members of the local community that this seemingly massive blue grey mudstone in places holds water, observed exiting exposures as seeps and springs. However, given its stratigraphic position at the base of the targeted succession in this study and the relatively low hydraulic conductivities measured relative to known high yield aquifers, the Mangaweka Mudstone Formation is considered hydrogeological basement in this study. Rare occurrences of natural gas seeps are also noted emanating from Mangaweka Mudstone Formation by residents, although the author could not confirm their existence during the field survey.

The Pleistocene marine succession underlying the productive Late Quaternary fill should not be entirely dismissed as hydrogeological basement during regional groundwater investigations. Instead, it should be included as a necessary component during conceptualisation of the groundwater system. Furthermore, continued stratigraphic work is necessary in the WB to define the transition from Pouakai Group to Holocene sediments, currently left ill-defined due to the

complicated nature of this recent phase in the WB's evolution. This clarification would enable more accurate definition and subdivision of the productive Late Quaternary fill including accurate introduction and definition of a lower base. Broadly, hydraulic conductivity reduces with increasing age due to the physical and geochemical changes of compaction and cementation during diagenesis. This results in steadily decreasing hydrogeological importance of units with age, due to lower hydraulic conductivity, progressively greater drilling depths and associated costs required for groundwater extraction. Of course, even the oldest hydrostratigraphic units crop out on the surface somewhere, facilitating groundwater recharge. Therefore, every hydrostratigraphic unit occurs as an unconfined unit in the hill country at shallow depth transitioning to a confined unit at depth farther south beneath the coastal and alluvial plains.

Water use and demand is concentrated on the plains where the older marine succession is at depth overlain by thick and highly productive Late Quaternary fill. This has largely led to the concentration of past groundwater investigations on the Kairanga-Manawatu Plains.

The first influx of coarse greywacke detritus to the eastern WB signaling the beginning of rapid emergence of the main axial range is just above and below the Pakihikura Pumice (1.58 Ma) (Milne 1968). From this time onward we see periodic deposition of coarse greywacke gravel sheets prograding outward from the uplifting paleo-axial range in a broad apron, extending as far west as the Rangitikei River. These gravels are so extensive that we see them commonly reworked into nearshore, shallow marine environments of the Mid Quaternary WB succession, forming basal transgressive lags and conglomeratic type A shellbeds. Pourewa Stream and Turakina River are also both prime examples of the extent of these gravels, both occurring just beyond the reach of the main sediment pathways from the axial range, with headwaters located in soft marine Pliocene sediment. Nevertheless, they contain considerable greywacke gravel fill, reworked

and incorporated from more easterly sources during various phases of their evolutionary history.

Hydrogeological literature places considerable importance on gravel and conglomerate units (Q2-Q10), mapping their extent of observable outcrop and correlating/extrapolating their ongoing occurrence in the subsurface beneath the Kairanga Plains (Te Punga 1952; Russell 1989; Bekesi 1998; Schumacher 1999; Taylor et al. 2001; Begg et al. 2005; Zarour 2008; Hughes & Kennedy 2009; Clement 2011). This emphasis is well placed, consistent with field observations gathered by Kampman and Caldwell (1985), Reynolds (1992), Cussins (1994) and during this study. However, why are we limiting ourselves to Q10 and in some instances Q12 (McCarron & Zarour 2005) gravel and conglomerate units? Furthermore, why are units that are clearly already defined in the geological literature (Te Punga 1952; Milne 1973) being given new, seemingly arbitrary names (Foxton, Himatangi, Opiki, Palmerston North, Linton aquifers)? There appears to be a disconnect between the considerable wealth of literature focused on the WB and the few hydrogeological studies conducted relatively more recently, seemingly in isolation from one another.

Toms Conglomerate occurs before the Onepuhi Tephra (570 ka) within the Rangitikei succession and is lithologically quite similar to an Ohakean gravel unit (Q2), albeit with a greater level of weathering. The similarity is so pronounced that in many cases the angle of dip and stratigraphic position need to be used to differentiate between <50 ka gravel and Toms Conglomerate (>570 ka gravel), often found in direct contact with one another. If we were to use this unit to re-adjust our hydrogeological standpoint on what constitutes high yield Late Quaternary fill, we would find we have almost doubled our amount of viable fill in the Rangitikei District. Clearly, any proposed re-definition should be carefully considered as it has far-reaching consequences.

The recognition, definition and exploitation of a separate seemingly isolated Nukumaruan aquifer within the Nukumaru Limestone and Nukumaru Brown Sand members (Fleming 1953) in Kai Iwi Valley and Whanganui (Evans et al. 2006) is in the authors opinion a somewhat narrow and limited perspective. The sediments forming this aquifer are not an isolated deposit within the WB, in fact they have clear equivalents in the present study area, namely the Mangamako Shell bed and Waipuru Shell beds, that occur as thin sandy coquina lenses within weakly consolidated, coarse sands with hydraulic conductivities as high as 400m/day. This may seem insignificant given the tremendously high hydraulic conductivity encountered in the Late Quaternary fill (2000 m/day). Yet when one accounts for the thickness of these sediments, 30–100 m, we obtain transmissivities of up to 40,000 m^2/day. To place this into some type of context, the highest hydraulic conductivity from the Nukumaruan Aquifer currently supplying drinking water to Whanganui City measured during pumping tests by Evans et al. (2006) was 75 m/day with maximum transmissivities of 2,295 m^2/day. Groundwater yields of 4 - 11.6 m/day have been obtained from the Late Miocene-Early Pliocene Matemateaonga Formation (typically considered hydrogeological 'basement'), stratigraphically below the Nukumaruan Aquifer (Allis et al. 1997).

Any assessment of groundwater resources in the WB would benefit greatly from taking a broader initial perspective to place local groundwater classification into regional context. This is not to take away from the important and useful work of Evans et al. (2006), but to suggest that end users of these scientific reports do not view a single local study in isolation of the regional setting; the importance of which is emphasized in early works of Feldmeyer et al. (1943), Te Punga (1952) and Fleming (1953).

If we think about the Nukumaruan aquifer in Whanganui from a wider geological perspective, it can provide a useful example, enabling an appreciation of the sedimentary basin on which we find ourselves living today. This sedimentary unit

was deposited within a shallow, near-shore, high-energy environment on the western margin of a sedimentary basin, the depocentre of which was undergoing a slow southward migration.

If we were to follow these nearshore deposits east at the time of their deposition, we would encounter progressively deeper water, finer grained deposits until crossing over the centre of the basin to the opposing side where once again, we would find coarse, marginal, high energy deposits. The WB is characterised by a mud depocentre occurring at shelf depths, similar to the contemporary mud depocentre on the south Taranaki Bight today. This depocentre is surrounded by coarse gravelly and shelly sands, deposited and sorted in nearshore environments by wave action while fine material is carried further out in suspension to deeper water. The depocentre has tracked south through geological time and with it so has its assortment of laterally adjacent depositional environments. Superimposed on this broad picture are seventy depositional cycles (Carter & Naish 1998; Naish et al. 1998; Grant et al. 2018), related to Quaternary climatic fluctuations resulting in water depth variations of up to 120m.

If we map the pattern of shifting depositional environments through geological time, we will understand where the chronologically equivalent shallow, marginal marine counterparts occur and as such, where potential hydrogeological reservoirs are located, analogous to the Nukumaruan aquifer suppling Whanganui City today. Developing a complete understanding of basin history will be the most important contribution to understanding the region's subsurface natural resources. What's more, we have somewhat of a head start, thanks to the insightful works of Feldmeyer et al. (1943), Te Punga (1952) and Fleming (1953), which continue to form the basis of natural resource investigation in our region today. A true testament to the ongoing relevance of work deeply entrenched in basic stratigraphy and fieldwork.

9.2 Sequence stratigraphy

The Whanganui Basin fill provides the perfect opportunity to investigate sequence stratigraphic concepts. The influence of eustatic sea level fluctuations on sedimentation was recognised over 60 years ago during early mapping of the basin (Fleming 1953). Advances in the application of radiometric, paleomagnetic, fission track and isotopic dating techniques have led to development of a basin wide chronostratigraphic framework, culminating in the correlation of the basin fill to the high resolution astronomically tuned $\delta^{18}O$ record (Naish et al. 1998).

Sequence stratigraphy is an important aspect of this thesis, despite not forming the basis of any single chapter. In particular, chapters 4, 5 and 7 make good use of sequence stratigraphic concepts during the definition, correlation and investigation of individual cycles within the basin fill. This study draws from a large and extensive body of work dealing with the sequence stratigraphy of the WB succession (Carter et al. 1991; Abbott 1994; Naish et al. 1996; Naish et al. 1998; Naish et al. 2005). For this reason, we have not endeavored to focus on sequence stratigraphy, instead taking a step back to delve into the fundamental geology and hydrogeology of the study area and fill in the gaps between existing high-level maps.

We present a complete lithostratigraphy not based on cyclothems, but on easily recognizable marker horizons. Formations typically include several cyclothems and the sequence boundaries commonly do not align perfectly with formational boundaries (Table 9.2). Furthermore, the author suggests mapping cyclothems across the heavily eroded Whanganui-Manawatu hill country to be impractical. The lithostratigraphic framework presented in this thesis is focused on providing a useful reference for mapping in the basin, in particular the recognition of

Table 9.2: Stratigraphic nomenclature of the study area including associated Whanganui Basin cyclothems (WB cycles), total number of cycles and marine oxygen isotope stages (MIS). Data from Naish and Kamp (1995), Saul et al. (1999) and Pillans et al. (2005).

Superior Oil Company NZ (1943)		Fleming (1953) Whanganui		Te Punga (1952) Rangitikei		Potter (1984) Bussell (1984) Rangitikei		This study Rangitikei		WB Cycles	Total no Cycles	MIS
RECENT		POUAKAI GROUP	Brunswick Frm.	UPPER RANGITIKEI FORMATION	Mangaone Sandstone	POUAKAI GROUP	Westoe Frm.	POUAKAI GROUP	Westoe Frm.	44	1	9
			Kaiatea Frm		Halcombe Conglomerate Waituna Conglomerate		Halcombe Conglomerate Frm.		Halcombe Conglomerate Frm.	43	1	10
		SHAKESPEARE GROUP	Landguard Frm Putiki Shellbed Mosstown Sand Karaka Siltstone Upper Castlecliff Shellbed Shakespeare Cliff Sand Shakespeare Cliff Siltstone Tainui Shellbed Pinnacle Sand Lower Castlecliff Shellbed Seafield Sand		Rangitawa Fossil Beds Kakariki Conglomerate Ruamahanga Conglomerate Onepuhi Fossil Beds Toms Conglomerate	SHAKESPEARE GROUP	*Mingaroa Fossil Bed Mb.* *Upper Kakariki Shell Conglomerate Mb.* *Te Hiiri Shellbed Mb.* *Rangitawa Fossil Bed Mb.* Mangatapu Frm *Kakariki Conglomerate Mb.* *Pryce Shellbed Mb.* *Ruamahanga Conglomerate Mb.* *Otapatu Shellbed Mb.* *Onepuhi Fossil Beds Mb.* Tokorangi Frm *Toms Shellbeds Mb.* *Toms Conglomerate Mb.*	SHAKESPEARE GROUP	*Mangatapu Frm.* *Ruamahanga Conglomerate Mb.* *Tokorangi Frm.* *Toms Conglomerate Mb.*	42 41 40 39	2 2	14-10 16-14
OTAKI												
CASTLECLIFFIAN	Kimbolton Ash	KAI IWI GROUP	Upper Kai Iwi Siltstone Kupe Frm Upper Westmere Siltstone Kaikokopu Frm. Lower Westmere Siltstone Omapu Shellbed Lower Kai Iwi Siltstone Kaimatira Pumice Sand		Shell Creek Fossil Beds Waitapu Shell Conglomerate Potaka Pumice		*Shell Creek Fossil Bed Mb.* Reu Reu Frm. Waiomio Frm. (Abbott 1992)	KAI IWI GROUP	Reu Reu Frm. *Waiomio Shellbed Mb.* Waiomio Frm. *Waitapu Shell Conglomerate Mb.* Kaimatira Pumice Sand Frm. *Potaka Pumice Mb.*	38 37 36 35 34	3 2	26-16 28-26
	Coutts Creek Horizon	OKEHU GROUP	Upper Okehu Siltstone Okehu Shell Grit Lower Okehu Siltstone Butlers Shell Conglomerate Makirikiri Tuff		Mangapipi Fossil Beds Pakihikura Pumice		Undifferentiated	OKEHU GROUP	*Rewa Frm.* *Mangapipi Conglomerate Mb.* *Mangapipi Mb.* Makirikiri Tuff Frm *Pakihikura Mb.*	33 32 31 30 29 28 27 26 25 24 23 22	6 6	44-28 56-44
	Basal Ash	MAXWELL GROUP	Upper Maxwell Frm Mangahou Siltstone Middle Maxwell Frm Pukekiwi Shell Sand Lower Maxwell Frm Tewkesbury Frm					MAXWELL GROUP	Upper Maxwell Frm Rataiti Frm	22 21 20 19	2 2	58-56 61-58
NUKUMARUAN	Waipuru Shellbed	NUKUMARU GROUP	Waipuru Shellbed	MIDDLE RANGITIKEI FORMATION	Waipuru Fossil Beds	RANGITIKEI GROUP	Vinegar Hill Frm *Waipuru Shellbed Mb.*	RANGITIKEI GROUP	Vinegar Hill Frm *Waipuru Shellbed Mb.*	19 18 17 16	4	68-61
	Mangamako Shellbed		Mangamako Shellbed		Mangamako Fossil Beds		Mangaonoho Frm *Mangamako Shellbed Mb.*		Mangaonoho Frm *Mangamako Shellbed Mb.*	15 14 13 12 11	5	80-68
	Ohingaiti Sand		Ohingaiti Sand		Ohingaiti Sandstone		Orangipongo Frm *Ohingaiti Sand Mb.*		Orangipongo Frm *Ohingaiti Sand Mb.*	10 9 8 7	4	88-80
	Tuha Sand	OKIWA GROUP	Kuranui Limestone		Tuha Sandstone		Makohine Frm *Tuha Sand Mb.*		Makohine Frm *Tuha Sand Mb.*	6 5 4 3	4	96-88
	Hautawa Shellbed		Hautawa Shellbed Te Rama Shellbed Parihauhau Shellbed				Tikapu Frm *Hautawa Shellbed Mb.*		Tikapu Frm *Hautawa Shellbed Mb.*	2	1	98-96
	Basal Sand		Te Rimu Sand		Basal Sandstone		Mangarere Frm. *Te Rimu Sand Mb.*		Mangarere Frm. *Te Rimu Sand Mb.*	1	1	100-98
WAITOTARAN	Mangamahu Concretions	PAPARANGI GROUP	Wilkies Shellbed Makokako Sand	LOWER RANGITIKEI	Mangaweka Concretionary Mudstone	PAPARANGI GROUP	Mangaweka Mudstone (Journeaux et al. 1996)	PAPARANGI GROUP	Mangaweka Mudstone	-	7	G20-100
	Mangaweka Mudstone Frm.		Mangaweka Mudstone Paparangi Sandstone									

Note: 1) Individual cycles sometimes span across formation boundaries. 2) The upper contact of the Rangitikei Group as defined by Naish and Kamp (1995) does not correlate to the upper contact of the Flemings (1953) Nukumaru Group.

horizons that attain prominence in the landscape/section and there use for subdividing the basin fill into groups, formations and members. Chapter 3 describes the marker horizons used to produce the 1:25 000 geological map series presented in Appendix B.

References

Abbott ST 1994. Sequence Stratigraphy, Sedimentology and Paleoecology of Pleistocene Cyclothems in the Castlecliff Section, Wanganui Basin, New Zealand, Unpublished PhD Thesis. James Cook University of Northern Queensland, Australia. 297 p.

Allis RG, Zhan X, Evans C, Kroopnick P 1997. Groundwater flow beneath Mt Taranaki, New Zealand, and implications for oil and gas migration. New Zealand Journal of Geology and Geophysics 40: 137-149.

Begg JG, Palmer A, Gyopari M 2005. Geological synopsis of the Manawatu-Horowhenua area for a review of the region's hydrogeology. Institue of Geological and Nucelar Sciences Client Report 2005/172, Lower Hutt, New Zealand. 22 p.

Bekesi G 1998. The development of an Aquifer Vulnerability Assessment Methodology with Application to the Manawatu Area of New Zealand. Unpublished PhD Thesis, Victoria University of Wellington, Wellington, New Zealand. 256 p.

Carter RM, Naish TR 1998. A review of Wanganui Basin, New Zealand: Global reference section for shallow marine, Plio-Pleistocene (2.5-0 Ma) cyclostratigraphy. Sedimentary Geology 122(1-4): 37-52.

Carter RM, Abbott ST, Fulthorpe CS, Haywick DW, Henderson RA 1991. Application of Global Sea - Level and Sequence - Stratigraphic Models in Southern Hemisphere Neogene Strata from New Zealand. Special Publication of the International Association of Sedimentologists(12): 41-65.

Clement AJH 2011. Holocene Sea-Level Change in the New Zealand Archipelago and the Geomorphic Evolution of a Holocene Coastal Plain Incised-Valley System: The Lower Manawatu Valley, North Island, New Zealand. Unpublished PhD Thesis, Massey University, Palmerston North, New Zealand. 459 p.

Cussins AP 1994. Hydrology and hydraulic characteristics of the unconfined aquifers of the Otaki-Te Horo area. Unpublished MSc Thesis, Victoria University, Wellington, New Zealand. 136 p.

Evans C, Holmes G, Mains D, Boothway D 2006. Groundwater Resources of the Wanganui District. Report prepared for Wanganui District Council by MWH New Zealand Ltd, Project Number Z1107300, Wanganui, New Zealand. 38 p.

Feldmeyer AE, Jones BC, Firth CW, Knight J 1943. The geology of the Palmerston-Wanganui Basin, "West side", North Island, New Zealand. Unpublished Report

of the Superior Oil Company of New Zealand, Petroleum Report Series 171, Ministry of Economic Development, Wellington, New Zealand. 46 p.

Fetter CW 2001. Applied Hydrogeology. 4th ed. New Jersey, United States of America, Waveland Press Inc. 588 p.

Fleming CA 1953. The geology of Wanganui subdivision. New Zealand Geological Survey Bulletin 52. Wellington, New Zealand. 362 p.

Gaber MS 2005. Michigan Flowing Well Handbook. Michigan Department of Environmental Quality, Water Bureau, Drinking Water and Environmental Health Section, Well Construction Unit, Michigan, United States of America. 45 p.

Grant GR, Sefton JP, Patterson MO, Naish TR, Dunbar GB, Hayward BW, Morgans HEG, Alloway BV, Seward D, Tapia CA and others 2018. Mid- to late Pliocene (3.3-2.6 Ma) global sea-level fluctuations recorded on a continental shelf transect, Whanganui Basin, New Zealand. Quaternary Science Reviews 201: 241-260.

Hughes GR, Kennedy DM 2009. Late Pleistocene sea-level oscillations (MIS 10-2) recorded in shallow marine and coastal plain sediments of the southern Wanganui Basin, New Zealand. Quaternary Research 71: 477-489.

Journeaux TD, Kamp PJJ, Naish TR 1996. Middle Pliocene cyclothems , Mangaweka region , Wanganui Basin , New Zealand : A lithostratigraphic framework. New Zealand Journal of Geology and Geophysics 39(1): 135-149.

Kampman I, Caldwell KJ 1985. Groundwater Resources of the Waitohu, Otaki and Mangaone. Manawatu Catchment Board Report No 65, Palmerston North, New Zealand. 22 p.

McCarron C, Zarour H 2005. State of the environment of the Manawatu-Wanganui Region – 2005. Technical Report Five – groundwater, 2004/EXT/609. 1-67, Horizons Regional Council, Palmerston North, New Zealand. 73 p.

Milne JDG 1968. The geology and soils of the Apiti District. Unpublished MSc thesis, Victoria Universtiy of Wellington, New Zealand. 122 p.

Milne JDG 1973. Upper Quaternary geology of the Rangitikei drainage basin, North Island, New Zealand. Unpublished PhD Thesis. Victoria University of Wellington, Wellington, New Zealand. 472 p.

Naish TR, Kamp PJJ 1995. Pliocene-Pleistocene marine cyclothems , Wanganui Basin , New Zealand : a lithostratigraphic framework. New Zealand Journal of Geology and Geophysics 38: 223-243.

Naish TR, Kamp PJJ, Alloway BV, Pillans BJ, Wilson GS, Westgate JA 1996. Integrated tephrochronology and magnetostratigraphy for cyclothemic marine strata, Wanganui Basin: Implications for the Pliocene-Pleistocene boundary in New Zealand. Quaternary International 34-36(95): 29-48.

Naish TR, Abbott ST, Alloway BV, Beu AG, Carter RM, Edwards AR, Journeaux TD, Kamp PJJ, Pillans BJ, Saul G and others 1998. Astronomical calibration of a southern hemisphere Plio-Pleistocene reference section, Wanganui Basin, New Zealand. Quaternary Science Reviews 17(8): 695-710.

Naish TR, Field BD, Zhu H, Melhuish A, Carter RM, Abbott ST, Edwards S, Alloway BV, Wilson GS, Niessen F and others 2005. Integrated outcrop, drill core, borehole and seismic stratigraphic architecture of a cyclothemic, shallow marine depositional system, Wanganui Basin, New Zealand. Journal of the Royal Society of New Zealand 35(1-2): 91-122.

Pillans BJ, Alloway B, Naish TR, Westgate J, Abbott S, Palmer AS 2005. Silicic tephras in Pleistocene shallow-marine sediments of Wanganui Basin, New Zealand. Journal of the Royal Society of New Zealand 35(1-2): 43-90.

Reynolds TI 1992. Kapiti Coast sub-region - Groundwater review. Wellington Regional Council Publication No WRC/CI-T-92/44, Wellington, New Zealand. 44 p.

Russell W 1989. Groundwater-Manawatu Plains, GCNZ Consultants Report. In: Zrour, H. (2008) Groundwater Resources in the Manawatu - Wanganui Region. Technical Report 2008/EXT/948, Horizons Regional Council, Palmerston North, New Zealand. Pp. 130-133.

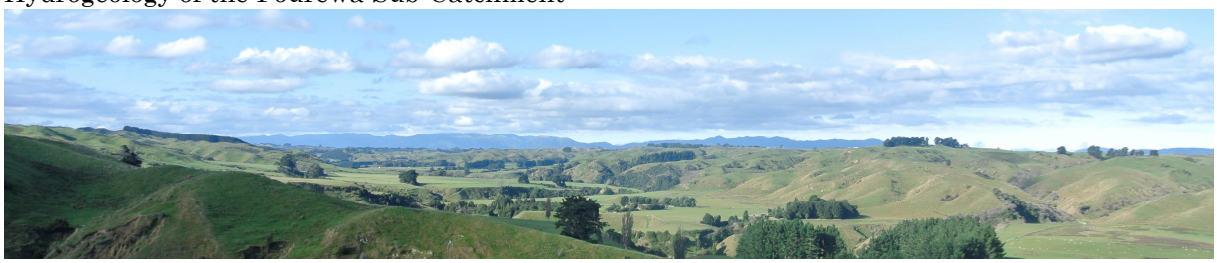
Saul G, Naish TR, Abbott ST, Carter RM 1999. Sedimentary cyclicity in the marine Pliocene-Pleistocene of the Wanganui basin (New Zealand): Sequence stratigraphic motifs characteristic of the past 2.5 m.y. Geological Society Of America Bulletin 111(4): 524-537.

Schumacher J 1999. Groundwater in the Lower Manawatu Valley (Palmerston North area), New Zealand. Unpublished MSc thesis, University of Waikato, Hamilton, New Zealand. 308 p.

Taylor CB, Trompetter VJ, Brown LJ, Bekesi G 2001. The Manawatu aquifers, North Island, New Zealand: Clarification of hydrogeology using a multidisciplinary environmental tracer approach. Hydrological Processes 15(17): 3269-3286.

Te Punga MT 1952. The geology of Rangitikei Valley. New Zealand Geological Survey Memoir 8, Wellington, New Zealand. 46 p.

Zarour H 2008. Groundwater Resources in the Manawatu–Wanganui Region Technical Report 2008/ET/948. Horizons Regional Council, Palmerston North, New Zealand. 262 p.



Chapter 10

Conclusion

The hydrogeology of the Pourewa sub-catchment is intricately related to its geographic location within the wider Whanganui groundwater basin. Basin fill comprises c. 4500m of Late Miocene-Quaternary marine sediments, including important aquifer units that supply agricultural, industrial and urban water supply schemes throughout the wider Manawatu-Whanganui Region.

Over the last c. 1.6 Ma, Mesozoic basement has pierced the Cenozoic basin fill of the lower North Island to form the main axial range. During uplift, gravel derived from the proto-axial range has periodically flooded into adjacent sedimentary basins, forming extensive alluvial fans. Contemporaneous volcanic eruptions in the TVZ have provided an important source of volcaniclastic sediment, transported by paleo-fluvial systems draining the central North Island.

WB fill has been deposited unconformably above a faulted shelf of Mesozoic basement that drops off steeply toward the paleo-basin depocentre west of the Turakina-Rangitikei interfluve. Pliocene–Early Pleistocene subsidence has transitioned into a marginally compressional regime characterised by a series of en echelon faults displaying scissor type movement, reverse reactivation and large lateral changes in throw.

The WB is characterised by a mud depocentre occurring at shelf depths, similar to the contemporary south Taranaki Bight today. The mud depocentre transitions landward into coarse gravel, shell and sand deposits, sorted by wave and tidal energy, whilst fine clay and silt is transported farther basinward. The basin depocentre has migrated southeastward through geological time. Sedimentation has occurred throughout climatically forced Quaternary sea level fluctuations, characterised by water depth variations of up to 120m. As a result, the WB contains a vertical stratigraphic succession of alternating coarse- and fine-grained sediments deposited within relatively shallow and deep-water depositional environments. Many of the formations within the basin succession encompass several individual sea level cycles separated by erosional unconformities. At the time of deposition, each cycle would have been characterised by a full suite of longitudinally and latitudinally adjacent depositional environments and associated facies, representing a shelf to shoreline transect across the basin. This suite of depositional environments and resultant facies are often times only partially preserved due to variations in uplift, accommodation space, erosion and paleogeography.

Tectonic uplift along the basin's northern and eastern margins has produced shore-normal tilting of the basin succession, forming gently inclined dip slopes oriented toward the modern day, offshore depocentre. Deep fluvial incision by rivers draining the central North Island and main axial range have partially exposed the basin succession, providing good outcrop within the major NE-SW oriented river valleys. The basin fill represents an abundant and relatively unexplored groundwater resource. Late Quaternary alluvial fill has been superimposed upon the gently tilted Plio-Pleistocene marine strata, providing the most productive shallow unconfined aquifer system in the study area. Local basement highs have channeled and constrained paleo-fluvial systems, resulting in valleys

characterised by highly productive, shallow, local groundwater systems that are intricately connected to the underlying regional WB groundwater system.

The shallow unconfined system is highly susceptible to pollution, due to its connection with surface drainage and a strong association with landforms characterised by recent landuse intensification. In the case of the Whanganui Basin, polluted waterways are but the surface expression of a polluted shallow groundwater system, in that the two are inseparable.

In contrast to the Late Quaternary valley fill, the Pleistocene sandstone and conglomerate aquifers of the marine basin fill are characterised by lower porosities and hydraulic conductivities. Longer residence times within these aquifers allows for depletion of oxygen and promotion of microbially facilitated denitrification. Reduction of nitrate requires the presence of suitable electron donors (clay and organic matter) in the sub-surface. In general, the marine basin fill is characterised by a higher nitrogen attenuation capacity than the shallow unconfined, valley fill.

This situation highlights a potential need to reduce stock numbers in river valley landscapes underlain by Late Quaternary valley fill with low nitrogen attenuation capacity. In contrast, better utilisation of hill country landscapes could possibly take advantage of their higher nitrogen attenuation capacity. Any change in management regime within the hill country would require careful consideration, due to the sensitivity of hill country soil types and the susceptibility of particular land areas to erosion and soil degradation.

This thesis presents an investigation into a single sub-catchment of the Rangitikei River with the goal of developing a conceptual hydrogeological model and providing geological input to aid council, landowners and researchers dealing with resource management issues in the Manawatu-Whanganui Region today.

Significant outcomes of this work include:

- Compilation of a 1:25 000 geological map series of the central Rangitikei with accompanying text, structural interpretation and 3D geological model (Rees et al. 2019a).

- Analysis of the physical and geochemical properties of major rock types in the central Rangitikei (Rees et al. 2019c, 2020c). Recognition of key hydrostratigraphic units and their importance within the regional hydrostratigraphy.

- Presentation of a geological history and model of landscape evolution within the Pourewa Stream sub-catchment and its relationship to the modern day hydrogeology of the area (Rees et al. 2019c).

- Development of a conceptual hydrogeological model for the Pourewa Stream sub-catchment, encompassing data from the wider geological survey. Presentation of the key hydrostratigraphic units within the Pourewa Stream sub-catchment and analysis of their structural and stratigraphic relationships.

- Preliminary spring survey in the central Rangitikei, including the identification of important hydrogeological controls on spring locations and their importance in understanding the regional hydrostratigraphy (Rees et al. 2019c).

- Addition of new geological and tephrostratigraphic data to aid stratigraphic correlation in the wider WB (Rees et al. 2019b, 2020a). Incorporation of datasets from the Pohangina and Oroua river catchments and integration into a basin history and interpretation of Quaternary paleogeography.

- Compilation of a revised stratigraphic framework for the central Rangitikei, with direct application to continued high level mapping in the eastern WB (Rees et al. 2019a).

- Regional application of the conceptual hydrogeological model within the wider Rangitikei hill country and WB (Rees et al. 2020b). Investigating Quaternary landslide distribution and its relationship to the structure, stratigraphy and hydrogeology of the Whanganui Basin fill.

- Investigation of landscape evolution in the Rangitikei hill country and wider Whanganui Basin (Rees et al. 2019c, 2020b). Revealing the influence of hydrogeology and structure on landscape forming processes.

Ultimately, these research outputs serve as a basis for future and ongoing analysis of the Manawatu-Whanganui Region's natural resources. Specifically to aid with investigations into regional and local groundwater systems and continued high level geological mapping of the WB.

10.1 Future Research

The limitations of this study provide scope for a large variety of future research projects. Proposed avenues for ongoing research include:

- Continued high-level spring survey of the central Rangitikei. This should entail a large-scale survey of local residents whom provide an incredible and under utilised resource. Summer provides the most convenient time to survey springs as the rivers are being recharged by baseflow and the ground is dry, making springs stand out (green grass, wet areas). This should be

followed up by a winter inspection, including flow gauging and water sampling. Flow gauging could be set up with v notch weirs and data logging systems for year round data capture. A spring survey will provide vital information on groundwater flow and variability through time.

- Flow gauging of the Pourewa Stream at multiple points. Geochemical analysis of the stream and spring water at these points. This will provide baseline data for developing a water balance and numerical hydrological model for the Pourewa sub-catchment.

- Ground investigation of the Late Quaternary valley fill by: ground penetrating radar (GPR), rotary core drilling, electrical resistivity survey (ER) and electricalmagnetic survey (EM), to constrain the depth and variation within this highly productive aquifer.

- Continued laboratory analysis of a wider range of sedimentary facies including: hydraulic conductivity, effective porosity, grain size distribution, mineralogy and geochemistry. This will provide further constraint on the natural variation within the WB succession.

- Installation of piezometers for a targeted water sampling regime to better understand the migration of nitrate from the farm to the river and the interplay between surface water and groundwater.

- Field survey of soils in the Pourewa Stream area, providing high-level maps to inform landuse management.

References

Rees CJ, Palmer AS, Palmer JA 2019a. The geology of the central Rangitikei, Whanganui Basin, lower North Island, New Zealand. 4 sheets+44p.

Rees CJ, Palmer JA, Palmer AS 2019b. Whanganui Basin, an archive of prehistoric earthquakes? Waitapu Shell Conglomerate (0.9 Ma), North Island, New Zealand. New Zealand Journal of Geology and Geophysics 62(2): 195-216.

Rees CJ, Palmer JA, Palmer AS, Singh R 2019c. Landscape evolution and hydrogeochemical characteristics of the Pourewa Stream catchment, Lower North Island, New Zealand. New Zealand Journal of Geology and Geophysics 62(2): 147-170.

Rees CJ, Palmer JA, Palmer AS 2020a. Tephrostratigraphic constraints on the timing of sedimentation and tectonism in the Whanganui Basin, New Zealand. New Zealand Journal of Geology and Geophysics 63(2): 262-280.

Rees CJ, Palmer AS, Palmer JA 2020b. Litho-structural controls on Quaternary landslide distribution in the Rangitikei hill country, North Island, New Zealand. New Zealand Journal of Geology and Geophysics 63(1): 90-109.

Rees CJ, Palmer JA, Palmer AS, Singh R 2020c. Variation in saturated hydraulic conductivity at the outcrop scale, the Whanganui Basin, New Zealand. Groundwater 58(4): 622-637.